

JUN 11 1993

ORNL-6746

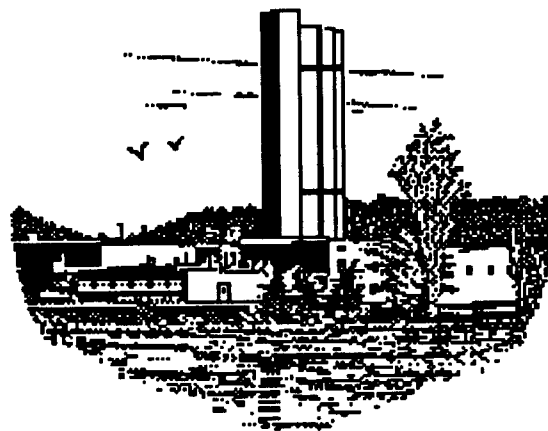
ornl

**OAK RIDGE
NATIONAL
LABORATORY**

MARTIN MARIETTA

PHYSICS DIVISION

**PROGRESS REPORT
for Period Ending September 30, 1992**



**MANAGED BY
MARTIN MARIETTA ENERGY SYSTEMS, INC.
FOR THE UNITED STATES
DEPARTMENT OF ENERGY**

This report has been reproduced directly from the best available copy.

Available to DOE and DOE contractors from the Office of Scientific and Technical Information, P.O. Box 62, Oak Ridge, TN 37831; prices available from (615) 576-8401, FTS 626-8401.

Available to the public from the National Technical Information Service, U.S. Department of Commerce, 5285 Port Royal Rd., Springfield, VA 22161.

This report was prepared as an account of work sponsored by an agency of the United States Government. Neither the United States Government nor any agency thereof, nor any of their employees, makes any warranty, express or implied, or assumes any legal liability or responsibility for the accuracy, completeness, or usefulness of any information, apparatus, product, or process disclosed, or represents that its use would not infringe privately owned rights. Reference herein to any specific commercial product, process, or service by trade name, trademark, manufacturer, or otherwise, does not necessarily constitute or imply its endorsement, recommendation, or favoring by the United States Government or any agency thereof. The views and opinions of authors expressed herein do not necessarily state or reflect those of the United States Government or any agency thereof.

PHYSICS DIVISION

PROGRESS REPORT for Period Ending September 30, 1992

J. B. Ball Director

F. E. Bertrand	Section Leader
S. Datz	Section Leader
D. K. Olsen	Section Leader
F. Plasil	Section Leader
R. L. Robinson	Section Leader
M. R. Strayer	Section Leader

Edited by: S. J. Ball

Date Published: March 1993

OAK RIDGE NATIONAL LABORATORY
Oak Ridge, Tennessee 37831
managed by
MARTIN MARIETTA ENERGY SYSTEMS, INC.
for the
U.S. DEPARTMENT OF ENERGY
under Contract No. DE-AC05-84OR21400

Previous reports in this series are as follows:

ORNL-2718	Period Ending March 10, 1959
ORNL-2910	Period Ending February 10, 1960
ORNL-3085	Period Ending February 10, 1961
ORNL-3268	Period Ending January 31, 1962
ORNL-3425	Period Ending May 21, 1963
ORNL-3582	Period Ending January 31, 1964
ORNL-3778	Period Ending December 13, 1964
ORNL-3924	Period Ending December 31, 1965
ORNL-4082	Period Ending December 31, 1966
ORNL-4230	Period Ending December 31, 1967
ORNL-4395	Period Ending December 31, 1968
ORNL-4513	Period Ending December 31, 1969
ORNL-4659	Period Ending December 31, 1970
ORNL-4743	Period Ending December 31, 1971
ORNL-4844	Period Ending December 31, 1972
ORNL-4937	Period Ending December 31, 1973
ORNL-5025	Period Ending December 31, 1974
ORNL-5137	Period Ending December 31, 1975
ORNL-5306	Period Ending June 30, 1977
ORNL-5498	Period Ending December 31, 1978
ORNL-5787	Period Ending June 30, 1981
ORNL-6004	Period Ending September 30, 1983
ORNL-6120	Period Ending September 30, 1984
ORNL-6233	Period Ending September 30, 1985
ORNL-6326	Period Ending September 30, 1986
ORNL-6420	Period Ending September 30, 1987
ORNL-6508	Period Ending September 30, 1988
ORNL-6578	Period Ending September 30, 1989
ORNL-6660	Period Ending September 30, 1990
ORNL-6689	Period Ending September 30, 1991

CONTENTS

INTRODUCTION	xix
1. HOLIFIELD HEAVY ION RESEARCH FACILITY	
Overview – <i>R. L. Robinson and C. M. Jones</i>	1
ACCELERATOR OPERATIONS AND DEVELOPMENT	
Accelerator Operations – <i>G. D. Alton, M. R. Dinehart, D. T. Dowling, D. L. Haynes, C. A. Irizarry, C. M. Jones, R. C. Juras, S. N. Lane, C. T. LeCroy, M. J. Meigs, G. D. Mills, S. W. Mosko, S. N. Murray, D. K. Olsen, B. A. Tatum, and N. F. Ziegler</i>	3
Tandem Accelerator – <i>G. D. Alton, M. R. Dinehart, D. L. Haynes, C. M. Jones, R. C. Juras, S. N. Lane, C. T. LeCroy, M. J. Meigs, G. D. Mills, S. N. Murray, and N. F. Ziegler</i>	4
A Simple, Inexpensive Voltage Grading Resistor for Large Electrostatic Accelerators – <i>D. L. Haynes, C. M. Jones, R. C. Juras, M. J. Meigs, J. E. Raatz, and J. B. Schroeder</i>	4
Performance Characteristics of a Multiple-Sample, Cesium-Sputter, Negative Ion Source – <i>G. D. Alton and M. T. Johnson</i>	4
A Simple Positive/Negative Surface Ionization Source – <i>G. D. Alton, M. T. Johnson, and G. D. Mills</i>	6
A Scaled Sigmund Theory Model for Determining Sputter Ratios – <i>G. D. Alton, D. H. Olive, M. L. Pinkham, and J. R. Olive</i>	8
Feasibility Studies for the Design of a Plasma Stripper – <i>G. D. Alton and D. Smithe</i>	10
FACILITY OPERATIONS AND DEVELOPMENT	
HHIRF Experiments – <i>R. L. Robinson</i>	12
Computer Systems – <i>W. T. Milner, J. W. McConnell, C. N. Thomas, and R. L. Varner</i>	14
Users Group Activities – <i>R. L. Auble</i>	19
The Joint Institute for Heavy Ion Research – <i>R. L. Robinson, J. H. Hamilton, and C. R. Bingham</i>	19
The HHIRF Program Advisory Committee – <i>R. L. Robinson</i>	23
2. THE RADIOACTIVE ION BEAM PROJECT	
Introduction – <i>D. K. Olsen</i>	25

High-Voltage Platform System for RIB Injection – <i>R. C. Juras, G. D. Alton, M. R. Dinehart, D. T. Dowling, D. L. Haynes, S. N. Lane, C. T. LeCroy, M. J. Meigs, G. D. Mills, S. W. Mosko, S. N. Murray, D. K. Olsen, C. A. Reed, B. A. Tatum, and H. Wollnik</i>	26
Tandem Accelerator Transmission Efficiency Studies – <i>C. M. Jones, M. R. Dinehart, R. C. Juras, C. T. LeCroy, M. J. Meigs, and S. N. Murray</i>	29
Optical Design of the First-Stage Mass Separator – <i>H. Wollnik, G. D. Alton, C. M. Jones, and D. K. Olsen</i>	30
Rib Injector Beam Line I-2 – <i>D. T. Dowling, G. D. Alton, D. L. Haynes, C. M. Jones, R. C. Juras, M. J. Meigs, G. D. Mills, S. W. Mosko, D. K. Olsen, B. A. Tatum, and H. Wollnik</i>	33
Mass-Analyzer Magnet Field Calculations – <i>B. A. Tatum, D. K. Olsen, and H. Wollnik</i>	34
Cross Sections for Production of Radioactive Ion Beams – <i>R. L. Robinson, L. Rayburn, C. Baktash, J. B. Ball, C. M. Jones, I. Y. Lee, F. K. McGowan, and D. K. Olsen</i>	35
Residual Radioactivity Following a Bombardment with Protons – <i>L. Rayburn and R. L. Robinson</i>	37
Progress with the Mark-I Target/Ion Source – <i>G. D. Alton, D. L. Haynes, G. D. Mills, and D. K. Olsen</i>	38
Time-Release Properties of Ion-Implanted Species: Diffusion Modeling – <i>G. D. Alton, H. K. Carter, I. Y. Lee, C. M. Jones, J. Kormicki, and D. K. Olsen</i>	40
ORIC Development – <i>S. W. Mosko, M. R. Dinehart, D. T. Dowling, S. N. Lane, C. T. LeCroy, S. N. Murray, D. K. Olsen, and B. A. Tatum</i>	42
Computation Studies of New Central Region for ORIC – <i>H. Blosser, L. Lee, F. Marti, and D. K. Olsen</i>	43
ORIC Beam Lines – <i>D. T. Dowling, S. N. Lane, S. W. Mosko, D. K. Olsen, and B. A. Tatum</i>	44
Tandem Accelerator Beam-Parameter Measurements – <i>C. M. Jones, R. C. Juras, M. J. Meigs, and D. K. Olsen</i>	45

3. LOW/MEDIUM ENERGY NUCLEAR PHYSICS

NUCLEAR STRUCTURE STUDIES VIA ELASTIC, INELASTIC, AND CHARGE EXCHANGE REACTIONS

Study of the Nuclear Excitation of the Isovector Giant Dipole Resonance by Inelastic Scattering – <i>D. H. Olive, J. R. Beene, F. E. Bertrand, R. L. Auble, M. L. Halbert, D. J. Horen, and R. L. Varner</i>	47
Study of One- and Two-Phonon Giant Resonance Strength in ²⁰⁸Pb with Intermediate Energy ³⁶Ar and ⁸⁴Kr Scattering – <i>J. R. Beene, F. E. Bertrand, D. J. Horen, M. L. Halbert, D. C. Hensley, D. Olive, M. Thoennessen, R. L. Auble, W. Mittag, Y. Schutz, K. Katori, W. Kühn, and R. Holzmann</i>	50

Systematics of Isospin Character of Transitions to the 2_1^+ and 3_1^- States in $^{90,92,94,96}\text{Zr}$ – D. J. Horen, R. L. Auble, J. Gomez del Campo, G. R. Satchler, R. L. Varner, J. R. Beene, Brian Lund, V. R. Brown, P. L. Anthony, and V. A. Madsen	52
Different Effects of Valence Neutrons on the Isospin Character of Transitions to the First 2^+ and 3^- States of $^{90,92,94,96}\text{Zr}$ – D. J. Horen, R. L. Auble, J. Gomez del Campo, R. L. Varner, J. R. Beene, G. R. Satchler, Brian Lund, V. R. Brown, P. L. Anthony, and V. A. Madsen	53
Isospin Character of the Transition to the 0.803-MeV State in ^{206}Pb from π^\pm Scattering at 180 MeV – D. J. Horen, C. L. Morris, S. J. Seestrom, F. W. Hersman, J. R. Calarco, M. Holtrop, M. Leuschner, Mohini Rawool-Sullivan, R. W. Garnett, S. J. Greene, M. A. Plum, and J. D. Zumbro	53
Lifetime Measurement of the 1.897-MeV, 3_1^- State in ^{96}Zr – D. J. Horen, R. L. Auble, J. R. Beene, I. Y. Lee, D. Cline, C. Y. Wu, M. Devlin, R. Ibbotson, and M. Simon	53
Measurement of the Lifetime of the 0.918-MeV, 2_1^+ State of ^{94}Zr – C. Y. Wu, D. Cline, M. Devlin, R. Ibbotson, M. Simon, D. J. Horen, and R. L. Auble	54
Measurements of the Lifetimes of Excited States in ^{100}Mo – R. L. Auble, D. J. Horen, D. Cline, C. Y. Wu, M. Devlin, R. Ibbotson, and M. Simon	54
NUCLEAR STRUCTURE STUDIES VIA TRANSFER, CAPTURE, AND COULOMB EXCITATION REACTIONS	
Possible Two-Phonon Quadrupole State in ^{232}Th – F. K. McGowan and W. T. Milner	55
Magnetic Dipole Strength in ^{46}Ca Observed with 180° Electron Scattering – J. P. Connelly, H. Crannell, L. W. Fagg, J. T. O'Brien, M. Petraitis, D. I. Sober, S. Raman, J. R. Deininger, and S. E. Williamson	56
Mechanism of (n,γ) Reaction at Low Neutron Energies – S. Raman and J. E. Lynn	56
Thermal-Neutron Capture by Silicon Isotopes – S. Raman, E. T. Journey, J. W. Starner, and J. E. Lynn	57
NUCLEAR STRUCTURE VIA COMPOUND NUCLEUS REACTIONS	
Test of Predicted Deformation-Driving Effects in ^{173}Re – N. R. Johnson, J. C. Wells, F. K. McGowan, D. F. Winchell, I. Y. Lee, P. Semmes, C. Baktash, J. D. Garrett, Y. A. Akovali, R. Bengtsson, R. Wyss, W. C. Ma, W. B. Gao, C.-H. Yu, and S. Pilotte	57
Transition Probabilities up to $I = 36^+$ in ^{160}Yb – N. R. Johnson, F. K. McGowan, D. F. Winchell, J. C. Wells, C. Baktash, L. Chaturvedi, W. B. Gao, J. D. Garrett, I. Y. Lee, W. C. Ma, S. Pilotte, and C.-H. Yu	59
Low-Spin Identical Bands in Neighboring Odd-A and Even-Even Nuclei: A Challenge to Mean-Field Theories – C. Baktash, J. D. Garrett, D. F. Winchell, and A. Smith	60
X-Ray Yields of Superdeformed States in ^{193}Hg – D. M. Cullen, I. Y. Lee, C. Baktash, J. D. Garrett, N. R. Johnson, F. K. McGowan, and D. F. Winchell	60

Lifetimes of Low Spin States in the Superdeformed Band of ^{192}Hg – I. Y. Lee, C. Baktash, D. M. Cullen, J. D. Garrett, N. R. Johnson, F. K. McGowan, D. F. Winchell, and C. H. Yu	61
Lifetime Measurements for Continuum Gamma Rays in ^{164}Yb and ^{170}Hf – I. Y. Lee, H. Xie, C. Baktash, W. B. Gao, J. D. Garrett, N. R. Johnson, F. K. McGowan, and R. Wyss	61
Level Repulsion and Chaos in the Nuclear Quantum System – J. D. Garrett	61
High Spin Studies of ^{181}Au – C.-H. Yu, H. Q. Jin, J. M. Lewis, W. F. Mueller, L. L. Riedinger, C. Baktash, J. D. Garrett, N. R. Johnson, I. Y. Lee, F. K. McGowan, and D. Winchell	62
On the Question of Spin Fitting and Quantized Alignment in Rotational Bands – C. Baktash, W. Nazarewicz, and R. Wyss	63
Search for Hyperdeformation in the Light Hg Isotopes – P. F. Hua, D. G. Sarantites, J. Barreto, A. Kirov, L. Sobotka, C. Baktash, D. M. Cullen, I. Y. Lee, J. D. Garrett, N. R. Johnson, F. K. McGowan, and W. C. Ma	64
The First Spectroscopy of ^{182}Au – D. M. Cullen, C. Baktash, I. Y. Lee, J. D. Garrett, N. R. Johnson, F. K. McGowan, P. F. Hua, D. G. Sarantites, J. Barreto, A. Kirov, and L. Sobotka	64
The Mass Dependence of Moments of Inertia of Rapidly-Rotating Nuclei – D. F. Winchell, D. O. Ludwigsen, and J. D. Garrett	65
High-Spin Structure of ^{167}W and ^{168}W – K. Theine, A. P. Byrne, H. Hübel, M. Murzel, R. Chapman, D. Clarke, K. Khazaie, J. C. Lisle, J. N. Mo, J. D. Garrett, H. Ryde, and R. Wyss	65
High Spin States in Neutron Rich Nuclei from Spontaneous Fission – K. Butler-Moore, S. Zhu, X. Zhao, J. H. Hamilton, A. V. Ramayya, Q. Lu, W.-C. Ma, L. K. Peker, J. Kormicki, J. K. Deng, P. Gore, D. Shi, E. F. Jones, H. Xie, W. B. Gao, J. D. Cole, R. Aryaeinejad, I. Y. Lee, N. R. Johnson, F. K. McGowan, C. E. Bemis, G. Ter-Akopian, and Yu. Oganessian	65
First Evidence for States in Hg Nuclei with Deformations Between Normal- and Super-Deformation – W. C. Ma, J. H. Hamilton, A. V. Ramayya, L. Chaturvedi, J. K. Deng, W. B. Gao, Y. R. Jiang, J. Kormicki, X. W. Zhao, N. R. Johnson, J. D. Garrett, I. Y. Lee, C. Baktash, F. K. McGowan, W. Nazarewicz, and R. Wyss	66
New High-Spin Excitation Modes in ^{184}Hg – J. K. Deng, W. C. Ma, J. H. Hamilton, A. V. Ramayya, J. Kormicki, X. W. Zhao, W. B. Gao, I. Y. Lee, J. D. Garrett, N. R. Johnson, D. Winchell, M. Halbert, and C. Baktash	66

NUCLEAR STRUCTURE STUDIES VIA RADIOACTIVE DECAY

Search for the α Decay of ^{190}Hg and the α-Decay Branches of ^{186}Hg and ^{188}Hg – K. S. Toth, Y. A. Akevali, C. R. Bingham, H. K. Carter, Y. Hatsukawa, P. F. Mantica, and M. Zhang	67
Study of Platinum Nuclei with the ATLAS Fragment Mass Analyzer – K. S. Toth, C. N. Davids, B. B. Back, K. Bindra, C. R. Bingham, W. Chung, D. J. Henderson, T. Lauritsen, D. M. Moltz, A. V. Ramayya, J. D. Robertson, and W. B. Walters	68

Alpha Decays of Light Uranium Isotopes – K. S. Toth, H. J. Kim, J. W. McConnell, C. R. Bingham, and D. C. Sousa	69
Investigation of Short-Lived Rare Earth Nuclei – K. S. Toth, J. M. Nitschke, D. C. Sousa, K. S. Vierinen, and P. A. Wilmarth	69
Identification of the the β-Decay Branch of ^{147}Tm – K. S. Toth, D. C. Sousa, P. A. Wilmarth, J. M. Nitschke, and K. S. Vierinen	70
Alpha-Decaying Low-Spin Levels in ^{155}Lu and ^{157}Lu – K. S. Toth, K. S. Vierinen, J. M. Nitschke, P. A. Wilmarth, and R. M. Chasteler	71
PHYSICS WITH RADIOACTIVE BEAMS	
North American Radioactive Beam Initiatives – J. D. Garrett	72
Exotic Nuclear Shapes and Configurations that Can Be Studied at High Spin Using Radioactive Ion Beams – J. D. Garrett	72
Prospects for Studies of Astrophysical Interest with Radioactive Ion Beams – J. D. Garrett	72
HEAVY-ION REACTION MECHANISM STUDIES, FUSION AND FISSION	
Large Deformation in $A \sim 170$ Nuclei at High Excitation Energies – M. Thoennessen, J. R. Beene, F. E. Bertrand, C. Baktash, M. L. Halbert, D. J. Horen, D. C. Hensley, D. G. Sarantites, W. Spang, D. W. Stracener, and R. L. Varner	73
Angular Momentum Effects in Subbarrier Fusion – M. L. Halbert and J. R. Beene	73
Fusion Near the Coulomb Barrier: Nonstatistical Effects and γ-Ray Multiplicity – J. R. Beene, M. L. Halbert, and M. R. Thoennessen	74
Evidence for Long Formation Times in Near Barrier Fusion Reactions – M. Thoennessen, J. R. Beene, R. L. Auble, F. E. Bertrand, C. Baktash, M. L. Halbert, D. J. Horen, D. G. Sarantites, W. Spang, and D. W. Stracener	76
Charged Particles as Probes to Study Entrance-Channel Effects in the Composite System ^{164}Yb – J. L. Barreto, D. G. Sarantites, R. J. Charity, N. G. Nicolis, L. G. Sobotka, D. W. Stracener, D. C. Hensley, J. R. Beene, M. L. Halbert, and C. Baktash	77
Analysis of Light Particles Emitted in Coincidence with Evaporation Residues for the $^{79}\text{Br} + ^{27}\text{Al}$ System at 11 MeV/Nucleon – J. Gomez del Campo, J. P. Wieleczko, E. Chávez, D. Shapira, M. Korolija, H. Kim, C. Volant, A. D'Onofrio, K. Teh, and J. Shea	77
The $^{14}\text{N} + ^{10}\text{B}$ System Measured at $E(^{14}\text{N}) = 248$ MeV – M. E. Ortiz, E. R. Chávez, A. Dacal, J. Gomez del Campo, Y. D. Chan, and R. G. Stokstad	79
Energy Sharing in Binary Reactions Induced by ^{19}F on ^{64}Ni at 118 MeV – A. Brondi, G. de Angelis, A. D'Onofrio, G. LaRana, R. Moro, V. Roca, G. Spadaccini, F. Terrasi, M. Vigilante, R. Alba, G. Bellia, A. Del Zoppo, G. Russo, P. Sapienza, and J. Gomez del Campo	79

Proton-Proton Correlations: Determination of the Characteristic Source Size and the Lifetime from a Deep Inelastic $^{58}\text{Ni} + ^{58}\text{Ni}$ Reaction at 15 MeV/Nucleon – <i>M. Korolija, D. Shapira, J. Gomez del Campo, E. Chávez, and N. Cindro</i>	80
Status of Soft Photon Experiment – <i>R. Clark, C. Erd, J. Gomez del Campo, A. Ray, J. Schukraft, D. Shapira, M. Tincknell, and C. Woody</i>	80
Particle Multiplicity Dependence of High-Energy Photon Production in a Heavy-Ion Reaction – <i>L. G. Sobotka, L. Gallamore, A. Chbihi, D. G. Sarantites, D. W. Stracener, W. Bauer, D. R. Bowman, N. Carlin, R. T. DeSouza, C. K. Gelbke, W. G. Gong, S. Hannuschke, Y. D. Kim, W. G. Lynch, R. Ronningen, M. B. Tsang, F. Zhu, J. R. Beene, M. L. Halbert, and M. Thoennesen</i>	85
The Mechanism for the Disassembly of Excited ^{16}O Projectiles into Four Alpha Particles – <i>R. J. Charity, J. L. Barreto, L. G. Sobotka, D. G. Sarantites, D. W. Stracener, A. Chbihi, N. G. Nicolis, R. Auble, C. Baktash, J. R. Beene, F. Bertrand, M. Halbert, D. C. Hensley, D. J. Horen, C. Ludemann, M. Thoennesen, and R. Varner</i>	85
DETECTOR, INSTRUMENTATION, AND COMPUTER DEVELOPMENT	
Upgrade of the HILI Detector System and Its Commissioning at the Texas A&M Cyclotron – <i>D. Shapira, M. Korolija, and J. Gomez del Campo</i>	86
Octal Amplifier and Discriminator Module for the Silicon Diode Detector Array in the HILI – <i>J. L. Blankenship, J. Gomez del Campo, and D. Shapira</i>	86
Development of the ORNL BaF₂ Array – <i>P. E. Mueller, J. R. Beene, F. E. Bertrand, J. L. Blankenship, M. L. Halbert, D. J. Horen, D. H. Olive, and R. L. Varner</i>	87
Hybrid Ion Chamber for the Texas A&M Cyclotron Spectrograph – <i>J. L. Blankenship, R. L. Auble, J. R. Beene, F. E. Bertrand, and D. Shapira</i>	89
Compton-Suppression Tests on Ge and BGO Prototype Detectors for GAMMASPHERE – <i>A. M. Baxter, T. L. Khoo, M. E. Bleich, M. P. Carpenter, I. Ahmad, R.V.F. Janssens, E. F. Moore, I. G. Bearden, J. R. Beene, and I. Y. Lee</i>	90
 4. HIGH-ENERGY NUCLEAR AND PARTICLE PHYSICS	
CERN WA93 and WA98 Experiments – <i>WA93 Collaboration</i>	91
Status Report of WA80 Proton Data Analysis – <i>WA80 Collaboration</i>	92
Transverse Energy and Forward Energy Production in a High-Energy Nuclear Collision Model – <i>Jing-Ye Zhang, Xiaochun He, Chia C. Shih, Soren P. Sorensen, Cheuk-Yin Wong</i>	93
Hadronic Model for the Space-Time Development of High-Energy Nuclear Collisions – <i>Soren P. Sorensen, Chao Wei-Qin</i>	94
Preconceptual Design of PHENIX Experiment for RHIC – <i>PHENIX Collaboration</i>	94
Monte Carlo Simulations of the PHENIX Detector at RHIC – <i>T. C. Awes, H. J. Kim, J. Kreke, X. C. He, F. E. Obenshain, F. Plasil, S. Saini, S. Sorensen, G. R. Young</i>	98

Low Energy Response of Pb Glass Calorimeters for RHIC – T. C. Awes, A. Lebedev, A. Nyanin	101
PHENIX Muon Spectrometer – PHENIX Collaboration	104
Simulations of the Performance of the PHENIX Muon Detector – PHENIX Collaboration	107
Limited Streamer Tubes for Muon ID – H. J. Kim, J. G. Kreke, F. E. Obenshain, G. R. Young	108
Calorimeter Optimization Experiment (RD-10/RD-45 Project) – S. H. Aronson, M. J. Murtagh, M. Starks, X.T. Liu, G. A. Pettit, Ziyang Zhang, L. A. Ewell, J. C. Hill, F. K. Wohn, J. B. Costales, M. N. Namboodiri, T. C. Sangster, J. H. Thomas, A. Gavron, L. Waters, W. L. Kehoe, S. G. Steadman, T. C. Awes, F. E. Obenshain, S. Saini, G. R. Young, J. Chang, S.-Y. Fung, J. H. Kang, J. Kreke, Xiaochun He, E. C. Cornell, C. F. Maguire	109
Development of Monolithic Electronics for RHIC and CERN WA98 – T.C. Awes, G.R. Young, G.T. Alley, C.L. Britton, M. N. Ericson, M.L. Simpson, A.L. Wintenberg	109
ORNL Activities in Support of the SSC GEM Collaboration – M. L. Bauer, C. L. Britton, S. M. Chae, L. G. Clonts, H. O. Cohn, C. C. Eberle, Y. Efremenko, A. Gordeev, J. L. Heck, Yu. Kamyshkov, A. Nikitin, D. Onoprienko, F. Plasil, K. F. Read, M. J. Rennich, A. Savin, K. Shmakov, A. Smirnov, E. Tarkovski, R. A. Todd, A. L. Wintenberg, K. G. Young	110
Calorimetry Development for the GEM Experiment at the SSC – S. M. Chae, H. O. Cohn, C.C. Eberle, Y. Efremenko, A. Gordeev, J. L. Heck, Yu. Kamyshkov, A. Nikitin, D. Onoprienko, F. Plasil, M. J. Rennich, A. Savin, K. Shmakov, A. Smirnov, E. Tarkovski, R. A. Todd, K. G. Young	111
ORNL Activities in Support of the GEM Central Tracker – C. Britton, L. Clonts, K. Read, and A. Wintenberg	113
Neutral-Strange-Particle Production in 200-GeV/c $p/\pi^+/K^+$ Interactions on Au, Ag, and Mg – International Hybrid Spectrometer Consortium	114
Measurement of the Lifetime of B-Hadrons and a Determination of V_{cb} – L3 Collaboration	114
Search for Lepton Flavor Violation in Z^0 Decays – L3 Collaboration	114
Measurement of the Strong Coupling Constant α_s for Bottom Quarks at the Z^0 Resonance – L3 Collaboration	115
A Direct Determination of the Number of Light Neutrino Families from $e^+e^- \rightarrow \nu\bar{\nu}\gamma$ at LEP – L3 Collaboration	115
Electroweak Parameters of the Z^0 Resonance and the Standard Model – LEP Collaborations	115
Search for the Neutral Higgs Boson at LEP – L3 Collaboration	115
Studies of Hadronic Event Structure and Comparisons with QCD Models at the Z^0 Resonance – L3 Collaboration	116

5. ACCELERATOR-BASED ATOMIC PHYSICS

Electron-Positron Pair Production in Coulomb Collisions of Ultrarelativistic Sulfur Ions with Fixed Targets – <i>C. R. Vane, S. Datz, P. F. Dittner, H. F. Krause, C. Bottcher, M. R. Strayer, R. Schuch, H. Gao, and R. Hutton</i>	117
Knock-On Electrons Produced in Collisions of 6.4-TeV Sulfur Ions with Fixed Targets – <i>C. R. Vane, S. Datz, P. F. Dittner, H. F. Krause, R. Schuch, H. Gao, and R. Hutton</i>	119
Saddle-Point Shifts in Ionizing Collisions – <i>V. D. Irby, S. Datz, P. F. Dittner, N. L. Jones, H. F. Krause, and C. R. Vane</i>	120
Observation of Interference in Resonant Coherent Excitation – <i>H. F. Krause, S. Datz, P. F. Dittner, N. L. Jones, and C. R. Vane</i>	121
Scattering of Axially Channeled Ions in a Very Thin Silicon Crystal – <i>H. F. Krause, J. R. Barrett, J. Gomez del Campo, S. Datz, P. F. Dittner, N. L. Jones, and C. R. Vane</i>	123
Dissociative Recombination of Vibrationally Cold H₃⁺ in an Ion Storage Ring – <i>S. Datz, M. Larsson, H. Danared, J. R. Mowat, P. Sigray, G. Sundström, L. Bieström, A. Filevich, A. Källberg, S. Mannervik, and K. G. Rensfelt</i>	124
Possible Two-Electron Excitation in C³⁺ Following 1 MeV/u Collisions with Atomic Targets: Z = 2, 10, 18, and 36 – <i>D. F. Deveney, Q. C. Kessel, R. J. Fuller, M. P. Reaves, S. Shafroth, and N. L. Jones</i>	125
Angular Distribution of Charge-Exchange Collisions at Very Low Energies – <i>N. Keller, R. D. Miller, M. Westerlind, L. R. Andersson, S. B. Elston, I. A. Sellin, and C. Biedermann</i>	128
Design and Performance of a Novel Position-Sensitive Electron Spectrometer – <i>R. D. Miller, N. Keller, L. Liljebj, I. A. Sellin, and M. Westerlind</i>	130
Coincidence Detection of Electrons Ejected at Large Angles and Target Recoil Ions Produced in Multiply Ionizing Collisions for the 1 MeV/u O⁴⁺ + Ar Collision System – <i>C. C. Gaither, M. Breinig, J. W. Berryman, B. F. Hasson, and J. D. Richards</i>	130
Photodetachment Studies of Few-Electron Atomic Negative Ions – <i>D. J. Pegg, J. Dellwo, C. Y. Tang, and G. D. Alton</i>	131
EN Tandem Operations – <i>P. F. Dittner and N. L. Jones</i>	132

6. ATOMIC PHYSICS IN SUPPORT OF FUSION

Very-Low Energy Collisions of Multicharged Ions with Rydberg Atoms in Merged Beams – <i>C. C. Havener, M. A. Haque, and P. A. Zeijlmans van Emmichoven</i>	133
Backscattering in Electron-Impact Excitation of Multiply Charged Ions – <i>X. Q. Guo, E. W. Bell, J. S. Thompson, G. H. Dunn, M. E. Bannister, R. A. Phaneuf, and A. C. H. Smith</i>	134
Crossed-Beams Electron-Impact Ionization Cross Section Measurements of Si⁹⁺ Ions – <i>M. E. Bannister, D. C. Gregory, C. C. Havener, R. A. Phaneuf, P. A. Zeijlmans van Emmichoven, E. W. Bell, X. Q. Guo, N. Djuric, J. S. Thompson, and M. Sataka</i>	136

Analysis of Low-Energy Electron Emission Arising During Slow Multicharged Ion-Surface Interactions – P. A. Zeijlmans van Emmichoven, C. C. Havener, I. G. Hughes, D. M. Zehner, and F. W. Meyer	137
Incident-Ion Charge-State Dependence of Electron Emission During Slow Multicharged Ion-Surface Interactions – I. G. Hughes, C. C. Havener, S. H. Overbury, M. T. Robinson, D. M. Zehner, P. A. Zeijlmans van Emmichoven, and F. W. Meyer	139
Neutralization of Slow Multicharged Ions Above a Cesium Au Surface – F. W. Meyer, L. Folkerts, I. G. Hughes, S. H. Overbury, D. M. Zehner, and P. A. Zeijlmans van Emmichoven	140
ECR Source Facility Upgrade Project – F. W. Meyer and J. W. Hale	141

7. THE UNISOR PROGRAM

Installation of NMR Coils at UNISOR/NOF – P. F. Mantica, Jr., N. J. Stone, M. L. Simpson, J. K. Deng, Y. S. Xu, H. K. Carter, L. A. Rayburn, and D. Shi	143
Modification of a β^--γ-γ Picosecond Lifetime System for Lifetime Measurements at UNISOR – P. K. Joshi, P. F. Mantica, E. F. Zganjar, S. J. Robinson, and W. B. Walters	144
Development of a New Picosecond Lifetime Measurement System Using the β^+ – X-Ray Coincidence – P. K. Joshi, P. F. Mantica, Jr., E. F. Zganjar, and S. J. Robinson	145
Lifetime Measurements in $^{118,120}\text{Xe}$ – P. F. Mantica, Jr., P. K. Joshi, S. J. Robinson, E. F. Zganjar, R. L. Gill, W. B. Walters, D. Rupnik, H. K. Carter, J. Kormicki, and C. R. Bingham	146
Development of a New Picosecond Lifetime Measurement System Using X-Ray – X-Ray Coincidence – P. K. Joshi, P. F. Mantica, Jr., E. F. Zganjar, and S. J. Robinson	147
Lifetimes of the O_2^+ Configuration in ^{186}Hg and ^{188}Hg – P. K. Joshi, P. F. Mantica, Jr., D. Rupnik, W. B. Walters, C. R. Bingham, A. V. Ramayya, J. H. Hamilton, S. J. Robinson, E. F. Zganjar, R. L. Gill, H. K. Carter, J. Kormicki, and W. C. Ma	147
Gamma-Ray Spectroscopy on ^{72}Br – W. C. Ma, T. Brown, A. V. Ramayya, J. H. Hamilton, L. Chaturvedi, J. Kormicki, Q. M-Lu, N. Severijns, P. Schuurmans, L. Vanneste, P. F. Mantica, Jr., and H. K. Carter	148
Nuclear Orientation of ^{96}Tc – M. R. Papantonakis, P. F. Mantica, Jr., J. Kormicki, K. Builer-Moore, A. V. Ramayya, J. H. Hamilton, J. K. Deng, W. C. Ma, A. Lahamer, and W. D. Hamilton	149
Level Structure of Odd-Odd ^{114}I – B. E. Zimmerman, W. B. Walters, P. F. Mantica, Jr., H. K. Carter, J. Kormicki, J. Rikavska, N. J. Stone, and B. D. Kern	150
Nuclear Orientation of ^{116}Sb – B. E. Zimmerman, W. B. Walters, P. F. Mantica, Jr., H. K. Carter, J. Kormicki, M. G. Booth, J. Rikavska, N. J. Stone, C. R. Bingham, and B. D. Kern	151

Non-Saturation of B(E2) Strength in Mid-Shell Xe Isotopes – P. F. Mantica, Jr., W. B. Walters, P. K. Joshi, E. F. Zganjar, S. J. Robinson, R. L. Gill, D. Rupnik, H. K. Carter, J. Kormicki, and C. R. Bingham	152
Decay of ^{123}Ba – Y. Hatsukawa, P. F. Mantica, Jr., B. E. Zimmerman, W. B. Walters, and H. K. Carter	153
Studies of the Onset of Deformation in the Very-Neutron Deficient Isotopes of Pr, Nd, Pm, and Sm – J. Breitenbach, R. A. Braga, J. L. Wood, P. B. Semmes, and J. Kormicki	154
Particle + Triaxial Rotor Model Calculations for Odd-Mass Pr Isotopes above $N = 82$ – P. F. Mantica, Jr. and W. B. Walters	155
Shape Coexistence and Electric Monopole Transitions in ^{184}Pt – Y. Xu, K. S. Krane, M. A. Gumin, M. Jarrio, J. L. Wood, E. F. Zganjar, and H. K. Carter	157
Spins and Magnetic Dipole Moments of New Isomers in ^{184}Au by Time Integral and Time Resolved Nuclear Orientation – N. J. Stone, J. R. Stone, M. G. Booth, W. B. Walters, B. E. Zimmerman, C. R. Bingham, K. S. Krane, J. Deng, B. D. Kern, H. K. Carter, Y. Hatsukawa, and P. F. Mantica, Jr.	157
Search for Coexisting $K^\pi=2^+$ Bands in ^{186}Pt – J. McEver, J. Breitenbach, J. L. Wood, J. Schwarzenberg, and R. A. Braga	158
Complete Spectroscopy in the $^{187\text{m}}\text{gTl}$ Decay: The Structure of ^{187}Au – D. Rupnik, E. F. Zganjar, and J. L. Wood	159
Nuclear Structure Studies of ^{187}Ir – M. A. Gumin, K. S. Krane, Y. Xu, T. Lam, E. F. Zganjar, J. B. Breitenbach, B. E. Zimmerman, H. K. Carter, and P. F. Mantica, Jr.	159
Nuclear Magnetic Dipole and Electric Quadrupole Moments of ^{187}Tl from Laser Spectroscopy and Their Interpretation in the Strutinsky and Particle-Plus-Rotor Models – H. A. Schuessler, E. C. Benck, F. Buchinger, H. Iimura, R. Wyss, J. Rikovska, H. K. Carter, J. Kormicki, and C. R. Bingham	160
Decay of Mass-Separated ^{199}Bi – M. Zhang, C. R. Bingham, J. Ding, B. E. Zimmerman, H. K. Carter, J. Kormicki, P. Mantica, Jr., L. Rayburn, P. K. Joshi, J. L. Wood, and S. Shastry	161
Production Rates of Isotopes and Resultant Radioactivity for Radioactive Ion Beam (RIB) Targets – L. Rayburn	162

8. THEORETICAL AND COMPUTATIONAL PHYSICS

ATOMIC PHYSICS

Electromagnetic Pair Production in Relativistic Heavy-Ion Collisions – C. Bottcher and M. R. Strayer	165
The Coulomb Three-Body Problem: A Progress Report – C. Bottcher and D. R. Schultz	165
Parametric Correlations and Diffusion in Quantum Spectra – X. Yang and J. Burgdörfer	166

Electron-Electron Interaction and Two-Center Effects in Projectile Ionization at Backward Emission Angles – J. Wang, C. O. Reinhold, and J. Burgdörfer	166
Torus Quantization of Symmetrically Excited Helium – J. Müller, J. Burgdörfer, and D. Noid	167
High <i>l</i>-State Population in O⁷⁺ Produced in Ion-Solid Collisions – J. Kemmler, J. Burgdörfer, and C. O. Reinhold	167
Coulomb-Born Theory of (e,2e) Collisions – J. H. Macek	167
Anomalous <i>n</i>-Dependence of Low-Energy Electron Capture from Atomic Hydrogen by Multicharged Ions – J. H. Macek and S. Y. Ovchinnikov	168
Perturbation Theory with Arbitrary Boundary Conditions for Charged-Particle Scattering: Application to (e,2e) Experiments in Helium – J. H. Macek and J. Botero	168
Close-Coupling Calculations for the Electron-Impact Excitation of Zn⁺ – M. S. Pindzola, N. R. Badnell, R.J.W. Henry, D. C. Griffin, and W. L. van Wyngaarden	168
Electron-Impact Excitation of Ions – D. C. Griffin, M. S. Pindzola, and N. R. Badnell	169
Electron-Impact Ionization of Ca⁺ – N. R. Badnell, D. C. Griffin, and M. S. Pindzola	169
Convergence of the Close-Coupling Method for the 3p⁵3d² Configuration in Ti³⁺ – D. C. Griffin, M. S. Pindzola, and N. R. Badnell	169
Ionization and Recombination in Transition Metal Ions – N. R. Badnell, M. S. Pindzola, D. C. Griffin, and H. P. Summers	170
Electron-Impact Ionization Data for the Nickel Isonuclear Sequence – M. S. Pindzola, D. C. Griffin, C. Bottcher, M. J. Buie, and D. C. Gregory	170
Dielectronic Recombination Between Hyperfine Levels of the Ground State of Bi⁸²⁺ – M. S. Pindzola, N. R. Badnell, and D. C. Griffin	170
Electron-Impact Ionization of the Tungsten Atom – M. S. Pindzola and D. C. Griffin	171
Ejected-Electron Spectra in Proton-Atomic Hydrogen Collisions – D. R. Schultz, R. E. Olson, C. O. Reinhold, M. W. Gealy, G. W. Kerby, III, Y.-Y. Hsu, and M. E. Rudd	171
Differential Cross Sections for State-Selective Electron Capture in 25-100 keV Proton-Helium Collisions – D. R. Schultz, C. O. Reinhold, R. E. Olson, and D. G. Seely	171
Classical Description and Calculation of Ionization in Collisions of 100 eV Electrons and Positrons with He and H₂ – D. R. Schultz, L. Meng, and R. E. Olson	172

COMPUTATIONAL PHYSICS

Calculations of Periodic Trajectories for the Hénon-Heiles Hamiltonian Using the Monodromy Method – K.T.R. Davies, T. E. Huston, and M. Baranger	172
---	-----

Evaluation of Integrals Using General Partial-Fraction Expansions – <i>K.T.R. Davies, J.-S. Wu, and R. W. Davies</i>	172
Extension of the Monodromy Method to Conservative Maps: The Standard Map – <i>K.T.R. Davies and M. Baranger</i>	173
Extension of the Monodromy Method to Dissipative Systems – <i>K.T.R. Davies and</i> <i>M. Baranger</i>	174
Chaos Educational Project – <i>K.T.R. Davies</i>	175
Implementation of Muon-Induced Fission on Massively Parallel Supercomputers – <i>V. E. Oberacker, J. C. Wells, A. S. Umar, C. Bottcher, and M. R. Strayer</i>	176
A Numerical Implementation of the Dirac Equation on a Hypercube Multicomputer – <i>J. C. Wells, A. S. Umar, V. E. Oberacker, C. Bottcher,</i> <i>M. R. Strayer, J.-S. Wu, J. Drake, and R. Flanery</i>	177
Solution of the Helmholtz-Poincaré Wave Equations Using the Coupled Boundary Integral Equations and Optimal Surface Eigenfunctions – <i>M. F. Werby,</i> <i>M. K. Broadhead, M. R. Strayer, and C. Bottcher</i>	177
Spline Techniques for Solving Relativistic Conservation Equations – <i>D. J. Dean,</i> <i>C. Bottcher, M. R. Strayer, and G. Gatoff</i>	178
Monte Carlo Study of One-Hole Band Structure in the t-J Model – <i>T. Barnes</i> <i>and M. D. Kovarik</i>	178
I = 3/2 π Scattering in the Nonrelativistic Quark Potential Model – <i>T. Barnes,</i> <i>E. S. Swanson, and J. Weinstein</i>	178
On the Excitation Spectrum of Heisenberg Spin Ladders – <i>T. Barnes, E. Dagotto,</i> <i>J. Riera, and E. S. Swanson</i>	179
Development of Relativistic Hydrodynamics for Heavy-Ion and Astrophysics Applications – <i>Z. Eitzen, D. J. Dean, M. R. Strayer, and M. W. Guidry</i>	179
NUCLEAR PHYSICS	
Dyson’s Equations for Nucleon-Pion-Delta Interactions: Toward a Self-Consistent Solution in Nuclear Matter – <i>K.T.R. Davies</i>	180
Retardation and Dispersive Effects in the Nuclear Mean Field – <i>C. Mahaux,</i> <i>K.T.R. Davies, and G. R. Satchler</i>	180
Analysis of an Unusual Potential Ambiguity for $^{16}\text{O}+^{16}\text{O}$ Scattering – <i>M. E. Brandan,</i> <i>K. W. McVoy, and G. R. Satchler</i>	181
Elastic Scattering of ^{11}Li and ^{11}C from ^{12}C at 60 MeV/Nucleon – <i>J. J. Kolata,</i> <i>M. Zahar, R. Smith, K. Lamkin, M. Belbot, R. Tighe, B. M. Sherrill, N. A. Orr,</i> <i>J. S. Winfield, J. A. Winger, S. J. Yennello, G. R. Satchler, and A. H. Wuosmaa</i>	181
Temporal Nonlocality of Nuclear and Atomic Mean Fields – <i>C. Mahaux and</i> <i>G. R. Satchler</i>	181
Further Studies of the Excitation of the Even Zr Isotopes by 70 MeV ^6Li and Other Ions – <i>D. J. Horen and G. R. Satchler</i>	181

A “Toy” Model to Illustrate the Dispersive and Retardation Properties of a Mean Field – V. A. Madsen and G. R. Satchler	182
Where are Pion Inelastic Interactions Localized? – R. L. Varner and G. R. Satchler	183
A New Effective Interaction for Peripheral Heavy-Ion Collisions – G. R. Satchler	183
Local Potential and S-Matrix Analysis of Pion-Nucleus Scattering – G. R. Satchler, M. B. Johnson, and R. S. Mackintosh	184
Origin of the Soft p_T Spectra – G. Gatoff and C. Y. Wong	185
Effect of Boundary on Momentum Distribution of Quarks in a Quark-Gluon Plasma – C. Y. Wong	185
The Transverse Profile of a Color Flux Tube – C. Y. Wong and G. Gatoff	185
Nuclear Stopping Power and Recoiling Nucleons – B. A. Li and C. Y. Wong	186
Formation and Decay of Toroidal and Bubble Nuclei and Nuclear Equation of State – H. M. Xu, J.B. Natowitz, C. A. Gagliardi, R. E. Tribble, C. Y. Wong, W. G. Lynch, and P. Danielewicz	186
Nonappearance of Dehnen-Shahin Resonances in the Positronium Continuum – C. W. Wong and C. Y. Wong	186
Effect of Quark-Gluon Plasma Boundary on the Momentum Distribution of Quarks – C. Y. Wong	186
Do Nucleons in Abnormal-Parity States Contribute to Deformation? – K. H. Bhatt, C. W. Nestor, Jr., and S. Raman	187
Hartree-Fock-Bogoliubov Calculations in Connection with Radioactive Ion Beam Facility – D. R. Kegley, V. E. Oberacker, M. R. Strayer, and A. S. Umar	187
Study of Nuclear Dissipation Via Muon-Induced Fission: A Relativistic Lattice Calculation – V. E. Oberacker, A. S. Umar, J. C. Wells, M. R. Strayer, and C. Botcher	187
Studies of Electromagnetic Lepton-Pair Production with Capture in Relativistic Heavy-Ion Collisions – J. C. Wells, V. E. Oberacker, A. S. Umar, C. Botcher, and M. R. Strayer	188
Dynamical Calculation of Central Energy Densities in Relativistic Heavy-Ion Collisions – D. J. Dean, A. S. Umar, and M. R. Strayer	189
Solution of a Class of Sturm-Liouville Problems Using the Galerkin Method with Global Basis Functions – C. Botcher, M. R. Strayer, and M. F. Werby	189
Can Molecules be Seen by Two Photons? – T. Barnes	189
Two-Photon Couplings of Quarkonia with Arbitrary J^{PC} – T. Barnes	190
Quark Born Diagrams: Meson-Meson Scattering Amplitudes from the Nonrelativistic Quark Potential Model – T. Barnes	190

NUCLEAR STRUCTURE AND ASTROPHYSICS

Some General Constraints on Identical Band Symmetries – M. W. Guidry, M. R. Strayer, C.-L. Wu, and D. H. Feng	190
The Fermion Dynamical Symmetry Model – C.-L. Wu, D. H. Feng, and M. W. Guidry	191
Nuclear Superdeformation and the Supershell Fermion Dynamical Symmetry Model – C.-L. Wu, D. H. Feng, and M. W. Guidry	191
The Fermion Dynamical Symmetry Model and Identical Bands – M. W. Guidry, C.-L. Wu, and D. H. Feng	192
The Dynamical Pauli Effect – M. W. Guidry, C.-L. Wu, and D. H. Feng	192
Network Calculations for the Production of Heavy Elements – R. Igharas, D. J. Dean, M. R. Strayer, M. W. Guidry, and F.-K. Thielemann	193
Heavy-Ion Transfer Reactions to High-Spin States in the Particle-Rotor Model – R. W. Kincaid, H. Schecter, M. R. Guidry, S. Landowne, R. Donangelo, and G. Leander	194
Nuclear Deformations as a Spontaneous Symmetry Breaking – W. Nazarewicz	194
Proton Emission from Nuclei Beyond the Proton Dripline – S. Åberg, W. Nazarewicz, J. R. Beene, and G. R. Satchler	195
New Vistas in Superdeformation – W. Nazarewicz	195
Diabaticity of Nuclear Motion: Problems and Perspectives – W. Nazarewicz	196
Triaxiality and Alternating M1 Strengths in f-p-g Shell Nuclei – S. L. Tabor, T. D. Johnson, J. W. Holcomb, P. C. Womble, J. Döring, and W. Nazarewicz	198
Magnetic Dipole Strength in Superdeformed Nuclei – I. Hamamoto and W. Nazarewicz	198
First Evidence for States in Hg Nuclei with Deformations Between Normal- and Super-Deformation – W. C. Ma, J. H. Hamilton, A. V. Ramayya, L. Chaturvedi, J. K. Deng, W. B. Gao, Y. R. Jiang, J. Kormicki, X. W. Zhao, N. R. Johnson, I.-Y. Lee, F. K. McGowan, C. Baktash, J. D. Garrett, W. Nazarewicz, and R. Wyss	199
Rotational Band Structure in ⁷⁵Se – T. D. Johnson, T. Glasmacher, J. W. Holcomb, P. C. Womble, S. L. Tabor, and W. Nazarewicz	199
Analysis of a Three-Dimensional Cranking in a Simple Model – W. Nazarewicz and Z. Szymanski	200
Collective Dipole Rotational Bands in ¹⁹⁷Pb – R. M. Clark, R. Wadsworth, E. S. Paul, C. W. Beausang, I. Ali, A. Astier, D. M. Cullen, P. J. Dagnall, P. Fallon, M. J. Joyce, M. Meyer, N. Redon, P. H. Regan, J. F. Sharpey-Schafer, W. Nazarewicz, and R. Wyss	200
Static Multipole Deformations in Nuclei – W. Nazarewicz	200
On the Question of Spin Fitting and Quantized Alignment in Rotational Bands – C. Baktash, W. Nazarewicz, and R. Wyss	201

Octupole Correlations, Spin Assignments, and Identical Bands in ^{193}Hg – <i>J. F. Sharpey-Schafer, D. M. Cullen, M. A. Riley, A. Alderson, I. Ali, T. Bengtsson, M. A. Bentley, A. M. Bruce, P. Fallon, P. D. Forsyth, F. Hanna, S. M. Mullins, W. Nazarewicz, R. Poynter, P. Regan, J. W. Roberts, W. Satula, J. Simpson, G. Sletten, P. J. Twin, R. Wadsworth, and R. Wyss</i>	201
The Influence of Pairing on the Properties of the A=190 Superdeformed Bands – <i>P. Fallon, W. Nazarewicz, M. A. Riley, and R. Wyss</i>	201
Anomalies in the Odd-Even Difference in the Moments of Inertia of Rotational Bands – C. Baktash, J. D. Garrett, I. Hamamoto, W. Nazarewicz, and D. F. Winchell	202
Triaxial Hexadecapole Deformations in Atomic Nuclei – S. Åberg and W. Nazarewicz	204
Nuclear Superdeformation: Past, Present, and Future – W. Nazarewicz	204
 9. LASER AND ELECTRO-OPTICS LAB	
Development of an Infrared Interferometer/Polarimeter System for ITER – <i>C. H. Ma and D. P. Hutchinson</i>	207
CO₂ Laser Thomson Scattering Alpha Particle Diagnostic – R. K. Richards, D. P. Hutchinson, and C. H. Ma	208
 10. COMPILATIONS AND EVALUATIONS	
Controlled Fusion Atomic Data Center – H. B. Gilbody, D. C. Gregory, C. C. Havener, M. I. Kirkpatrick, E. W. McDaniel, F. W. Meyer, T. J. Morgan, R. A. Phaneuf, M. S. Pindzola, D. R. Schultz, and E. W. Thomas	211
Nuclear Data Project – Y. A. Akevali, M. R. Lay, M. J. Martin, S. Rab, and M. R. Schmorak	212
 11. PUBLICATIONS	213
 12. PAPERS PRESENTED AT SCIENTIFIC AND TECHNICAL MEETINGS	241
 13. GENERAL INFORMATION	259

INTRODUCTION

This report covers the research and development activities of the Physics Division for the 1992 fiscal year, beginning October 1, 1991, and ending September 30, 1992. The activities of this Division continue to be concentrated in the areas of experimental nuclear physics, experimental atomic physics, and theoretical nuclear and atomic physics. In addition, there are smaller programs in particle physics, plasma diagnostics, and data compilation and evaluation.

This year has seen a significant change in the direction of the research programs supported by the Holifield Facility. In mid-year, funding was received to reconfigure the accelerators into a dedicated radioactive ion beam (RIB) facility--the first such facility in North America. To effect this transition, user operations of the HHIRF were concluded in June and efforts redirected to the new mission. A summary of Facility activities, along with supporting activities of the Joint Institute for Heavy Ion Research, is given in Chapter 1. The RIB project is described in Chapter 2.

The experimental nuclear physics program covers a broad spectrum of activities centered largely, but not exclusively, on the use of heavy ions. Particularly emphasized are programs in nuclear structure, nuclear reaction spectroscopy of giant resonances, and low-energy reaction phenomena. Results from this past year's work are presented in Chapter 3.

The relativistic heavy ion experimental program continues at CERN and at the Brookhaven AGS. In addition to experimental results from high-energy, heavy ion and particle physics programs, the activities of the Division in support of the new PHENIX (RHIC) and GEM (SSC) detector collaborations are included in Chapter 4. Also included in this chapter is a summary of the effort in experimental particle physics.

A continuing major area of experimental research for the Division is atomic physics. This activity comprises two groups: one on accelerator-based atomic physics, centered primarily at the EN-tandem and the Holifield Facility, but extending to ultrarelativistic energies at the CERN SPS; and one on atomic physics in support of fusion energy, based primarily at the ECR ion source facility. These programs also operate, respectively, the EN-tandem and the ECR Ion Source Facility as "user resources." A report on the activities of the accelerator-based research is given in Chapter 5, and the program in support of fusion is described in Chapter 6.

The UNISOR program, since its inception, has been associated intimately with the Division and, most particularly, with the Holifield Facility. A summary of the research of this consortium is included in Chapter 7.

The theoretical physics activity in the Division concentrates on the areas of atomic physics, nuclear physics, and physics at the nuclear-particle interface, with a particular emphasis on applications of high-performance computing. These efforts, which represent independent studies as well as support to the experimental program, are presented in Chapter 8. Included in this chapter are the results of work associated with the Center for Computationally Intensive Physics and work involving long-term theory visitors of the Joint Institute for Heavy Ion Research.

The Division efforts in the development of Tokamak diagnostics for the Fusion Energy program are described in the work of the Laser and Electro-Optics Lab in Chapter 9.

The Division operates two efforts in data compilation and evaluation. The work of the Atomic Physics Data Center and our effort as part of the National Nuclear Data Center are summarized in Chapter 10.

The report concludes with general information on publications, Division activities, and personnel changes.

J. B. Ball
January 1993

1. HOLIFIELD HEAVY ION RESEARCH FACILITY

OVERVIEW

R. L. Robinson and C. M. Jones

The past year has been one of dramatic transition preparing the way for propelling the Holifield facility into an exciting new area of nuclear physics. At the end of June, the facility ceased operation for the research program and its staff redirected their efforts into modifying the accelerators to produce radioactive ion beams (RIBs). DOE, early this year, approved "Accelerator Improvement Modification (AIM)" funds of \$2.4 million, over the three years FY 1992-94, for this upgrade. The present schedule calls for production of the first RIB in early 1995. At that time the facility will resume its operation as a national user facility.

The Holifield RIB Facility will provide RIBs with masses up to 80 with suitable energies and intensities for nuclear structure and nuclear astrophysics studies. Because the required two accelerators are already in place, the cost for the modification is modest, and the schedule short. (No other U.S. facility has such a fortunate juxtaposition.) Light ions from the ORIC cyclotron will be used to bombard a thick target to produce nuclear reactions leading to radioactive products. Radioactive nuclei of one mass will be selected, converted to negative ions and accelerated with the 25 MV tandem accelerator. The major new components are two high voltage platforms, the target/ion source where the RIBs are produced, a magnetic dipole for mass selection, a negative-ion charge-exchange canal, and two beam lines to link the ORIC, the RIB production area, and the tandem accelerator together. The two high voltage platforms

will be located in an existing heavily shielded target area ideally located between the ORIC cyclotron and the tandem accelerator. The target/ion source, mass separator, and charge exchange canal will be located on one of the high voltage platforms; electronics for these components will be mounted on the other platform. Details of the project can be found in Chapter 2.

During the first nine months of FY 1992, the Holifield facility served as a national research facility by providing 2616 hours of beam for research to 137 scientists from 35 institutions (see Table 1.1). As in FY 1991, these hours were all provided with the tandem accelerator with no coupled operation because of budgetary limitations. In spite of the reduced budget and schedule, performance and reliability of the tandem accelerator continued to be good and no significant problems were encountered.

A contract was signed late in the fiscal year with Danfysik for construction of the Recoil Mass Spectrometer (RMS). This is a new generation device to separate reaction products, with high efficiency and high-mass resolution, from the primary beam at zero degrees. It is unique in its capability to provide this separation for essentially all inverse reactions. The RMS is an excellent complement to the RIB facility because it can be used to detect nuclei which are produced with small cross sections very far from the valley of stability.

A new target room is planned for housing the RMS and future associated detector systems. Funds have been approved, conceptual design completed, and work on construction drawings has been initiated.

2 Physics Division Progress Report

Table 1.1. Distribution of users who participated in research programs at the Holifield during the twelve-month period between October 1, 1991, and September 30, 1992

Institution	Number of Researchers	Institution	Number of Researchers
U.S. UNIVERSITIES		NATIONAL LABORATORIES	
Berea College	1	Argonne National Laboratory	2
Eastern Kentucky University	1	Brookhaven National Laboratory	1
Georgia Institute of Technology	7	Idaho National Energy Laboratory	2
Louisiana State University	3	NASA/GSFC	7
McGill University	1	Oak Ridge National Laboratory	33
Michigan State University	1		
Mississippi State University	6		45
ORAU	3		
Oregon State University	2		
Princeton University	2	NON-U.S. INSTITUTIONS	
Rutgers University	3	AERE (United Kingdom)	1
SW Missouri State University	2	Dubna (Russia)	1
SUNY	1	JAERI (Japan)	2
Tennessee Technological University	4	University of Leuven (Belgium)	2
Texas A&M University	2	Oxford University (United Kingdom)	4
University of Kentucky	2	University of Hannover (Germany)	2
University of Maryland	2	Ecole Polytechnique (France)	1
University of North Carolina	1	University of Tokyo (Japan)	1
University of Pittsburgh	5		14
University of Tennessee	9		
Vanderbilt University	15		
Washington University	5		
	78	Total	137

ACCELERATOR OPERATIONS AND DEVELOPMENT

ACCELERATOR OPERATIONS

*G. D. Alton, M. R. Dinehart, D. T. Dowling,
D. L. Haynes, C. A. Irizarry, C. M. Jones,
R. C. Juras, S. N. Lane, C. T. LeCroy, M. J. Meigs,
G. D. Mills, S. W. Mosko, S. N. Murray,
D. K. Olsen, B. A. Tatum, and N. F. Ziegler¹*

As a result of decreased funding, accelerator operation was further curtailed in FY 1992. No coupled-operation beams were provided and it was necessary to reduce the accelerator operations staff by another person so that a substantial fraction of accelerator operation was performed with only three full-time accelerator operators. In spite of these changes, accelerator utilization efficiency, defined as hours of beam available for research/(hours of beam available for research plus tuning plus unscheduled maintenance), exceeded 80% and 2616 hours of beam time were provided for the research program. Complete operating statistics for FY 1992 are shown in Table 1.2 and a list of beams provided for research is given in Table 1.3. Operation for the experimental program was terminated on July 30, 1992.

Another important task related to operations was completion of the hazard screening documentation which constitutes the first phase of a new Laboratory safety documentation initiative.

1. Consultant.

Table 1.3. Beams provided for research for the period October 1, 1991, through September 30, 1992

Ion Species	Maximum Energy (MeV)
¹² C	150
¹⁶ O	191
¹⁷ O	47
²⁴ Mg	172
²⁸ Si	150
³¹ P	158
³² S	220
³⁴ S	175
³⁶ S	159
³⁵ Cl	195
⁴⁵ Sc	205
⁴⁶ Ti	246
⁴⁸ Ca	213
⁵⁶ Fe	450
⁵⁸ Ni	246
⁶⁴ Ni	237
⁷⁸ Se	270
⁷⁹ Br	370
¹⁰⁷ Ag	550
¹²⁷ I	400

Table 1.2. Tandem accelerator utilization for the period October 1, 1991, through September 30, 1992

	Hours	Percent
Beam available for research (tandem-alone and coupled operation)	2616	30
Accelerator tuning (includes scheduled startup-shutdown)	342	4
Machine studies (includes conditioning not required for specific experiments)	296	3
Total operating time	3254	37
Unscheduled maintenance	305	3
Scheduled maintenance	1034	12
Scheduled shutdown	4191	48

4 Physics Division Progress Report

TANDEM ACCELERATOR

*G. D. Alton, M. R. Dinehart, D. L. Haynes,
C. M. Jones, R. C. Juras, S. N. Lane, C. T. LeCroy,
M. J. Meigs, G. D. Mills, S. N. Murray,
and N. F. Ziegler¹*

Performance and reliability of the tandem accelerator continued to be good, and no significant problems were encountered during this period of operation on a reduced schedule. Terminal potentials up to 23 MV were used during operation for the experimental program.

Of the seven tank openings which occurred during this period, three were planned for scheduled maintenance and four were required for unscheduled maintenance. Three of the unscheduled openings were required to repair high-voltage power supplies. A broken charging chain caused the fourth opening. This chain had been in service since April 1979 and had 62,605 hours of operation. No damage was caused by the broken chain; it was quickly replaced with a spare chain removed in 1984.

An important development during this year was an improved understanding of how to install titanium sublimation pump elements ("slugs") in the terminal stripper pump. The resulting installation improvement and an associated modification of the elements resulted in a significant reduction in stripper pump outgassing time following the installation of new elements.

The prototype voltage-grading resistors discussed in the previous progress report² continued to function well with no apparent spark-induced damage. Installation of a complete resistor-based voltage-grading system based on this design is planned for FY 1994.

Operation of the SF₆ storage and recirculation system continued to be without incident. SF₆ inventory losses for the year were about 0.5%.

In response to a request from a user, the energy-analyzing magnet calibration³ was checked by performing an absolute beam energy measurement for a 71.2 MeV ¹⁶O⁴⁺ beam using the time-of-flight method described in Ref. 3. The measured value of 71.21 ± 0.06 MeV was in good agreement with the value of 71.23 MeV obtained using the observed NMR value and the calibration function measured in 1986.³

1. Consultant.

2. D. L. Haynes, C. M. Jones, R. C. Juras, M. J. Meigs, J. E. Raatz, and J. B. Schroeder, *Phys. Div. Prog. Report for Period Ending Sept. 30, 1991*, ORNL-6689, pg. 6.

3. D. K. Olsen, K. A. Erb, C. M. Jones, W. T. Milner, D. C. Weisser, and N. F. Ziegler, *Nucl. Instr. and Meth.* **A254**, 1 (1987).

A SIMPLE, INEXPENSIVE VOLTAGE GRADING RESISTOR FOR LARGE ELECTROSTATIC ACCELERATORS¹

*D. L. Haynes, C. M. Jones, R. C. Juras,
M. J. Meigs, J. E. Raatz,² and J. B. Schroeder²*

A simple, inexpensive voltage-grading resistor installation for electrostatic accelerators is described. Functional tests in the Holifield Heavy Ion Research Facility 25-MV tandem accelerator indicate that this system is insensitive to spark-induced damage at operating potentials up to 24 MV.

1. Abstract of published paper: *Nucl. Instr. and Meth.* **A320**, 400 (1992).

2. National Electrostatics Corporation, Middleton, Wisconsin 53562.

PERFORMANCE CHARACTERISTICS OF A MULTIPLE-SAMPLE, CESIUM-SPUTTER, NEGATIVE-ION SOURCE

G. D. Alton and M. T. Johnson¹

A multiple-sample, cesium-sputter, negative-ion source which permits sample changes without disruption of on-line tandem accelerator operations is described. The source is equipped with provisions for remotely selecting and moving into the beam position any one of sixty samples by means of stepping motors equipped with absolute shaft encoders. A spherical-sector cesium ionizer is used to produce the cesium beam for sputtering the sample material. The source is equipped with a three-element electrode system which has been designed to increase the perveance for cesium ion beam generation and to improve negative-ion-beam extraction from the source. (Details of the mechanical design features and optics of the three-element electrode system have been previously discussed in Refs. 2 and 3.) Data pertinent to

source operation and the dependence of negative-ion yields on certain source operational parameters were determined during this fiscal year.

A thin layer of cesium can reduce the work function to very low values; the magnitude of the work function change depends on the value of the intrinsic work function, as well as the characteristics of the adsorbate (Refs. 4 and 5). Maximum negative-ion yields are realized whenever minimum work function surfaces are achieved. Thus, an understanding of the dependence of negative-ion yields on source operational parameters, such as ionizer heater current, cesium oven temperature, and sputter-probe voltage, is essential for optimum and efficient, as well as stable, source operation. The dependence of negative-ion yields on each of these three parameters was carefully determined for source operation with C, Cr, and Ni samples.

Negative-ion yield versus ionizer heater current. In order to evaporate cesium in ionic form, it is necessary to heat the ionizer to a critical temperature of ~1100°C. Typically, the cesium ion beam intensities exhibit very abrupt onsets which occur when the critical temperature (~1100°C) is reached. This phenomenon is illustrated in Fig. 1.1, which displays relative negative-ion yield versus ionizer temperature. Such behavior is characteristic of most, if not all, surface-ionization processes.

Negative-ion yield versus cesium oven temperature. A thorough knowledge of the correlation between negative-ion yield and cesium oven temperature is required in order to realize optimum negative-ion yields, as well as to maintain stability of source operation. The cesium oven temperature controls the rate at which cesium strikes the hot

ionizer surface. If the cesium oven temperature is too low, the negative-ion yields will be low. If the cesium oven temperature is too high, the negative-ion yields also decrease and severe sparking may result as a consequence of the high flux of neutral cesium entering the extraction region of the source. The maximum negative-ion current for the elements considered was found at oven temperatures close to 200°C.

Negative-ion yield versus ionizer voltage. The ionizer voltage also affects the negative-ion current due to the increase in sputtering rate with cesium ion energy. A sputtering voltage too low relative to optimum cesium flow rate conditions reduces the negative-ion yield from the standpoint of the number of particles sputtered, as well as greater interference between the sputtered target particles and the effective cesium layer. In contrast, a voltage which is too high can detrimentally disturb the cesium layer by sputtering away the cesium monolayer too quickly, resulting in an increasing work function and a decrease in the probability for negative ion formation. At some ionizer voltage, the cesium oven-temperature-limited regime will be reached; at this point, the ion current will no longer increase, while the sputter rate will continue to increase. The dependence of relative ion yield on ionizer voltage for C⁻ is shown in Fig. 1.2. For this case, the maximum in the negative-ion yield versus ionizer voltage has not been reached. According to theory, the total negative-ion yield from sources of this type should increase strongly with ionizer voltage ($\propto V^{5/2}$).

Experience during test stand operation indicates that the source is simple to operate, reliable, and capable of producing a wide spectrum of negative ions. However, to date, the source has only been used

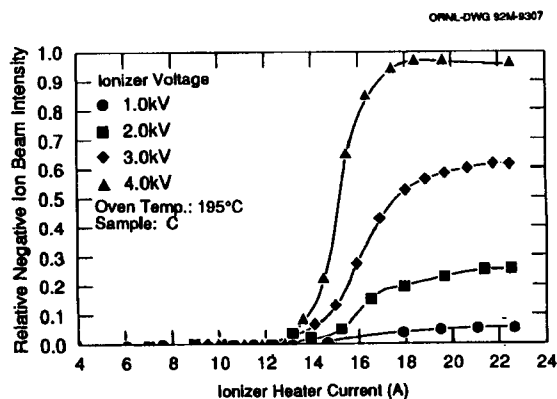


Fig. 1.1. Relative negative-ion current as a function of ionizer heater current.

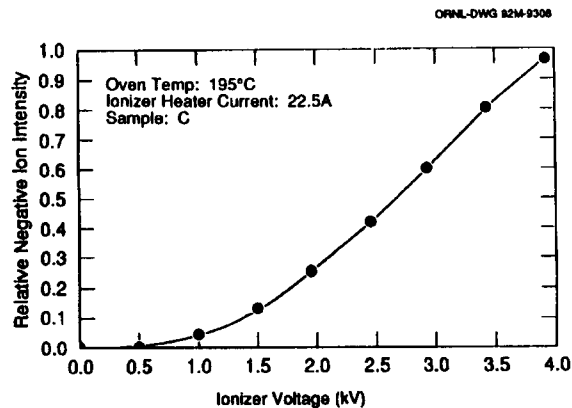


Fig. 1.2. Relative C⁻ negative-ion yield as a function of ionizer voltage.

6 Physics Division Progress Report

to produce negative-ion beams of C^- , Cu^- , and Ni^- for the purpose of determining the operational characteristics of the source. With the source operated at optimum cesium oven temperature, a sputter probe potential of -2000 V and the intermediate electrode operated at -1800 V, negative-ion yields of C^- , Cu^- , and Ni^- are observed to be equal to or greater than the spherical-geometry ionizer source described in Refs. 6 and 7. The source has not been extensively used for a large number of species or to determine maximum yield capability of the source for a particular species. However, the source appears to be superior to the previous spherical-surface source design (Refs. 6 and 7) in terms of negative-ion-beam intensity, ease of operation, and operational stability. The source will undergo further evaluation in the months to come and will be the subject of a future report which will include an extended list of negative-ion species. After this period of operation, more definitive information will be available regarding the maximum absolute negative-ion yields that can be achieved under optimum operating conditions.

1. Science and Engineering Research Semester participant, Hamline University, St. Paul, MN.
2. G. D. Alton, R. M. Beckers, and J. W. Johnson, Phys. Div. Progress Report ,ORNL-6578 (1989), p. 9.
3. G. D. Alton, M. T. Johnson, and G. D. Mills, to be published in Nucl. Instr. and Meth.
4. G. D. Alton, Surf. Sci. **175**, 226 (1986).
5. J. K. Nørskov and B. I. Lundqvist, Phys. Rev. **B19**, 5661 (1979); G. D. Alton, R. M. Beckers, and J. W. Johnson, Nucl. Instr. and Meth. **A244**, 148 (1986).
6. G. D. Alton and G. D. Mills, IEEE Trans. Nucl. Sci. **NS-32** (5), 1822 (1985).
7. G. D. Alton, J. W. McConnell, S. Tajima, and G. J. Nelson, Nucl. Instr. and Meth. **B24/25**, 826 (1987).

A SIMPLE POSITIVE/NEGATIVE SURFACE IONIZATION SOURCE

*G. D. Alton, M. T. Johnson,¹ and
G. D. Mills*

During the fiscal year, the versatile, spherical-geometry, self-extraction surface ionization source, described previously,^{2,3} was assembled, vacuum

tested, and operated both as a positive and as a negative surface-ionization source. The source utilizes direct-surface ionization to form either positive or negative-ion beams resulting from interactions between highly electropositive or electronegative atoms or molecules and a spherical-sector surface ionizer maintained at $\sim 1100^\circ\text{C}$. The efficiencies for forming Cs^+ or UF_6^- in the respective modes of operation are, according to theory, very high. For positive ion generation, the surface ionizer is chosen to be a high-work-function metal such as Mo, Ta, or W; while for negative ion formation, a LaB_6 surface ionizer is selected. The design features and performance of the source for each of these modes of operation are discussed in this report.

The positive or negative surface ionization source, shown schematically in Fig. 1.1 of Ref. 2, can be converted quickly and easily to and from positive or negative modes of operation by simply interchanging the surface ionizer. The body of the source is identical to the standard cesium-sputter negative-ion sources described in Refs. 4-7. Conversion to either a positive or negative surface-ionization source is accomplished by retrofitting the standard negative-ion source with the appropriate spherical-sector ionizer and ionizer-heater assembly. The ionizer assembly electrode structure is insulated from the source housing so that a positive or negative potential of ± 1 to ± 5 kV can be applied for initial acceleration of ions formed on the hot ionizer surface. The respective ionizers are made of Ta for positive and LaB_6 for negative ion generation. The ionizers are identical in size and shape and have diameters of 19 mm and spherical radii of 29.3 mm. The ionizer electrode structure is designed to focus the ion beam through the ion exit aperture, where the beam is further accelerated to ~ 20 keV. An annular heater is used to heat the ionizer to 1100°C . The annular heater design permits easy exchange of the ionizer material when converting from positive to negative or negative to positive modes of operation. Operational parameters for each mode of operation were determined. These results are discussed separately below.

In order to optimize source operation, the correlation between Cs^+ ion beam intensity and ionizer current, cesium oven temperature and initial acceleration voltage must be measured. The dependence of Cs^+ ion beam current on each of these parameters was determined.

The cesium ion-beam intensity, I , is dependent upon the potential difference, V_{ex} , between the ionizer and extraction electrode. Figure 1.3 illustrates this dependence. The theoretical values were calcu-

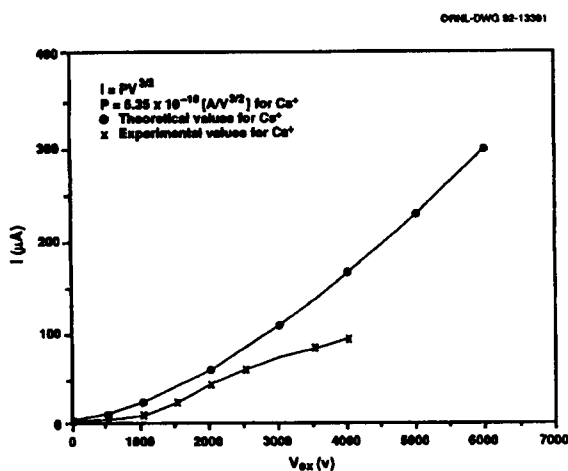


Fig. 1.3. Comparison of observed and theoretical/predicted space-charge limited beam Cs+ intensities I as a function of ionizer voltage V_{ex} .

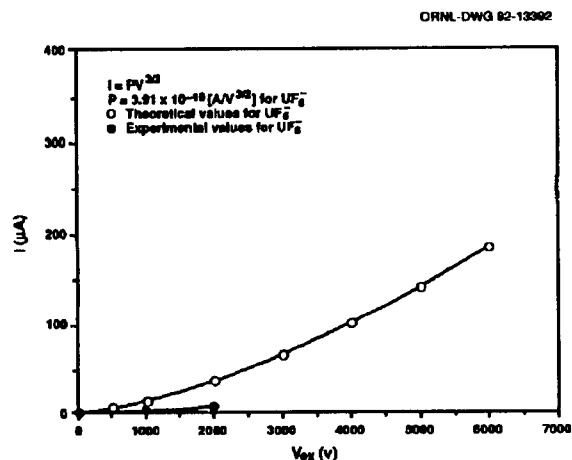


Fig. 1.4. Comparison of observed and theoretically predicted space-charge-limited UF_6 ion beam intensities as a function of ionizer voltage.

lated from the Child-Langmuir relation. The Cs+ beam intensity is space-charge-limited in regions where space-charge-limited conditions exist. Above this region, there is a transition region. This transition region occurs because the source is now being operated in the temperature-limited regime where space charge is not in full effect. In this region, the cesium ion-beam intensity is limited by the rate of arrival of cesium on the hot ionizing surface. The discrepancies between theory and experiment for Cs+ generation are, in part, attributable to slight misalignment of the spherical-sector ionizer with respect to the ion exit aperture.

Analogous measurements were made for UF_6 generation with the source operated in the negative-surface-ionization mode. Many molecules have remarkably high electron affinities that should easily be ionized by the low-work-function LaB_6 surface. However, in practice, the ideal low-work-function surface was found to be difficult to maintain, resulting in unstable beam intensities and low ionization probabilities. Attempts were made to characterize the source for creation of UF_6 beams. Unfortunately, satisfactory stable operation at high intensity levels were never achieved due to apparent chemical reactions between the UF_6 and F_2 with the LaB_6 and due to coating of the LaB_6 ionizer surface with decomposition products (UF_4) and sputter deposits which raised the work function of the ionizer. Low beam intensities were observed to be more stable. Comparisons are made in Fig. 1.4 of observed and theoretical space-charge-limited UF_6 ion beam intensities

as a function of ionizer voltage. A maximum beam intensity of $5 \mu A$ UF_6 was achieved. However, the flow rate of UF_6 required for beam intensities of this magnitude and, consequently, the pressure in the ion source, was found to be very high ($\sim 5 \times 10^{-5}$ Torr). The negative-ion yields were also observed to be very erratic, suggesting that the LaB_6 was easily poisoned by high UF_6 pressures in the source. On disassembly of the source, UF_4 decomposition products and sputter deposits were found on the LaB_6 ionizer. The results from these tests are disappointing.

Operation of the source for the production of cesium ion beams has proven to be simple and reliable. The intrinsic high brightness of the Cs+ source makes it a viable candidate for a number of applications, including microfocused ion-beam surface analysis such as SIMS. The design characteristics of the source make it easy to remove parts for routine maintenance, as well as interchanging the low-work-function substrate. Test stand operation has proved that the source can produce stable positive ion beams of varying intensities up to 200 microamps. However, the negative-ion mode of operation proved to be disappointing, with erratic and unstable operation.

1. Science and Engineering Research Semester participant, Hamline University, St. Paul, MN.
2. G. D. Alton, Phys. Div. Prog. Report, ORNL-6689 (1991), p. 8.
3. G. D. Alton, M. T. Johnson, and G. D. Mills, to be published in *Nucl. Instr. and Meth.*

4. G. D. Alton, Nucl. Instr. and Meth. A244, 133 (1986).
5. G. D. Alton and G. D. Mills, IEEE Trans. Nucl. Sci. NS-32, 1822 (1985).
6. G. D. Alton, R. M. Beckers, and J. W. Johnson, Nucl. Instr. and Meth. A244, 146 (1986).
7. G. D. Alton and J. W. McConnell, Nucl. Instr. and Meth. A268, 445 (1988).

A SCALED SIGMUND THEORY MODEL FOR DETERMINING SPUTTER RATIOS

G. D. Alton, D. H. Olive,¹ M. L. Pinkham,² and J. R. Olive¹

The Sigmund model³ is the most widely accepted and used theoretical model for estimating sputter ratios, i.e., the number of atoms ejected from a surface per incident ion as a result of energetic particle bombardment. Despite the universal appeal of an analytical approximation to the sputtering process, estimates from this theory are known to deviate from experimental observation, often by factors of five or more, depending on the projectile target combination and energy regimes over which the sputtering takes place. In order to effect sputtering, a minimum of energy must be transferred by the projectile to the lattice structure. The Sigmund theory does not account for this threshold effect. During the fiscal year, an improved scaling technique was developed⁴ over that reported previously.⁵ The deviations between theory and experiment are, in part, attributable to approximations and deletions made in developing the theory and perhaps the assumption of homogeneously distributed or amorphous targets; most targets exhibit microstructure, e.g., metals are usually polycrystalline. We have developed a simple scaling technique that can be used to bring theory and experimental observation into better agreement, which includes the threshold effect.

The modified theory takes the form

$$S(E, \theta) = A_1(E) \frac{0.042 \alpha S_n(E)}{U_o(\cos\theta)^F} \quad (\text{for } E \leq 1000 \text{ eV}) \quad (1)$$

$$S(E, \theta) = \frac{A_2 0.042 \alpha S_n(E)}{U_o(\cos\theta)^F} \quad (\text{for } E > 1000 \text{ eV}) \quad (2)$$

where

a is a tabulated function of the ratio of the target mass M_2 to projectile mass M_1 ,

U_o is the heat of sublimation of the target,

θ is the angle between the incident projectile and the surface normal,

F usually has values between 1 and 1.7, depending on the ratio of target to projectile mass.

$$S_n(E) = 4\pi Z_1 Z_2 e^2 a_{12} [M_1 / (M_1 + M_2)] s_n(\epsilon),$$

Z_1, Z_2 are the respective projectile and target atomic numbers,

$$a_{12} = 0.8853 a_o (Z_1^{2/3} + Z_2^{2/3})^{-1/2}$$

a_o is the radius of the first Bohr orbit,

$s_n(\epsilon)$ is the projectile stopping power in the target,

$$\epsilon = \frac{a_{12} M_2 E}{Z_1 Z_2 e^2 (M_1 + M_2)},$$

and A_1, A_2 are scaling parameters. (The original theory does not include such scaling factors.) In this formulation, we incorporate the following approximation for the stopping power.

$$s_n(\epsilon) = \frac{1/2 \ln(1 + \epsilon)}{\epsilon + 0.14 \epsilon} \quad (3)$$

This expression, derived by Wilson et al.⁶ is supposed to be applicable within the high- and low-energy regimes. However, we did not find this to be the case.

Good agreement between Sigmund theory and experiment, with the approximation of expression (3) used for $s_n(\epsilon)$, was found over the complete high-energy regime by linearly scaling Eq. (2) by a factor A_2 . Two methods are used to determine A_2 . A_2 can either be determined from experimental data for projectile energies $E \geq 1000$ eV or by least squares fits to experimental sputter ratio versus projectile atomic number data for a given energy and particular target material, again at projectile energies $E \geq 1000$ eV. In either case, the scaling parameter A_2 is derived by determining the sputter ratio for the projectile of

interest and dividing it by the unscaled Sigmund theory value. The latter technique can be used to obtain scaling parameters for projectiles for which there is no known sputter information. The scaling factor A_2 , in general, was not found to depend on projectile energy E for the high-energy case. This was not the case for projectile energies $E_{th} \leq E \leq 1000$ eV. A function $G(E)$ was found to be necessary in order to bring Eq. (1) into agreement with experiment.

For this energy regime, G was found to depend on the energy of the projectile E in the following way:

$$G(E) = a_0 + a_1 E + a_2 E^2 + a_3 E^3 + a_4 E^4. \quad (4)$$

The constants a_j are averages derived from linear least-squares fits to several sets of experimental data (normalized to unity at $E = 1000$ eV) for neon, argon, krypton, and xenon projectiles interacting with a variety of targets over the low-energy regime $E_{th} \leq E \leq 1000$ eV. The fits were heavily weighted with an average threshold value E_{th} of 24 eV in order to force the sputter ratio S to be zero at E_{th} independent of projectile and target material. The function $G(E)$ is required to have a value at 1000 eV of unity. A_2 is then used as a linear scaling factor for both the low- and high-energy regimes, so that $A_1(E) = G(E) A_2$.

Figure 1.5 displays the function $G(E)$ as determined by least squares fits to many sets of projectile/target sputter data, taken from Ref. 7. Shown in comparison are least squares fits to several sets of

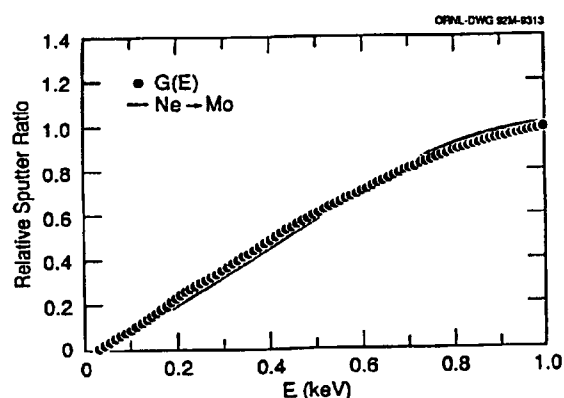


Fig. 1.5. Comparisons of the normalized function $G(E)$ derived from least squares fits to many sets of projectile/target experimental data with least-squares fits to normalized neon projectile/Mo target sputter data. The experimental data for both functions were taken from the compilations of Ref. 7.

normal incidence Ne projectile Mo target sputter data, also taken from Ref. 7, normalized to unity at 1000 eV. As noted, the two normalized curves are in close agreement and are typical of the agreement found between many other projectile/target combinations with the function $G(E)$. As noted, both functions were initiated at a threshold value of $E_{th} = 24$ eV. This threshold value is used for all projectile/target combinations and is an average of the several threshold values reported in Ref. 7.

Figure 1.6 compares sputter ratios derived from the two theories with experimental data taken from Ref. 7 for Ar projectiles incident normal to the surface of an Ag target. As noted, the scaled theory agrees substantially better with experimental data than unscaled theory for all cases considered. This is found to be true in general.

1. Graduate student, Vanderbilt University, Nashville, Tennessee.
2. Undergraduate student, Loyola University, New Orleans, Louisiana.
3. P. Sigmund, *Phys. Rev.* **184**, 383 (1969).
4. G. D. Alton, D. H. Olive, M. L. Pinkham, and J. R. Olive, to be published in *Radiation Effects and Defects in Solids*.
5. G. D. Alton and J. R. Olive, *Phys. Div. Prog. Report, ORNL-6578* (1989), p. 14.
6. W. D. Wilson, L. G. Haggmark, and J. P. Biersack, *Phys. Rev.* **B15**, 2458 (1977).

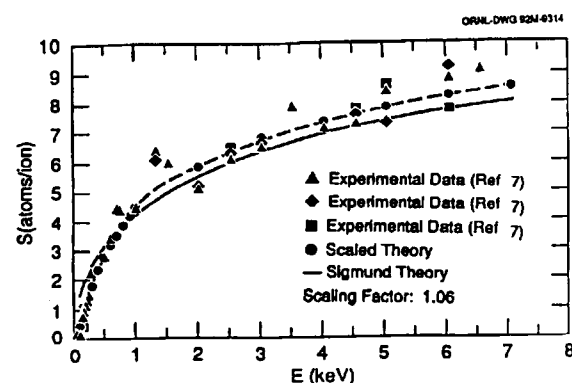


Fig. 1.6. Comparisons of calculated sputter ratios for Ar projectiles at normal incidence on Ag with the experimental data taken from Ref. 7 as a function of projectile energy. --- scaled Sigmund theory; — unscaled Sigmund theory; ▲, ◆, ■ experimental data.

7. All data taken from the compilations of H. H. Anderson and H. L. Bay, "Sputtering Yield Measurements," Chapter 4 in *Sputtering by Particle Bombardment 1*, Vol. 47, *Topics in Applied Physics*, ed. R. Behrish, Springer-Verlag, New York (1981).

FEASIBILITY STUDIES FOR THE DESIGN OF A PLASMA STRIPPER

G. D. Alton and D. Smithe¹

The advantages of a fully ionized hydrogen plasma over conventionally utilized gas and foil strippers in terms of charge state and beam quality for producing highly ionized heavy-ion beams has recently been elucidated computationally^{2,3} and a Z-pinch device initially designed for measuring stopping powers has recently been employed as a pulsed-mode heavy-ion stripper.⁴ Preliminary design studies for a plasma stripper for potential use in increasing the charge states of energetic heavy ion beams were completed during the fiscal year. Magnet design codes, plasma dispersion solvers, and particle-in-cell (PIC) simulation codes, such as MAGIC,⁵ have been used to arrive at the first step in the design of an advanced stripper based on ECR technology. Three areas were emphasized in the study: (1) the magnetic field used to confine the plasma; (2) the generation of ambipolar electric fields in the plasma; and (3) the microwave radiation heating of the plasma.

The advanced concept design utilizes a minimum-B magnetic mirror geometry with a multi-cusp, magnetic-field, with a high number of cusps to assist in confining the plasma radially, and special tailored mirror fields in the end zones. The magnetic field is designed to achieve a large plasma volume with

constant mod-B, so that a large fraction of the plasma reaches the ECR resonant condition with the microwave power source used for plasma heating. This design enables the generation and heating of energetic electrons over a large volume, rather than heating electrons at very localized ECR zone regions, typical of more abrupt B-minimum mirror configurations. Figure 1.7 displays magnetic field intensity profiles for cusp magnetic fields with $N = 6$ and $N = 16$ poles. As noted, the volume over which the central magnetic field is zero increases with an increase in the number of poles. Thus, a high number of poles coupled with a classical solenoidal magnetic field along the z-axis is used in the design to achieve a large uniformly distributed ECR zone. In addition, it was discovered, in this feasibility study, that it is fairly simple to tailor the mirror fields such that the axial magnetic field is nearly uniform except in a very localized region within the mirror end zone. The magnetic field profile for the axial magnetic field of the device is shown schematically in Fig. 1.8. Thin solenoidal coils are used to flatten the profile near the mirror coils which are used to confine the plasma in the end zones.

1. Mission Research Corporation, 8560 Cinderbed Road, Newington, Virginia 22122.

2. G. D. Alton, R. A. Sparrow, and R. E. Olson, *Phys. Rev. A* **45**, 5957 (1992).

3. G. D. Alton, R. A. Sparrow, and R. E. Olson, *Phys. Div. Prog. Report, ORNL-6689 (1991)*, p. 10.

4. K. G. Dietrich, D. H. H. Hoffmann, E. Boggasch, J. Jacoby, H. Wahl, M. Elfers, C. R. Haas, V. P. Dubenkov, and A. A. Golubev, submitted to *Phys. Rev. Lett.*

5. "MAGIC User's Manual," Mission Research Corporation, MRC/WDC-R0-282 (1991).

ORNL-DWG 92-14375

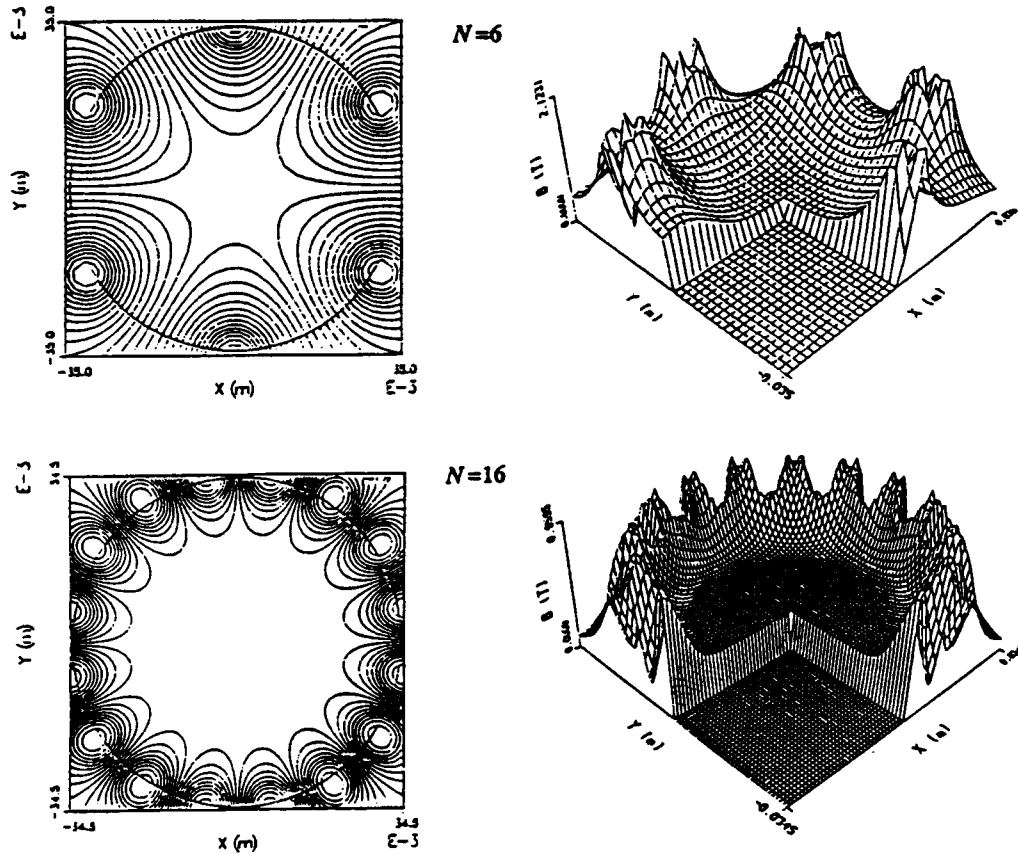


Fig. 1.7. Magnetic field lines and field magnitudes for radial plasma confinement using multi-cusp fields with $N = 6$ and 16 cusps. Note that as the number of cusps increases, the zero-field volume increases, thereby increasing the ECR zone volume. Standard ECR ion sources typically use cusp fields of $N = 6$ poles.

ORNL-DWG 92M-14381

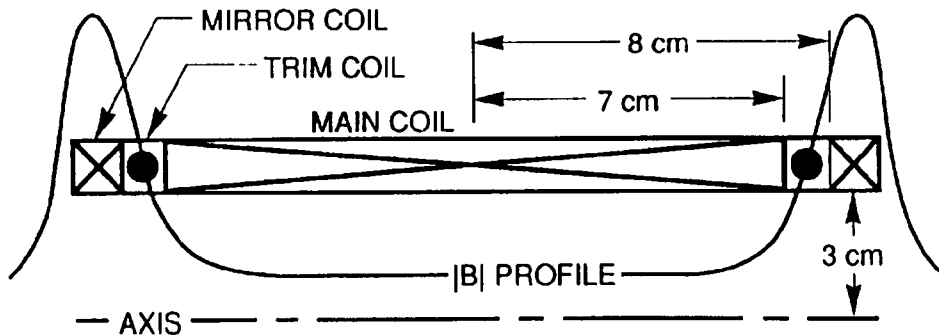


Fig. 1.8. Plasma stripper coil design for axial field, showing locations of main, mirror and trim coils. A diagram of the magnetic field magnitude is also shown to illustrate the effect of the trim coils in providing a flat central field region.

FACILITY OPERATIONS AND DEVELOPMENT

HHIRF EXPERIMENTS

R. L. Robinson

The Holifield Facility served, as over the past ten years, as a national research center until the end of June at which time it ceased operation as a user

facility. Experiments performed during the nine months of operation are listed in Table 1.4. Several of these 36 experiments were performed in more than one part giving a total of 40 runs. Experiments with a prefix H were those recommended by PAC; those with a prefix D were those granted discretionary time; those with a prefix A purchased accelerator time.

Table 1.4. Experiments completed at the HHIRF during the period of October 1, 1991 to June 30, 1992

Title	Spokesman	Run No.	Target Station	Beam		Research Hours
				Type	E(MeV)	
Coulomb Excitation of First 3 ⁻ and 2 ⁺ States in ⁹⁶ Zr	D. Horen (ORNL)	D082	Compact Ge Ball	³² S	105	23
Continuum Gamma-Ray Spectra in Cold Fusion Reactions	J. Beene (ORNL)	D085	Spin Spectrometer	⁵⁸ Ni	246	83
				⁶⁴ Ni	237	
Lifetime of Superdeformed States in ¹⁹² Hg	I. Y. Lee (ORNL)	D086	Compact Ge Ball	³⁶ S	159	62
Decay of ¹⁸⁴ Au to ¹⁸⁴ Pt	K. Krane (Oregon SU)	D087	UNISOR	¹⁶ O	160	21
Beam Energy Scale Check Using ¹⁶ O + ¹⁴⁸ Sm	M. Halbert (ORNL)	D088	Spin Spectrometer	¹⁶ O	66,69,71	18
Energetic Particle Intensity and Composition Experiment	D. Reames (NASA/GSFC)	A001	1.6-m Chamber	⁵⁶ Fe	400	20
				¹⁰⁷ Ag	550	
Energetic Particle Intensity and Composition Experiment	D. Reames (NASA/GSFC)	A002	1.6-m Chamber	⁵⁶ Fe	450	32
				¹⁰⁷ Ag	550	
Heavy Ion Irradiation of Superconducting Materials	D. Christen (ORNL)	A003	1.6-m Chamber	¹⁰⁷ Ag	575	30
Spins and Magnetic Dipole Moments of New Isomers in ¹⁸⁴ Au by Time Integral and Time Resolved Nuclear Orientation and NMR/ON	N. J. Stone (Oxford U)	H320	UNISOR-NOF	¹² C	150	65
Effect of the h _{9/2} Orbital on the Shapes of Nuclei near Z = 82	H. Schuessler (Texas A&M U)	H324	UNISOR	¹⁶ O	190	40
Testing the Role of the Intruder Proton i _{13/2} Orbit in ¹⁸¹ Au	C. Yu (U Tennessee)	H332	Spin Spectrometer-Ge	³⁵ Cl	164,168	123
Study of Shape Coexistence in ¹⁹⁵ Pb by Nuclear Orientation	C. Bingham (U Tennessee)	H334	UNISOR-NOF	¹⁶ O	155,170	114

Table 1.4. (Continued)

Title	Spokesman	Run No.	Target Station	Beam		Research Hours
				Type	E(MeV)	
Deformation and Triaxiality of Odd-Mass $^{123,125}\text{Xe}$	W. Walters (U Maryland)	H335	UNISOR	^{32}S	180,200	83
Intruder Bands in ^{183}Pt	W. Ma (Vanderbilt U)	H338	Compact Ge Ball	^{34}S	163,167	113
Collisional and Radiative Decay of Short-Lived Selected $n = 2$ States Excited by Resonant Coherent Excitation in Crystal Channels	S. Datz (ORNL)	H339	Atomic-43	^{24}Mg	150-170	73
High Spin Spectroscopy of ^{178}Ir	C. H. Yu (U Tennessee)	H342	Compact Ge Ball	^{45}Sc	250	113
Correlations between the Proximity of Intruder Orbitals and the Onset of Shape Coexistence: Spectroscopy Studies of $^{116,122}\text{Xe}$	P. Mantica (ORAU)	H344	UNISOR	^{32}S	175,220	77
The α Reduced Width of ^{180}Pb and the $Z = 82$ Shell Gap	K. Toth (ORNL)	H347	Velocity Filter	^{79}Br	340-370	106
Study of Octupole Deformation in the Actinide Region	J. Saladin (U Pittsburgh)	H348	Spin Spectrometer-Ge	^{13}C	67	93
Search for Internal-Pair Formation EO Transitions as a Mechanism to Depopulate Superdeformed Bands: The $^{192}\text{Tl} \rightarrow ^{192}\text{Hg}$ Decay	E. Zganjar (Louisiana SU)	H349	UNISOR	^{16}O	145	104
Study of the Decay of Superdeformed States	I. Y. Lee (ORNL)	H351	Compact Ge Ball	^{36}S	159	169
Mixed Symmetry States in Nuclei With Shape Coexistence and Search for Super Large Oblate-Prolate Competition in Light Br Nuclei	J. Hamilton (Vanderbilt U)	H353	UNISOR	^{16}O	55,61 184,191	124
Evidence of Conversion Electron Decay in Super-deformed ^{193}Hg from X-ray Measurements	D. Cullen (ORNL)	H354	Compact Ge Ball	^{48}Ca	213	48
Lifetime Measurements of the Deformed States in $^{184,186,188}\text{Hg}$	P. Joshi (Louisiana SU)	H356	UNISOR	^{16}O	170	60
Determination of the ^{190}Hg and ^{192}Hg Alpha Reduced Widths; Influence of Neutron Number on the $Z = 82$ Gap	K. Toth (ORNL)	H357	UNISOR	^{16}O	130,150,170	84
Time Scale of Fission by the X-ray Clock Method	D. Sarantites (Washington U)	H358	Compact Ge Ball	^{32}S	165	109

14 Physics Division Progress Report

Table 1.4. (Continued)

Title	Spokesman	Run No.	Target Station	Beam		Research Hours
				Type	E(MeV)	
Laser Spectroscopy of Promethium	H. Schuessler (Texas A&M U)	H359	UNISOR	¹⁹ F	190	37
Entrance Channel Effects in Fusion Reactions: Nuclear Structure or Nuclear Reaction?	C. Baktash (ORNL)	H360	Compact Ge Ball	³² S	165	116
Nuclear Orientation of ¹¹⁶ I and ¹¹⁴ Sb	W. Walters (U Maryland)	H361	UNISOR-NOF	³² S	220	57
Lifetime Measurements in ^{120,126} Xe	P. Mantica	H362	UNISOR (ORAU)	³² S	175	48
High Energy Ion Bombardment of Polymers for Conductivity Enhancement	L. Bridwell (SW Missouri SU)	H363	1.6-m Chamber	¹²⁷ I	399	12
Extending the High-spin Scheme of ¹⁷⁹ Ir and Searching for Highly-deformed Bands	H. Jin (Rutgers U)	H364	Compact Ge Ball	³¹ P	150,154	108
Shape Coexistence and Electric Monopole Transitions in ^{179,177} Pt and ^{179,177} Ir	J. Schwarzenberg (Georgia Tech)	H365	UNISOR	¹² C	150	63
Excited States in the N = Z+1 Nucleus ⁷³ Kr	D. Winchell (ORNL)	H366	Spin Spectrometer +Ge	¹⁷ O	47	127
Strongly Deformed Shapes and Softness in the Very Neutron-Deficient Nd and Pm Isotopes	J. Breitenbach (Georgia Tech)	H367	UNISOR	⁴⁶ Ti	245,250	26
The Identification of Mixed-Symmetry States in, and the Level Structures of, the N = 80 Isotones: Ce, Nd and Sm	R. B. Piercey (Mississippi SU)	H368	UNISOR-NOF	⁵¹ V ¹² C	225 150	35
						2616

COMPUTER SYSTEMS

*W. T. Milner, J. W. McConnell
C. N. Thomas¹, R. L. Varner*

Network Expansion

C. N. Thomas¹ and R. L. Varner

Terminal communications equipment and cabling in Buildings 6003 and 6008 have been replaced. This

equipment provides faster and more reliable communications as well as direct telnet access to host computers. The Physics Ethernet network has been extended into Building 6007 and terminal communications equipment installed. Terminal lines have been pulled to six offices and are available for use. Work is in progress to extend the FDDI network into Building 6003. All optical fibers are in place and electronic components are on hand. Work should be completed in December. New Terminal communications equipment has also been installed in the 6000B high bay

area to improve reliability and provide telnet access to host computers.

Data Acquisition System Development

*J. W. McConnell, R. L. Varner, W. T. Milner,
and C. N. Thomas¹*

Development

As reported last year,² we are developing a high-capacity VME/UNIX-based data acquisition system. This system is designed to control data acquisition for detector systems such as the HILI or the BaF₂ array used by the local experimental groups. The system is relatively portable, so that it can be used by groups with experimental programs at other facilities. It controls up to 8 CAMAC crates in addition to reading out FASTBUS and FERA ECLbus. In addition to serving our current needs for portable data acquisition systems we may provide for the radioactive ion beam facility. This work has consisted of three principal parts: (1) the development and adaptation of workstation software for network and interprocess communication, data recording, display and analysis, (2) the development of a simple front-end programming language for specifying event readout, and (3) the development of a VME based front-end system for event recognition and readout.

Architecture

The acquisition system has two major components, a front-end readout processor and a back-end workstation. The architectural model we use (Fig. 1.9) is one of a "server" (the front end) of events and control busses, and a "client" (the workstation), which records events and makes control requests of the server. The front end processes each event by responding in real time to event triggers generated by the detector system. It holds events until its buffers are full and then transmits them to the workstation, which provides load-leveling needed for reasonable response of the workstation. It also responds to requests from users of the workstation to perform CNAF's, FASTBUS operations, and various acquisition control operations.

The workstation receives the event stream, distributes the stream to client tasks which write the

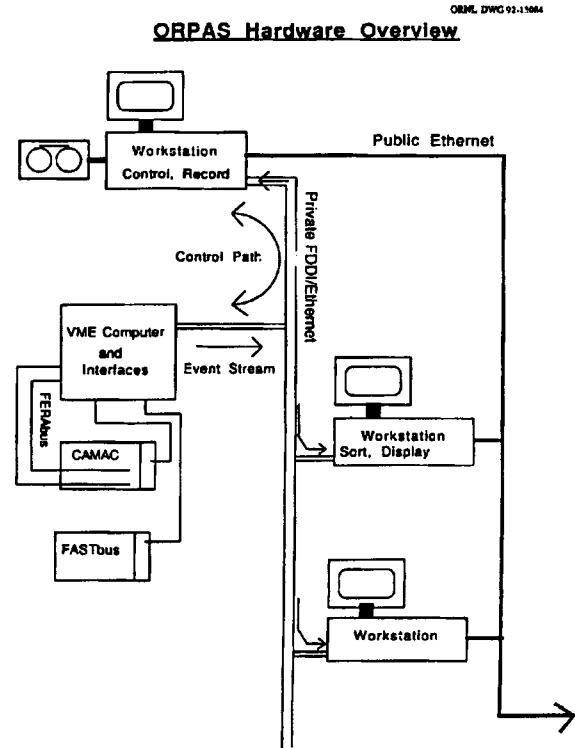


Fig. 1.9. Oak Ridge Physics Acquisition System (ORPAS) hardware overview.

events to tape and make histograms. These clients include the SCANU and LEMO programs of UPAK.^{3,4} The workstation is also used to download code and control the software components of the front-end system.

Ethernet Communications

The connection from the VME host to the workstation is via thinwire Ethernet initially, to be replaced by a Fiber Distributed Data Interconnect (FDDI) in the next year. We use a locally written network protocol. It is connectionless and supports both a "reliable" (ACK/NAK) transmission and an "unreliable" transmission. The unreliable transmission is used for event data in which some small loss of events is acceptable as long as the loss is measured. The reliable transmission is inefficient, as there is one ACKnowledgment for each transmitted packet. The protocol was deliberately made simple, first to simplify its implementation in the VME and second, because we may adopt a standard protocol in the implementation of the FDDI.

Workstation Implementation

The workstation is a DECstation 5000/125 with 600 Mbyte and 1.6 Gbyte disks and 96 Mbytes of memory, as well as a second Ethernet controller and FDDI interface. The large memory is needed only to support large user histogramming tasks. The recording medium is an Exabyte 8500 tape (8mm, 5-Gbyte capacity and 500-Kbyte/s writing speed) using the SCSI bus. The choice of the DECstation and Exabytes allows us to make substantial use of the UPAK software already developed here for data processing under UNIX.

We created the workstation software (Fig. 1.10) to gracefully integrate the UPAK software into the acquisition environment. The major software component is a network data receiver which deposits data into a shared memory segment (SHM), access to which is synchronized using UNIX semaphores (SEM). Each instance of a receiver can support up to 10 clients. Among the clients are LEMO and SCANU from the UPAK. The new L003 event format presently precludes us from safely using the CHIL-based SCAN package, although it too has been modified to also use the shared memory event input. LEMO has been extended to support copying the SHM data stream to tape, including such features as automatic header generation, display of the new L003 format, and event stream modification for output to other clients. In addition, all the clients can now write messages to a UNIX message queue from which a common, time-stamped log can be produced for later diagnosis of the run. All clients now monitor the ratio of events they receive to events sent by the front end, to measure deadtime losses contributed by the Ethernet event data protocol. All these facilities are implemented with C and Fortran callable interfaces and will be easy to include in future utilities. There are also a number of tools to control the front end, as well as timed scaler readout.

Front-end Programming Language - PAC

A front-end programming language PAC (stands for Physics Acquisition Code) has been designed and implemented which enables the user to easily specify how the parameters of an "event" are to be read out by the front-end processor. The PAC program, which performs a function similar to the Event Handler program in the earlier Concurrent data acquisition system, consists of two main parts: (1) a hardware description list and (2) a conditional readout section.

ORPAS Data Flow Diagram

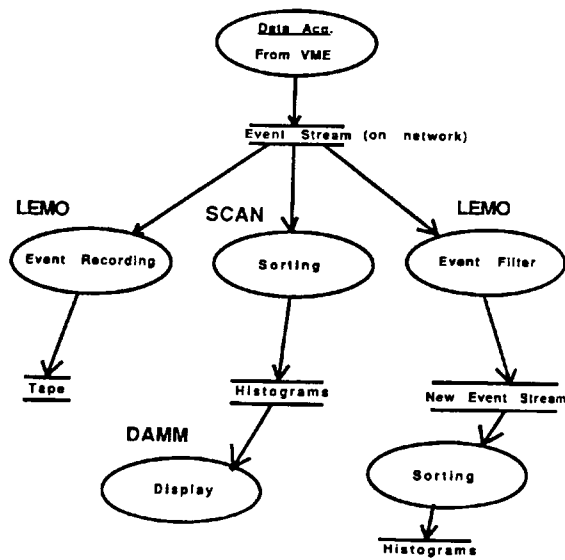


Fig 1.10. ORPAS - Data flow diagram for complete system.

The hardware description list specifies in a compact way (with implied loops, etc.) the hardware types and locations of all devices (ADCs, TDCs, gated latches, scalars, etc.) to be read as well as associated parameter numbers and names (referenced in any subsequent conditional readout section). Any parameters (gated latches, etc.) which are to be saved for testing in the conditional readout section are also specified. All devices given in the hardware description list are read for every event unless they are subsequently specified to be read conditionally. In summary, the hardware description list specifies the following:

- (1) Kind of module (CAMAC, FERA, FASTBUS, etc.),
- (2) Model No. for FASTBUS and FERA modules,
- (3) Locations of devices (crate, slot, sub-addr),
- (4) Function codes to read/clear CAMAC modules,
- (5) Parameter numbers associated with each device,
- (6) Parameter names associated with each device,
- (7) Identification of gated latch devices,
- (8) Initializing CNAFs - executed at RUN-time and
- (9) End-of-Event CNAFs - executed at end of event.

The conditional readout section provides for the testing of gated latch bits and, depending on the result

of the tests, the execution of actions of the following form:

- (1) An entire event may be killed.
- (2) All devices of a given FASTBUS or FERA Model number may be read.
- (3) Individual CAMAC sub-addresses may be read.
- (4) Write or no-data CNAFs may be executed.

A PAC compiler has been written which runs in the workstation, reads in the user-written source code, performs extensive diagnostics and generates tabulated instructions (object code) which can be downloaded into the front-end processor. Software running in this processor performs the actual data acquisition via VME interfaces to the various front-end crates (CAMAC, FERA and FASTBUS). The PAC object code serves as the guide to event readout.

The Front-end Readout System

The VME based front-end readout system (Fig. 1.11) consists of a Force Computers CPU-40B/4 with onboard Ethernet interface, a Kinetics Systems 2917 CAMAC interface, a LeCroy 1131 interface to FASTBUS and an event trigger input/output module. An interface to FERA readout devices will be added in the near future. The workstation communicates with the VME system via Ethernet.

The software system uses the VMEPROM real-time kernel supplied with the CPU-40B. A new system services trap handler was developed which handles the most time-critical functions and passes the remainder to VMEPROM. VMEPROM is a multitasking kernel and the initial boot load from the workstation loads four tasks and allocates a memory segment for the data acquisition parameters. These tasks are (1) an Ethernet driver providing communication with the workstation, (2) a memory manager which allows the workstation to load, execute and kill additional tasks, (3) a CAMAC driver which executes CAMAC operations directed by the workstation, and (4) a FASTBUS driver which executes commands to the FASTBUS segment manager/interface. A library of FORTRAN callable routines allow user FORTRAN programs to access CAMAC and FASTBUS devices.

For data acquisition (see Fig. 1.12 for a data flow diagram), the workstation loads two additional tasks into the CPU-40B. The first task is the real-time readout. The PAC compiler downloads tables of parameters to a memory segment in the CPU-40B.

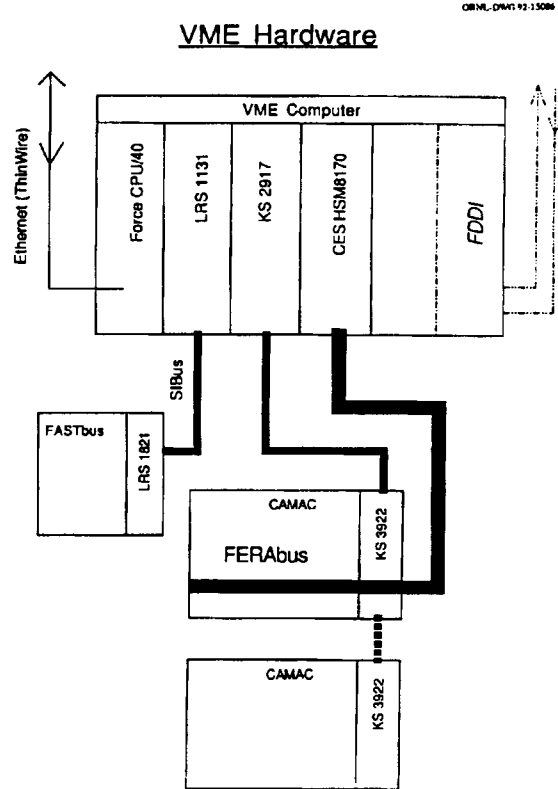


Fig. 1.11. ORPAS - VME hardware.

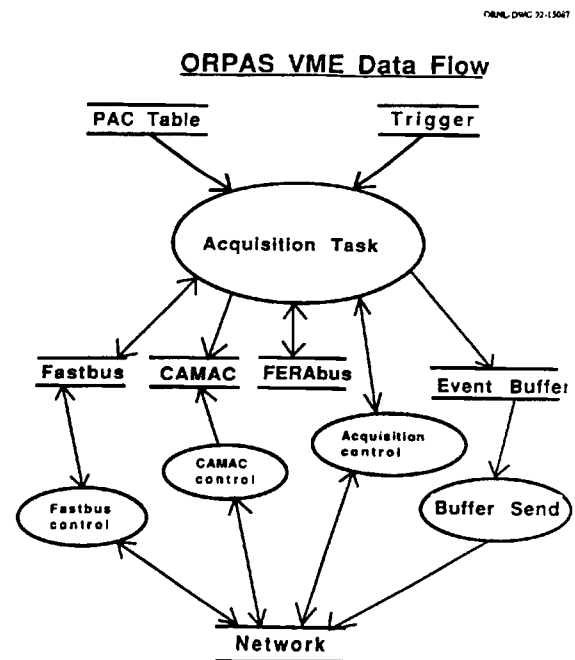


Fig. 1.12. ORPAS - VME data flow diagram.

After the acquisition parameters are loaded, the readout task must be initialized. During the initialization phase, the initialization list specified by the PAC is executed, run-time hardware dependent execution lists are built from PAC specifications, and lists of functions to be executed in response to the Event signal input are built. Any errors detected during this process are reported to the workstation and data acquisition is inhibited. The second task receives data buffers from the readout task and formats these buffers into Ethernet packets which are transmitted to the workstation.

Status

The system has now been used for two experiments at Texas A&M Cyclotron Institute with the HILI detector. The system has performed well and can take data at more than 2500 events/sec and transfer data at up to 60% of the Ethernet bandwidth (on the order of 700 Kbytes/sec). We are working to improve the performance and usefulness of all aspects of the VME system, as well as to provide a suitable data acquisition environment on the workstation. We are also working to provide online documentation, as well as to make the system easily portable by non-UNIX experts.

Our use of UNIX and industry standard network interfaces are expected to make it possible for us to include additional DECStations as clients of the front end, as well as implement other workstation types.

GAMMASPHERE Software Development Activities

R.L. Varner and W.T. Milner

We have been involved in the past year in the development of software for the GAMMASPHERE being constructed at Lawrence Berkeley Laboratory (LBL). Our involvement is of two kinds, the development of the "base" software for histogramming and display on workstations during GAMMASPHERE data acquisition, and participation in the GAMMASPHERE Software Working Group, a committee to assist users in specifying and supplying software to enhance the available base software at GAMMASPHERE.

The base software specification was agreed to in January of 1992 at LBL. The Oak Ridge Physics Division agreed to provide a complete sorting, histogramming and display software package to run on the workstations which provide the user interface to the GAMMASPHERE. The software will consist of the current version UPAK^{2,3,4} data analysis software with suitable enhancements for operation in a data acquisition environment.⁵ This software will be ported to SUN workstations, and integrated with the datastream from the LBL event building system. That effort has now begun, using a SUN workstation provided to ORNL by the GAMMASPHERE project. This task is projected to be completed by the time the full implementation of GAMMASPHERE is complete.

The GAMMASPHERE Software Working Group was established by the GAMMASPHERE project director to allow the user community of GAMMASPHERE to focus its requests and contributions to the GAMMASPHERE software effort. To smooth the interface of the committee with the base software development, a representative of each national laboratory involved in the base software was appointed. The member from Oak Ridge is Robert Varner. The chairman of the committee is R. B. Piercey of Mississippi State University (MSU). The committee met at Mississippi State University, to organize and discuss the initial directions of the committee's work.

The main items of interest to the committee were the representation and processing of the n-dimensional gamma-ray data which GAMMASPHERE is designed to produce, as well as the portability of the available analysis software. To better focus the issues, the committee has formed working groups on the following topics:

- 1) Histogram formats
- 2) Graphical user interfaces
- 3) Parallel programming

The working groups in which ORNL is active are the histogram format committee and the graphical user interface committee. The common histogram format is viewed as necessary to create sharable tools and an extensible system. The graphical user interface committee will study the extension of the software ORNL will provide, by including a graphical user interface for some of the tools. The parallel

programming committee is looking into styles and degrees of parallelism which might enhance the processing of GAMMASPHERE data.

The working group on the common histogram format consists of R. B. Piercey (MSU), R. L. Varner (ORNL), R. MacLeod (Chalk River), R. A. Belshe (LBL), and M. P. Carpenter (ANL). The focus of this subcommittee is to develop a common, extensible histogram format which could be used to develop common tools throughout the GAMMASPHERE user community and, perhaps, the nuclear physics community at large. This format emphasizes saving complete information about each histogram with the histogram, including sufficient information to recreate the original sort, create a display, and even save annotations. This information is saved with each histogram as a linked list, which allows one to save only the required DATA record, or even include customized information in additional records.

The work of this committee is continuing and we expect to publish a first version of the format in the near future.

1. Oak Ridge Associated Universities.
2. R. L. Varner et al. in Phys. Div. Prog. Rep. for Period Ending Sept. 30, 1991, ORNL-6689, p. 20.
3. HHIRF Newsletter No. 34, page 5 (1987).
4. HHIRF Newsletter No. 46, page 5 (1992).
5. J. W. McConnell, R. L. Varner, W. T. Milner, and C. N. Thomas, "Data Acquisition System Development," this report.

USERS GROUP ACTIVITIES

R. L. Auble

The Executive Committee of the HHIRF Users Group met on December 12, 1991, February 14, 1992, and June 5, 1992 to provide guidance on operation of the HHIRF and recommendations for making the transition to a radioactive-ion-beam facility. Committee members for 1991 and 1992 are listed in Table 1.5.

The Executive Committee has taken an active role in organizing a workshop to examine apparatus requirements for the RIB facility, and has provided recommendations on phase-out of existing apparatus, interim dormitory operation, restructuring of the users group, and beams to be considered for initial operation.

Table 1.5. Users Group Executive Committee

1991

Carroll Bingham, University of Tennessee
 Doug Cline, University of Rochester
 Tom Cormier², Wayne State University
 John Rasmussen, Lawrence Berkeley Laboratory
 Demetrios Sarantites¹, Washington University
 Ken Toth, Oak Ridge National Laboratory

1992

Cyrus Baktash², Oak Ridge National Laboratory
 Tom Cormier¹, Wayne State University
 Doug Cline, University of Rochester
 John Rasmussen, Lawrence Berkeley Laboratory
 Demetrios Sarantites, Washington University
 Bill Walters, University of Maryland

¹Chairperson

²Chairperson-elect

Although operation of the Holifield as a national user facility was suspended in June 1992, the committee felt that it was essential to maintain continuity by establishing a RIB Users Group and keeping the Executive Committee active in the development phase of the RIB project. Therefore, membership request cards were distributed to potential RIB users and an election will be held to elect two new members to the Executive Committee for 1993. The members of the Nominating Committee were J. D. Garrett (ORNL) - chairperson, M. A. Riley (Florida State University), P. D. Parker (Yale University), E. F. Zganjar (Louisiana State University), and J. X. Saladin (University of Pittsburgh).

THE JOINT INSTITUTE FOR HEAVY ION RESEARCH

*R. L. Robinson, J. H. Hamilton,¹ and
C. R. Bingham²*

The Joint Institute for Heavy Ion Research is a collaborative endeavor between the University of Tennessee, Vanderbilt University, and ORNL. About two-thirds of its funding comes from the State of Tennessee through the Science Alliance at the University of Tennessee. The remainder is provided by Vanderbilt University, DOE, and ORNL. The Joint Institute is housed in two buildings which are adjacent to the Holifield Facility.

20 Physics Division Progress Report

It has continued to fulfill its mission as defined in its Agreement between the three sponsoring institutes:

“to promote and support heavy-ion research at the Holifield Facility by providing an intellectual center and physical support for researchers who work at the Holifield Facility, to the mutual benefit of sponsors and participants, in the field of heavy ion research.”

This is done in three ways: 1) support of workshops and meetings, 2) support of guests, and 3) operation of a dormitory facility.

Full or partial support was provided to the guests noted in Table 1.6. The average length of appointment during FY 1992 for the 60 guests was over 3 months. The primary effort was in the area of nuclear structure theory with the purpose of assisting in the creation of a nuclear structure theory effort at the Laboratory. The mainstay of this was support for a senior nuclear structure theorist (Witek Nazarewicz) and support for a post doc (filled by Ramon Wyss until April 1992).

Support was provided for the meetings noted in Table 1.7. The International Symposium on Reflections and Directions in Low Energy Heavy-Ion Physics celebrated operation of twenty years for UNISOR and ten years for the Joint Institute for Heavy Ion Research. Speakers at this two-day symposium reflected, in part, on the accomplishments in low-energy, heavy-ion science and then emphasized the new directions and opportunities to be explored with low-energy, heavy-ion facilities. Areas covered included properties of nuclei far from stability, high-spin states, hot dipoles, transfer, reaction mechanisms, and atomic physics. A final session focused on research at new facilities, such as one with radioactive ion beam capabilities, and a new generation recoil mass spectrometer.

Among the developments reported at the Second International Conference on On-Line Nuclear Orientation and Related Topics were new initiatives to search for violations of parity and time-reversal invariance in nuclei, successful theoretical approaches leading to the understanding of E2/M1 mixing ratios

and M1 moments, and the latest advances in the application of nuclear magnetic resonance to oriented nuclei. Also reported was a wealth of new spectroscopic information obtained from on-line nuclear-orientation measurements using both gamma-ray and particle detection.

The Workshop on the Microscopic Origin of Nuclear Deformation consisted of lectures on various aspects of nuclear deformation. Subjects covered included the role of proton-neutron interactions, the comparison and relation between shell model, algebraic, and geometrical pictures of nuclear deformation, and the phenomenon of spontaneous symmetry breaking. The goal was to summarize the present knowledge of the origin of nuclear deformations, and also discuss new directions in this field of research.

The purpose of the International Workshop on Nuclear Structure Models was to review and evaluate various theoretical approaches to nuclear structure. The first part of the workshop consisted of formal, but pedagogical, presentations on ten different groups of nuclear structure models. The second part of the workshop was devoted to evaluations of the different models.

The Satcherfest had talks which highlighted major advances in the areas of direct, inelastic, particle-transfer, and fusion reactions, dispersion relations, semiclassical scattering, effective interactions, optical models, and giant resonances. It was fitting that this meeting commemorated the 65th birthday of Ray Satchler who has over several decades, been one of the major contributors to these areas.

The program of the First Symposium on Nuclear Physics in the Universe emphasized the new interface between Astrophysics, Nuclear Physics, and Atomic Physics that is promised by radioactive ion beam facilities. This was particularly timely as the Holifield Facility is in the process of converting to this area of research.

The dormitory provided lodging for 230 guests who stayed for a total of 1425 person-nights.

-
1. Vanderbilt University.
 2. University of Tennessee .

Table 1.6. Guest scientists at the Joint Institute for Heavy Ion Research during the period of October 1991 - September 1992

Name	Institute	Length of Appointment
S. Aberg	Lund Univ. (Sweden)	6 weeks
A. Balantekin	Univ. of Wisconsin	5 days
K. Bhatt	Univ. Mississippi	17 days
J. Blankenship	ORNL/JHIR	1 year
M. Brack	Univ. of Regensburg (Germany)	10 days
A. Bulgac	Michigan State Univ.	10 days
P. Butler	Univ. of Liverpool (England)	1 week
A. Champagne	Univ. of North Carolina	2 days
E. Chavez-Lomeli	Nat. Univ. of Mexico (Mexico)	7 months
D. Cullen	Univ. of Liverpool (England)	11 months
J. Dellwo	Univ. of Tennessee	2 months
J. Dobaczewski	Warsaw Univ. (Poland)	1 month
J. Draayer	Louisiana State Univ.	1 week
A. Faessler	Univ. Tubingen (Germany)	1 week
D. Feng	Drexel Univ.	1 week
S. Frauendorf	NBI (Denmark)	4 days
G. Gatoff	ORNL	11 months
J. Goerres	Univ. of Notre Dame	2 days
A. Goodman	Tulane Univ.	1 week
W. Greiner	Univ. of Frankfurt (Germany)	3 days
S. Gupta	Bhabha Atomic Res. Centre (India)	3 weeks
I. Hamamoto	Lund Univ. (Sweden)	10 days
K. Heyde	Inst. for Nuclear Physics (Belgium)	1 week
I. Hughes	JET Joint Undertaking (England)	8 months
V. Irby	Univ. of Missouri	9 months
R. Janssens	ANL	1 day
M. Korolija	Ruder Boskovic Inst. (Yugoslavia)	1 year
V. Madsen	Oregon State Univ.	5 months
C. Mahaux	Univ. of Liege (Belgium)	2 weeks
J. Maruhn	Univ. of Frankfurt (Germany)	19 days
F. McGowan	ORNL	1 year
J. Mueller	Univ. of Frankfurt (Germany)	1 year
P. Mueller	Univ. of Illinois	1 year
W. Nazarewicz	Warsaw Univ. (Poland)	1 year
V. Oberacker	Vanderbilt Univ.	1 week
T. Otsuka	Univ. of Tokyo (Japan)	3 days
V. Pashkevich	JINR (Russia)	10 days
S. Pittel	Univ. of Delaware	1 day
S. Rab	Kuwait Inst. Sci. Res. (Kuwait)	4 months
A. Ray	Texas A&M Univ.	3 months
S. Rohozinski	Warsaw Univ. (Poland)	10 days
S. Saini	ORNL	1 year
K. Schmid	Univ. of Tubingen (Germany)	10 days
M. Schmorak	ORNL	1 year
M. Schulz	Univ. of Missouri	13 days
M. Smith	California Inst. of Tech.	2 days
J. Stone	Oxford Univ. (United Kingdom)	1 month

22 Physics Division Progress Report

Table 1.6. (Continued)

Name	Institute	Length of Appointment
N. Stone	Oxford Univ. (United Kingdom)	1 month
D. Stracener	Washington Univ.	3 days
S. Szymanski	Warsaw Univ. (Poland)	6 weeks
F. Thielemann	Harvard Univ.	1 day
M. Vallieres	Drexel Univ.	11 days
R. Vogelaar	Princeton Univ.	2 days
M. Wiescher	Univ. of Notre Dame	2 days
D. Winchell	Univ. of Pittsburgh	1 year
R. Wyss	Royal Inst. of Tech (Sweden)	8 months
P. Zeijlman	Utrecht Univ. (The Netherlands)	11 months
V. Zelevinsky	NBI (Denmark)	10 days
J. Zhang	Inst. of Modern Phys. (China)	1 year
W. Zhao	Inst. of High Energy Phys. (China)	3 months

Table 1.7. Meetings sponsored by the JHIR during FY 1992

Meeting	Date	Attendees	Chairmen
International Symposium on Reflections and Directions in Low Energy Heavy-Ion Physics	October 14-15, 1991	120	J. H. Hamilton
Second International Conference on On-Line Nuclear Orientation and Related Topics	October 16-19, 1991	75	K. S. Krane
Workshop on Microscopic Origin of Nuclear Deformation	November 25, 1991	30	D. H. Feng M. W. Guidry W. Nazarewicz
Workshop on Nuclear Structure Models	Mar. 16-25, 1992	64	R. Bengtsson J. P. Draayer W. Nazarewicz
Satchlerfest: A Symposium on Nuclear Reactions	April 15-16, 1992	50	M. R. Strayer
First Symposium on Nuclear Physics in the Universe	September 24-26, 1992	100	M. W. Guidry M. R. Strayer

**THE HHIRF PROGRAM
ADVISORY COMMITTEE**

R. L. Robinson

The last meeting, until at least 1994, of the Holifield Program Advisory Committee (PAC-18) was held November 6, 1991. Normally the PAC has been requested to recommend approval for those experiments which proposed the strongest physics. However, because of the unusual situation of cessation of user operation in June 1992, the PAC members were requested to temper their decisions with the need to complete outstanding experiments and to provide data for dissertations based on programs already in progress at the Holifield Facility.

PAC-18 reviewed 20 proposals requesting 1792 hours of beam time. It approved 1200 of these hours. Because of the termination of operation, 384 hours approved by this PAC and preceding PACs could not be accommodated.

Members of PAC-18 were: J. P. Draayer (Louisiana State University), J. C. Hardy (Chalk River National Laboratory), M. B. Lewis (ORNL), C. J. Lister (Yale University), W. G. Lynch (Michigan State University), and J. C. Waddington (McMaster University). Observers of the meeting were J. B. Ball (Director, ORNL Physics Division), R. L. Auble (HHIRF Liaison Officer), and D. G. Sarantites (Chairman, Executive Committee of the HHIRF Users Group). The meeting was chaired by R. L. Robinson (HHIRF Scientific Director).

2. THE RADIOACTIVE ION BEAM PROJECT

INTRODUCTION

D. K. Olsen

During FY 1992, the ORNL proposal¹ to reconfigure and develop the HHIRF accelerator system to be a first-generation radioactive ion beam RIB facility was approved and funded as a FY 1992-93-94 AIP project. Consequently, on June 30, the HHIRF shut down as a national user facility for research with stable heavy ion beams and the operating and development technical personnel began developing the ORNL RIB facility. The Directive for the project was signed by the Oak Ridge Field Office on September 30, 1992. First experiments with low-intensity radioactive beams are scheduled for the first half of calendar year 1995. An important milestone will occur at the end of 1993. At that time, the RIB injector will be completed, the Mark-I target-ion source will be tested, and the ORIC beam lines will be reconfigured. This should allow the optimization of RIB production with ORIC beams and, perhaps, allow some experiments with 300-KV RIBs accelerated with the new RIB injector.

The overall physics program and conceptual design for the RIB project are described in the FY 1990 (ORNL-6660) and FY 1991 (ORNL-6689) Physics Division Progress Reports. During FY 1992, substantial progress was made toward reconfiguring the HHIRF accelerator system and developing a RIB facility. Most of the work has focused on the goal of accelerating ORIC-produced RIBs with the new injector. In particular, the following progress was made:

1. A detailed layout of the mechanical and electrical equipment for the new RIB injector has been completed. A specification for the HV platform system for the RIB injector has been completed. Procurement of the HV platform system is under way.
2. A detailed physics design of the first-stage mass separator on the new RIB injector has been completed, including a third-order calculation of the beam transport with the GIOS code.
3. The transmission through the tandem as a function of injection voltage was measured to specify the minimum RIB injector voltage.
4. Much of the preparation work on room C111 required to install the HV platform has been completed.
5. A NEPA categorical exclusion was obtained for the RIB project and other immediate ES&H issues were resolved.
6. HETC and PACE calculations were completed in order to better understand the expected radioactive atom yields with ORIC beams and resulting residual radiation.
7. The detailed engineering of the Mark-I target-ion source has been nearly completed and components are being procured.
8. A concept for a second target-ion source based on direct-negative extraction with plasma sputtering has been developed.
9. The ORIC radiation safety system was simplified, improved, and approved for intense light-ion acceleration with the internal ion source.
10. Operation of ORIC with an internal ion source was restored. A $K = 75 \text{ H}_2^+$ ions. Beam was circulated and individual turns were measured in the ORIC central region.
11. Calculations were completed, in collaboration with Michigan State University, for a new ORIC

central region configuration for intense light ion beam acceleration and extraction.

12. An optical and engineering design of the light-ion beam line (number 1 and 9) from ORIC to the RIB injector has been completed.
13. Specifications for the beam line 9 and first-stage mass-separator dipole magnets are nearly complete.
14. The tandem beam energy-analyzing system was studied for use as a mass separator. Adequate tandem voltage stability was demonstrated without beam, using the new terminal-potential stabilizer.
15. A concept was developed for a universal low-intensity RIB diagnostic based on a good/bad Faraday cup for integral current measurements and a channeltron measurement of secondary electrons for individual-ion measurements.
16. A detailed plan was developed for a beam-line 12 diagnostic to measure elemental beam intensities within an isobaric mass chain. The diagnostic is based on an insertable tape system and gamma ray detector.

1. "A Proposal for Physics with Exotic Beams at the Holifield Heavy Ion Research Facility," eds. J. D. Garrett and D. K. Olsen (ORNL, February 1991).

HIGH-VOLTAGE PLATFORM SYSTEM FOR RIB INJECTION

*R. C. Juras, G. D. Alton, M. R. Dinehart,
D. T. Dowling, D. L. Haynes, S. N. Lane,
C. T. LeCroy, M. J. Meigs, G. D. Mills,
S. W. Mosko, S. N. Murray, D. K. Olsen,
C. A. Reed,¹B. A. Tatum, and H. Wollnik²*

The RIB target-ion source will be mounted on a new injector which operates at potentials up to negative 300 kV with respect to ground potential. The purpose of the injector is to preaccelerate RIBs for isobaric mass separation and for efficient injection into the 25-MV tandem electrostatic accelerator. Because calculations have shown that radiation produced in some RIB targets would severely damage

solid-state electronics in the proximity of the RIB target-ion source, the injector will consist of a two-platform system. The RIB target-ion source and related beam line will be mounted on a source platform and a second instrumentation platform, biased at the same potential as the RIB target-ion source platform, will house electronics associated with the RIB injector. A shield wall will separate the platforms. The layout of the RIB high-voltage platform system is shown in Figs. 2.1 and 2.2.

The target-ion source will be operated at potentials up to ± 60 kV with respect to platform potential. Beams of protons or light ions from the ORIC will be transported from ground potential to the RIB target-ion source through a ground-to-platform-potential acceleration tube, followed by a platform-to-source-potential acceleration tube. Radioactive ion beams produced in the source by reactions between the ORIC beam and a thick target will be accelerated to platform potential and mass analyzed through a symmetric split-pole flat-field double-focusing magnet. This mass-analyzed beam will be charge exchanged, if necessary, and accelerated to ground potential through an acceleration tube, ready for separation of neighboring elements of the RIB isobar, and injection into the tandem accelerator.

Each injector platform will have areas for equipment at platform potential and equipment at source potential. Electrical signal and power cables will be transported through the grounded shield wall between platforms in two high-voltage conduits. One conduit will be biased at platform potential and the other will be biased at source potential. Two motor-generator sets, each capable of supplying up to 40 kVA of isolated power, will supply electrical power to the two areas.

The injector will be biased at acceleration potential by a 300-kV, 1-mA power supply. Stability of injector acceleration potential is an important injector design consideration since RIB beams must be separated from neighboring elements of the RIB isobar. The output voltage of the high-voltage power supply must have extremely low ripple and noise components, specified to be less than 0.004%. The injector will be designed to minimize causes of injector voltage fluctuations, such as corona currents and time-varying leakage currents.

A deionized water system between ground and platform potentials will be used to cool equipment on the injector platform. To minimize current loading of the high-voltage power supply, water lines to the platform will be coiled to decrease conductance to

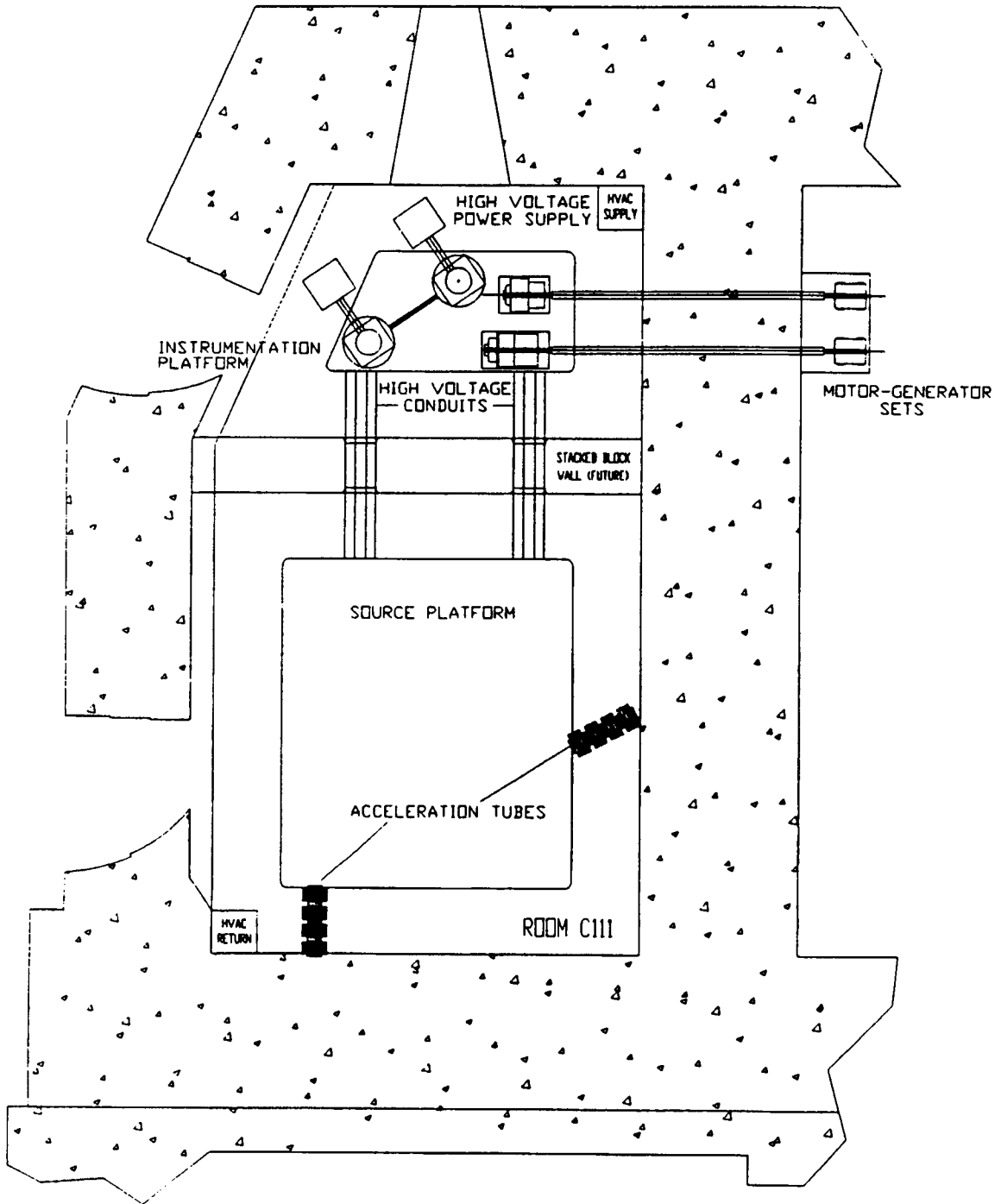


Fig. 2.1. High-voltage platform system conceptual layout floor plan.

ORNL-DWG 92-15712

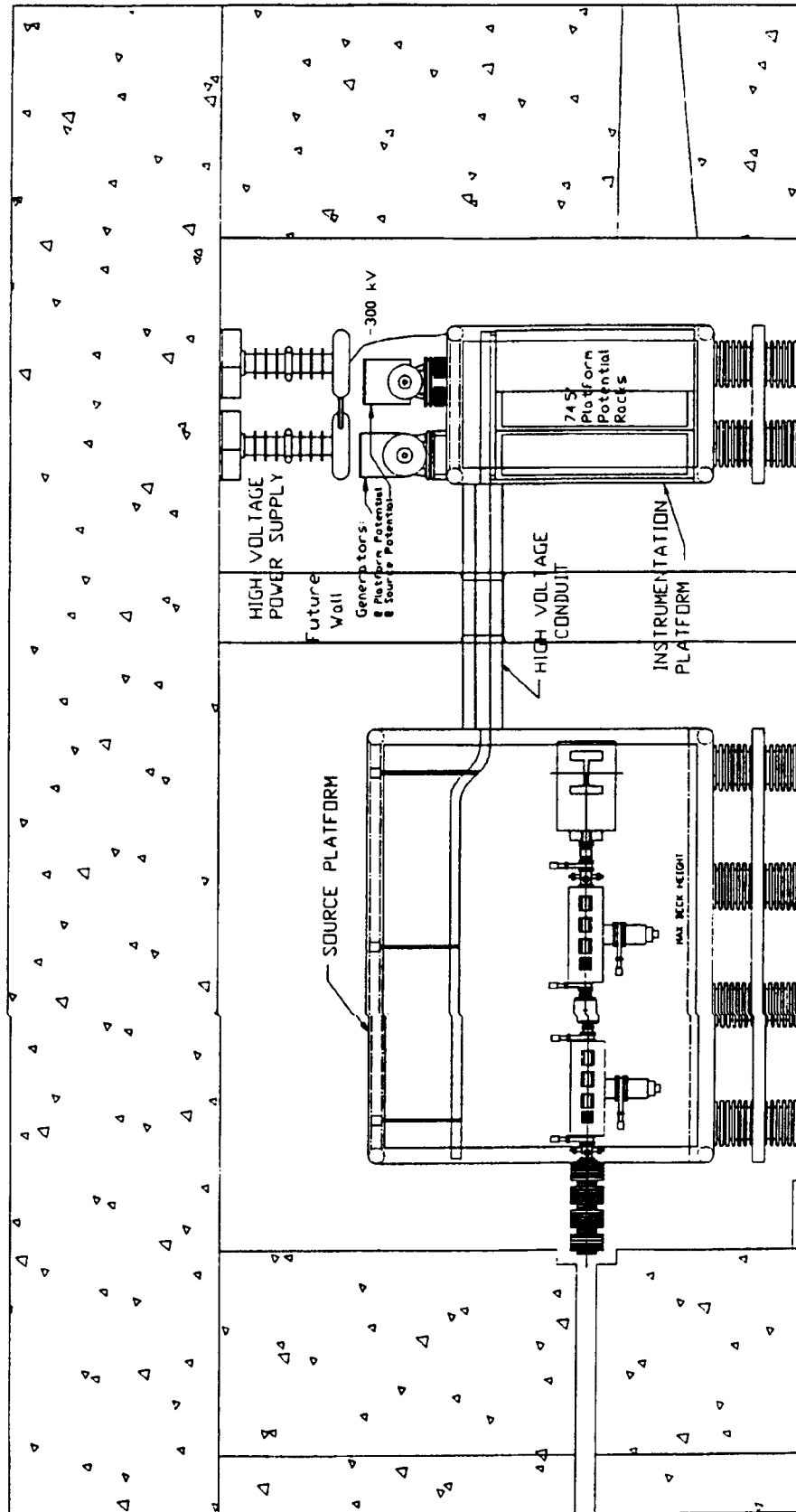


Fig. 2.2. High-voltage platform system conceptual layout elevation plan.

ground. Control of RIB injector components will be done by an extension of the existing CAMAC-based tandem-accelerator control system. CAMAC crates at platform potential and at platform-plus-source potential will communicate with ground-potential equipment through fiber-optic CAMAC serial highways. A detailed specification to procure the injector platforms, acceleration tubes, motor-generator sets, high-voltage conduits, and high-voltage power supply has been completed and procurement is in progress.

Preparations of room C111 for the high-voltage platforms include stripping all protrusions from the walls of the room and providing a smoothly contoured grounded surface on the walls, floor, and ceiling. Shielding blocks between the north and south portions of room C111 and shield blocks between room C111 and the cyclotron vault have been removed. A new shield wall in a more optimal location will be built between platforms before operation with full-power ORIC beams. Air conditioning of room C111 will be improved to control humidity.

1. UNISOR, Oak Ridge Associated Universities.
2. University of Giessen, Giessen, Germany.

TANDEM ACCELERATOR TRANSMISSION EFFICIENCY STUDIES

*C. M. Jones, M. R. Dinehart, R. C. Juras,
C. T. LeCroy, M. J. Meigs, and S. N. Murray*

An important design decision for the RIB facility concerns the maximum required operating potential for the high-voltage platform to be installed in room C111. One element in this decision was the beam energy required for injection into the tandem accelerator. Specifically, the RIB high-voltage platform must provide sufficient injection energy for efficient beam transmission through the tandem accelerator.

From a theoretical viewpoint, this question may be understood in terms of the dependence of the normalized phase-space acceptance of the tandem accelerator low-energy acceleration tube on injection energy. This question has been addressed by Larson and Jones¹ with the following result: For a system with the geometry of the HHIRF tandem accelerator, the low-energy acceleration tube normalized phase-space acceptance is remarkably insensitive to injection

energy if the injection system can provide a beam waist at the entrance of the low-energy acceleration tube which is approximately equal in diameter to the beam waist at the terminal stripper. In practice, this is not possible over a wide range of injection energies because only one lens was provided between the image waist of the mass analyzing magnet and the entrance of the low-energy acceleration tube.² This lens was positioned to provide good matching for beams of approximately 300 keV and cannot be easily moved because of its location with respect to the pressure vessel boundary.

The present injector platform of the tandem accelerator was specified as a 500 kV platform to provide appropriate velocities for beam bunching with light ion beams. In practice, it has been operated at 280 kV to provide 300 keV beams for tandem accelerator injection. The question to be addressed experimentally was the following: Given the existing geometry and location of ion-optic elements, what is the effect of injection energies less than 300 keV on beam transmission efficiency, i.e., how much can the injection energy be lowered before transmission efficiency is significantly affected? This question was answered by a series of measurements for beams which are typical of those expected with the RIB facility. For each beam, the overall optimized tandem-acceleration transmission efficiency, defined as accelerated beam intensity/injected beam intensity, was measured for injection energies of 100, 200, and 300 keV. The essential result of these measurements is that transmission efficiency was significantly affected at 100 keV, but not at 200 keV. A summary of the measured beams and the ratio of transmission efficiency at 200 keV to that at 300 keV is given in Table 2.1. As noted in the table, the average ratio of transmission efficiencies is $98 \pm 3.6\%$, indicating that the tandem injection energy can be lowered to 200 keV without a significant effect on tandem-accelerator transmission efficiency.

Another variable shown in Table 2.1 is "Injection-Line Electrostatic Steerers ON or OFF." This variable refers to the electrostatic steerers in the beam line that is used to transport beam from the injector to the tandem accelerator. This entry is in response to an observation that transmission efficiency appears to be improved by approximately 7% when these steerers are turned off, suggesting that these steerers introduce undesirable aberrations into the beam. This observation is consistent with the idea that these steerers operate in a mode in which the electrostatic potential at the median plane of each steerer element

Table 2.1. Summary of transmission efficiency measurements as a function of injection energy.

<u>Beam</u>	<u>Terminal Stripping Mode</u>	<u>Injection Line Electrostatic Steerers</u>	<u>Ratio of Transmission Efficiencies at 200 keV and 300 keV</u>
205 MeV $^{45}\text{Se}^{7+}$	Subequilibrium Gas	On	0.928
110 MeV $^{16}\text{O}^{5+}$	Subequilibrium Gas	On	0.976
110 MeV $^{16}\text{O}^{5+}$	Subequilibrium Gas	Off	0.983
140 MeV $^{58}\text{Ni}^{6+}$	Subequilibrium Gas	On	1.036
140 MeV $^{58}\text{Ni}^{6+}$	Subequilibrium Gas	Off	0.964
290 MeV $^{58}\text{Ni}^{13+}$	Foil	Off	0.958
300 MeV $^{107}\text{Ag}^{14+}$	Foil	Off	1.018
Average			0.980 ± 0.036

is elevated above ground potential; that is, the steerers act as weak, planar einzel lenses. As indicated in Table 2.1, most of the transmission measurements were performed with the steerers off.

OPTICAL DESIGN OF THE FIRST-STAGE MASS SEPARATOR

H. Wollnik,¹ G. D. Alton, C. M. Jones, and D. K. Olsen

The optical design of the radioactive-beam transport system on the high-voltage platform of the RIB injector has been completed. This includes the design of the first stage of a multi-stage high-dispersion system to separate the different elements in an isobaric mass chain. The second stage will be part of the negative-ion injection line from the RIB injector to the tandem accelerator. Figure 2.3 shows both a horizontal view and a stretched vertical view of the overall optical layout on the source high-voltage platform, including characteristic ion trajectories for

1. J. D. Larson and C. M. Jones, Nucl. Instr. and Meth. **140**, 489 (1977).

2. W. T. Milner, G. D. Alton, D. C. Hensley, C. M. Jones, R. F. King, J. D. Larson, C. D. Moak, and R. O. Sayer, IEEE Trans. Nucl. Sci. NS-22 (3), 1697 (1975).

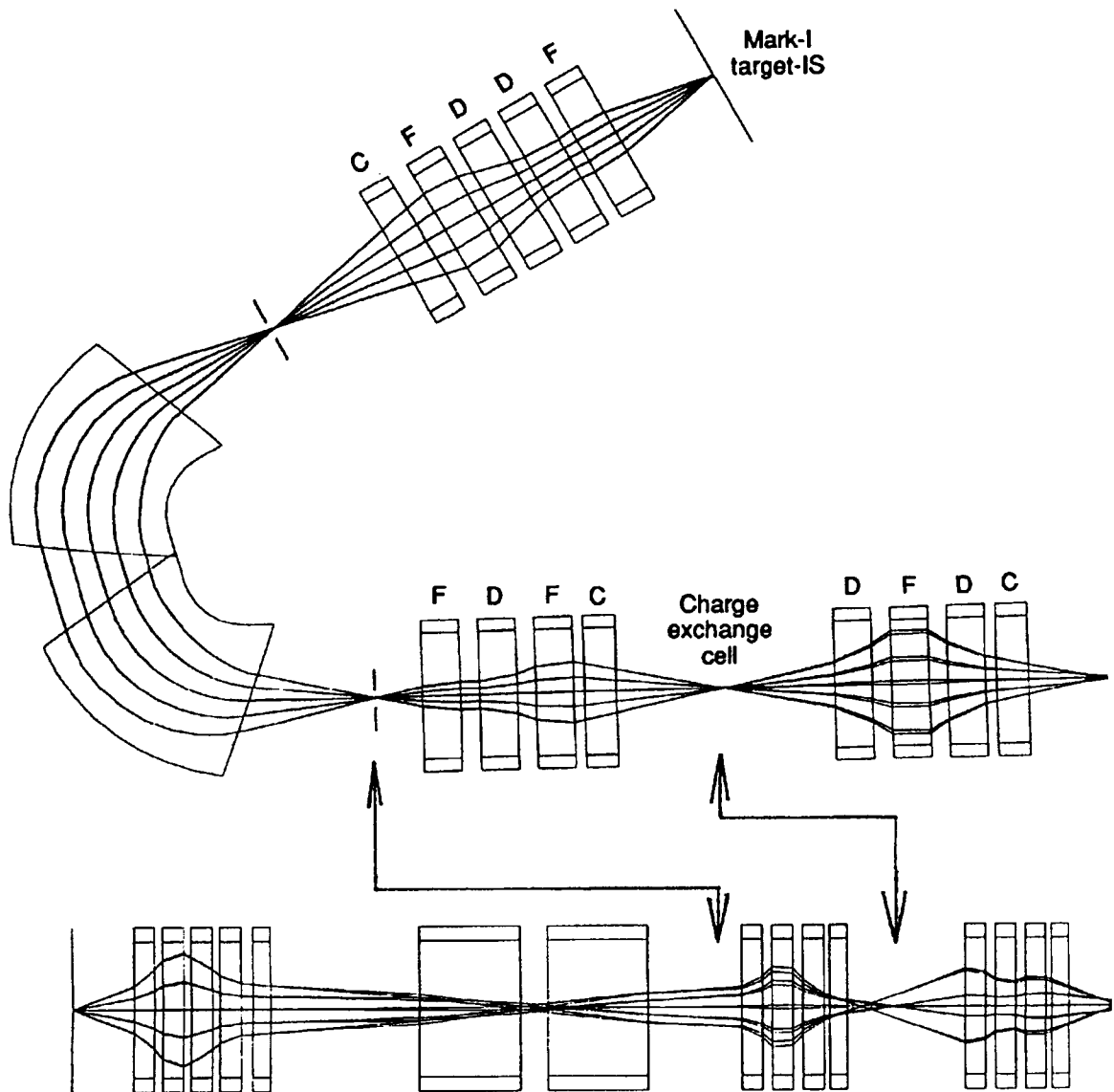


Fig. 2.3. Third-order GIOS calculation of Mark-I target-ion source RIB envelopes through the beam transport system on the RIB injector.

the Mark-I target-ion source. These trajectories were calculated to third order with the code GIOS.²

The design is space constrained. Four quadrupole singlets and a multipole correction element will focus a round beam with an emittance of 0.4π mm mrad ($x = y = \pm 0.2$ mm, $x' = y' = \pm 2$ mrad) from the Mark-I target-ion source into a horizontal waist with a beam width of about $x = \pm 0.2$ mm, and a beam height of about $y = \pm 8$ mm at the entrance slit of a symmetric

split-pole dipole magnet³ with a 50-mm air gap, 558.8-mm radius, and four edge angles of 20.3 degrees each. The object and image distances will be 517.6 mm. The four quadrupole singlets with apertures of ± 30 mm will allow a variable magnification of the ion source virtual image onto the entrance slit of the dipole magnet. In the horizontal plane at the center of dipole, the beam will be parallel as shown in Fig. 2.3, having a width of about ± 30 mm, whereas

in the vertical plane, a waist will be formed of about ± 5 mm. This arrangement greatly reduces space-charge effects in the vicinity of the entrance slit and at the same time reduces the geometric aberrations in horizontal plane from angular divergences in the vertical plane. Fig. 2.4 shows contour plots as well as intensity distributions projected into the vertical and horizontal directions on the focal plane of the split dipole assuming ions of masses ^{230}U and ^{231}U and perfect alignment of all optical elements. The two beams are calculated to have a FWHM of about ± 0.1 mm and a height of about ± 8.0 mm and are separated by about 30 mm, giving a mass resolution in the order of $1/2000$. Slits at this position should collimate an isobaric mass chain with very low background. The mass-separated ions will then be accelerated to 300 KV and provide the object for the second-stage mass separator. For this purpose, the beam spot at the exit slit will be refocused to a roughly round beam by a

quadrupole triplet and steered to the center of a charge-exchange canal of 120 mm length and 8 mm diameter. A second quadrupole triplet and steerers will then focus the negative-ion beam out of the charge-exchange canal onto the entrance of the 300-KeV acceleration tube leading the ions to ground potential.

1. University of Giessen, Giessen, Germany.
2. H. Wollnik et al., Nucl. Instr. and Meth. A258 408 (1987).
3. H. Wollnik et al., Rad. Nucl. Beams, eds. W. Myers et al., World Scientific, Singapore, 603 (1989).

ORNL-DWG 92-15714

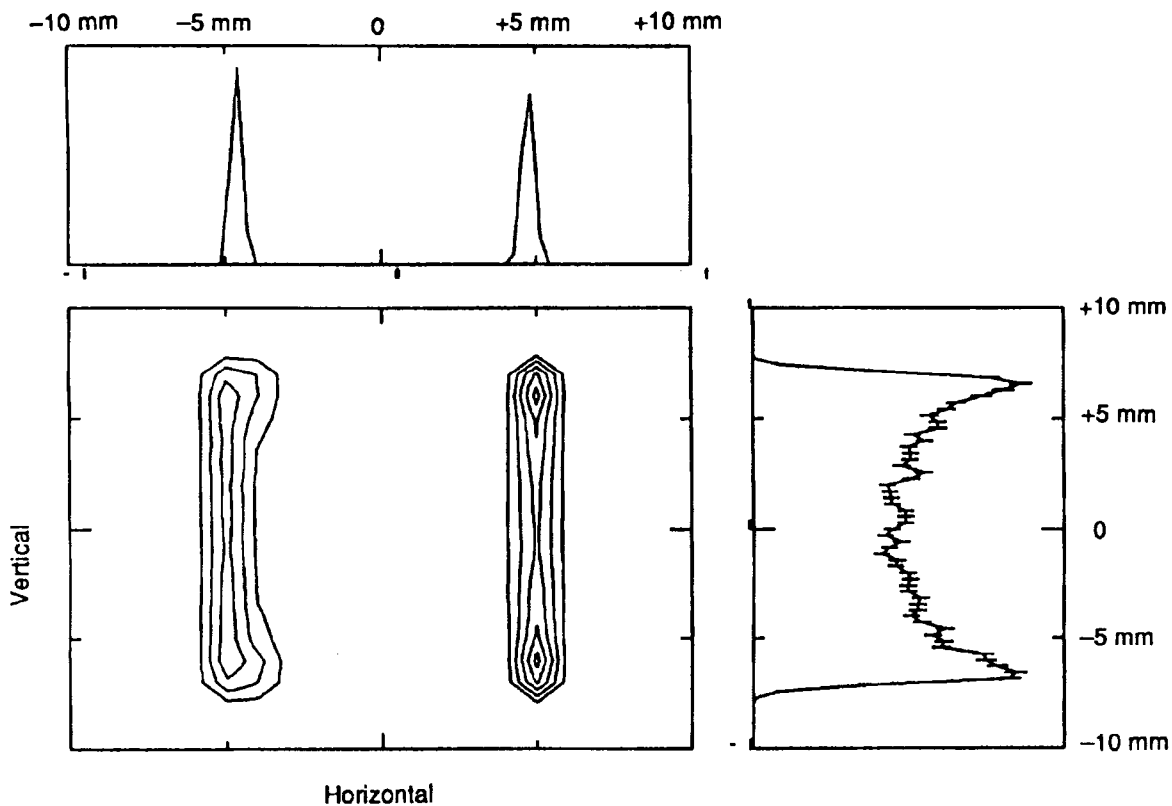


Fig. 2.4. Third-order GIOS calculation of the RIB spot for ^{230}U and ^{231}U beams on the focal plane of the first-stage mass separator.

RIB INJECTOR BEAM LINE I-2

*D. T. Dowling, G. D. Alton, D. L. Haynes,
C. M. Jones, R. C. Juras, M. J. Meigs, G. D. Mills,
S. W. Mosko, D. K. Olsen, B. A. Tatum,
and H. Wollnik¹*

Substantial progress has been made in the mechanical design of the RIB beam line on the source HV platform. This beam line includes the first-stage mass separator and has been labeled I-2. The conceptual design of this beam line has been completed and is shown in Fig. 2.5. The major components are the RIB target-ion source, the symmetric split-pole mass-analyzing magnet, the charge-exchange cell, the electrostatic focusing elements, and the beam diagnostic elements. The target-ion source and the mass-analyzing magnet are discussed elsewhere in this report.

All steering and focusing elements of beam line I-2 will be housed in large vacuum chambers at three

locations. This approach reduces the overall length requirements of the beam line while also providing more convenient servicing of components in the case of radioactive contamination. The design of the three chambers will be identical with the exception of the electrostatic element-mounting flange. The chambers will be interchangeable and the replacement of any of the three could be accomplished with a single spare chamber. The three chambers will use "quick" vacuum connections and electrical connections so that chamber removal may be accomplished in the shortest possible time.

The RIB target-ion source will be followed by one of these optics chambers. This chamber will house four electrostatic quadrupole singlets, an electrostatic multi-pole steerer/corrector, and a turbomolecular pumping station. The second and third optics chambers are positioned on either side of the charge-exchange cell. These two chambers will each house three electrostatic quadrupole singlets, an

ORNL-DWG 92-15715

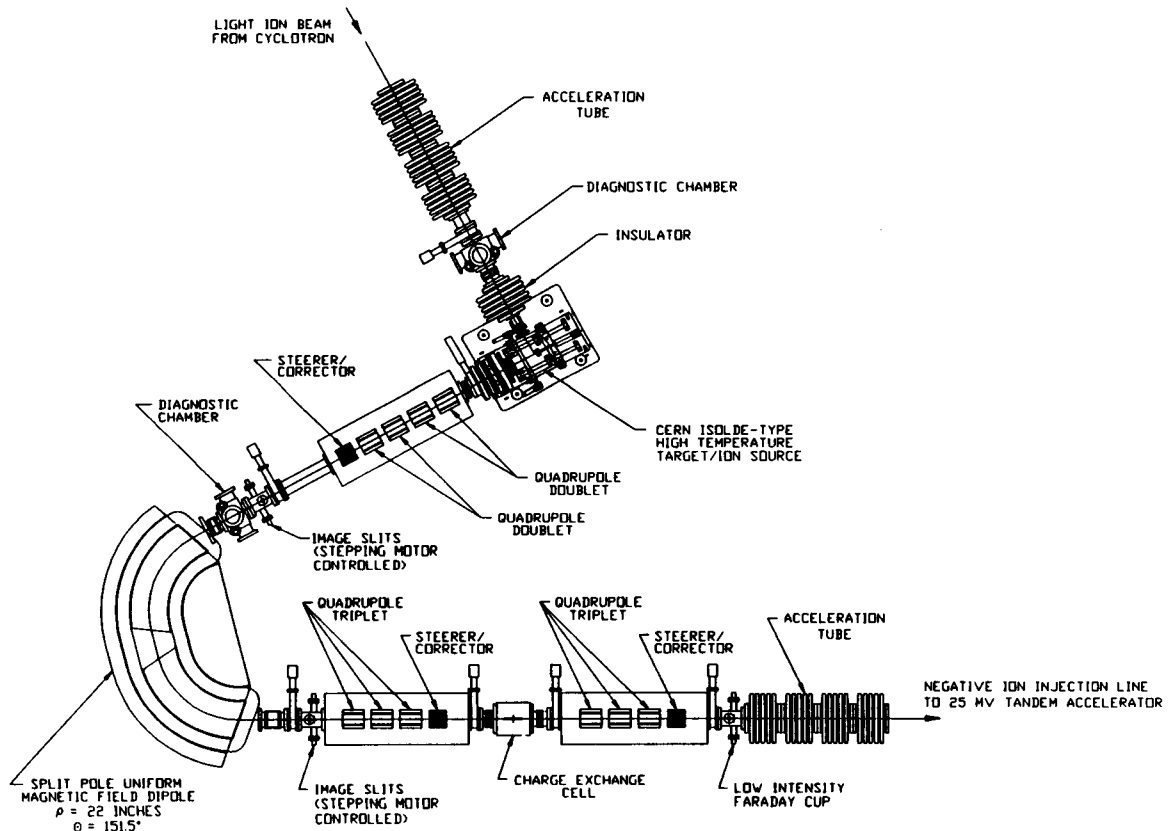


Fig. 2.5. Schematic drawing of the target-ion source and isotope-separation system for the Oak Ridge Radioactive Ion Beam Facility

electrostatic multi-pole steerer/corrector, a turbomolecular pumping station, and beam diagnostics. The charge-exchange canal may be one of the higher maintenance components, and is being designed to use quick connections.

The remaining components are the beam-diagnostic elements, some of which are not shown in Fig. 2.5 because the designs are still being finalized. Associated with the mass-analyzing magnet are object and image slit systems which may be rotatable and will be remotely operable. Immediately following each of the slit systems will be beam diagnostics which are presently undefined. In addition, the charge-exchange cell will have beam diagnostics at both its entrance and exit. The final diagnostics station will be a low-intensity Faraday-cup assembly positioned just before the entrance of the last acceleration tube.

1. University of Giessen, Giessen, Germany.

MASS-ANALYZER MAGNET FIELD CALCULATIONS

B. A. Tatum, D. K. Olsen, and H. Wollnik¹

Two-dimensional magnetic field calculations were performed to optimize the RIB first-stage split-pole mass analyzing dipole. These three primary aspects of the magnet design were studied: cross-section field homogeneity, fringe-field effects at the magnet ends, and fringe-field effects in the center of the magnet between the two sets of pole tips.

To achieve the desired mass-separation capabilities, a field homogeneity of at least 1 part in 3000 is required within a good field region of 4 cm centered on the central trajectory. This field quality is only attainable by careful shaping of the pole tips and design and placement of pole-tip shims. Furthermore, the yoke must be designed to prevent saturation because the maximum magnet excitation will exceed one Tesla in the gap. Thus, magnet field calculations were performed to optimize the pole-tip cross-section and yoke design. Figure 2.6 shows the optimized magnet cross-section geometry and field profile at maximum excitation. The field homogeneity is better than 1 part in 6000. The pole width is 23 cm and the shims are 20.0 mm x 0.9 mm.

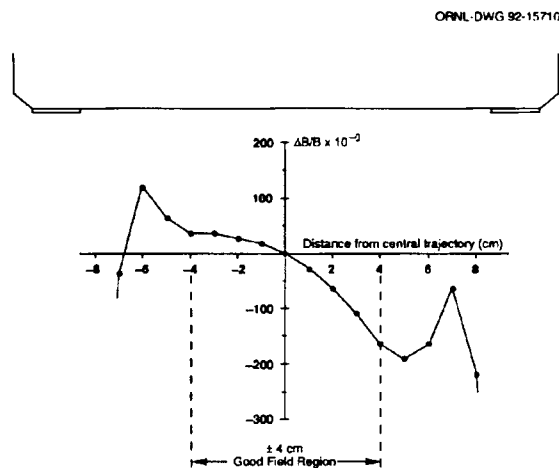


Fig. 2.6. Pole geometry and 2D calculated magnetic field profile of the first-stage, split-pole, mass-analyzing magnet.

An understanding of fringe fields is necessary because they affect the effective path length of the magnet. Fringe fields vary at different excitation levels and thus alter the ability to focus the beam through the analyzing magnet onto the image slits. Thus, magnetic field end calculations were performed to optimize field clamps and shape the pole tip ends to minimize saturation fringing effects. Figure 2.7 shows a plot of the optimized magnet-end geometry and corresponding field at maximum excitation. The 2-cm-wide field clamp located 9.5 cm from the pole-tip end minimizes the tail on the magnetic field. The pole ends are shaped to approximate a radius of 0.8 times the half-gap. This minimizes saturation and contains the effective field boundary to be 20.8 mm from the magnet edge. Quantification of the end effects permits trimming of the magnet poles to achieve the desired effective path length.

Fringe fields are also present at the center of the magnet between the poles and there is no space for field clamps to control these fields. Because of the proximity of the poles to one another, the fringe fields vary from the inner to the outer radius of the poles. This was simulated by varying the distance between the pole edge and the symmetry line at the center of the split-pole magnet. The results are shown in Fig. 2.8 which shows a 2-cm variation in the effective field boundary at maximum excitation, assuming that the pole end is shaped the same as in the previous end-field calculation. Thus the pole tips must be trimmed

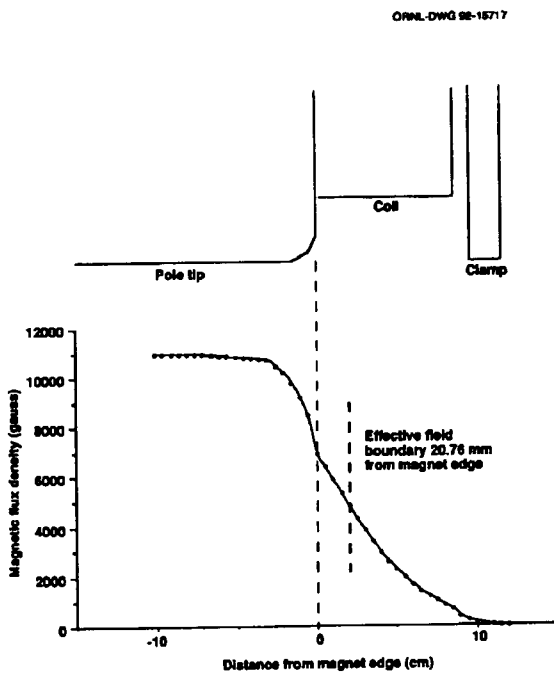


Fig. 2.7. End geometry and 2D calculated magnetic field fall off at the outside ends of the first-stage, split-pole, mass-analyzing magnet. The gap is 5 cm and the effective field boundary is 20.8 mm from the magnet edge.

in the center of the magnet and the edge angles adjusted to attain the desired effective path length.

1. University of Giessen, Giessen, Germany.

CROSS SECTIONS FOR PRODUCTION OF RADIOACTIVE ION BEAMS (RIB)

*R. L. Robinson, L. Rayburn,¹ C. Baktash,
J. B. Ball, C. M. Jones, I. Y. Lee,² F. K. McGowan,
D. K. Olsen*

One of several considerations in the selection of RIBs is the cross section for its production using light ions from the ORIC cyclotron. Unfortunately, a library search revealed that there are few relevant measured cross sections. Thus, we have explored the possibility of using two programs, PACE³ and HETC,⁴ to calculate the cross sections. PACE is a Monte Carlo, statistical-model evaporation code that determines the relative population of residual products following particle evaporation from a compound nucleus. HETC is a Monte Carlo, high-energy nucleon-meson transport code; it has the disadvantage that it is only applicable for protons, but has the merit of including spallation as well as fusion in the determination of cross sections.

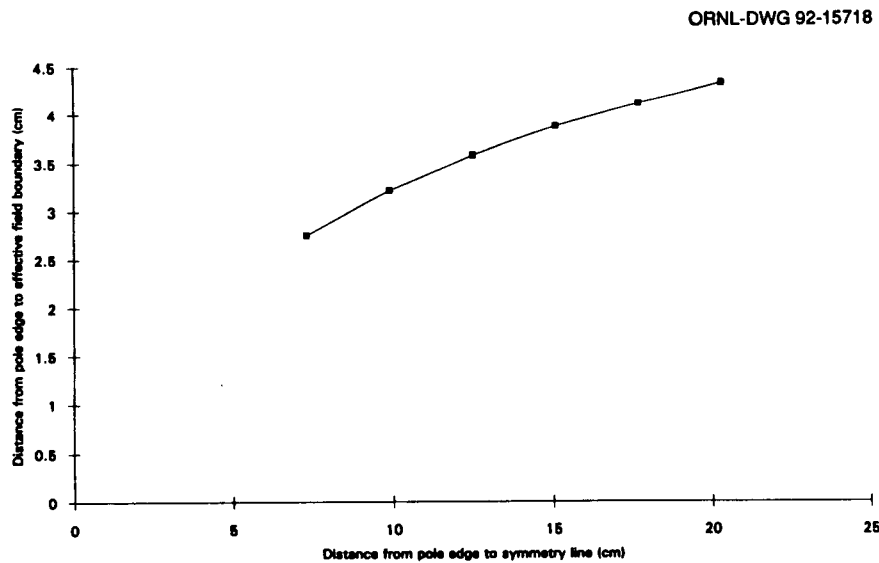


Fig. 2.8. Effective field boundary location from the pole edge as a function of the location of the symmetry line from the pole edge in the center of the first-stage, split-pole, mass-analyzing magnet.

Table 2.2. Number of cases with ratio R falling within the listed ranges, where R is the ratio of the peak of the experimental cross section divided by the peak of the calculated cross using the two codes PACE and HETC. The cases are for different channels resulting from the projectile-target combinations noted.

Projectile/ target	$R = \sigma_{\text{exp}}/\sigma_{\text{cal}}$				Total Cases
	$0.67 \leq R \leq 1.5$	$0.5 \leq R \leq 2.0$	$0.4 \leq R \leq 2.5$	$0.33 \leq R \leq 3.0$	
p/ ^{63,65} Cu	PACE	8	9	11	11
	HETC	6	8	10	10
p/ ⁴³ Sc	PACE	2	2	3	3
	HETC	2	2	2	2
p/ ²⁷ Al	PACE	0	1	2	2
	HETC	2	2	2	2
^{3,4} He/ ^{63,65} Cu, ⁶⁴ Zn	PACE	2	6	9	11
	HETC	2	6	9	11
^{3,4} He/ ²⁷ Al	PACE	1	2	3	4
	HETC	1	2	3	4

To obtain a measure of the reliability of the two codes, their predictions for the peak of the cross section for different exits channels were compared to experimental results from the projectile-target combinations listed in Table 2.2. Some guidelines indicated by the limited comparison in this table are:

1. For protons on nuclides around mass 60, predictions of peak cross sections by either HETC or PACE are within a factor of 1.5 of the measured values over one-half of the time and the majority are within a factor of 2.
2. The predictions for PACE for ^{3,4}He projectiles on targets of about mass 60 are not as good as for protons; half of the cases have predictions within a factor of two of the measured values and the majority are within a factor of 2.5.
3. Based on only two cases, HETC did better than PACE for the p+²⁷Al reaction.

Predictions by PACE of peak cross sections and energies at which the peaks occur are given in Table 2.3 for a variety of interesting RIBs with A=37-73. Although ⁶⁴Ge is an especially desirable beam, the cross section of 0.5 mb is probably too small to yield

Table 2.3. Predictions by the PACE code for peak cross sections and projectile energies at which the peaks occur.

Reactions	σ_{peak} (mb)	E_{peak} (MeV)
⁴⁰ Ca(p, α) ³⁷ K	50	21
⁵⁸ Ni(p,n) ⁵⁸ Cu	80	16
⁶⁴ Zn(p,2n) ⁶³ Ga	35	30
⁶⁴ Zn(p,n) ⁶⁴ Ga	200	14
⁶⁴ Zn(³ He,3n) ⁶⁴ Ge	0.5	50
⁷⁰ Ge(p,3n) ⁶⁸ As	25	40
⁷⁰ Ge(p,2n) ⁶⁹ As	180	29
⁷⁰ Ge(p,n) ⁷⁰ As	500	15
⁷⁰ Ge(³ He,3n) ⁷⁰ Se	12	38
⁷⁰ Ge(³ He,2n) ⁷¹ Se	160	23
⁷² Ge(p,3n) ⁷⁰ As	400	40
⁷⁴ Se(p,3n) ⁷² Br	25	46
⁷⁴ Se(p,2n) ⁷³ Br	180	30

a reasonable beam intensity for nuclear structure studies.

1. Oak Ridge Associated Universities.
2. Lawrence Berkeley Laboratory.
3. Some details on the approach of PACE calculations are found in reference: A. Gavron, Phys. Rev. **C21**, 230 (1980).
4. ORNL Report, CCC-178C (1991).

RESIDUAL RADIOACTIVITY FOLLOWING A BOMBARDMENT WITH PROTONS

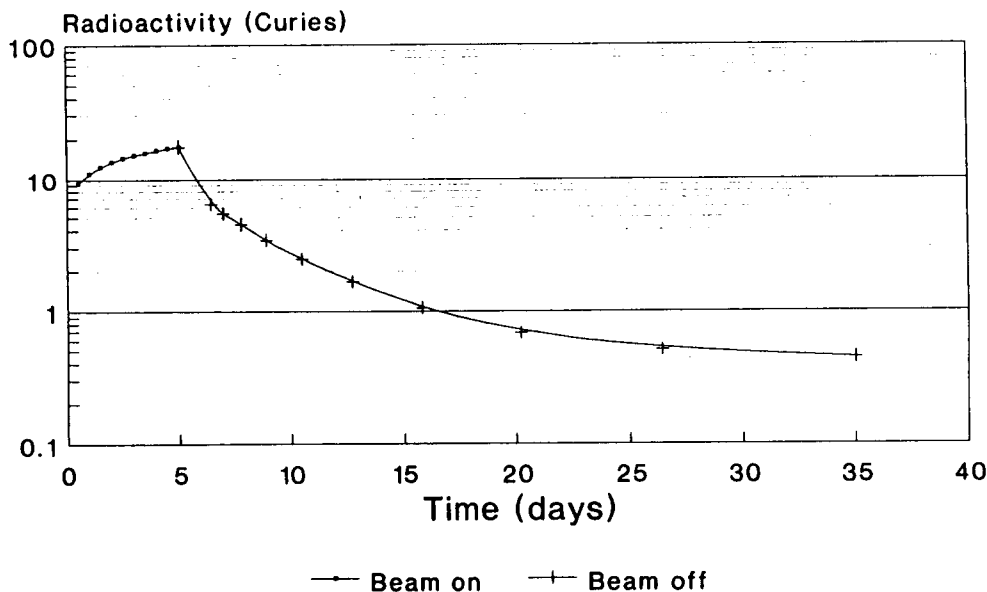
L. Rayburn and R. L. Robinson

To obtain a sense of the residual radioactivity following bombardment of a thick target with a proton beam to produce a RIB, we have made use of a special feature of the HETC code. This code, which calculates cross sections for all residual channels resulting from the interaction of energetic protons with target nuclides, has the additional capability of calculating the gamma rays emitted from these residual products as a function of time. As part of this process, the code includes extensive tables that give

half-lives and gamma rays emitted by radioactive isotopes.

The calculation for the residual radioactivity using HETC has been done for a likely scenario in which there is a hypothetical five day bombardment to produce a ^{68}As radioactive beam. Assumed conditions are: a 43-MeV beam of protons with current of 47 μA (beam power of 2 kW), and a 800 mg/cm^2 target of $\text{Zr}_5^{70}\text{Ge}_3$ (an energy loss in the target of 7 MeV). Figure 2.9 shows the results of the calculations assuming all of the radioactivity remains in the target area. The peak level of activity of 18 curies gives rise to a radiation level of about 14 rem/hr at 1 meter from the target. After one week of cooling, the level of activity is reduced about an order of magnitude.

Present plans are to place a 1-mil-thick Re window before and after the target. Activation of the windows would increase the level of activity by another 5 curies at the end of the bombardment described in the preceding paragraph; this gives a radiation level of 3 rem/hr at 1 meter. If the beam stop were ^{12}C , the only product with a sufficiently long half life to be a problem would be ^7Be ($T_{1/2} = 53$ days). It would contribute approximately 0.5 curies at the end of the bombardment with a corresponding radiation level of about 150 mrem/hr at one meter.



Calculate with HETC

Fig. 2.9. Level of activity at the target/ion source from activation of the $\text{Zr}_5^{70}\text{Ge}_3$ target material if all reaction products remain in the target area. The activity is plotted for 5 days of bombardment with a 47- μA beam of 43-MeV protons. The target thickness is 800 mg/cm^2 .

PROGRESS WITH THE MARK-I TARGET/ ION SOURCE

*G. D. Alton, D. L. Haynes, G. D. Mills,
and D. K. Olsen*

Steady progress has been made toward the completion of engineering drawings for the high-temperature ISOLDE-type ion source assembly¹ that will be used for initial RIB generation. As reported previously,² the high-temperature version of the CERN ISOLDE source was selected as the first source because of its low emittance ($\sim 2\pi$ mm.mrad (MeV)^{1/2}), relatively high ionization efficiency, and capability for producing a broad range of radioactive species. Of equal importance, the source assembly has been engineered for remote installation, removal, and servicing as required for safe handling of highly radioactive target material, source components, and ancillary equipment. The source assembly also permits easy modification to lower temperature versions and conversion from electron-impact ionization to either thermal, positive, or negative surface ionization. The choice of this particular source was also made based on its successful employment for RIB generation for many years at the CERN-ISOLDE facility.³ In designing this source, particular emphasis was placed on the materials of construction, the thermal transport properties of the source, the size and geometry of the target, the number of species that the source can be used to process, and the ionization efficiency. Equal attention was given to design features which facilitate assembly and disassembly of contaminated components.

The assembly incorporates many of the engineering features used in the CERN ISOLDE design and has been engineered to enable remote installation and removal in high-radiation fields and the transport of contaminated source assemblies to and from servicing and storage areas. For installation, the assembly will be lowered by a remotely controlled overhead hoist mechanism onto locator pins on a linear motion carriage. The carriage will be pushed forward and clamped against the vacuum interface flange by a remotely controlled pneumatic actuator mechanism. The source assembly will plug into the interface flange, during which all electrical, gas feed, coolant, vacuum, and temperature monitoring connections will be mated together. Then the vacuum seal between the source chamber and ORIC beam line will also be made by remote actuation of a similar pneumatic clamping device. The vacuum chambers

can then be remotely pumped down or vented. To remove the source assembly, the procedure will be reversed. For servicing and storage, the source will simply be lifted from the linear-motion carriage by means of an electrically driven hoist and transported along an overhead track to a separated cask.

Following pump down, the source will be out-gassed by incrementally adding power to both the target reservoir and to the cathode until the source achieves a steady-state vacuum level at the anticipated operating temperature. The high-temperature components of the source are shown schematically in Figs. 2.10 and 2.11. A collimated ORIC ion beam will pass through a thin Re window and produce RIBs with refractory target material. The Ta target reservoir, vapor transport tubing, and internal surfaces of the source will be lined with Ir or Re metal. The target thickness will be chosen to maximize RIB production and minimize residual-radiation production. Most of the beam will exit the target through a second Re window and stop in a cooled C beam stop. This technique will also reduce the power deposited in the target and simplify temperature control problems.

The target material reservoir will be positioned within the inner diameter of a series-connected, resistively heated, three-cylinder coaxial Ta tube which can be heated to temperatures exceeding 2100°C. The power required to heat the assembly to 2100°C is estimated to be 5.5 kW (11 V at 500 A). Temperature control will be maintained within $\pm 2^\circ\text{C}$ by use of current-feedback circuitry driven by a two-color pyrometer. The electron-emitter cathode is also made of Ta and will be resistively heated to thermionic emission temperatures. The resulting electron beam, typically ≥ 250 mA, will be accelerated by a potential difference of 300 V through the perforated anode plate into the cylindrical cavity of the anode structure and will ionize the radioactive gas. The electron beam will be collimated by adjusting the coaxially directed, solenoidal magnetic fields to optimize the RIB ionization efficiency. The cathode power required to achieve thermionic-emission temperature will be about 2 kW (400 A at 5 V).

Engineering drawings for all of the target/ion source high-temperature components have been completed and components are being purchased. The high-temperature components for two of the four assemblies will be coated with Ir or Re to test the use of a chemically-inert material to reduce surface-adsorption delays. The remaining components of the source assembly are nearing completion. The total

ORNL-DWG 92-15719

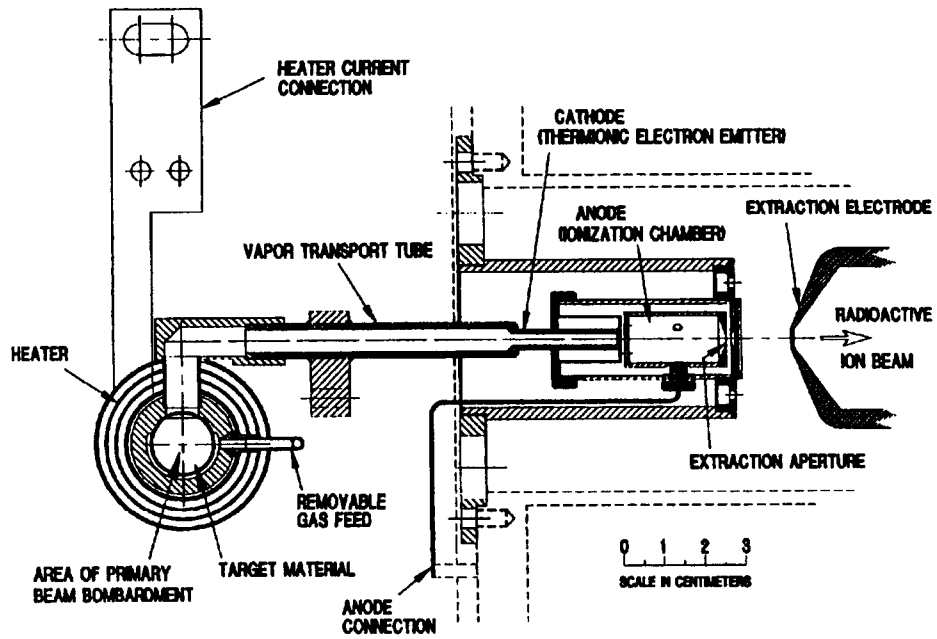


Fig. 2.10. Side view of the Mark-I high-temperature target-ion source.

ORNL-DWG 92-15720

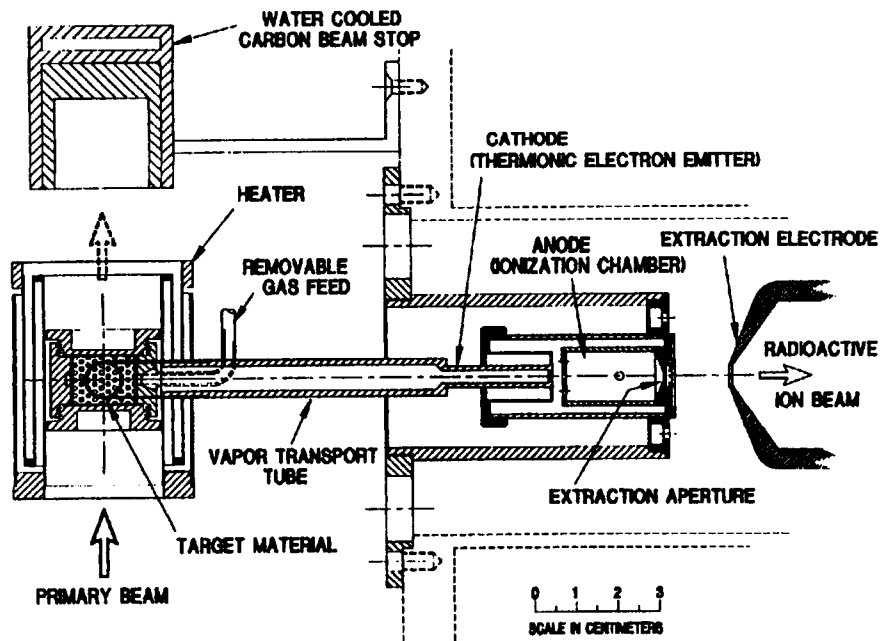


Fig. 2.11. Top view of the Mark-I high-temperature target-ion source.

power required to heat the target material and cathode and to ionize the vaporous material transported from the target to the ionization chamber will be of the order of 5.5 kW. Table 2.4 provides a list of the power

Table 2.4. Power supplies for the Mark-I target-ion source.

Power Supply	Rating
Acceleration	60 kV at 2 mA
Extraction	30 kV at 2 mA
Anode	400 V at 1.5 A
Cathode	6 V at 500 A
Target	15 V at 1000 A
Magnet Coils	20 V at 50 A (3 each)

supplies required to operate the source. All power supplies have been selected and will be procured during the present fiscal year.

1. S. Sundell, to be published in NIM.
2. G. D. Alton, D. L. Haynes, G. D. Mills, and D. K. Olsen, *Physics Division Progress Report, ORNL-6689*, March 1992, p. 209.
3. H. L. Ravn and B. W. Allardyce, *Treatise on Heavy Ion Science*, ed. D. A. Bromley, Vol. VIII, *Nuclei Far From Stability (Plenum Press, New York, 1989)*, p. 363.

TIME-RELEASE PROPERTIES OF ION-IMPLANTED SPECIES: DIFFUSION MODELING

G. D. Alton, H. K. Carter,¹ I. Y. Lee,² C. M. Jones, J. Kormicki,³ and D. K. Olsen

Experiments continued to measure the time-release characteristics of stable ion beams implanted in candidate refractory target materials for forming RIBs. This information is needed to select the most appropriate target materials for generating initial RIBs. The experiments are performed with the UNISOR facility using the HHIRF tandem accelerator to implant species of interest into selected target materials maintained at elevated temperatures within the UNISOR FEBIAD-type ion source.⁴ These ex-

periments have provided thermal time-release data and realistic estimates of release efficiencies for beams such as ³⁵Cl from Zr₅Si₃ and ⁷⁵As, ⁷⁹Br, and ⁷⁸Se from Zr₅Ge₃.⁵ The principal processes whereby radioactive atoms are lost between initial formation and use are associated with diffusion, surface adsorption, and ion source inefficiencies.

Measurements were made of the FEBIAD ion source target temperature as a function of source operating parameters and target beam power. These experiments were conducted in an effort to establish typical target temperatures during ion implantation-release experiments. The high temperature is responsible for diffusion of implanted species from the target materials. This information was incorporated into a diffusion model which was developed to understand the diffusion process and radioactivity decay losses for short-lived species.

The time and temperature-dependent release of radioactive atoms embedded in a chemically dissimilar target material implies the presence of a binary diffusion mechanism. Whenever there is a concentration gradient of impurity atoms or vacancies in a solid material, the atoms or vacancies will move through the solid until equilibrium is reached. The net flux of the particular species J is related to the gradient of the concentration n by the phenomenological relation of Fick.⁷ A modified form of Fick's first law, which accounts for radioactive decay losses, can be written as

$$J = -D\nabla n - n\lambda t, \quad (1)$$

where D is the diffusion coefficient, $\lambda = 1/\tau_{1/2}$ where $\tau_{1/2}$ is the RIB half life, and n is time dependent. The time-dependent form of Eq. 1, referred to as Fick's second law, can be expressed as

$$\frac{\partial n}{\partial t} = D\nabla^2 n - n\lambda t. \quad (2)$$

The diffusion process is not only driven by the concentration gradient, but also by the activation energy or barrier height H_A required to move the atoms from site to site through the solid. The diffusion coefficient is usually found to vary with temperature according to

$$D = D_0 \exp(-H_A/kT). \quad (3)$$

The activation energy H_A must be supplied to the atom through lattice vibrations to enable the particle

to move from site to site through interstitial or vacancy diffusion processes. The diffusion constant D_0 is related to the vibrational frequency and lattice parameters of the solid crystal. Higher temperatures result in faster release times for atoms distributed within the solid. This necessitates the use of refractory target materials in order to avoid high pressures in the ion source which adversely affects the ionization efficiency.⁷ In principle, Eq. 2 can be solved for the particular target geometry and simulation studies of the diffusion release of Cl ions implanted in Zr_5Si_3 and As, Br, and Se in Zr_5Ge_3 were made for the UNISOR geometry.

Figure 2.12 illustrates the expected time-dependence of the fractional release of ion-implanted stable and radioactive atoms from the surface of a solid. The curves are a numerical solution to the one-dimensional form of Eq. 2. The atoms are assumed to be implanted to an average depth of $18 \mu\text{m}$ in a depth profile predicted by TRIM simulations.⁸ The diffusion constant D was adjusted so that the calculated release profiles approximate those observed experimentally. In principle, these calculations can be used to provide diffusion coefficients appropriate for the particular target-RIB combination. The radioactive atoms are assumed to have half lives of 60 s and 30 s. The beam-on side of the curves reflects a balance

between ion implantation growth and diffusion release at the sample surface. The beam-off side of the curves reflects release of the implanted atoms at the surface through diffusion. The dashed curves are targets which are assumed to be heated solely by power from the UNISOR FEBIAD ion source cathode, anode, and electron beam with negligible beam on target. In the FEBIAD source, the target temperature is governed by adsorption of radiation from the cathode electron bombardment and beam heating effects. Target temperatures were measured as a function of source operating parameters by using a two-color optical pyrometer and found to be about 1645°C for normal positioning of the target relative to the source anode. Similar measurements were made as a function of beam power on target. Sample temperatures were found to increase linearly with beam power. The measured relationship between rise in sample temperature ΔT and beam power is shown in Fig. 2.13. Diffusion release is calculated to be marginally affected by beam heating as indicated by the full lines on Fig. 2.12.

Further modeling studies and measurements will be completed during FY 1993. These studies will attempt to determine diffusion coefficients of refractory target materials by comparing experiment and theory and thereby estimating the characteristic re-

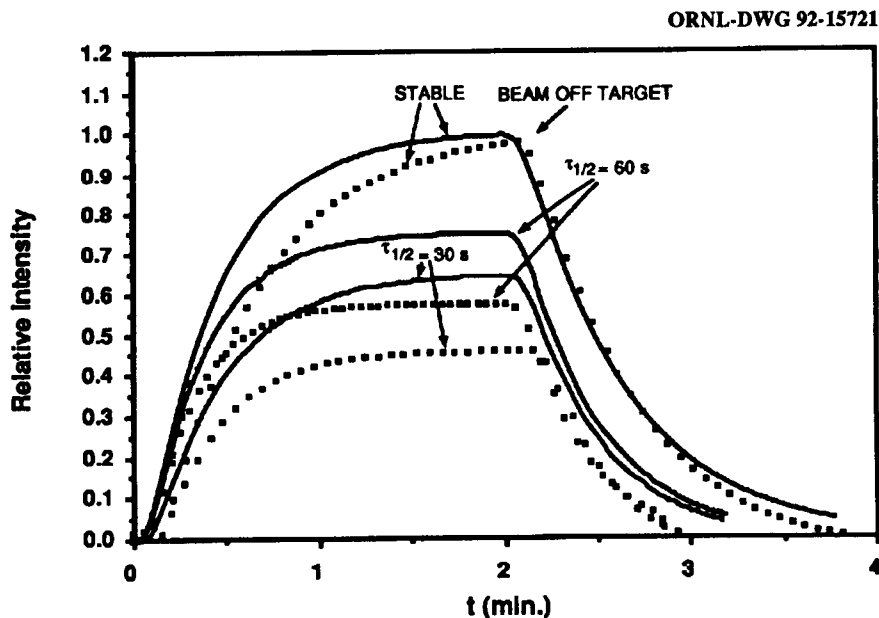


Fig. 2.12. Theoretical time-dependent release profiles of stable and radioactive As atoms implanted into Zr_5Ge_3 with and without beam heating effects. The solid curves are for beam power = 20 W and target temperature = 1745°C , whereas the dashed curves are for beam power = 0 and target temperature = 1645°C .

ORNL-DWG 92-15722

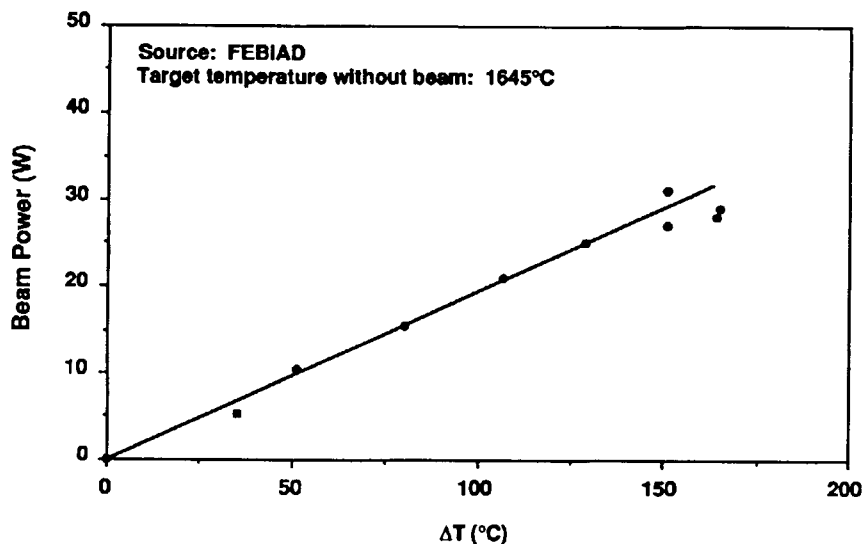


Fig. 2.13. Experimentally measured change in UNISOR target temperature as a function of ion tandem accelerator beam power.

lease time as a function of ion-implantation depth, as well as decay losses of short-lived nuclei. Adsorption processes can also be readily incorporated into the model.

ORIC DEVELOPMENT

*S. W. Mosko, M. R. Dinehart, D. T. Dowling,
S. N. Lane, C. T. LeCroy, S. N. Murray,
D. K. Olsen, and B. A. Tatum*

ORIC. The ORIC is undergoing reconfiguration for acceleration of intense light-ion beams with the internal ion source. This beam will produce radioactive atoms in the target-ion source. In order to reduce ORIC activation, graphite beam interceptors were added to the rf system to limit the axial beam aperture and to protect the interior of the accelerating system from spurious beams. In addition, a graphite septum was installed on the deflector and a combination of graphite and tantalum shields were added to the magnetic channels in the beam-extraction system.

A new, moveable radial-beam aperture was installed in the central region of the cyclotron in order to reduce phase acceptance for ions from the internal source. This "phase clipper" was installed on the front of the dee in a track that is opposite the one used for the puller electrode. Previously, the puller was driven by a split-phase motor with hard-wired controls. Since split-phase motors cannot instantly reverse direction of rotation, fine adjustment was difficult. New drives were installed for both the clipper

1. UNISOR, Oak Ridge Associated Universities.
2. Lawrence Berkeley Laboratory.
3. Oak Ridge Associated Universities and Vanderbilt University (permanent address, Institute of Nuclear Physics, Cracow, Poland).
4. R. Kirchner, *Nucl. Instr. and Meth.* **B26**, 204 (1987).
5. G. D. Alton, H. K. Carter, I. Y. Lee, C. M. Jones, J. Kormicki, and D. K. Olsen, *Nucl. Instr. and Meth.* **B66**, 492 (1992).
6. See, for example, *Diffusion in the Condensed State*, J. S. Kirkaldy and D. J. Young (The Institute of Metals, London, 1987) Ch. 1.
7. P. Decroock, M. Huyse, P. Van Duppen, M. Loiselet, G. Ryckewaert, *Proc. 10th Int. Workshop on ECR Sources*, CONF-9011136, Knoxville, TN, November 1-2, 1990, p. 259.
8. TRIM - the Transport of Ions in Matter, J. F. Ziegler, IBM Research, Yorktown Heights, New York 10598, USA.

and the puller using capacitor-splitter motors controlled by an existing programmable logic controller. The new system has triac outputs controlling the motors and position feedback potentiometers feeding 12-bit analog-to-digital converter modules. The operator interface is via a programmable keyboard with readout on a new CRT page in the existing cyclotron control system.

A collaboration is under way with H. G. Blosser, L. Lee, and F. Marti of Michigan State University to study the central region of ORIC and to determine what modifications might be implemented to improve ion-beam transmission efficiency through the acceleration and extraction processes. Good efficiency is vital for minimizing activation of accelerator parts during acceleration of high-intensity light-ion beams. Preliminary results were used to determine possible locations for effective use of radial-beam clipper apertures (phase clippers). These studies also show a need to improve the internal ion source geometry and puller location for optimum acceleration on the first orbits. A new power supply was purchased for supplying arc power in the internal ion source. The new supply is rated at 2 A and 5 kV with both voltage and current regulation, or limiting, modes of operation.

Target-ion source room. One of the ORIC experiment rooms, C111, was chosen as the RIB target-ion source area, and reconfiguration is under way. This room was formerly split into two areas, C111N and C111S, by a stacked block wall. The wall has been removed. All experimental equipment, wiring, piping, and beam line shield-wall plugs are in the process of being removed. It will be necessary to eliminate all perturbations from floor and wall surfaces to permit installation of smooth conducting surfaces that will comprise the ground planes surrounding the high-voltage platforms that will house the target-ion source and peripheral equipment.

Radiation safety system. The demolition of wiring in C111 resulted in disruption of the HHIRF radiation safety system, RSS. Further disruption occurred through the need to reconfigure the cyclotron RSS for stand-alone operation and for dealing with high radiation expectations in both the cyclotron room and the target-ion source room. Consequently, a new radiation-safety configuration was developed and implemented.

Cyclotron beams are now restricted to the cyclotron vault, C109, and the target-ion source room, C111. All beam lines leading to other rooms or areas were terminated or removed and the respective shield-

wall plugs were sealed. The shield-wall plugs and stacked-block portion of the wall between C109 and C111 were removed. The two rooms are now treated as a single radiation zone and both rooms must be secure to satisfy operation interlock requirements. The selector switch system which formerly permitted selection of a target area to be secured along with C109 has been eliminated. The large experimental room, C110, is currently inactive. The UNISOR and spin spectrometer rooms, C113 and C114, are now operable as tandem accelerator target areas only, and have no ties to the cyclotron RSS.

COMPUTATION STUDIES OF NEW CENTRAL REGION FOR ORIC

H. Blosser,¹ L. Lee,¹ F. Marti,¹ and D. K. Olsen

A new central region concept was designed with the goal of obtaining a well-centered intense beam. A major change from the present design is the decrease of the distance from the source slit to the puller face with the purpose of increasing the electric field at the slit. In the present configuration, the distance is approximately 2.7 cm, while in the new design, shown in Fig. 2.14, for a $k = 75$ molecular hydrogen beam, it has been reduced to 1.0 cm. The peak electric field

ORNL-DWG 92-15723

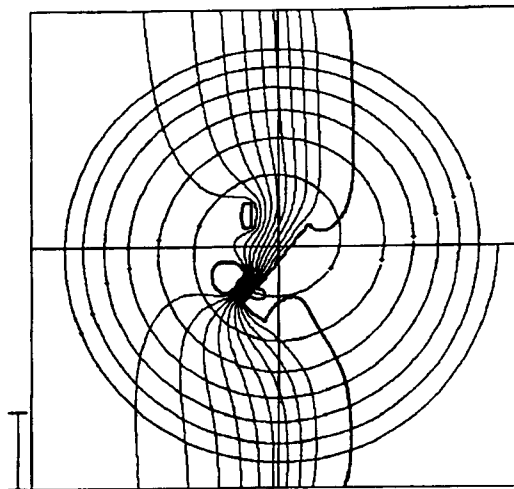


Figure 2.14. The central ray trajectory for the first six turns superimposed on the electric field equipotential lines.

is still significantly lower than peak fields obtained routinely at other cyclotrons. Orbit studies have shown that a starting time of 20 degrees RF before peak voltage is the optimum choice to decrease orbit center spread and maximize intensity. A range of orbits ± 10 degrees around this central ray time will have good centering and good vertical motion behavior. This range is larger than what is needed to obtain single-turn extraction for high extraction efficiency. Phase selection on the first or second turn will be implemented to decrease losses at extraction.

1. National Superconducting Cyclotron Laboratory, Michigan State University, East Lansing, Michigan 48824.

ORIC BEAM LINES

*D. T. Dowling, S. N. Lane, S. W. Mosko,
D. K. Olsen, and B. A. Tatum*

The ORIC beam transport system is being upgraded to interface with the RIB Project. As part of this activity, both a reconfigured beam-line 1 and a

new beam-line 9, shown in Fig. 2.15, have been designed to transport intense light-ion beams from the cyclotron to the RIB target/ion source. The position of the target/ion source was chosen by balancing the RIB mass-separator system-optics requirements with the retention of flexibility and simplicity in the ORIC beam transport system. It is currently envisioned that light-ion beams from the cyclotron will be transported only to the heavily shielded RIB target/ion source room C111. This fact enables the existing beam transport system to be reconfigured and optimized for the RIB project. However, the capability of transporting an ORIC beam to room C110, which is also heavily shielded, is being retained, but would require modifications to the existing radiation safety system.

Beam-line 1 will remain essentially the same from an optical standpoint. Quadrupole-doublet magnets 1 and 2 will retain their current position, while the horizontal beam switching magnet, BSM-1, will be moved approximately 60 inches down stream. The beam will be bent 11.46 degrees by BSM-1 into the new beam-line 9. The beam will then be focused using a quadrupole triplet, bent upward using a new bending magnet, and transported to the RIB target/ion source. The vertical bend angle will be 13° and is required to accommodate the elevation of the RIB beam line, 87 inches from the floor in room C111.

ORNL-DWG 92-15724

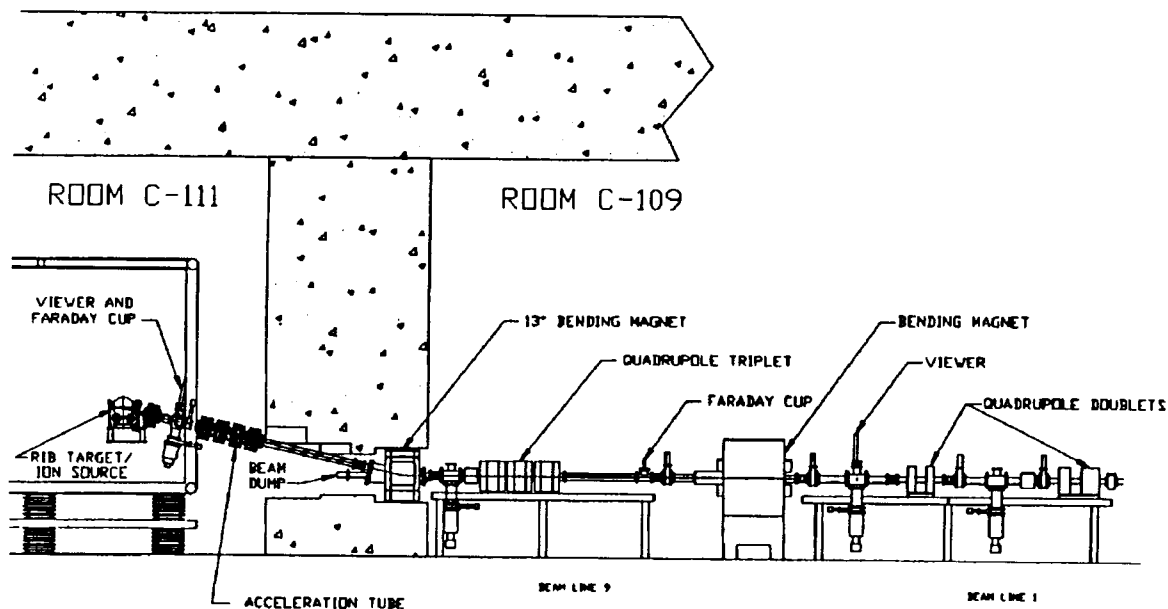


Fig. 2.15. Reconfigured beam line to transport intense, light-ion beams from ORIC to the RIB target-ion source.

The final design layouts for the new ORIC beam lines are nearing completion. The diagnostics requirements have been finalized and the beam-optics requirements are known. Existing magnetic elements are being utilized where possible, resulting in the need to purchase only one magnetic element, the 13-degree, vertical-bend dipole. The two beam lines will be constructed, almost exclusively, of aluminum components to reduce residual radiation problems, and the currently-used oil diffusion pump stations will be replaced with either cryopumps or turbomolecular pumps.

TANDEM ACCELERATOR BEAM-PARAMETER MEASUREMENTS

*C. M. Jones, R. C. Juras, M. J. Meigs,
and D. K. Olsen*

One of the challenges which must be addressed in the design and development of the new, radioactive-ion-beam facility is separation of the radioactive beams of interest from isobaric contaminant beams. One possible solution to this problem is use of the tandem accelerator energy-analyzing magnet as a mass analyzer.

Mass separation with a system of this kind is based on the physical separation of ions of differing mass at the image plane of the system. The degree to which this mass-dependent separation is useful depends on the mass-independent size of the beam at the image plane, or more accurately, the mass-independent beam intensity distribution projected on the image plane. With this motivation, a series of preliminary measurements has been completed with beams whose mass and energy are typical of those expected for the new facility.

A detailed discussion of the experimental methods used for these measurements, as well as a detailed discussion of the experimental results, is beyond the scope of this report. The essential results of the measurements of bending plane parameters at the image plane may be summarized as follows:

- The magnitude of the apparent collective beam motion has an upper limit of about 0.5 mm peak-to-

peak with a dominant frequency of 2.3 Hz. This apparent collective motion appears to have at least two components:

1. A component which appears only in the image-bending plane and is thought to be due to tandem terminal voltage fluctuations.
2. A component which appears at both the object and image planes and is thought to be either an artifact of the measurement technique or real beam motion resulting from ion-optic component power-supply fluctuations.

Contributions of this apparent motion to beam size measurements were reduced by an averaging technique.

- Beam emittance for a 90% beam fraction is typically $0.3\text{-}0.5\pi$ mm mrad for gas stripping and 1.0π mm mrad for foil stripping.

- Beam widths for a 90% beam fraction are typically 0.5 to 1.0 mm for gas stripping and 1.4 mm for foil stripping.

- With the addition of a quadrupole lens upstream of the analyzing magnet, beam widths for a 90% beam fraction in the range 0.2 to 0.3 mm are thought to be achievable with gas stripping. The corresponding mass resolution would be 1 part in 11,000 to 16,500. With a full-width-half-maximum criterion, the corresponding mass resolution would be 1 part in 16,000 to 24,000.

- More work is required to estimate achievable beam widths with foil stripping.

In addition, it was determined that conventional "slit control" does not appear to be required for stable operation of the tandem accelerator. Adequate control of the terminal voltage potential appears to be possible using only a generating voltmeter. Thus, there is no apparent lower intensity limit to beams which can be accelerated in the tandem accelerator.

3. LOW/MEDIUM ENERGY NUCLEAR PHYSICS

NUCLEAR STRUCTURE STUDIES VIA ELASTIC, INELASTIC, AND CHARGE EXCHANGE REACTIONS

STUDY OF THE NUCLEAR EXCITATION OF THE ISOVECTOR GIANT DIPOLE RESONANCE BY INELASTIC SCATTERING

*D. H. Olive,¹ J. R. Beene, F. E. Bertrand,
R. L. Auble, M. L. Halbert,
D. J. Horen, and R. L. Varner*

During this year significant progress has been made in the analysis of data related to the isovector giant resonance research program. The goal of this program is to characterize the nuclear excitation of the isovector giant dipole resonance through a systematic study of inelastic scattering using medium-energy light ions and lower-energy heavy ions. In previous reports the Coulomb excitation of isovector dipole and quadrupole resonances using medium energy (60, 84, and 95 MeV/nucleon) heavy ions has

been described.^{2,3,4} An understanding of the excitation of isovector resonances via the nuclear force is of equal importance.

Traditionally the study of the nuclear excitation of isovector resonances by hadronic probes has proved difficult due to the strong excitation of isoscalar resonances in the same energy region (Fig. 3.1, left). With heavy ions at sufficiently high bombarding energies (>50 MeV/nucleon), the excitation cross sections for isovector states are comparable to those of isoscalar states. This, however, results mainly from Coulomb excitation and does not yield much information about the nuclear interaction. Fortunately the ground state γ decay is dominated by E1 transitions that allows us to isolate the GDR, even where there is a large non-dipole background. We have shown that by gating on these gamma rays decaying to the ground state, the IVGDR can be

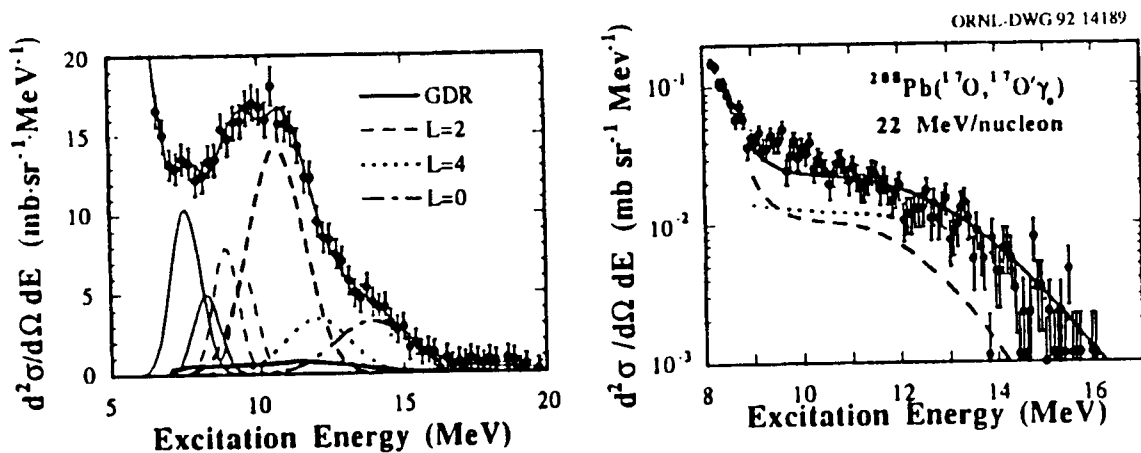


Fig. 3.1. (Left) Inelastic singles spectrum for the $^{208}\text{Pb}(^{17}\text{O}, ^{17}\text{O}')$ reaction at 22 MeV/nucleon. A smooth background has been subtracted. The position and width of all peaks were taken from high resolution (p,p') work, except the IVGDR that was calculated using the photonuclear strength. (Right) The corresponding ground state γ -ray coincidence spectrum of the reaction $^{208}\text{Pb}(^{17}\text{O}, ^{17}\text{O}')$. The histogram is data, the heavy solid curve is the contribution from the GDR alone.)

picked out quite well in all nuclei^{2,3} and the isovector giant quadrupole resonance can be isolated in nuclei near closed shells.⁴

The effectiveness of this technique is illustrated in Fig. 3.1 where inelastic singles data is shown on the left along with the multipole decomposition. The corresponding ground-state γ -decay coincidence spectrum is shown on the right where the GDR is seen to dominate. This technique provides an enhancement of approximately 100 to 1 for the IVGDR relative to the isoscalar quadrupole and should ultimately provide direct information on the radial form of the GDR transition potential.

In order to examine the effects of the nuclear interaction in the excitation of the GDR we use the deformed optical potential model with a radial form of the nuclear part of the transition potential^{5,6} for excitation of the target GDR given by

$$\delta U(r) = \frac{-2\alpha_1}{A} \left\{ [Z f_0^n(r) - N f_0^p(r)] + c [Z f_1^n(r) + N f_1^p(r)] \right\} \quad (1)$$

where $f_j^i(r)$ for $i = n, p$, and $j = 1, 0$ refer to neutron and proton and isovector and isoscalar pieces, respectively, and c is a constant determining the strength of the isovector piece of the interaction. Equation (1) is a phenomenological expression, but its form is based on the folding model. Guided by the folding model, we can make an estimate of the quantity c in terms of the projectile neutron and proton densities, ρ_p^i , and the volume integrals, J_j , of the central part of the nucleon-nucleon interaction:

$$c \sim \frac{J_1}{J_0} \left(\frac{\rho_p^n - \rho_p^p}{\rho_p^n + \rho_p^p} \right)_R \leq 0. \quad (2)$$

The form of the $f(r)$ in the collective model depends on the macroscopic model one chooses to represent the dipole oscillation. For the Goldhaber-Teller model,

$$f_j^i(r) = \frac{dU_j^i(r)}{dr_i} \quad (3)$$

where $U_j^i(r)$ represents the neutron and proton ($i = n, p$) parts of the isoscalar or isovector ($J = 0, 1$) pieces of the optical potential.⁸

The significant feature of equation (1) is realized by noting that $c \leq 0$ for all projectiles. For a strictly isoscalar ($T=0$) probe (e.g., α or ^{16}O) the second term in equation (1) vanishes ($f_1^{n,p} = 0$). For $T \neq 0$ probes (e.g., ^3He or ^{17}O) the second term is finite and less than zero. The effect is a reduction of the GDR excitation by $T \neq 0$ probes relative to isoscalar probes with the same kinematics. Figure 3.2 shows this effect comparing angular distributions of the differential cross section for ^{16}O , an isoscalar probe, and ^{17}O , an isovector probe as a function of c .

An initial experiment has been performed to quantitatively determine the effect shown in Fig. 3.2 using 22 MeV/nucleon ^{16}O and ^{17}O projectiles to excite the GDR in ^{208}Pb . The inelastically scattered oxygen ions were detected with the HHIRF broad range spectrograph and coincident gamma rays were detected using the ORNL BaF_2 array. During the past year the analysis of this data was almost completed. Preliminary results are shown in Fig. 3.3. The angular distribution data shows the reduction of the GDR strength by a factor of 1.45 ± 0.10 for the ^{17}O reaction integrated over the entire angle range. This investigation of the difference between GDR excitation with an isoscalar probe and neighboring $N \neq Z$ projectiles provides a sensitive probe of the structure of the transition potential in nucleus-nucleus collisions and how it is related to the nucleon-nucleon interaction.

An experiment to study the IVGDR in ^{208}Pb and ^{40}Ca using 140-MeV polarized protons has been approved at the Indiana University Cyclotron. Similar to the first experiment, ground-state gamma rays will be measured in coincidence with inelastically scattered protons detected in the spectrograph. The measured cross sections will provide direct information on the isovector proton-nucleus interaction. Simultaneous measurements of analyzing powers will also be made, which should provide additional sensitivity to the radial shape of the GDR transition density as well as the strength of the isovector interaction. Although these two studies should shed much light on the nuclear interaction, several experiments will be needed to fully complete this systematic investigation.

1. Partial support provided by Vanderbilt University and Oak Ridge Associated Universities under the Laboratory Graduate Research Program.

2. J. R. Beene et al., *Phys. Rev. C* **41**, 920 (1990).

3. J. R. Beene et al., *Phys. Rev. C* **39**, 1307 (1989).

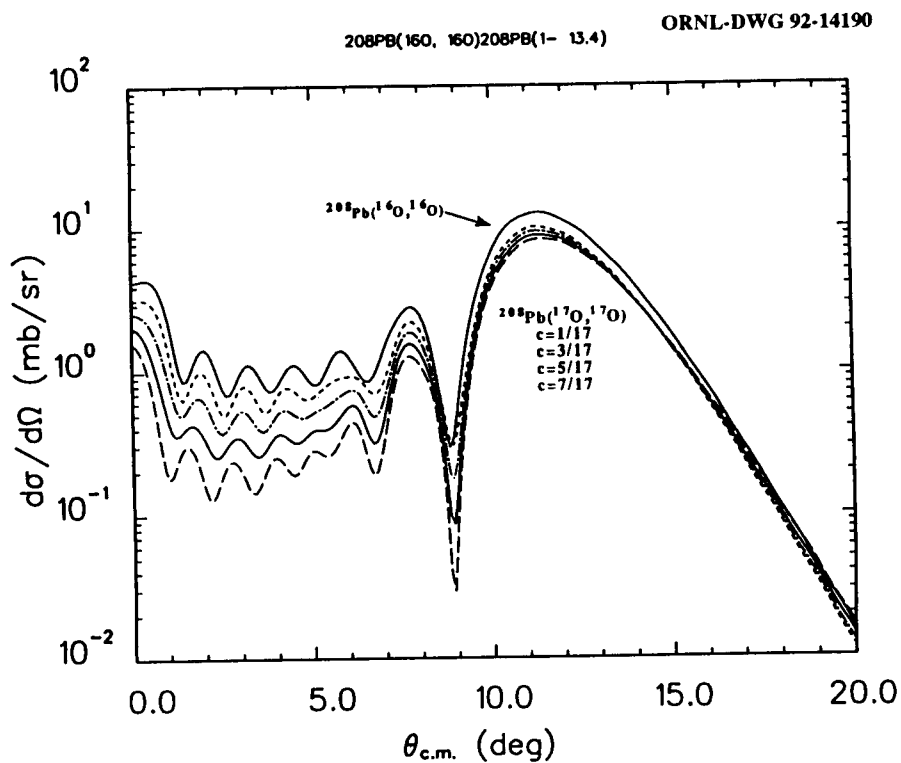


Fig. 3.2. A DWBA calculation of the angular distribution of the 1^- ($E^* = 13.4$) differential cross section for $^{16,17}\text{O}$ projectiles on ^{208}Pb at 22 MeV/nucleon.

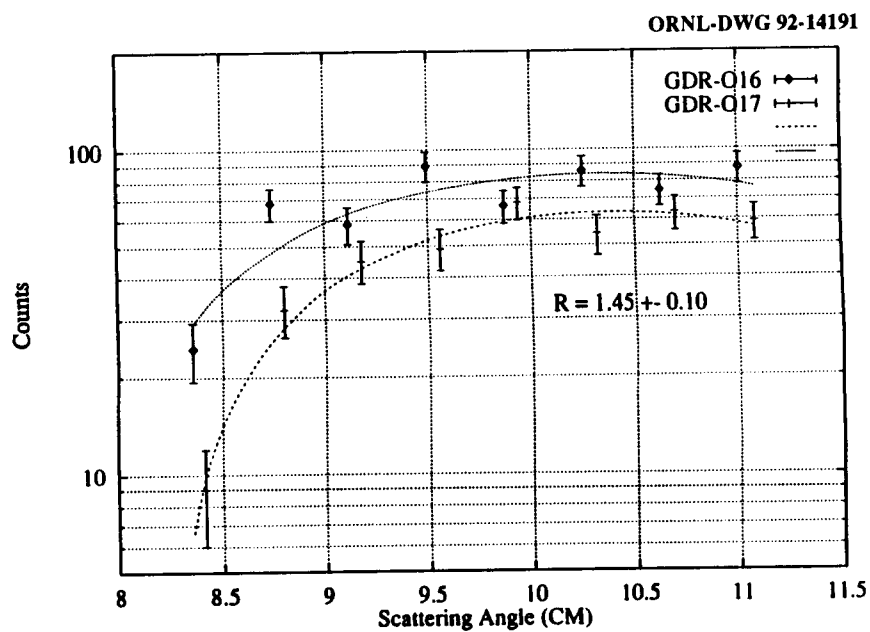


Fig. 3.3. Angular distribution of $^{208}\text{Pb}(^{16}\text{O}, ^{16}\text{O}\gamma_0)$ and $^{208}\text{Pb}(^{17}\text{O}, ^{17}\text{O}\gamma_0)$ at 22 MeV/nucleon. The two data sets are normalized to the 2^+ state in ^{208}Pb . R represents the relative GDR strength in the two reactions integrated over all angles.

4. J. R. Beene and F. E. Bertrand, p. 159 in *The Spectroscopy of Heavy Nuclei 1989, Inst. Phys. Conf. Ser. No. 105* (Proceedings, Int. Conf. on Spectroscopy of Heavy Nuclei, Crete, Greece, 1989).

5. G. R. Satchler, *Nucl. Phys. A* **472**, 215 (1987).

6. G. R. Satchler, *Direct Nuclear Reactions* (Oxford University Press, Oxford, 1983).

STUDY OF ONE- AND TWO-PHONON GIANT RESONANCE STRENGTH IN ^{208}Pb WITH INTERMEDIATE ENERGY ^{36}Ar AND ^{84}Kr SCATTERING

J. R. Beene, F. E. Bertrand, D. J. Horen, M. L. Halbert, D. C. Hensley,¹ D. Olive,² M. Thoennessen,³ R. L. Auble, W. Mittig,⁴ Y. Schutz,⁴ K. Katori,⁴ W. Kühn,⁵ and R. Holzmann⁶

Cross sections for Coulomb excitation of giant resonances in a target nucleus increase rapidly with both the velocity and nuclear charge of the projectile. At high enough energies, the excitation probabilities, particularly for the GDR, become large enough that multiple excitation of the giant modes might be expected.

In 1986 we began a series of experiments which exploited the large giant-resonance excitation cross sections produced by 84 MeV/nucleon ^{17}O beams at the GANIL facility. We have recently extended this program with experiments using higher-Z beams, studying $^{208}\text{Pb}(^{36}\text{Ar}, ^{36}\text{Ar}')$ at 95 MeV/nucleon and $^{208}\text{Pb}(^{86}\text{Kr}, ^{86}\text{Kr}')$ at 60 MeV/nucleon, also at the GANIL facility.

These experiments involved detection of the inelastically-scattered projectile in the magnetic spectrometer SPEG in coincidence with γ rays detected in an array of 228 BaF_2 detectors. This array was made up of detectors from the ORNL array, the TAPS collaboration, and the GSI.

A singles spectrum for 95 MeV/nucleon ^{36}Ar scattering is shown along with results from our earlier ^{17}O scattering experiments in Fig. 3.4. A dramatic increase in peak to continuum is seen even compared to the 84 MeV/nucleon ^{17}O scattering. The total cross section in the GR bump is almost 15 b/sr while the continuum cross section is only about 120 mb/MeV at 30 MeV of excitation.

Figure 3.5 shows the calculated total (angle integrated) cross section as a function of bombarding energy for Coulomb excitation of a selection of

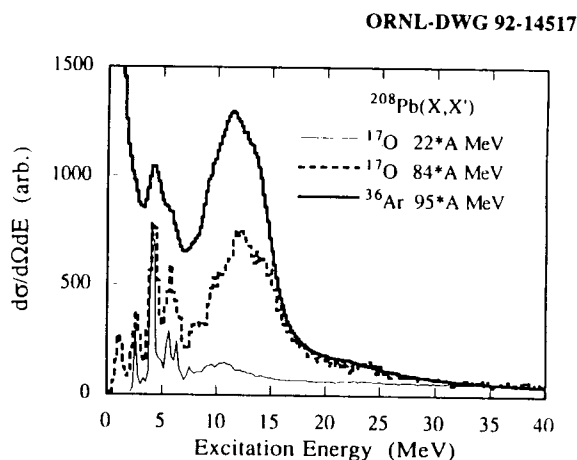


Fig. 3.4. Comparison of the excitation of ^{208}Pb by the inelastic scattering of ^{17}O at 22 (thin solid curve) and 84 (dotted curve) MeV/nucleon, and ^{36}Ar at 95 MeV/nucleon (heavy solid curve). Spectra are normalized to match yields in the 35-40 MeV region.

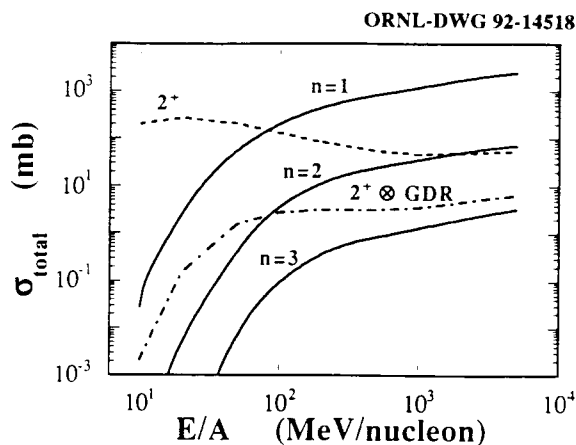


Fig. 3.5. Total cross section for Coulomb excitation of some one-, two-, and three-phonon states in ^{208}Pb by ^{86}Kr scattering. The excitations involving only the GDR (solid lines) are labeled by the phonon number, n .

one-, two-, and three-phonon states in ^{208}Pb with ^{86}Kr beams. All the multiple excitations shown involve the GDR, but the mixed two-phonon $2^+ \otimes \text{GDR}$ state is included along with multiple GDR excitations. The $3^- \otimes \text{GDR}$ state involving the low-lying (2.61 MeV) octupole state has a similar energy dependence, with a slightly smaller cross section. It is clear that, provided sensitive and definitive enough detection

and identification methods are available, the mixed two-phonon states and even the two-phonon GDR \otimes GDR state, might be profitably studied with relatively low-energy beams, where high-resolution spectroscopic studies can be performed using the magnetic spectrometers available at facilities like GANIL. Data on the excitation strength, width, and decay properties of such states are of great interest, as they carry potentially new information about resonance damping, anharmonicities, and phonon-phonon interactions.

Our intermediate-energy experiments on two-phonon states rely on two tools for identification of the states. One is the expected dependence on the projectile Z of the excitation cross section. Two-phonon excitation cross sections at a given projectile velocity scale as Z^4 , while one-phonon excitations scale as Z^2 [12]. Consequently we acquired data with the highest energy ^{36}Ar and ^{86}Kr beams available at GANIL (95 and ~ 60 MeV/nucleon, respectively). Our existing ^{17}O data provides a third Z comparison. To illustrate this point, the calculated peak differential cross sections for these three projectile combinations for excitation of the GDR \otimes GDR state are ~ 1 mb/sr (^{17}O), ~ 50 mb/sr (^{36}Ar) and 60 mb/sr (^{86}Kr) and ~ 1 mb/sr, ~ 30 mb/sr and 160 mb/sr, respectively, for the $2^+ \otimes$ GDR. The other identification tool is the electromagnetic de-excitation of the GDR phonon, which has already been discussed extensively in the preceding article.

Figure 3.6 illustrates schematically how we use the electromagnetic decay of the GDR phonon to isolate and identify two-phonon strength. The horizontal scale (excitation energy) is obtained from the energy of the inelastically scattered ion. The coincident total γ -ray energy (ΣE_γ) measured in the BaF_2 arrays is plotted on the vertical axis. The locus along which all the excitation energy is accounted for by detected γ radiation is the 45° dash-dotted line. The region expected to be occupied by events corresponding to decay of the various one- and two-phonon states involving the GDR are indicated on the figure along with numbers which are relative yields in our experimental geometry (including γ -detection efficiency) for ^{208}Pb ($^{86}\text{Kr}, ^{86}\text{Kr}'$) at 60 MeV/nucleon, normalized to the Kr- $\gamma\gamma$ triple-coincidence yield for the decay of the $n=2$ GDR in Pb.

Some very preliminary results of the analysis of these data are shown in Fig. 3.7. The upper panel shows the one-fold γ yield from ^{208}Pb ($^{86}\text{Kr}, ^{86}\text{Kr}'\gamma$) in the range of E_γ from 12 to 18 MeV, as a function of excitation energy. This corresponds to a rectangular slice of Fig. 3.6 projected onto the horizontal axis.

ORNL-DWG 92-14519

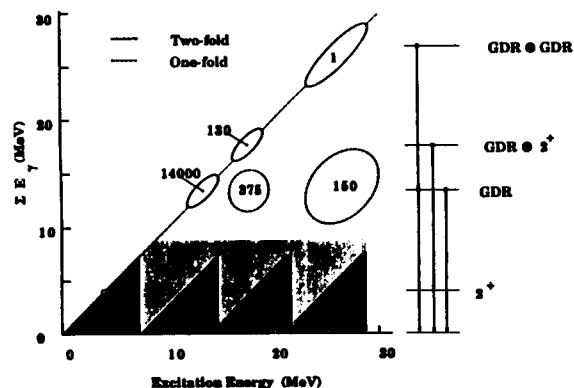


Fig. 3.6. A schematic illustration of the experimental method employed to isolate two phonon strength in a heavy-ion scattering spectrum by γ -decay coincidence. The shaded region at the bottom of the plot represents a region of intense γ background from decays following emission of one or more neutrons.

ORNL-DWG 92-14520

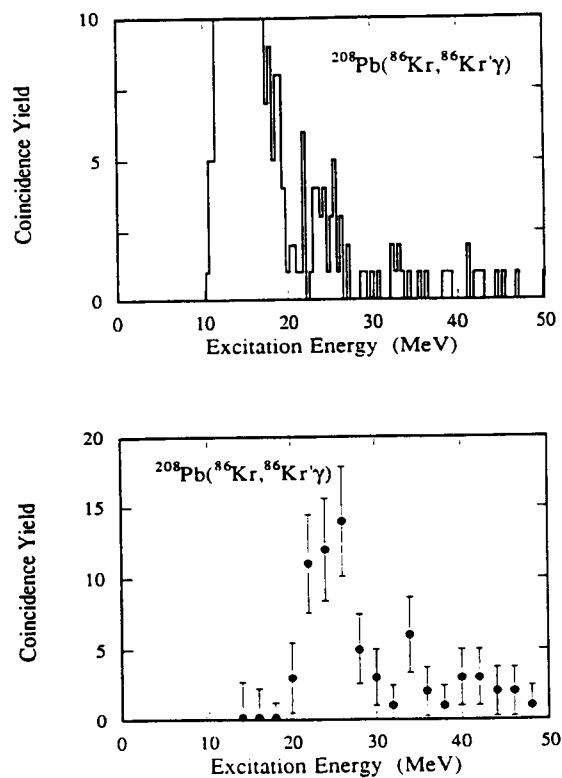


Fig. 3.7. ^{208}Pb ($^{86}\text{Kr}, ^{86}\text{Kr}'\gamma$) coincidence spectra. See text for discussion.

Unfortunately the resolution in excitation energy is poor due to a combination of difficulties in the determination of ^{86}Kr momentum and from target inhomogeneities, and as a result the mixed two-phonon states ($2^+ \otimes \text{GDR}$ expected at about 17.5 MeV and the $3^- \otimes \text{GDR}$ at ~ 15.6 MeV) are not resolved from the GDR. However, a distinct structure centered at an excitation energy of 25 MeV is observed. Its properties are more clearly seen in the lower part of Fig. 3.7 from which γ decays consistent with direct decays to the ground state (i.e., all excitation accounted for by E_γ) have been removed. We interpret the structure at ~ 24 MeV as resulting from the two-phonon GDR \otimes GDR state – as would be expected from the qualitative picture in Fig. 3.6. The distribution of coincidence yield in Fig. 3.7 is not a direct representation of the GDR \otimes GDR strength distribution, but is related to it in a direct and straightforward way by the dynamics of the Coulomb excitation process. From a preliminary analysis of the data in Fig. 3.7 we infer a GDR \otimes GDR strength distribution centered at 26 MeV with a width of about 6 MeV.

Preliminary indications are that the γ -decay yield from the two-phonon GDR is somewhat higher than our simplest predictions. This would indicate that either the excitation cross section is larger than expected, or the γ -decay branch from the two-phonon state is larger than our simplest expectations based on a harmonic vibrator picture.

SYSTEMATICS OF ISOSPIN CHARACTER OF TRANSITIONS TO THE 2_1^+ AND 3_1^- STATES IN $^{90,92,94,96}\text{Zr}$ ¹

D. J. Horen, R. L. Auble, J. Gomez del Campo, G. R. Satchler, R. L. Varner, J. R. Beene, Brian Lund,² V. R. Brown,³ P. L. Anthony,³ and V. A. Madsen⁴

Differential cross sections for exciting the 2_1^+ and 3_1^- states of $^{90,92,94,96}\text{Zr}$ with 70-MeV ^6Li ions have been measured. Calculations of the cross sections have been performed using a deformed optical model potential (DOMP) with OMP deduced from fits to the elastic data, as well as a folding model with an effective nucleon-nucleon interaction with a Yukawa form factor obtained from fits to the elastic data and transition densities obtained from open-shell RPA calculations. The DOMP fits to the data yield values of M_n/M_p which are in good agreement with those predicted using the RPA. For the 2_1^+ states, we find M_n/M_p increases from less than N/Z to greater than N/Z in going from ^{90}Zr to ^{96}Zr . However, for the 3_1^- states M_n/M_p remains less than N/Z for all cases, a result which is in disagreement with previous works. The folding model, with the RPA transition densities, provides good agreement with the 2_1^+ measurements, but underpredicts the cross sections for the 3_1^- states. A reanalysis of the earlier data from excitation of these states by (α, α') reactions removes much of the apparent discrepancies between those measurements and other measurements, including the ones reported here. The localization of the ^6Li interaction is also discussed.

1. Office of Waste Management and Remedial Actions, ORNL.

2. Partial support provided by Vanderbilt University and Oak Ridge Associated Universities under the Laboratory Graduate Research Program.

3. Michigan State University, East Lansing, MI.

4. GANIL, Caen, France.

5. University of Giessen, Germany.

6. GSI, Darmstadt, Germany.

7. J.R. Beene et al., *Phys. Rev. C* **38**, 1307 (1989)

8. J.R. Beene et al., *Phys. Rev. C* **41**, 920 (1990).

9. A. Bertulani and G. Baur, *Phys. Rept.* **16**, 299(1988), and references therein.

1. Abstract of paper submitted to *Physical Review C*.

2. Yale University, New Haven, CT.

3. Lawrence Livermore National Laboratory, Livermore, CA.

4. Oregon State University, Corvallis, OR.

**DIFFERENT EFFECTS OF VALENCE
NEUTRONS ON THE ISOSPIN
CHARACTER OF TRANSITIONS TO THE
FIRST 2^+ and 3^- STATES OF $^{90,92,94,96}\text{Zr}^1$**

*D. J. Horen, R. L. Auble, J. Gomez del Campo,
R. L. Varner, J. R. Beene, G. R. Satchler,
Brian Lund,² V. R. Brown,³ P. L. Anthony,³
and V. A. Madsen⁴*

We have used the $^{90,92,94,96}\text{Zr}(^6\text{Li},^6\text{Li})$ reaction at $E = 70$ MeV to deduce the ratio of M_n/M_p for transitions to the first 2^+ and 3^- excited states. For the first 2^+ state, we find M_n/M_p increases from less than N/Z to greater than N/Z going from ^{90}Zr to ^{96}Zr . However, for the 3^- state we find that M_n/M_p is significantly smaller than N/Z for all four isotopes, a result which is in sharp disagreement with previous work. We find that our measured values of M_n/M_p are well reproduced by random-phase-approximation calculations including pairing.

-
1. Abstract of paper to be published in *Physics Letters B*.
 2. Yale University, New Haven, CT.
 3. Lawrence Livermore National Laboratory, Livermore, CA.
 4. Oregon State University, Corvallis, OR.

**ISOSPIN CHARACTER OF THE
TRANSITION TO THE 0.803-MeV STATE IN
 ^{206}Pb FROM π^\pm SCATTERING AT 180 MeV¹**

*D. J. Horen, C. L. Morris,² S. J. Seestrom,²
F. W. Hersman,³ J. R. Calarco,³ M. Holtrop,³
M. Leuschner,⁴ Mohini Rawool-Sullivan,⁴
R. W. Garnett,⁴ S. J. Greene,² M. A. Plum,²
and J. D. Zumbro⁵*

Elastic and inelastic π^\pm scattering by ^{206}Pb has been studied to measure the isospin character of transitions to bound states. The data have been interpreted using both distorted wave impulse approximation and optical model potentials. The data for the collective states at 2.647 MeV (3^-) and 4.111 MeV (2^+) are well reproduced with $\delta_l^+ = \delta_l^- = \delta_l^p$, i.e., assuming that these transitions are isoscalar. For the 0.803-MeV, 2^+ level we deduce $M_n/M_p = 2.6 \pm 0.3$

which is in excellent agreement with a value obtained from inelastic heavy-ion scattering.

-
1. Abstract of published paper: *Phys. Rev. C* **46**, 499 (1992).
 2. Los Alamos National Laboratory, Los Alamos, NM.
 3. University of New Hampshire, Durham, NH.
 4. New Mexico State University, Las Cruces, NM.
 5. University of Pennsylvania, Philadelphia, PA.

**LIFETIME MEASUREMENT OF THE
1.897-MeV, 3_1^- STATE IN ^{96}Zr**

*D. J. Horen, R. L. Auble, J. R. Beene, I. Y. Lee,¹
D. Cline,² C. Y. Wu,² M. Devlin,² R. Ibbotson,²
and M. Simon²*

Recently, there have been two centroid-shift measurements of the half-life of the 1.897-MeV, 3_1^- state in ^{96}Zr which give values of 50 ± 7 ps (Ref. 3) and 46 ± 15 ps (Ref. 4). These yield a $B(E3)\uparrow \approx 0.25 e^2b^3$ which makes this one of the fastest E3 transitions known thus far. An inelastic proton scattering measurement gave $B(E3)\uparrow = 0.183 e^2b^3$ (Ref. 5). A study of the $^{96}\text{Zr}(^6\text{Li},^6\text{Li}')$ reaction at 70 MeV^{6,7} suggests unreasonably low values of M_n/M_p for this transition if the $B(E3)\uparrow \approx 0.25 e^2b^3$.

We have bombarded ^{96}Zr with 105-MeV ^{32}S ions using the University of Rochester tandem Van de Graaff accelerator. Photons from recoiling ^{96}Zr ions were measured at 0° with a Ge detector in coincidence with backscattered ^{32}S ions that were detected in an annular avalanche counter. The lifetime of the 3_1^- state was determined from measurements of the shifted and unshifted peaks of the 0.147-MeV transition as a function of the stopping distance.

Preliminary data analysis indicates that the half-life of the 1.897-MeV state is about 64 ps, i.e., about 28% longer than that reported from the centroid-shift measurements. This means that $B(E3)\uparrow \approx 0.2 e^2b^3$, a value close to that obtained in the (p,p') scattering.

-
1. Present address: Lawrence Berkeley Laboratory, Berkeley, CA.
 2. Nuclear Structure Laboratory, University of Rochester, Rochester, NY.

3. H. Mach et al., *Phys. Rev. C* **42**, R811 (1990).
4. H. Ohm et al., *Phys. Lett.* **241**, 472 (1990).
5. M. M. Stautberg et al., *Nucl. Phys. A* **104**, 67 (1967).
6. D. J. Horen et al., "Systematics of Isospin Character of Transitions to the 2_1^+ and 3_1^- States in $^{90,92,94,96}\text{Zr}$," this report.
7. D. J. Horen et al., "Different Effects of Valence Neutrons on the Isospin Character of Transitions to the First 2^+ and 3^- States of $^{90,92,94,96}\text{Zr}$," this report.

MEASUREMENT OF THE LIFETIME OF THE 0.918-MeV, 2_1^+ STATE OF ^{94}Zr

C. Y. Wu,¹ D. Cline,¹ M. Devlin,¹ R. Ibbotson,¹ M. Simon,¹ D. J. Horen, and R. L. Auble

In trying to deduce the isospin character of the transition to the 0.918-MeV, 2_1^+ state in ^{94}Zr using inelastic scattering of 70-MeV ^6Li ions^{2,3} it was found that the data were not sufficiently accurate to search independently on both the $B(E2)\uparrow$ and the nuclear deformation length. There have been two Coulomb-excitation measurements of the $B(E2)\uparrow$ which differ by about 50%, i.e., $0.081 \pm 0.17 e^2b^2$ and $0.056 \pm 0.014 e^2b^2$ (Ref. 4). Hence, we have undertaken a measurement of the lifetime of the 2_1^+ state using the plunger technique.

The University of Rochester tandem Van de Graaff was used to provide 105-MeV ^{32}S ions which were scattered from a self-supporting ^{94}Zr target. The backscattered ^{32}S ions were detected in an annular avalanche counter and coincidences were recorded with photons detected in a Ge detector placed at 0° .

Our preliminary value for the half-life of the 0.918-MeV state is 8 ps which is in better agreement with the value of $B(E2)\uparrow = 0.056 e^2b^2$.

1. Nuclear Structure Research Laboratory, University of Rochester, Rochester, NY.

2. D. J. Horen et al., "Systematics of Isospin Character of Transitions to the 2_1^+ and 3_1^- States in $^{90,92,94,96}\text{Zr}$," this report.

3. D. J. Horen et al., "Different Effects of Valence Neutrons on the Isospin Character of Transitions to the First 2^+ and 3^- States of $^{90,92,94,96}\text{Zr}$," this report.

4. S. Raman et al., *At. and Nucl. Data Tables* **36**, 1 (1987).

MEASUREMENTS OF THE LIFETIMES OF EXCITED STATES IN ^{100}Mo

R. L. Auble, D. J. Horen, D. Cline,¹ C. Y. Wu,¹ M. Devlin,¹ R. Ibbotson,¹ and M. Simon¹

There exists a discrepancy between the measured $B(E3)\uparrow$ for the 1.908-MeV, 3_1^- state in ^{100}Mo and that calculated using the measured half-life combined with the adopted photon branching ratios.² Since this $B(E3)\uparrow$ is considerably enhanced over the single-particle value (similar to the case for ^{96}Zr), we have measured the lifetime of the 1.908-MeV level (and several other states) using the plunger technique. The incident beam obtained from the University of Rochester tandem accelerator was 105-MeV ^{32}S . Data were obtained for the 2^+ levels at 0.535 and 1.064 MeV, the 4^+ level at 1.136 MeV and the 3_1^- state at 1.908 MeV. These data are presently being analyzed, and suggest lifetimes consistent with those previously reported.²

1. Nuclear Structure Laboratory, University of Rochester, Rochester, NY.

2. B. Singh and J. A. Szucs, *Nucl. Data Sheets* **60**, 1 (1990).

NUCLEAR STRUCTURE STUDIES VIA TRANSFER, CAPTURE, AND COULOMB EXCITATION REACTIONS

POSSIBLE TWO-PHONON QUADRUPOLE STATE IN ^{232}Th

F. K. McGowan¹ and W. T. Milner

For nearly thirty years a significant issue in the nuclear structure of deformed nuclei has been whether or not two-phonon collective excitations exist in a spheroidal nucleus. In the level spectra of many deformed nuclei, low-lying excitations are observed that may be approximately described as one-phonon β and γ vibrations. Odd-parity collective modes of low frequency corresponding to octupole shape oscillations have also been observed as a systematic feature in nuclei.

Recently, strong evidence for the existence of the two-phonon γ vibration² with $K = 4$ has been established in ^{168}Er at an excitation energy $2.5E(2^+_{\gamma})$ and the ratio of $B(E2, 4_{2\gamma} \rightarrow 2_{\gamma})/B(E2, 2_{\gamma} \rightarrow 0)$ is between 0.52 and 1.61. Using the HI Coulomb excitation reaction, the Heidelberg group³ have observed a two-phonon γ vibration with $K = 4$ in ^{232}Th at an excitation

energy of 1414 keV [$1.8E(2^+_{\gamma})$]. The branching ratio decay of this state into the one-phonon γ band is consistent with $K = 4$ assignment.

The Coulomb excitation reaction, induced by light ions, selectively excites 2^+ and 3^- states by direct E2 and E3 Coulomb excitation. Twenty-five states in ^{232}Th have been observed with 18-MeV ^4He ions on a thick target. Eleven 2^+ states between 774 and 1554 keV and three 3^- states in Fig. 3.8 are populated by direct E2 and E3, respectively. The remaining states are either weakly excited by multiple Coulomb excitation and/or populated by the γ -ray decay of the directly excited states. Singles spectra were taken at $\theta = 0^\circ, 55^\circ,$ and 90° with 53 to 70×10^6 counts in each spectrum. That gives good γ -ray angular distribution data for most all transitions in Fig. 3.8. Spin assignments are based on γ -ray distributions. Reduced transition probabilities have been deduced from the γ -ray yields. The $B(E2)$ values for excitation of the 2^+ states range from 0.024 to 3.5 W.u. (222 W.u. for the first 2^+ state). For the 3^- states, the $B(E3, 0 \rightarrow 3^-)$ values are 1.7, 11, and 24 W.u.

ORNL-DWG 92M-10234R

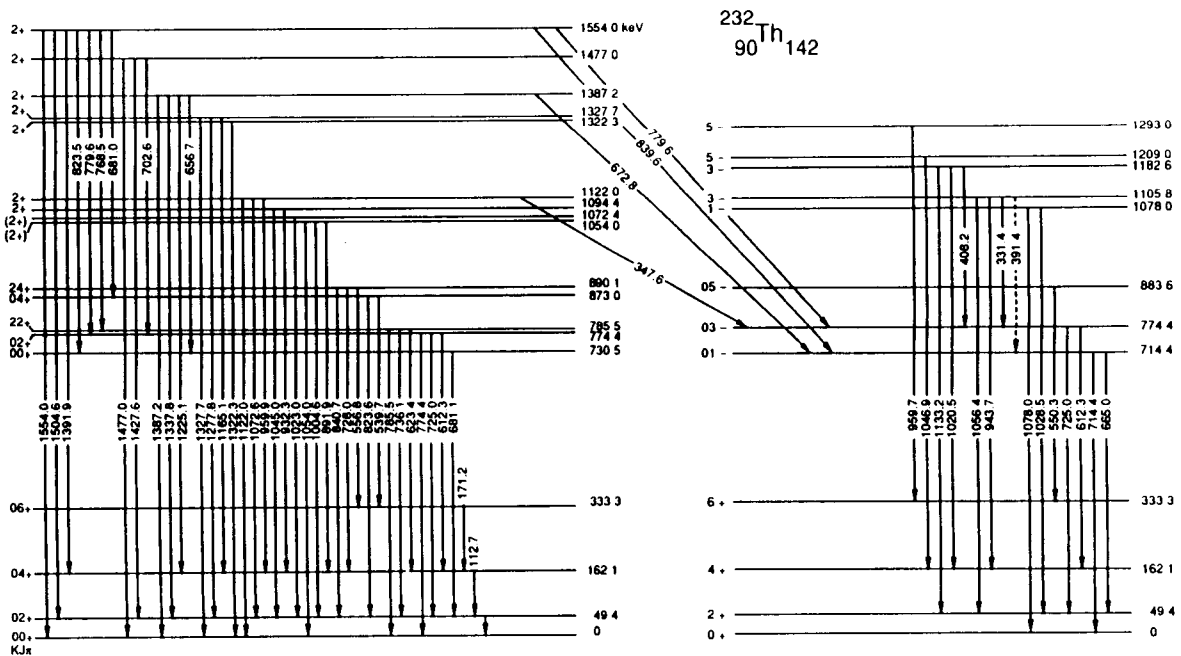


Fig. 3.8. ^{232}Th level scheme from Coulomb excitation.

A possible two-phonon state at 1554 keV, which is nearly harmonic, decays to 4 members of the one-phonon states, to the ground state band, and to the $K = 0^-$ octupole band. The $B(E2)$ value for excitation of this state is 0.66 ± 0.05 W.u. and the $B(E1)$ values for decay of this state are (2 and 6) $\times 10^{-4}$ W.u. The $B(E2)$ values between the two- and one-phonon vibrational states range between 16 and 53 W.u. which are an order of magnitude larger than the $B(E2)$ values between the one- and zero-phonon states.

In the extraction of these $B(E2)$ values, the weak excitation of the states 0_β , 4_β , 4_γ , 1^- , and 5^- by multiple Coulomb excitation did introduce several corrections. For example, the 823.6 keV γ ray appears in two locations of the level scheme $2 \rightarrow 0_\beta$ and $4_\beta \rightarrow 2$ with nearly identical angular distributions. Likewise, the 681 keV γ ray appears in the level scheme at $0_\beta \rightarrow 2$ and $2 \rightarrow 4_\beta$. The 779.7 keV γ ray appears in the $2 \rightarrow 2_\beta$ and $2 \rightarrow 3^-$ transitions. The inclusion of the $4_\beta \rightarrow 2$ intensity reduces the $2 \rightarrow 0_\beta$ intensity by 15%. An extreme scenario concerning the $4_\beta \rightarrow 2$ intensity (disregarding known branching ratio data) could reduce $B(E2, 2 \rightarrow 0_\beta)$ from 41 W.u. to 20 W.u. The $B(E2, 2 \rightarrow 2_\beta) = 53$ W.u. is based on $E2/M1 = 6.25$. An analysis with $E2/M1 = 10^{-2}$ leads to $B(E2, 2 \rightarrow 2_\beta) = 0.6$ W.u. and the $B(M1, 2 \rightarrow 2_\beta)$ is very large, $2 \times 10^{-1} \mu_N^2$, which is 2 to 3 orders of magnitude larger than eight other $B(M1)$ values extracted from the data on ^{232}Th . This latter choice of $E2/M1 = 10^{-2}$ is rather unlikely. These large $B(E2)$ values between the two- and one-phonon vibrational states disagree with our present understanding of collectivity in nuclei, viz., the $B(E2)$ between two-phonon and one-phonon states is approximately equal to the $B(E2)$ between one-phonon and zero-phonon states.

The $B(E1)$ values for nine transitions between the positive and negative parity states range between 10^{-6} to 6×10^{-4} W.u. The latter value is a relatively fast E1 transition and the occurrence of large E1 transition rates is a more common phenomenon than expected. Although no stable octupole deformation is predicted in this mass region, one is forced to question whether such E1 transition rates can unambiguously be taken as evidence for octupole instability. The $B(E1)$ branching ratios for transitions from the 3^- and 1^- states to the ground-state band have large deviations from the Alaga-rule predictions. These deviations can be understood by the strong Coriolis coupling between the states of the octupole quadruplet in deformed nuclei.

1. Partial support provided by Joint Institute for Heavy Ion Research, ORNL.

2. H. G. Börner et al., *Phys. Rev. Lett.* **66**, 691 (1991).

3. W. Korten et al., *Proc. Int. Conf. on Nuclear Structure through Static and Dynamic Moments*, ed. H. H. Bolotin (Conference Proceedings Press, Melbourne, 1987), p. 61.

MAGNETIC DIPOLE STRENGTH IN ^{46}Ca OBSERVED WITH 180° ELECTRON SCATTERING¹

*J. P. Connelly,² H. Crannell,² L. W. Fagg,²
J. T. O'Brien,² M. Petraitis,² D. I. Sober,²
S. Raman, J. R. Deininger,³ and S. E. Williamson³*

Results are presented from a search for $M1$ strength in ^{46}Ca by means of 180° electron scattering at low momentum transfer. We report the presence of a 1^+ state at 13.02 ± 0.04 MeV with a reduced electromagnetic transition strength. The excitation energy of this level is ~ 2 MeV higher than strong 1^+ states seen in other even-even calcium isotopes. No evidence was seen for $M1$ strength in the 10 MeV excitation energy region where strength is predicted by shell model calculations.

1. Abstract of published paper: *Phys. Lett.* **B277**, 383 (1992).

2. Catholic University of America, Washington, DC.

3. University of Illinois, Urbana, IL.

MECHANISM OF (n,γ) REACTION AT LOW NEUTRON ENERGIES¹

S. Raman and J. E. Lynn²

We discuss the interplay between direct capture, valence capture, and compound-nuclear capture in attempting to explain the vast amount of capture data for light-mass nuclei.

1. Abstract of published invited paper: *Beijing International Symposium on Fast Neutron Physics*, edited by Sun Zuxun, Tang Hongqing, Xu Jincheng, and Zhang Jingshang (World Scientific, Singapore, 1992), p. 107.

2. Los Alamos National Laboratory, Los Alamos, NM.

THERMAL-NEUTRON CAPTURE BY SILICON ISOTOPES¹

S. Raman, E. T. Jurney,² J. W. Starner,²
and J. E. Lynn²

We have studied primary and secondary γ rays (46 in ²⁹Si, 107 in ³⁰Si, and 33 in ³¹Si) following thermal-neutron capture by the stable ²⁸Si, ²⁹Si, and ³⁰Si isotopes. Almost all of these γ rays have been incorporated into corresponding level schemes consisting of 12 excited levels in ²⁹Si, 28 in ³⁰Si, and 9 in ³¹Si. In each case, the observed γ rays account for nearly 100% of all captures. The measured neutron separation energies for ²⁹Si, ³⁰Si, and ³¹Si are 8473.56

± 0.04 , 10609.24 ± 0.05 , and 6587.40 ± 0.05 keV, respectively. The measured thermal-neutron capture cross sections for ²⁸Si, ²⁹Si, and ³⁰Si are 169 ± 4 , 119 ± 3 , and 107 ± 3 mb, respectively. In all three cases, primary electric-dipole (*E1*) transitions account for the bulk of the total capture cross section. We have calculated these *E1* partial cross sections using direct-capture theory. The agreement between theory and experiment is satisfactory.

1. Abstract of published paper: *Phys. Rev. C* **46**, 972 (1992).

2. Los Alamos National Laboratory, Los Alamos, NM.

NUCLEAR STRUCTURE VIA COMPOUND NUCLEUS REACTIONS

TEST OF PREDICTED DEFORMATION - DRIVING EFFECTS IN ¹⁷³Re

N. R. Johnson, J. C. Wells,¹ F. K. McGowan,²
D. F. Winchell,² I. Y. Lee,³ P. Semmes,¹
C. Baktash, J. D. Garrett, Y. A. Akaoli,
R. Bengtsson,⁴ R. Wyss,⁵ W. C. Ma,⁶ W. B. Gao,⁶
C. Y. Yu,⁷ and S. Pilotte⁷

In recent years there has been much discussion—and occasionally some controversy—about the interpretation of the properties of light W-Re-Ir-Os-Pt nuclei. For example, for some of the odd-A isotopes of these nuclei, the behavior of B(M1)/B(E2) ratios for strongly coupled bands, the shoulder or extra peak in a plot of the dynamical moment of inertia, band crossing frequencies, and the apparent aligned angular momentum in some of the bands have been used as bases for invoking rotation alignment of $h_{9/2}$ protons. Self-consistent cranking calculations, however, indicate that in such nuclei as ¹⁷⁰W (Ref. 8) and ¹⁷²Os (Ref. 9) the 1/2[541] orbital does not play an active role in the rotation-alignment process below $\hbar\omega \approx 0.45$ MeV.

Often, the conflicting explanations of features in even-mass nuclei are best attacked through studies of their odd-A neighbors where many bands built on single-particle states are observed. The nucleus ¹⁷³Re is such a case on which γ - γ coincidence spectroscopy

measurements have been done by Bark et al.¹⁰ and Hildingsson et al.¹¹ to establish bands built on the $\pi h_{11/2}, 9/2$ [514], the $\pi d_{5/2}, 5/2^+$ [402], the $\pi i_{13/2}, 1/2^+$ [660], and the $\pi(h_{9/2}), 1/2^-$ [541] Nilsson states. The richness of these data has been complemented by refined total Routhian surface (TRS) calculations by Wyss et al.¹² They¹² find that the $\pi h_{9/2}$ surfaces have a single well-defined minimum providing an essentially unchanged deformation as the rotational frequency increases through and beyond the point of alignment of $i_{13/2}$ neutrons. On the other hand, the $\pi d_{5/2}$ and $\pi h_{11/2}$ surfaces begin at a lower deformation than the $\pi h_{9/2}$, but show significant deformation increases (~25%) at the modest rotational frequencies achieved before the backbend. Thus these TRS calculations support the idea that large deformation changes may occur within some bands and contribute to the unusual alignment patterns in this region of nuclei. To test for the possibility of large deformation changes in ¹⁷³Re we have carried out Doppler-shift recoil-distance lifetime measurements in this nucleus. In the preliminary analyses of the data carried out to this point, we have concentrated on the $d_{5/2}$ band and here we report on the preliminary results.

The ¹⁷³Re in these experiments was produced in the reaction ¹⁵⁰Sm(²⁷Al,4n)¹⁷³Re at a bombarding energy of 125 MeV. At this incident energy, the recoil velocity was $v/c = 1.20\%$. The 1.02 mg/cm² Sm target was enriched to 99.9% in mass 150. For the “zero-distance” measurement a target of 1.02 mg/

cm² ¹⁵⁰Sm evaporated onto a 42 mg/cm² Pb backing was employed. The data were recorded with a BGO Compton-suppressed Ge detector located at 0° with respect to the beam direction. Only γ - γ coincidence data were stored with the requirement that there be a trigger from at least one of an array of six Ge detectors located at 90° with respect to the beam. Coincidence spectra were taken at 23 target-stopper separations ranging from 0 to 2200 mm.

The computer program LIFETIME¹³ was used to extract lifetimes from the normalized decay curves. This program, containing the minimization routine MINUIT,¹⁴ adjusts the initial level populations and transition rates to obtain best fits for both shifted and unshifted intensities as a function of target-stopper separation. We have determined the lifetimes in both signatures of the 5/2⁺[402] band to high spins and have extracted transition quadrupole moments (Q_t) for all of the stretched E2 transitions and B(M1) values for most of the M1 transitions between the two signatures. The Q_t values are shown in Fig. 3.9 and the B(M1) values in Fig. 3.10.

Based on the results in Fig. 3.9 we can conclude that a significant change of deformation occurs in the 5/2⁺[402] band of ¹⁷³Re at very low rotational frequencies. Between the 13/2 → 9/2 and 15/2 → 11/2 transitions (corresponding to $\hbar\omega \approx 160$ keV) there is a dramatic jump of about 40% in the range of Q_t values, assuming that at the lower frequencies there is a scatter about the value $Q_t \approx 5.8$ and at the higher frequencies there is a scatter about the value $Q_t \approx 8.3$. This corresponds to a change of deformation from $\beta_2 \approx 0.22$ to $\beta_2 \approx 0.29$.

This large increase in quadrupole deformation can account for the properties of the 5/2⁺[402] band (e.g., crossing frequencies and alignment gains). However, the rather sharp increase in B(M1) values at just the same frequency where the Q_t values increase is an interesting and unexpected phenomenon. In an attempt to understand this behavior, estimates for the M1/E2 properties have been made based on the particle-rotor model¹⁵ using the Woods-Saxon potential. Two deformations have been considered, $\beta_2 = 0.205$ and $\beta_2 = 0.25$, which correspond to an intrinsic core quadrupole moment Q_0 of 5.5 b and 6.9 b, respectively. Calculations were made at each deformation, both in the strong coupling limit (i.e., with no Coriolis mixing) and with Coriolis mixing included.

Qualitatively, these calculations agree with the trends of the experimental B(M1)/B(E2) ratios and also roughly reproduce the absolute M1 and E2 transition rates at the lowest spins ($I = 7/2$ to $13/2$) for

a nearly pure 5/2⁺[402] band at the smaller deformation. In Fig. 3.10, the curve A shows the strong coupling limit, while Coriolis mixing with the 7/2⁺[404] band is included in curve B. At the larger deformation, these two Nilsson orbitals are expected to lie closer in energy, producing greater Coriolis mixing and further reducing the M1 rates (curve C). While the jump in E2 rates can be attributed to a shape change, it is difficult to understand how the M1 rates

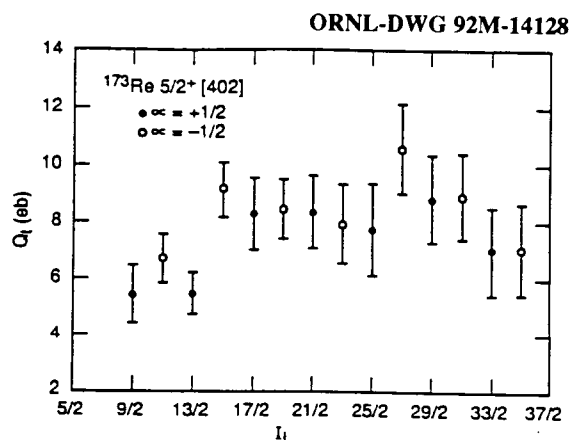


Fig. 3.9. Plot of the transition quadrupole moments as a function of initial spin for the 5/2⁺[402] band of ¹⁷³Re.

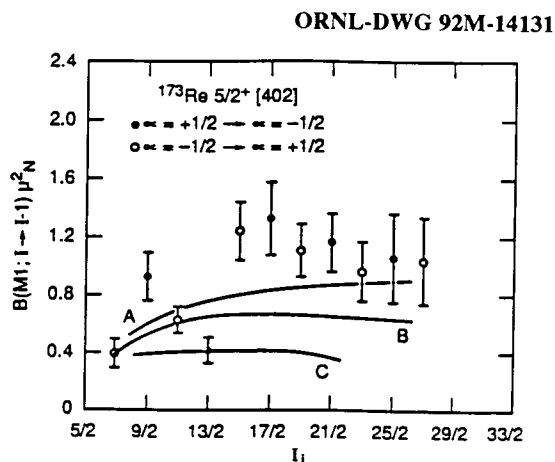


Fig. 3.10. Plot of the B(M1) values (in μ_N^2) as a function of initial spin for the M1 transitions between the two signatures of the 5/2⁺[402] band in ¹⁷³Re. The solid lines are calculated values with the particle-rotor model for the following conditions: A (strong coupling limit and $\beta^2 = 0.21$ and 0.25); B (with Coriolis mixing and $\beta^2 = 0.21$); C (with Coriolis mixing and $\beta^2 = 0.25$).

could also increase so much. The M1 properties of the $5/2^+[402]$ and $7/2^+[404]$ orbitals should change very little if the deformation increases to $\beta_2 = 0.29$, and thus cannot explain the M1 enhancement. If some alignment of $i_{13/2}$ neutrons also occurs, this should increase the M1 rate (by decreasing the effective core g_R factor), but such an alignment is difficult to reconcile with the large deformation implied by the E2 rates. Finally, we note that the idea of rotation-alignment by a pair of $h_{9/2}$ protons offers no solution because the effective core g_R would increase and, therefore, cause a reduction in $B(M1)$.

TRANSITION PROBABILITIES UP TO $I = 36^+$ IN ^{160}Yb

*N. R. Johnson, F. K. McGowan,¹ D. F. Winchell,¹
J. C. Wells,² C. Baktash, L. Chaturvedi,³
W. B. Gao,³ J. D. Garrett, I. Y. Lee,⁴ W. C. Ma,³
S. Pilotte,⁵ and C.-H. Yu⁵*

In last year's annual report we⁶ presented preliminary results from Doppler-broadened line shape (DBLS) experiments on high-spin states in ^{160}Yb , a nucleus lying just at the onset of permanent deformation and known to be very soft with respect to deformation changes, especially in the γ degree of freedom. The analyses of these measurements have since been completed and the results were reported at a recent conference.⁷

For these DBLS experiments the ^{160}Yb was produced in the reaction $^{120}\text{Sn}(^{44}\text{Ca},4n)^{160}\text{Yb}$ at a beam energy of 200 MeV. The beam was provided by the 25-MV Tandem Accelerator at Oak Ridge. Measurements were made on two different targets. In one case, 1.05 mg/cm² ^{120}Sn evaporated onto a 10 mg/cm² Au backing was employed and in the other, the same thickness of ^{120}Sn was used, but the backing was 28 mg/cm² Pb. We collected these γ -ray data in the coincidence mode with the Oak Ridge Compton Suppression Spectrometer System which consists of 20 Compton-suppressed Ge detectors. Four of the detectors are located at 45° with respect to the beam direction and four at 135°. The data stored are from coincidences in each of these detectors with any other detector.

Averages of the Q_i values determined for both the gold-backed and lead-backed targets have been taken and the results for the $I = 22^+$ through 36^+ states in the yrast sequence of ^{160}Yb are plotted in Fig. 3.11. The solid points for the states up to $I = 22^+$ in Fig. 3.11 are from our⁸ earlier recoil-distance measurements. They show an appreciable dropoff of collectivity in the frequency range $\hbar\omega = 0.26\text{--}0.36$ MeV, a phenomenon which is accounted for – at least qualitatively – in terms of cranked shell model and cranked Hartree-Fock-Bogoliubov calculations. Note that we^{8,9} have also observed loss of collectivity at similar rotational frequencies in other light ytterbium nuclei near $N = 90$.

In recent years there has been much speculation on what happens to the collectivity of these light

1. Tennessee Technological University, Cookeville, TN.

2. Partial support from the Joint Institute for Heavy Ion Research, ORNL.

3. Present address: Lawrence Berkeley Laboratory, Berkeley, CA.

4. UNISOR, Oak Ridge Institute of Science Education, ORNL.

5. Joint Institute for Heavy Ion Research, ORNL.

6. Vanderbilt University, Nashville, TN.

7. University of Tennessee, Knoxville, TN.

8. J. Recht, Y. K. Agarwal, K. P. Blume, M. Guttormsen, H. Hübel, H. Kluge, K. H. Maier, A. Maj, N. Roy, D. J. Decman, J. Dudek, and W. Nazarewicz, Nucl. Phys. A440 (1985) 336.

9. J. C. Wells, N. R. Johnson, C. Baktash, I. Y. Lee, F. K. McGowan, M. A. Riley, A. Virtanen, and J. Dudek, Phys. Rev. C 40 (1989) 725.

10. R. A. Bark, G. D. Dracoulis, A. E. Stuchbery, R. P. Byrne, A. M. Baxter, F. Riess, and P. K. Weng, Nucl. Phys. A501 (1989) 157.

11. L. Hildingsson, W. Klamra, Th. Lindblad, G. G. Linden, C. A. Kalfas, S. Kossionides, C. T. Papadopoulos, R. Vlastou, J. Gizon, D. Calrke, F. Khazaie, and J. N. Mo, Nucl. Phys. A513 (1990) 394.

12. R. Wyss, W. Satula, W. Nazarewicz, and A. Johnson, Nucl. Phys. A511 (1990) 324.

13. J. C. Wells, M. P. Fewell, and N. R. Johnson, ORNL Technical Memo ORNL-TM-9105, 1985 (unpublished).

14. F. James and M. Roos, Comput. Phys. Commun. 10 (1975) 343.

15. S. E. Larsson, G. Leander, and I. Ragnarsson, Nucl. Phys. A307 (1978) 189.

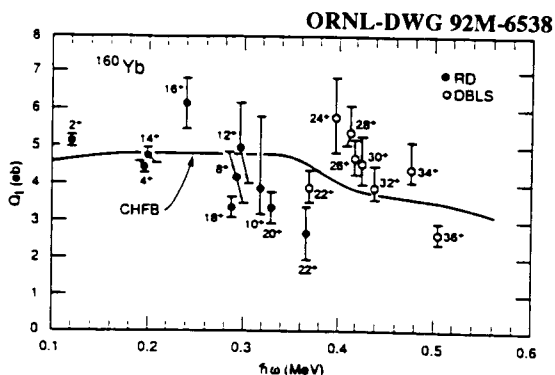


Fig. 3.11. Transition quadrupole moments (Q_2) for members of the yrast sequence in ^{160}Yb . The solid lines are from the earlier recoil-distance measurements⁸ and the open circles are from the current Doppler-broadened line shape experiments.

ytterbium nuclei at frequencies above 0.36 MeV. Our results in Fig. 3.11 indicate rather strongly that in the range of $\hbar\omega \approx 0.36\text{--}0.50$ MeV there is a regaining of collective behavior comparable to that of the lower members of the yrast sequence. The solid curve in Fig. 3.11 is based on deformation parameters from cranked Hartree-Fock-Bogoliubov calculations of Wyss and Bengtsson.¹⁰ It is clear that above $\hbar\omega \approx 0.30$ MeV there is at best only modest agreement between experiment and theory.

1. Partial support from the Joint Institute for Heavy Ion Research, ORNL.

2. Tennessee Technological University, Cookeville, TN.

3. Vanderbilt University, Nashville, TN.

4. Present address: Lawrence Berkeley Laboratory, Berkeley, CA.

5. University of Tennessee, Knoxville, TN.

6. N. R. Johnson et al., *Phys. Div. Prog. Rep. for Period Ending Sept. 30, 1991*, ORNL-6689, p. 43.

7. N. R. Johnson et al., in *Proceedings of the International Conference on Nuclear Structure at High Angular Momentum*, ed. D. Ward and J. Waddington, in press.

8. M. P. Fewell et al., *Phys. Rev. C* **31**, 1057 (1985); and *C* **37**, 101 (1988).

9. F. K. McGowan, N. R. Johnson, C. Baktash, I. Y. Lee, Y. Schutz, J. C. Wells, and A. Larabee, *Nucl. Phys. A* **539**, 276 (1992).

10. R. Wyss and R. Bengtsson, private communication.

LOW-SPIN IDENTICAL BANDS IN NEIGHBORING ODD-A AND EVEN-EVEN NUCLEI: A CHALLENGE TO MEAN-FIELD THEORIES¹

C. Baktash, J. D. Garrett, D. F. Winchell,²
and A. Smith³

A comprehensive study of odd-A rotational bands in normally-deformed rare-earth nuclei indicates that a large number of seniority-one configurations (30% for odd-Z nuclei) at low spin have moments of inertia nearly identical (within 1%) to that of the seniority-zero configuration of the neighboring even-even nucleus with one less nucleon. It is difficult to reconcile these results with conventional models, based on the traditional picture of nuclear pair correlation in vogue for more than three decades, which predict variations of about 15% in the moments of inertia of configurations differing by one unit in seniority.

1. Abstract of published paper: *Phys. Rev. Lett.* **69**, 1500 (1992).

2. Partial support from the Joint Institute for Heavy Ion Research, ORNL.

3. Participant in the Oak Ridge Science and Engineering Research Semester from Saint Joseph's College, Rensselaer, IN.

X-RAY YIELDS OF SUPERDEFORMED STATES IN ^{193}Hg ¹

D. M. Cullen,² I. Y. Lee,³ C. Baktash, J. D. Garrett,
N. R. Johnson, F. K. McGowan,²
and D. F. Winchell²

The K_{α} -x-ray yields associated with the superdeformed and normal-deformed bands in ^{193}Hg have been measured. The results indicate an excess yield of K_{α} -x rays in coincidence with the superdeformed cascade relative to that in coincidence with the normal-deformed cascade. The internal conversion of known transitions along the superdeformed cascade cannot account for the ob-

served K_{α} -x-ray yield. It is likely that this excess x-ray yield is associated with low-energy interband-M1 transitions competing with the low-spin superdeformed-E2 transitions.

-
1. Abstract of paper submitted as a Brief Report to *Physical Review C*.
 2. Partial support from the Joint Institute for Heavy Ion Research, ORNL.
 3. Present address: Lawrence Berkeley Laboratory, Berkeley, CA.

LIFETIMES OF LOW SPIN STATES IN THE SUPERDEFORMED BAND OF ^{192}Hg ¹

I. Y. Lee,² C. Baktash, D. M. Cullen,³ J. D. Garrett, N. R. Johnson, F. K. McGowan,³ D. F. Winchell,³ and C. H. Yu⁴

Lifetimes associated with the two lowest gamma-ray transitions of the superdeformed band in ^{192}Hg were measured using the recoil-distance method. It was found that these states have the same collective E2 decay strength as the high-spin states. From these lifetimes and the branching ratios to the normally-deformed states, the amplitude of the wave function corresponding to the normally-deformed shape was derived. The derived variation of the barrier penetrability as a function of spin is consistent with theoretical calculations.

-
1. Abstract of paper submitted to *Physical Review Letters*.
 2. Present address: Lawrence Berkeley Laboratory, Berkeley, CA.
 3. Partial support from the Joint Institute for Heavy Ion Research, ORNL.
 4. University of Tennessee, Knoxville, TN.

LIFETIME MEASUREMENTS FOR CONTINUUM GAMMA RAYS IN ^{164}Yb AND ^{170}Hf ¹

I. Y. Lee,² H. Xie,³ C. Baktash, W. B. Gao,³ J. D. Garrett, N. R. Johnson, F. K. McGowan,⁴ and R. Wyss⁵

Lifetimes of states associated with the ridges in the E_{γ} - E_{γ} correlation spectrum of ^{164}Yb and ^{170}Hf

were measured by the Doppler-shift attenuation method. The results indicate a reduction of the quadrupole collectivity associated with gamma rays with energy from 0.7 to 0.9 MeV and an enhancement of collectivity for those above 0.9 MeV. The reduced and the enhanced collectivity can be understood as rotationally-induced modifications of the occupation of high-j orbitals originating from below and above the Fermi surface respectively. The effect of rotational damping on the lifetimes of continuum states also is discussed.

-
1. Abstract of paper submitted to *Nuclear Physics*.
 2. Present address: Lawrence Berkeley Laboratory, Berkeley, CA.
 3. Vanderbilt University, Nashville, TN.
 4. Partial support from the Joint Institute for Heavy Ion Research, ORNL.
 5. Joint Institute for Heavy Ion Research, ORNL.

LEVEL REPULSION AND CHAOS IN THE NUCLEAR QUANTUM SYSTEM

J. D. Garrett

Recent analyses of the spacing of nuclear levels having the same spin and parity indicate¹ a systematic progression from a Poisson to a Wigner distribution (often associated² with ordered and chaotic behavior, respectively) with increasing excitation energy, see Fig. 3.12. However, even at low excitation energies where the average spacing is about 300 keV and the distribution is basically Poisson, deviations are observed for small spacings, see Fig. 3.12c. Such deviations are attributed to the level repulsion associated with the mixing of closely-spaced states having the same quantum numbers. These data indicate that this mixing apparently becomes increasingly important in deformed rare earth nuclei for separations less than about 60 keV. For higher excitation energies where the average level spacing is of the same order as or larger than the level repulsion (shown in Fig. 3.12b and 3.12a, respectively), the level-spacing distribution is Wigner shaped.

These systematics illustrate the intimate relation between the mixing of nuclear states and quantum chaos. In the limit of strong mixing, neighboring states contain little specific nuclear structure information (other than the average level spacing); there-

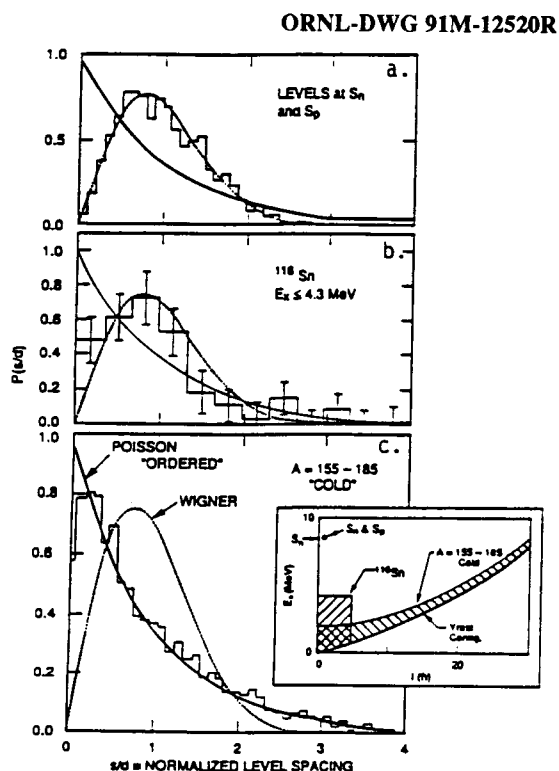


Fig. 3.12. Comparison of level-spacing distributions (histograms) for (a) levels with the same I^π at the neutron and proton threshold,² (b) for ^{116}Sn ,³ and (c) for "cold" deformed rare-earth nuclei.¹ Curves corresponding to Poisson and Wigner distributions (often associated² with "ordered" and "chaotic" behavior, respectively) are shown for each experimental distribution. The insert indicates the range of excitation energy, E_x , and angular momentum, I , associated with each data set.

fore, they are said to be chaotic. In the opposite limit, where the low-lying states are reasonably pure, neighboring states have distinctively different wave functions, hence they are termed ordered.

1. J. D. Garrett et al., in Proc. Strasbourg Conf., ed. J. Dudek (AIP, 1992, NY), in press.

2. R. Haq et al., *Phys. Rev. Lett.* **48**, 1086 (1982).

3. S. Raman et al., *Phys. Rev. C* **43**, 521 (1991).

HIGH SPIN STUDIES OF ^{181}Au

C.-H. Yu,¹ H. Q. Jin,¹ J. M. Lewis,¹ W. F. Mueller,¹
L. L. Riedinger,¹ C. Baktash, J. D. Garrett,
N. R. Johnson, I. Y. Lee,² F. K. McGowan,³
and D. Winchell³

High-spin states were populated using the reaction $^{150}\text{Sm}(^{35}\text{Cl},4n)^{181}\text{Au}$ at a beam energy of 164 MeV. The experiment was carried out at the Oak Ridge National Laboratory, and the γ rays were detected by the Spin Spectrometer consisting of 20 Compton-suppressed Ge detectors and a 52-element NaI multiplicity filter. About 75 million double- or higher-fold coincidence events were collected in the experiment. A preliminary data analysis extends our previously established⁴ $\pi i_{13/2}$ and $\pi h_{9/2}$ decay sequences in ^{181}Au to higher angular momenta, making a systematic analysis of configuration-dependent shapes possible for the light Au isotopes.

Figure 3.13 shows the aligned angular momenta for the $\pi i_{13/2}$ and $\pi h_{9/2}$ bands in $^{181,183,185,187}\text{Au}$. An interesting feature displayed in this figure is the gradual disappearance of a band crossing in the $\pi i_{13/2}$ band with decreasing neutron number. This crossing, clearly established⁵ in ^{187}Au and understood as the $h_{9/2}$ proton crossing, is completely absent in ^{181}Au , in which a gradual alignment gain dominates the entire $\pi i_{13/2}$ sequence instead (see Fig. 3.13). Such an evolution of proton crossing as a function of neutron number is a typical example that shows the strong influence of nuclear collective degrees of freedom (shape variations) on single-particle motions. The neutron Fermi levels of these Au nuclei are in the mid- or upper portion of the $i_{13/2}$, $h_{9/2}$, and $f_{7/2}$ subshells. The decrease of neutron number is therefore expected to increase the quadrupole deformation due to the occupation of fewer up-sloping levels. Indeed, the gradual alignment observed in the $\pi i_{13/2}$ band in the lightest ^{181}Au is an indication of a larger quadrupole deformation with its obviously larger moments of inertia. The calculated⁶ total Routhian surfaces also predict smaller γ deformation for lighter Au isotopes (e.g., ^{181}Au) compared to the heavier isotopes. Cranked shell-model calculations show that in this mass region, the proton $h_{9/2}$ crossing occurs at a higher frequency with increasing quadrupole deformation and decreasing γ deformation. The missing crossing in the $\pi i_{13/2}$ band of ^{181}Au thus can

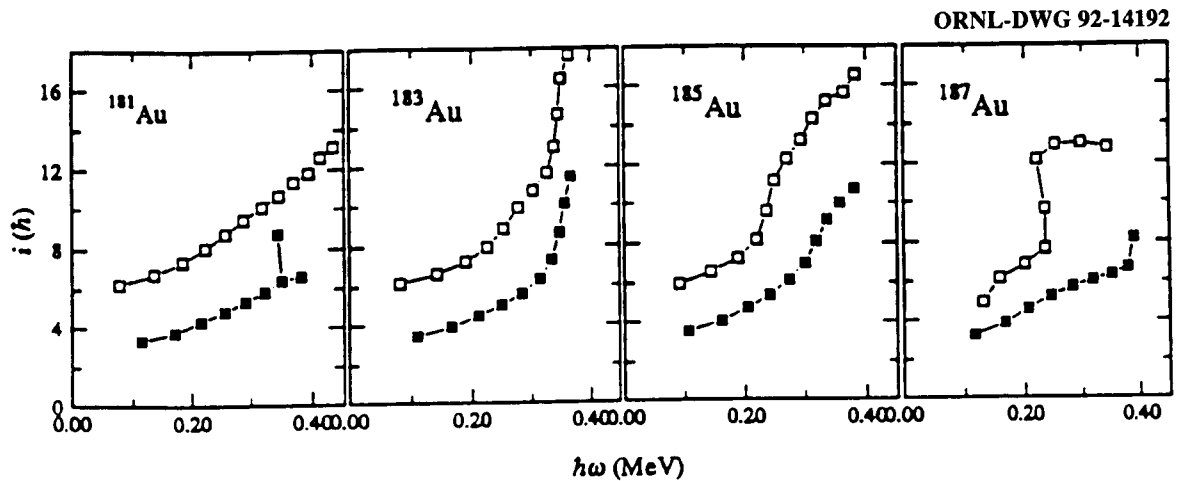


Fig. 3.13. Aligned angular momenta as a function of rotational frequency for $^{181,183,185,187}\text{Au}$. The open and closed symbols denote the $\pi_{113/2}$ and $\pi_{h9/2}$ bands, respectively. The reference configuration used is parametrized by the Harris formula using $J^{(1)} = 22 \hbar^2/\text{MeV}$, and $J^{(2)} = 90 \hbar^4/\text{MeV}$. Data for ^{183}Au , ^{185}Au , and ^{187}Au are taken from Refs. 7, 8, 5, respectively.

be understood, since the crossing frequency may be beyond 0.45 MeV where the experimental data stop.

1. University of Tennessee, Knoxville, TN.
2. Present address: Lawrence Berkeley Laboratory, Berkeley, CA.
3. Partial support from the Joint Institute for Heavy Ion Research, ORNL.
4. H. Q. Jin et al., p. 26 in *University of Tennessee Annual Report* (1988).
5. J. K. Johansson et al., *Phys. Rev. C* **40**, 132 (1989).
6. R. Wyss, W. Nazarewicz et al., private communication.
7. L. Zhou et al., p. 21 in *University of Tennessee Annual Report* (1988).
8. A. J. Larabee et al., *Phys. Lett.* **B169**, 21 (1986).

ON THE QUESTION OF SPIN FITTING AND QUANTIZED ALIGNMENT IN ROTATIONAL BANDS¹

C. Baktash, W. Nazarewicz,² and R. Wyss²

Several methods employed to parameterize the spins of the superdeformed bands in terms of their

observed gamma-ray energies are closely examined. It is pointed out that, since the proposed fitting procedures are variants of the Harris expansion formula, they cannot be applied to determine the unknown spins of the *excited* bands due to the possible presence of non-zero initial alignments. A comprehensive study of the normally-deformed excited bands indicates that no correlation exists between the fitted spins and the experimentally known values. Therefore, there is no firm evidence for the presence of anomalous relative alignments between the superdeformed identical bands in the Hg region. Additionally, a critical review of several of the models and scenarios that purport to explain the origin of the identical bands, or the patterns of the fitted alignments, is presented. It is concluded that none of these models can satisfactorily explain the identical moments of inertia in neighboring nuclei and the systematics of the observed or fitted alignments. Thus, the important question of the microscopic origin of the identical bands remains to be investigated.

1. Abstract of paper submitted to *Nuclear Physics*.
2. Joint Institute for Heavy Ion Research, ORNL.

SEARCH FOR HYPERDEFORMATION IN THE LIGHT Hg ISOTOPES

*P. F. Hua,¹ D. G. Sarantites,¹ J. Barreto,¹
A. Kirov,¹ L. Sobotka,¹ C. Baktash, D. M. Cullen,²
I. Y. Lee,³ J. D. Garrett, N. R. Johnson,
F. K. McGowan,² and W. C. Ma⁴*

Recent total Routhian surface calculations⁵ by Nazarewicz have indicated that hyperdeformed states (major to minor axis ratio $\approx 3:1$) may form the yrast line in the light Hg isotopes at relatively low spin values of $I \approx 30-40 \hbar$. There exists a non-negligible chance that these states would survive fission and become accessible to experimental observation. Motivated by these predictions, we have undertaken an experimental study of the high-spin structures in ^{182}Hg , which were populated using the reaction $^{154}\text{Gd}(^{32}\text{S},4n)$ at a beam energy of 165 MeV. This experiment was performed at the HHIRF with 12 Compton-suppressed Ge detectors in the compact-geometry configuration. Four BaF_2 detectors, inserted in anti-Compton shields, served as a multiplicity filter to select the high-spin events. In addition, a segmented tubular plastic counter allowed identification of the evaporated charged particles and, indirectly, the fission fragments. In this arrangement, it was possible to construct two-dimensional gamma-gamma matrices, from which contributions of the exit channels involving fission and charged-particle emission were removed. One such matrix was constructed and examined for the presence of regularly spaced cascades of gamma rays. Although a few candidates were found that gave the appropriately large moment of inertia, we could not unambiguously establish that they originated from a single rotational band. These results indicate an upper limit of 1% for the population of a discrete hyperdeformed band in ^{182}Hg . Further analysis of these data is in progress.

This matrix was also analyzed to construct a partial level scheme for ^{182}Hg . So far, we have established five normally-deformed rotational bands that extend to a maximum spin of $I = 22$. These data offer a valuable opportunity to extend the shape-coexistence studies of Hg nuclei to very neutron-deficient isotopes.

3. Present address: Lawrence Berkeley Laboratory, Berkeley, CA.

4. Vanderbilt University, Nashville, TN.

5. W. Nazarewicz, in *Proceedings of the International Conference on Nuclear Structure at High Angular Momentum*, Ottawa, May 1992.

THE FIRST SPECTROSCOPY OF ^{182}Au

*D. M. Cullen,¹ C. Baktash, I. Y. Lee,² J. D. Garrett,
N. R. Johnson, F. K. McGowan,¹ P. F. Hua,³
D. G. Sarantites,³ J. Barreto,³ A. Kirov,³
and L. Sobotka³*

A detailed study of the odd-odd nucleus ^{182}Au has been made for the first time. This work was carried out at the Holifield Heavy Ion Research Facility, utilizing the Compact-Ball array of 20 Compton-suppressed gamma-ray spectrometers. Channel selection was obtained via multiplicity information from a group of BaF_2 detectors placed around the Compact Ball in a plane perpendicular to the beam direction. Furthermore, a specially constructed plastic-scintillator detector, developed by Sarantites et al.,⁴ was placed inside the beam tube. This detector surrounded the target, giving information on the number of charged particles emitted and was used to veto fission events by tagging a particular charged-particle exit channel.

^{182}Au was populated with the reaction $^{154}\text{Gd}(^{32}\text{S},p3n)^{182}\text{Au}$ at a beam energy of 165 MeV. The target consisted of a 1 mg/cm² self-supporting foil of ^{154}Gd . A symmetrized gamma-gamma coincidence matrix with 68×10^6 events was produced from these data. Two rotational bands containing about 7 or 8 transitions have been observed for the first time in ^{182}Au . These bands extend up to spins assumed to be around $26 \hbar$ from a comparison with the neighboring odd-odd nuclei. The bands also appear in coincidence with each other, and the dipole cross-over transitions are observed. A more detailed analysis is presently being carried out, and DCO ratios are being measured to determine the multipolarity of the gamma rays.

1. Washington University, St. Louis, MO.

2. Partial support from the Joint Institute for Heavy Ion Research, ORNL.

1. Partial support from the Joint Institute for Heavy Ion Research, ORNL.

2. Present address: Lawrence Berkeley Laboratory, Berkeley, CA.

3. Washington University, St. Louis, MO.

4. See P. F. Hua et al., "Search for Hyperdeformation in the Mass $A \approx 182$ Region," this report.

THE MASS DEPENDENCE OF MOMENTS OF INERTIA OF RAPIDLY-ROTATING NUCLEI¹

*D. F. Winchell,² D. O. Ludwigsen,³
and J. D. Garrett*

An analysis of high-spin moments of inertia for the yrast sequences of deformed nuclei from $A = 72-184$ indicates that, within each deformed mass region, the moment of inertia is surprisingly constant. In contrast, between the different deformed mass regions the $A^{5/3}$ dependence of the moment of inertia, expected for a macroscopic rotor, is approximately restored.

1. Abstract of published paper: *Phys. Lett.* **B289**, 267 (1992).

2. Partial support from the Joint Institute for Heavy-Ion Research, ORNL.

3. Participant in the University of Tennessee Science Alliance Undergraduate Summer Program from Beloit College, Beloit, WI.

HIGH-SPIN STRUCTURE OF ¹⁶⁷W AND ¹⁶⁸W¹

*K. Theine,² A. P. Byrne,^{2,3} H. Hübel,² M. Murzel,²
R. Chapman,⁴ D. Clarke,^{4,5} F. Khazaie,^{4,5}
J. C. Lisle,⁴ J. N. Mo,⁴ J. D. Garrett, H. Ryde,⁶
and R. Wyss^{7,8}*

Excited states in ¹⁶⁷W and ¹⁶⁸W, populated in the ¹⁴²Nd(³⁰Si,xn) reaction, were investigated at high spins using the ESSA30 array with 29 Compton-suppressed Ge detectors. The level schemes are extended to higher spins and several new rotational bands are identified. The results are discussed in comparison with existing data on the neighboring $N = 93$ and 94 isotones and on the $Z = 74$ W isotopes. A theoretical analysis is presented within the framework of a pairing-self-consistent cranked shell model

using shape parameters obtained from total-routhian-surface calculations.

1. Abstract of paper submitted to *Nuclear Physics A*.

2. Institut für Strahlen-und Kernphysik, Universität Bonn, Germany.

3. Present address: Australian National University, Canberra, Australia.

4. Schuster Laboratory, University of Manchester, Manchester, U.K.

5. Present address: NNC Ltd., Knutsford, U.K.

6. University of Lund, Lund, Sweden.

7. Manne Siegbahn Institute of Physics, Stockholm, Sweden.

8. Joint Institute for Heavy Ion Research, ORNL.

HIGH SPIN STATES IN NEUTRON RICH NUCLEI FROM SPONTANEOUS FISSION¹

*K. Butler-Moore,² S. Zhu,² X. Zhao,²
J. H. Hamilton,² A. V. Ramayya,² Q. Lu,²
W.-C. Ma,² L. K. Peker,² J. Kormicki,² J. K. Deng,²
P. Gore,² D. Shi,² E. F. Jones,² H. Xie,²
W. B. Gao,² J. D. Cole,³ R. Aryaeinejad,³ I. Y. Lee,
N. R. Johnson, F. K. McGowan,⁴ C. E. Bemis,
G. Ter-Akopian,⁵ and Yu. Oganessian⁵*

One fragment- γ - γ and three γ - γ coincidence measurements of the prompt γ -rays from the fragments produced in the spontaneous fission (SF) of ²⁵²Cf and very recently of ²⁴²Pu were carried out with a 20 Ge detector ball at HHIRF. With our high statistics, γ - γ coincidences, where the two gates are on transitions in the two partner fragments, were extracted. Comparing the ²⁵²Cf and ²⁴²Pu data allowed unique placements of many transitions. New, higher spin states were observed in many nuclei, up to 16^+ in some of the heavy partners. Levels in several nuclei were observed for the first time. Studies of the fission process included measured relative branchings to the 1n to 6n channels. Much data remains to be analyzed. These data provide new insights into the changing structures at higher spins of many neutron-rich nuclei and the fission process.

1. Abstract of paper to be published in *Proceedings International Conference on Nuclei Far From Stability and Atomic Masses*, Germany, July, 1992.

2. Vanderbilt University, Nashville, TN.
3. Idaho National Engineering Laboratory, Idaho Falls, ID.
4. Partial support from the Joint Institute for Heavy Ion Research, ORNL.
5. Joint Institute for Nuclear Research, Dubna, Russia.

FIRST EVIDENCE FOR STATES IN Hg NUCLEI WITH DEFORMATIONS BETWEEN NORMAL- AND SUPER-DEFORMATION¹

W. C. Ma,² J. H. Hamilton,² A. V. Ramayya,²
 L. Chaturvedi,² J. K. Deng,² W. B. Gao,²
 Y. R. Jiang,² J. Kormicki,² X. W. Zhao,²
 N. R. Johnson, J. D. Garrett, I. Y. Lee, C. Baktash,
 F. K. McGowan,³ W. Nazarewicz,⁴ and R. Wyss⁴

High-spin states in ¹⁸⁶Hg with a quadrupole deformation of $\beta_2 = 0.34(4)$ have been established from measured gamma-ray coincidences and lifetimes. These data, which provide the first evidence for a deformation midway between normal- and super-deformed, can be interpreted in terms of the [651 1/2] and [770 1/2] neutron configurations.

-
1. Abstract of paper accepted for publication in *Physical Review C*.
 2. Vanderbilt University, Nashville, TN.
 3. Partial support from the Joint Institute for Heavy Ion Research, ORNL.
 4. Joint Institute for Heavy Ion Research, ORNL.

NEW HIGH-SPIN EXCITATION MODES IN ¹⁸⁴Hg

J. K. Deng,¹ W. C. Ma,¹ J. H. Hamilton,¹
 A. V. Ramayya,¹ J. Kormicki,¹ X. W. Zhao,¹
 W. B. Gao,¹ I. Y. Lee, J. D. Garrett, N. R. Johnson,
 D. Winchell,² M. Halbert, C. Baktash

The region of neutron-deficient Hg isotopes presents an extraordinarily rich variety of shape evolution and shape coexistence phenomena. The under-

standing of these nuclei has recently been deepened rapidly through extensive experimental and theoretical efforts devoted to this region. The coexistence between different structures at low spins and low excitation energies in the ¹⁸²⁻¹⁸⁸Hg isotopes is experimentally well established.³ Our previous experiments for ¹⁸⁶Hg revealed higher-spin states up to 32 \hbar (Ref. 4), and five new rotational bands were found. To further understand the properties of these new bands we need to study the high-spin states in ¹⁸⁴Hg and other neighboring nuclei.

A new ¹⁸⁴Hg γ - γ coincidence experiment was performed recently at Holifield Heavy Ion Research Facility. The high-spin structure of ¹⁸⁴Hg was populated by using the ¹⁵⁶Gd(³²S,4n) reaction at the tandem accelerator at ORNL, with a beam energy of 160 MeV as selected in the previous experiment.⁵ A self-supporting stacked ¹⁵⁶Gd target, with total thickness of 1085 $\mu\text{g}/\text{cm}^2$, was used. In-beam γ -ray coincidence events were detected with the Spin Spectrometer which included 18 Ge detectors and 54 NaI counters as sum-energy and multiplicity filter. Only the events with multiplicity ≥ 12 were collected. They were decomposed later into 149 million double-coincidence events.

New transitions in ¹⁸⁴Hg were identified by their coincidence relations with previously established transitions.^{5,6} The higher-spin states in the ¹⁸⁴Hg yrast band were extended up to (26⁺). Seven new rotational bands were observed for the first time in these data. The 8⁻ isomeric state and bands built on it, as found in the N = 106 isotone chain,⁷ were not found. Theoretical calculations based on the framework of CSM are currently underway.

-
1. Vanderbilt University, Nashville, TN.
 2. Partial support from the Joint Institute for Heavy Ion Research, ORNL.
 3. J. H. Hamilton et al., *Rep. Prog. Phys.* **48**, 631 (1985).
 4. W. C. Ma et al., submitted to *Physical Review Letters*.
 5. W. C. Ma et al., *Phys. Lett.* **167B**, 277 (1986).
 6. J. D. Cole et al., *Phys. Rev. Lett.* **37**, 1185 (1976).
 7. J. H. Hamilton, p. 387 in *Proceedings International Symposium on Heavy Ion Physics and Its Applications*, Lanzhou, Oct. 1990.

NUCLEAR STRUCTURE STUDIES VIA RADIOACTIVE DECAY

SEARCH FOR THE α DECAY OF ^{190}Hg AND THE α -DECAY BRANCHES OF ^{186}Hg AND ^{188}Hg

*K. S. Toth, Y. A. Akovali, C. R. Bingham,¹
H. K. Carter,² Y. Hatsukawa,³ P. F. Mantica,²
and M. Zhang¹*

In a discussion⁴ of α -decay half-lives of even-even nuclei in the lead mass region it was noted that Hg isotopes appear to have decay rates that are slower than those of Pb nuclides. The result is unexpected since there should be a hindrance effect of the $Z = 82$ closed shell on the Pb α -decay half-lives. We decided to provide additional data on the subject by remeasuring the α branching ratios of the two heaviest known Hg α emitters, namely ^{186}Hg and ^{188}Hg , since for each of these isotopes only one experimental determination of its α branch was available. As part of the investigation we also attempted to identify the α decay of ^{190}Hg .

Natural tungsten was bombarded with ^{12}C ions extracted from the Holifield Heavy Ion Research Facility 25-MV Tandem accelerator. Three bombarding energies were selected in turn to maximize yields for the Hg nuclides, and the UNISOR on-line isotope separator was used to mass separate reaction products. These were collected on a movable tape system which was programmed to transport radioactivities to an array of α -particle and γ -ray detectors following a preset collection time. Collection and counting times were optimized for the half-life of the mercury nuclide being investigated. The Ge γ -ray detectors were calibrated for energy and absolute efficiency with an NBS standard Eu source while the Si(Au) α -particle detector was calibrated with ^{240}Pu and ^{244}Cm sources whose absolute disintegration rates were known.

Figure 3.14 shows the α -particle spectra recorded at $A = 186$ [part (a)], $A = 188$ [part (b)], and $A = 190$ [part (c)]. For ^{186}Hg the intensities of the strong 112.1- and 251.5-keV γ rays were used together with the adopted⁵ decay scheme to calculate the isotope's (EC+ β^+)-decay strength. By comparing this intensity with that of the 5094-keV α transition [see Fig. 3.14(a)] the ^{186}Hg α branch was deduced to be 1.8×10^{-4} . This branch agrees with the available⁵ value of 1.6×10^{-4} . For ^{188}Hg the most intense γ -ray transition

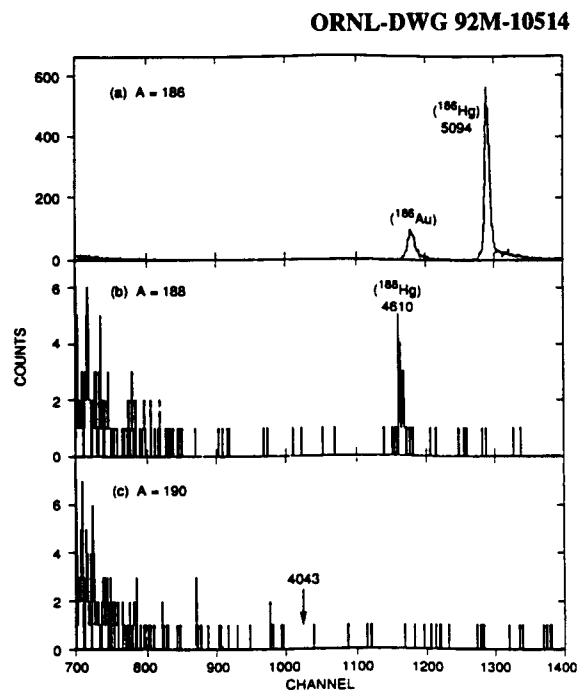


Fig. 3.14. Alpha-particle spectra recorded for mass-separated sources produced in ($^{12}\text{C} + \text{natW}$) bombardments.

(66.7 keV) is obscured by K x rays and we are currently evaluating intensities for the other, much weaker, ^{188}Hg γ rays with which to determine the (EC+ β^+)-decay strength. In the meantime, based on the adopted⁶ decay scheme, we converted our $\text{K}\alpha_1$ and $\text{K}\beta_2$ x-ray intensities to a number related to the ^{188}Hg (EC+ β^+)-decay strength. From this and the intensity of the 4610-keV α transition [see Fig. 3.14(b)] we deduced a preliminary ^{188}Hg α branch of 4.2×10^{-7} which agrees with the available⁶ value of 3.7×10^{-7} . In Fig. 3.14(c) we indicate by an arrow the expected location of the ^{190}Hg α peak if its energy is indeed 4043 keV as predicted⁷ from systematics. The $A = 190$ data were accumulated for two days but no α group was seen in the vicinity of that energy. The ^{190}Hg (EC+ β^+)-decay strength was determined based on the isotope's adopted⁷ decay scheme and the intensity of its strongest γ ray, 142.6 keV. We then deduced an upper limit of 3.4×10^{-9} for the ^{190}Hg α branch by assuming that a peak with 5 counts close to

the predicted energy would have provided us with clear cut evidence for the α decay of ^{190}Hg . The previously available upper limit⁷ is 5×10^{-7} .

1. University of Tennessee, Knoxville, TN.
2. UNISOR, Oak Ridge Associated Universities, Oak Ridge, TN.
3. Japan Atomic Energy Research Institute, Tokai, Ibaraki 319-11, Japan.
4. K. S. Toth et al., *Phys. Rev. Lett.* **53**, 1623 (1984).
5. R. B. Firestone, *Nucl. Data Sheets* **55**, 583 (1988).
6. B. Singh, *Nucl. Data Sheets* **59**, 133 (1990).
7. B. Singh, *Nucl. Data Sheets* **61**, 243 (1990).

STUDY OF PLATINUM NUCLEI WITH THE ATLAS FRAGMENT MASS ANALYZER

K. S. Toth, C. N. Davids,¹ B. B. Back,¹ K. Bindra,² C. R. Bingham,³ W. Chung,⁴ D. J. Henderson,¹ T. Lauritsen,¹ D. M. Moltz,⁵ A. V. Ramayya,² J. D. Robertson,⁶ and W. B. Walters⁷

The fragment mass analyzer (FMA)⁸ at the Argonne National Laboratory has recently undergone a series of commissioning tests using beams from the ATLAS facility. One such test involved the study of short-lived neutron-deficient platinum α -emitting isotopes produced in ^{32}S irradiations of ^{144}Sm . Following their traversal through the FMA, fusion reaction products were implanted in a Si(Au) detector placed behind a parallel plate avalanche counter (PPAC) located at the focal plane of the FMA. The subsequent α -particle decays of these recoils were then investigated, with spectra recorded both during bombarding and counting intervals. During the counting intervals a beam sweeper was used to deflect the ^{32}S ions off the ^{144}Sm target. The M/q resolution of the FMA was found to be about one part in 350. Excellent beam rejection was accomplished by means of a time-of-flight measurement between the PPAC and the surface barrier detector.

Two bombarding energies, 164 and 200 MeV, were used to emphasize the production of (^{173}Pt and ^{172}Pt) and of (^{171}Pt and ^{170}Pt), respectively. The half-lives of ^{173}Pt and ^{172}Pt were determined to be 290(60) ms and 110(20) ms in agreement with values adopted^{9,10} for the two isotopes. In Fig. 3.15 we show the spectrum accumulated in the 200 MeV irradiation

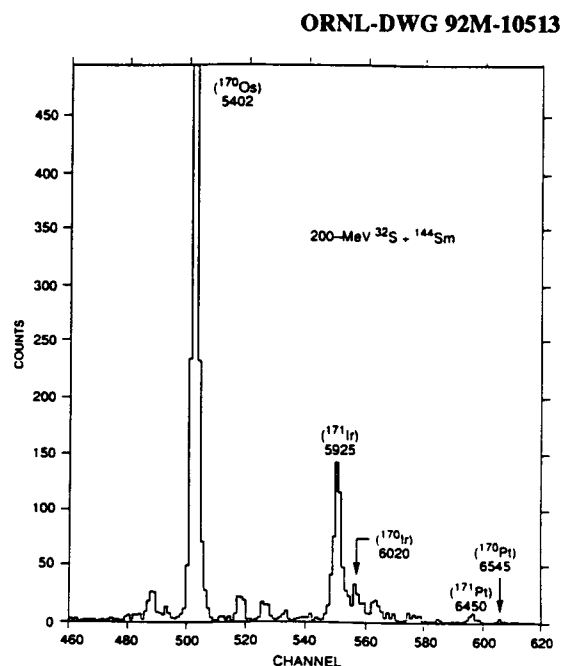


Fig. 3.15. Alpha-particle spectrum of reaction products implanted in a Si(Au) detector following their traversal through the ATLAS fragment mass analyzer.

when the beam was both on and off the ^{144}Sm target. While the α peaks of ^{171}Pt and ^{170}Pt are clearly present in Fig. 3.15, one sees the low cross sections encountered for these extremely proton-rich ($^{32}\text{S},5n$) and ($^{32}\text{S},6n$) reaction products. For ^{171}Pt half-lives of 40(10) ms and 20(6) ms have been reported;¹¹ our estimate of ~ 45 ms favors the first of these two values. In the case of ^{170}Pt , only three α -decay events were observed when the beam was deflected off the target. Since they were all registered in the first 10-ms time bin of the 80-ms counting interval used in the A = 171 and A = 170 measurements, our results support the one available half-life determination¹² for ^{170}Pt , namely 6^{+5}_{-2} ms. We plan to have an experiment in the near future wherein the bombarding and counting times will be optimized to obtain a better half-life measurement for ^{170}Pt with which to improve our understanding of α -decay rates in this mass region.

1. Argonne National Laboratory, Argonne, IL.
2. Vanderbilt University, Nashville, TN.
3. University of Tennessee, Knoxville, TN.
4. Notre Dame University, Notre Dame, IN.
5. Lawrence Berkeley Laboratory, Berkeley, CA.

6. University of Kentucky, Lexington, KY.
7. University of Maryland, College Park, MD.
8. C. N. Davids and J. D. Larson, *Nucl. Instrum. Methods B40/41*, 1224 (1988).
9. V. S. Shirley, *Nucl. Data Sheets* **54**, 589 (1988).
10. W. Gongqing, *Nucl. Data Sheets* **51**, 577 (1987).
11. V. S. Shirley, *Nucl. Data Sheets* **43**, 127 (1984).
12. S. Hofmann et al., *Z. Phys. A299*, 281 (1981).

ALPHA DECAYS OF LIGHT URANIUM ISOTOPES¹

K. S. Toth, H. J. Kim, J. W. McConnell,
C. R. Bingham,² and D. C. Sousa³

With the use of a velocity filter, the α -particle decays of ²²⁴U and ²²⁵U were studied in ¹⁹F bombardments of ²⁰⁹Bi. The data obtained for these two isotopes are compared with those of previous investigators, and the α -decay rates of ^{222,224,226}U are discussed within the context of partial α half-lives for even-even nuclei with $Z \geq 84$.

1. Abstract of published paper: *Phys. Rev. C* **45**, 856 (1992).

2. University of Tennessee, Knoxville, TN.

3. Eastern Kentucky University, Richmond, KY.

INVESTIGATION OF SHORT-LIVED RARE EARTH NUCLEI

K. S. Toth, J. M. Nitschke,¹ D. C. Sousa,²
K. S. Vierinen,¹ and P. A. Wilmarth¹

We have investigated the nuclear structure characteristics of neutron-deficient rare-earth nuclei near the proton drip line by studying the decay properties of short-lived isotopes produced in bombardments of Ru, Mo, and Nb targets with ⁵⁸Ni and ⁶⁴Zn ions extracted from the Lawrence Berkeley Laboratory SuperHILAC. Products of interest were mass separated with the OASIS on-line facility³ and then assayed with particle and γ -ray detectors. Herein we

discuss recent results dealing with the decays of ¹⁴⁵Dy, ¹⁵⁵Lu, ¹⁵⁷Lu, and ¹⁵⁴Tm.

While ¹⁴⁵Dy is a well-characterized⁴ β -delayed-proton emitter, essentially no information is available concerning levels in its (EC + β^+)-decay daughter with only four γ rays having been assigned⁵ to ¹⁴⁵Dy. We have observed numerous γ rays following ¹⁴⁵Dy (EC + β^+) decay and have also made a thorough dissection of its β -delayed-proton spectrum, including the detection of protons in coincidence with positrons, x rays, and γ rays. The γ -ray coincidences show that, in addition to the ground state, the first 2^+ level in ¹⁴⁴Gd is fed by the proton decays. Population of these two levels demonstrates that there are states in ¹⁴⁵Dy with very different spins that emit β -delayed protons. A comparison of the experimental final-state feedings with values predicted by statistical model calculations shows that the assignments for these ¹⁴⁵Dy precursors are consistent with the $vs_{1/2}$ (ground state) and $vh_{1/2}$ (isomer) orbitals expected from systematics. Indeed, we have identified a 108.1-keV γ ray which decays with a 6(2)-s half-life rather than the 14.5(10)-s value that we observe for most of the other intense ¹⁴⁵Dy transitions. Because the predominant number of γ rays decay with the longer half-life, which agrees with published⁵ values for ¹⁴⁵Dy, it must represent the decay of the $h_{1/2}$ isomer while the new 6-s half-life must be due to the decay of the $s_{1/2}$ ground state. In Fig. 3.16 we show a partial ¹⁴⁵Dy decay scheme that involves low-lying single-proton levels in ¹⁴⁵Tb associated with the 108.1-keV transition which is at the base of a three- γ -ray cascade, 184.5 \rightarrow 145.1 \rightarrow 108.1 keV. In addition, there is a cross-over transition, 253.1 keV, which is in coincidence with the 184.5-keV γ ray but not with the other two. A sequence of four states, 0.0, 108.1, 253.1, and 437.7 keV, is then established and, on the basis of single-proton level systematics for $N = 82, 84$, and 86 odd- A Tb, Ho, and Tm nuclei, one would propose assignments of $s_{1/2}$, $d_{3/2}$, $d_{5/2}$, and $g_{7/2}$, respectively, for these states. However, we also observe an intense 437.7-keV γ ray, not in coincidence with any strong transitions. It therefore appears to de-excite the 437.7-keV level directly to the base state (either ground or first-excited state) for the ¹⁴⁵Tb low-spin levels. This 437.7-keV cross-over transition implies that the base state is $d_{3/2}$ and not $s_{1/2}$ and that the level sequence in this $N = 80$ nucleus is $d_{3/2}$, $s_{1/2}$, $d_{5/2}$, and $g_{7/2}$.

We recently discovered evidence⁶ of second, lower-energy, α groups from ¹⁵⁵Lu and ¹⁵⁷Lu (see also Refs. 7 and 8). These data provide information

on the ground and first-excited states in these Lu isotopes. The new groups have low heavy-ion-induced production yields so they must originate from levels with spins lower than those of states emitting the previously known higher-energy α groups. These latter transitions, 5648- (^{155}Lu) and 4988-keV (^{157}Lu), based on their allowed α -decay rates,⁶ proceed from $h_{11/2}$ states to the same proton levels (ground states) in ^{151}Tm and ^{153}Tm , respectively. While α branches for the new 5579- (^{155}Lu) and 4924-keV (^{157}Lu) groups are not known, the 140-ms half-life⁶ of the ^{155}Lu transition, when compared to β -decay rates of nearby nuclei, indicates that, for it, α decay predominates. If its branch is assumed to be 79% (that of the 5648-keV ^{155}Lu emitter) then its α width of 0.066 MeV indicates an unhindered decay from a low-spin ($d_{3/2}$ or $s_{1/2}$) state to the $s_{1/2}$ isomer in ^{151}Tm . Since the same decay patterns ($h_{11/2} \rightarrow h_{11/2}$ and $s_{1/2} \rightarrow s_{1/2}$) are seen for the α -emitting $h_{11/2}$ and $s_{1/2}$ states in Tm and Ho odd-A isotones, one surmises that the 4924-keV ^{157}Lu transition also feeds the ^{153}Tm $s_{1/2}$ isomer. Initial and final level energies and α -decay Q-values then are such that the $h_{11/2}$ levels cannot be the ground states in ^{155}Lu as they are in Tm and Ho with $N = 84$

and 86. Instead, they have to be ~ 22 keV above the low-spin ($d_{3/2}$ or $s_{1/2}$) ground states.

In a series of ^{64}Zn bombardments of ^{94}Mo and ^{92}Mo we investigated the decay properties of the high- and low-spin ^{154}Tm isomers (probable spin assignments of 9^+ and 2^- , respectively). The $8^+ \rightarrow 6^+ \rightarrow 4^+ \rightarrow 2^+ \rightarrow 0^+$ γ -ray cascade⁹ in ^{154}Yb was observed, together with the well-established⁹ 5031-keV (9^+ level) and 4956-keV (2^- level) α transitions. In our irradiations of ^{92}Mo , ^{154}Tm could be produced directly only from heavier Mo isotopes present in the target material. Instead, most of this nuclide originated from the β decay of ^{154}Yb and the yield of the high-spin isomer was therefore greatly suppressed *via-à-vis* the low-spin state. In these experiments with the ^{92}Mo target, coincidences between α particles and γ rays revealed a new, very weak, α transition (associated with the 2^- state) which populates a low-spin ^{150}Ho level at ~ 130 keV previously seen¹⁰ in the β decay of ^{150}Er . Its intensity is $\sim 2 \times 10^{-3}$ that of the 4956-keV transition.

ORNL-DWG 92M-10512

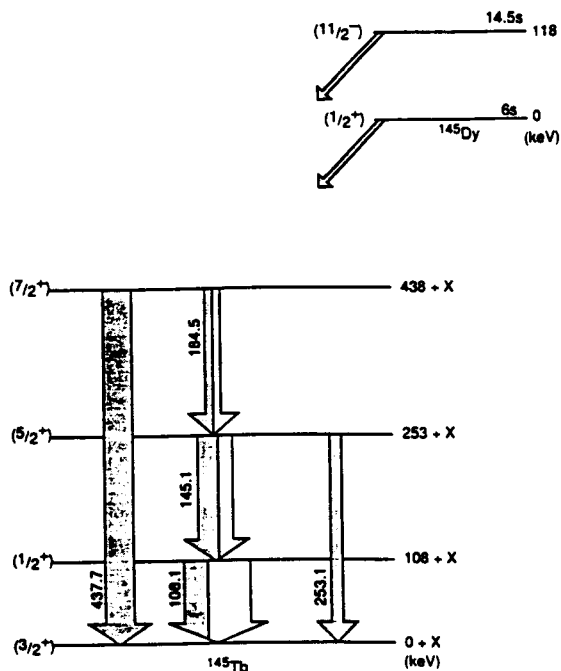


Fig. 3.16. Partial ($\text{EC} + \beta^+$)-decay scheme of ^{145}Dy .

1. Lawrence Berkeley Laboratory, Berkeley, CA.
2. Eastern Kentucky University, Richmond, KY.
3. J. M. Nitschke, *Nucl. Instrum. Methods* **206**, 341 (1983).
4. D. Schardt et al., p. 229 in *Proc. of the 7th Inter. Conf. on Atomic Masses and Fundamental Constants*, Darmstadt-Seeheim (1984).
5. L. K. Peker, *Nucl. Data Sheets* **49**, 1 (1986).
6. K. S. Toth et al., *Z. Phys. A* **340**, 343 (1991).
7. S. Hofmann et al., *Z. Phys. A* **333**, 107 (1989).
8. M. Lewandowski et al., *Z. Phys. A* **340**, 107 (1991).
9. R. G. Helmer, *Nucl. Data Sheets* **52**, 1 (1987).
10. K. S. Toth et al., *Phys. Rev. C* **35**, 620 (1987).

IDENTIFICATION OF THE β -DECAY BRANCH OF $^{147}\text{Tm}^1$

K. S. Toth,² D. C. Sousa,² P. A. Wilmarth,³
J. M. Nitschke,³ and K. S. Vierinen³

The $h_{11/2}$ ground state of ^{147}Tm has been known^{4,5} for about a decade to be a direct proton emitter. While cross-section measurements, barrier-penetration calculations, and gross β -decay half-life predictions have all indicated that the radioactivity's dominant decay mode is ($\text{EC} + \beta^+$) decay, this particular branch has not been observed. Here in we report the identi-

fication of the ^{147}Tm ($\text{EC} + \beta^+$) decay in a series of ^{58}Ni irradiations of ^{92}Mo with the use of the OASIS on-line separator facility⁶ at the Lawrence Berkeley Laboratory's SuperHILAC.

Two sets of irradiation and counting cycles were used, namely, 1.28 and 4 s. A comparison of low-energy photon spectra from these two experiments showed the presence of Er K_{α_1} x rays in the 1.28-s data set but not in the 4-s results. Also, a 0.6-s component was noted in the decay curve of the annihilation radiation seen in the 1.28-s irradiations. Because the ^{147}Tm β -decay energy is higher than those of the other $A = 147$ isobars investigated here, we set gates on the annihilation-radiation peak and looked at coincident γ rays to emphasize the ^{147}Tm contribution. Figures 3.17(a) and 3.17(b) show these coincident spectra for the 1.28- and 4-s data, respectively. In addition to γ rays belonging to ^{147}Er , ^{147}Ho , and ^{147}Dy , an 80.9-keV transition (and Er K_{α_1} x rays) is clearly seen in Fig. 3.17(a) while in Fig. 3.17(b) the γ ray is scarcely visible. We therefore assign the 80.9-

keV γ ray to the β decay of the ^{147}Tm $h_{11/2}$ ground state and propose that it connects the ^{147}Er first-excited $d_{3/2}$ neutron-hole level with its $s_{1/2}$ ground state. This placement is based on systematics of $s_{1/2}$, $d_{3/2}$, and $h_{11/2}$ neutron-hole states in this mass region that were recently updated⁷ following our study of the β decay of ^{145}Ho ($h_{11/2}$), the $N = 79$ isotope just below ^{147}Tm . The 80.9-keV energy for the $d_{3/2}$ level in ^{147}Er fits well into the overall picture, i.e., this level is at 1.58 keV in ^{141}Sm , and then increases in excitation energy to 45.1 and 66.3 keV in ^{143}Gd and ^{145}Dy , respectively. As in the case of ^{145}Ho decay,⁷ the $d_{3/2}$ level in ^{147}Er is probably populated by a γ ray from the higher-lying $d_{5/2}$ state; however, we could not observe this $d_{5/2} \rightarrow d_{3/2}$ transition nor any other γ rays which could be assigned to ^{147}Tm decay.

1. Summary of a paper submitted to *Physical Review C*.
2. Eastern Kentucky University, Richmond, KY.
3. Lawrence Berkeley Laboratory, Berkeley, CA.
4. O. Klepper et al., *Z. Phys.* **A305**, 125 (1982).
5. P. O. Larsson et al., *Z. Phys.* **A314**, 9 (1983).
6. J. M. Nitschke, *Nucl. Instrum. Methods* **206**, 341 (1983).
7. K. S. Vierinen et al., *Phys. Rev. C* **39**, 1972 (1989).

ORNL-DWG 89-15172R

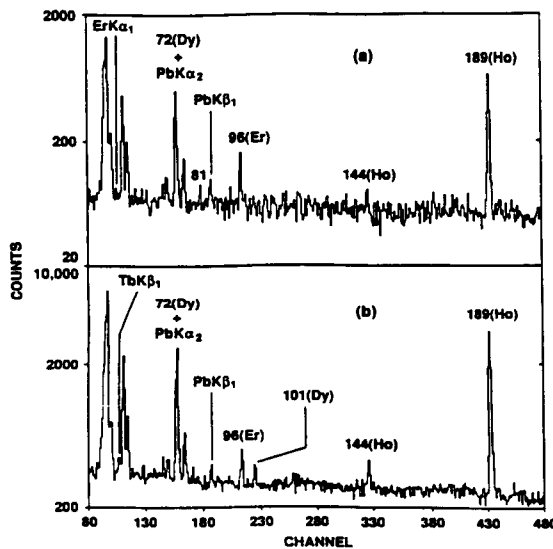


Fig. 3.17. Gamma-ray spectra observed in coincidence with annihilation radiation for $A = 147$ nuclides during 1.28-s [part (a)] and 4-s [part (b)] counting cycles. The 81-keV γ ray in part (a) is assigned to ^{147}Tm ($\text{EC} + \beta^+$) decay. Transitions assigned to the decays of ^{147}Dy , ^{147}Ho , and ^{147}Er are labeled by their elemental symbols.

ALPHA-DECAYING LOW-SPIN LEVELS IN ^{155}Lu AND ^{157}Lu ¹

K. S. Toth, K. S. Vierinen,² J. M. Nitschke,²
P. A. Wilmarth,² and R. M. Chasteler²

Using an on-line mass separator, the α -particle decays of ^{155}Lu and ^{157}Lu were investigated. A new α -emitting level in ^{157}Lu was identified [$T_{1/2} = 5.7(5)$ s, $E_{\alpha} = 4924(20)$ keV]. In addition, a half-life of 140(20) ms was measured for the recently discovered second, low-lying, α -decaying level [$E_{\alpha} = 5579(5)$ keV] in ^{155}Lu .

1. Abstract of published paper: *Z. Phys.* **A340**, 343 (1991).
2. Lawrence Berkeley Laboratory, Berkeley, CA.

PHYSICS WITH RADIOACTIVE BEAMS

NORTH AMERICAN RADIOACTIVE BEAM INITIATIVES¹

J. D. Garrett

After a brief review of existing radioactive beam facilities in North America, two new initiatives (the Oak Ridge Radioactive Ion Beam Facility and the IsoSpin Laboratory) are described in some detail. An evaluation of which nuclei these facilities will be able to study, that cannot be studied with stable targets and beams, also is presented.

1. Abstract of paper to be published in *Proceedings of the Workshop on the Techniques of Secondary Nuclear Beams*, Dourdan, France, March 1992.

EXOTIC NUCLEAR SHAPES AND CONFIGURATIONS THAT CAN BE STUDIED AT HIGH SPIN USING RADIOACTIVE ION BEAMS¹

J. D. Garrett

The variety of new research possibilities afforded by the culmination of the two frontier areas of nuclear structure: high spin and studies far from nuclear stability (utilizing intense radioactive ion beams) are discussed. Topics presented include: new regions of exotic nuclear shape (e.g., superdeformation, hyperdeformation, and reflection-asymmetric shapes); the population of and conse-

quences of populating exotic nuclear configurations; and complete spectroscopy (i.e., the overlap of state of the art low- and high-spin studies in the same nucleus). Likewise, the various beams needed for proton- and neutron-rich high spin studies are also discussed.

1. Abstract of paper to be published in *Proceedings of the Workshop on the Techniques of Secondary Nuclear Beams*, Dourdan, France, March 1992.

PROSPECTS FOR STUDIES OF ASTROPHYSICAL INTEREST WITH RADIOACTIVE ION BEAMS¹

J. D. Garrett

Realistic estimates of the new nuclei that will become accessible for study with the planned new generation of radioactive beam facilities are compared with the predicted paths of the various nucleosynthetic processes. These facilities should permit studies of essentially the complete set of nuclei associated with the rp- and p-processes, the CNO cycle, and big-bang nucleosynthesis, as well as the r-process below $A \cong 150$.

1. Abstract of paper to be published in *Proceedings of the Nuclei in the Cosmos 1992 Conference*, Karlsruhe, Germany, July 5-10, 1992.

HEAVY-ION REACTION MECHANISM STUDIES, FUSION AND FISSION

LARGE DEFORMATION IN A ~ 170 NUCLEI AT HIGH EXCITATION ENERGIES¹

*M. Thoennessen,² J. R. Beene, F. E. Bertrand,
C. Baktash, M. L. Halbert, D. J. Horen,
D. C. Hensley,³ D. G. Sarantites,⁴ W. Spang,⁵
D. W. Stracener,⁴ and R. L. Varner*

The γ -ray decay of the giant dipole resonances was measured in coincidence with fission fragments following the fusion reaction $^{16}\text{O} + ^{159}\text{Tb}$ forming ^{175}Ta at 123.4 MeV excitation energy. A large splitting of the giant dipole resonance (GDR) energies in the compound system was observed corresponding to a large deformation of $\beta = 0.55$.

1. Abstract of published paper: *Phys. Lett.* **B282**, 288 (1992).

2. Michigan State University, East Lansing, MI.

3. Office of Waste Management and Remedial Actions, ORNL.

4. Washington University, St. Louis, MO.

5. Laboratoire National Saturne, F-91191 Gif-sur-Yvette Cedex, France.

ANGULAR MOMENTUM EFFECTS IN SUBBARRIER FUSION

M. L. Halbert and J. R. Beene

Further investigations have been carried out of the fusion reactions $^{64}\text{Ni} + ^{100}\text{Mo}$ and $^{16}\text{O} + ^{148}\text{Sm}$ at energies near the Coulomb barrier in order to improve the analysis of the low- ℓ region of the angular-momentum distributions.¹ Old data^{1,2} were re-examined and new data were obtained on fusion of $^{16}\text{O} + ^{148}\text{Sm}$. In the following, k denotes the coincidence fold – i.e., the number of NaI detectors that fired in a given event.

(1) The analysis of Ref. 1 discarded data with $k < 3$ because these events did not provide a good estimate of event timing needed for time-of-flight separation of neutrons and γ rays. New scans of the data tapes made with no restrictions on k showed that

there in fact had been no significant losses due to the $k < 3$ condition.

(2) These tape scans also provided k spectra without rejection of late-arriving pulses (presumably due to neutrons). The effect on the k spectra of removal of neutron pulses was studied at all five ^{64}Ni beam energies (235, 225, 220, 215, and 210 MeV lab) and both ^{16}O beam energies (81.3 and 71.2 MeV lab). It has already been noted^{2,3} that at ^{64}Ni energies of 235 and 220 MeV, the principal difference between the k distributions obtained with and without off-line neutron rejection was a shift toward lower k values. This shift is about two units in k and is consistent with what is known about the neutron efficiency of the NaI detectors in the Spin Spectrometer.³ Careful comparisons of the spectra with and without neutron rejection have now been made for every data set; similar results were obtained for the k shifts.

(3) For the pairs of k spectra with the best counting statistics, the neutron-rejected spectra show a slightly steeper slope on the high side of the peak. The slight broadening with the neutrons included is probably due to finite width of the Spin Spectrometer response function for neutrons. To investigate this point, the k response for neutrons was represented by a Poisson distribution with mean value equal to the average number of neutrons detected; since this number is the same as the shift in k , the broadening can be included without adding any additional parameters. Though the choice of the Poisson distribution may seem arbitrary, it is actually a realistic choice. For a mean value of $k \sim 2$, the neutron response should show a significant probability for $k = 0$ (no neutrons detected) and a tail on the high- k side (if a neutron scatters once in the Spin Spectrometer, it has a good chance of scattering again); the Poisson distribution fulfills these expectations. Empirically, the improvement in fit when the neutron broadening is taken into account is shown by a reduction in the chi-squared per degree of freedom to values substantially closer to unity. Figure 3.18 shows the best-fit k shifts from this type of analysis.

(4) Our measured cross-section fractions for the xn exit channels in the ^{16}O -induced reaction at the lower of the two beam energies disagree with similar data measured by another technique.^{4,5} One possible explanation of the disagreement is an inconsistency in beam energy scales among the three measure-

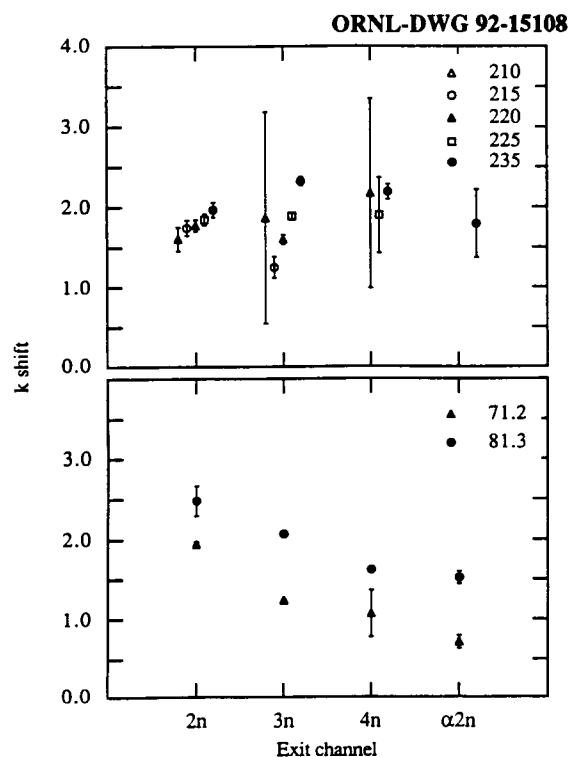


Fig. 3.18. The shift in the k distributions due to neutron detection for the reactions $^{64}\text{Ni} + ^{100}\text{Mo}$ (upper part) and $^{16}\text{O} + ^{148}\text{Sm}$ (lower part). The five ^{64}Ni and the two ^{16}O beam energies (lab) are indicated. The effect of the broadening due to the neutron response was taken into account as described in the text.

ments. As a check, the absolute calibration of the HHIRF tandem energy scale was re-measured⁶ with a 71.23-MeV ^{16}O beam by the time-of-flight method.⁷ At the same time spectra from $^{16}\text{O} + ^{148}\text{Sm}$ were recorded with a large number of Ge counters in the Spin Spectrometer at this beam energy and also at 68.54 and 66.06 MeV. The analyzing-magnet calibration and hence the beam-energy scale were found⁶ to be identical within $(0.03 \pm 0.08)\%$ of what they had been in 1986. Analysis of the reaction data is in progress to check the xn fractions.

1. M. L. Halbert, J. R. Beene, D. C. Hensley, K. Honkanen, T. M. Semkow, V. Abenante, D. G. Sarantites, and Z. Li, *Phys. Rev. C* **40**, 2558 (1989).

2. M. L. Halbert, J. R. Beene, D. C. Hensley, K. Honkanen, T. M. Semkow, V. Abenante, D. G. Sarantites, and Z. Li, in *Phys. Div. Prog. Rep. for Period Ending Sept. 30, 1990*, ORNL-6660, p. 73.

3. M. L. Halbert and J. R. Beene, *Proceedings of the XIV Symposium on Nuclear Physics, Cuernavaca, Mexico, January 7-10, 1991*, ed. M.-E. Brandan (World Scientific, Singapore, 1991), p. 105.

4. R. G. Stokstad, Y. Eisen, S. Kaplanis, D. Pelte, U. Smilansky, and I. Tserruya, *Phys. Rev. C* **21**, 2427 (1980).

5. D. E. DiGregorio, M. diTada, D. Abriola, M. Elgue, A. Etchegoyen, M. C. Etchegoyen, J. O. Fernández Niello, A.M.J. Ferrero, S. Gil, A. O. Macchiavelli, A. J. Pacheco, J. E. Testoni, P. R. Silveira Gomes, V. R. Vanin, R. Liguori Neto, E. Crema, and R. G. Stokstad, *Phys. Rev. C* **39**, 516 (1989).

6. C. M. Jones, R. C. Juras, and M. J. Meigs (private communication).

7. D. K. Olsen, K. A. Erb, C. M. Jones, W. T. Milner, D. C. Weissner, and N. F. Ziegler, *Nucl. Instrum. and Methods A* **254**, 1 (1987).

FUSION NEAR THE COULOMB BARRIER: NONSTATISTICAL EFFECTS AND γ -RAY MULTIPLICITY

*J. R. Beene, M. L. Halbert,
and M. R. Thoennessen¹*

The dynamics of the fusion of heavy nuclei near and below the Coulomb barrier has proved to be much more interesting than would have been guessed a decade ago. One example of the unexpected richness of phenomena which has recently been uncovered in the study of fusion reactions at low energy is the apparent contradiction of the Bohr independence hypothesis in the decay of fused systems formed, at the same excitation energy and angular momentum, by fusion reactions with very different entrance channel asymmetries. Provocative early work in this area was reported by the Argonne National Laboratory group and by a Giessen-Argonne-Heidelberg collaboration.^{2,3,4,5} They compared the decay of rare-earth compound systems produced by ^{12}C - and ^{16}O -induced (i.e., very asymmetric) reactions with the decay of those produced by ^{64}Ni projectiles (i.e., a nearly symmetric entrance channel). The main ex-

perimental difficulty in making a meaningful comparison between two such reactions is the very much larger range of entrance-channel angular momenta involved in the Ni-induced reaction, if the bombarding energy is chosen to match excitation energy. This difficulty is dealt with by γ -ray multiplicity techniques using a 4π crystal-ball γ -detection array.

In an earlier report (ORNL-6689) we have discussed results on the ratio of exit-channel cross sections, $\sigma_{xn}/\Sigma\sigma_{xn}$, as a function of angular momentum, ℓ , for the $^{164}\text{Yb}^*$ nucleus formed by the $^{16}\text{O} + ^{148}\text{Sm}$ and $^{64}\text{Ni} + ^{100}\text{Mo}$ reactions. These reactions were studied at HHIRF using the ORNL Spin Spectrometer. An example of these data is shown in Fig. 3.19, which shows relative exit channel (xn) cross sections plotted against γ -ray fold, i.e. the number of detectors in the Spin Spectrometer which were triggered in an event. The fold from the 3n exit channel is increased by 2.5 units to account for the character of the ^{161}Yb level scheme. The lower part of the figure, corresponding to a $^{164}\text{Yb}^*$ excitation energy of 49 MeV, shows a departure from the expected compound nucleus behavior above a γ -ray fold $k_{\text{eff}} \sim 17$. This effect is almost identical to that reported in Ref. 3. A new and interesting feature is provided in Fig. 3.19a, which shows similar data taken at a slightly lower bombarding energy, corresponding to an excitation energy 9 MeV lower. In contrast to the 49 MeV data, there is no statistically significant difference between the two entrance channels.

Subsequent analysis has uncovered another difference in the decay of these excited ^{164}Yb systems formed by different entrance channels. In Fig. 3.20 the relative cross section for the $\alpha 2n$ exit channel is plotted, again as a function of γ -ray fold. Here an excess $\alpha 2n$ yield is found in the ^{16}O induced reaction, with the difference between the two entrance channels decreasing at high fold, in contrast to the xn results in Fig. 3.19.

It was established in the 1970's that an approximately linear relationship exists between the angular momentum of the states populated in a reaction and the γ -ray multiplicity observed in the subsequent decay. The transformation of distributions in γ -ray multiplicity to distribution in ℓ have been done almost universally by assuming that the observed relationship between average values of multiplicity and ℓ , can be extended to imply a functional (i.e., one to one) relationship between the ℓ and M treated as variables; i.e.,

$$M_\gamma = f(\ell). \quad (1)$$

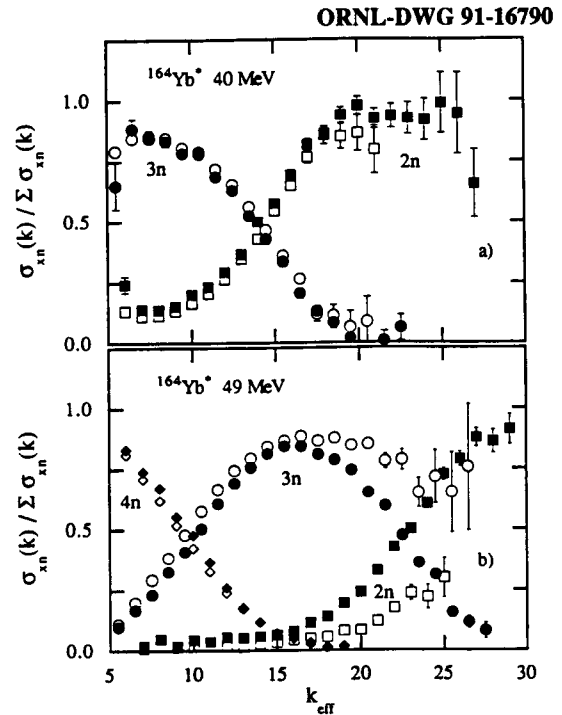


Fig. 3.19. Fractional xn cross sections, $\sigma_{xn}/\Sigma\sigma_{xn}$, for the $^{64}\text{Ni} + ^{100}\text{Mo}$ (filled symbols) and $^{16}\text{O} + ^{148}\text{Sm}$ (open symbols) as a function of gamma ray fold. The two panels are for two different ^{164}Yb excitation energies (see text).

Such a relationship leads to a straightforward mapping from a distribution in M_γ to a distribution in angular momentum ℓ . We have investigated such transformations using statistical-model calculations to define the relationship between the initial angular momentum and mean multiplicity. Even if we relax the normal assumption that the relation in equation (1) is linear (polynomial approximations up to 3rd order were used), we find that a transformation based on equation (1) with its form fit to statistical-model results – preserves and in some cases even enhances the entrance-channel dependent decay effect seen in Fig. 3.19b.

It is well known that the relationship implied by equation (1) is false. A point in M_γ space maps to a distribution in ℓ space and vice-versa. It is also clear that for most purposes the error introduced in the final ℓ distributions by the assumptions of a one to one mapping is of negligible importance. This is not clear for the ratio of cross section data like that in Fig. 3.19 and Ref. 3. We felt that before the data in Figs. 3.19 and 3.20 could be seriously considered to show a

violation of the independence hypothesis, the effect of this distributed mapping should be investigated.

We have done this by using the full information provided by Monte-Carlo statistical models to construct $\ell \rightarrow M_\gamma$ mapping, and unfolding techniques to transform the cross section distributions. The mapping from M_γ to k (multiplicity to fold) is well understood experimentally. We have found that Monte-Carlo calculations based on GEANT reproduce these experimental results accurately. We therefore combined the Monte-Carlo statistical model and detector response codes to directly relate γ -ray-fold distributions to angular-momentum distributions.

The results of this investigation were surprising, and cast doubt on the significance of the entrance-channel effect shown in Fig. 3.19. Reasonable statistical-model parameters can be found which fully account for the differences between the ^{64}Ni and ^{16}O induced results! By implication, this observation casts doubt on the results in Ref. 3 as well.

The effect on the αn ratio shown in Fig. 3.20, however, survives the transformation to ℓ . Rather than a failure of the independence hypothesis, however, we interpret this result as a manifestation of the well known propensity of ^{16}O to break up into $^{12}\text{C} + \alpha$ prior to fusion. Our results can be accounted for

quantitatively by applying breakup-fusion or incomplete-fusion models. It is very surprising, however, that this process continues to be important at such low bombarding energies [$E_{\text{Lab}}(^{16}\text{O}) = 80$ MeV and 70 MeV]. It appears that the tendency of light heavy ions like ^{16}O to break up must be taken into account even in near-barrier reactions.

1. Michigan State University, East Lansing, MI.
2. W. Kühn et al., *Phys. Rev. Lett.* **51**, 1858 (1983).
3. A. Ruckelshausen et al., *Phys. Rev. Lett.* **56**, 2356 (1986).
4. R.V.F. Janssens et al., *Phys. Lett.* **B181**, 16 (1986).
5. F.L.H. Wolfs et al., *Phys. Rev. C* **39**, 865 (1989).

EVIDENCE FOR LONG FORMATION TIMES IN NEAR BARRIER FUSION REACTIONS¹

M. Thoennesen,² J. R. Beene, R. L. Auble, F. E. Bertrand, C. Baktash, M. L. Halbert, D. J. Horen, D. G. Sarantites,³ W. Spang,⁴ and D. W. Stracener³

We measured high-energy γ rays from the decay of the GDR built on highly-excited states in ^{164}Yb at $E_{\text{ex}} = 49$ MeV formed in two different reactions. While standard statistical model calculations can describe the γ -ray spectrum from the $^{16}\text{O} + ^{148}\text{Sm}$ reaction, they fail to reproduce the γ -ray spectra from the more symmetric reaction $^{64}\text{Ni} + ^{100}\text{Mo}$. A simple model which includes particle evaporation and γ -ray decay during the formation process can account for the differences when large fusion times ($\sim 2 \times 10^{-20}$ s) are assumed.

1. Abstract of paper to be submitted to *Physical Review C*.

2. Michigan State University, East Lansing, MI.

3. Washington University, St. Louis, MO.

4. Institut für Kernphysik, Forschungszentrum Jülich, Germany.

ORNL-DWG 92-14513

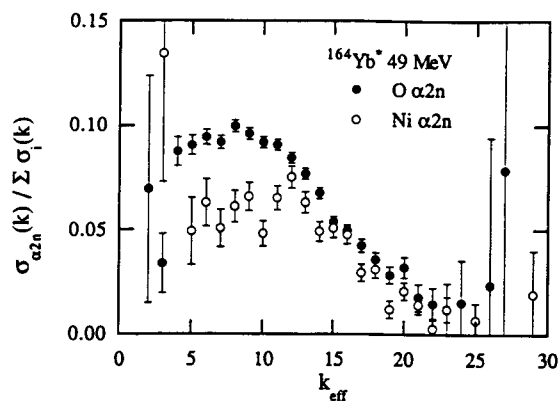


Fig. 3.20. Cross section ratios, as in Fig. 3.19, for the αn exit channel. Solid points are for the $^{16}\text{O} + ^{148}\text{Sm}$ entrance channel. Open points are for $^{64}\text{Ni} + ^{100}\text{Mo}$.

CHARGED PARTICLES AS PROBES TO STUDY ENTRANCE-CHANNEL EFFECTS IN THE COMPOSITE SYSTEM ^{164}Yb

*J. L. Barreto,¹ D. G. Sarantites,¹ R. J. Charity,¹
N. G. Nicolis,¹ L. G. Sobotka,¹ D. W. Stracener,¹
D. C. Hensley,² J. R. Beene, M. L. Halbert,
and C. Baktash*

Entrance-channel effects have been studied by comparing measured charged particle and γ -ray multiplicities in coincidence with residue nuclei (identified by discrete transitions), from both mass symmetric and asymmetric reactions. The systems studied are $^{64}\text{Ni} + ^{100}\text{Mo}$ and $^{16}\text{O} + ^{148}\text{Sm}$, both of which would produce the ^{164}Yb compound nucleus with 52 MeV of excitation energy. In the $(\alpha 2n)$ exit channel, the center of mass α -particle angular distribution is symmetric around 90° in the Ni-induced reaction, indicating emission from a fully equilibrated system. The extracted anisotropies show no evidence for an enhancement of α -particle emission in the low-energy region, which indicates emission from a nearly spherical system. However, the corresponding angular distribution of the ^{16}O -induced reaction shows a strong forward component, which is a clear signature of a non-statistical contribution to the residue cross section.

1. Washington University, St. Louis, MO.

2. Office of Waste Management and Remedial Actions, ORNL.

ANALYSIS OF LIGHT PARTICLES EMITTED IN COINCIDENCE WITH EVAPORATION RESIDUES FOR THE $^{79}\text{Br} + ^{27}\text{Al}$ SYSTEM AT 11 MeV/NUCLEON

*J. Gomez del Campo, J. P. Wieleczko,¹ E. Chávez,²
D. Shapira, M. Korolija,³ H. Kim, C. Volant,⁴
A. D'Onofrio,⁵ K. Teh,⁶ and J. Shea⁷*

An important step in the understanding of nuclear collisions in the intermediate energy domain (10-100 MeV/nucleon) is the ability to study reaction products by means of exclusive measurements with appropriate gates to isolate the various competing reaction mechanisms. Such a study is reported here for products of the reaction $^{79}\text{Br} + ^{27}\text{Al}$ produced by bombardment of an ^{27}Al target with a ^{79}Br beam of

930 MeV, obtained from coupled-accelerator operation of HHIRF. Light particles (protons, deuterons, tritons, and alphas) were measured in coincidence with evaporation residues (ER) of $Z = 36-43$ by means of the large detector array HILI.⁸

The light particles were detected with a hodoscope array composed of 192 plastic scintillators that were calibrated with recoil protons produced by an ^{16}O beam on a polypropylene target. The calibration for particles of higher Z and M was done as described in Ref. 8. Additional checks were carried out by comparing the alpha-particle and $Z = 1$ spectra obtained with the hodoscope to those obtained from calibrated Si detector telescopes. For example, for the case of singles α spectra measured for the $^{58}\text{Ni} + ^{58}\text{Ni}$ reaction at 500 MeV bombarding energy with Si detectors placed at similar laboratory angles as the hodoscopes, agreement of the measured energy spectra was found within 2 MeV. We estimate the overall energy resolution to be better than 5%. The hodoscopes alone provide Z identification; the mass was determined by time of flight using the cyclotron RF and the time signal of each plastic detector.

Energy spectra for p, d, t, and α are shown in Fig. 3.21 by the open circles. These spectra were obtained by summing all the counts from each element of the hodoscope for all laboratory angles between 2.8 and 24 deg. The spectra in Fig. 3.21 have the constraint of being in coincidence with fragments of $Z = 36-43$, detected with the ionization chamber of the HILI system. The energy cutoffs seen in Fig. 3.21 (about 8 MeV for p's and 20 MeV for α 's) are consistent with the energy threshold imposed by the 0.5 mm thickness of the ΔE element of the plastic hodoscopes.

Since the light particles are in coincidence with fragments which have Z 's characteristic of ER of the compound nucleus, the proper calculation to compare with the data is the Hauser-Feshbach theory, assuming that the particles are emitted by a compound nucleus formed at equilibrium in a complete fusion reaction. These calculations were performed using the Monte Carlo code LILITA;⁹ however, substantial modifications were needed to improve the agreement with the low-energy part of the experimental spectrum. The most important modification was to introduce explicit optical-model transmission coefficients using the optical-model parameters of Ref. 10. (The original version of LILITA has a simple parameterization for low excitation energies plus a sharp cutoff for high excitation energies.) Results are shown as solid lines in Fig. 3.21 where the normalization factor for each curve is indicated in the figure. The same experimental constraints placed by the

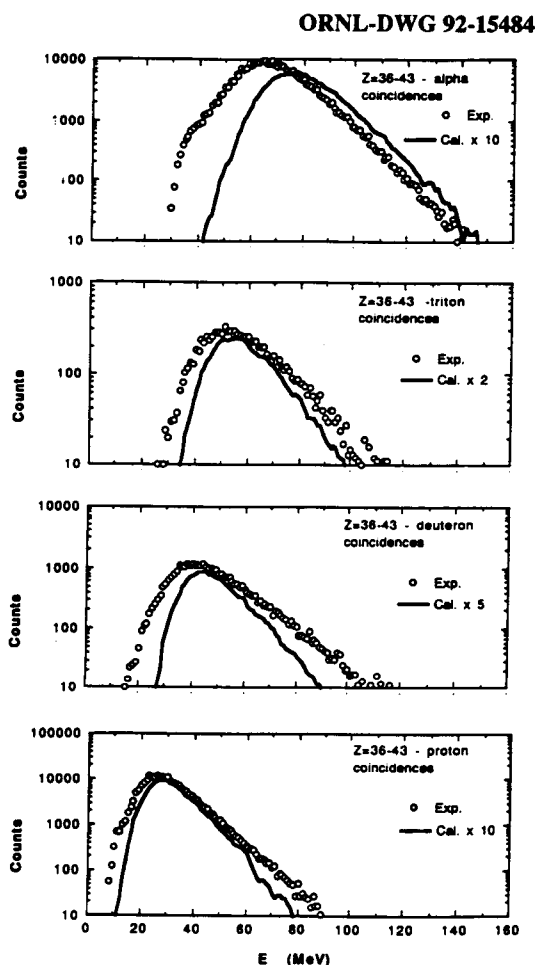


Fig. 3.21. Experimental energy spectra (dots) for light particles emitted in coincidence with evaporation residues of $^{79}\text{Br} + ^{27}\text{Al}$ at 11 MeV/nucleon. The solid lines are predictions of code LILITA discussed in the text.

HILI system on the spectra have been applied to the calculation.

From the comparisons shown in Fig. 3.21, it can be seen that except for the low-energy part of the alpha spectrum the calculated shapes are in reasonable agreement with the experiment. The yield, however, has some serious problems. The calculations predict correctly that the yield of deuterons and tritons is an order of magnitude lower than that of the protons and alpha particles, as seen from Fig. 3.21. Also the relative yields of p's and α 's seem to be well reproduced. However, the yields of deuterons and tritons are clearly overpredicted by factors of 2 and 5,

respectively. Some of the yield discrepancies can be attributed to the fact that the data contain components other than complete fusion that are not in the simulation. If an analysis is done with higher-fold coincidences, the relative yields are in better agreement, as was shown previously in analysis of the ER.¹¹

In more detail, it can be seen from Fig. 3.21 that for the $Z = 1$ particles there is a slight disagreement in the low-energy part of the spectra that may support the idea that the emission barriers are lower than predicted by normal optical models due to deformation effects on the compound nucleus (claims made in Ref. 12 and references therein). Clearly for the case of the alphas the discrepancy is more important and will require very large deformations to explain it (effective radius of the compound nucleus about 1.5 times that of the normal shape). The low-barrier effect observed in the present experiment is more pronounced for the α channel than for the protons, but the opposite is reported in Ref. 12. Also the high-energy slopes are lower than predicted for deuterons and tritons.

Another interesting feature of Fig. 3.21 is the slope of the high-energy part of the spectra. The slopes for protons and alpha particles are reasonably well reproduced with a value of the level-density parameter $a = A/12$. Lower values, such as $A/8$, produce substantially bigger slopes that deviate strongly from the data. The experimental slopes are not as well reproduced for deuterons and tritons which, together with the fact that the relative yields are not well reproduced either, may be indicative of a problem with the optical-model parameters. The value of $a = A/12$ is in agreement with other analyses¹²⁻¹⁴ although it has also been suggested¹⁵⁻¹⁶ that a should increase with decreasing excitation energy up to the Fermi-gas limit of $A/8$. The present comparisons support values substantially lower than $A/8$.

Coming back to the lower energy region, it can be seen in Fig. 3.21 that there is a clear discrepancy at very low energies which can be understood by invoking very large deformation of the compound nucleus. In particular, for the alpha-particle channel, emission barriers as low as those of ^{27}Al ($E_{\text{cm}} \sim 4.5$ MeV) are required to reproduce the data. One appealing explanation that requires further analysis is that of preequilibrium-shape emission for which emission from a dinuclear configuration, resembling the entrance channel, occurs before a fully-equilibrated compound nucleus is formed. Well-known effects such as incomplete fusion have been considered, but,

even for a channel losing up to two α particles, the predictions do not account for the lower emission barrier.

1. GANIL, Caen, France.
2. IFUNAM, Mexico City, Mexico.
3. Partial support from the Joint Institute for Heavy Ion Research, ORNL.
4. Centre d'Etudes de Saclay, Gif-sur-Yvette, Cedex, France.
5. Istituto Nazionale di Fisica Nucleare, Naples, Italy.
6. GSI, Darmstadt, Germany.
7. University of Maryland, College Park, MD.
8. D. Shapira et al., *Nucl. Instrum. Methods Phys. Res. A* **301**, 76 (1991).
9. J. Gomez del Campo and R. G. Stokstad, ORNL/TM-7295 (1981).
10. C. M. Perey and F. G. Perey, *Atom. Data and Nucl. Data Tables* **17**, 1 (1976).
11. J. P. Wieleczko et al., *Phys. Div. Prog. Report for Period Ending Sept. 30, 1989*, ORNL-6578, p. 85.
12. W. E. Parker et al., *Phys. Rev. C* **44**, 774 (1991).
13. S. M. Grimes, *Z. Physik.* **A343**, 125 (1992).
14. A. Bracco et al., *Phys. Rev. Lett.* **62**, 2080 (1989).
15. W. E. Ormond et al., *Phys. Rev. C* **40**, 1510 (1989).
16. R. Wada et al., *Phys. Rev. C* **39**, 497 (1989).

THE $^{14}\text{N} + ^{10}\text{B}$ SYSTEM MEASURED AT $E(^{14}\text{N}) = 248 \text{ MeV}^1$

*M. E. Ortiz,² E. R. Chávez,² A. Dacal,²
J. Gomez del Campo, Y. D. Chan,³
and R. G. Stokstad³*

Total and differential cross sections for reactions induced by ^{14}N on ^{10}B have been measured at a ^{14}N bombarding energy of 248 MeV ($\sim 18 \text{ MeV/A}$) for products from $Z = 3$ to 11. The study of saturation effects on the angular momentum and the identification of the non-fusion cross sections constitute the aim of the present work. Energy, angular, and Z distributions are presented and compared to Hauser-Feshbach calculations for the fusion components and

a sum-rule model for the non-fusion components. The extracted critical angular momentum is $21 \pm 2 \hbar$ and is the same as at lower energies. The experimental total reaction cross section is in agreement with an optical model calculation.

1. Abstract of published paper: *Revista Mexicana de Física* **38**, 543 (1992).
2. Instituto de Física, Universidad Nacional Autónoma de Mexico, Mexico.
3. Lawrence Berkeley Laboratory, Berkeley, CA.

ENERGY SHARING IN BINARY REACTIONS INDUCED BY ^{19}F ON ^{64}Ni AT 118 MeV¹

*A. Brondi,² G. de Angelis,² A. D'Onofrio,²
G. LaRana,² R. Moro,² V. Roca,² G. Spadaccini,²
F. Terrasi,² M. Vigilante,² R. Alba,³ G. Bellia,³
A. Del Zoppo,³ G. Russo,³ P. Sapienza,³
and J. Gomez del Campo*

Complex fragments have been detected in singles and in γ -particle coincidence measurements for the $^{19}\text{F} + ^{64}\text{Ni}$ system, at 118 MeV incident energy. Cross sections for the excited states of the complex fragments were measured detecting the characteristic γ -transitions deexciting these states. The measurement of cross sections for the population of the ground and excited states of ^{18}O and ^{13}C , as well as of the production cross sections of heavy residues in coincidence with these ejectiles, as a function of the total dissipated energy, indicate an evolution of energy sharing, with increasing mass transfer, from equipartition to thermal equilibrium.

1. Abstract of paper to be published in *Nuclear Physics A*.
2. Istituto Nazionale di Fisica Nucleare, Napoli, Italy.
3. Dipartimento di Fisica dell'Università, Catania, Italy.

**PROTON-PROTON CORRELATIONS:
DETERMINATION OF THE
CHARACTERISTIC SOURCE SIZE AND
THE LIFETIME FROM A DEEP INELASTIC
 $^{58}\text{Ni} + ^{58}\text{Ni}$ REACTION AT 15 MeV/
NUCLEON¹**

*M. Korolija,^{2,3} D. Shapira, J. Gomez del Campo,
E. Chávez,⁴ and N. Cindro³*

Triple p-p-fragment coincidences from the $^{58}\text{Ni} + ^{58}\text{Ni}$ reaction at 850 MeV have been measured. The average source size (r_0) and the average particle emission time (τ) have been deduced from the directional dependence of the p-p correlation function. The ambiguity in the determination of the parameters r_0 and τ has been resolved by extracting the parameters r_0 and τ from a simultaneous fit to the p-p correlation functions subsets for which the components of the p-p relative momentum (Δp), parallel or perpendicular to the relative velocity between the p-p *c.o.m.* and the source (v_{rel}), are small. This analysis yields values of (2.5 ± 0.2) fm and $3.6_{-1.0}^{+2.3} * 10^{-22}$ s for the parameters r_0 and τ .

1. Abstract of paper to be submitted to *Physical Review C*.

2. Partial support from the Joint Institute for Heavy Ion Research, ORNL.

3. Rudjer Boskovic Institute, Croatia.

4. Instituto de Física, UNAM, Mexico.

STATUS OF SOFT PHOTON EXPERIMENT

*R. Clark,¹ C. Erd,² J. Gomez del Campo, A. Ray,³
J. Schukraft,⁴ D. Shapira, M. Tincknell,⁵
and C. Woody⁶*

Experiment E855, a search for new sources of "soft" photons (transverse momentum < 50 MeV), was conducted at Brookhaven in March of 1990. A beam of protons of energy 10 and 18 GeV was used to bombard Be and W targets at the AGS. Some theorists claim that partial or complete quark deconfinement would lead to a slight excess of just such photons,⁷ and hence, provide supporting evidence for the existence of quark-gluon plasma.

To isolate the signal of interest one has to remove all known sources of photons in this energy regime, which include hadronic decays, bremsstrahlung, and the decay of excited nuclei. Of the hadronic decays, the overwhelming contribution is due to π^0 's, each of which decays into 2 photons. Figure 3.22 shows the dominance of the π^0 's compared with the other hadronic species. In this figure and the ones which follow, the abscissa is the transverse momentum, p_T ,

ORNL-DWG 92-15088

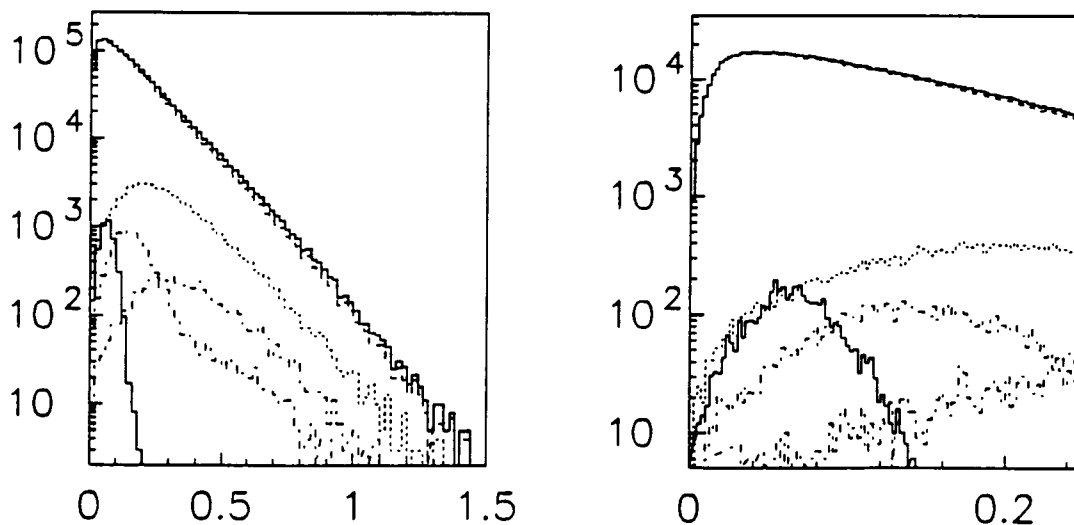


Fig. 3.22. LUND Monte Carlo calculation of contributions to the hadron decay background in p-W interactions at 18 GeV as a function of p_T : upper dashed curve, π^0 ; dotted curve, η ; dot-dashed curve with peak < 0.2 GeV/c, η' ; other dot-dashed curve, ω ; lower solid curve, Σ^0 ; upper solid curve, total.

in GeV/c, and the ordinate is yield in arbitrary units. The only exception is the ordinate of Fig. 3.25, which shows a differential cross section.

The experimental setup and the objective were reported previously.^{8,9} This report lists further progress made in the analysis and in particular presents results from the detectors positioned at large angles.

During the past year the contribution to the photon spectra due to bremsstrahlung has been calculated. Also, we have determined the dN/dy rapidity distributions, where N is the number of photons emitted as a function of y , the rapidity (for photons $y = \log(\cot \frac{\theta}{2})$ and for particles with mass, $y = \frac{\theta}{1} \log \frac{E + p_z}{E - p_z}$). This quantity is important in estimating the contribution from the π^0 decays to our photon spectra. As expected, the distributions were essentially gaussian, the widths of which agree remarkably well with the LUND Model, an event generator for high energy collisions that we frequently use as a guide.

We have utilized GEANT, a detector simulation software package, to systematically study various aspects of our detectors' response, and we have corrected the data accordingly. Although much of this work is complete, still outstanding is the determination of the effect of the individual-crystal constant-fraction discriminator efficiencies on the overall p_T spectra as well as the effect of energy leakage.

The parameterization of the π^0 p_T spectra presently used for the Be data is given by:

$$f(y, p_T) = a_1 p_T \exp(-a_2 m_T) \exp \frac{-(y - a_3)^2}{2a_4^2}, \quad (1)$$

where $\sqrt{m_{\pi^0}^2 + p_T^2}$ and a_i denote the parameters. The p_T dependence of Equation (1) has been shown to be valid for charged pions in similar energy regimes,¹⁰ and it is assumed that the π^0 's may be parameterized as the average between the π^+ 's and the π^- 's. As for the y dependence in the equation, it is based on the measured photon spectrum, which was in excellent agreement with a gaussian shape. Since LUND indicates that the π^0 distribution behaves similarly, a_3 , the peak of the gaussian, was assumed

to be the same as measured for the photons and, therefore, not allowed to vary in the fitting procedure.

A second exponential term was needed to fit the tungsten data. We have assumed a p^0 distribution given by,

$$f(y, p_T) = a_1 p_T [\exp(-a_2 m_T) + a_5 \exp(-a_6 m_T)] \exp \frac{-(y - a_3)^2}{2a_4^2}. \quad (2)$$

Since our data focuses on the low p_T end, the systematic error introduced by using a double exponential is insignificant, although, admittedly, this question needs to be studied further.

Figure 3.23 shows the result of the various fits for the tungsten data and Fig. 3.24 shows the same data plotted at a finer range in p_T . At wider angles [more negative rapidities ($y_{cm} = 0$ corresponds to 18° in the lab, and $y_{cm} = -1.84$ is $\theta_{lab} = 90^\circ$)] it is evident that there is a low p_T component to the spectrum that can't be accounted for by the π^0 's.

It should be pointed out that the data shown in Figs. 3.23 and 3.24 have been arbitrarily normalized such that the peak occurs at about 10 for all displayed spectra. In reality, the yield at the widest angle is about 30% as much as at the peak. If this component is due to the isotropically decaying W nuclei, it would be most prominent just where it is seen in the figures. Since the fits have yet to be finalized, a subtraction of nuclear γ 's hasn't been carried out yet.

The Be fit is as good as the W at the high p_T end, but it doesn't show the excess at very low p_T for the wider angles that is seen in tungsten. Figure 3.25 shows the photon spectrum at $y_{cm} = 0$ for both Be and W photons from the fitted π^0 distribution, the bremsstrahlung and the sum of the two also displayed. The data doesn't show the characteristic asymptotic behavior of the bremsstrahlung because it hasn't yet been adjusted for the constant-fraction discriminator efficiencies. Figure 3.26 is the same as Fig. 3.25 except for data taken at $\theta_{lab} = 90^\circ$.

Although there are a few corrections yet to be performed to the data and it must undergo a thorough and systematic error analysis, the tentative judgment is that within the expected experimental errors, no anomalous excess of low p_T photons is seen for either Be or W, and the large-angle photon spectra indicate

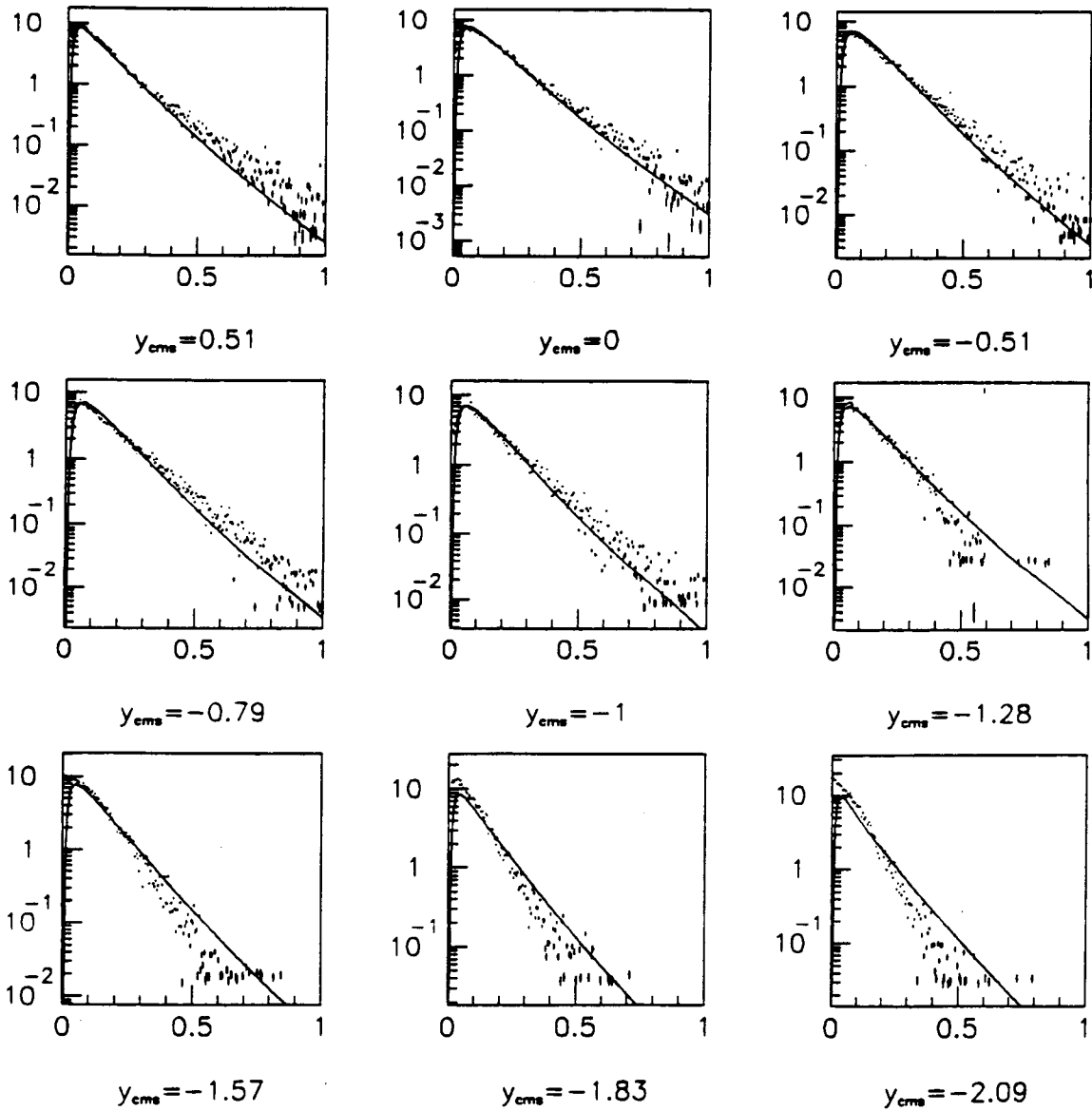


Fig. 3.23. W data shown with photons generated from π^0 distribution; the ordinate is arbitrarily normalized.

ORNL-DWG 92-15090

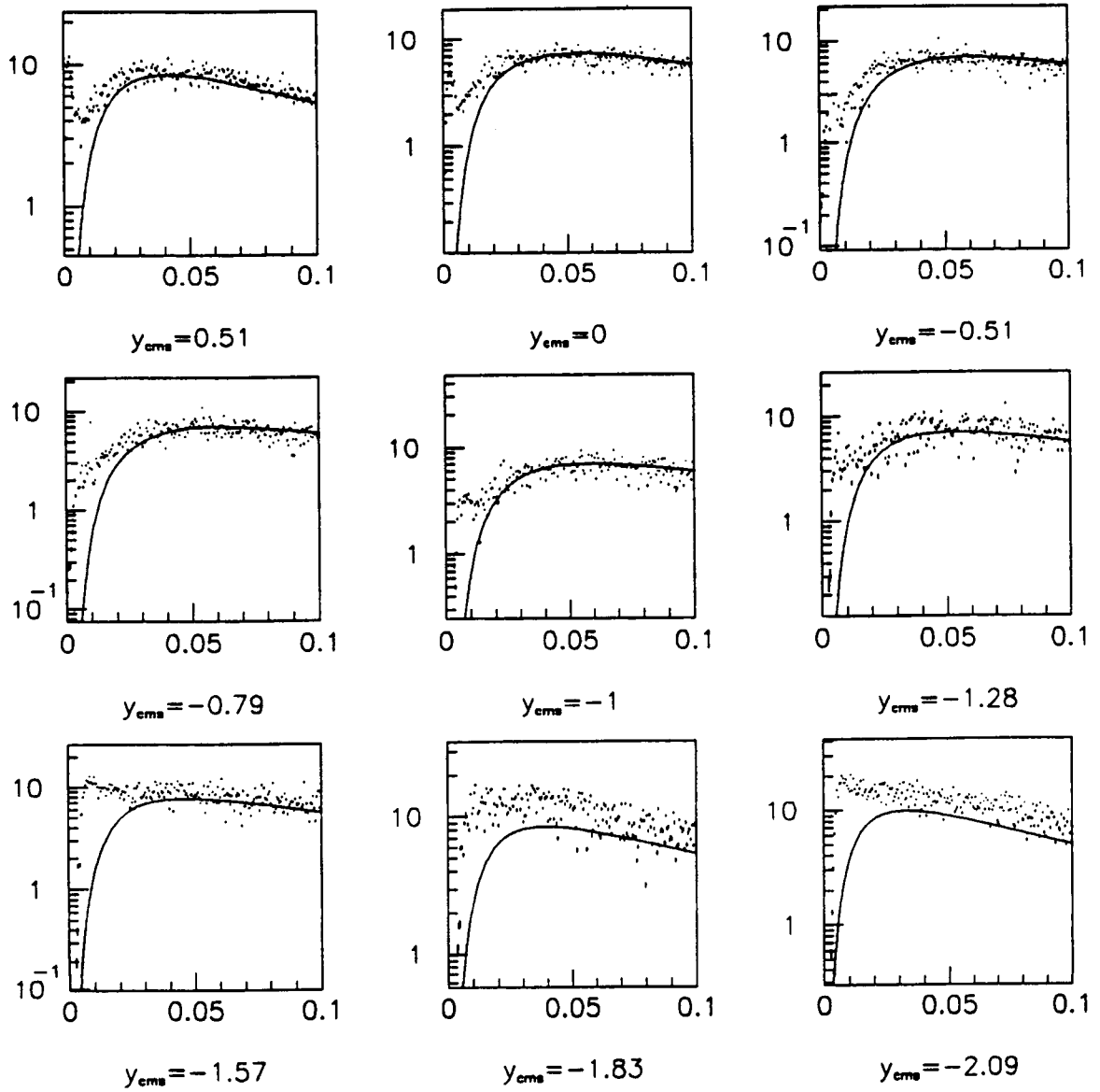


Fig. 3.24. W data shown with the fitted distribution with an expanded abscissa (photon transverse momenta).

ORNL-DWG 92-15091

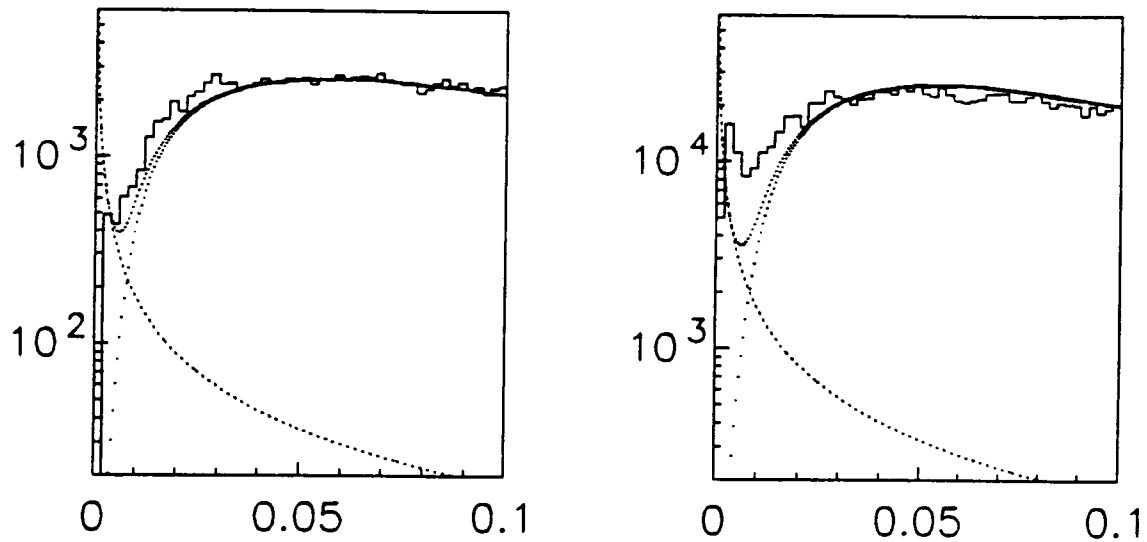


Fig. 3.25. p-Be(W) data shown left(right) at $\theta_{\text{lab}} = 18^\circ$ ($y_{\text{cm}} = 0$). With the data is plotted the fitted π^0 distribution, the bremsstrahlung (asymptotic at $p_T = 0$) and the sum of the two. Here the ordinate is $\frac{d^2\sigma}{dydp_T}$ in mb/GeV/c.

ORNL-DWG 92-15092

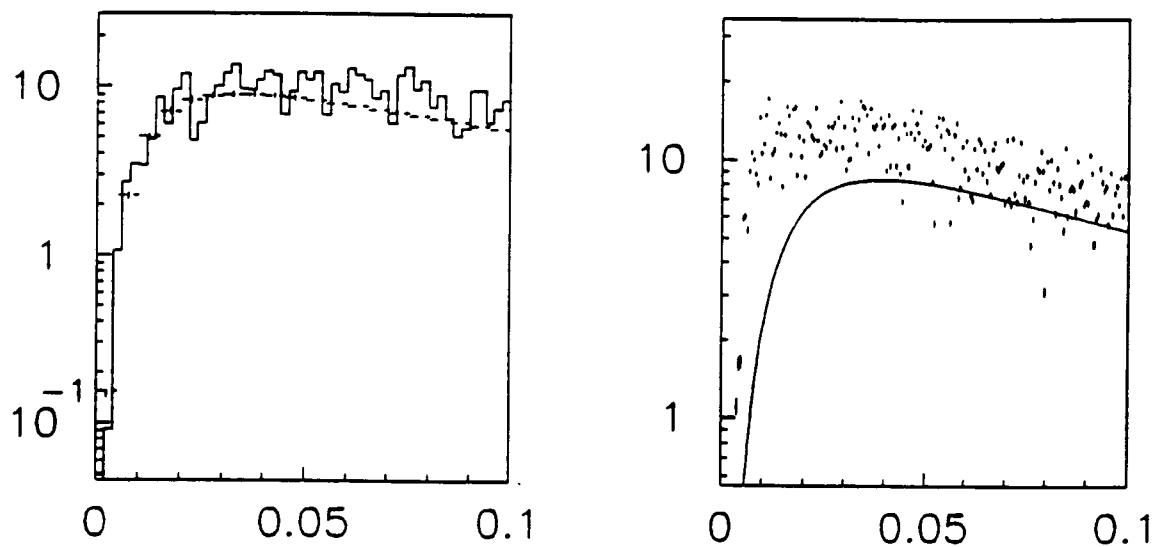


Fig. 3.26. p-Be(W) data shown left(right) at $\theta_{\text{lab}} = 90^\circ$ ($y_{\text{cm}} = -1.83$). An excess possibly due to nuclear γ 's in the W data is present.

the presence of a significant contribution of gamma rays from nuclear decays for the W target.

1. Vanderbilt University, Nashville, TN.
2. European Space Agency, Astrophysics Division, Noordwijk, The Netherlands.
3. Variable Energy Cyclotron Center, Calcutta, India.
4. CERN, Geneva, Switzerland.
5. Purdue University, West Lafayette, IN.
6. Brookhaven National Laboratory, Upton, NY.
7. J. A. Thompson, ed., *Proceedings of the Pittsburgh Workshop on Soft Lepton Pair and Photon Production* (Nova Science Publishers, Inc, New York, 1992).
8. R. Clark et al., *Phys. Div. Prog. Rep. for Period Ending Sept. 30, 1990*, ORNL-6660, p. 72.
9. R. Clark et al., *Phys. Div. Prog. Rep. for Period Ending Sept. 30, 1991*, ORNL-6689, p. 67.
10. T. Abbott et al., *Phys. Rev. Lett.* **66**, 1567 (1991).

PARTICLE MULTIPLICITY DEPENDENCE OF HIGH-ENERGY PHOTON PRODUCTION IN A HEAVY-ION REACTION¹

L. G. Sobotka,² L. Gallamore,² A. Chbihi,² D. G. Sarantites,² D. W. Stracener,² W. Bauer,³ D. R. Bowman,³ N. Carlin,³ R. T. DeSouza,³ C. K. Gelbke,³ W. G. Gong,³ S. Hannuschke,³ Y. D. Kim,³ W. G. Lynch,³ R. Ronningen,³ M. B. Tsang,³ F. Zhu,³ J. R. Beene, M. L. Halbert, and M. Thoennessen³

The production of high-energy photons in an intermediate energy heavy-ion reaction ($65 \text{ MeV/nucleon } ^{40}\text{Ar} + ^{93}\text{Nb}$) is studied by characterizing the events, which produce the photons, by the forward and backward, light and heavy, charged-particle production. While the absolute yield of high-energy photons increases with increasing charged particle multiplicity, the spectral shape is found to be almost independent of multiplicity. This indicates that the fundamental photon production mechanism is insensitive to the impact parameter but that the production process is more probable for the more violent collisions. This is expected for an incoherent nucleon-nucleon bremsstrahlung mechanism but not for a statistical mechanism. This work also provides a

comparison of two observables that have been suggested as impact parameter selectors: the high-energy photon yield and the charged-particle multiplicity. We find that the photon yield, binned by particle multiplicity, does not scale as would be expected if both techniques truly measured the impact parameter. This observation can be explained by large fluctuations in the particle multiplicity at fixed impact parameter.

1. Abstract of published paper: *Phys. Rev. C* **44**, R2257 (1991).
2. Washington University, St. Louis, MO.
3. Michigan State University, East Lansing, MI.

THE MECHANISM FOR THE DISASSEMBLY OF EXCITED ^{16}O PROJECTILES INTO FOUR ALPHA PARTICLES¹

R. J. Charity,² J. L. Barreto,² L. G. Sobotka,² D. G. Sarantites,² D. W. Stracener,² A. Chbihi,² N. G. Nicolis,² R. Auble, C. Baktash, J. R. Beene, F. Bertrand, M. Halbert, D. C. Hensley,³ D. J. Horen, C. Ludemann,⁴ M. Thoennessen,⁵ and R. Varner

The decay of excited ^{16}O projectiles into the four-alpha-particle exit channel has been investigated. The projectiles, with bombarding energies of $E/A = 25 \text{ MeV}$, were excited through peripheral interactions with ^{159}Tb target nuclei. The distribution of relative angles between the four alpha particles in their center of mass frame was compared to simulations of ^{16}O decay by various mechanisms. The relative angles are found to be consistent with either a disassembly via sequential evaporation of alpha particles or by a prompt disintegration process. The data are not consistent with a sequential decay sequence initiated by the fission of the projectile into two ^8Be fragments.

1. Abstract of paper accepted for publication in *Physical Review C*.
2. Washington University, St. Louis, MO.
3. Office of Waste Management and Remedial Actions, ORNL.
4. Human Resources Division, ORNL.
5. Michigan State University, East Lansing, MI.

DETECTOR, INSTRUMENTATION, AND COMPUTER DEVELOPMENT

UPGRADE OF THE HILI DETECTOR SYSTEM AND ITS COMMISSIONING AT THE TEXAS A&M CYCLOTRON

D. Shapira, M. Korolija,¹ and J. Gomez del Campo

In July 1991, the HILI was disassembled and shipped to the Texas A&M Cyclotron (TAMU) at College Station, Texas, and has been reassembled and readied for operation on a dedicated beam line at TAMU. The HILI now has eight ionization chambers for heavy-fragment detection. An array of Si-strip detectors to be used in front of several hodoscope elements has been purchased and tested. The noise level in each individual channel has to be low enough to discriminate 150-keV signals left by fast protons in the Si detector. We are now testing the electronic signal-processing package developed especially for that array. Three test runs have been performed and changes were made in the beam line that greatly improved the quality of the beam delivered. A new data acquisition system based on a DEC 5000 workstation operating under UNIX has been put together. The data analysis and reduction programs for the HILI have been rewritten and debugged as have the numerous programs that provided for smooth control and operation of the HILI during data acquisition (e.g., setup and other communication with the FastBus ADCs, pedestal acquisition and storage, control and matching of high voltages on 192 phototubes, etc.). We expect to start calibration measurements in November 1992 and take first data in early 1993.

1. Partial support from the Joint Institute for Heavy Ion Research, ORNL.

OCTAL AMPLIFIER AND DISCRIMINATOR MODULE FOR THE SILICON DIODE DETECTOR ARRAY IN THE HILI

*J. L. Blankenship,¹ J. Gomez del Campo,
and D. Shapira*

An array of 72 silicon-diode detectors is to be used in front of nine plastic scintillators in the hodo-

scope of the HILI detector system, now located at the Texas A&M University Cyclotron. Each plastic scintillator will have eight transmission-type silicon diodes in a close-packed 4-by-2 array in front of it. The silicon diodes provide improved angular resolution for light charged particles sensed by the plastic scintillator and a second measure of dE/dx for heavier charged particles.

An eight-channel preamplifier, amplifier, and discriminator module has been designed for this silicon-diode array. A total of nine modules are required for the 72 silicon-diode detectors. The analog signal from each of the eight charge-sensitive preamplifiers is amplified and applied to a summing amplifier for processing by a spectroscopy-type shaping amplifier. This approach reduces the number of spectroscopy amplifiers required, but increases the noise referred to the input by a factor of approximately three. Each analog signal is separately amplified, shaped by a high-pass filter, and applied to a fast leading-edge discriminator. The discriminator output is an emitter-coupled-logic (ECL) signal which is applied to a non-retriggerable, monostable multivibrator. The multivibrator provides a 500-ns differential ECL logic signal on a front-panel connector. The individual discriminator output signals enable identification of which one of the eight diode elements produced the signal at the analog sum output. Each of the eight channels of logic signals is also applied to an ORgate, and the resulting ECL logic signal is also provided at the front-panel connector. The discriminator threshold is adjustable from 0 to 1.0 volt by a front-panel potentiometer, and can be monitored by a test point on the front panel.

The module is constructed in conformance to the VXI specifications for the D-size module, except for the P1 connector-pin assignments. Connectors P2 and P3 are not used. Therefore, the P1 connector must provide the voltages required by the module, namely +12, -12, +5, and -5.2 volts, as well as the detector bias voltage. This module does not use the data and control lines defined in the VXI specifications in this design. A specialized backplane was designed for this system, which provides the required voltages on only the P1 connector. The large area provided by this module enables a circuit layout which exhibits no measurable crosstalk between the fast risetime (1ns),

ECL-logic signals and the low-level analog signals of the charge-sensitive preamplifier inputs.

1. Partial support from the Joint Institute for Heavy Ion Research, ORNL.

DEVELOPMENT OF THE ORNL BaF₂ ARRAY

*P. E. Mueller,¹ J. R. Beene, F. E. Bertrand,
J. L. Blankenship,¹ M. L. Halbert, D. J. Horen,
D. H. Olive,² and R. L. Varner*

During the past three years we have assembled, developed, and operated an array of 77, 6.5-cm x 20-cm, right-hexagonal-prism BaF₂ crystals, each coupled to a HAMAMATSU R2059 quartz-window photomultiplier tube with integral voltage-divider base and magnetic shield. These detectors are mounted in four 19 packs. The array was commissioned in July 1989 and has since been used in approximately 25 experiments at six different accelerator facilities. These experiments utilized light and heavy ion beams ranging in energy from a few MeV/nucleon to 95 MeV/nucleon. The experimental conditions required a BaF₂ gamma-ray detection system with very fast timing for time-of-flight discrimination between photons and much more abundant low-energy neutrons, pulse-shape discrimination for charged particles and high-energy neutrons, and good energy resolution. Among the more important results from these experiments was the first definitive observation of the two-phonon giant dipole resonance and the isolation of the isovector giant quadrupole resonance.

This success notwithstanding, our future plans are limited by the solid angle coverage we can achieve with the present array. In particular, experiments where neutral meson decays are either studied directly or are present as a background require larger crystal stacks (more elements) to be feasible. We therefore have requested funds to expand our array to 192 detectors.³ These detectors will be mounted either in ten 19 packs or in five 37 packs as required by each experiment (see Fig. 3.27). We also plan to provide each BaF₂ detector with a charged-particle veto (CPV). Each CPV will be an independent detector consisting of a hexagonal piece of thin plastic scintillator coupled by a lightguide to its own photomultiplier tube. Each plastic scintillator will

cover the face of one BaF₂ detector. The CPVs will provide charged-particle suppression on line.

While the performance of our present array has been superb, we have noticed a gradual deterioration of its energy resolution. Over a two-year period the resolution [$\Delta E(\text{FWHM})/E$, $E = 898 \text{ keV}$] of the BaF₂ detectors under experimental conditions has increased by an average of 13%. During the same time the gain of the BaF₂ detectors has decreased. If this decrease in gain resulted from a decrease in the number of primary scintillation photons, and/or photoelectrons, it should be related to the increase in resolution by Poisson statistics. The observed increase in resolution is actually somewhat less than would be predicted by this relationship for the majority of the detectors.

Bench tests of one fourth of the photomultiplier tubes were conducted by measuring their resolution at $E = 662 \text{ keV}$ when coupled to the same test BaF₂ crystal that was used three to four years earlier during their acceptance tests. This test crystal had never been used in an experiment. The resolution of the photomultiplier tubes has degraded by an average of 30% with respect to their acceptance tests. Individual photomultiplier tube resolution increased between 10% and 40%. Several of these photomultiplier tubes were further tested by measuring their resolution when coupled to the same NaI(Tl) crystal that had also been used in their acceptance tests. The average increase in resolution was 10%.

NaI(Tl) has ten times the light output of BaF₂. Therefore, for the same energy gamma ray, a small noise background in the photomultiplier tube would make a larger contribution to energy resolution when measured with a BaF₂ crystal than when measured with a NaI(Tl) crystal. Photomultiplier tube resolutions measured with the test BaF₂ crystal did not show any deviation from the predicted $1/\sqrt{E}$ behavior in the limited energy range from 662 keV to 1836 keV. A deviation would indicate a contribution to the resolution from a constant noise background added in quadrature with the photomultiplier tube signal.

The wavelength of maximum emission for NaI(Tl) is 415 nm. The wavelength of maximum emission for the slow component of BaF₂ (which contains most of the light) is 310 nm. A wavelength-dependent reduction in photocathode quantum efficiency could also account for the different increases in photomultiplier tube resolution measured with NaI(Tl) and BaF₂. Ion bombardment of the photocathode is a possible cause of quantum efficiency reduction. Evidence of ion bombardment is the

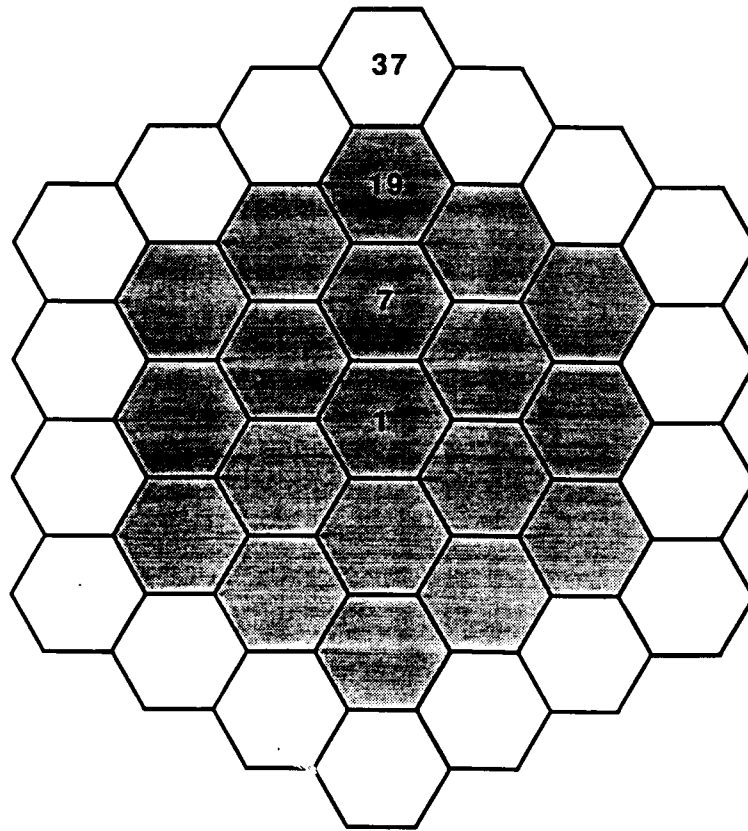


Fig. 3.27. Front view of a planned 37 pack of BaF_2 detectors. The shaded region shows the present 19 pack configuration.

presence of afterpulses in the photomultiplier tube signal.

The phenomenon of afterpulsing occurs when a gas atom between the photocathode and the first dynode is ionized by a photoelectron. The ion is accelerated back into the photocathode, ejecting many secondary electrons which behave just like the original photoelectron but are delayed by the ion drift time. The photomultiplier signal then consists of a primary pulse followed by an afterpulse. Similar processes can also occur along the dynode chain where the probability of ionization is higher (due to higher electron flux) but the subsequent amplification is lower.⁴ Since the ionization of gas atoms is a statistical process, afterpulsing also directly degrades photomultiplier tube resolution.

Gas inside a photomultiplier tube can either remain from the manufacturing process (residual gas), or, in the case of helium, leak directly through the glass envelope. Pure quartz (fused silica) is

significantly more permeable to helium than other glasses. Quartz window photomultiplier tubes are known to be particularly susceptible to inleakage of helium and the resultant afterpulsing.⁵

Observation with a 400 MHz microchannel-plate oscilloscope reveals distinct afterpulses starting 300 nsec after the primary pulse of many of our photomultiplier tubes, indicating the presence of helium. Averaging thousands of signals with a 500 MHz digitizing oscilloscope shows that, in addition to a broad peak around 300 nsec after the spike of the primary pulse, there is also a long tail which rides on the long tail of the primary pulse. The broad peak of the afterpulse is associated with the spike (fast light component) of the primary pulse. The long tail of the afterpulse is associated with the long tail (slow light component) of the primary pulse.

The magnitude of the afterpulse suggests that afterpulsing can make a *significant* direct contribution to resolution (in addition to causing long-term

photocathode degradation), particularly at the nominal integrating gate widths of 1500 nsec. The effect of afterpulsing is seen by measuring resolution with different integrating gate widths (see Fig. 3.28). Because of the long decay time of the slow component (600 nsec), the fractional resolution in a non-afterpulsing photomultiplier tube decreases with increasing gate width out to times on the order of 3 μ sec. Resolution then increases for longer gate widths since more noise is included in the gate without any significant additional inclusion of signal. By contrast, this minimum occurred at only 600 nsec for a selected photomultiplier tube that showed pronounced afterpulsing. This can be similarly understood as due to the introduction of afterpulsing noise at gate widths larger than 300 nsec.

Our present efforts are directed at correlating quantitative measurements of afterpulsing with resolution for all the photomultiplier tubes in our array. The conclusions of this study will have important consequences for future photomultiplier tube procurement, operation, and (perhaps) periodic replacement.

1. Partial support from the Joint Institute for Heavy Ion Research, ORNL.

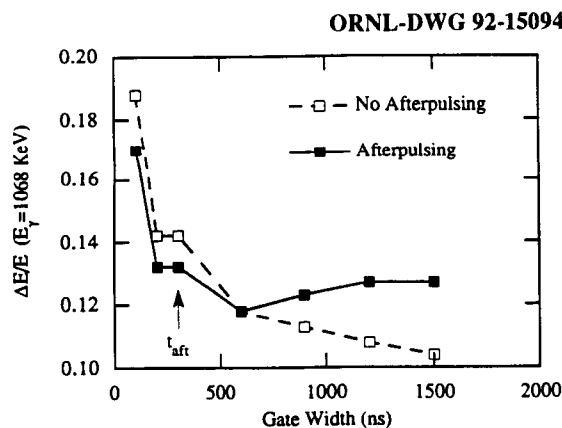


Fig. 3.28. Energy resolution as a function of integrating gate width for two different BaF₂ detectors. The open boxes show the expected behavior for a photomultiplier tube with no afterpulsing. The solid boxes show a minimum in resolution at 600 nsec for a photomultiplier tube with afterpulsing. t_{af} indicates the start of the afterpulse at 300 nsec after the primary pulse due to inleakage of helium.

2. Partial support provided by Vanderbilt University and Oak Ridge Associated Universities under the Laboratory Graduate Research Program.

3. Letter of intent to the Department of Energy, 10 April 1992.

4. Thorn EMI Electron Tubes catalog PMC/86.

5. Hamamatsu publication RES-0791-02, second edition.

HYBRID ION CHAMBER FOR THE TEXAS A&M CYCLOTRON SPECTROGRAPH

J. L. Blankenship,¹ R. L. Auble, J. R. Beene, F. E. Bertrand, and D. Shapira

Texas A&M University (TAMU) is replacing its Enge Spectrograph with a magnetic spectrograph originally designed and built for use at Oxford University. The focal-plane detector for the Oxford spectrograph is a hybrid ion chamber with a sensitive volume of 10.5-cm high, 49.5-cm deep, and 37-cm wide. The existing entrance window has a clear opening of 6 cm x 30 cm. The total energy signal is obtained from the charge induced on the cathode, Frisch grid, and field-shaping electrodes by the remaining positive ions after the electrons have drifted to the anode. Measurements of particle energy loss (ΔE) are made by two anode segments, each of which is 6.7-cm deep. The electrons collected from the remaining anode depth are not sensed electronically. The horizontal location of the track is measured at two depths by position-sensitive proportional counters (PSPC's) spaced 15 cm apart, with the two ΔE anodes between them.

The hybrid ion chamber has been tested at ORNL and changes in the design have been made to improve detector performance and adapt the chamber to the energy range of the TAMU Superconducting Cyclotron. New front and back cover plates have been designed. A plastic scintillator will be located at the rear window to stop particles which pass through the ion chamber, and thus will provide part of the total energy information. The new front cover plate will provide coupling to the transition chamber which will continue the vacuum flight path from the last spectrometer element to the entrance window of the ion chamber. Drawings of these parts are complete, and construction is under way at TAMU.

The design of the field-shaping electrode structure has been changed to provide a more robust

construction and to allow quick replacement of field-shaping wires at the front and rear windows. Stainless steel rods of 1.6-mm diameter are used as field-shaping electrodes on each side of the drift region. The voltage-divider resistors which fix the potential of the field-shaping electrodes are now located on a terminal strip, along with bypass capacitors, and the charge signal from the field-shaping electrodes is now available for addition to the charge signals from the cathode and the Frisch grid. Using a movable, collimated alpha source, we found that the charge signal induced by the positive ions was strongly dependent on horizontal position if the charge signal was obtained only from the anode and Frisch grid. At 15 cm from the chamber center, measured horizontally, the charge signal was found to drop to 70 per cent of that signal measured at the chamber center. This distance corresponds to the edges of the entrance window. This measurement demonstrates the importance of including the charge signal induced on the field-shaping electrodes.

The large quantity of Delrin plastic used in the original construction of the ion chamber presents a challenge to keeping the gas free of impurities which trap electrons and reduce electron mobility. After a month of conditioning, the reduced electric field at which near-complete electron collection could be obtained in isobutane was found to be 2.5 V/Torr-cm. This value was found to hold between 50 and 150 Torr of isobutane. This condition is achieved at 100 Torr for 3500 V on the cathode, 700 V on the Frisch grid, and anode at ground potential.

An improved system of grounding was installed in the ion chamber to reduce crosstalk between the proportional counters, the anodes, and the Frisch grid. A 2.5-cm-wide strip of printed-circuit board, clad on both sides with copper, extends from the front plate along both outer sides of the Delrin support structure to the rear, 3 mm below the anode plane, and is electrically bonded to the front cover. Filter capacitors are bonded to this ground bus with minimum lead length, thus minimizing lead inductance.

Modification of the ion chamber at ORNL has been completed, and the chamber has been returned to TAMU. Following completion of the new front and rear chamber windows/covers, beam tests will be made.

1. Partial support from the Joint Institute for Heavy Ion Research, ORNL.

COMPTON-SUPPRESSION TESTS ON GE AND BGO PROTOTYPE DETECTORS FOR GAMMASPHERE¹

A. M. Baxter,² T. L. Khoo,² M. E. Bleich,²
M. P. Carpenter,² I. Ahmad,² R.V.F. Janssens,²
E. F. Moore,² I. G. Bearden,³ J. R. Beene, and
I. Y. Lee⁴

Measurements are described of the Compton suppression of two prototype detectors for GAMMASPHERE. The prototypes consist of a large (75% efficient) n-type germanium detector with a BGO Compton-suppression shield. A peak-to-total ratio of 0.678(2) is achieved with a ⁶⁰Co source. This is the best ratio reported to date for a detector of this kind. The results are compared with those obtained from Monte Carlo simulations. The simulations can predict the observed peak-to-total ratios if a significant background from scattered photons is included.

1. Abstract of published paper: *Nucl. Instrum. Methods Phys. Res.* A317, 101 (1992).

2. Argonne National Laboratory, Argonne, IL.

3. Purdue University, West Lafayette, IN.

4. Present address: Lawrence Berkeley Laboratory, Berkeley, CA.

4. HIGH-ENERGY NUCLEAR AND PARTICLE PHYSICS

CERN WA93 AND WA98 EXPERIMENTS

WA93 Collaboration

*P. Donni,¹ E. Durieux,¹ M. Izycki,¹
M. Martin,¹ L. Rosselet,¹ N. Solomey,¹
R. Bock,² H. H. Gutbrod,² B. W. Kolb,²
H. R. Schmidt,² S. Kachroo,³ N. K. Rao,³
S.S. Sambyal,³ V. Antonenko,⁴ S. Fokin,⁴
M. Ippolitov,⁴ K. Karadjev,⁴ A. Lebedev,⁴
V. Manko,⁴ S. Nikolaev,⁴ A. Vinogradov,⁴
H. Löhner,⁵ I. Lund,⁵ G. Claesson,⁶
A. Eklund,⁶ S. Garpman,⁶ H. A. Gustafsson,⁶
J. Idh,⁶ A. Oskarsson,⁶ I. Otterlund,⁶
K. Söderström,⁶ E. Stenlund,⁶
H. J. Whitlow,⁶ F. Berger,⁷ D. Bock,⁷
G. Clewing,⁷ L. Dragon,⁷ R. Glasow,⁷
G. Hölker,⁷ K.-H. Kampert,⁷ T. Peitzman,⁷
M. Purschke,⁷ R. Santo,⁷ K. Steffens,⁷
P. Steinhäuser,⁷ D. Stüken,⁷ T. C. Awes,
F. E. Obenshain, F. Plasil, S. Saini,
G. R. Young, M. M. Agarwal,⁸ V. S. Bhatia,⁸
I. S. Mitra,⁸ B. S. Garcha,⁸ K. B. Bhalla,⁹
S.K. Gupta,⁹ S. Lokanathan,⁹ S. Mukherjee,⁹
S. Ramiwala,⁹ X. He,¹⁰ S. P. Sorensen,¹¹
N. Van Eijndhoven,¹² R. Kamermans,¹²
S. Chattopadhyay,¹³ A. Das,¹³
M.R.D. Majumdar,¹³ T. Ghosh,¹³
G.S.N. Murthy,¹³ M. N. Rao,¹³
B. C. Sinha,¹³ D. K. Srivastava,¹³
M. D. Trivedi,¹³ Y. P. Vijoyi¹³*

The CERN WA93 experiment is the successor to the WA80 experiment in which ORNL has participated since 1984. The primary purpose of WA93 is to extend the data set obtained by WA80 and, in addition, to implement new detector systems commissioned primarily for use in the upcoming WA98 experiment. WA98 will be the successor to experiment WA93 and will be performed using the lead beams at CERN. It was described in last year's progress report under the title "Proposal for a Large-

Acceptance Hadron and Photon Spectrometer" (Ref. 14).

During this reporting period, two WA93 runs have taken place. The first run was carried out in October and November 1991, and the second run took place in April 1992. The primary change in WA93 relative to WA80 is the removal of the Plastic Ball and the addition of a large magnet ("Goliath") needed for particle tracking, which is performed by means of multistep avalanche counters (MSACs). In addition, a photon multiplicity detector (PMD) built by Indian members of the collaboration was also commissioned. The ORNL designed and built Mid-Rapidity Calorimeter (MIRAC) and Zero-Degree Calorimeter (ZDC), as well as the nearly 4000-element lead-glass photon detector, were retained from experiment WA80 for operation in WA93. Prior to the first WA93 run, the radiation-damaged scintillator of the ZDC had to be replaced since its performance had degraded to an unacceptable level. The radiation damage was a result of the combined effect of the continuous low-level uranium activity from the ZDC absorber plates, as well as the higher level radiation doses received from the full intensity heavy-ion beams stopped in the ZDC. The replacement of the ZDC scintillator plates turned out to be a difficult (and expensive) operation due to the presence of uranium oxide powder from the corroded depleted-uranium absorber plates.

The first WA93 run (October–November 1991) was only a partial success. This was, in part, due to the fact that the new detector systems had not been thoroughly studied in test beams and some (e.g., MSACs) did not perform as expected. It was also due partly to numerous beam delivery problems. The second WA93 run (April 1992) was much more productive than the first run. However, while the performance of the MSACs continued to improve during the run, their efficiency never exceeded 80%. Nevertheless, during both runs a large amount of photon data was obtained.

In early April 1992, the SPSL Committee approved the P260 proposal, leading to experiment

WA98. This approval, however, was extended to only part of the experiment (photon measurements). The committee withheld approval of the tracking portion of the proposal, pending presentation of results from the WA93 runs. The actual design of WA98 continues to undergo changes. MIRAC will continue in operation, but will be reconfigured. The size of the lead-glass array will be expanded to 10,000 elements, and ORNL-designed monolithic electronics will be installed on it for readout. A larger PMD will be constructed. The ZDC will be decommissioned and replaced by a calorimeter capable of withstanding the increased exposure to radiation damage which will take place with lead beams. The Plastic Ball will be reinstalled. It is expected that experiment WA98 will first be operated in 1994.

1. University of Geneva, Switzerland
2. GSI, Darmstadt, Germany.
3. University Jammu, India.
4. Kurchatov Inst., Moscow, USSR.
5. KVI, Goningen, The Netherlands.
6. University of Lund, Sweden.
7. University of Münster, Germany.
8. Punjab University, Chandigarh, India.
9. University Rajasthan, Jaipur, India.
10. University Tennessee, Knoxville.
11. Adjunct research participant from the University of Tennessee, Knoxville.
12. University of Utrecht, The Netherlands.
13. VECC, Calcutta, India.
14. *Phys. Div. Prog. Rep. for Period Ending Sept. 30, 1991*, ORNL-6689, p.80.

STATUS REPORT OF WA80 PROTON DATA ANALYSIS

WA80 Collaboration

R. Albrecht,¹ T. C. Awes, P. Beckmann,²
 F. Berger,² R. Bock,¹ G. Claesson,³
 G. Clewing,² L. Dragon,² A. Eklund,³
 R. L. Ferguson, A. Franz,⁵ S. Garpman,³
 R. Glasow,² H. A. Gustafsson,³
 H. H. Gutbrod,¹ J. Idh,³ P. Jacobs,⁴
 K. H. Kampert,² B. W. Kolb,¹
 P. Kristiansson,³ I. Y. Lee, H. Löhner,²
 I. Lund,¹ F. E. Obenshain, A. Oskarsson,³
 I. Otterlund,³ T. Peitzmann,² S. Persson,³
 F. Plasil, A. M. Poskanzer,⁴ M. Purschke,²

H. G. Ritter,⁴ S. Saini, R. Santo,²
 H. R. Schmidt,¹ R. Schmidt,³ T. Siemiarczuk,¹
 S. P. Sorensen,⁶ E. Stenlund,³
 M. L. Tincknell, G. R. Young

The WA80 collaboration has published results of calorimetric measurements of transverse and forward energy distributions in previous years.⁷ The setup included a midrapidity calorimeter (MIRAC) and a zero-degree calorimeter (ZDC). The reactions were induced by 60-GeV/c/A oxygen, 200-GeV/c/A oxygen, and 200-GeV/c/A sulphur beams from the CERN SPS bombarding different targets. Analysis of WA80's 200-GeV/c proton data taken in 1988 will provide additional understanding of the reaction mechanisms in high-energy collisions; this analysis is presently underway.

The experimental minimum-bias cross sections have been compared with the Fritiof 1.7 calculations and Glauber theory predictions (see Table 4.1). All the cross sections and spectra have been corrected for background effects by subtracting the normalized results from runs on an empty aluminum target frame. The background corrections to the raw minimum-bias cross sections are typically between 20% to 30% and only affect the E_T spectra for the most peripheral events (i.e., E_T less than 2.5 GeV).

Preliminary transverse energy E_T spectra (measured using MIRAC) were obtained for the targets ^{nat}C , ^{27}Al , ^{nat}Cu , ^{nat}Ag , and ^{197}Au (see Fig.4.1). Several parameterizations have been tested to fit the E_T spectra by using the single- and double-gamma distributions.^{8,9} A single-gamma distribution (with three parameters) does not fit the E_T spectra well. A better fit to the E_T spectra can be obtained with the double-gamma distribution, at the cost of introducing two

Table 4.1. Comparison of WA80 pA minimum-bias (MB) cross sections with Fritiof 1.7 and Glauber theory predictions.

Target	MB Cross Section (mb)		
	Fritiof	Glauber	WA80
C	221.5	235.3	245.9
Al	402.0	410.3	351.0
Cu	755.8	756.3	809.9
Ag	1103	1085	1178
Au	1701	1628	1760

ORNL-DWG 92-15105

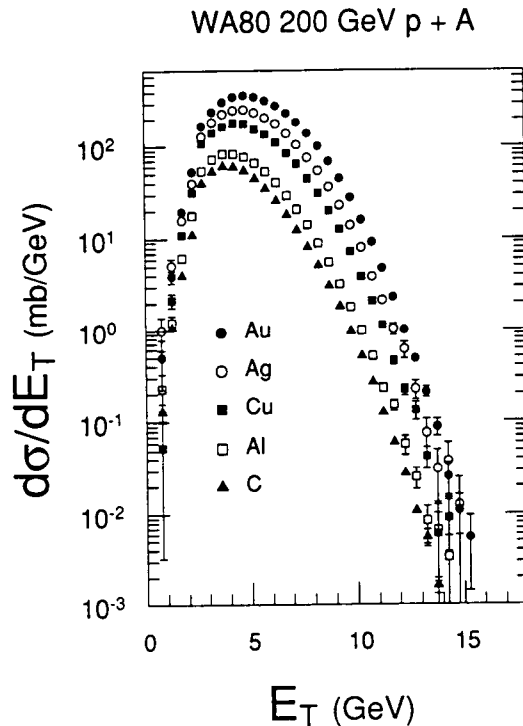


Fig. 4.1. Transverse energy spectra (minimum bias) for 200-GeV/c proton-induced reactions on ^{nat}C , ^{27}Al , ^{nat}Cu , ^{nat}Ag , and ^{197}Au target. The error bars reflect the statistical error only, and the spectra have been corrected for distortions caused by background events.

additional free parameters in the fit procedure. A clear physics interpretation of these parameters is lacking. An alternative approach is to use folding models to get effective nucleon-nucleon E_T spectra from p+A reactions. The A+A spectra can then be built up from the effective nucleon-nucleon E_T spectra by using properties of p+A and A+A collisions.

MIRAC covered a pseudorapidity range of $1.6 < \eta < 6.0$. It had a full azimuthal coverage in the pseudorapidity interval $2.4 < \eta < 5.5$, for both the WA80 proton and heavy-ion runs. Preliminary pseudorapidity distributions were obtained using different event selection criteria. These were fit well using a Gaussian distribution, and a target-mass dependence of the $dE_T/d\eta$ distributions was established. The distribution shifts backwards further in pseudorapidity space, with greater target mass. This is consistent with WA80's heavy-ion data.⁷

In addition, some of the Monte Carlo code predictions have been compared with our data. This will be explored more in further data analysis.

1. GSI, Darmstadt, Germany.
2. University of Münster, Germany.
3. University of Lund, Sweden.
4. LBL, Berkeley, Calif.
5. University of Tennessee, Knoxville.
6. Adjunct research participant from the University of Tennessee, Knoxville.
7. R. Albrecht et al., WA80 Collaboration, *Phys. Rev. C* **44**, 2739 (1991) and references therein.
8. M. J. Tannenbaum, *Inter. Journal of Mod. Phys. A* **4**, 3377 (1989).
9. T. Abbott et al., E-802 Collaboration, *Phys. Rev. C* **45**, 2933 (1992).

TRANSVERSE ENERGY AND FORWARD ENERGY PRODUCTION IN A HIGH-ENERGY NUCLEAR COLLISION MODEL¹

Jing-Ye Zhang,² Xiaochun He,² Chia C. Shih,²
Soren P. Sorensen,³ Cheuk-Yin Wong

Distributions of transverse energy, forward energy, and dE_T/d from 60 A GeV and 200 A GeV ^{16}O -induced and 200 A GeV ^{32}S -induced nuclear collision with Al, Cu, Ag, and Au are calculated by a high-energy nuclear collision model and compared to recent experimental data from the WA80 Collaboration at CERN. The high-energy nuclear collision Monte Carlo model, which is based on the concept of independent, multiple nucleon-nucleon collisions, describes the experimental data well at forward rapidity and midrapidity.

1. Abstract of published paper: *Phys. Rev. C* **46**, 748 (1992).
2. University of Tennessee, Knoxville.
3. Adjunct research participant from the University of Tennessee, Knoxville.

HADRONIC MODEL FOR THE SPACE-TIME DEVELOPMENT OF HIGH-ENERGY NUCLEAR COLLISIONS

Soren P. Sorensen¹ Chao Wei-Qin²

Since 1986, ORNL's High-Energy Reactions Group has, as part of the CERN WA80 collaboration, accumulated a large amount of calorimeter data from high-energy nuclear collisions. Most of these data have now been analyzed and published. In an attempt to understand better the physics underlying the data, we have started a theoretical attempt to model the space-time development of high-energy nuclear collisions. The emphasis in the model has been put on investigating how much information about the energy densities attained can be obtained from the available data on transverse energy and forward energy.

The model is based on a completely hadronic scenario in which the energy lost in the binary collisions between the initial nucleons is used to generate pions with p_T and rapidity distributions obtained from free nucleon-nucleon collisions. The pions emerge after a formation time τ_0 in their own rest frame. The subsequent rescattering between nucleons and pions is treated with special care by a novel method, which is Lorentz-frame independent.

We find that the maximal energy density at SPS energies [$\sqrt{s} < 20$ GeV] is 30-50% smaller than predicted by use of the Bjorken formula. This is caused by the finite collision time of approximately 1 fm/c, which is comparable to the formation time. At RHIC energies the collision time will be much smaller, and the energy densities will be closer to the Bjorken model predictions. These considerations assume that no rescattering takes place.

If, however, the rescattering is turned on, the measured transverse energies change considerably, whereas, the maximal energy density does not. This is because the maximal energy density is reached early in the collision before rescattering has any effect.

We have also made systematic studies of the effects on the energy density of different formation times, stopping powers, bombarding energies, and colliding nuclei. Figure 4.2 shows a typical develop-

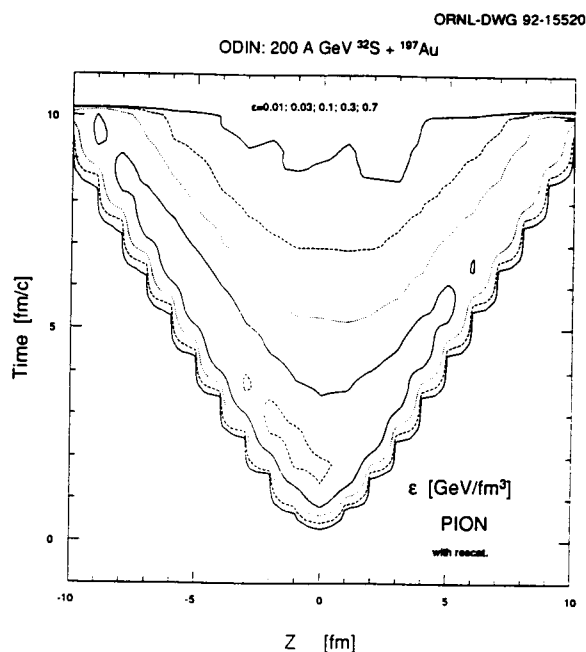


Fig. 4.2. The longitudinal space and time development of the local energy density in a central collision of 200 A GeV ³²S+¹⁹⁷Au.

ment of the energy density as a function of the time and longitudinal coordinate.

1. Adjunct research participant from the University of Tennessee, Knoxville.

2. Institute of High Energy Physics, Beijing, P.R.C., and CCAST, Beijing, P.R.C.

PRECONCEPTUAL DESIGN OF PHENIX EXPERIMENT FOR RHIC

PHENIX Collaboration

J. C. Gregory,¹ T. Shiina,¹ Y. Takahashi,¹
 M. Tocci,¹ S. K. Gupta,² S. H. Aronson,³
 M. Fatyga,³ S. Gavin,³ W. Guryan,³ J. Harder,³
 S. Kahn,³ E. Kistenev,³ P. Kroon,³ M. J. Murtagh,³
 E. O'Brien,³ L. Paffrath,³ S. Rankowitz,³
 S. Rescia,³ T. K. Shea,³ M. Tanaka,³

- M. J. Tannenbaum,³ C. L. Woody,³ P. Beery,⁴
 Sun-Yiu Fung,⁴ Ju-Hwan Kang,⁴ R. Seto,⁴
 Xixiang Bai,⁵ Kexing Jing,⁵ Xiaoping Liu,⁵
 Zuhua Liu,⁵ Yajun Mao,⁵ Benhao Sa,⁵ Zuxun Sun⁵
 Yude Wan,⁵ Zhongqi Wang,⁵ Jincheng Xu,⁵
 Xiaoze Zhang,⁵ Yuming Zheng,⁵
 Shuhua Zhou,⁵ C. Y. Chi,⁶ B. Cole,⁶ J. Dodd,⁶
 Qiming Li,⁶ S. Nagamiya,⁶ T. Nayak,⁶ W. Sippach,⁶
 P. Stankus,⁶ O. Vossnack,⁶ Fuqiang Wang,⁶
 Yufeng Wang,⁶ Yuedong Wu,⁶ Xihong Yang,⁶
 W. A. Zajc,⁶ Wenlong Zhan,⁶ L. C. Dennis,⁷
 A. D. Frawley,⁷ X. T. Liu,⁸ G. Peitit,⁸ Z. Zhan,⁸
 H. Iwata⁹ A. Sakaguchi,⁹ T. Sugitate,⁹ Y. Sumi,⁹
 R. Aryaeinejad,¹⁰ R. DeVries,¹⁰ J. Cole,¹⁰
 M. Drigert¹⁰ Zheng-dong Cheng,¹¹
 Shao-min Chen,¹¹ Qi-ming Li,¹¹ Jun-guang Lu,¹¹
 De-wu Wang,¹¹ Wei-qin Zhao,¹¹ Zhi-peng Zheng,¹¹
 Yu-can Zhu,¹¹ V. V. Ammosov,¹² A. Denisov,¹²
 A. Durum,¹² V. Gapienko,¹² Yu. Galiitsky,¹²
 Yu. Gutnikov,¹² A. Ivanilov,¹² V. I. Kochetkov,¹²
 B. Korablev,¹² A. Kozelov,¹² V. V. Makeev,¹²
 E. Melnikov,¹² Yu. Mikhailov,¹² V. Onuchin,¹²
 Yu. Pischalnikov,¹² Yu. Protopopov,¹²
 V. I. Rykalin,¹² K. Shestermanov,¹² A. Starkov,¹²
 D. Strustymov,¹² A. Surkov,¹² V. Zaetz,¹²
 A. Zaichenkov,¹² Ruirong He,¹³ Genming Jin,¹³
 Yixiao Luo,¹³ Baowan Wei,¹³ Hongfei Xi,¹³
 Feng Ye,¹³ Wenlong Zhan,¹³ Jingyu Zhang,¹³
 Y. Akiba,¹⁴ H. Hamagaki,¹⁴ S. Homma,¹⁴ H. Sako,¹⁴
 M. Sekimoto,¹⁴ L. A. Ewell,¹⁵ J. C. Hill,¹⁵
 H. Skank,¹⁵ W. Thomas,¹⁵ F. K. Wahn,¹⁵
 L. Anatori,¹⁶ A. Baldin,¹⁶ A. Malakhov,¹⁶
 Z. Pavel,¹⁶ A. Sergei,¹⁶ R. Sergei,¹⁶ D. Vladimir,¹⁶
 A. Yuri,¹⁶ J. Chiba,¹⁷ Y. Mori,¹⁷ M. Nomachi,¹⁷
 O. Sasaki,¹⁷ H. Sakamoto,¹⁷ T. Shintomi,¹⁷
 K. H. Tanaka,¹⁷ K. S. Sim,¹⁸ S. Belyaev,¹⁹
 S. Fokin,¹⁹ M. Ippolitov,¹⁹ K. Karadjev,¹⁹
 A. Lebedev,¹⁹ V. Manko,¹⁹ A. Nyanine,¹⁹
 A. Vinogradov,¹⁹ H. Enyo,²⁰ H. Kaneko,²⁰
 J. Costales,²¹ Z. Koenig,²¹ L. Hansen,²¹
 N. Namboodiri,²¹ C. Sangster,²¹ J. Thomas,²¹
 S. Tonse,²¹ R. Yamamoto,²¹ R. Zasadzinski,²¹
 J. G. Boissevain,²² T. A. Carey,²² A. Gavron,²²
 H. van Hecke,²² B. Jacak,²² J. Kapustinsky,²²
 M. Leitch,²² J. Lillberg,²² P. L. McGaughey,²²
 J. Moss,²² J. Simon-Gillo,²² W. E. Sondheim,²²
 J. P. Sullivan,²² L. Waters,²² P. N. Kirk,²³
 Z. F. Wang,²³ Jaingchen Yu,²³ E. F. Zganjar,²³
 S. Garpman,²⁴ H.-A. Gustafsson,²⁴ A. Oskarsson,²⁴
 I. Otterlund,²⁴ K. Soderstrom,²⁴ E. Stenlund,²⁴
 J. Barrette,²⁵ S. K. Mark,²⁵ L. Nikkinen,²⁵
 L. Normand,²⁵ M. Rosati,²⁵ F. Berger,²⁶
 R. Glasow,²⁶ K.-H. Kampert,²⁶ Th. Peitzmann,²⁶
 R. Santo,²⁶ E. Takada,²⁷ P. Braun-Munzinger,²⁸
 G. David,²⁸ T. Hemmick,²⁸ B. Hong,²⁸
 W. J. Llope,²⁸ S. Panitkin,²⁸ M. Rao,²⁸ J. Stachel,²⁸
 N. Xu,²⁸ Y. Zhang,²⁸ C. Zou,²⁸ T. Awes, Hee Kim,
 F. Obenshain, F. Plasil, S. Saini, G. R. Young,
 Shang-lian Bao,²⁹ Jia-ehr Chen,²⁹
 Dong-xing Jiang,²⁹ Lun-cun Wei,²⁹
 N. K. Abrosimov,³⁰ N. N. Chernov,³⁰
 V. G. Ivochkin,³⁰ L. M. Kochenda,³⁰
 G. A. Rjabov,³⁰ V. Schegelski,³⁰
 D. M. Seliverstov,³⁰ N. Smirnov,³⁰
 E. M. Spiridenkov,³⁰ A. Vorobyov,³⁰ O. Dietzsch,³¹
 N. Cansian de Silva,³¹ E. M. Takagai,³¹
 N. Carlin,³¹ R. Matheus,³¹ A. Szanto de Toledo,³¹
 J. C. Kim,³² Xiao-chun He,³³ J. Kreke,³³
 S. Sorensen,³³ G. Torshizi,³³ R. Hayano,³⁴
 T. Ishikawa,³⁴ H. Sakurai,³⁴ K. Shigaki,³⁴
 H. Tamura,³⁴ I. Arai,³⁵ Y. Igarashi,³⁵ T. Ikeda,³⁵
 M. Ise,³⁵ S. Kato,³⁵ H. Kitayama,³⁵ A. Kumagai,³⁵
 K. Kurita,³⁵ Y. Miake,³⁵ Y. Nagasaka,³⁵
 H. Tobinai,³⁵ K. Tomizawa,³⁵ S. Ueno,³⁵ K. Waki,³⁵
 K. Yagi,³⁵ Y. Yamashita,³⁵ E. Cornell,³⁶
 C. Maguire,³⁶ A. V. Ramayya,³⁶
 J. Barris,³⁷ M. Bennett,³⁷ A. Chikanian,³⁷
 G. Diebold,³⁷ B. Shiva Kumar,³⁷ J. Mitchell,³⁷
 J. Nagle,³⁷ A. Oulette,³⁷ K. Pope,³⁷ S. Borenstein,³⁸
 W. L. Kehoe,³⁹ K. Kimura⁴⁰

The PHENIX Preliminary Conceptual Design Report (PCDR) was submitted to Brookhaven National Laboratory and RHIC management on June 29, 1992. Subsequent reviews by the BNL/RHIC Technical Advisory Committee and Program Advisory Committee were held in August and September 1992, respectively. The collaboration will submit a formal Conceptual Design Report to BNL in January 1993, with the intent to begin final engineering and construction of PHENIX by the latter part of 1993.

The PHENIX collaboration consists of about 275 scientists, engineers, and graduate students from 41 institutions in 10 countries. The collaboration is still growing.

The PHENIX collaboration at RHIC was formed under a common interest to measure as many potential signatures of the quark-gluon plasma (QGP) as possible, to see if any or all of the physics variables show a simultaneous anomaly due to the formation of the QGP. We concentrate our efforts on electromagnetic radiation and selected aspects of hadron emission from relativistic heavy-ion collisions. We emphasize the importance of searching in parallel for

several markers of deconfinement, our hypothesis being that formation of the QGP will have many identifying marks, with no single signal assured of success. A key theme is the measurement of continuum electromagnetic radiation from the strongly-interacting system created in the collision. This radiation is observed in the form of real and virtual photons (via $\gamma^* \rightarrow l^+l^-$, $l = e$ or μ). We will be sensitive to this continuum from the high p_T and m_T range, above 4 GeV, where perturbative QCD should serve as a quantitative point of reference, down through the range from 1-3 GeV and below, where radiation from a QGP is expected to be largest. Creation of a plasma with a large latent heat or large initial temperature will result in large amounts of radiation emitted. Similarly, we would be sensitive to a system with a long-lived mixed phase, the more so the higher the QCD critical temperature happens to be. We will also detect l^+l^- decays of vector mesons, a particularly useful class of hadrons for probing the matter created at RHIC and sensing changes in it. In the hadron sector, we will perform measurements of π^\pm and K^\pm spectra, measurements of small Δq correlations, and measurements of specific decays such as $\phi \rightarrow K^+K^-$. This gives us capabilities to observe strange particles (K^\pm) and particles carrying strange quarks (ϕ, η). The production of both types of particles is predicted to be modified in the presence of a plasma or mixed phase with temperature T approaching m_s , the strange quark mass. We will also study two-particle correlation measurements, which yield information on the space-time size and shape of the system at hadronization. Observation of a particularly large system or one exhibiting a shape asymmetry, characteristic of a long hadronization time, would be expected to be correlated with observing significant thermal electromagnetic radiation (e.g., in the form of copious photon emission at $p_T \sim T_{crit}$). By measuring hadrons, we can also test ideas concerning the expected chiral-restoring transition of strongly interacting matter via comparison of $\phi \rightarrow e^+e^-$ and $\phi \rightarrow K^+K^-$ decay channels, which requires a comparison of lepton and hadron decay modes under the same set of reaction conditions.

We will search for a QGP through the programmatic study of a broad array of potential signatures as a function of energy density in both A + A and p + A collisions. Since some of the potential signatures involve rare processes and small effects, we have designed the detector to be capable of taking data at the highest luminosities expected to be provided at RHIC. An isometric view of the PHENIX detector, as proposed in the PCDR, is shown in Fig.4.3.

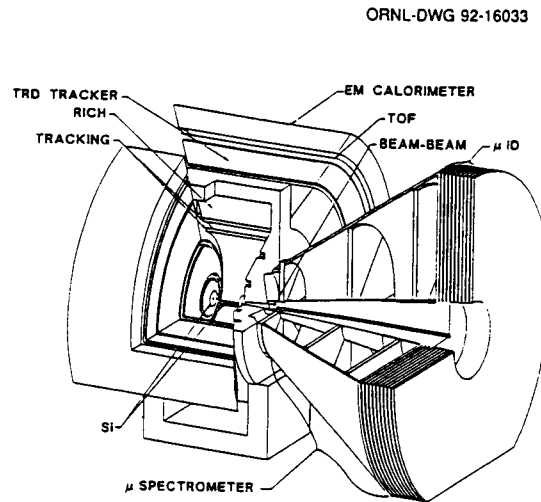


Fig. 4.3. Overview of the PHENIX detector showing the location of detector subsystems.

We have chosen an axial field magnet with two opposing electron detectors in order to have uniform p_T acceptance for dielectrons. Electrons and positrons are detected by this two-arm spectrometer, each arm subtending 90° in azimuth (ϕ) and ± 0.35 units in pseudorapidity (η), roughly equivalent to a polar angle (θ) acceptance of $\pm 20^\circ$ centered at θ equal to 90° . The solid angle of each arm is 0.94 sr. Within this aperture, which is to be fully active for electrons, are subsets for photons ($\Delta\phi = 45^\circ$, $\Delta\eta = \pm 0.35$ for Pb glass and $\Delta\phi = 90^\circ$, $\Delta\eta = \pm 0.15$ for CsI or BaF₂) and for hadrons ($\Delta\phi = 30^\circ$, $\Delta\eta = \pm 0.35$). For muons, a cone within θ equal to 37° around the beam direction is instrumented.

The detector consists of two magnets and a number of detector subsystems, which are summarized in the table below.

The detector will use the Major Facility Hall (MFH) at RHIC for final assembly and operation. Beneficial occupancy of the MFH in January, 1994, is required in order to complete the detector for operations in September, 1997.

1. University of Alabama, Huntsville.
2. BARC, Bombay, India .
3. Brookhaven National Laboratory, Upton, NY.
4. University of California - Riverside, CA.
5. China Institute of Atomic Energy, Beijing, P.R.C.
6. Columbia University, Nevis Laboratory, Irvington, NY.

Table 4.2. Summary of the detector subsystems for the standard version of PHENIX.

Element	$\Delta\eta$	$\Delta\phi$	Ch#	Purpose, special features, etc.
Magnet:central	± 0.5	360°		1.0 Tm for ++; 0.41 Tm for +-
muon	1.1-2.5	360°		0.95 Tm for $\eta = 2$; 0.41 Tm for $\eta = 1.3$
Beam-beam	$\pm 3.1-4$	360°	0.1K	Start timing, on-line vertex decision
Si strip	± 2	120°	23K	$dN/d\eta$, accurate vertex decision
Si pad	$\pm 1.6-3.8$	360°	23K	$d^2N/d\eta d\phi$
Drift chambers	± 0.35	$90^\circ \times 2$	13K	Good momentum resolution, $\Delta m/m = 0.4\%$ at the ϕ
Pad chambers	± 0.35	$90^\circ \times 2$	47K	Pattern recognition, tracking for non-bend direction
TE chambers	± 0.35	$90^\circ \times 2$	43K	Pattern recognition, dE/dx and TRD
RICH	± 0.35	$90^\circ \times 2$	6.4K	Electron ID and tracking, PM tube based
TOF	± 0.35	30°	2K	$\sigma < 100$ ps; good hadron ID
EM Cal	± 0.35	$90^\circ \times 1.5$	18K	Good e/π separation
Pb-glass	± 0.35	45°	10K	Photon detection
CsI/BaF ₂	± 0.05	90°	3K	High resolution photon detection
Muon chambers	1.1-2.5	360°	17K	Tracking for muons
Muon identifier	1.1-2.5	360°	10K	Steel absorbers and streamer tubes for μ /hadron separation

7. Florida State University, Tallahassee .
8. Georgia State University, Atlanta.
9. Hiroshima University, Japan.
10. Idaho National Engineering Laboratory, Idaho Falls, ID.
11. Institute of High Energy Physics, Academia Sinica, Beijing, P.R.C.
12. Institute of High Energy Physics, Protovino, Russia.
13. Institute of Modern Physics, Academia Sinica, Lanzhou, P.R.C.
14. Institute for Nuclear Study, University of Tokyo, Japan.
15. Iowa State University, Ames.
16. Joint Institute for Nuclear Study, Dubna, Russia.
17. KEK, Institute for High Energy Physics, Tsukuba, Japan.
18. Korea University, Seoul, Korea.
19. Kurchatov Institute, Moscow, Russia.
20. Kyoto University, Japan.
21. Lawrence Livermore National Laboratory, Livermore, CA.
22. Los Alamos National Laboratory, Los Alamos, NM.
23. Louisiana State University, Baton Rouge.
24. Lund University, Sweden.
25. McGill University, Montreal, Canada.
26. University of Münster, Germany.
27. National Institute of Radiation Science, Chiba-ken, Japan.
28. State University of New York - Stony Brook, NY.
29. Peking University, Beijing, P.R.C.
30. St. Petersburg Nuclear Physics Institute, Leningrad, Russia.
31. University of São Paulo, Brasil.
32. Seoul National University, Seoul 151-742, Korea..
33. University of Tennessee, Knoxville.
34. University of Tokyo, Japan.
35. University of Tsukuba, Japan.
36. Vanderbilt University, Nashville, TN.
37. Yale University, New Haven, CT.
38. York College - CUNY, Jamaica, NY.
39. Massachusetts Institute of Technology, Cambridge.
40. Nagasaki, Japan.

MONTE CARLO SIMULATIONS OF THE PHENIX DETECTOR AT RHIC

*T.C. Awes, H. J. Kim, J. Kreke,¹ X. C. He¹
F. E. Obenshain, F. Plasil, S. Saini, S. Sorensen,²
G. R. Young*

The design of the PHENIX detector for RHIC is currently in an intensive simulation phase in order to evaluate and optimize the detector elements and the experimental configuration within the constraints of a fixed construction budget. In general, two rather different simulation approaches are followed depending on the issues to be addressed. A standardized approach is to use the GEANT simulation package which can track the particles of simulated events in full detail through all of the active and inactive media of the experiment. This approach is extremely useful in order to evaluate the expected performance of the detector elements themselves, as deployed in the detector configuration, with full events. It is also useful in order to investigate sources of background, as might be produced by particles showering in portions of the detector. Such a GEANT-based simulation framework called PISA, which includes the full PHENIX geometry, has been set up by C.F. Maguire of Vanderbilt University. However, due to the extremely large particle multiplicities at RHIC and the large amount of CPU time necessary to track all particles fully, it is generally not feasible to simulate fully more than a few thousand events using GEANT. Since the emphasis of the PHENIX experiment is to concentrate on electromagnetic probes which have low count rates, this generally means that many millions of events must be simulated in order to approach the level of significance where physics will be done. For this reason, a second simulation approach is to use efficient Monte Carlo generators in which the physics signals and the backgrounds are parameterized appropriately in order to make parametric studies of the physics performance for various detector options.

Such efficient Monte Carlo simulations have been described previously for analysis of the photon detection results within PHENIX.³ The simulation code which was developed for this purpose has been adapted to simulate either the electron-pair or muon-pair performance of the PHENIX experiment. The code uses an efficient event generator which produces only those particles which decay to produce leptons in the final state, and which includes backgrounds which might be identified falsely as leptons.

The code has been implemented on the ORNL Intel/i860 Hypercube in order to obtain sufficient numbers of simulated events in short (~1- to 2-day) simulation runs.

Results of such simulations for the electron-pair measurement within PHENIX are shown in Fig. 4.4. The results are shown for 12.8×10^6 central Au+Au events in which a multiplicity of $dN/dy=375$ has been assumed for each pion charge state. This corresponds to about three days of running at RHIC at design luminosity. The PHENIX detector electron coverage consists of two arms, each subtending 90 degrees in ϕ with a 45-degree opening between the arms, and covering the pseudorapidity region of $|\eta| < 0.35$. Electrons are assumed to be tracked and identified if their momentum exceeds 100 MeV/c; softer electrons are trapped in the central magnetic field. For these simulations it has been assumed that, according to design, pions will be misidentified as electrons with 10^{-4} probability and that 0.5% of the photons will convert to e^+e^- pairs and not be eliminated by means other than a pair-mass cut. The results of Fig. 4.4 show the invariant mass spectrum for opposite-sign electron pairs after imposing a Dalitz pair rejection criteria in which all electrons which form an opposite-sign pair with invariant mass less than 50 MeV/c² are eliminated from the pair list. This Dalitz rejection criteria has been optimized through such Monte Carlo studies. It is observed that the electron-pair invariant-mass spectrum is dominated by a large combinatorial background which is seen to be attributed mainly to the background due to Dalitz electrons. This is the case in spite of the attempted rejection of Dalitz pairs. In fact, the Dalitz rejection provides a background suppression by about a factor of three only, due to the fact that many of the electrons to be associated to a Dalitz pair fall below the 100-MeV electron threshold or out of the detector acceptance. The results indicate the importance of finding a method to improve the rejection of Dalitz pairs. It is currently under investigation whether it is feasible to include an inner detector to identify electrons whose momentum is below the electron arm threshold in order to improve the Dalitz rejection capabilities.

The results of Fig. 4.4 are shown integrated over the transverse momentum of the pair. In Fig. 4.5 the simulation results are analyzed quantitatively for the ρ , ω , and ϕ resonances as a function of the transverse momentum of the resonance. It is seen that due to the large combinatorial backgrounds, the peak/total ratios for these resonances are quite low for transverse

ORNL-DWG 92-15016

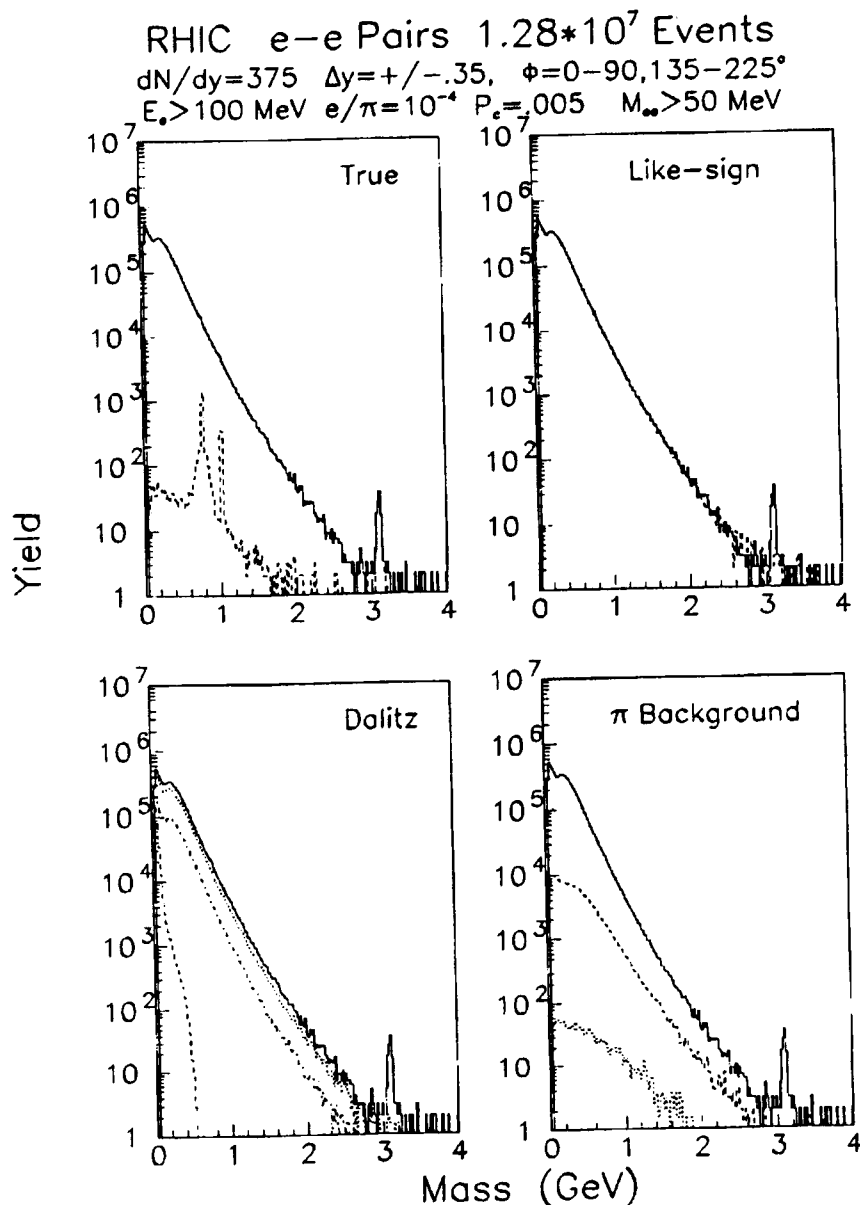


Fig. 4.4. Simulation of electron-pair measurements in the PHENIX detector at RHIC for 12.8×10^6 central Au+Au events. The solid curve is the same in each panel and shows the expected experimental result for the invariant-mass spectra for opposite-sign pairs. In the upper left panel, the true pair signal is shown by the dashed curve in which the ρ , ω , η , and J/ψ resonances can be seen on top of a continuum due to $D\bar{D}$ decays. No ρ - ω mixing is assumed. The like-sign pair combinatorial-mass distribution is shown by the dashed curve in the upper right panel. In the lower left panel the contribution of true opposite-sign electron pairs from Dalitz decays of the π^0 and η is shown by the dashed curve. It is seen to fall several decades below the combinatorial spectrum; only the latter can be measured. The dotted curve indicates the combinatorial background due to a Dalitz decay electron with any opposite-sign electron, while the dashed-dotted curve indicates the same for all combinations of Dalitz electrons only. The lower right panel shows the contribution to the combinatorial background due to misidentified electrons (e.g., charged hadrons) with anything (dashed curve) or misidentified electrons paired with themselves (dotted curve).

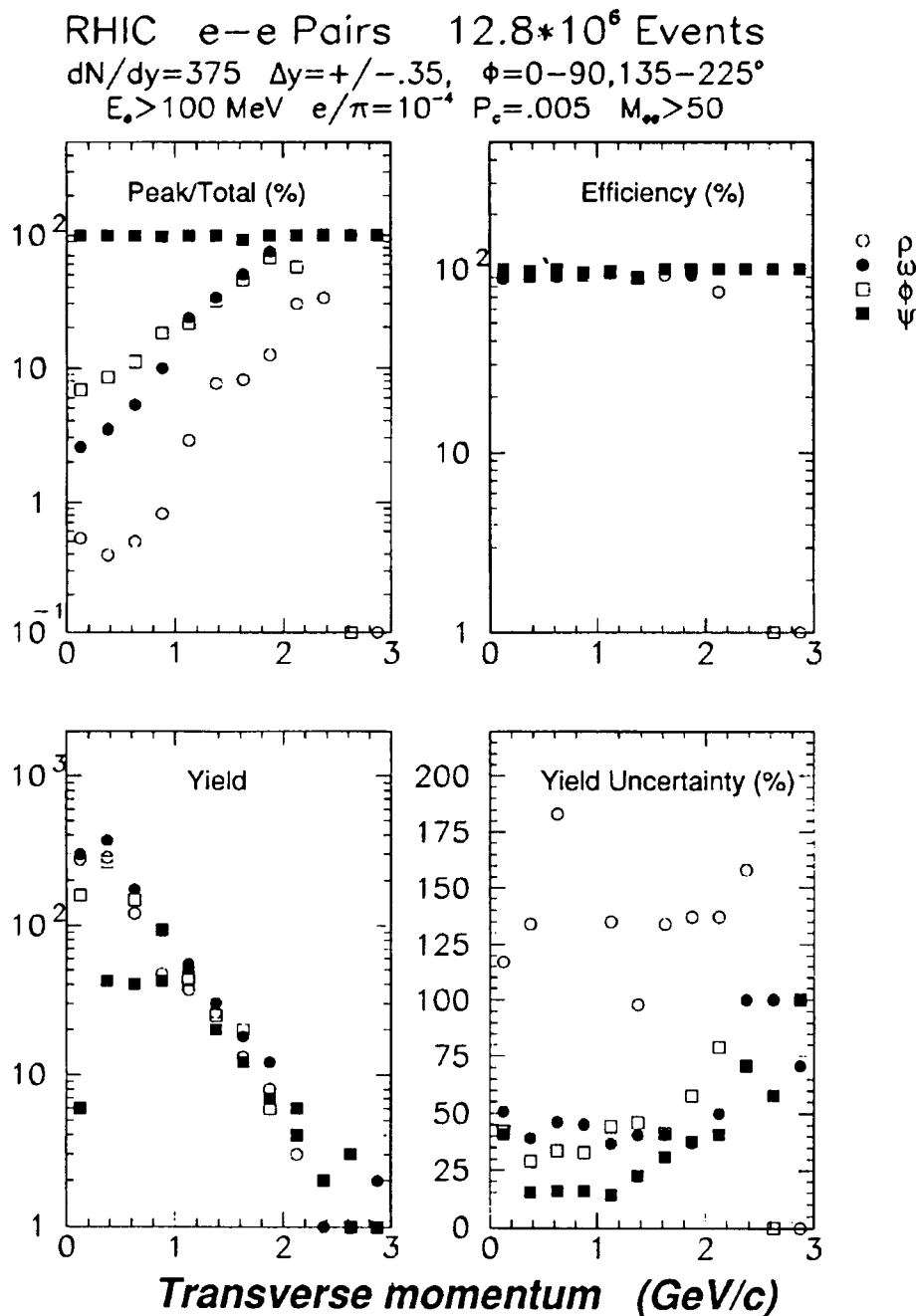


Fig. 4.5. The expected performance of the PHENIX detector electron-pair measurement as a function of the pair transverse momentum for the ρ (open circles), ω (closed circles), and ϕ (open squares) resonances for 12.8×10^6 central Au+Au events. The results were analyzed after Dalitz pair suppression by first eliminating all electron candidates which form an opposite-sign pair with pair mass less than 50 MeV. The upper left panel shows the peak/total ratio integrated over the region of $\pm 2\sigma$ about the peak. The upper right panel shows an estimated (comparing runs with/without Dalitz rejection) efficiency that the Dalitz rejection does not reject true pairs. The lower left panel shows the accepted true yield as a function of transverse momentum. The lower right panel indicates the statistical uncertainty to extract the true yield after background subtraction.

momenta below about 2 GeV/c. Only the J/ψ resonance appears without combinatorial background. As a result of these combinatorial backgrounds, the statistical errors for extracting the resonance cross section from the large background (equal to $\sqrt{(2-Q)/(QN)}$, where Q is the peak/total ratio and N is the number of counts in the peak) are relatively large, even with the large number of accumulated events and even though the yields in the peaks are themselves large. The conclusion to be drawn from these simulations is that with the PHENIX electron detection system as presently designed, extracting the ρ and ω resonance production via their electron-pair decay will be quite difficult for central Au+ Au collisions at RHIC. The extraction of the ρ production cross sections is probably not possible, and by implication, neither will be the more difficult extraction of thermal electron pairs due to decay of virtual photons. In order to improve the PHENIX electron-pair measurement substantially, it would be necessary to increase the electron detection coverage significantly, which is not feasible financially, or to improve the Dalitz rejection capabilities in order to eliminate this overwhelming background.

1. University of Tennessee, Knoxville.
2. Adjunct research participant from the University of Tennessee, Knoxville.
3. "Monte Carlo Simulations of Photon Measurements for the PHENIX Detector at RHIC," *Phys. Div. Prog. Rep. for Period Ending Sept. 30, 1991*, ORNL-6689, p. 96.

LOW ENERGY RESPONSE OF Pb GLASS CALORIMETERS FOR RHIC

T.C. Awes, A. Lebedev,¹ A. Nyanin¹

The emphasis of the PHENIX detector at RHIC is to concentrate on the detection of electromagnetic probes of the relativistic heavy-ion collision. As part of the PHENIX experiment, it is intended to use the 10,000 element Pb-glass detector array presently being assembled for use in the WA98 experiment with Pb beams at CERN. A portion of this system has already been used with the oxygen and sulphur beams at CERN to perform a search for excess direct photons, which would be expected due to thermal radiation in the event of formation of a quark-gluon plasma

(QGP). The prospects for QGP formation are considered more favorable at RHIC due to the expected increase in energy density. Within the PHENIX experiment, the Pb-glass array will be used in a similar search for excess direct photons. It will also provide an important component of the electron identification system in PHENIX which will be used to study the production of virtual photons and vector mesons through their electron-pair decay.

The response of the Pb-glass detector has previously been measured thoroughly at CERN for energies and operating conditions appropriate for the fixed-target operation at CERN. At the RHIC collider the Pb-glass detector will be deployed at midrapidity, with the result that the average particle energies in the detector will be considerably lower. In order to investigate the Pb-glass response in operating conditions more appropriate to RHIC, measurements were made in the A2 test beam at BNL. The tests were made with a 7x7 module array of Pb-glass elements (each 4x4x40 cm³, 16 radiation lengths). The Pb glass was provided by the Kurchatov Institute, together with Russian FEU-84 photomultipliers and bases for readout. Tests were performed with gain settings corresponding to about 2 MeV/channel (compared to settings of 20 MeV/channel for CERN operation) using positive and negative beams of electrons, muons, pions, and protons from 0.5 GeV/c to 4 GeV/c. The tests were performed with varying angles of incidence up to 20 degrees, as expected in the Pb-glass configuration within PHENIX. A main purpose of the tests was to determine the expected energy resolution and typical number of active modules, to estimate occupation probabilities, for the PHENIX detector settings. It was also desired to provide an initial data set for development of shower identification algorithms and to determine the electron/pion discrimination capabilities of the Pb glass for the low-energy particles typical of RHIC. In addition, timing measurements were made to investigate the possibility to use the Pb glass for a low-resolution time-of-flight measurement for particle identification at low momentum. The configuration of the test beam line consisted of a fast start counter followed by two Cerenkov counters operated with nitrogen in threshold mode and set to trigger on electrons but not pions or muons. A fast stop counter was placed 12.85 m downstream of the start detector immediately in front of the Pb glass. The fast timing detectors had rms timing resolutions of about 80 ps.

The energy resolution of the Pb glass is shown in Fig. 4.6 for electrons of 0.5 GeV/c to 4 GeV/c at

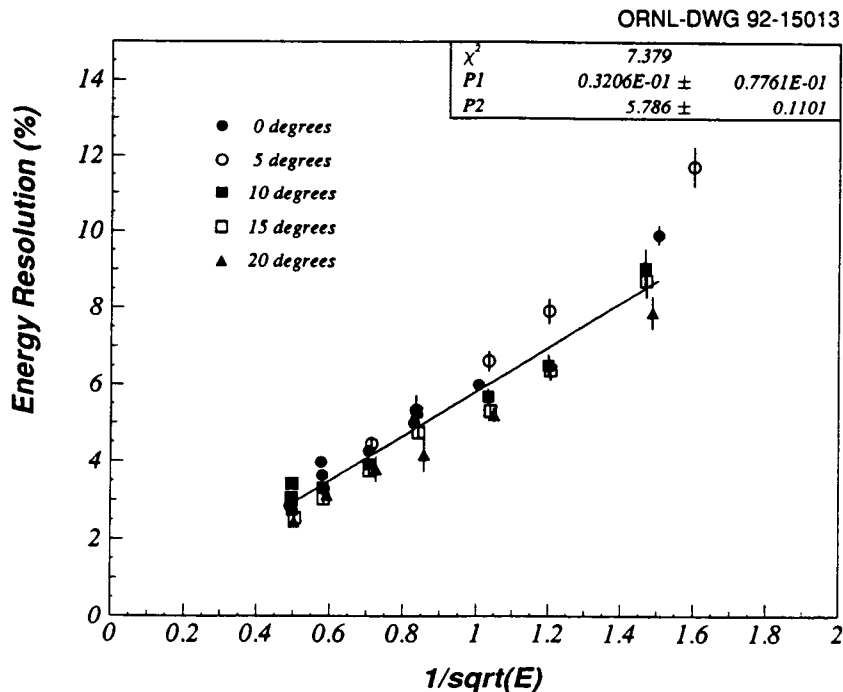


Fig. 4.6. Pb-glass energy resolution as a function of $1/\sqrt{(E)}$ for electrons of incident momenta of 0.5 to 4 GeV/c at various angles of incidence.

angles of incidence of 0, 5, 10, 15, and 20 degrees. In order to keep the shower well-contained in the Pb glass array, the array was displaced by 1/2 of a module width for each 5-degree change in orientation of the array. Thus, the beam was centered on the central module for 0 degrees incidence, but centered on the adjacent module for 10 degrees incidence, and centered on the next-to-adjacent module for 20 degrees incidence. The beam profile was diffuse with a nearly uniform illumination over a single module size of $4 \times 4 \text{ cm}^2$ as defined by the beam counters. After correction for the beam resolution (assumed to be removed in quadrature), an energy resolution of $5.8\%/\sqrt{(E)}$ is measured with no constant term. If the beam resolution correction is not performed, an energy resolution of $5.9\%/\sqrt{(E)} + 0.8\%$ is obtained. This may be compared to a resolution of $7.4\%/\sqrt{(E)} + 1.4\%$ measured at CERN with the same Pb-glass elements but at higher incident energies and correspondingly higher gains. There was no observed degradation of the energy resolution with increasing angle of incidence. In fact, the results shown in Fig. 4.6 suggest an improved energy resolution with increasing angle of incidence. However, this result is explained by the fact that the energy resolution of the

modules adjacent to the center module, into which the beam was shifted, had better intrinsic resolution (as observed when measured at 0 degrees incidence during gain-matching of all modules). This is shown in Fig. 4.7, where the measured resolution at 2 GeV/c for 0-degree incidence is shown versus the measured number of photoelectrons/GeV. A clear correlation between resolution and the number of photoelectrons is observed. An average value of 622 photoelectrons/GeV was measured for all Pb-glass modules, while the center module which dominates most of the test results was on the low-performance side with only 484 photoelectrons/GeV.

The most interesting aspect of the Pb-glass test beam measurements was the timing results. For these measurements, the analog output of the center module was split with timing information obtained using a constant fraction discriminator on one of the split signals and the other output sent to the ADC. The discriminator was set with a threshold at about 15 mV, corresponding to an energy deposit of about 50 MeV. In Fig. 4.8 the timing resolution as a function of the energy deposited in the module is shown for positron beams summed over all incident momenta and for pions of 1 GeV/c. The timing resolution may

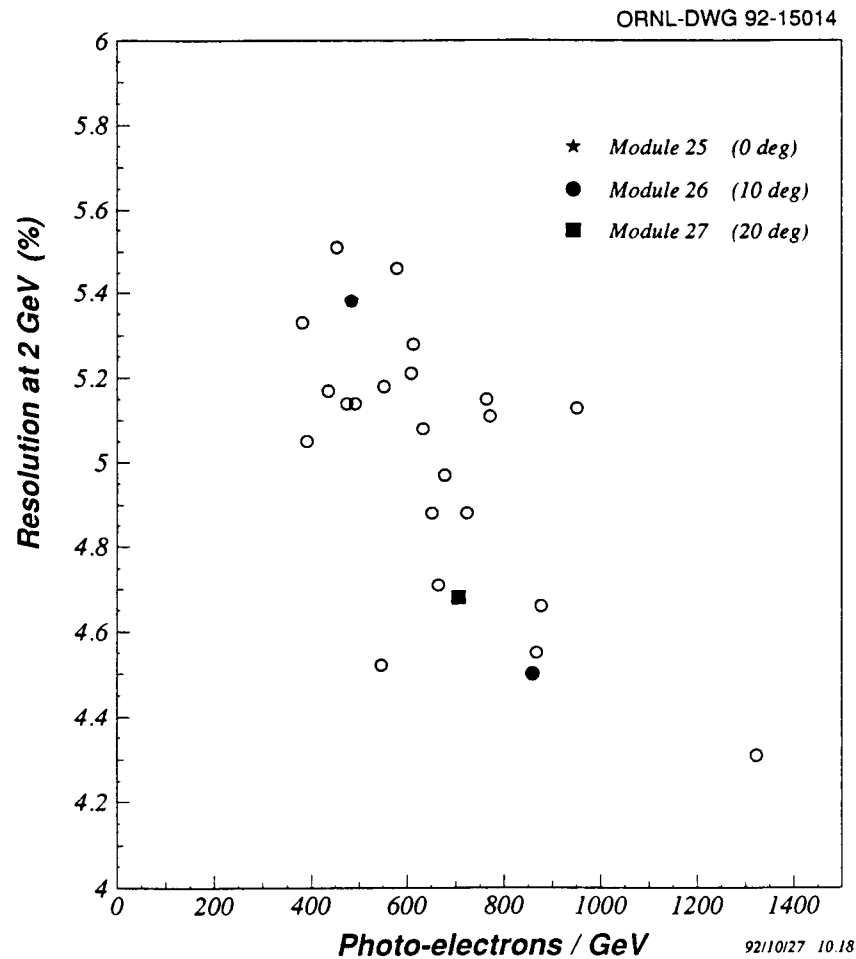


Fig. 4.7. Energy resolution versus the number of photoelectrons/GeV for each of the central 5x5 Pb-glass modules. The energy resolution is for electrons at normal incidence on the center of each module at 2 GeV/c. Module 25 was the center module for 0° incidence.

be fit to the form $\delta t = \delta t_0 + \delta t_1 / \sqrt{(N_{pe} * E_{Dep})}$, where N_{pe} is the number of photoelectrons/GeV and E_{Dep} is the energy deposited in the module. The fitted results give a constant term contribution of $\delta t_0 = 75$ ps, which is presumably due to intrinsic fluctuations in the shower localization. The second term, which improves with photon statistics, has a value of $\delta t_1 = 3.75$ ns, which corresponds to about 1/4 to 1/3 of the signal risetime. The same dependence of the timing resolution on the deposited energy is obtained for pions and protons for energies up to and slightly above the minimum ionizing peak at 500 MeV. There was insufficient timing data to draw conclusions for hadrons which deposit greater energy.

The most surprising aspect of the Pb-glass timing results was the observation that the pion and proton timing signal generally arrived sooner than that of an electron with similar energy deposit. For example, in the region of the minimum-ionizing peak, the pion signal arrived about 800 ps before the electron signal. The interpretation of this effect is that the showering electron produces light at the front of the Pb glass which is then transmitted at a reduced velocity of c/n , where n is the Pb-glass index of refraction, compared to a minimum-ionizing pion which can traverse the length of the Pb glass with a velocity c and put Cerenkov light directly into the photomultiplier from the back of the Pb glass. (Ac-

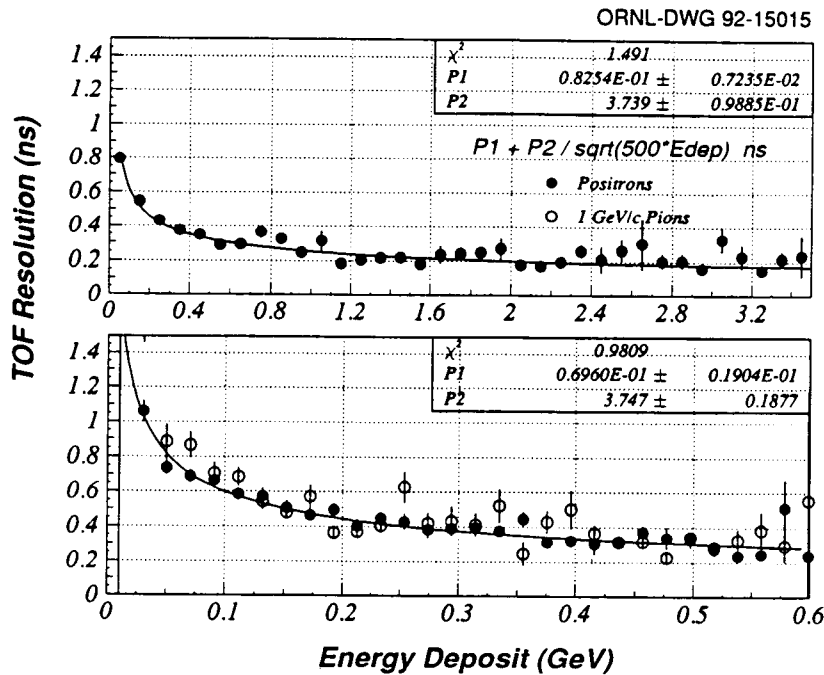


Fig. 4.8. Single Pb-glass module timing resolution as a function of the energy deposited in the module for electrons of incident momenta 0.5 to 4 GeV/c and pions of 1 GeV/c.

tually due to emission at the Cerenkov angle, the light from the electron shower must also travel a path length increased by a factor $1/n$, further delaying the signal arrival time, although this correction factor also applies to light generated by a minimum-ionizing pion.) Thus, the signal arrival time in the Pb glass provides information about the depth at which the energy is deposited in the Pb glass. Due to this effect, it appears possible to obtain discrimination between hadrons and electrons (or photons) on the basis of signal arrival time in regions of momenta where there is no difference in time of flight. On the other hand, this sensitivity to the depth of the shower may complicate the use of the Pb-glass timing information for actual time of flight measurements. Additional tests are planned to study this effect.

PHENIX MUON SPECTROMETER

*PHENIX Collaboration**

A muon endcap-spectrometer, with large solid angle acceptance and high rate capability, is proposed for the PHENIX detector at RHIC to detect muon pairs with broad kinematical coverage. Muon pair detection appears to offer a tractable solution for lepton-pair detection at rapidities greater than one. Muon pairs can span a range in invariant and transverse mass from 1 to 10 GeV/c². This approach, using an endcap spectrometer with full azimuthal coverage at forward rapidity, y , also allows us to obtain useful counting statistics in the mass region above 4 GeV/c², where perturbative QCD should be applicable. We can then move to lower mass using the same detector to examine the regime where nonperturbative effects and plasma may be seen. This spectrometer could also be used for measurements of the A_{target} , P_T , and x_F dependences of lepton-pair emission in p-A collisions. These measurements take advantage of the unique capabilities of RHIC to provide p-A collisions at high \sqrt{s} . Such studies can shed light on modifica-

1. Kurchatov Institute, Moscow, Russia .

tions of structure functions in nuclei and are an integral part of a program seeking to understand lepton-pair and photon emission in A-A collisions.

Several authors¹ have suggested that there may be a modification of properties of vector mesons immersed in dense strongly-interacting matter. These include changes in mass, width, branching ratio, and yield of vector mesons. One suggestion for demonstrating deconfinement is the observation of suppression of the yields for certain heavy vector mesons.

The proposed spectrometer will detect vector mesons over a large range of rapidity ($1 < y < 3$) and p_T (0 GeV/c up to the statistics limit, which should be > 5 GeV/c for the J/ψ). The acceptance and resolution are sufficiently good to measure the cross section not only for J/ψ and ψ' , which are expected to be suppressed, but also for Ψ production, which is expected to be a "control" for vector meson suppression due to size effects.

Vector-meson suppression depends on the local energy density and, thus, screening radius; therefore, an experiment requires large rapidity coverage in order to take advantage of the variation of dE_T/dy with rapidity. Measurements at several values of \sqrt{s} will be necessary to observe a large variation in the maximum dE_T/dy for a given system. Good statistics are needed, which implies large acceptance. The need for large acceptance becomes acute for lower \sqrt{s} , since the luminosity at RHIC decreases there, as does the lifetime for intra-beam scattering. Suppression effects should disappear at sufficiently high p_T , because the $q\bar{q}$ pair leaves the plasma before it can separate to a radius at which screening affects formation of the relevant state. This behavior is usually predicted to occur at p_T around 5 GeV/c, again placing a premium on acceptance if "control" points are to be accessible experimentally.

The muon endcap spectrometer consists of three main sections: a hadron absorber thick enough to remove most hadrons but thin enough to permit good mass resolution and kinematic acceptance, a magnetic spectrometer providing good acceptance and mass resolution of $< 2-3\%$, and a muon identifier to complete rejection of hadrons to the 10^{-4} level or better.

The purpose of the absorber is to attenuate the hadronic flux entering the tracking region to acceptable levels. The particular design depends upon the magnet chosen for PHENIX. The axial-field magnet has steel pole tips at forward rapidities $|y| \geq 1.0$ and for the present design it is $\sim 4\lambda$ thick. This serves as the hadron absorber. If further calculations of the field configuration in the central spectrometer section in-

dicates that some of the steel could be removed from the $|y| \geq 1.0$ region, it would be preferable to replace as much of this steel as possible with other materials; for example, a low-Z material such as Al_2O_3 could be used for the first $2-3\lambda$ in order to minimize the multiple-scattering which dominates the resolution below 3 GeV/c² invariant mass. Simulations indicate that tracking through the magnet is not a problem since the integrated effect of the field is less than the effect of multiple scattering. Leakage calculations indicate that $1-2\lambda$ of copper will have to be added to the steel in order to reduce shower leakage into the muon tracking chambers to an acceptable level.

The shower products exiting the pole tip are dominated by soft e^+ , e^- , and gammas, which can be easily suppressed by installing 10 radiation lengths of lead after the pole tip. Whether a graded absorber or a monolithic one of steel is used, presently depends upon magnet developments.

Following the absorber is the muon tracking region. This consists of a large magnet and tracking chambers. The magnet being designed at the present time is shown in Fig. 4.9 and gives nearly complete acceptance in ϕ . It is a piston and lamp-shade configuration where the magnetic field is radial everywhere along the beam line. The polar-angle acceptance depends on the configuration of the poles for the central-region magnet and the muon magnet design. It includes all polar angles in the range $8.75^\circ < \theta < 37^\circ$.

The tracking chambers, as presently conceived, use drift chamber technology, which may be most suitable with the radial geometry. The chambers would be arranged in three stations, each with 6 detector planes. As an alternative, wire chambers with strip and/or pad readout could be constructed with the wires parallel to the field direction. It is likely that the wire chambers can be constructed with fewer radiation lengths of material, say, less than two percent.

Behind the tracking system will be a second hadron absorber for muon identification. This system will consist of steel layers interspersed with either proportional or streamer tubes. These may be read out using pads or by digital strips positioned along and normal to the wire direction. Which method is preferable (or necessary) depends upon further study related to the ability of any given system to connect a deep hit in the muon-identifier with the correct particle out of the several dozen present in the tracking section.

The inner absorber will eliminate most of the background in the muon spectrometer portion of the detector. However, several percent of the hadrons,

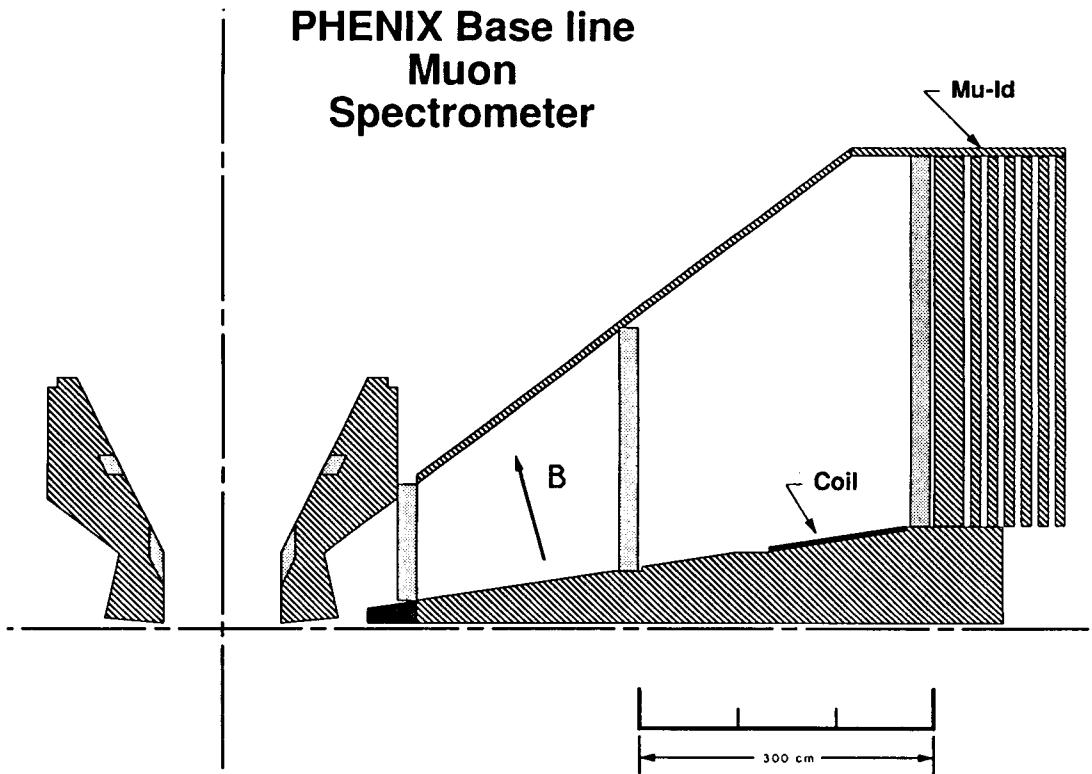


Fig. 4.9. A section of the dimuon spectrometer is shown in relation to the main axial-field magnet (see PHENIX write-up). The iron yoke of the main magnet serves as the muon inner absorber. The muon magnet and tracking chambers are shown on the right. The muon identifier is the last element of the spectrometer.

particularly pions, will not be absorbed and will be detected in the outer absorber. In addition, some secondaries from showers starting late in the absorber will also enter the tracking section, as will a significant number of neutrons. Thus, the outer absorber must function as a "muon identifier," capable of discriminating between muons and the background of pions and other hadrons. The ideal muon identifier comprises >6 layers of absorber plates alternating with gas proportional tubes or streamer tubes. The exact configuration of plates needs to be optimized, but at least 10λ are needed. Our Monte Carlo studies indicate that the muon identifier needs effective pattern recognition in order to reject hadrons at the level required. The front layers may have to be instrumented with streamer tubes with pad readout in order to obtain good three-dimensional pattern recognition and to associate a hit deep in the muon identifier with the correct particle entering, since there are several

dozen particles entering the forward muon identifier per event. It may be possible to instrument the deep layers in a less expensive manner with proportional tubes in alternating x and y layers with readout in yes-no mode, because the showers caused by hadrons are dilute there. We hope that directional information from deep hits is sufficient to resolve which entering particle matches the deep hit, because that would allow us *not* to instrument the first 2-3 of the muon identifier. This would save considerable money. We will study this design issue to optimize performance versus cost.

We have investigated the ability of the muon identifier to provide a fast trigger signal, by making Monte Carlo studies using as few as two parameters, neither of which would require a long time to process, either in terms of signal collection times or calculation times. We find that satisfactory results are obtained by using only two parameters—total number

of hits and deepest plane registering a hit. Our Monte Carlo results indicate that more than 95% of the pions can be rejected while rejecting only about 10% of the muons over the range from 1 to 10 GeV. We will study this topic further in order to improve the acceptance for the muons. Additional cuts on tracking chamber hits and a vertex constraint would be applied before a muon candidate would be accepted. Tagging muons at trigger level is most important in reducing interaction rates for p-A and low mass A-A cases, as well as for peripheral Au+Au collisions.

*For a complete list of authors, see article "Preconceptual Design of PHENIX Experiment for RHIC."

1. T. Matsui and H. Satz, *Phys. Lett. B* **178**, 416 (1986); B.Svetitsky, *Phys. Lett. B* **227**, 450 (1989); "The Nuclear Equation of State, Part B: QCD and the Formation of the Quark—Gluon Plasma," edited by W.Greiner and H.Stöcker, Plenum Press, New York, 1989, p. 257.

SIMULATIONS OF THE PERFORMANCE OF THE PHENIX MUON DETECTOR

*PHENIX Collaboration**

At the current stage in the development of the PHENIX detector for the RHIC accelerator, large-scale Monte Carlo simulations are of great importance for the evaluation of the performance of the various detector components. At ORNL we have been responsible, in collaboration with Tennessee, Georgia State, Vanderbilt, and Los Alamos, for the simulation of the muon detector. This detector consists of a tracking element with a lamp shade magnet, followed by a large, instrumented block of steel serving as a muon identifier.

The early work was focused on evaluating the acceptance and dimuon invariant mass resolutions. The current detector design will accept all muons with scattering angles between 9 and 35 degrees with energies above 2 GeV. At the same time, pions and kaons with the same kinematics will be suppressed by $\approx 3 \times 10^{-4}$. Based on the measured positions of the muons in three drift chambers and the vertex position, determined by the vertex detector, we have developed a novel method for determining the momentum vector at the vertex. The method is based on a

Chebyshev polynomial expansion in the measured quantities. It is especially well suited for second-level trigger purposes, since it is very fast and does not require any fitting.

The tracking of particles through the detector will impose three problems: (1) correlation of hits within the drift planes of a tracking station, (2) correlation of hits between tracking stations, and, finally, (3) correlations between tracks found in the muon identifier and the spectrometer. At the moment, we have solved problem 1 and are working on 2. The algorithm used for solving problem 1 is based on the principal component method and seems to be able to handle hit densities of up to 15-20%. We anticipate hit densities of 5-10% from our GEANT studies.

The whole feasibility of the muon detector hinges on the magnitude of the vector meson yield compared to the underlying combinatorial background of muons originating from sources other than vector meson decay or correlated dimuon production. The most important source is decay muons from pion decay. Through GEANT calculations at Vanderbilt and Los Alamos and high-gain Monte Carlo simulations at ORNL, we have found that even if the combinatorial background will be a most annoying feature. The signal-to-noise ratio will still be above 1 for invariant masses from 3 GeV and up.

Figure 4.10 shows the invariant dimuon mass distributions for both all unlike-sign accepted muon pairs and the original signal consisting of vector mesons and Drell-Yan pairs. No background is present at the Y (9.4 GeV). The J/ψ (3.1 GeV) is clearly seen above the background, whereas the ψ' (3.7 GeV) just makes it. The ρ (0.8 GeV) and ϕ (1.0 GeV) seem to be completely covered below the background, but one is able to recover their yield to within 10-20% by performing the proper background subtraction based on like-sign muon pairs. We note that no cuts to remove background muons have been made in this spectrum.

*For a complete list of authors, see article "Preconceptual Design of PHENIX Experiment for RHIC."

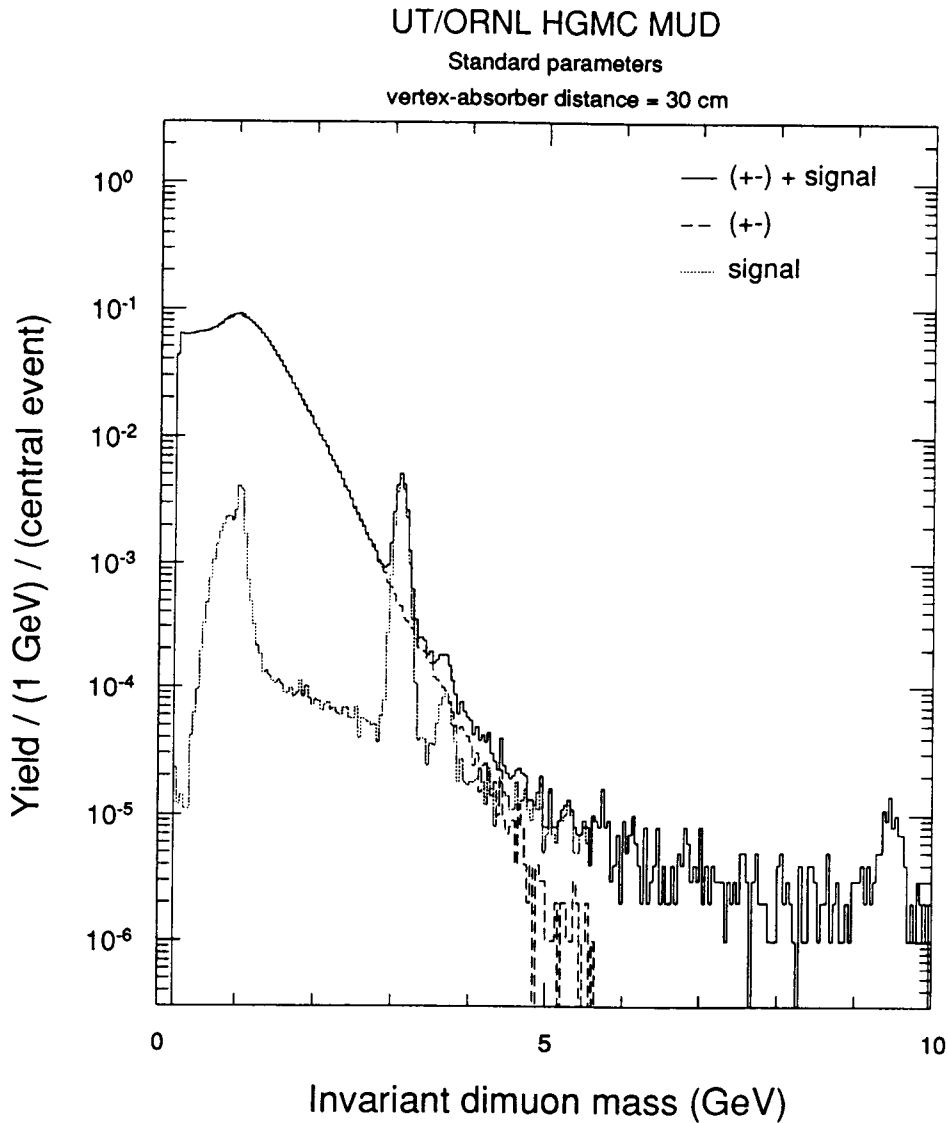


Fig. 4.10. Invariant dimuon mass distributions. See text for details.

LIMITED STREAMER TUBES FOR MUON ID

*H. J. Kim F. E. Obenshain
J. G. Kreke¹ G. R. Young*

Limited Streamer Tubes (LST) are the leading detector candidate for the muon-identification section of the PHENIX detector. We have purchased 160 LSTs from a commercial vendor for evaluation. The

tubes are 8.4-cm wide, 148-cm long; and they are being evaluated at the test facility which was set up during the summer (1992). These LSTs are rugged, reliable, simple, and inexpensive, and are widely used in experiments where charged-particle detection over large surface area is required, e.g., hadron calorimeters, muon identifiers, etc. The magnitude and shape of cosmic-ray, gamma-ray, and beta-particle induced pulses from the plastic LST (supplied by Hodotector, Inc., of Houston, Texas) observed at the

test facility are in good accord with expected results. Having completed the evaluation of detector characteristics and found the performance to be satisfactory, these LST are being instrumented into a ten-layer, muon identifier interleaved with steel plates. Once assembled and thoroughly tested using cosmic rays, this prototype muon identifier will be taken to the AGS facility at Brookhaven National Laboratory for in-beam test experiments. We will study range, trajectory, shower pattern, and shower size for relativistic charged particles that traverse or partially traverse the ten-layer detector. We plan to utilize results from this study to design the muon identifier for the PHENIX experiment at RHIC.

-
1. University of Tennessee, Knoxville.

CALORIMETER OPTIMIZATION EXPERIMENT (RD-10/RD-45 PROJECT)

*S. H. Aronson,¹ M. J. Murtagh,¹ M. Starks,¹
X.T. Liu,² G. A. Pettit,² Ziyang Zhang,²
L. A. Ewell,³ J. C. Hill,³ F. K. Wohn,³
J. B. Costales,⁴ M. N. Namboodiri,⁴
T. C. Sangster,⁴ J. H. Thomas,⁴ A. Gavron,⁵
L. Waters,⁵ W. L. Kehoe,⁶ S. G. Steadman,⁶
T. C. Awes, F. E. Obenshain, S. Saini,
G. R. Young, J. Chang,⁷ S.-Y. Fung,⁷
J. H. Kang,⁷ J. Kreke,⁸ Xiaochun He,⁸
E. C. Cornell,⁹ C. F. Maguire,⁹*

The RD-10 calorimeter optimization experiment conducted at the AGS at Brookhaven National Laboratory, in the spring of 1991, resumed this spring under the project designation RD-45. This year's experiment concentrated on iron absorber studies with calorimeter thicknesses of 4.8 and 8.2. The layout was the same as for RD-10, with the exception of the addition of a third Cerenkov counter. This counter was placed between the beam hodoscopes, as close as possible to the calorimeter, and was used to better identify pions, thus reducing the number of misidentified decay muons incident on the calorimeter. Incident particle momenta were 1.5, 2, 3, 4, 6, and 8 GeV/c for the thinner calorimeter and 3, 4, 6, and 8 GeV/c for the thicker calorimeter. Because of the low leakage count rate with the relatively thick calorimeter configurations, the secondary-level muon

trigger was not implemented, and only the 4-inch lead curtain was used at the four highest energy runs. Secondary-level triggers did include the electron trigger and the leakage trigger; a minimum bias (no secondary) trigger was also used for survey and normalization purposes.

-
1. BNL, Upton, NY.
 2. Georgia State University, Atlanta.
 3. Iowa State University, Ames.
 4. LLNL, Livermore, CA.
 5. LANL, Los Alamos, NM.
 6. MIT, Cambridge, MA.
 7. University of California, Riverside.
 8. University of Tennessee, Knoxville.
 9. Vanderbilt University, Nashville, TN

DEVELOPMENT OF MONOLITHIC ELECTRONICS FOR RHIC AND CERN WA98

*T.C. Awes, G.R. Young, G.T. Alley,¹ C.L. Britton,¹
M.N. Ericson,¹ M.L. Simpson,¹ A.L. Wintenberg¹*

Work has continued on development of monolithic electronics circuits for use in reading out the large number of channels to be encountered in the RHIC PHENIX detector, and on those under construction for the photon calorimeter for the CERN WA98 experiment. Activities for this year concentrated on testing of ADC circuits and of a large, integrated readout chip which represented one possible solution for partitioning the overall readout chain. The goal remains to reduce the entire chain, including preamplifier, amplifier/shaper, sampler/analog storage unit, readout amplifier, and ADC plus output buffer, to one or two circuits implemented entirely in monolithic form. We prefer to do this in CMOS where possible, in order to minimize power consumption and provide access to a widely used fabrication technology.

Testing of the various ADCs using different construction methods indicated that a successive approximation (SAR) ADC with 11 bits differential nonlinearity and 5-microsecond conversion time was achieved. This is encouraging, but this ADC does require a considerable amount of silicon area, limiting its usefulness in a design where 16 or 32 channels of readout must be included on a single silicon substrate. Accordingly, work on a multichannel Wilkinson

ramp-down-type ADC, encompassing at least 16 channels converting in parallel, was begun. This design will require longer conversion times than the SAR design, but should afford greater economy in silicon area usage and system cost.

Testing of an integrated readout chip, which included everything from preamp to ADC, indicated that all components functioned, but that clocking noise from the analog memory units interfered excessively with preamp behavior. Accordingly, a separated-function design with preamp/amp/shaper on one substrate, and all other functional blocks on another, was begun.

A block diagram of the readout system for the 10,000 element lead-glass detector for CERN experiment WA98 was prepared. This includes two 10-bit ADC channels separated by a factor of 8 in gain. This is well matched to the intrinsic resolution of the lead-glass [$6\%/ \sqrt{E}$], as well as to the dynamic range requirement of operation from 2 MeV (pedestal range) up to 40 GeV, as dictated by the fixed-target nature of WA98. The circuit also includes a TAC/ADC channel used to measure flight times from the target to the lead glass with a precision better than 50 psec, over a full range of 50 nsec in flight time. This time measurement will be a new capability for the photon detectors used in the WA80/93/98 experiments. It will help in distinguishing minimum-ionizing particles, which only pass through the detector, from ~500-MeV photons, which yield a similar pulse-height signal. It will also help with the general problem of separating hadrons from photons in the lead-glass detector.

1. ORNL I&C Division.

ORNL ACTIVITIES IN SUPPORT OF THE SSC GEM COLLABORATION

*M. L. Bauer,¹ C. L. Britton,¹ S.M. Chae,²
L. G. Clonts, H. O. Cohn, C.C. Eberle,²
Y. Efremenko,³ A. Gordeev,³ J. L. Heck,²
Yu. Kamyshev,³ A. Nikitin,³ D. Onoprienko,³
F. Plasil, K. F. Read, M. J. Rennich,² A. Savin,³
K. Shmakov,³ A. Smirnov,³ E. Tarkovski,³
R. A. Todd,¹ A. L. Wintenberg,¹ K. G. Young,¹*

During this reporting period, ORNL continued to play a major role in the GEM calorimeter group. Yuri Kamyshev was in charge of coordinating the

overall GEM calorimetry effort. In the course of the year, several difficult technology choices were made by the collaboration. At the time of the submission of the *Letter of Intent* in the fall of 1991, two technologies were under consideration for both the electromagnetic and the hadronic calorimeter sections. Barium fluoride crystals and liquid argon were the two competing technologies for the electromagnetic calorimeter, and scintillating fibers and liquid argon were considered for the hadron calorimeter.

It was recognized that the most important potential disadvantage of the barium fluoride crystals was the possibility that their performance might suffer as a result of radiation damage. An expert panel was convened to study the problem and to provide guidance for an intense R&D program, in which ORNL participated. A schedule was established regarding R&D progress and decision deadlines. Criteria on which the decision was to be based were generated. A similar procedure was followed for the liquid-argon electromagnetic calorimeter option. In this case, the most significant potential problem was in the area of engineering.

In late spring of 1992, it was recognized that the liquid-argon electromagnetic calorimeter would not be able to provide the excellent resolution required by GEM. Consequently, it was decided that liquid krypton would be used in the electromagnetic section should the cryogenic liquid option be chosen. At the same time, so-called "hybrid" options were studied. While the barium fluoride crystals are naturally matched to the projective scintillating fiber hadronic towers, it is also natural to consider a large cryostat, in which both electromagnetic and hadronic sections would be contained. With the selection of krypton for the electromagnetic portion, however, the appeal of an all-cryogenic liquid system diminished, since it would have been too expensive to fill such a large system with liquid krypton. Thus, consideration was given to a "hybrid" system consisting of a liquid krypton electromagnetic section backed by a scintillating fiber hadronic section.

The *Baseline 1* document of the GEM collaboration, prepared in April 1992, featured primarily an all-liquid-argon calorimeter and mentioned some of the other combinations described above. This baseline GEM design was presented to the SSC Program Advisory Committee in July 1992. The committee expressed concern regarding the approach that GEM was taking to calorimetry and suggested that GEM may not be able to reach desired physics performance under any of the proposed scenarios.

In August 1992, the expert panel on barium fluoride radiation damage concluded that the proposed strategy (preradiation of the crystals) was not likely to be successful. However, the panel also pointed out that an alternative strategy (annealing *in situ*) was very promising. This was followed up with intensive R&D, which confirmed the panel's conclusion.

The electromagnetic calorimetry decision was made in early September, 1992, and the liquid krypton option was selected. The ORNL group believes that this choice was unfortunate, since it regards the potential performance of a barium fluoride system to be superior and more closely matched to GEM performance objectives.

In early October, 1992 the second major GEM calorimetry decision was made. It was decided that a "hybrid" system would be proposed. The ORNL group welcomed this decision, since a large part of its effort was devoted to scintillating fiber calorimetry R&D and since it was assumed that the hybrid system would consist of a liquid krypton electromagnetic calorimeter backed by a scintillating fiber hadronic calorimeter. Unfortunately, this assumption turned out to be wrong. What GEM management had in mind was to place a substantial portion of the hadronic section of the calorimeter inside the cryostat. Thus, the scintillating fiber option was essentially relegated to the role of a hadronic shower "tail-catcher."

During the year, the ORNL effort has concentrated on barium fluoride R&D (radiation damage studies, performance simulations, engineering, prototype design and production, beam test, etc.) and on scintillating fiber R&D (engineering design, beam tests, simulations, fiber radiation damage studies). Consequently, the GEM technology choices have come as a disappointment. As a result, ORNL has declined the offer to play the lead engineering role in GEM calorimetry. Instead, the ORNL group, together with ITEP colleagues working at ORNL, plans to play a major role in the design and construction of the scintillating fiber "tail-catcher," and in the "forward" calorimeter system, where a choice of technology has not yet been made and where the radiation damage problems are expected to be very severe.

In addition to ORNL's activity in GEM calorimetry described above, ORNL participates actively in the design and implementation of electronics associated with the central tracker.

2. Martin Marietta Energy Systems Engineering Division.

3. Consultant under subcontract from ITEP, Moscow.

CALORIMETRY DEVELOPMENT FOR THE GEM EXPERIMENT AT THE SSC

*S.M. Chae,¹ H. O. Cohn, C.C. Eberle,¹
Y. Efremenko,² A. Gordeev,² J. L. Heck,¹
Yu. Kamyshkov,² A. Nikitin,² D. Onoprienko,²
F. Plasil, M. J. Rennich,¹ A. Savin,²
K. Shmakov,² A. Smirnov,² E. Tarkovski,²
R. A. Todd,³ K. G. Young³*

During 1992, ORNL has played an important role in the design and optimization of electromagnetic and hadron calorimetry for the GEM experiment at the SSC. Emphasis was placed on two major areas; engineering and Monte Carlo simulation studies. A group of physicists and engineers from the Institute of Theoretical and Experimental Physics (ITEP) of Moscow, Russia, which is currently on assignment at ORNL, played an essential role in these studies. This group was supported by the SSC Laboratory with FY1992 R&D funds, and it operated in collaboration with ORNL Physics and I&C Divisions, and with the Martin Marietta Energy Systems Engineering Division.

The following studies were performed at ORNL:

Comparative MC studies of different EM calorimeter options for the detection of a neutral Higgs decaying into two gammas. Higgs mass reconstruction from $H^0 \rightarrow \gamma\gamma$ decay was studied for BaF₂ and LAr/Kr electromagnetic calorimeters.⁴ The best energy resolution in the 80- to 150-GeV Higgs mass region was shown to be achieved with a BaF₂ calorimeter. In the end-cap calorimeter region, the choice of technology does not significantly impact the total energy resolution (Fig. 4.11).⁵ The accuracy of decay-vertex reconstruction for $H^0 \rightarrow \gamma\gamma$ in the different calorimeter options was estimated. Reconstruction at different collider luminosities was considered. Calorimeter performance for jet measurements, for π^0 rejection,⁶ and for $\epsilon-\pi$ discrimination was studied.

Effects of cracks and of dead material on calorimeter performance. The effects of cracks and of dead material on the performance of different electromagnetic calorimeter options was studied for

1. ORNL I&C Division.

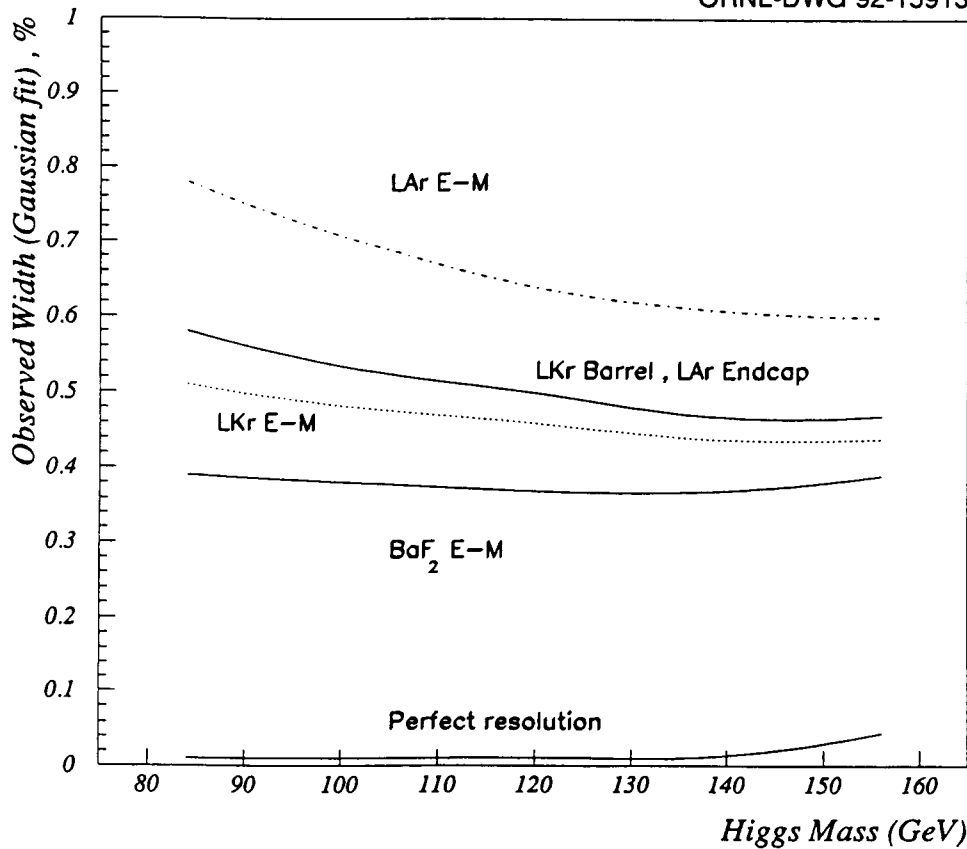


Fig. 4.11. Higgs mass reconstruction obtained with PHYTHI5.6; $M_H = 150$ GeV and with the assumption of perfect position resolution. The energy resolution was taken for LAr, $7.5\%/\sqrt{E} + 0.4\%$; LKr, $5.0\%/\sqrt{E} + 0.4\%$; and BaF₂, $2.5\%/\sqrt{E} + 0.5\%$.

$H^0 \rightarrow \gamma\gamma$ decay. It was shown that all options would have similar detection efficiencies for $H^0 \rightarrow \gamma\gamma$ (about 65%) without taking into account possible interactions in the central tracker. Interactions in the tracker will reduce the efficiency to about 50%. Separately, the influence of dead material in front of and behind the EM calorimeter was considered for electron and gamma response. Response corrections resulting from a "massless gap" were studied, and estimates of the accuracy of missing E_T measurements due to losses in cryostat walls were performed.⁷

Simulation of BaF₂ calorimeter performance. With the help of the light-transport Monte Carlo code LTRANS,⁸ requirements for crystal uniformity were defined in order to optimize the energy resolution.^{9,10} Studies of different coatings of BaF₂ crystals resulted in the establishment of a method to equalize crystal response in order to meet requirements for crystal uniformity. It was shown that light annealing of

radiation effects in BaF₂ crystals could be performed with a UV source and with quartz optical fibers. Studies of calibration options for BaF₂ crystals via isolated electrons, noninteracted hadrons, and an RFQ system were performed with the help of Monte Carlo simulations.

Beam tests with various calorimeter prototypes. ORNL staff members participated in the preparation of LAr/Kr calorimeter prototypes with accordion and parallel-plate geometries for beam test measurements at the AGS at BNL.¹¹ Simulation of beam test results for spaghetti-calorimeter modules was performed with the help of the GEANT Monte Carlo code.

Monte Carlo study of the performance of the forward Cerenkov calorimeter. Cerenkov light-collection efficiency in quartz fibers was calculated by means of the LTRANS code for different crossing angles, impact parameters, and particle velocities.

The response of a Cu/quartz-fiber calorimeter to electrons, pions, muons, and jets with energies of 10 and 100 GeV was simulated for different fiber/absorber ratios.

Engineering design studies. Designs of various calorimeter options and of various calorimeter components were performed. These include design of a scintillating-fiber hadron calorimeter with a BaF₂ crystal EM section, design of the details of a number of hybrid calorimeter configurations with LKr EM sections and scintillating-fiber hadronic sections, and design of a scintillating-tile "massless" gap as the forward part of the hadron calorimeter. Experimental setups for the study of the variation of attenuation length of fibers vs radiation dose and for the measurements of uniformity of light yield of scintillating tiles were designed and constructed.

1. Martin Marietta Energy Systems Engineering Division.
2. Consultant under subcontract from ITEP, Moscow.
3. ORNL I&C Division.
4. *Simulations for LKr EM Calorimeter*, GEM Calorimeter Group Meeting, BNL, GEM TN-92-119.
5. *Pointing and Light Higgs Mass Reconstruction with LKr/LAr EM Calorimeter*, Higgs to GammaGamma Task Force Meeting, SSCL, GEM TN-92-139.
6. *π^0 Rejection Using Shape Analysis with Pb/LKr EM Calorimeter*, EM Calorimeter Meeting, Stony Brook, N.Y., GEM TN-92-183.
7. *Missing E_T in Cryostat Walls*, Task Force on a Hybrid Calorimeter, GEM TN-92-213.
8. "Light Transport Code LTRANS," A. Savin, K. Shmakov, E. Shoumilov, E. Tarkovski, in preparation.
9. *Simulations on BaF₂ Response Uniformity*, GEM Calorimeter Group Meeting, Tucson, GEM TN-92-84.
10. *Local Nonuniformity of the BaF₂ Crystals*, Calorimeter Group Meeting, SSCL, GEM TN-92-143.
11. *GEM Baseline Calorimeter: Noble Liquid Integrated Calorimeter, The Liquid Argon Test*, 3rd International Conference on Calorimetry in High Energy Physics, Corpus Christi, Texas, Sept. 1992.

ORNL ACTIVITIES IN SUPPORT OF THE GEM CENTRAL TRACKER

*C. Britton,¹ L. Clonts,¹ K. Read,
and A. Wintenberg¹*

ORNL is active in the central tracker group for the proposed GEM detector at the SSC. Hardware activities include collaboration between the I&C and Physics Divisions of ORNL in order to develop radiation hard readout electronics for the Interpolating Pad Chambers (IPC) which surround the silicon microstrip tracker.

The front-end IPC readout electronics consist of a preamp followed by an analog memory unit (AMU), followed by a flash ADC. ORNL's primary hardware contribution will be development of the AMU design. Further IPC readout hardware contributions are possible. The AMU is a switched capacitor array. Due to its close proximity to the interaction point, it must be fabricated using a process resistant to 1-Mrad accumulated dose. The 16-channel AMU is 128 cells deep. The channel pitch is 310 μm , and the cell length is 34 μm . The AMU uses two 6-bit decoders to serve as a 7-bit decoder. The dynamic range is 10 bits.

Efforts this year have concentrated on selecting a foundry for the first radiation hard prototype fabrication run. This year ORNL signed nondisclosure agreements with Harris and UTMC for their radiation hard processes. They obtained process models to simulate the effects of radiation damage on the circuits. An AMU prototype design was developed this summer using the Harris AVLSI-RA process. The design should be submitted for fabrication by the end of 1992. The prototype run will yield two alternate designs of the AMU with different decoding schemes on a single wafer. The first chip will be an 8-channel prototype with 128 cells per channel. Four channels will use a voltage-write, voltage-read topology. The other four channels will employ a voltage-write, charge-read topology. One 6-bit decoder will control the first 64 channels. The other 6-bit decoder will control the remaining 64 channels. The second chip will be logically identical to the first except that the two decoders will control alternate channels.

During the spring of 1993, the prototype chips will be tested for performance and radiation hardness and will be characterized in order to refine the design. A major goal is to ascertain whether or not the Harris

AVLSI-RA process is satisfactory and whether or not the UTMIC 1.2- μm UTE-R process is preferable to the Harris process. Another goal is to assess the relative merits of the voltage-write, voltage-read and voltage-write, charge-read topologies.

Monte Carlo simulations of the tracker performance have been performed. A powerful local Silicon Graphics workstation is used for this purpose. Work is in progress to contribute to the development of the central tracker off-line reconstruction code.

1. ORNL I&C Division.

**NEUTRAL-STRANGE-PARTICLE
PRODUCTION IN 200-GeV/c $p/\pi^+/K^+$
INTERACTIONS ON Au, Ag, and Mg¹**

*International Hybrid Spectrometer Consortium
Including H. O. Cohn
(For a complete list of authors, see Ref.1)*

We have used the Fermilab 30-in. bubble-chamber-hybrid spectrometer to study neutral-strange-particle production in the interactions of 200-GeV/c protons and π^+ and K^+ mesons with nuclei of gold, silver, and magnesium. Average multiplicities and inclusive cross sections for K^0 and Λ are measured, and a power law is found to give a good description of their A dependence. The exponent characterizing the A dependence is consistent with being the same for K^0 and Λ production, and also the same for proton and π^+ beams. Average K^0 and Λ multiplicities, as well as their ratio, have been measured as functions of the numbers of projectile collisions v_p and secondary collisions v_s in the nucleus, and indicate that rescattering contributes significantly to enhancement of Λ production but not to K^0 production. The properties of events with multiple K^0 's or Λ 's also corroborate this conclusion. K^0 rapidities are in the central region and decrease gently with increasing v_p , while Λ rapidities are in the target-fragmentation region and are independent of v_p . K^0 and Λ multiplicities increase with the rapidity loss of the projectile, but their rapidities do not.

1. Abstract of published paper: *Phys. Rev. D* **45**, 734 (1992).

**MEASUREMENT OF THE LIFETIME OF
B-HADRONS AND A DETERMINATION
OF $|V_{cb}|$ (Ref.1)**

*L3 Collaboration
Including H. O. Cohn, Yu. Kamyshev,² F. Plasil,
and K. F. Read
(For a complete list of authors, see Ref.1)*

From a fit to the impact parameter distribution of lepton tracks from semileptonic b decay, the lifetime of B hadrons produced in e^+e^- collisions at the Z^0 is measured to be 1.32 ± 0.08 (stat.) ± 0.09 (syst.) ps. Combined with an earlier measurement of the branching ratio $\text{Br}(B \rightarrow l\nu X)$, the CKM matrix element $|V_{cb}|$ is determined to be 0.046 ± 0.002 (exp.)^{+0.004}_{-0.003} (theory).

1. Abstract of published paper: *Phys. Lett. B* **270**, 111 (1991).
2. Consultant under subcontract from ITEP, Moscow.

**SEARCH FOR LEPTON FLAVOR
VIOLATION IN Z^0 DECAYS¹**

*L3 Collaboration
Including H. O. Cohn, Yu. Kamyshev,² F. Plasil,
and K. F. Read
(For a complete list of authors, see Ref.1)*

We have searched for lepton flavor violation in Z^0 boson decays into lepton pairs, $Z^0 \rightarrow \mu\tau$, $Z^0 \rightarrow e\tau$, and $Z^0 \rightarrow e\mu$. The data sample is based on an integrated luminosity of 10.4 pb^{-1} corresponding to 370,000 Z^0 's produced. We obtain upper limits on the branching ratios of 4.8×10^{-5} for the $\mu\tau$, 3.4×10^{-5} for the $e\tau$, and 2.4×10^{-5} for the $e\mu$ decay modes at the 95% confidence level.

1. Abstract of published paper: *Phys. Lett. B* **271**, 453 (1991).
2. Consultant under subcontract from ITEP, Moscow.

**MEASUREMENT OF THE STRONG
COUPLING CONSTANT α_s
FOR BOTTOM QUARKS AT THE Z^0
RESONANCE¹**

L3 Collaboration

*Including H. O. Cohn, Yu. Kamyshev,² F. Plasil,
and K. F. Read*

(For a complete list of authors, see Ref.1)

We have measured the ratio of the strong coupling constants α_s for bottom quarks and light quarks at the Z^0 resonance in order to test the flavor independence of the strong interaction. The coupling strength α_s has been determined from the fraction of events with three jets, measured for a sample of all hadronic events, and for inclusive muon and electron events. The b purity is evaluated to be 22% for the first data set and 87% for the inclusive lepton sample. We find $\alpha_s(b)/\alpha_s(\text{udsc}) = 1.00 \pm 0.05$ (stat.) ± 0.06 (syst.).

-
1. Abstract of published paper: *Phys. Lett. B* 271, 461 (1991).
 2. Consultant under subcontract from ITEP, Moscow.

**A DIRECT DETERMINATION OF THE
NUMBER OF LIGHT NEUTRINO FAMILIES
FROM $e^+e^- \rightarrow \nu\bar{\nu}\gamma$ AT LEP¹**

L3 Collaboration

*Including H. O. Cohn, Yu. Kamyshev,² F. Plasil,
and K. F. Read*

(For a complete list of authors, see Ref.1)

The L3 detector at LEP has been used to determine the number of light neutrino families by measuring the cross section of single photon events in e^+e^- collisions at energies near the Z^0 resonance. We have observed 61 single photon candidates with more than 1.5 GeV of deposited energy in the barrel electromagnetic calorimeter, for a total integrated luminosity of 3.0 pb^{-1} . From a likelihood fit to the single photon cross sections, we determine $N_\nu = 3.2 \pm 0.46$ (statistical) ± 0.22 (systematic).

-
1. Abstract of published paper: *Phys. Lett. B* 275, 209 (1992).
 2. Consultant under subcontract from ITEP, Moscow.

**ELECTROWEAK PARAMETERS OF THE Z^0
RESONANCE AND THE STANDARD
MODEL¹**

*LEP Collaborations: ALEPH, DELPHI, L3,
and OPAL*

*Including H. O. Cohn, Yu. Kamyshev,² F. Plasil,
and K. F. Read*

(For a complete list of authors, see Ref.1)

The four LEP experiments have each performed precision measurements of Z^0 parameters. A method is described for combining the results of the four experiments, which takes into account the experimental and theoretical systematic errors and their correlations. We apply this method to the 1989 and 1990 LEP data, corresponding to approximately 650,000 Z^0 decays into hadrons and charged leptons, to obtain precision values for the Z^0 parameters. We use these results to test the standard model and to constrain its parameters.

-
1. Abstract of published paper: *Phys. Lett. B* 276, 247 (1992).
 2. Consultant under subcontract from ITEP, Moscow.

**SEARCH FOR THE NEUTRAL HIGGS
BOSON AT LEP¹**

L3 Collaboration

*Including H. O. Cohn, Yu. Kamyshev,² F. Plasil,
and K. F. Read*

(For a complete list of authors, see Ref.1)

A search for the standard neutral Higgs boson is described. Data collected during 1990 and 1991, corresponding to 408,000 hadronic decays of the Z^0 , were used. At the 95% confidence level we exclude the existence of the minimal standard model Higgs boson in the mass range $0 \leq M_{H^0} < 52 \text{ GeV}$.

-
1. Abstract of published paper: *Phys. Lett. B* 283, 454 (1992).
 2. Consultant under subcontract from ITEP, Moscow.

**STUDIES OF HADRONIC EVENT
STRUCTURE AND COMPARISONS
WITH QCD MODELS AT THE Z^0
RESONANCE¹**

L3 Collaboration

*Including H. O. Cohn, Yu. Kamyshkov,² F. Plasil,
and K. F. Read*

(For a complete list of authors, see Ref.1)

The structure of hadronic events from Z^0 decay is studied by measuring event shape variables, factorial moments, and the energy flow distribution. The distributions, after correction for detector effects and initial and final state radiation, are compared with the predictions of different QCD Monte Carlo programs with optimized parameter values. These Monte Carlo programs use either the second-order matrix element or the parton shower evolution for the perturbative QCD calculations and use the string, the cluster, or the independent fragmentation model for

hadronization. Both parton shower and $O(\alpha_s^2)$ matrix element based models with string fragmentation describe the data well. The predictions of the model based on parton shower and cluster fragmentation are also in good agreement with the data. The model with independent fragmentation gives a poor description of the energy flow distribution. The predicted energy evolutions for the mean values of thrust, sphericity, aplanarity, and charge multiplicity are compared with the data measured at different center-of-mass energies. The parton shower based models with string or cluster fragmentation are found to describe the energy dependences well while the model based on the $O(\alpha_s^2)$ calculation fails to reproduce the energy dependences of these mean values.

1. Abstract of published paper: *Z. Phys. C* **55**, 39 (1992).

2. Consultant under subcontract from ITEP, Moscow.

5. ACCELERATOR-BASED ATOMIC PHYSICS

ELECTRON-POSITRON PAIR PRODUCTION IN COULOMB COLLISIONS OF ULTRARELATIVISTIC SULFUR IONS WITH FIXED TARGETS

*C. R. Vane, S. Datz, P. F. Dittner, H. F. Krause,
C. Bottcher, M. R. Strayer,
R. Schuch,¹ H. Gao,¹ and R. Hutton²*

At ultrarelativistic energies, peripheral collisions between heavy, highly charged atoms produce extremely intense, rapidly varying electromagnetic fields which are expected to give rise to copious lepton-pair formation. These collisions are fundamentally different from those involving singly charged projectiles because the coupling constant $Z\alpha$ can be large (≥ 0.5) in heavy systems. Lepton pair production in these systems is especially interesting because the collision strength can be varied continuously, from regions of low charge and energy where past applications of low-order perturbative methods are suitable, to higher energy and charge regimes where first-order perturbative calculations are known to occasionally give unphysical results.

We report here new measurements using an improved efficiency apparatus and comparisons with theory for angular and momentum distributions of 1–17 MeV/c positrons from electron-positron pairs generated by 6.4 TeV sulfur ions in peripheral collisions with fixed targets of Al, Pd, and Au. Fully stripped 6.4 TeV sulfur ions from the CERN Super Proton Synchrotron (SPS) accelerator were passed through thin foil targets in a high-vacuum chamber centered in the 14-cm gap of a 1-meter-long, CERN standard dipole bending magnet located upstream of the large nuclear physics collaboration experiment WA93. Electrons and positrons generated by ions in the targets were separated in the nearly uniform vertical magnetic field and transported 180° along circular arcs to one of two identical arrays of discrete detectors mounted on either side of the ion beam in the plane containing the chosen target.

Electron and positron counts were stored as functions of detector position for two settings of

magnetic field (0.18 and 0.45 T) corresponding to detected momenta of 1.0–6.7 MeV/c and 2.5–17 MeV/c, respectively. Data were collected for targets of: 75 $\mu\text{g}/\text{cm}^2$ polypropylene $(\text{CH}_2)_x$; 180 $\mu\text{g}/\text{cm}^2$ Al; 4.9 mg/cm^2 Pd; and 0.6, 1.5, and 4.7 mg/cm^2 Au. The very thin targets ($<10^{-3}$ radiation length) were used to minimize backgrounds from direct knock-on (KO) electrons and to avoid significant multiple Coulomb scattering of low energy electrons and positrons. Less than one sulfur ion in ten thousand underwent nuclear charge-changing collisions in these targets. Signals from the WA93 Zero Degree Calorimeter (ZDC) were used in our experiment to identify, count, and provide coincidence timing for full energy projectile sulfur ions. Sulfur ions from the SPS were delivered in roughly uniform spills of 5.1-sec length with 10^5 to 10^6 ions per spill. For the 1.5 mg/cm^2 Au target, typical counting rates for 1–6.7 MeV/c positrons and electrons (primarily KO's) detected in coincidence with projectile ions were (1–10)/sec and (100–1000)/sec, respectively. Positron and electron yields/ion were found to vary linearly with Au target thickness from 0.6 to 4.7 mg/cm^2 , indicating that backgrounds from higher-order scattering processes like pair conversion of projectile-target γ rays in the same target are not significant.

Results of measurements of single positrons detected in coincidence with full-energy sulfur ions are reported here. Analysis of electron data collected in coincidence with positrons and ions may be complicated by possible interference of simultaneously ejected KO electrons and will be treated at a future date.

The variation of intensity with vertical displacement is related to the angular distribution of ejected positrons or electrons. The measured distribution represents a projection of the source angular differential cross section on a limited vertical aperture determined by the height of the detector array. Electrons and positrons from pairs exhibit distributions that peak sharply in the forward direction. Instead of attempting to deconvolute measured distributions, we have mapped selected angular differential cross sections through the magnetic analyzing field to the

detector plane and compared the resulting calculated distributions with the data. Using a computer simulation which incorporates effects of multiple Coulomb scattering, and assuming a simple exponential form for the angular cross section ($d\sigma/d\Omega \sim \exp(-\theta/w)$, where θ is the polar angle), we have determined $1/e$ angular widths (w) which most closely reproduce the data, as a function of horizontal position (i.e., positron momentum). Results of these simulation fits are displayed in Fig. 5.1 for positrons from a 1.5 mg/cm^2 Au target. Figure 5.1 also shows results for similar angular widths calculated in an exact Monte Carlo evaluation of the two-photon terms in lowest-order QED calculations³ for structureless nuclei. Widths from simulation fits to the data differ from the theoretical results by only $\sim 1\text{-}2^\circ$, well within the experimental median angular resolution of 3° .

Since the angular distribution for positron emission is peaked so narrowly in the forward direction, the horizontal intensity distribution on the detector array directly represents the momentum distribution. We have summed counts in nine sets of detectors grouped according to horizontal position and plot the resulting momentum distributions in Fig. 5.2, at the two field settings. The solid line histograms show measured cross sections corrected for the fractions of positrons lying outside the vertical acceptance of each detector group. These corrections were made assuming theoretical angular distributions as presented in Fig. 5.1. Theoretical $d\sigma/dp$ cross sections are displayed in Fig. 5.2 as smooth curves. Results of First Born approximation calculations⁴ which employ Sommerfeld-Maue wavefunctions for the free electron and positron are displayed by the dashed line. To construct this curve, cross sections for 200 GeV $p + U$ have been interpolated and scaled according to Z_p^2 and Z_T^2 where Z_p and Z_T are the projectile and target nuclear charges. Finally, comparing positron yields per sulfur ion for Al, Pd, and Au, we find that the measured cross sections vary as Z_T^2 as predicted by all lowest order calculations.

1. Manne Siegbahn Institute of Physics, Stockholm, Sweden.

2. University of Lund, Lund, Sweden.

3. C. Botcher and M. R. Strayer, *Phys. Rev. D* **39**, 1330 (1989); M. J. Rhoades-Brown and J. Weneser, *Phys. Rev. A* **44**, 330 (1991).

4. P. B. Eby, *Phys. Rev. A* **43**, 2258 (1991); **39**, 2374 (1989).

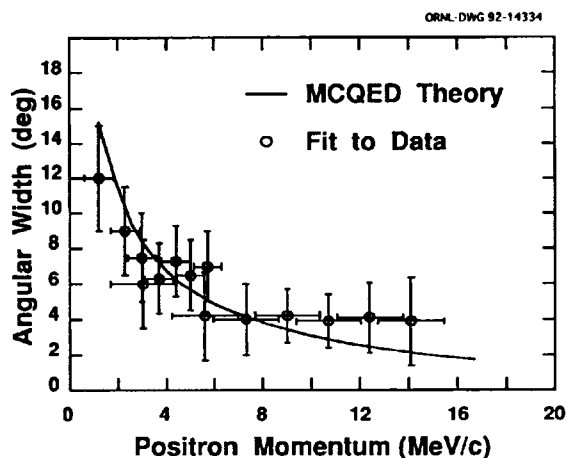


Fig. 5.1. Angular $1/e$ widths for $d\sigma/d\Omega$ plotted as a function of positron momentum for 6.4 TeV S + Au. Data points (o) are results of simulation fits to measured vertical intensity distributions as described in the text. Error bars indicate observed fitting uncertainty dominated by experimental angular resolution set by detector size. Theoretical results (—) of Ref. 3.

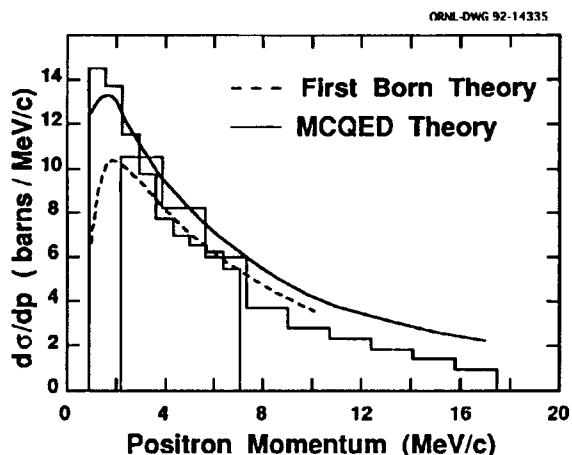


Fig. 5.2. Measured positron differential cross sections compared with theoretical results. Overlapping solid line histograms are measured cross sections for field settings of 0.18 and 0.45 Tesla, corrected for incomplete detection of the full angular emission distributions as described in the text. Relative uncertainty in cross sections is $\leq \pm 10\%$. Smooth curves represent results of Ref. 3 (—) and interpolations of scaled First Born calculation results (---) given in Ref. 4.

**KNOCK-ON ELECTRONS
PRODUCED IN COLLISIONS OF
6.4-TeV SULFUR IONS WITH
FIXED TARGETS**

*C. R. Vane, S. Datz, P. F. Dittner, H. F. Krause,
R. Schuch,¹ H. Gao,¹ and R. Hutton²*

Secondary electron emission in collisions of ions with atoms and solids has been a topic of considerable theoretical and experimental interest for many years. Significant progress has been made in understanding the energy and angular distributions observed for these ejected electrons for a wide variety of projectile-target systems. These include partially stripped ions up to several MeV/u and heavy, many-electron targets, which have shown surprisingly complex spectra depending on the precise charge state and energy of the projectile ions. However, except for cosmic ray studies, almost no measurements or detailed calculations exist at extreme relativistic collision energies.

In recent experiments³ studying the formation of electron-positron pairs in peripheral Coulomb collisions of ultrarelativistic heavy-ion projectiles with target atoms, we have simultaneously collected data on high-energy (> 0.6 MeV) electrons ejected in binary ion-electron collisions. At relativistic energies, these direct collision secondary electrons are usually referred to as delta rays (especially when identified from tracks in emulsions) or as knock-on (KO) electrons. Cross sections for KO production are generally relatively large with observed KO yields depending strongly on the ranges of detected electron energies and emission angles.

Knock-on data were collected using the same apparatus described previously³ for targets of: $75 \mu\text{g}/\text{cm}^2$ - polypropylene (CH_2)_x; $180 \text{ mg}/\text{cm}^2$ - Al; and $0.6, 1.5,$ and $4.7 \text{ mg}/\text{cm}^2$ - Au. The very thin targets were used to maintain acceptable counting rates from KO electrons and to reduce multiple Coulomb scattering. Signals from the WA93 Zero Degree Calorimeter were employed for normalization and for coincidence measurements with KO electrons detected in our magnetic spectrometer. Electron counts detected in coincidence with unscattered, full-energy ions were stored as functions of detector position for two settings of magnetic field (0.18 and 0.45 T) corresponding to detected electron momenta of 1.0–6.7 MeV/c and 2.5–17 MeV/c, respectively.

Instead of attempting to deconvolute measured counting distributions, we have mapped selected Born approximation cross sections for KO production,

doubly differential in energy and angle, through the magnetic analyzing field to the detector plane and compared the resulting calculated counting distributions with the data. These calculations were carried out using a Monte Carlo simulation routine which incorporates effects of multiple Coulomb scattering from uniformly distributed launch sites along the ion's path in the solid targets.

Because high-energy KO electrons tend to be emitted in the forward direction, there is little energy/angular mixing in trajectories through the magnetic analyzing field, and the horizontal counting distribution on the detector array (with minor loss of resolution) directly reflects the momentum distribution. We have summed counts in nine sets of detectors grouped according to horizontal position and plot in Fig. 5.3, overlapping histograms of the resulting momentum distributions at the two field settings for KO electrons from a $1.5 \text{ mg}/\text{cm}^2$ Au target. Dashed line histograms in Fig. 5.3 display results of the computer simulation calculations described above. We note general good absolute agreement between measurements and calculations, well within an estimated experimental error of $\pm 25\%$. Measured distributions from all other targets (including CH_2 and Al) are similar, except for increased low-energy KO contributions for the thickest Au target where multiple Coulomb scattering becomes important. This

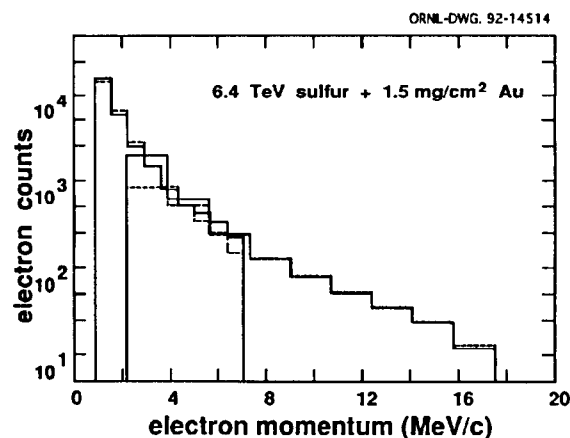


Fig. 5.3. Momentum distributions for KO electrons from a $1.5 \text{ mg}/\text{cm}^2$ Au target. Overlapping solid-line histograms display measured absolute yields for 0.18 T and 0.45 T magnetic analyzing fields. Dashed-line histograms show corresponding simulation results.

implies that target binding, averaged over all electrons, has little effect on the final high-energy KO momentum distributions investigated here.

The measured KO vertical displacement distribution for 1.0 – 2.5-MeV electrons from 1.5 mg/cm² Au target is shown in Fig. 5.4a along with simulation results. The observed nearly uniform distributions arise from a relatively narrow angular cut imposed by the vertical height accepted by the detector array, when compared to an initial launch mean polar angle of approximately 37° corresponding to 1.5-MeV electrons. Figure 5.4b shows similar results for higher energy (10 – 12 MeV) electrons. Here, the classical kinematical launch angle would be ~ 17°. Again, we

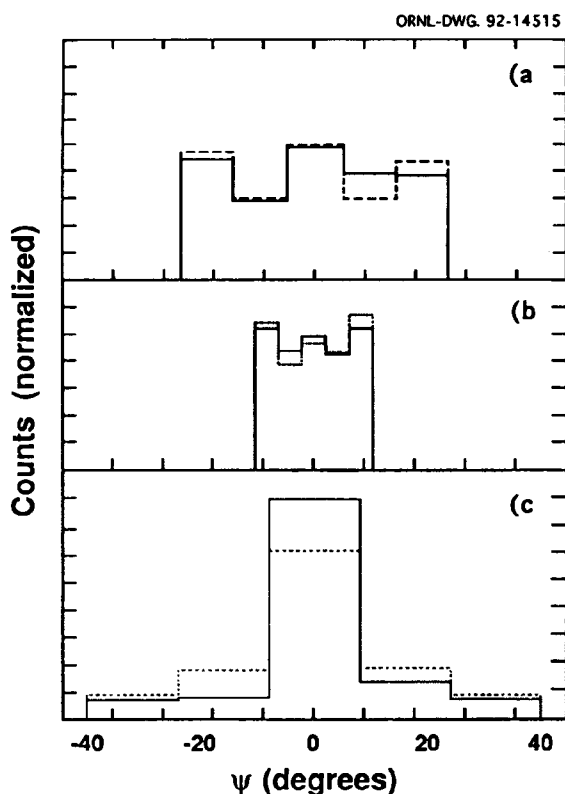


Fig. 5.4. Vertical KO electron distributions at the detector plane generated by selecting detectors with positions corresponding to specific electron energies. Solid-line histogram shows measured distribution of counts. Dashed-line histograms show simulation results. Angle ψ is the projected vertical launch angle, measured in the detector plane. (a) 1.0 – 2.5-MeV electrons. (b) 10 – 12-MeV electrons. (c) 0.6 – 1.0-MeV electrons.

note that there is generally good agreement between experiment and calculations.

At the lowest energy range detected, 0.6 – 1.0 MeV, the measured vertical distribution is significantly more “forward peaked” than predicted by our simple calculations. A comparison of simulation results and measurements is shown in Fig. 5.4c. We suspect that this effect is due in part to secondary scattering of higher energy electrons, launched at larger polar angles, into the forward direction, with production of even lower energy electrons spread over all angles. Secondary scattering effects, except for multiple Coulomb scattering, are not included in the simulations. At 0.6-MeV target binding effects may also become significant, although we observe little variation in electron distributions for light versus heavy targets. It is interesting to note that the observed angular distributions of secondary electrons measured in experiments⁴ at much lower energies also show some of the tendencies seen here. For bare projectiles, electron energy spectra, integrated over emission angles, tend to agree with Born and binary encounter calculations, even at relatively low collision energies. Angular distributions, on the other hand, are usually not well predicted. There tend to be more electrons observed in the forward and backward directions than calculated.⁴

1. Manne Siegbahn Institute of Physics, Stockholm, Sweden

2. University of Lund, Lund, Sweden

3. See previous article, this report.

4. J. E. Turner and C. E. Klots, *Proceedings, Third Int'l Symposium on Microdosimetry*, Stresa, Italy, 1971, pub. by Comm. European Communities Luxembourg, 1972; P. B. Eby and S. H. Morgan, Jr., *Phys. Rev. A* 5, 2536 (1972).

SADDLE-POINT SHIFTS IN IONIZING COLLISIONS

V. D. Irby,¹ S. Datz, P. F. Dittner, N. L. Jones, H. F. Krause, and C. R. Vane

Experimental studies of electrons ejected in ionizing collisions of C⁺, C²⁺, and C³⁺ projectiles and He and Ne targets have been made for incident projectile energies of 83, 100, and 150 keV/u. The data exhibit pronounced maxima in the 10° ejected-electron en-

ergy spectra and projectile-charge dependent shifts of these maxima which strongly supports the hypothesis of a "saddle-point" ionization mechanism.^{2,3}

Experiments were carried out at the ORNL EN Tandem accelerator facility. Ejected-electron energy spectra were obtained utilizing a new high-resolution spectrometer that was designed by J. P. Giese⁴ and assembled by U. Bechthold.⁵ It is twice the size of the Swenson spectrometer⁶ and incorporates piezoelectric inchworm motors to translate and rotate the microchannel plate detector. The differentially pumped target consists of an inner and outer gas cell with slots cut every 10° in both cells to allow passage of the ejected electrons. In addition, both the inner and outer cells are electrically isolated, allowing for acceleration/deceleration of electrons produced in the target region.

Figure 5.5 illustrates the results obtained for 150 keV/u C^{q+} ions incident on He at an ejection angle of 10°. The upper, middle, and lower curves are for C⁺, C²⁺, and C³⁺, respectively. As can be seen, the data exhibit projectile-charge dependent shifts of the maxima in the ejected-electron energy spectra. These shifts correspond to the decrease in the "saddle-point" velocity, v_{sp} ,

$$v_{sp} = v_p / (1 + Q_p / Q_t)$$

(where v_p is the projectile velocity, Q_p is the projectile charge, and Q_t is the charge on the ionized target) as the projectile charge increases. The saddle-point is,

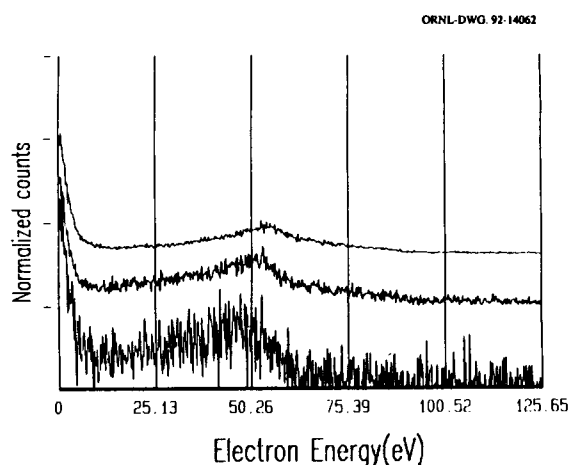


Fig. 5.5. Ejected-electron energy spectra for 150-keV/u C^{q+} ions incident on He taken at 10°. Individual spectra were background subtracted and normalized to the incident ion flux.

by definition, the position at which the Coulomb force exerted on the electron by the target ion is equal and opposite to that exerted by the projectile ion.

1. JHIR, Oak Ridge, TN.
2. R. E. Olson, T. J. Gay, H. G. Berry, E. B. Hale, and V. D. Irby, *Phys. Rev. Lett.* **59**, 36 (1987).
3. V. D. Irby, *Phys. Rev. A* **39**, 54 (1989).
4. J. P. Giese, private communication (1992).
5. U. Bechthold, Diploma Thesis, University of Frankfurt (1992).
6. J. K. Swenson, *Nucl. Instr. Meth Phys. Res.* **B10/11**, 899 (1985).

OBSERVATION OF INTERFERENCE IN RESONANT COHERENT EXCITATION

H. F. Krause, S. Datz, P. F. Dittner,
N. L. Jones, C.R. Vane

When an ion moves parallel to the atomic strings inside a crystalline solid, the ion experiences a static electric field variation as it passes each substrate atom. The spatial variation appears as a periodic time-varying electric field in the projectile frame. The fundamental perturbation frequency, ν experienced by the ion, is ν/D where ν is the ion speed and D is the distance between lattice atoms. In reality, the spatial electric field is not a pure sinusoid, therefore in general, the ion is also perturbed at integral multiples of the fundamental frequency, $K(\nu/D)$, where $K = 1, 2, \dots, N$. When any perturbation frequency matches an excitation frequency of the projectile ion, for example the $N = 1$ to $N = 2$ transition frequency of a one-electron ion, a fraction of the incident ground-state ions becomes excited. This phenomenon, called resonant coherent excitation (RCE), has been demonstrated and extensively studied for swift, low- Z ($4 < Z < 10$) one- and two-electron ions moving in face-centered-cubic (FCC) lattices such as Ag and Au.¹ The interesting consequences that can occur in RCE for non-FCC crystals have not been studied, heretofore.

The $\langle 111 \rangle$ axis in a diamond lattice such as silicon or germanium illustrates the importance of phase in the RCE process. The $\langle 111 \rangle$ axial channel in either an FCC or a diamond lattice is bounded by an equilateral array of three atomic strings. In each string, the distance D between atoms is $\sqrt{3} A$, where

A is the unit cell dimension ($A = 5.431 \text{ \AA}$ in silicon). A $\langle 111 \rangle$ string in the FCC structure only has atoms indicated by "1" (solid dots) in Fig. 5.6. A $\langle 111 \rangle$ string in the diamond structure has additional atoms indicated by "2" (open circles) that are displaced from atoms 1 by the distance $D/4$. RCE can occur in a given harmonic when the impact-parameter-dependent Fourier coefficient of the longitudinal or transverse electric field, $f_i = \int E(r) e^{ik \cdot r} dr$, is non-zero. By comparing the location of either atoms 1 or atoms 2 with the sinusoidal integrand of the Fourier amplitude in the $K=4$ and 6 harmonics shown in Fig 5.6, we see that the integral is non-zero for either harmonic, if $E(r)$ is non-zero. The Fourier amplitude for either atoms 1 or 2 alone, f_1 or f_2 , of course increases for closer encounters with the string. In Fig. 5.6, we can also see that the Fourier amplitudes for atoms 1 and 2 add in the $K = 4$ harmonic (constructive interference, $f_1 + f_2$), but cancel in the $K = 6$ harmonic (destructive interference, $f_1 - f_2$). Since the interference occurs within each $\langle 111 \rangle$ string surrounding the axial channel and for every impact parameter, it must also occur for all axial channeling impact parameters (i.e., in the superposition of the three surrounding strings that have different translational phase factors). More generally for a diamond crystal in the $\langle 111 \rangle$ direction, constructive and destructive interference should occur for the harmonic sequences $K = 4, 8, 12, \dots$ and $K = 2, 6, 10, \dots$, respectively. Incomplete destructive

interference could occur if (1) the channeled projectile were deflected significantly within the distance D , (2) the crystal had correlated defects, or (3) the thermal vibration amplitudes for atoms in the string were significant.

In the experiment, ion beams of C and N were accelerated by the Oak Ridge EN Tandem Accelerator. Hydrogen-like ions formed by post-stripping were narrowly collimated before entering a thin Si crystal (3000 \AA in the $\langle 111 \rangle$ direction). Ions emerging from the crystal were charge state analyzed using a parallel-plate electrostatic deflector. Separated charge states were detected using a one-dimensional solid-state position-sensitive detector. Evidence of hydrogen-like $N = 1$ to 2 excitation in RCE was detected by studying the velocity dependence of the emergent charge state fraction, since excited ions ionize rapidly inside the crystal.¹ The emergent charge fraction for N^{6+} between 12 – 42 MeV is shown in Fig. 5.7. Referring to Fig. 5.7, we see resonance dips for $K = 5$ and 7 harmonic excitation with monotonically decreasing strength. The measured strengths below 20 MeV do not accurately track calculated Fourier coefficients for RCE because single-electron capture cross sections for N^{6+} rapidly increase at the lowest velocities. The predicted constructive $K = 8$ dip is surprisingly strong, given the high harmonic and the lack of charge state frozenness around 14 MeV. Also as predicted, we do not observe

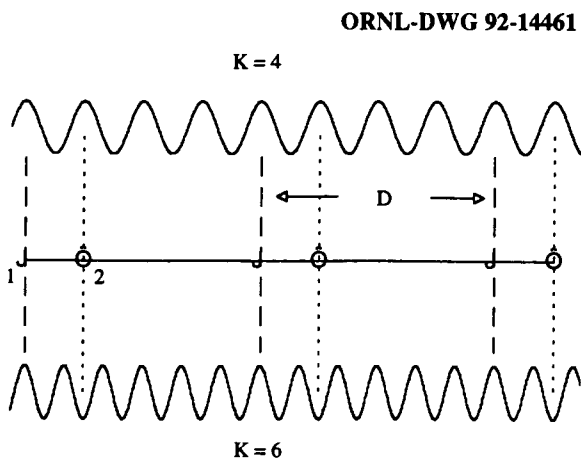


Fig. 5.6. Two repetitions of an atomic string along the $\langle 111 \rangle$ axial direction of a diamond lattice that consists of atomic substrings 1 and 2. The sinusoidal integrands of the Fourier amplitude of electric field are shown for the $K = 4$ and 6 constructive and destructive harmonics.

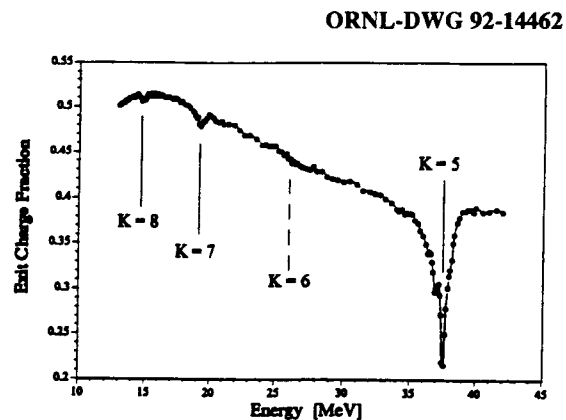


Fig. 5.7. The N^{6+} emergent charge state fraction for one-electron ions channeled along the Si $\langle 111 \rangle$ axis. The location of RCE resonances for the $K = 5, 6, 7,$ and 8 harmonics are indicated. The $K = 6$ resonance that would normally be about half the size of the large $K = 5$ resonance is missing because of destructive interference in the $N = 1$ to 2 electric dipole transition amplitude.

a sharp resonance dip in the $K = 6$ harmonic at 26.2 MeV, where charge state frozenness is not a problem.

In this experiment, we have demonstrated that RCE selection rules occur in the case of a diamond lattice. The selection or propensity rules are the consequence of complete destructive or constructive interference in the quantum mechanical transition amplitude for excitation. This demonstration of atomic interferometry proves the fundamental importance of phase coherence in RCE at a transition frequency of order 10^{17} Hz.

1. C. D. Moak et. al., *Phys. Rev. A* **19**, 977 (1979).

SCATTERING OF AXIALLY CHanneled IONS IN A VERY THIN SILICON CRYSTAL

H. F. Krause, J. R. Barrett,¹ J. Gomez del Campo, S. Datz, P. F. Dittner, N. L. Jones, and C. R. Vane

Atomic collision processes such as excitation, ionization and electron capture are often studied at high energy using ion channeling techniques and very thin crystalline targets. For such crystals, the angular distribution of emergent ions indicates the unique trajectory inside the crystal. An understanding of the trajectories can simplify the interpretation of atomic physics experiments and/or suggest directions for more sophisticated coincidence studies performed with angular correlation. No complete study of axial channeling angular distributions at high energy has been reported heretofore.

We measured high-resolution (FWHM = 4 millidegrees) two-dimensional angular distributions for 0.5–2.5-MeV/u C^{q+} ions ($q = 4–6$) axially channeled in a thin silicon crystal (1730 Å). The angular distribution measured for 20-MeV C^{6+} channeled in the $\langle 100 \rangle$ direction is shown in Fig. 5.8. The crystal was oriented so that the four atomic strings associated with the $\langle 100 \rangle$ axis are congruent with the corners of Fig. 5.8. We see that the complicated angular distri-

bution is correlated with the string locations. Islands, due to a rainbow effect, are also observed. More complicated structure is revealed in one-dimensional projected cuts² that pass through 0° . A complete analysis of our $\langle 100 \rangle$ data indicates that the angular distributions depend strongly on the crystal thickness, the ion velocity, and the entrance charge state. To clarify the interpretation, we have also measured the exit charge state distributions for entering C^{q+} ions ($q = 4–6$), at each energy.

Extensive Monte Carlo modeling using the channeling code, LAROSE, has been performed. All observed angular distributions are closely duplicated in the calculations by assuming only a Moliere scattering potential. Small discrepancies in the experimental and calculated angular distributions, barely noticeable in a plot as coarse as Fig. 5.8, are probably due to small inaccuracies of this potential.

Using LAROSE, now experimentally verified, we have been able to establish that transverse axial oscillations are the root cause of all angular effects observed. The transverse oscillation frequency, 7.4×10^{13} Hz for protons in Si $\langle 100 \rangle$, accurately scales with the q/M of the projectile, where q is the ionic charge state and M is the projectile mass. Using this information, we have discovered that normalized angular distributions calculated for H^+ in Si $\langle 100 \rangle$, each specified by a wavelength parameter λ , can be used to predict the angular distributions for C^{q+} , even in the case of very different experimental conditions. The normalization parameter λ , is given by

$$\lambda = t \cdot f(q,M)/v \quad (1)$$

where t is the $\langle 100 \rangle$ crystal thickness [cm], $f(q,M)$ is the transverse oscillation frequency [Hz] scaled from H^+ ions, and v is the projectile velocity [cm/s]. Given the complexity of axial channeling angular distributions, it is remarkable that this scaling formula is so simple. We plan to exploit this simplicity in the design of future atomic physics experiments.

-
1. Retired, ORNL Solid State Division.
 2. H. F. Krause, to be published.

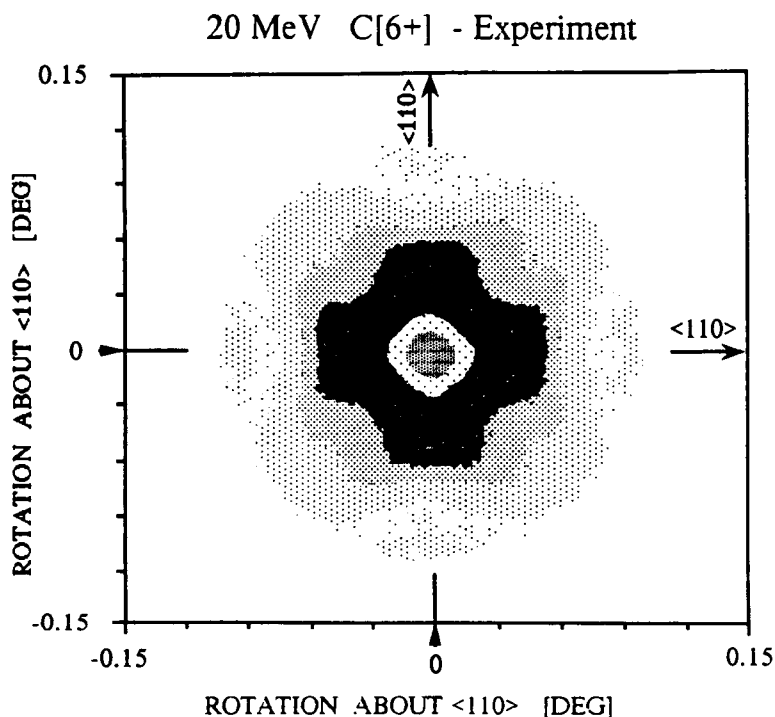


Fig. 5.8. The measured two-dimensional angular distribution for 20-MeV C^{6+} ions axially channeled in the $\langle 100 \rangle$ direction of a 1730-Å-thick silicon crystal. Cuts through the intensity distribution at a percentage of the maximum count are plotted as contours at the following levels: 2.5, 5, 10, 20, and 50%. Atomic strings that define the axial channel lie along $\langle 100 \rangle$ directions, rotated 45° from the $\langle 110 \rangle$ directions.

DISSOCIATIVE RECOMBINATION OF VIBRATIONALLY COLD H_3^+ IN AN ION STORAGE RING

*S. Datz, M. Larsson,¹ H. Danared,² J. R. Mowat,³
P. Sigraý,² G. Sundström,¹ L. Bieström,²
A. Filevich,⁴ A. Källberg,² S. Mannervik,²
and K. G. Rensfelt²*

We have utilized the Heavy Ion Storage Ring at the Manne Siegbahn Institute of Physics in Stockholm, Sweden, to study the dissociative recombination (DR) of H_3^+ , i.e., $H_3^+ + e \rightarrow H_2 + H$ or $H + H + H$. Aside from fundamental interest in this reaction, the rate is of great interest for astrophysics. The molecular ion has been identified in the Jovian atmosphere and in interstellar clouds. Through its ability to protonate carbon, oxygen, and other heavy atoms, the H_3^+ molecule is thought to be the precursor of nearly a

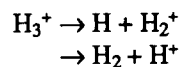
hundred interstellar molecules. For it to survive loss by dissociative recombination requires a small cross section and, in fact, calculations verify this assumption. However, numerous experiments, utilizing techniques ranging from flowing afterglows to merged electron-ion beams, indicated cross sections which were orders of magnitude higher than anticipated. Experimental results varied over three orders of magnitude, and sober assessment of results indicated uncertainties of a factor of 500.

The problem is the degree of internal excitation of the H_3^+ present as it leaves the ion source. Vibrational excitation of the H_3^+ could open a DR channel by curve crossing which would lead to an enormous rate at approximately zero kinetic energy. In interstellar space, the time between collisions is long compared to radiative lifetimes necessary to relax the H_3^+ to the $v = 0$ state. The longest-lived vibrational state has a radiative lifetime of ~ 1 sec. We utilize the

storage ring to circulate the H_3^+ long enough to reach $v = 0$, and then use the merged electron beam in the cooler to study the recombination rate.

The H_3^+ was injected into the ring at 300 keV/amu via an RFQ. The beam ($10^7 - 10^8$ ions) was accelerated to a full energy of 12 MeV/amu. Flat-top was reached in 2 seconds. The beam half-life for destruction by residual gas collision was ~ 2 sec, but this was no problem. In fact, it was necessary to wait for eight seconds before making a measurement because of pileup in the detector. During this time, the beam was "cooled" by the electron beam set at zero relative energy (cooling time was $\sim 1-2$ sec). The electron beam energy was then switched to desired relative collision energy for 0.5 sec, back to zero for 1 sec. The cycle was repeated three times for each beam dump. The ring was filled four times a minute. The reason for the cycling was to avoid "drag" of the beam energy by the electron beam.

The signal was detected by a solid state surface barrier detector placed beyond the first dipole directly in line with the electron cooler leg so that only neutral fragments would strike it. Collisions of the H_3^+ with residual gas molecules ($p = 5 \times 10^{-11}$ Torr) yield neutral fragments:



which give pulse heights of one-third and two-thirds of the full energy, respectively. DR results in all neutral fragments which simultaneously strike the detector and give a pulse height equal to the full energy.

The results are shown in Fig. 5.9. The low-energy region from 0.002 to 0.2 eV is in reasonable agreement (a factor of two) with the latest results of Mitchell et al.,⁵ who used a single-pass merged beam with an ion trap source to store the H_3^+ for ~ 10 ms before injection. A new feature which had not been previously observed, is the bump centered at 9 eV. This can be shown to be due to vertical transitions from the $n = 0$ state of H_3^+ onto a repulsive portion of the H_3 potential. The presence of H_3^+ in states $n > 0$ is precluded by the shape and position of this feature. The cross section in the low energy region, although lower than many previous reports, remains high compared to expectations based on astrophysical observation.

1. Royal Institute of Technology, Stockholm, Sweden.

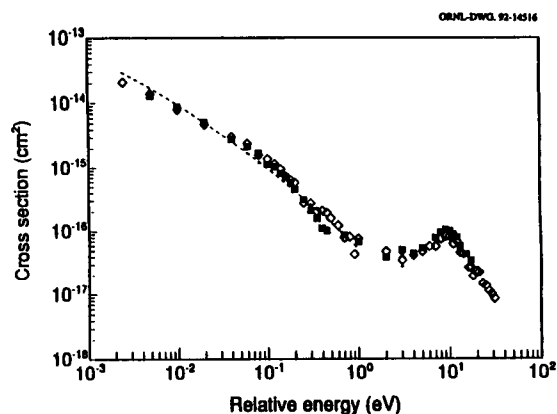


Fig. 5.9. Cross section for dissociative recombination of H_3^+ versus relative energy: open squares - electron beam faster than the ion beam; closed squares - electron beam slower than the ion beam.

2. Manne Siegbahn Institute of Physics, Stockholm, Sweden.

3. North Carolina State University, Raleigh, North Carolina.

4. CNPA, TANDAR, 1429 Buenos Aires, Argentina.

5. J. B. A. Mitchell, *Phys. Rep.* **186**, 215 (1990).

POSSIBLE TWO-ELECTRON EXCITATION IN C^{3+} FOLLOWING 1 MeV/u COLLISIONS WITH ATOMIC TARGETS: $Z = 2, 10, 18, \text{ AND } 36$

*D. F. Deveney,¹ Q. C. Kessel,¹ R. J. Fuller,¹
M. P. Reaves,¹ S. Shafrath,² and N. L. Jones*

The projectile Auger-electron spectra following collisions of Li-like carbon projectile ions with single He-atom targets provides unique information on the ion-atom many-body collision interaction. The identification of Auger peaks in the emitted electron spectra with intermediate-autoionizing (AI) configurations of the projectile states formed by the collision can help to decipher the role which specific individual interactions play. Possible interactions are: The projectile electron with the target electron (electron-electron or e-e) interaction, the projectile electron with the target nucleus (electron-nucleus or e-n) interaction, the projectile nucleus with the target electron (nucleus-electron or n-e) interaction, and various combinations thereof. For fast collisions in the impulse approximation, target electrons can be viewed as "quasi-free," and one possible n-e interac-

tion is the capture of a target electron onto the projectile ion. Combining this capture in various combinations with the aforementioned interactions can result in resonant, nonresonant, and uncorrelated capture channels and processes such as: resonant transfer and excitation (RTE), nonresonant transfer excitation (NTE) and uncorrelated transfer and excitation (UTE) such as 2eTE, which is uncorrelated two-electron transfer and excitation.³⁻⁶

In this work, we investigate the Auger electron spectra of C^{3+} following collisions with different Z atomic targets at 1 MeV/u. The investigation focuses on the relative intensities of Auger peaks between 220 and 260 eV (projectile frame) in going from collisions with He, Ne, and Ar to Kr targets.

The experiment was performed using 12 MeV C^{3+} beams from the EN Tandem accelerator. Electrons emitted at 10° in the laboratory frame entered a parallel-plate, double-pass electron spectrometer that was designed and constructed by Giese and Bechthold⁷ and was based on the Swenson design.⁸ Figure 5.10 shows an entire, typical, Auger electron spectrum obtained in this case from the collision of C^{3+} with Kr. In Fig. 5.11, spectra from all four targets are plotted after being normalized in each individual case to the beam-current integration and target gas pressure.

The three prominent peaks that appear in the He target spectra of Fig. 5.11 are the peaks that were used to energy calibrate the spectrometer. These peaks, the $1s2s^2(^2S)$, $\{1s(2s2p)^3P\}^2P$, and $\{1s(2s2p)^1P\}^2P$, are singly excited states that can relax nonradiatively

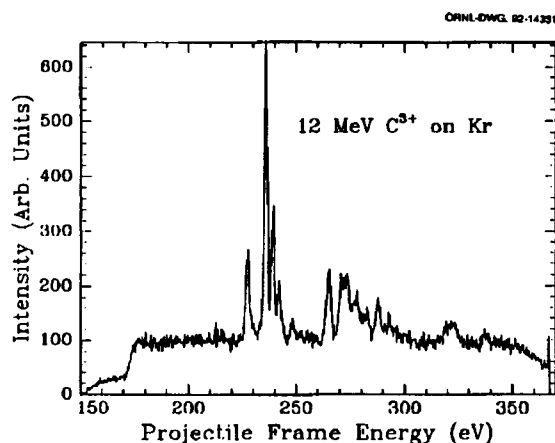


Fig. 5.10. Auger electron spectrum obtained at 10° (laboratory frame of reference) for 12 MeV C^{3+} on Kr collisions.

to the $\{1s^2(^1S) + e_c \ell_c\}^2L$ ground state (g.s.) resulting in Auger electron energies of 227.5, 235.9, and 339.3 eV, respectively.⁹⁻¹¹ The formation of these three AI states are the result of ion-atom interactions that can include single 1s projectile excitation by either the target nucleus (e-n) or the target electron (e-e) or possibly even a more intricate process where a projectile electron is ionized, again by the target nucleus or by a target electron, followed by a capture of a target electron to the projectile (n-e). The solid line in Fig. 5.12 is a simulation of the three singly excited doublets, using Auger transition rates of the excited AI state to the g.s., calculated from an atomic struc-

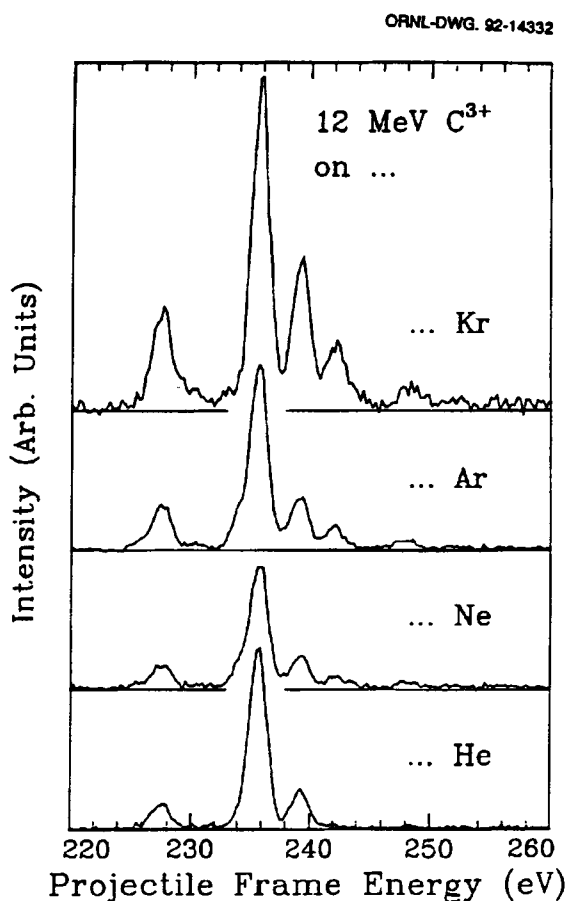


Fig. 5.11. The 220 to 260 eV energy region of the projectile Auger electron spectra for collisions with He, Ne, Ar, and Kr targets. Beginning with Ne targets, the two Auger peaks at 242.1 and 248.3 eV are apparent. These two Auger peaks are consistent with the decay to ground state of the doubly excited AI configurations $\{1s(2p^2)^1D\}^2D$ and $\{1s(2p^2)^1S\}^2S$, respectively.

ture code by Cowan¹² and fit to Gaussian line shapes with 2 eV FWHM for comparison with the data.

In the Auger electron spectra of higher Z targets, also shown in Fig. 5.11, two peaks at 242.1 and 248.3 eV appear. Beginning with Ne targets, the two peaks first appear and increase in intensity with Ar and Kr targets. The first singly excited AI configuration after the (1s2s2p) configuration is (1s2s3s), which relaxes to the g.s. with an Auger electron of energy ~270 eV. However, the terms of the first doubly excited configuration of C³⁺ 1s2p², ²D, and ²S relax to the g.s. with Auger electron energies¹³ that agree well with those observed in the experiment. In Fig. 5.12, the calculated transition rates for the ²D and the ²S are shown by the dashed line (reduced by a factor of ten).

Neither resonant or nonresonant interactions are likely to lead to the AI configurations discussed above. A resonance between a target He electron and the carbon projectile for an Auger electron of roughly 240 eV will occur at roughly 5.3 MeV beam energy. Owing to the spread of the resonance due to the Compton profile of the target, it might extend to 12 MeV, but it will not be significant. Nonresonant processes involving the capture of target electrons by the projectile nucleus will also be insignificant at this beam energy.

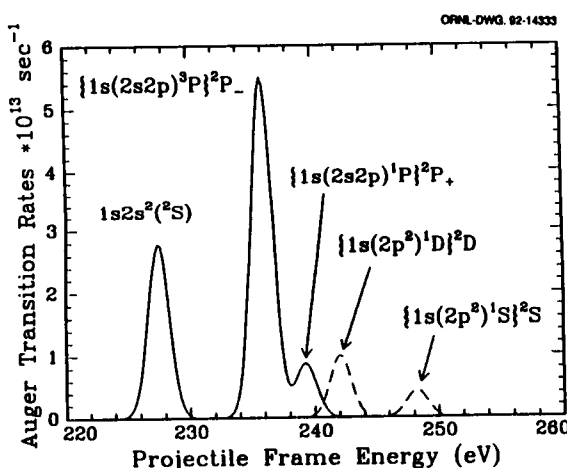


Fig. 5.12. Simulated Auger electron spectrum from singly (solid line) and doubly excited (dashed line) AI configurations of the C³⁺ projectile. The Auger electron transition rates were calculated using the atomic structure code by Cowan,¹² and the energies were taken from Refs. 9 and 13.

Direct excitation mechanisms such as e-e and e-n, however, can be significant. The beam energy thresholds for C³⁺ 1s to 2p, e-e, and e-n excitations are 7.1 MeV and 324 eV, respectively, so that at 12 MeV both e-e and e-n interactions may be involved.

As a function of the target Z, it is expected that the increased number of target electrons will influence the screening and effective Z' of the target so that e-n becomes a more complicated function of the impact parameter. The e-e excitation will also be more complex. It is unclear, however, to what degree these effects, and possibly others, have for the Ne, Ar, and Kr targets where the doubly excited states are formed with intensities approaching those of the singly excited states.

1. Department of Physics, University of Connecticut, Storrs, Connecticut.

2. Department of Physics, University of North Carolina, Chapel Hill, North Carolina.

3. D. Brandt, *Phys. Rev. A* **27**, 1314 (1983).

4. A. Tanis, *Nucl. Instr. Meth. Phys. Res. A* **262**, 52 (1987).

5. See for example the review articles in the section Symposium of Correlated Transfer/Excitation and Autoionization from the XVI International Conference on the Physics of Electronic and Atomic Collisions. Editors: A. Dalgarno, R. S. Freund, P. M. Koch, M. S. Lubell and T. B. Lucatorto, (New York, New York 1989)

6. U. Y. Hahn, *Phys. Rev. A* **40**, 2950 (1989).

7. J. P. Giese and U. Bechthold, private communication.

8. J. K. Swenson, *Nucl. Instr. Meth. Phys. Res. B* **10/11**, 899 (1985).

9. N. Stolterfoht, *Phys. Rep.* **146**, 315 (1987).

10. S. M. Shafroth et al., *Nucl. Instr. Meth. Phys. Res. B* **56/57**, 129 (1991).

11. S. M. Shafroth et al., Astracts, Seventeenth International Conference on the Physics of Electronic and Atomic Collisions, Brisbane, Australia, 1991, edited by I. E. McCarthy, W. R. MacGillivray and M. C. Standage (Griffith University).

12. R. D. Cowan, "The Theory of Atomic Structure and Spectra" (The University of California Press, 1985).

13. R. Bruch, K. T. Chung, W. L. Luken, and J. C. Culbertson, *Phys. Rev. A* **31**, 310 (1985).

ANGULAR DISTRIBUTION OF CHARGE-EXCHANGE COLLISIONS AT VERY LOW ENERGIES

*N. Keller,¹ R. D. Miller,¹ M. Westerlind,¹
L. R. Andersson,¹ S. B. Elston,² I. A. Sellin,²
and C. Biedermann³*

The investigation of collisions between highly charged ions and atoms at very low energies (eV/u range) has become a very active research field over the last decade. Differential and total cross sections for charge exchange are, for example, important in such areas as fusion research and astrophysical model calculations.

While many measurements in the past were performed using heavy, multi-electron projectiles and targets, only a few experiments investigated less complex collision systems. One particular interesting case is the collision system $C^{4+} \rightarrow He$. In the 1970s, it was found that at collision energies below 20 keV double-electron capture occurs more frequently than single-electron capture.⁴ In fact, at the lowest recorded energy (500 eV), the cross sections are over a magnitude apart.⁵

We present here experimental results for the $C^{4+} \rightarrow He$ collision system at energies below 1 keV. At lower energies, rainbow and other interference patterns in the angular differential cross sections become more resolvable, thus allowing one to extract detailed information about the potentials and interaction dynamics.

A high-energy ion beam (30-MeV Cl^{5+}) from the EN Tandem Van de Graaff Accelerator at the Oak Ridge National Laboratory collides with a methane gas target in order to produce highly charged recoil ions. These ions are extracted out of the production gas cell by an electric field. The strength of the field determines the secondary projectile ion energy. After further acceleration, they pass through a Wien filter for charge and mass analysis, and are then decelerated back to their initial energy. The selected ions, in our case C^{4+} , are then directed onto a He gas jet. The charge-exchanged C^{2+} ions are energy analyzed by a 63° cylindrical electrostatic analyzer to determine their energy gain values. A multi-channelplate with a resistive anode mounted downstream of the analyzer is used as a detecting device.

While the energy gain is recorded in the plane of dispersion, the scattering angle can simultaneously be monitored in the perpendicular direction. Because of the two-dimensional recording, angular plots cor-

responding to different energy gain values can be chosen in the analyzing procedure.

Figure 5.13 shows an energy-gain spectra for double-electron capture taken at a collision energy of 800 eV. The corresponding angular region covers angles between 0° and 2°. The energy-gain peak is centered around $\Delta E \approx 30$ eV, indicating that the two electrons are captured into the ground state of C^{2+} ($1s^2 2s^2$). The Q value of this collision process is 33.4 eV.

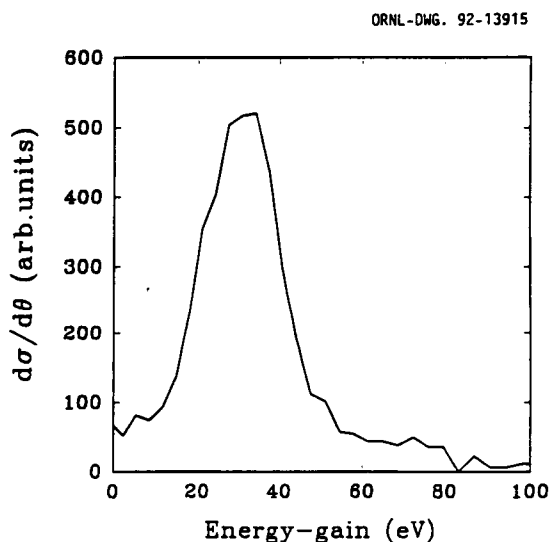


Fig. 5.13. Energy-gain spectra for double-electron capture within projectile scattering angles of 0° and 2° in 800 eV $C^{4+} \rightarrow He$ collisions.

The measured energy-gain value is in accordance with earlier investigations by other authors.⁶ Because of a rather moderate energy resolution of our analyzer ($\Delta E/E \approx 2\%$), we are not able to resolve any oscillation towards lower energy-gain values in the spectrum as observed by Cederquist et al.⁶ In Fig. 5.14, the angular differential cross sections are shown for the three recorded energies 400, 600, and 800 eV. The corresponding window in the energy-gain spectrum was chosen to fully cover the main double-capture peak. The angular distributions show an oscillatory pattern with the strongest peak situated at scattering angles around 2°. These oscillations have been explained as a Stueckelberg interference pattern.^{7,8} The frequency of the Stueckelberg oscillations, which can be expressed as the areas between the branches of the classical deflection function, is usu-

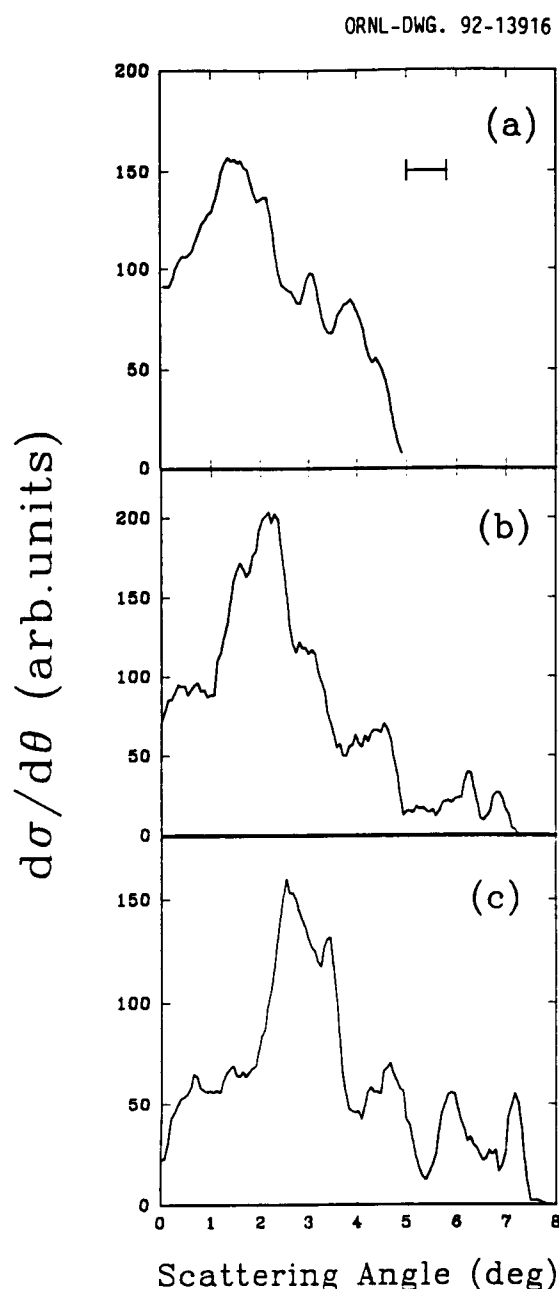


Fig. 5.14. Angular distributions for double-electron capture in $C^{4+} \rightarrow He$ collisions at 800 (a), 600 (b), and 400 eV (c). The horizontal bar in part (a) marks the FWHM of the incident C^{4+} beam.

ally too high to be observable in any experimental setup. The present collision system $C^{4+} \rightarrow He$, however, is one of the few cases where the resolution of the oscillatory patterns is in reach. Angular differential cross sections for double-electron capture in

$C^{4+} \rightarrow He$ collisions have been measured by Cocke et al.⁹ and Barat et al.¹⁰ for collision energies at 1.5 keV and 9.6 keV, respectively. A comparison between the angular distributions of Cocke et al. at 1.5 keV and our highest recorded energy (800 eV) shows an approximate scaling behavior. At 800 eV, the strongest peak is situated at $\theta \approx 2^\circ$, the other maxima can be seen at angles 3° , 4° , and 4.5° . Further maxima at larger angles could not be observed since the upper limit of our angular acceptance is $\pm 8^\circ$. Assuming a scaling behavior such that the angular differential distribution remains essentially unchanged if plotted against the reduced angle $\tau = E\theta$, we note a correspondence between the 2° peak at 800 eV and the 1° peak at 1.5 keV. This correspondence is also observed for the secondary maxima. It is, however, not quite as perfect as for the strongest peak. It should also be noted that the assumed scaling behavior does not transform itself further down to the two other recorded energies of 400 eV and 600 eV. For example, the main peak at 800 eV is located at 2° . In the angular distribution for 400 eV, it has not shifted to 4° , but rather to angles around 3° . A similar behavior can be observed for the secondary structures (3° , 4° , and 4.5° at 800 eV; 4.7° , 5.9° , and 7.3° at 400 eV). This deviation from a true scaling behavior is not too surprising. For it to be valid, it is assumed that the incoming interaction potential can be approximated in first order by a flat curve. This is no longer the case for low-energy collisions where such effects as polarization and core-penetration become important.

1. Department of Physics, University of Tennessee, Knoxville.
2. Adjunct staff member from the Department of Physics, University of Tennessee, Knoxville.
3. Manne Siegbahn Institute of Physics, Stockholm, Sweden.
4. J. Goldhar, R. Mariella, Jr., and A. Javan, *Appl. Phys. Lett.* **29**, 96 (1976).
5. H. J. Zwally and D. W. Koopman, *Phys. Rev. A* **2**, 1851 (1970).
6. H. Cederquist et al., *J. Phys. B* **18**, 3951 (1985).
7. H. Danared and A. Bárány, *J. Phys. B* **19**, 3109 (1986).
8. A. Bárány et al., *J. Phys. B* **19**, L427 (1986).
9. C. L. Cocke et al., *Nucl. Instrum. Meth. Phys. Res.* **B24/25**, 97 (1987).
10. M. Barat et al., *J. Phys. B* **23**, 2811 (1990).

DESIGN AND PERFORMANCE OF A NOVEL POSITION-SENSITIVE ELECTRON SPECTROMETER

*R. D. Miller,¹ N. Keller,¹ L. Liljeby,² I. A. Sellin,³
and M. Westerlind¹*

A spherical electrostatic spectrometer has been designed, via computer simulation, and constructed to be used in the angular- and energy-distribution measurements of electrons arising from ion-atom or photon-atom collisions. Several novel features have been incorporated in the design of the spectrometer which enable the simultaneous collection of all angles in a scattering plane (defined as the plane perpendicular to that containing the projectile beam axis and the spectrometer symmetry axis) with an angular resolution (detector pixel size limited) of $\approx 2.5^\circ$ (can be improved to $\approx 0.6^\circ$) and the collection of $\approx 1.5\%$ of the analyzer pass energy with a resolution of $\approx 0.5\%$. A gas jet is employed with the source volume being ≈ 0.5 mm³. Electrons are detected by a position-sensitive detector (PSD) while a time-of-flight (TOF) detector allows for the charge state determination of the ionized target atom. Further computer simulations and initial tests of the spectrometer are presently being performed.

1. Department of Physics, University of Tennessee, Knoxville.

2. Manne Siegbahn Institute of Physics, Stockholm, Sweden.

3. Adjunct staff member from the Department of Physics, University of Tennessee, Knoxville.

COINCIDENT DETECTION OF ELECTRONS EJECTED IN LARGE ANGLES AND TARGET RECOIL IONS PRODUCED IN MULTIPLY IONIZING COLLISIONS FOR THE 1 MeV/u O^{q+} + Ar COLLISION SYSTEM

*C. C. Gaither,¹ M. Breinig,² J. W. Berryman,¹
B. F. Hasson,¹ and J. D. Richards¹*

A specific problem of recent theoretical and experimental interest in the field of ion-atom collision physics is the determination of the energy and angular distributions of electrons ejected in multiply ionizing collisions between fast heavy ions and neu-

tral noble gas targets. Theoretical studies using the n-body Classical Trajectory Monte Carlo (nCTMC) method have predicted that a substantial number of energetic electrons will be emitted at large angles, relative to the incident beam direction, in fast collisions in which multiply charged, target-recoil ions are produced.³

In our experiments, we have measured the angular distributions of electrons ejected from the target into an angular region from approximately 45° to 135° , relative to the incident beam direction, in multiply ionizing collisions between 1 MeV/u O^{q+} (q = 4, 7) projectiles and Ar gas targets. These measurements have been performed for electrons with energies of 179 eV, 345 eV, and 505 eV. The angular distributions have been measured in coincidence with target Ar recoil ions of charge state 4+ or greater, 3+, and 2+. Additionally, measurements of the energy distributions of electrons ejected into specific angular regions have been performed.

Ion beams of 1 MeV/u O^{q+} (q = 4, 7) from the ORNL EN Tandem Van de Graaff Accelerator interact with Ar gas targets. Electrons ejected between $\sim 45^\circ$ and $\sim 135^\circ$ in the laboratory frame, relative to the incident beam direction, are energy analyzed by a cylindrical mirror electrostatic electron energy analyzer (CMA), and the ejection angles of the energy-analyzed electrons are recorded with a two-dimensional position-sensitive detector. The recoil ions resulting from the ion-atom collisions are extracted by a small electric field of approximately 6 V/cm and directed into a time-of-flight (TOF) recoil-ion spectrometer.

Argon LMM satellite Auger electrons appear as a peak in the energy spectrum of electrons ejected at all large angles. The center of this peak is found at an electron energy of ≈ 179 eV. Electrons of 179 eV energy, ejected at large angles, are preferentially produced in coincidence with recoil ions of charge state 4+. Electrons of 345 eV energy and 505 eV energy ejected at large angles are preferentially produced in coincidence with recoil ions of charge state 3+. The angular distributions for these electrons are strongly peaked in the forward direction; essentially no electrons are observed at angles larger than 90° .

Absolute cross sections for ejecting electrons into specific angular ranges, in coincidence with recoil ions of charge state 4+ or greater, are presented in Fig. 5.15 for the O⁴⁺ + Ar collision system. Qualitatively, the angular distributions of electrons ejected at large angles for the O⁷⁺ + Ar collision system are similar.

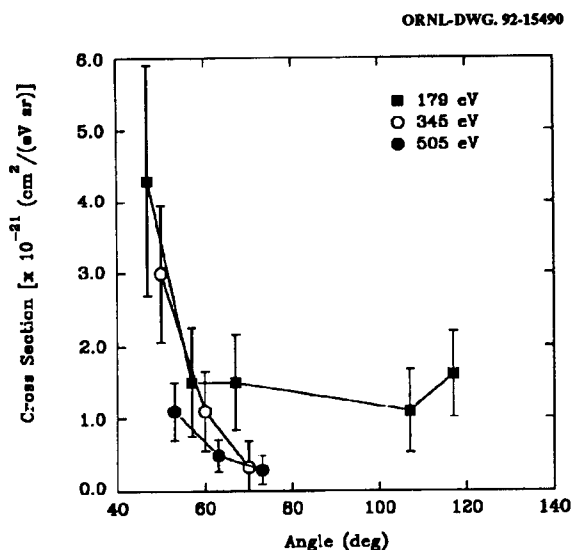


Fig. 5.15. Cross section for producing 179 eV, 345 eV, and 505 eV electrons in coincidence with recoil ions of charge state 4+ or greater for the $O^{4+} + Ar$ collision systems.

The data for both collision systems are consistent with projectile- and target-electron binary-encounter processes being the dominant large-angle electron production mechanism. We find no evidence of energetic electrons being ejected at large angles by mechanisms other than Auger and binary-encounter-type processes.

1. Department of Physics, University of Tennessee, Knoxville.
2. Adjunct staff member from the Department of Physics, University of Tennessee, Knoxville.
3. R. E. Olson, J. Ullrich, and H. Schmidt-Böcking, *Phys. Rev. A* **39**, 5572 (1989).

PHOTODETACHMENT STUDIES OF FEW-ELECTRON ATOMIC NEGATIVE IONS

*D. J. Pegg,¹ J. Dellwo,² C. Y. Tang,³
and G. D. Alton*

Energy- and angular-resolved spectroscopic measurements have been made on electrons detached from few-electron negative ions, such as Li^- , Be^- , and B^- . Energies, yields, and angular distributions of the ejected photoelectrons were measured using a crossed

laser-negative ion beam apparatus. Electron affinities, asymmetry parameters, and photodetachment cross sections were determined from these measured quantities.

A detailed investigation of the saturation characteristics of the photodetachment of Li^- and D^- ions was made in order to determine the range of laser powers over which the photoelectron yields are approximately proportional to the photon fluxes (see Fig. 5.16). Cross section measurements were made in this unsaturated regime. Results are shown in Fig. 5.16. The cross section ratio, $\sigma(Li^-)/\sigma(D^-)$, was measured to be 1.98 ± 0.15 , 1.84 ± 0.11 , and 2.97 ± 0.28 at photon energies of 1.871, 2.077, and 2.442 eV, respectively. An absolute scale for these measurements was established by normalizing the measured ratios to theoretical $\sigma(H^-)$ cross sections, which are known to better than 3%. The measured absolute cross sections, $\sigma(Li^-)$, then become 73.5 ± 6.0 , 63.5 ± 5.7 , and 89.8 ± 9.5 Mb. As a check, we have used the fitted saturation curves shown in Fig. 5.16 to extract an apparent cross section ratio at each laser power, and then extrapolated the ratio data to zero laser power. This produced a result of 1.86 at 2.077 eV, which is consistent with the value of 1.84 ± 0.11 obtained in the unsaturated regime. We have begun measuring the cross section ratios, $\sigma(B^-)/\sigma(Li^-)$ and $\sigma(Be^-)/\sigma(D^-)$. Early results are encouraging.

Preliminary measurements of the angular distribution of photoelectrons associated with the degenerate channels: $h\nu + Be^-(2s2p^2^4P) \rightarrow Be(2s2p^3P) + e^-(\epsilon s, d)$ and the electron affinity of the metastable

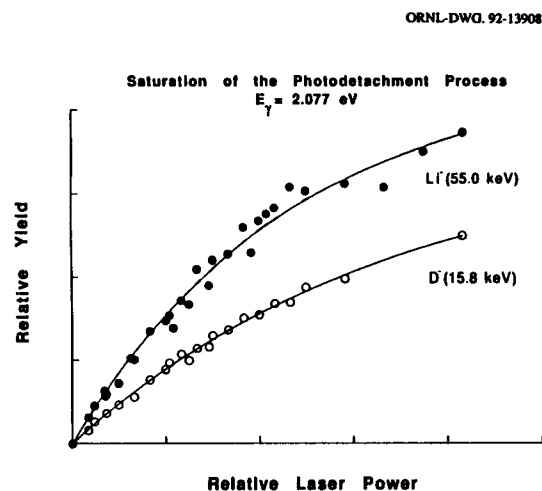


Fig. 5.16. Saturation curves for Li^- and D^- photodetachment.

Be(2^3P) atom have been made. Data are shown in Figs. 5.17 and 5.18. At a photon energy of 2.076 eV, the asymmetry parameter has a measured value of $\beta = 0.41 \pm 0.04$. The spectral data in Fig. 5.18 shows the peak associated with the photodetachment of the metastable Be $^-$ ion referenced to similar peaks associated with the photodetachment of the metastable He $^-$ ion. The latter peaks allows one to accurately

determine, in situ, the ion beam energy which is required in the frame transformation. The preliminary Be electron affinity result is 264 ± 13 meV.

1. Adjunct staff member from the Department of Physics, University of Tennessee, Knoxville.
2. Graduate student from the Department of Physics, University of Tennessee, Knoxville.
3. Postdoctoral Research Associate, University of Tennessee, Knoxville.

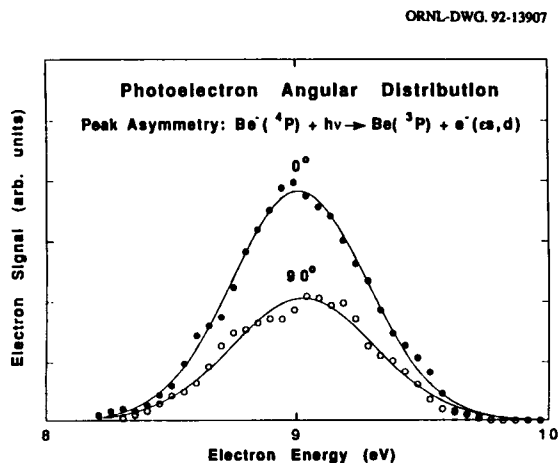


Fig. 5.17. Photodetachment of Be $^-$: photoelectron yields for horizontal (upper) and vertical (lower laser) polarization.

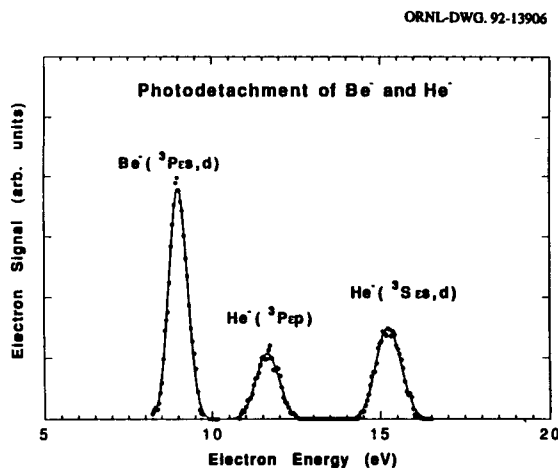


Fig. 5.18. Photodetachment electron spectra of Be $^-$ and He $^-$ ions. Photon energy of 2.076 eV and ion beam energy of 45.46 keV.

EN TANDEM OPERATIONS

P. F. Dittner and N. L. Jones

During the past year, the EN Tandem operated for 1450 hours in support of the accelerator-based atomic physics program. Operation was between 0.46 and 7.21 MV on the terminal, accelerating beams of ions from hydrogen through silver. In March, work was completed on the new column voltage gradient system. This upgrade has resulted in less variation in gradient, better spark protection of the resistors, more fault tolerant resistors, easier testing and replacement, and a reduction by a factor of ten in replacement resistor price. After initial adjustments to the new system, the machine was conditioned to 6.5 MV and returned to use for experiments. Early this fall, the machine was conditioned to 7.29 MV with no sparking. The ion source cooling system was converted to air cooling utilizing Hilsch tubes. This successful conversion has eliminated the use of CFC's at this facility. A CAD workstation has been purchased for system drawing maintenance and design. Beam line vacuum systems have continued to be upgraded. A new beam line was constructed for use in channeling experiments. The facility was utilized by the ORNL Physics Division staff, researchers from other ORNL divisions, and by outside users from the University of North Carolina, Kansas State University, University of Connecticut, University of the South, University of Tennessee, University of Missouri, and foreign institutes such as the Manne Siegbahn Institute, Stockholm, Sweden, and the University of Fribourg, Switzerland.

6. ATOMIC PHYSICS IN SUPPORT OF FUSION

VERY-LOW ENERGY COLLISIONS OF MULTICHARGED IONS WITH RYDBERG ATOMS IN MERGED BEAMS

C. C. Havener, M. A. Haque,¹ and P. A. Zeijlmans van Emmichoven²

During the last year the ion-atom merged-beams apparatus has been modified to allow measurements with Rydberg H(D) atoms. For very low collision energies, electron capture from Rydberg atoms by multicharged ions is characterized by enormous cross sections, the predicted maximum being comparable to the geometric size of the Rydberg atom. When the collision velocity is greater than the orbital velocity of the Rydberg electron ($v_e = 1/n$ a.u., where n is the principal quantum number), Classical Trajectory Monte-Carlo (CTMC) calculations³ predict that the cross section scales as n^4 . For lower velocities where quantum sub-barrier transitions dominate, molecular effects of the quasi-molecule formed in the collision may be important. Indeed, recent calculations,⁴ which are based on a simple Landau-Zener model, suggest that rotational coupling between intermediate states formed in the collision results in an electron capture cross section that scales as n^5 up to n^7 , depending on the sublevel population of the initial state. We have initiated an effort to quantify these cross sections for the wide range of collision energies and charge states accessible to the ORNL ion-atom merged-beams apparatus.

A fast H(D) beam containing 0.15% in n shells between 11 and 24 is produced by collisional detachment of H^- in N_2 gas. A Rydberg field ionization stripper is used to truncate the n -shell population of the H(D)-excited states before merging with the multicharged ion beam. Measurements of the beam-beam signal as a function of the applied stripper electric field are used to infer the n -dependence of the capture cross section. Figure 6.1 shows two such measurements⁵; $O^{3+} + D$ at 321 eV/amu and $O^{5+} + D$ at 22 eV/amu. Also shown are estimates for the signal when the capture cross section is assumed to be proportional to n^3 , n^4 , or n^5 (assuming a $1/n^3$ initial

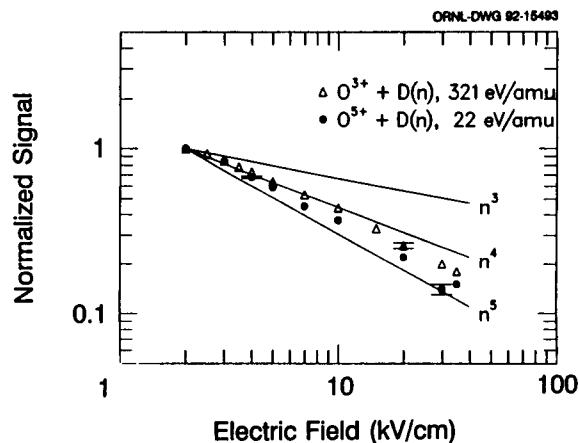


Fig. 6.1. The beam-beam signal as a function of the stripper electric field. The results are normalized at 2 kV/cm.

population of excited states for all n). As can be seen, the 321 eV/amu data suggests that the cross section generally scales as n^4 , as expected from CTMC calculations.³ Due to our experimental technique, ionization of the H Rydberg atoms by the multicharged ions, which has a weaker n -dependence, may contribute to the measured beam-beam signal at these higher collision energies, and could thereby reduce the observed scaling. The O^{5+} measurements at 22 eV/amu correspond to a velocity slightly less than v_e for the Rydberg n states considered here, and should therefore not be affected by ionization. As can be seen in the figure, the measurements show a slightly steeper n scaling for the electron capture cross section than n^4 .

Preliminary measurements have also been performed for O^{5+} at collision energies below 1 eV/amu which show even steeper n dependences, approaching the n^5 scaling recently predicted⁴ for statistically populated initial n -levels. According to the calculations, the n scaling is very dependent upon the initial state of the Rydberg atom. Indeed, scalings of up to n^7 are predicted for states with a dipole charge distri-

bution oriented along the beam axis. In the future we plan to produce Rydberg atoms via capture by H^+ in an attempt to produce such nonstatistical states.

1. ORAU/Office of Fusion Energy Historically Black Colleges and Universities Faculty Research participant.

2. University of Tennessee/Joint Institute for Heavy Ion Research; present address: Universidad del Pais Vasco, San Sebastian, Spain.

3. R. E. Olson, *J. Phys. B: Atom. Phys.* **13**, 483 (1980).

4. J. Macek and S. Y. Ovchinnikov, *Phys. Rev. Lett.* **69**, 2357 (1992).

5. C. C. Havener et al., to be published in the Proceedings of the VI International Conference on the Physics of Highly-Charged Ions, Manhattan, Kansas, Sept. 28-Oct. 2, 1992.

BACKSCATTERING IN ELECTRON-IMPACT EXCITATION OF MULTIPLY CHARGED IONS

X. Q. Guo,¹ E. W. Bell,¹ J. S. Thompson,^{1,2}
G. H. Dunn,¹ M. E. Bannister,
R. A. Phaneuf,² and A. C. H. Smith³

One of the important atomic processes occurring in fusion plasmas is the excitation of ions by electron impact, since it leads to energy loss through radiation. The radiation resulting from the subsequent radiative relaxation is often used as a spectroscopic diagnostic for such plasma. To date, electron-impact excitation cross sections have been measured for only a few ions,⁴ most of which are singly charged. Even fewer measurements exist of differential cross sections for near-threshold excitation. In the present fiscal year, we have performed measurements of absolute total cross sections for electron-impact excitation of Ar^{7+} ($3s \rightarrow 3p$) using the JILA merged-beams electron-energy-loss apparatus.⁵ The unique merged-beams configuration makes it possible to separate inelastically scattered electrons travelling forward or backward in the laboratory frame and, hence, to infer gross features of the differential scattering in the center-of-mass (CM) frame. By measuring the apparent cross sections as a function of the ion velocity (essentially, the velocity of the CM), it was found that over 90% of the inelastically scattered electrons for this system

were ejected in the backward direction in the CM frame.

The measured absolute total excitation cross section for the Ar^{7+} ($3s \rightarrow 3p$) resonant transition is plotted in Fig. 6.2. The error bars represent the total relative uncertainty at 90%-confidence level; the typical total absolute uncertainty is about 20%, indicated in Fig. 6.2 by the double error bars at the 18.62 eV point. The solid line in the figure is the result of a seven-state R-matrix close-coupling calculation⁶ after being convoluted with a 0.2 eV FWHM Gaussian representing the electron beam energy spread. The agreement between theory and experiment is quite good. However, given the experimental uncertainties, the structures in the theoretical curve calculated in the investigated energy range are not of sufficient magnitude to be resolved.

The apparent cross sections σ_{app} were measured as a function of the ion velocity at a fixed electron excitation velocity. Above the excitation threshold, the velocity of inelastically scattered electrons is the vector sum of the scattered electron velocity v_e' in the CM frame and CM velocity V_{cm} . When $V_{cm} + v_e' \cos$

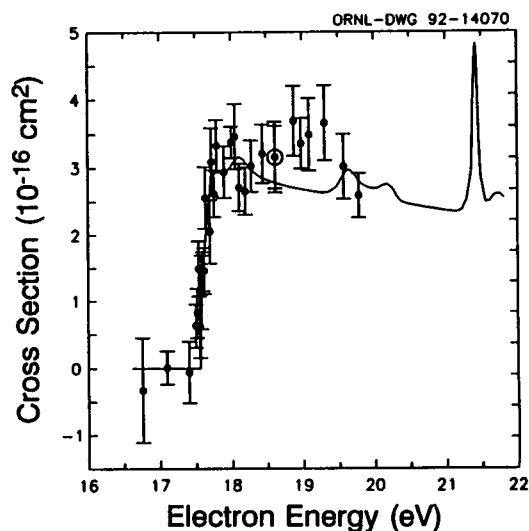


Fig. 6.2. The measured total excitation cross sections for Ar^{7+} ($3s \rightarrow 3p$). The solid curve represents a close-coupling calculation (Ref. 6) convoluted with the electron energy spread. Error bars are at 90%-confidence level.

$\theta < 0$, where θ is the electron scattering angle in the CM frame, the scattered electron velocity in the lab frame will be in the backward direction; under this condition, inelastically scattered electrons will not reach the detector. Hence, for a given set of ion and electron velocities, electrons scattered through an angle larger than a certain critical angle θ_c (defined by $V_{cm} + v_e \cos \theta_c = 0$) will travel backward in the lab frame, resulting in a reduction in σ_{app} . For a fixed electron energy in the lab frame, as the ion (or CM) velocity is reduced, v_e increases, reducing θ_c and σ_{app} . Since the actual fractional reduction in the signal also depends on the differential cross section (DCS), one can infer gross features of the structure of the DCS by measuring σ_{app} as a function of the ion velocity. Figure 6.3 shows the measured σ_{app} plotted versus the energy of the ions for an incident electron energy of 27.15 eV in the lab frame. The velocity of

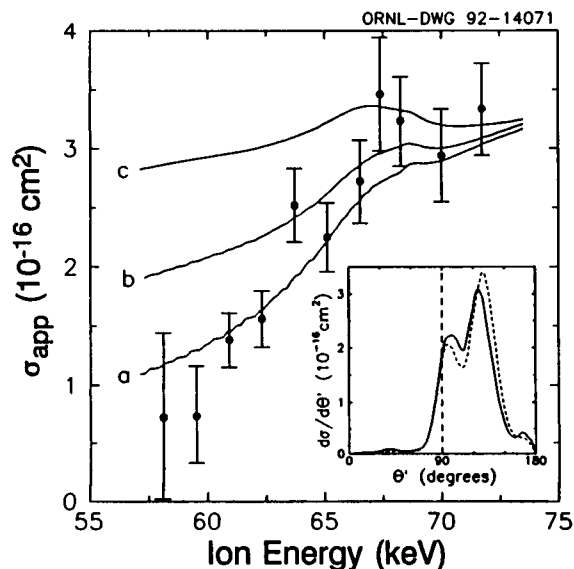


Fig. 6.3. Measured apparent cross sections as a function of laboratory ion energy and for a fixed laboratory electron energy of 27.15 eV. Error bars are shown at 90%-confidence level. Solid curves were obtained from modeling using relative differential cross sections from: (a) close-coupling calculations (Ref. 7), (b) isotropic, (c) partial-wave calculations (Ref. 8) with forward-peaked DCS. The total cross section for all three cases is as shown by the solid curve in Fig. 6.2. Inset, DCS from close-coupling (full curve, Ref. 7) and distorted-wave (dashed curve, Ref. 9) calculations.

the CM frame ranged from $(5.29 - 5.90) \times 10^5$ m/s over this ion energy range, and the corresponding range of v_e was $(2.65 - 6.1) \times 10^5$ m/s.

The solid curves in Fig. 6.3 represent modeling of the apparent cross section based on three different DCS. The modeling is the result of trajectory calculations for inelastically scattered electrons weighted by each of the three DCS in order to determine the fraction of inelastically scattered electrons that will reach the detector. This fraction is then multiplied by the appropriate total cross section (solid curve, Fig. 6.2) to obtain the apparent cross section. Only curve (a) of Fig. 6.3, which uses the close-coupling DCS (solid curve, inset of Fig. 6.3), agrees with the measured decrease of apparent cross section. Curve (b), using an isotropic DCS, and curve (c), using a forward-peaked partial-wave DCS,⁸ do not reproduce the decrease of σ_{app} with decreasing ion energy. Since neither an isotropic scattering distribution, nor anything more forward peaked comes close to describing the data, one is led to conclude that scattering is dominantly in the backward direction. Based on the comparison in Fig. 6.3, one could speculate that the DCS may be even more strongly backward peaked than the close-coupling theory predicts. Backscattering has also been recently inferred for the near-threshold excitation of O^{5+} ions.

1. Joint Institute for Laboratory Astrophysics, Boulder, CO.
2. Present address: Dept. of Physics, Univ. of Nevada, Reno, NV.
3. University College London.
4. G. H. Dunn, *Nucl. Fusion Supplement: Atomic and Plasma-Material Interaction Data for Fusion 2*, 25 (1992).
5. E. K. Wählin, J. S. Thompson, G. H. Dunn, R. A. Phaneuf, D. C. Gregory, and A. C. H. Smith, *Phys. Rev. Lett.* **66**, 157 (1991).
6. N. R. Badnell, M. S. Pindzola, and D. C. Griffin, *Phys. Rev. A* **43**, 2250 (1991).
7. D. C. Griffin, N. R. Badnell, and M. S. Pindzola (private communication).
8. Peaked at $\theta=0^\circ$, half height at $\theta=34^\circ$ resulting from a partial wave construction including partial waves only up to $l=2$; C. Bottcher (private communication).
9. R. E. H. Clark (private communication).

CROSSED-BEAMS ELECTRON-IMPACT IONIZATION CROSS SECTION MEASUREMENTS OF Si^{n+} IONS

M. E. Bannister, D. C. Gregory, C. C. Havener, R. A. Phaneuf,¹ P. A. Zeijlmans van Emmichoven,² E. W. Bell,³ X. Q. Guo,³ N. Djurić,³ J. S. Thompson,^{1,3} and M. Sataka⁴

Electron collision processes involving silicon ions are important in the study of both astrophysical and laboratory plasmas. Silicon ions will be present as plasma impurities in fusion reactors using silicon-containing alloys. In addition, the lowest Si charge states (Si^+ and Si^{2+}) occur in plasmas used in the fabrication of microelectronic components.

The only electron-impact-ionization cross section measurements previously reported⁵ were for Na-like Si^{3+} . The present work involves the measurement of cross sections for Si^+ , Si^{2+} , Si^{4+} , Si^{5+} , Si^{6+} , and Si^{7+} . These absolute cross section measurements utilized the ORNL ECR ion source and the ORNL electron-ion crossed-beams apparatus. The results and discussion of the data can be readily divided into two parts, with the measurements for Si^+ and Si^{2+} forming one group, and those for Si^{4+} through Si^{7+} the other. General features of the cross sections for each group will be noted, and one example from each group will be discussed in some detail.

The cross section data for electron-impact ionization of Si^{2+} ($1s^2 2s^2 2p^6 3s^2$) are plotted in Fig. 6.4 along with a distorted-wave (DW) calculation⁶ (solid curve) for ionization of ground state ($3s^2 \ ^1S$) Si^{2+} ions. The DW results were calculated in the average configuration approximation and include contributions from direct ionization of the 3s electrons (dashed curve) as well as $2p \rightarrow 3l$ and $2p \rightarrow 4l$ excitations leading to autoionization. The non-zero cross sections measured below the threshold for direct ionization (33.49 eV) of 3s electrons from the ground state are evidence that a significant number of Si^{2+} ions in the incident beam were in metastable states ($3s3p \ ^3P^o$). The assumption of a metastable fraction of 35-40% yields the best agreement between the data and DW calculations near the thresholds for the metastable and ground state ions. The DW calculations predict the excitation-autoionization (EA) contribution reasonably well, but seem to overestimate the contribution of direct ionization by about 10%. The ratio of the peak of the EA contribution to the peak of the direct ionization contribution is about 0.17. This is in line with other Mg-like ions⁷ (0.08 for Al^+ and

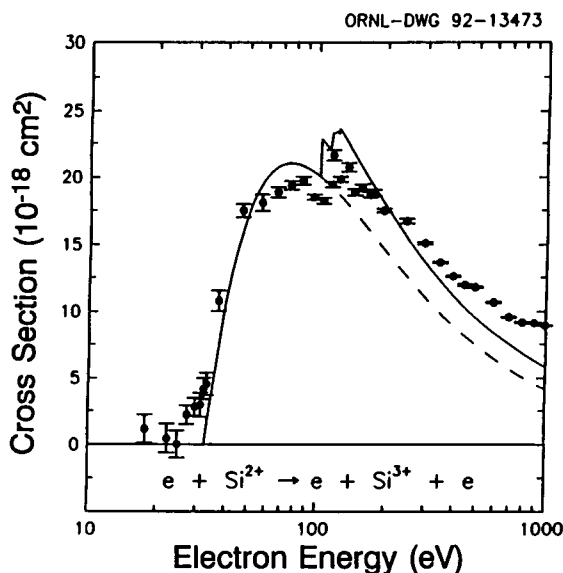


Fig. 6.4. Cross sections for electron-impact ionization of Si^{2+} . The points are the present measurements with relative uncertainties at the one standard deviation level. The solid curve is the distorted-wave (DW) calculation of Ref. 6 including excitation-autoionization (EA) of 2p electrons and direct ionization of 3s electrons. The dashed curve is the DW result for direct ionization above the EA threshold.

0.4 for S^{4+}), since we expect the ratio to increase with increasing charge state.

The measured cross sections for ionization of Si^+ ($1s^2 2s^2 2p^6 3s^2 3p$) also show a significant contribution of excitation-autoionization, and evidence of metastable ($3s3p^2 \ ^4P$) ions in the incident beam. The threshold for EA, however, essentially coincides with that for direct ionization of the 3p electron, and the EA contribution dominates the cross section near threshold. The metastable fraction in the Si^4 beam was estimated to be a maximum of 3%.

Figure 6.5 shows the measured ionization cross sections for Si^{6+} ($1s^2 2s^2 2p^4$) together with a DW calculation⁶ for direct ionization of 2p and 2s electrons of Si^{6+} . The cross section is typical of Si ions of the second group (Si^{4+} through Si^{7+}), which have an electronic configuration of $1s^2 2s^2 2p^n$ with $n=6,5,4,3$ with increasing charge. The ionization is dominated

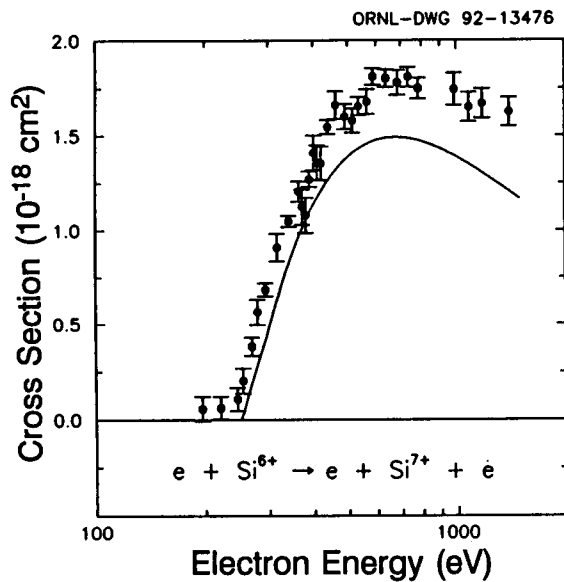


Fig. 6.5. Cross section for electron-impact ionization of Si^{6+} . The points are the present measurements with relative uncertainties at the one standard deviation level. The solid curve is the distorted-wave (DW) calculation of Ref. 6 for direct ionization of 2p and 2s electrons.

by direct processes, with little contribution from excitation-autoionization. The DW calculations underestimate the direct cross section by about 20% for this ion. The finite measured cross sections below the ground state threshold (246.5 eV) indicate a possible presence of metastable ions in the incident beam, which may account for the measured cross sections being 20% larger than the DW predictions.

The ionization cross sections for the other ions in the second group (Si^{4+} , Si^{5+} , and Si^{7+}) are very similar to that for Si^{6+} ; they are all dominated by direct ionization processes. Such behavior along an isonuclear sequence has been reported previously in publications on xenon and chromium,⁸ wherein it was noted that excitation-autoionization dominates when there are only one or two electrons in the outer subshell, and direct ionization dominates when the outer subshell is full or almost full.

In summary, absolute cross sections for electron-impact ionization of Si^{q+} ions ($q=1,2,4-7$) have been measured for the first time. The indirect processes of excitation-autoionization were found to be signifi-

cant only for Si^+ and Si^{2+} , while the ionization of Si^{4+} through Si^{7+} appeared to be dominated by direct processes.

1. Present address: Dept. of Physics, Univ. of Nevada, Reno, NV.

2. University of Tennessee/Joint Institute for Heavy Ion Research; present address: Universidad del Pais Vasco, San Sebastian, Spain.

3. Joint Institute for Laboratory Astrophysics, Boulder, CO.

4. Japan Atomic Energy Research Institute, Tokai, Japan.

5. D. H. Crandall et al., *Phys. Rev. A* **25**, 143 (1982).

6. M. S. Pindzola (private communication).

7. D. S. Belic et al., *Phys. Rev. A* **36**, 1073 (1987); A. M. Howald et al., *Phys. Rev. A* **33**, 3779 (1986).

8. D. C. Griffin et al., *Phys. Rev. A* **29**, 1729 (1984); M. Sataka et al., *Phys. Rev. A* **39**, 2397 (1989).

ANALYSIS OF LOW-ENERGY ELECTRON EMISSION ARISING DURING SLOW MULTICHARGED ION-SURFACE INTERACTIONS

P. A. Zeijlmans van Emmichoven,¹ C. C. Havener,¹ I. G. Hughes,¹ D. M. Zehner,² and F. W. Meyer

The above-surface neutralization of a slow multicharged ion of charge q proceeds via resonant neutralization, whereby q electrons from the conduction band are captured into Rydberg levels of the incident ion, leading to the creation of a multiexcited "hollow" atom. The subsequent deexcitation of such a "hollow" atom occurs via a cascade of intra-atomic Auger transitions, each step resulting in the emission of an electron. In addition to electrons arising from this Auger cascade, a significant contribution to electron production is expected due to above-surface neutralization when those electrons that have been captured into projectile Rydberg levels, but have not yet had time to deexcite, are "peeled" from the projectile as it penetrates the surface. Such peel-off electrons are expected to have energies in the range 5-15 eV. During the last year we have undertaken a search for these low energy electrons, which have so far eluded direct experimental observation in our laboratory. Measurements have been performed³ for

30-100 keV N^{2+} - N^{6+} ions incident at 20° with the surface on Cu(001) and Au(011) single crystals, for a series of observation angles. The interpretation of the spectra is complicated in that both potential and kinetic emission mechanisms contribute. The low-energy electron spectra appear to be comprised of at least two distinct components (Fig. 6.6). The first component constitutes a minor part of the overall electron emission, and appears around 15-20 eV in extreme forward angles. This "dynamic" component appears to be consistent with binary encounters between incident ions and metal electrons at the surface/vacuum interface. The second component at energies around 5-10 eV is the major contribution to the total electron yield. The intensity of this "sub-surface" component exhibits a cosine distribution, slightly skewed in the direction of the incident ion beam. This component we attribute mainly to bulk emission of target electrons with an enhanced contribution in forward angles, i.e., in the direction of motion of the incident ion. Electrons captured into Rydberg levels of the projectile which are "peeled" off as the incident ion impacts the surface would be expected to exhibit

just such a bias for emission into forward angles. We have, however, been unable to unambiguously attribute this additional component to such "peel-off" electrons, since both Auger emission close to the surface/vacuum interface and kinetic emission within the first few layers may also result in enhanced emission in forward angles.

For the 20° incidence case therefore, we were unable to find a distinct spectral feature attributable to low-energy peel-off electrons. It is possible however that the peel-off electrons are energetically indistinguishable from the kinetic emission peak and that the enhancement of kinetic emission in forward angles may be due to this component.

1. University of Tennessee/Joint Institute for Heavy Ion Research; present address: Universidad del Pais Vasco, San Sebastian, Spain.

2. Solid State Division, ORNL

3. P. A. Zeijlmans van Emmichoven et al., "Emission of Low-Energy Electrons from Multicharged Ions Interacting with Metal Surfaces," submitted to *Physical Review A*.

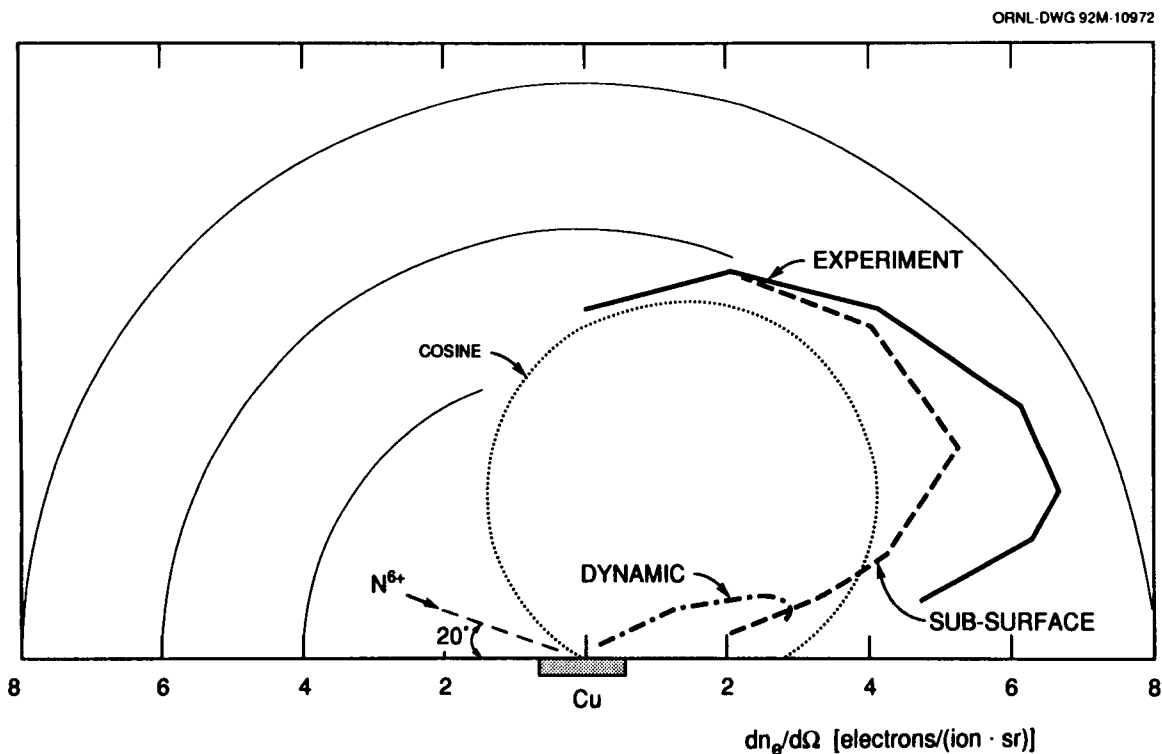


Fig. 6.6. Polar plot of the energy-integrated electron emission for 100-keV N^{6+} - Cu(001) collisions. Measured electron emission (solid line); "sub-surface" component (dashed line); "dynamic" component (dot-dashed line).

INCIDENT-ION CHARGE-STATE DEPENDENCE OF ELECTRON EMISSION DURING SLOW MULTICHARGED ION-SURFACE INTERACTIONS

*I. G. Hughes,¹ C. C. Havener, S. H. Overbury,²
M. T. Robinson,³ D. M. Zehner,³
P. A. Zeijlmans van Emmichoven,^{1,4}
and F. W. Meyer*

The total electron yield γ , defined as the average number of electrons emitted per incoming ion, arising in the interaction of multicharged ions with a metal surface may be composed of contributions from several distinct production mechanisms. Traditionally, it has been useful to define electron emission as

kinetic electron emission (KEE) or potential electron emission (PEE), depending on whether the ejected electrons are liberated by the conversion of kinetic or potential energy of the incident projectile. While KEE can occur only after the incident ion has impacted the target surface, PEE can already begin when the ion is at relatively large distances above the surface.⁵ During the past year we have carried out measurements of the total electron yield for N^{2+} , N^{5+} and N^{6+} ions in the velocity range 0.25 - 0.55 a.u. incident on a Au(011) single crystal. Characteristic variations in γ have been observed as a function of the incident azimuthal angle. These variations allow us to unambiguously separate the contributions of PEE and KEE to the total electron yield. Figure 6.7 shows our measurements of the total electron yield as a

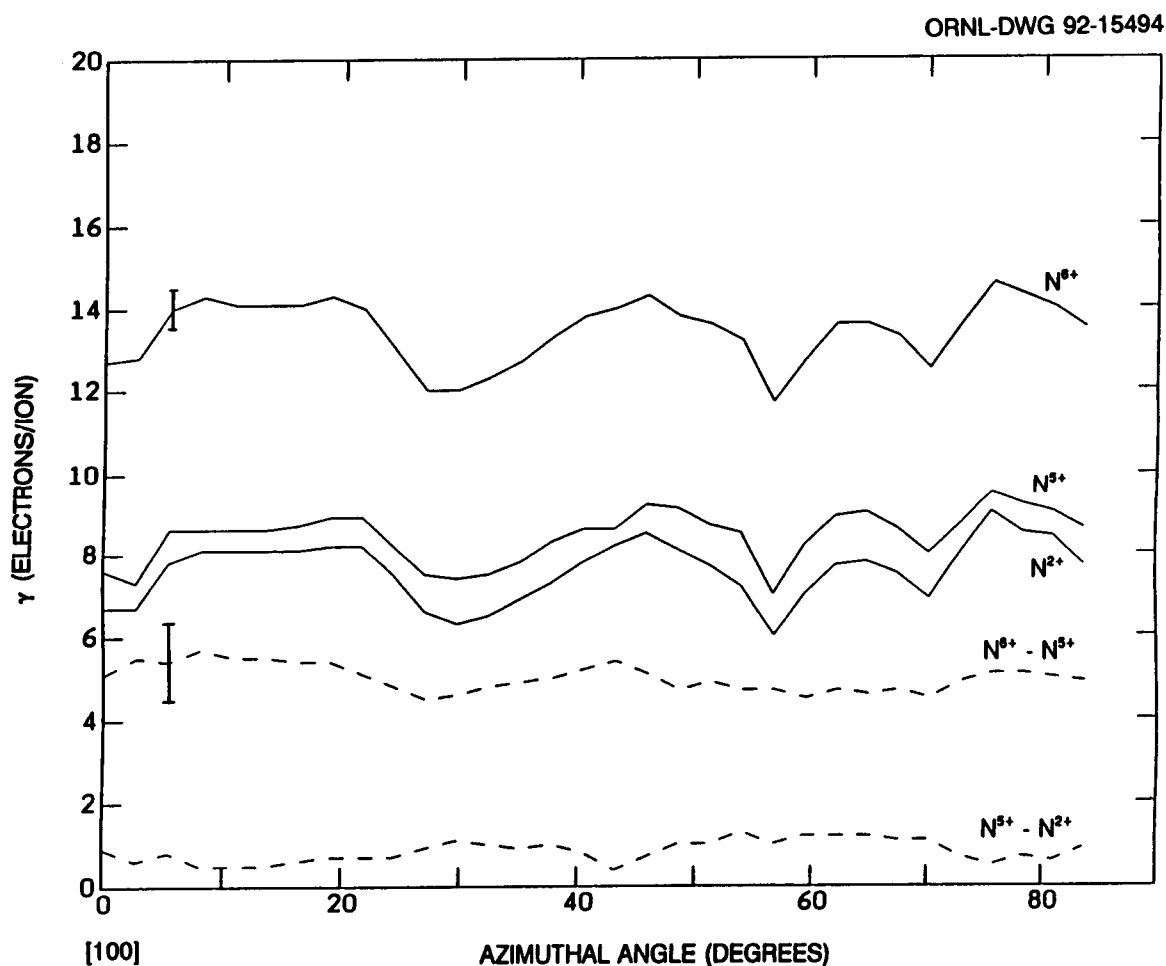


Fig. 6.7. Observed azimuthal variation in the total electron yield γ for 30 keV N^{2+} , N^{5+} , and N^{6+} ion incident at 20° along the [100] direction on a clean Au(011) single crystal.

function of the crystal azimuthal angle for 30 keV N^{2+} , N^{5+} and N^{6+} ions at 20° incidence. The amplitude of the azimuthal variations can be seen to be independent of the incident-ion charge state. The contribution to the total electron yield due to the initial ion charge state can be obtained by subtracting the spectra for N^{6+} and N^{5+} , and N^{5+} and N^{2+} incident ions, respectively. These charge state dependent contributions are also shown and can be seen to be essentially azimuthally invariant. Similar measurements of the azimuthal variations in the total electron yield were performed for 80 keV N^{5+} and N^{6+} . The amplitude of the variations was found to increase at the higher incident projectile energy. This is consistent with KEE being responsible for this component. Furthermore, the charge-state-dependent contribution at 80 keV was found to have the same magnitude as for 30 keV incident ions. This charge-state-dependent component we attribute to PEE. Using computer simulations of the projectile energy loss within the target we have been able to reproduce the observed variations. The results of our simulations are consistent with the conclusion that KEE arises predominantly in close collisions between incident ions and target atoms. In addition, the azimuthal invariance of PEE suggests that the electrons which constitute this component originate either above the target surface or within a short distance below the vacuum/surface interface. Since PEE is projectile-related emission, the emitted-electron intensity would be expected to decrease as the ion penetrates further into the target material where inelastic electron scattering becomes important. The fact that PEE is observed to be constant in the present energy regime suggests that PEE is complete within one electron inelastic mean-free-path of the surface. Assuming straight line trajectories, this indicates neutralization times of the order of 10^{-15} secs, which is consistent with previous measurements we have performed.⁶

1. Joint Institute for Heavy Ion Research, Holifield Heavy Ion Research Facility, Oak Ridge, TN 37831-6372, USA

2. ORNL Chemistry Division.

3. ORNL Solid State Division.

4. Current address: Departamento de Física de Materiales, Universidad del Pais Vasco, San Sebastián, Spain.

5. U. A. Arifov, L. M. Kishinevskii, E. S. Mukhamadiev, and E. S. Parilis, *Sov. Phys. Tech. Phys.* **18**, 118 (1973).

6. F. W. Meyer, S. H. Overbury, C. C. Havener, P. A. Zeijlmans van Emmichoven, and D. M. Zehner, *Phys. Rev. Lett.* **67**, 723 (1991); F. W. Meyer, S. H. Overbury, C. C. Havener, P. A. Zeijlmans van Emmichoven, J. Burgdörfer, and D. M. Zehner, *Phys. Rev. A* **44**, 7214 (1991).

NEUTRALIZATION OF SLOW MULTICHARGED IONS ABOVE A CESIATED AU SURFACE

*F. W. Meyer, L. Folkerts,¹ I. G. Hughes,¹
S. H. Overbury,² D. M. Zehner,³
and P. A. Zeijlmans van Emmichoven^{1,4}*

The critical distance above the surface at which conduction band electrons can start to neutralize incident multicharged projectiles by classical overbarrier transitions is inversely proportional⁵ to the metal work function. By varying the amount of Cs coverage on a Au single crystal target between 0 and 1 monolayers, we have been able to verify an up to 3.3 eV decrease of the surface work function relative to that for clean Au of 5.1 eV. This change should result in more than doubling the above-surface interaction time. At larger above-surface distances, however, the electron capture most likely occurs into higher principal quantum numbers of the projectile. The subsequent de-excitation cascade by which inner shells of the projectiles are populated may thus require more time. We have investigated the overall effect that lowering the work function has on the above-surface component of projectile K-Auger electron emission for grazing incidence N^{6+} ions interacting with a cesiated Au single crystal. In the range of incidence angles 0.3 - 1.4° , we have found that an enhancement of this component is indeed evident, and that there is significant dependence on incidence angle, as is illustrated in Fig. 6.8. The 5° incidence spectra shown in each panel is assumed to represent the peak shape obtained from sub-surface emission alone.

1. Joint Institute for Heavy Ion Research, Holifield Heavy Ion Research Facility, Oak Ridge, TN 37831-6372, USA

2. Chemistry Division, ORNL

3. Solid State Division, ORNL

4. Present address: Universidad del Pais Vasco, San Sebastian, Spain.

5. J. Burgdörfer, P. Lerner, and F. W. Meyer, *Phys. Rev.* **44**, 5674 (1991).

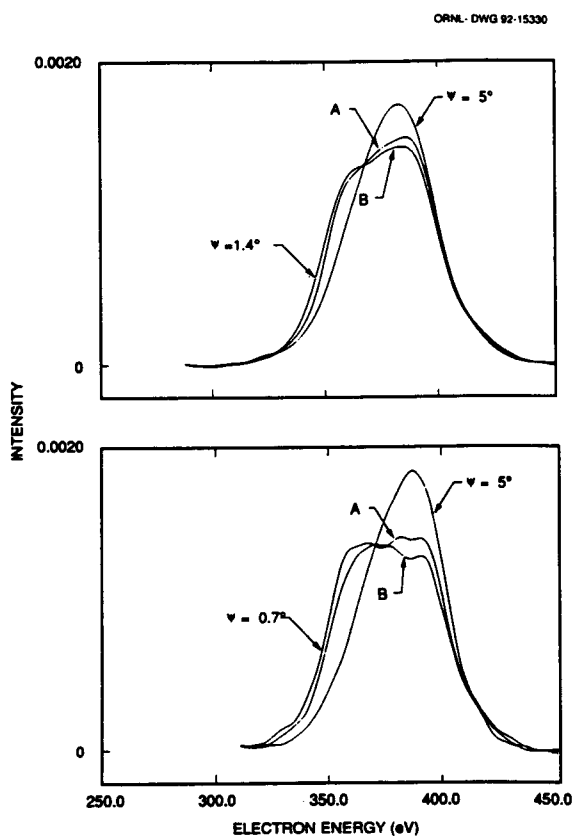
ECR SOURCE FACILITY UPGRADE
PROJECT*F. W. Meyer and J. W. Hale*

Fig. 6.8. Background subtracted N KLL Auger peaks for 60 keV N^{6+} incident on Au(011) at the indicated angles. Curves A: clean Au surface; curves B: cesiated Au surface. All peaks are normalized to the same total K-Auger electron yield of $1 e^-$ per ion.

As a part of the ORNL ECR source multicharged ion research facility upgrade project, a decision was made in early FY 1992 to purchase a CAPRICE ECR ion source from Centre Etudes Nucleaires-Grenoble, France. This ECR source will operate at the same frequency as the present ORNL ECR source, but will have significantly higher performance due to increased gradients in the radial and axial confining magnetic fields realized in this source design. Typical source performances determined during acceptance testing performed by ORNL staff at CEN-G were as follows (all for 20 kV source potential): for intermediate charge states - 500 μA of Ar^{8+} , 700 μA of N^{5+} , and 5 μA of Ta^{22+} ; and for high charge states - 5 μA of fully stripped N, 150 nA of Ar^{16+} , and 0.5 μA of Ta^{28+} . The new ECR source will be fully installed and become operational early in FY 1993.

7. THE UNISOR PROGRAM

The University Isotope Separator - Oak Ridge is a cooperative venture of universities, Oak Ridge Associated Universities, Oak Ridge National Laboratory, the U.S. Department of Energy, and the State of Tennessee. The primary purpose of the UNISOR consortium is to investigate the structures and decay mechanisms of rare, short-lived atomic nuclei which are prepared by means of a magnetic isotope separator coupled to the accelerators in the Holifield Heavy Ion Research Facility. The accounts which follow describe work at the UNISOR facility or work associated with UNISOR research performed principally by investigators outside the Physics Division. Research and development activities at UNISOR by Physics Division staff members are included in the Nuclear Physics Section.

INSTALLATION OF NMR COILS AT UNISOR/NOF

*P. F. Mantica, Jr.¹ N. J. Stone² M. L. Simpson³
J. K. Deng⁴ Y. S. Xu⁵
H. K. Carter¹ L. A. Rayburn¹ D. Shi⁴*

We have continued to implement new experimental apparatus and techniques to further research capabilities at the UNISOR Nuclear Orientation Facility (UNISOR/NOF). One such implementation is the installation of nuclear magnetic resonance (NMR) coils into the cryostat of the He dilution refrigerator, in order to increase the precision with which nuclear magnetic moment measurements can be made.

A single loop coil has been placed at the sample position using a support former, which is attached to the bottom of the 50 mK radiation shield and places the coils 1 cm from the center of the sample foil position. The coil was placed to allow the resulting resonating field, B_1 , to be perpendicular to the applied orienting field, B_{ext} . Operational tests of the coils were performed on an implanted $^{60}\text{CoFe}$ sample provided by Oxford University. Measurements were

taken by introducing modulated rf frequency to the sample foil at power levels (P) that involved a minimum level of non-resonant heating. Modulation of the rf frequency signal is required in order to affect an appreciable amount of sample nuclei, which are considered grouped in individual "spin packets," each packet requiring a different B_1 for destruction of the nuclear alignment.

The results of our tests are shown in Fig. 7.1. The destruction of anisotropy is given as the difference in the counting rates with frequency modulation (FM) on and off. For a B_{ext} of 0.3 T, the peak in the NMR spectrum was observed at 164.1 MHz for the $^{60}\text{CoFe}$ sample. This is in agreement with the previously measured results for this Co isotope impurity in a iron host, where the resonance frequency is defined by the following relation:

$$\nu = gB_{eff}/h,$$

where g is the nuclear g factor, B_{eff} is the effective magnetic field at the nucleus and h is Plank's constant. To confirm the actual observance of the resonance peak, we also measured the $^{60}\text{CoFe}$ resonance destruction at a reduced value of B_{ext} . Since the effective field is the sum of the B_{ext} and the hyperfine nuclear field B_{hf} , a reduction in B_{ext} will result in the movement of the resonance peak to a higher frequency, as the value of B_{hf} for Co in an iron lattice is -29.01 T. The resonance spectrum for $B_{ext} = 0.1$ T is also shown in Fig. 7.1, and the peak of the resonance was observed to increased to a frequency of 165.3 MHz.

Further development work on this technique is needed to allow for the detection of destruction for samples where the observed anisotropy is much less intense. This may include reduction of the coil-to-sample distance and/or reduction of the actual coil size to deliver maximum rf power to the sample.

1. UNISOR, Oak Ridge Institute for Science and Education, Oak Ridge, TN

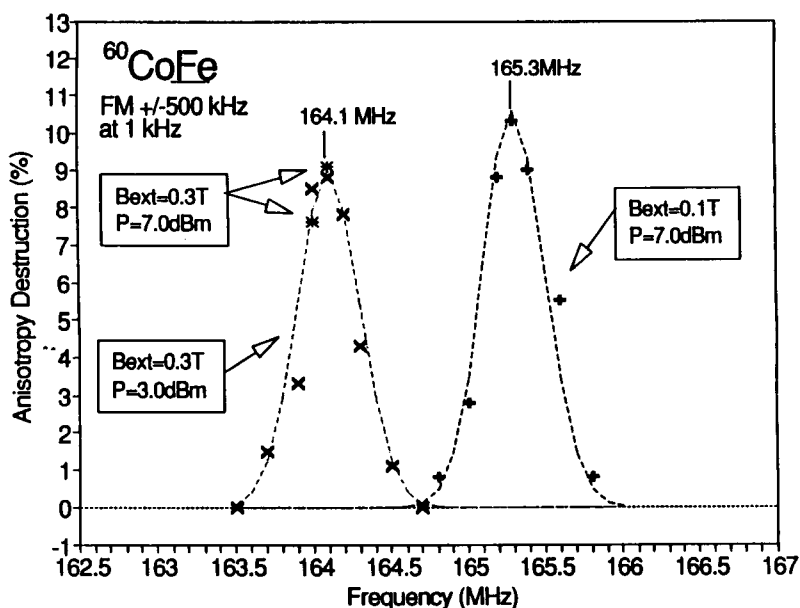


Fig. 7.1. NMR resonance spectrum for $^{60}\text{CoFe}$ taken at UNISOR/NOF.

2. Clarendon Laboratory, Oxford University, Oxford UK
3. Instrumentation & Controls Division, Oak Ridge National Laboratory, Oak Ridge, TN
4. Vanderbilt University, Nashville, TN
5. Oregon State University, Corvallis

MODIFICATION OF A β - γ PICOSECOND LIFETIME SYSTEM FOR LIFETIME MEASUREMENTS AT UNISOR

*P. K. Joshi¹ P. F. Mantica, Jr.² E. F. Zganjar¹
S. J. Robinson³ W. B. Walters⁴*

We have adapted the β - γ picosecond-lifetime system⁵ designed for neutron-rich isotopes at the TRISTAN isotope-separator facility for use on proton-rich isotopes at the UNISOR facility, where β^+ and electron capture populate states in the daughter nuclei.

The system uses a fast-slow coincidence circuit to define a triple coincidence between an initial β ray and a subsequent cascade of two γ rays. The fast

timing part consists of a thin (0.3 cm) NE-111A plastic scintillator ΔE β detector mounted on a Philips XP-2020 photomultiplier tube (PMT) and a conical BaF_2 crystal mounted on a Philips XP-2020Q PMT. The BaF_2 crystal has a thickness of 1.3 cm and upper and lower diameters of 1.9 and 2.5 cm, respectively. The energy resolution of the BaF_2 detector was measured to be 9.5% for the 662-keV transition in ^{137}Cs . For each detector, a Philips S-5632 voltage divider has been used, modified so that the dynode output signal is taken from the 9th dynode of the divider as prescribed in Ref. 5. The dynode signals are processed using Ortec 583 constant fraction discriminators, whose output is used as the start/stop signal for a time-to-pulse-height converter (TAC).

For the slow timing circuit, a Ge detector of large volume (35% efficient relative to NaI) and good energy resolution (FWHM < 2.0 keV at 1.33 MeV) is used to define the cascade sequence of interest. The timing performance of the system has been tested using a calibration source of ^{24}Na . The energy dependence of the FWHM and centroid position of the fast timing TAC peak are shown in Fig. 7.2.

The system can be readily placed on the 30° beam line of the UNISOR separator. Mass-separated samples are implanted in a moving tape, which trans-

ORNL DWG-92-15297

DEVELOPMENT OF A NEW PICOSECOND LIFETIME MEASUREMENT SYSTEM USING THE β^+ - X-RAY COINCIDENCE

P. K. Joshi¹ E. F. Zganjar¹ P. F. Mantica, Jr.²
S. J. Robinson³

A new system was developed at UNISOR to measure nuclear lifetimes in the picosecond range. This system is based on the design at TRISTAN⁴ and is a modification of the system in the previous contribution.⁵

At UNISOR, the nuclei produced are mainly proton rich and hence decay by β^+ emission and electron capture. If the excited level is fed via a β^+ decay path, the timing information is obtained by a coincidence between the β^+ and a γ -ray transition depopulating the level. However, if the level in question is 0^+ and if it depopulates only by internal conversion, as is the case for ^{186,188}Hg, then the only radiation which can be utilized as a fast trigger is the X ray which follows conversion of the $0_2^+ \rightarrow 0_1^+$ transition. Since all K X rays which originate from the internal conversion process are of the same energy, it is not possible to isolate the X rays whose origin is that particular transition. Hence, a Si(Li) detector was used to select a particular electron transition. To accomplish this, a triple coincidence was setup between the β^+ , the K conversion electrons and X rays following the K conversion. The timing information is obtained from the fast coincidence between the β^+ and the X rays, while the high resolution electron detector was used to select the transition of interest.

A Plastic scintillator, NE-411A, 1.3 cm in diameter and 0.3 cm thick coupled to a XP2020 photomultiplier tube was used to detect the β^+ particles. A BaF₂ crystal, semi-conical in shape with 2.5 cm and 1.9 cm diameters at base and top respectively, and 1.9 cm thick, was mounted on a XP2020Q photomultiplier tube to detect the X rays.

A timing resolution of 1.19 ns was achieved for the β^+ - X ray coincidence. The centroid shift method was employed to obtain the lifetime information from the TAC peaks.

We would like to thank Mark Whitley and Jim Blankenship, Physics Division, for their technical advice and material support.

1. Louisiana State University, Baton Rouge
2. UNISOR, Oak Ridge Institute for Science and Education, Oak Ridge, TN

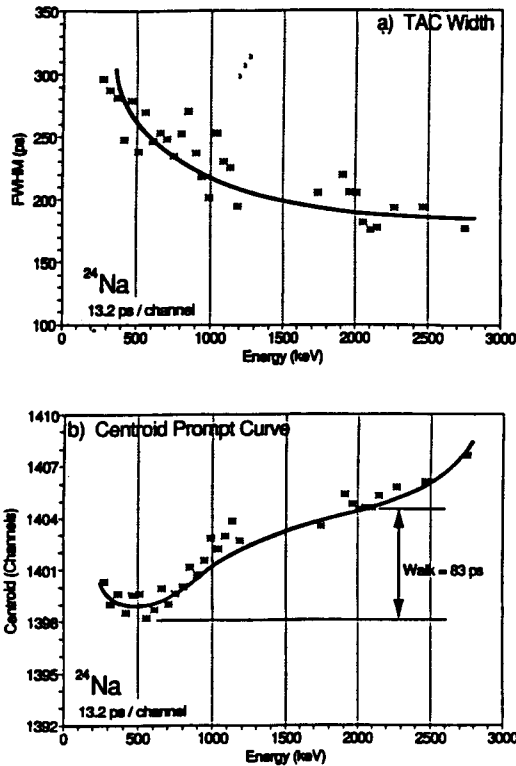


Fig. 7.2. Energy dependence of a) FWHM and b) centroid position determined for the β^+ - γ lifetime system using ²⁴Na.

ports the activity of interest to the center of the lifetime system. The sequential stepping of the tape is controlled by a LED and sensor to avoid tape slippage and variation of the sample position. The β^+ - γ lifetime system has been used successfully in the measurement of the lifetime of the first 2^+ states in ¹¹⁸Xe and ¹²⁰Xe.

We are grateful for the technical assistance provided by Jim Blankenship and Mark Whitley, Physics Division, and Ron Gill, Brookhaven National Laboratory.

1. Louisiana State University, Baton Rouge
2. UNISOR, Oak Ridge Institute for Science and Education, Oak Ridge, TN
3. Tennessee Technological University, Cookeville
4. University of Maryland, College Park
5. H. Mach *et al.*, *Nucl. Instrum. Methods Phys. Res. A* **280**, 49 (1989)

3. Tennessee Technological University, Cookeville
 4. H. Mach, R. L. Gill and M. Moszynski, *Nucl. Instrum. Methods Phys. Res. A* **280**, 49 (1989)
 5. P. K. Joshi, P. F. Mantica, Jr., E. F. Zganjar, S. J. Robinson and W. B. Walters, *current progress report*

LIFETIME MEASUREMENTS IN $^{118,120}\text{Xe}$

P. F. Mantica, Jr.¹ P. K. Joshi² S. J. Robinson³
 E. F. Zganjar² R. L. Gill⁴ W. B. Walters⁵
 D. Rupnik² H. K. Carter¹ J. Kormicki^{1,6}
 C. R. Bingham⁷

We have measured the lifetimes for levels in $^{118,120}\text{Xe}$ populated through the β^+/EC decay of $^{118,120}\text{Cs}$, respectively, using the new picosecond lifetime system at the UNISOR isotope separator. The major motivation for these new measurements was the employment of a different experimental technique to determine the lifetimes for the first 2^+ level in these nuclides, and to hopefully resolve the discrepancy in the RDDS lifetime measurements⁸ for the 2^+_1 level in ^{120}Xe .

Samples of $^{118,120}\text{Cs}$ were produced as recoils from the heavy-ion reaction between a ^{92}Mo target and a 175-MeV ^{32}S beam. Data was collected using the new UNISOR picosecond lifetime system. The system comprised a 0.3-cm thick NE-111A plastic scintillator ΔE β detector mounted on a Philips XP-2020 photomultiplier tube (PMT) and a 1.3-cm thick conical BaF_2 crystal mounted on a Philips XP-2020Q PMT for γ detection. These detectors were placed face-to-face in vertical positions relative to the beam line. Two Ge detectors were also incorporated into the system, and were placed face-to-face in horizontal positions.

Shown in Fig. 7.3 are the time-to-amplitude conversion (TAC) spectra for coincidences between β rays and the 322-keV 2^+_1 to 0^+_1 transition in ^{120}Xe , and for coincidences between β rays and the 338-keV transition in ^{118}Xe . The resulting lifetimes were determined using the centroid shift method, where the reference "prompt" TACs were constructed by gating on the region of the BaF_2 γ -ray spectrum just above the full-energy peak of interest. The use of a background gate as the reference TAC ensures that Compton events from higher energy γ rays will not influence the lifetime measurement. Since there is no dependence of the centroid position on γ -ray energy in the BaF_2 detector for the energy region from 250 to

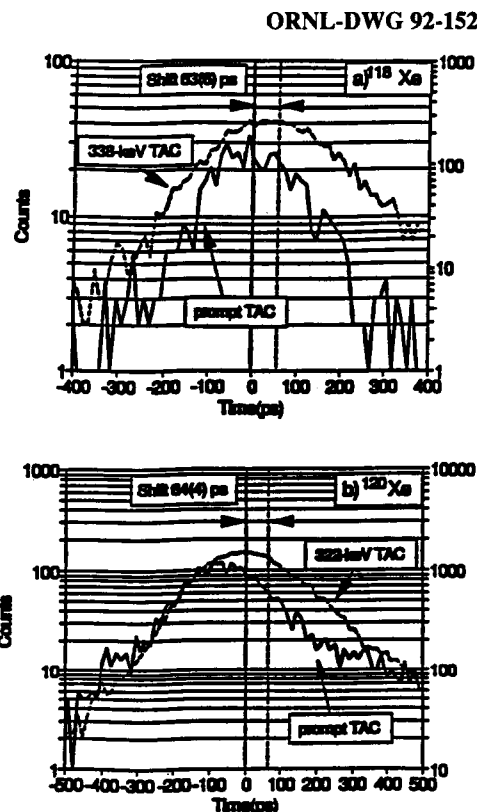


Fig. 7.3. Delayed and prompt TAC spectra for the measurement of the centroid shift for the 2^+_1 to 0^+_1 transitions in a) ^{118}Xe , and b) ^{120}Xe .

700 keV, as determined from prompt curve calibration measurements using ^{24}Na , the difference in the centroid position of the full-peak and background gates will yield directly the lifetimes of the 2^+_1 levels for $^{118,120}\text{Xe}$.

Although the result presented here for the lifetime of the 2^+_1 level in ^{118}Xe agrees with the adopted lifetime value,⁸ the lifetime value for the same level in ^{120}Xe is nearly a factor of 2 lower than the adopted value. The result for ^{120}Xe , however, is within the error limit of the most recent RDDS measurement by the Cologne group,⁹ who have reported a lifetime value of 75 ± 7 ps for the first excited 2^+ state in ^{120}Xe .

1. UNISOR, Oak Ridge Institute for Science and Education, Oak Ridge, TN
2. Louisiana State University, Baton Rouge
3. Tennessee Technological University, Cookeville
4. Brookhaven National Laboratory, Upton, NY
5. University of Maryland, College Park

6. Vanderbilt University, Nashville, TN
7. University of Tennessee, Knoxville
8. S. Raman *et al.*, *At. Data Nucl. Data Tables* **36**, 1 (1987)
9. A. Dewald *et al.*, *Proceedings of XXV Zakopane School of Physics* (Singapore, World Scientific, 1990) 152; Private communication 1992.

DEVELOPMENT OF A NEW PICOSECOND LIFETIME MEASUREMENT SYSTEM USING X-RAY - X-RAY COINCIDENCE

P. K. Joshi¹ E. F. Zganjar¹ P. F. Mantica, Jr.² S. J. Robinson³

Modification was made to the β^+ - X-ray coincidence system developed at UNISOR^{4,5} in order to accommodate the fact that many heavy proton-rich nuclei decay predominantly by the electron capture process rather than β^+ decay. Since the electron capture decay process is followed by emission of X rays, replacement of the β^+ plastic detector by a BaF₂ detector identical to the one used in the β^+ - X-ray coincidence system will allow for detection of these X rays. In this way a fast X-ray - X-ray coincidence is achieved, where one X ray follows the electron capture process and the second the internal conversion process. Since these X rays are of the same energy, the particular transition of interest is selected by using a Si(Li) detector gate on the appropriate conversion electron line. Hence a triple X-ray - X-ray - e⁻ coincidence is achieved where the timing information is extracted from the X-ray - X-ray fast coincidence.

One consequence, which evolves from use of the X-ray - X-ray fast coincidence, is that the start signal triggering the time-to-pulse-height convertor (TAC) can be an X ray from either the conversion process or the capture process. Should the X ray from the capture process trigger the TAC, a level lifetime longer than 5 ps would be indicated by a shift in the centroid of the TAC spectrum to a channel number above the prompt centroid position. However, should the X ray from the conversion process trigger the TAC, the centroid of the TAC spectrum would shift to a channel number below that of the prompt centroid position. Since the two BaF₂ detectors are identical in every respect, the two competing X-ray processes have an equal probability of triggering the start signal for the TAC. The resulting TAC spectrum, therefore,

will be the sum of the two TAC spectra, which are shifted in opposite directions relative to the prompt centroid position. The resulting TAC spectrum therefore will be wider than the prompt TAC spectrum. The level lifetime, τ , is then found simply by comparing the root-mean-square value σ of the two distributions. If σ_p and σ_t are the σ values of the prompt TAC spectrum and the TAC spectrum which results from lifetime of greater than 5 ps, then the lifetime τ is given by the following equation.

$$\sigma_t^2 = \sigma_p^2 + \tau^2.$$

1. Louisiana State University, Baton Rouge
2. UNISOR, Oak Ridge Institute for Science and Education, Oak Ridge, TN
3. Tennessee Technological University, Cookeville
4. P. F. Mantica, Jr., P. K. Joshi, E. F. Zganjar and S. J. Robinson, *current progress report*
5. P. K. Joshi, P. F. Mantica, Jr., E. F. Zganjar and S. J. Robinson, *current progress report*

LIFETIMES OF THE 0_2^+ CONFIGURATION IN ¹⁸⁶Hg AND ¹⁸⁸Hg

P. K. Joshi¹ S. J. Robinson² P. F. Mantica, Jr.³ E. F. Zganjar¹ D. Rupnik¹ R. L. Gill⁴ W. B. Walters⁵ H. K. Carter³ C. R. Bingham⁶ J. Kormücki^{3,7} A. V. Ramayya⁷ W. C. Ma⁷ J. H. Hamilton⁷

Coexisting bands of quite different deformation in ^{184,186,188}Hg have been known for some time from in-beam reaction^{8,9} and radioactive decay^{10,11} studies. The latter work also observed electric monopole (E0) transitions in these neutron-deficient Hg isotopes and precipitated the evolution of this region into a classic example of widely-occurring, nearly degenerate, nuclear shape coexistence.

A direct measure of the mixing of coexisting shapes in even-even nuclei is the E0 strength between the intruder state and the ground state.¹² Changes in the nuclear radius lead to non-vanishing values for the monopole strength function, $\rho(E0)$, and to measure $\rho(E0)$ experimentally, all that is needed is a measurement of the partial half-life of the 0_2^+ level. These Hg isotopes present a unique challenge to the measurement of 0_2^+ lifetimes in the picosecond range since the complexity of the decay demands a triple coincidence.

A lifetime measurement system developed at UNISOR¹³ was used to measure the lifetimes of the 0_2^+ configurations in ^{186}Hg and ^{188}Hg . For ^{186}Hg , the $(\beta^+ - X) - e^-$ triple coincidence, where X represents the X ray following internal conversion of the associated e^- , was used to determine the lifetime of the 0_2^+ state. This unique system has been thoroughly described.¹⁴ The lifetime for the 0_2^+ level in ^{188}Hg was measured using the triple coincidence $(X - X) - e^-$, where the first X represents the K X rays following the electron capture and the second is the same as above. The associated 2_2^+ -level lifetimes are determined in a similar manner. The mixing matrix element V_0 , calculated using the formalism of Kantele¹⁵ are 73_{-18}^{+9} keV for the 0_2^+ level in ^{188}Hg and ≥ 111 keV for the 0_2^+ level in ^{186}Hg . These results are presented in Table 7.1.

1. Louisiana State University, Baton Rouge
2. Tennessee Technological University, Cookeville
3. UNISOR, Oak Ridge Institute for Science and Education, Oak Ridge, TN
4. Brookhaven National Laboratory, Upton, NY
5. University of Maryland, College Park
6. University of Tennessee, Knoxville
7. Vanderbilt University, Nashville, TN
8. N. Rud, D. Ward, H. R. Andrews, R. L. Graham and J. S. Geiger, *Phys. Rev. Lett.* **31**, 1421-1423 (1973)
9. D. Protel, R. M. Diamond and F. S. Stephens, *Phys. Rev. Lett.* **B 48**, 102-104 (1974)
10. J. H. Hamilton *et al.*, *Phys. Rev. Lett.* **35**, 562-565 (1975)
11. J. D. Cole *et al.*, *Phys. Rev. Lett.* **37**, 1185-1188 (1976)
12. K. Heyde and R. A. Meyer, *Phys. Rev. C* **37**, 2170-2175 (1988)
13. P. K. Joshi *et al.*, *Nucl. Instrum. Methods Phys. Res.* to be submitted

14. J. Kantele, *Nucl. Instrum. Methods Phys. Res.* **A271**, 625-627 (1988)

15. J. Kantele, *Heavy Ions and Nuclear Structure* (Harwood Academic Pub.) 391-447 (1984)

GAMMA-RAY SPECTROSCOPY ON ^{72}Br

W. C. Ma¹ T. Brown¹ A. V. Ramayya¹
 J. H. Hamilton¹ L. Chaturvedi¹
 J. Kormicki^{1,3} Q. M-Lu¹ N. Severijns²
 P. Schuurmans² L. Vanneste²
 P. F. Mantica, Jr.³ H. K. Carter³

The first studies of the decay of ^{72}Br to ^{72}Se ,^{4,5} which reveal in ^{72}Se the first example of the coexistence of shapes with quite different deformations ($|\beta_2| \sim 0.1$ and $|\beta_2| \sim 0.3$), have been very important for the general understanding of nuclear structure. However, microscopic theoretical calculations^{6,7} predict a much greater richness of levels than seen in recent in-beam gamma-ray spectroscopy on ^{72}Se .⁸ Indeed, whereas the experimentally observed positive parity levels are dominated by a single band with large deformation, the theoretical calculations predict multiple band structures which are not seen experimentally. For ^{68}Ge on the other hand, the similar complex band structure which is predicted by these microscopic calculations, is nicely reproduced by the measurements.⁸ One thus wonders what is the difference between these two nuclei which were predicted to be quite similar theoretically. A possible explanation might be the fact that ^{72}Se is much closer to the island of ground-state superdeformation centered around $N = Z = 38$ (Ref. 9) and that the dominance of these reinforcing proton and neutron shell gaps at 38 is not included in the calculations yet. Thus, it remains interesting to study in more detail the level structure of ^{72}Se .

Table 7.1. Lifetimes and Monopole Strength Parameters

Nucleus	$E(0_2^+)$ keV	$T_{1/2}(0_2^+)$ ps	E0 branch	$T_{(1/2)p}(0_2^+)$ ps	$\rho^2(E0)^1$ $\times 10^3$	V_0 keV	$E(2_2^+)$ keV	$T_{1/2}(2_2^+)$ ps
^{188}Hg	824	288 ± 63	$\geq 58\%$	288_{-63}^{+207}	$5.5_{-2.3}^{+1.5}$	73_{-18}^{+9}	881	199 ± 44
^{186}Hg	523	≤ 52	72%	≤ 72	≥ 32	≥ 111	620	66 ± 37

A second problem pertaining to this nucleus is related to the question of mixed symmetry states.^{10,11} These states involve out of phase motions of the protons and neutrons which contribute to the collective excitations and represent some of the exciting current developments of the understanding of collective motions in nuclei. One of the important characteristics of such states are large enhanced M1 transition strengths, for example in $2^+_x \rightarrow 2^+_1$ transitions ($k > 1$). In the decay of ^{72}Br there are several 2^+ states which are candidates for mixed symmetry states. Moreover, this nucleus is particularly interesting because of the mixing of the two coexisting shapes that is known to occur at the 2^+_1 level.⁵ However, in order to warrant a nuclear orientation experiment, which would give information on the E2/M1 mixing ratios of the decay of the 2^+_x levels, too few definite spin assignments are available as yet.

In order to clarify both of the above discussed problems, we have carried out a more complete $\gamma\text{-}\gamma$ coincidence run to better establish the ^{72}Br decay scheme. The activity was produced with a 48-MeV, 60-particle-nA ^{16}O beam bombarding a Ni target, which was placed in front of a FEBIAD type ion source on the UNISOR mass separator. Data are currently being analyzed.

NUCLEAR ORIENTATION OF ^{96}Tc

M. R. Papantonakis¹ P. F. Mantica, Jr.²
 J. Kormicki^{2,3} K. Butler-Moore³ A. V. Ramayya³
 J. H. Hamilton³ J. K. Deng³ W. C. Ma³
 A. Lahamer¹ W. D. Hamilton⁴

We have studied the decay of ^{96}Tc using the UNISOR Nuclear Orientation Facility. A sample was prepared by diffusing ^{96}Tc activity ($t_{1/2} = 4.3$ d) into a 0.1-mm thick pure Fe foil at 830 °C under H_2 atmosphere. The sample was top-loaded into the $^3\text{He}/^4\text{He}$ dilution refrigerator, and data were collected at both warm ($T > 1$ K) and cold ($T \sim 7$ mK) temperatures at 30 minute cycles over a four-day period. Gamma-ray anisotropy measurements were made using Ge detectors placed at angles of 0, 45, 90, 135 and 180 degrees, relative to the applied external magnetic field. The directional distributions at each angle were normalized to the 0-degree distribution as a correction for the changing sample strength, and also to the 205-keV isotropic distribution from the decay of ^{95}Tc ($I = 1/2$) to correct for dead-time and amplifier pile-up effects.

The corrected distributions for the transitions in ^{96}Mo were then used to determine the A_2 and A_4 gamma-ray angular-distribution coefficients, where the deorientation coefficients, U_2 and U_4 , were found through the top-down analysis technique. The mixing ratio, δ , for each transition was then calculated using the analytical relation between A_2 , A_4 and δ . These mixing ratios are listed in Table 7.2.

A comparison of our new mixing-ratio determinations with those obtained from previous $\gamma\gamma$ angular-correlation measurements⁵ reveals good agreement for many of the transitions listed in Table 7.2. The one having the largest discrepancy is our new measurement for the 314-keV transition from the second 6^+ level. Previously, $\delta(314)$ was identified to be +0.27(5), whereas the results here find the mixing ratio with the opposite sign. Our new results point to the fact that both the 314- and 317-keV transitions, out of 6^+_2 the level at 2755 keV, have considerable M1 components. Since the 6^+_1 and 5^+_1 states are in an energy realm where they should be fully symmetric with regards to proton and neutron degrees of freedom, the large M1 strength for the transitions into these levels from the 6^+_2 state suggests that the 2755-

1. Vanderbilt University, Nashville, TN
2. University of Leuven, Belgium
3. UNISOR, Oak Ridge Institute for Science and Education, Oak Ridge, TN
4. W. E. Collins *et al.*, *Phys. Rev. C* **19**, 1457 (1974)
5. J. H. Hamilton *et al.*, *Phys. Rev. Lett.* **32**, 239 (1974)
6. A. Petrovici, K. W. Schmid, F. Grümmer and Amand Faessler, *Nucl. Phys.* **A504**, 277 (1989)
7. K. W. Schmid, Zheng Ren-Rong, F. Grümmer and Amand Faessler, *Nucl. Phys.* **A499**, 63 (1989)
8. L. Chaturvedi *et al.*, *Phys. Rev. C* **43**, 2541 (1991)
9. J. H. Hamilton, in *Treatise on Heavy Ion Science*, ed. A. Bromley (Plenum, New York, Vol. 8, p. 3, 1989)
10. J. H. Hamilton *et al.*, *Phys. Rev. Lett.* **53**, 2469 (1984)
11. W. D. Hamilton, *J. Phys.* **G16**, 745 (1990)

Table 7.2. Gamma-ray distribution coefficients and mixing ratios for transition in ^{96}Mo

E_γ	I_i	I_f	I_γ	U_2	U_4	A_2	A_4	δ	Q(%E2)	$\alpha(\gamma)$
314	6_2	6_1	2.43	0.9692	0.8974	-0.386(6)	-0.018(14)	-0.11(1)	1.1	+0.27(5)
317	6_2	5_1	1.40	0.9692	0.8974	+0.392(4)	+0.025(19)	-0.060(5)	0.36	< 0.13
885	6_2	4_2	0.10	0.9692	0.8974	-0.29(4)	-0.22(8)	-0.10(3)	1.0 [#]	
1127	6_2	4_1	15.2	0.9692	0.8974	-0.361(6)	-0.222(14)	-0.037(5)	0.13 [#]	-0.03(10)
812	6_1	4_1	82.0	0.9617	0.8909	-0.362(6)	-0.217(14)	-0.036(8)	0.13 [#]	-0.01(3)
569	5_1	4_2	0.92	0.9279	0.7704	+0.598(5)	+0.066(26)	-0.183(3)	3.25	
								-2.84(3)	89.0	
722	4_3	2_2	0.12	0.8721	0.6156	-0.42(3)	-0.27(9)	-0.03(3)	0.1 [#]	
481	3_1	2_2	0.08	0.7885	0.4188	+0.03(8)	+0.45(32)	+0.16(4)	2.6	
								-12(-4,+12)	99	
1200	3_1	2_1	0.37	0.7885	0.4188	-0.77(1)	+0.38(4)	+0.81(2)	39.7	+0.39(15)
								+2.12(8)	81.8	
719	2_2	2_1	0.20	0.4498 [*]	0.0395	-0.75(4)	+1.5(13)	+0.33(7)	10	+0.42(27)
								+1.1(1)	55	
1498	2_2	0_1	0.09	0.4498 [*]	0.0395	-0.59(2)	-1.07(15)	0.0 [#]		
778	2_1	0_1	99.7	0.6501	0.1725	-0.54(1)	-1.10(7)	0.0 [#]		

[#] Mixing is M3/E2

^{*} Deorientation coefficients determined assuming the 1498-keV transition is pure E2.

keV level has characteristics of a mixed-symmetry state.

1. Berea College, Berea, KY
2. UNISOR, Oak Ridge Institute for Science and Education, Oak Ridge, TN
3. Vanderbilt University, Nashville, TN
4. University of Sussex, Brighton, UK
5. *Nucl. Data Sheets* **35**, 281 (1982)

LEVEL STRUCTURE OF ODD-ODD ^{114}I

B. E. Zimmerman^{1,2} *W. B. Walters*¹
*P. F. Mantica, Jr.*³ *H. K. Carter*³ *J. Kormicki*^{3,6}
*J. Rikovska*⁴ *N. J. Stone*⁴ *B. D. Kern*⁵

In order to extend previous work on odd-odd nuclei near the $Z=50$ closed shell, we have investigated the structure of the odd-odd $Z=53$ nuclide ^{114}I (Ref. 7). The most important new result is the identification of highly converted transitions at 28.2 and 134.5 keV, which are placed in the level scheme shown in Fig. 7.4. The 135-keV transition has a K/L/

M ratio consistent with M3 multipolarity and is thought to be the isomeric transition de-exciting the high-spin isomer at 266 keV. The half-life of the conversion electrons associated with this transition is 6.2 s, which is the same value derived for the 103-keV transition which has been seen to be of E1 multipolarity. The multipolarity of the 28-keV transition has been determined to be $\Delta J = 2$, but we have not been able to determine whether the transition is of electric or magnetic nature.

From the data, we have been able to deduce that the ground state is most like a 1^+ member of a $\pi d_{5/2} \nu d_{3/2}$ multiplet while the first excited state is probably the 2^- member of a $\pi g_{7/2} \nu h_{11/2}$ multiplet. Depending on whether the 28-keV transition is E2 or M2, there are several combinations of single-particle orbitals that result in states with spins and parities of 4^+ and 7^+ or 4^- and 7^- . Further interpretation through the Interacting Boson-Fermion-Fermion Model (IBFFM) is in progress.

1. University of Maryland, College Park
2. Present address: University of Tennessee, Knoxville
3. UNISOR, Oak Ridge Institute for Science and Education, Oak Ridge, TN

ORNL DWG-92-15726

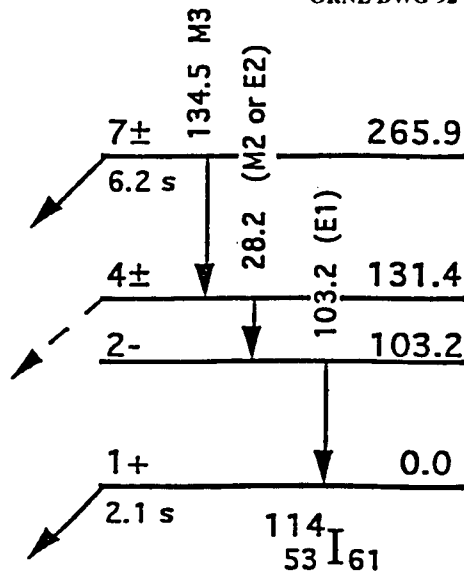


Fig. 7.4. Proposed level scheme for the decay of ^{114m}I .

- 4. Oxford University, UK
- 5. University of Kentucky, Lexington

- 6. Vanderbilt University, Nashville, TN
- 7. B. E. Zimmerman, W. B. Walters, P. F. Mantica, Jr., H. K. Carter, N. J. Stone, J. Rikovska and B. D. Kern, *Proceedings of the Conference on Nuclei Far from Stability, Bernkastel-Kues* (1992)

NUCLEAR ORIENTATION OF ^{116}Sb

B. E. Zimmerman^{1,2} W. B. Walters¹ P. F. Mantica, Jr.³ H. K. Carter³ J. Kormicki^{3,7} M. G. Booth⁴ J. Rikovska⁴ N. J. Stone⁴ C. R. Bingham⁵ B. D. Kern⁶

The odd-odd nucleus ^{116}Sb was studied via On-Line Nuclear Orientation (OLNO) to investigate the spin-lattice relaxation properties of the $^{116}\text{SbFe}$ system. The resulting plot of anisotropy versus inverse temperature (Fig. 7.5.) reveals little deviation between the experimental data and the calculated theoretical anisotropy curve, for which all of the orientation parameters are well-established from NMR measurements.⁸ This is interpreted as an indication that

ORNL DWG-92-15727

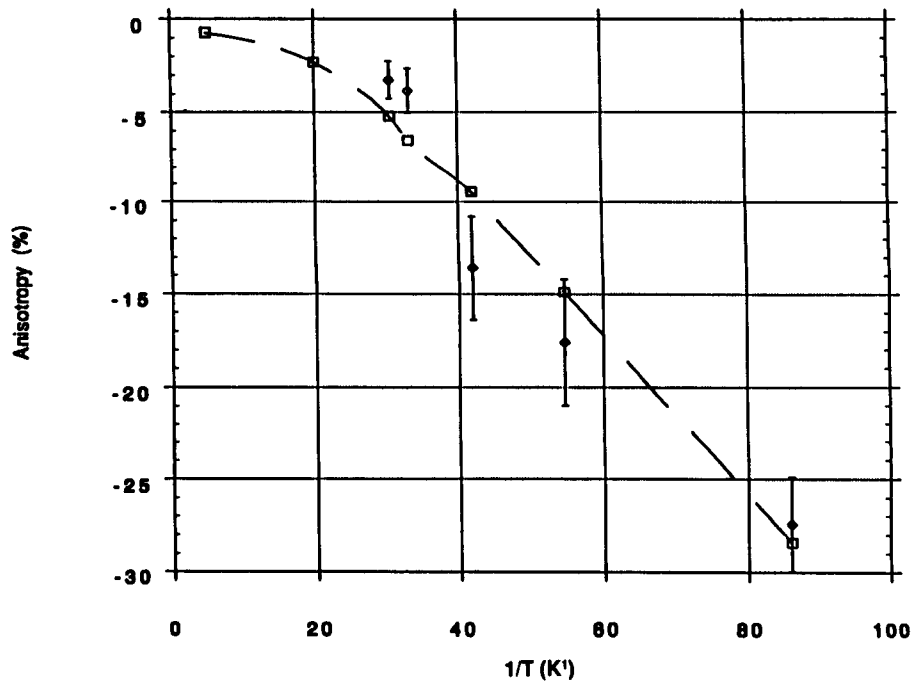


Fig. 7.5. Experimental anisotropies for ^{116}Sb decay (1293 keV line) with theoretical curve (without accounting for relaxation).

the system has reached full thermal equilibrium; that is, the nuclei are completely relaxed. This is in agreement with the results expected for a calculated spin-lattice relaxation time of ~ 200 s at 11.6 mK for a nucleus with a 950 s half-life. These results confirm that the Korringa Law is obeyed in this system and that the scaling rule $g^2 C_x = (\text{constant for all isotopes of the same element in the same host})$ can also be applied.

-
1. University of Maryland, College Park
 2. Present address: University of Tennessee, Knoxville
 3. UNISOR, Oak Ridge Institute for Science and Education, Oak Ridge, TN
 4. Oxford University, United Kingdom
 5. University of Tennessee, Knoxville
 6. University of Kentucky, Lexington
 7. Vanderbilt University, Nashville, TN
 8. V. R. Green, C. J. Ashworth, J. Rikovska, T. L. Shaw, N. J. Stone, P. M. Walker and I. S. Grant, *Phys. Lett. B* **177**, 159 (1986)

NON-SATURATION OF B(E2) STRENGTH IN MID-SHELL Xe ISOTOPES

*P. F. Mantica, Jr.¹ W. B. Walters² P. K. Joshi³
E. F. Zganjar³ S. J. Robinson⁴ R. L. Gilf⁵
D. Rupnik³ H. K. Carter¹ J. Kormicki^{1,6}
C. R. Bingham⁷*

The experimental electromagnetic transition rate between the ground state and the first excited 2^+ state in the even-even Xe isotopes below $N = 82$ appears to saturate⁸ as mid-shell neutron number is approached. This saturation effect has been considered a result of the filling of neutron orbitals⁹ which contribute very little to the total quadrupole moment. It has also been reproduced in the IBM-2 through the introduction of Pauli factors¹⁰ into the operators of the IBM-2 Hamiltonian. More recent measurements using the Recoil Distance Doppler Shift (RDDS) technique employing the Differential Decay Curve Analysis¹¹ have determined the mean lifetime of the 2^+ levels in ^{120,122,124}Xe to be shorter than that reported,⁸ suggesting there is no saturation of B(E2) values at mid-shell.

Recently, we have measured the lifetimes for levels in ^{118,120}Xe populated through the β^+ /EC decay of ^{118,120}Cs, respectively, using the new picosecond lifetime system at the UNISOR isotope separator.

The lifetimes for the first 2^+ level in these nuclides were determined to be 63 ± 6 and 64 ± 4 ps for ¹¹⁸Xe and ¹²⁰Xe, respectively. The resulting values for B(E2; $0_1^+ \rightarrow 2_1^+$) are shown in Fig. 7.6 for the new measurements and also for previous measurements that are given in Ref. 8. The B(E2) \uparrow presented here for the lifetime of the 2_1^+ level in ¹¹⁸Xe agrees with the adopted value;⁸ however, the B(E2) \uparrow value for the same level in ¹²⁰Xe is nearly a factor of 2 lower than the adopted value. Our new results for ¹²⁰Xe, however, are within the experimental uncertainty of the most recent RDDS measurement by the Cologne group,¹¹ which is also shown in Fig. 7.6.

Our new measurements, along with the most recent measurements from the Cologne group, suggest that there is no saturation of B(E2; $0_1^+ \rightarrow 2_1^+$) for the mid-shell Xe isotopes. To the contrary, these new B(E2) \uparrow data imply that there is a steady increase until mid-shell neutron number is reached, after which the B(E2) \uparrow values begin to decrease. This is clearly illustrated in Fig. 7.6. This is in agreement with the isotope shift data¹² available for the Xe isotopes below the $N=82$ closed shell, where the observed shift is linearly dependent on neutron number at least through $N=68$. Since the occupation of the relatively "flat" Nilsson orbitals by neutron numbers $64 \leq N \leq 70$ does not allow for a large increase in the B(E2) values for the Xe isotopes around mid-shell neutron number,⁹ it may prove important to consider the contribution from the proton [404]9/2 Nilsson orbital. This is a strongly up-sloping Nilsson orbital, which is indeed close to the Fermi surface for the mid-shell nuclides in this mass region, (where $\beta \geq 0.25$) as reflected in the ground-state intruder character of the odd-Z nuclides ¹¹⁹Cs.

Discussions of this topic with A. Dewald, S. Raman, W. Nazarewicz and I. Hammamoto are gratefully acknowledged.

-
1. UNISOR, Oak Ridge Institute for Science and Education, Oak Ridge, TN
 2. University of Maryland, College Park
 3. Louisiana State University, Baton Rouge
 4. Tennessee Technological University, Cookeville
 5. Brookhaven National Laboratory, Upton, NY
 6. Vanderbilt University, Nashville, TN
 7. University of Tennessee, Knoxville
 8. S. Raman *et al.*, *At. Data Nucl. Data Tables* **36**, 1 (1987)
 9. S. Raman *et al.*, *Phys. Rev. C* **43**, 556 (1991)

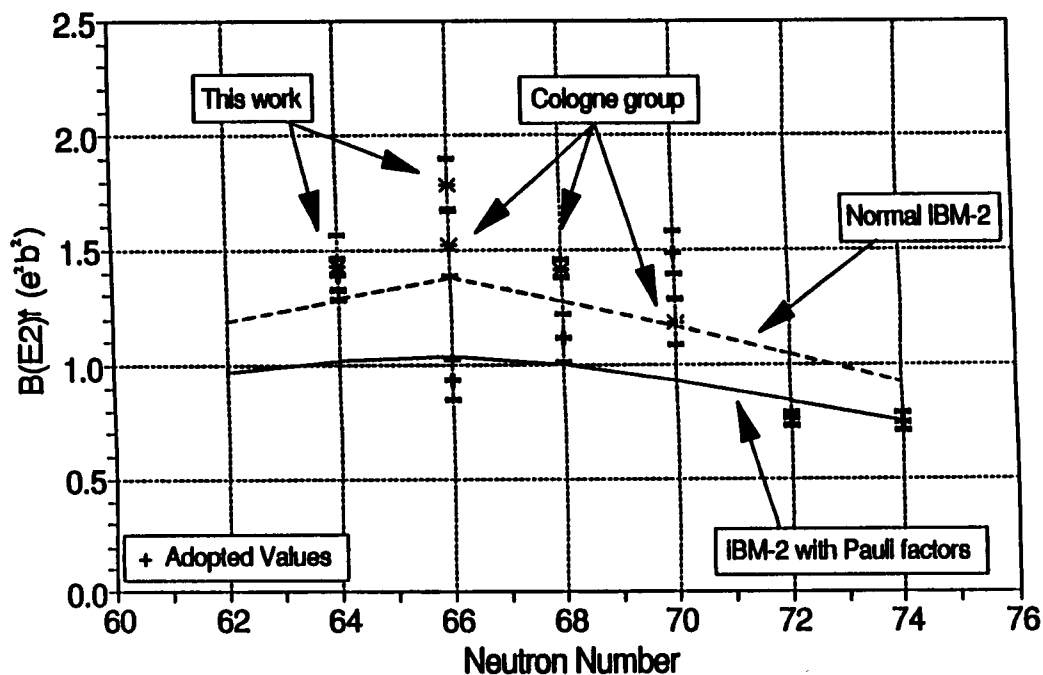


Fig. 7.6. Most recent experimental $B(E2)^\dagger$ values for the Xe isotopes below $N = 82$ compared to recent theoretical calculations predicting saturation at mid shell.

10. T. Otsuka *et al.*, *Phys. Lett.* **B247**, 191 (1990)
11. A. Dewald *et al.*, *Proceedings of XXV Zakopane School of Physics* (Singapore, World Scientific, 1990) 152; Private communication 1992
12. W. Borchers *et al.*, *Phys. Lett.* **B216**, 7 (1989)

DECAY OF ^{123}Ba

Y. Hatsukawa¹ P. F. Mantica, Jr.²
B. E. Zimmerman³ W. B. Walters³ H. K. Carter²

High-spin states of ^{123}Cs are well investigated⁴ by in-beam spectroscopic studies. However, the study of the low-spin states in ^{123}Cs from the decay of ^{123}Ba , using isotope separation techniques, is hampered by difficulties involved in ionizing Ba. Recently, a thermal ion source, based on the GSI design, has been adapted for use on the UNISOR separator. This new source has proven successful in the ionization of many rare-earth nuclei previously unattainable at the UNISOR separator, including the ionization of the Ba isotopes.

The investigation of the radioactive decay of ^{123}Ba ($t_{1/2} = 2.4$ m) to low-spin states in ^{123}Cs has been completed using the UNISOR isotope separator. The ^{123}Ba activity was produced in the heavy-ion reaction by ^{35}Cl bombardment of a ^{92}Mo target. The recoil products were ionized using the newly adapted thermal ion source, mass separated, and subsequently the desired $A=123$ activity was implanted into a moving tape system. The tape system was programmed to transport the radioactivity every 7 minutes to a counting station, which comprised a Si(Li) electron detector and two Ge detectors.

Gamma-ray and conversion-electron singles, time-dependent γ -ray singles and $\gamma\gamma$ coincidence data were collected at this counting station. Preliminary analysis of the multiscaled singles data has allowed for the assignment of 46 γ rays to the decay of ^{123}Cs ; these are listed in Table 7.3. The $\gamma\gamma$ coincidence results should serve to compliment the recent study of the decay of ^{123}Cs by Osa *et al.*⁵

1. Japan Atomic Energy Research Institute, Tokai, Japan

Table 7.3. Gamma rays assigned to the decay of ^{123}Cs .

Energy (keV)	Intensity (%)	$T_{1/2}$ (m)
20.4		
31.1	10900 (500)	2.0
35.7	1700 (150)	2.0
64.6	177 (7)	2.7
93.5	440 (30)	2.2
95.1	1000 (30)	2.2
116.6	480 (16)	2.3
120.4	220 (10)	2.2
124.1	630 (20)	2.1
137.6	240 (10)	2.1
201.3	675 (21)	2.3
333.8	72 (12)	
347.4	144 (12)	
370.7	500 (20)	2.0
373.1	273 (13)	
399.8	125 (11)	
405.1	90 (10)	
410.8	179 (12)	1.8
437.3	104 (10)	
484.5	244 (12)	
493.8	442 (17)	1.9
497.2	227 (13)	
546.9	155 (10)	
590.3	141 (10)	
607.7	95 (10)	
635.1	148 (10)	
670.3	83 (8)	
716.4	267 (15)	2.2
718.6	367 (17)	2.2
780.3	75 (10)	
782.1	54 (10)	
806.9	45 (9)	
810.8	119 (10)	
864.9	77 (10)	
874.0	40 (9)	
894.4	48 (10)	
991.0	51 (10)	
1068.3	17 (10)	
1074.4	23 (10)	
1207.3	59 (11)	
1540.1	43 (11)	
1542.5	60 (11)	
1657.4	123 (12)	
1669.0	240 (15)	
1675.8	51 (11)	
1698.6	74 (10)	
1762.3	180 (13)	
1821.5	60 (10)	

2. UNISOR, Oak Ridge Institute for Science and Education, Oak Ridge, TN

3. University of Maryland, College Park

4. J. R. Hughes *et al.*, *Phys. Rev. C* **45**, 2177 (1992)

5. A. Osa *et al.*, report KURRI-TR-348, 1991

STUDIES OF THE ONSET OF DEFORMATION IN THE VERY-NEUTRON DEFICIENT ISOTOPES OF Pr, Nd, Pm AND Sm

*J. Breitenbach*¹ *R. A. Braga*² *J. L. Wood*¹
*P. B. Semmes*³ *J. Kormicki*^{4,5}

Detailed $\gamma\gamma$, γX , $e\gamma$, and eX coincidence data and γ -, X -, and e -singles spectrum multiscaling data have been analyzed for the decays:

^{137}Eu (11 s) \rightarrow ^{137}Sm (45 s) \rightarrow ^{137}Pm (2.4 m) \rightarrow ^{137}Nd

^{135}Sm (10 s) \rightarrow ^{135}Pm (49 s) \rightarrow ^{135}Nd

^{133}Sm (3 s) \rightarrow ^{133}Pm (12 s) \rightarrow ^{133}Nd (70 s) \rightarrow ^{133}Pr

Low-lying levels for $^{133,135}\text{Pr}$ and $^{135,137}\text{Pm}$ are shown in Fig. 7.7. A level scheme for ^{133}Nd has been constructed containing 73 transitions: Previous decay information for $^{133}\text{Pm} \rightarrow ^{133}\text{Nd}$ did not report any γ rays. A low-spin β -decaying isomer in ^{133}Nd is established. Calculations using the Lund (triaxial Nilsson) model have been carried out. Results for ^{137}Pm are shown in Fig. 7.8. The rapid onset of deformation predicted⁶ to occur between ^{137}Pm and ^{135}Pm (cf. Fig. 7.7.) is not observed.

1. School of Physics, Georgia Institute of Technology, Atlanta

2. School of Chemistry, Georgia Institute of Technology, Atlanta

3. Tennessee Technological University, Cookeville

4. Vanderbilt University, Nashville, TN

5. UNISOR, Oak Ridge Institute for Science and Education, Oak Ridge, TN

6. G. A. Leander and P. Moller, *Phys. Lett. B* **110**, 17 (1982)

ORNL-DWG 92-15103

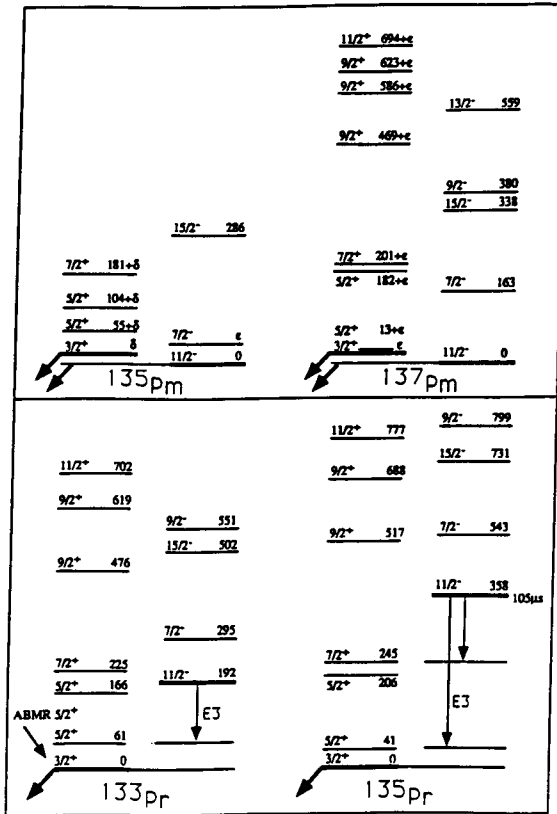


Fig. 7.7. Level systematics for the N=76 and N=74 Pm and Pr isotopes.

PARTICLE + TRIAXIAL-ROTOR MODEL CALCULATIONS FOR ODD-MASS Pr ISOTOPES ABOVE N = 82

P. F. Mantica, Jr.¹ W. B. Walters²

We have recently studied the level structure³ of ^{147}Pr , where we have identified several new levels below 1.2 MeV and have also made firm assignments of negative parity to several low-energy levels, paralleling similar low-energy negative-parity states⁴ identified in ^{145}Pr . The presence of these low-lying negative-parity states suggests that configurations having significantly different deformation, related to the highly-deformed region above N=90 and/or to reflection asymmetric region identified around ^{145}Ba , may manifest themselves at low energy in these nuclides. To further our study of ^{147}Pr and the other odd-A Pr isotopes above N = 82, we have attempted to reproduce the structures of these nuclides using the particle + triaxial-rotor model.

The low-energy positive-parity levels calculated using the particle + triaxial-rotor code for $^{145,147}\text{Pr}$ are shown in Fig. 7.9, where they are compared with the known experimental levels. The calculations involved the diagonalization of the deformed shell-model Hamiltonian to compute single particle energies and wavefunctions of a non-axially symmetric deformed Woods-Saxon potential. In these calculations, the deformation parameters (β_2, β_4, γ) used for the Woods-Saxon potential were extracted from Total Routhian Surface (TRS) calculations for the even-even neighbors of these odd-A Pr isotopes. The single-particle matrix elements were calculated by selecting all the Nilsson orbitals residing within ± 4 MeV of the Fermi surface. The residual pairing interaction was treated within the BCS approximation, where a standard value of the pairing strength parameter, G, was adopted for each isotope. The core 2_1^+ energy was estimated by taking the average of the 2_1^+ energies from the neighboring even-even core nuclei and the recoil terms in the particle + triaxial-rotor model Hamiltonian were treated as one-body operators.

A close comparison of the theoretical level energies to the actual experimental spacings suggests that the PTRM does quite well in predicting the level density at low-energy, especially in ^{147}Pr , where the triplet of states found to be within 100 keV of the ground state is well reproduced. However, the PTRM calculations presented here do not do as well in

ORNL-DWG 92-15104

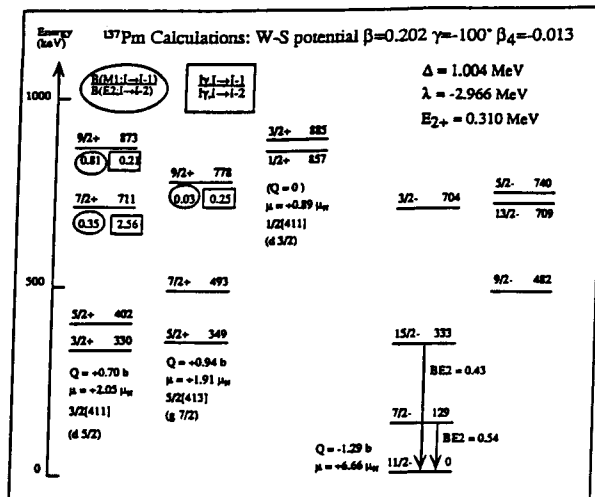


Fig. 7.8. Predicted level structure for ^{137}Pm .

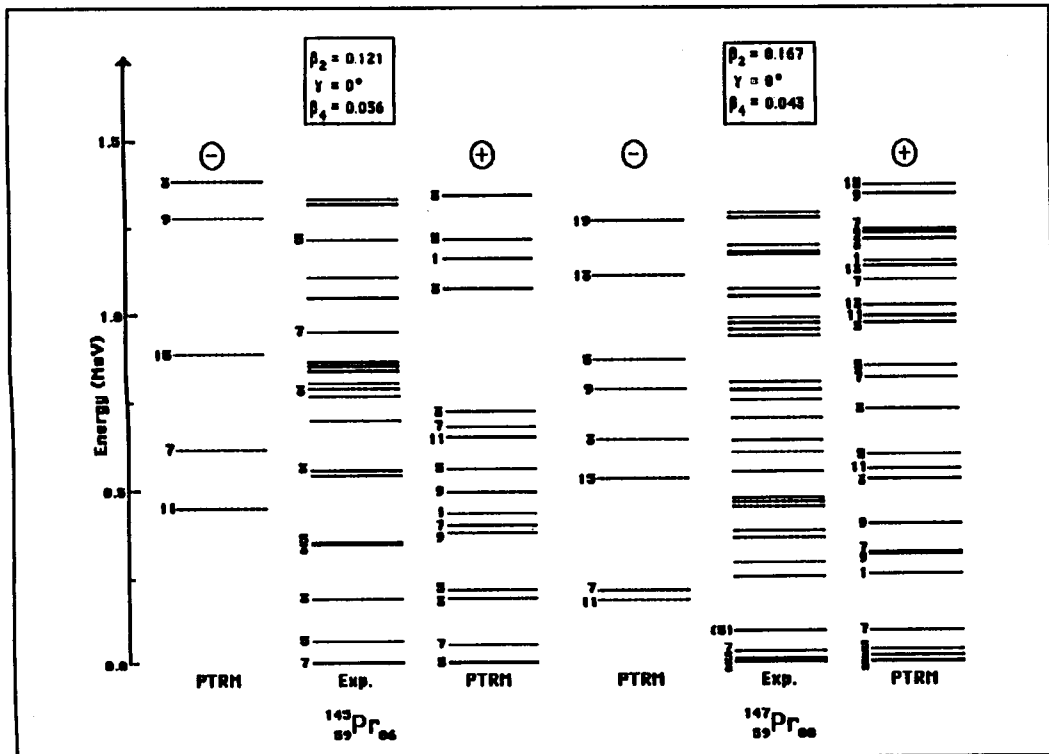


Fig. 7.9. Experimental levels in $^{145,147}\text{Pr}$ with the positive and negative parity levels calculated from the particle + triaxial-rotor model.

reproducing the low-lying levels of ^{145}Pr . The fact that there is better agreement for the case of ^{147}Pr may suggest that the even-even core nucleus for ^{145}Pr , ^{144}Ce , may not be properly represented as a good rotor.

The resulting wavefunctions for the states calculated at low energy in ^{147}Pr are highly mixed, with the majority of the contribution from the $[411]3/2$ and $[413]5/2$ orbitals. One interesting aspect of the calculations reported here is that there was very little change in the calculated wavefunctions for the low-energy levels in the range where $0.15 \leq \beta_2 \leq 0.18$. That these levels do form the pseudo-spin doublet $[312] 3/2, 5/2$ will only be mentioned since a detailed investigation into the pseudo $\text{SU}(3)$ symmetry limit has not been carried out at this time.

The negative-parity level structures for $^{145,147}\text{Pr}$ were also calculated and are shown in Fig. 7.9. One comment that can be made in regards to the negative parity levels in these Pr nuclides is the density of low-energy low-spin negative parity levels. The experimental levels shown in Fig. 7.9 are obtained from radioactive decay studies: specifically, the study of β

decaying parent nuclides having low spin (where, to define a reference frame, low spin is $I \leq 9/2$). For ^{145}Pr and ^{147}Pr , where the negative parity states have been identified from measurements of internal conversion coefficients, there is an apparent excess in low-spin negative-parity states at low energy, above that predicted from the particle + triaxial-rotor model. However, the code used in these calculations does not include provisions for the mixing of positive and negative parity states, as the octupole (β_3) degree of freedom is excluded from the calculations. Therefore, if these low-energy, low-spin negative-parity states arise from complex configuration mixing involving β_3 deformation, these levels would lie outside the particle + triaxial-rotor model space.

We would like to thank P. B. Semmes for his guidance in the use and interpretation of the output from the particle + triaxial-rotor code.

1. UNISOR, Oak Ridge Institute for Science and Education, Oak Ridge, TN
2. University of Maryland, College Park

3. P. F. Mantica *et al.*, to be submitted to *Phys. Rev. C*

4. E. M. Baum *et al.*, *Phys. Rev. C* **39**, 1514 (1989)

SHAPE COEXISTENCE AND ELECTRIC MONOPOLE TRANSITIONS IN ^{184}Pt

Y. Xu¹ K. S. Krane¹ M. A. Gummin¹ M. Jarrio²
J. L. Wood² E. F. Zganjar³ H. K. Carter⁴

Excited states of ^{184}Pt were studied through the radioactive decay of mass-separated ^{184}Au produced through the ($^{12}\text{C},\text{xn}$) reaction on a target of ^{181}Ta . The beam from the UNISOR separator was used to do gamma and conversion-electron spectroscopy and also was implanted into the UNISOR Nuclear Orientation Facility, enabling the study of the angular distribution of gamma rays from the decay of ^{184}Au oriented at low temperature. A report describing this work was given at the OLNO-2 Conference.⁵

Spectroscopy measurements have placed more than 150 gamma transitions among more than 50 excited states of ^{184}Pt . We observe 2 patterns of feeding of the high-lying states that correspond respectively to daughter states of high spin and low spin. Based on our measurements, we have concluded that the ^{184}Au decay proceeds through 2 isomers, probably of spins 3 and 6. In an effort to determine the half-lives of these decays, multiscaling data have been taken from the decay of ^{184}Au both produced directly and (in a separate experiment) following the decay of ^{184}Hg . It appears that the 2 half-lives are both close to 50 s, and data analysis is presently in progress to try to resolve this question.

Analysis of the decays from the low-lying states has revealed strong E0 transitions between states of the $K = 0^+$ bands and also between states of the $K = 2^+$ bands. We regard this as evidence for shape coexistence in both pairs of bands. These conclusions follow from combining the internal conversion results, which show evidence for E0+M1+E2 character for the transitions between the bands, with results from the nuclear orientation angular distributions from which the E2/M1 multipole mixing ratios can be extracted. Combining these two results permits the E0 contributions to the transitions to be obtained. These E0 admixtures serve as direct evidence for the coexisting

bands. Coexistence between the $K = 2^+$ bands represents a new feature of nuclear structure.⁶

1. Oregon State University, Corvallis

2. School of Physics, Georgia Institute of Technology, Atlanta

3. Louisiana State University, Baton Rouge

4. UNISOR, Oak Ridge Institute for Science and Education, Oak Ridge, TN

5. X. Yu *et al.*, *Hyperfine Interactions*, in press

6. Y. Xu *et al.*, *Phys. Rev. Lett.* **26**, 3853 (1992)

SPINS AND MAGNETIC DIPOLE MOMENTS OF NEW ISOMERS IN ^{184}Au BY TIME INTEGRAL AND TIME RESOLVED NUCLEAR ORIENTATION

N. J. Stone¹ J. R. Stone¹ M. G. Booth¹
W. B. Walters² B. Zimmerman^{2,3} C. R. Bingham⁴
K. S. Krane⁵ J. Deng⁶ B. D. Kern⁷
P. F. Mantica, Jr.⁸ H. K. Carter⁸ Y. Hatsukawa⁹

The existence of isomerism in ^{184}Au has been established in on-line studies at the NICOLE facility, ISOLDE, CERN, and confirmed in a previous UNISOR experiment. The detection of a highly converted M3 transition of energy 68 keV indicates that, provided no other transition is involved in the isomeric decay, the two levels involved have the same parity, and a spin difference of three. Low temperature nuclear orientation studies have been made at NICOLE in an attempt to elucidate the spins and moments of the long-lived states, but these were hampered by the fact that at ISOLDE there has been no direct Au beam and the activity was produced following implantation of ^{184}Hg [$t_{1/2} = 30.6$ s]. The decay of ^{184}Au is complex, as revealed by a previous detailed study¹⁰ at UNISOR. Many levels in the daughter ^{184}Pt are fed indirectly through both isomer and ground-state decay, thus making it difficult to extract information concerning the individual hyperfine interactions of the parents.

In the current study we have used the direct UNISOR ^{184}Au beam produced by the reaction of ^{12}C on ^{181}Ta at 150 MeV. It is known that the production ratio of the two long-lived states in this reaction differs from the ratio obtained from the Hg decay.

The experiment divided into three sections. In the first, ^{184}Au activity implanted into a prepared iron foil was oriented at temperatures down to 14.5 mK. Accurate anisotropy measurements were made on all transitions in the combined decay of the low- and high-spin isomers of ^{184}Au . Taking advantage of the detailed decay scheme study done at UNISOR, these measurements will yield level spin and gamma transition properties in the daughter ^{184}Pt as well as helping to establish the hyperfine interactions of the long-lived orienting states.

The second stage of the experiment saw the first use at UNISOR of the pulsed beam implantation method,¹¹ Time Resolved On-Line Nuclear Orientation (TR-OLNO), to observe the growth of orientation of the ^{184}Au activity as the nuclei relax, cooling to the Fe foil lattice temperature through the Korringa conduction electron relaxation mechanism. The relaxation time is a sensitive measure of the nuclear g-factor and, taken together with conventional orientation, can yield both the spin and moment of the oriented state. The activity was pulsed using a controlled beam stopper in the focal plane of the separator to give implantation for a period of 40 s followed by relaxation and decay for 216 s, the operation being repeated cyclically. Spectra taken during each of 32 successive 6-s time frames were added in successive cycles to allow observation of the growth of the anisotropy with good statistical quality. Data were taken with the dilution refrigerator at 16.7 mK and also at 1 Kelvin, the latter to study the decay of unoriented activity.

Finally, measurements were made on the spectroscopy beam line to improve knowledge of the half-lives of the long-lived states in ^{184}Au and to rule out the presence of additional isomers, which would be revealed only through the detection of highly converted low-energy transitions.

The data are still being analyzed in detail. Provisional TR-OLNO results, giving clear evidence for relaxation in ^{184}Au , are shown in Fig. 7.10.

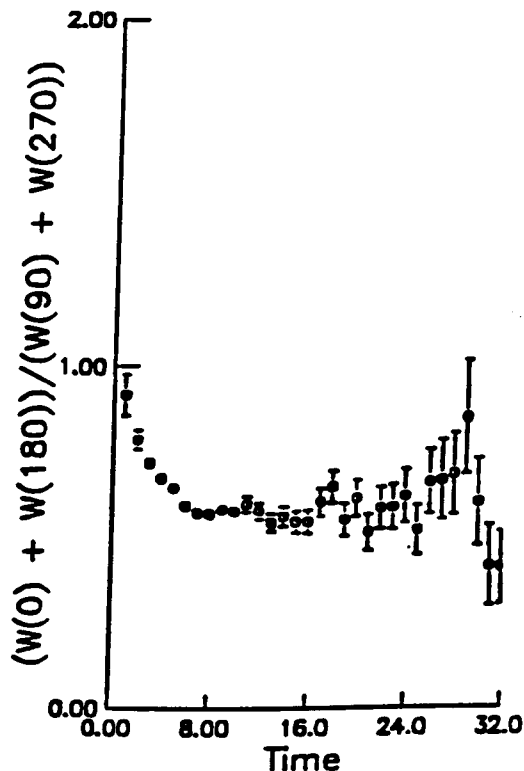


Fig. 7.10. Time resolved nuclear orientation of ^{184}Au 363 keV transition.

9. Japan Atomic Energy Research Institute, Tokai, Japan

10. Y. Xu, K. S. Krane, M. A. Gummin, M. Jarrio, J. L. Wood, E. F. Zganjar and H. K. Carter, *current progress report*

11. N. J. Stone, *Nucl. Instrum. Methods Phys. Res. B70*, 556 (1992)

SEARCH FOR COEXISTING $K^\pi=2^+$ BANDS IN ^{186}Pt

J. McEver¹ J. Breitenbach¹ J. L. Wood¹
J. Schwarzenberg¹ R. A. Braga²

As a continuation of the discovery³ of coexisting $K^\pi = 2^+$ bands in ^{184}Pt , the decay of ^{186}Au (11 m) to ^{186}Pt was studied by $\gamma\gamma$, γX , $e\gamma$ and eX coincidence and γ , X^- , and e -singles multiscaling spectroscopy. The ^{186}Au was produced by the $^{181}\text{Ta}(^{12}\text{C}, 7n)$ reaction. The signature³ for coexisting $K^\pi = 2^+$ bands will

1. Oxford University, UK
2. University of Maryland, College Park
3. Present address: University of Tennessee, Knoxville
4. University of Tennessee, Knoxville
5. Oregon State University, Corvallis
6. Vanderbilt University, Nashville, TN
7. University of Kentucky, Lexington
8. UNISOR, Oak Ridge Institute for Science and Education, Oak Ridge, TN

be E0 transitions feeding the established⁴ low-lying $K^\pi = 2^+$ band.

-
1. School of Physics, Georgia Institute of Technology, Atlanta
 2. School of Chemistry, Georgia Institute of Technology, Atlanta
 3. Y. S. Xu *et al.*, *Phys. Rev. Lett.* **68**, 3853 (1992)
 4. M. Finger *et al.*, *Nucl. Phys. A* **188**, 369 (1972); C. Hebbinghaus *et al.*, *ibid.* **A514**, 225 (1990)

COMPLETE SPECTROSCOPY IN THE ^{187m,g}Tl DECAY: THE STRUCTURE OF ¹⁸⁷Au

D. Rupnik¹ E. F. Zganjar¹ J. L. Wood²

The analysis of the extensive $^{187}\text{Tl} \rightarrow ^{187}\text{gHg} \rightarrow ^{187}\text{Au}$ and $^{187\text{m}}\text{Hg} \rightarrow ^{187}\text{Au}$ decays is complete and manuscripts are being prepared. The data was obtained at UNISOR using the $^{176}\text{Hf}(^{19}\text{F}, 8\text{n})^{187}\text{Tl}(\beta/\text{EC})^{187}\text{Hg}$ and $^{176}\text{Hf}(^{16}\text{O}, 5\text{n})^{187}\text{Hg}$ reactions. The beta decay of ^{187}Tl populates predominantly the $3/2^-$ ground state of ^{187}Hg (2.4 m) and, consequently, the low-spin states of ^{187}Au are populated by the decay of ^{187}Hg . The direct production of ^{187}Hg will populate preferentially the $13/2^+$ isomer in ^{187}Hg (1.7 m) and, consequently, more high-spin states in ^{187}Au are populated. The decay of $^{187\text{m}}\text{Hg}$ was analyzed first. About 430 transitions and 145 levels have been extracted from the data and assigned to the levels in ^{187}Au . The analysis of $^{187\text{m,g}}\text{Tl}$ decay brought these numbers up to about 490 and 180, respectively, mostly by introducing transitions and levels related to low spin. The higher complexity of the second analysis is due to the additional contamination from two sources: the $^{187}\text{Tl} \rightarrow ^{187}\text{Hg}$ decay and the internal transition of the $9/2^-$ $^{187\text{m}}\text{Tl}$ isomer.

A group of states have been located which correspond to several series of the core-particle couplings, as well as levels near 2 MeV, which correspond to a coupling between a proton and the states in the core with energy greater than the pairing gap. We have also identified a number of transitions, seen in the lower-spin part of the high-spin data,³ which lie in the domain of spins of the decay data.⁴ The analysis of these data has been the most complete of any odd-A nucleus that we have attempted. We have, on a routine basis, placed transitions with intensities as

low as 0.2 relative to 100 for the 233.4-keV transition. An extensive analysis of multiplets has yielded 52 transitions with differences in energy which are between 0.5 keV and 1 keV (instrumental resolution, FWHM, being ≈ 2 keV), and 83 transitions with separations ≤ 0.5 keV. A total of over 2000 coincidence gates were carefully analyzed to establish coincidence relations. Over 200 gamma-gated gammas and over 50 gamma-gated electrons were analyzed to extract the separate intensities of the multiplets which are not separable in the ungated spectra.

Conversion-electron spectra were analyzed and 279 conversion coefficients were established using combined gamma-gated electrons and gamma-gated gammas. Multipolarities, as well as both sets of intensities (from the decay of $^{187\text{m}}\text{Hg}$ and $^{187\text{g}}\text{Hg}$), were used to establish spins of the levels. Finally, an iteration procedure, employing both sets of gamma intensities, was used to separate the gamma intensities corresponding to the $3/2^-$ ground state and the $13/2^+$ isomeric state of the ^{187}Hg parent nucleus.

-
1. Louisiana State University, Baton Rouge
 2. School of Physics, Georgia Institute of Technology, Atlanta
 3. D. Rupnik, E. F. Zganjar and J. L. Wood, *ORNL-6689 Physics Division, Progress Report 91*, p. 120 (1991)
 4. C. Bourgeois, M. G. Poquet, N. Perrin, H. Segolle, F. Hannachi, G. Bastin and F. Beck Z. *Phys. A* **333**, 5 (1989)

NUCLEAR STRUCTURE STUDIES OF ¹⁸⁷Ir

*M. A. Gummin¹ K. S. Krane¹ Y. Xu¹ T. Lam²
E. F. Zganjar² J. B. Breitenbach³
B. E. Zimmerman^{4,6} H. K. Carter⁵
P. F. Mantica, Jr.⁵*

The nuclear structure of odd-proton ^{187}Ir was studied following the radioactive decay of mass-separated ^{187}Pt . Two experiments were done: a spectroscopy study in which gamma-ray and electron singles and gamma-gamma angular correlations were observed, and a nuclear orientation study in which gamma-ray angular distributions were measured from ^{187}Pt oriented at low temperature.

Based on these results, a new decay scheme has been constructed including approximately 92% of the decay intensity with levels up to about 2.4 MeV. A

new multiplet of levels has been confirmed in the 2.4-MeV region; no previous structure in this nucleus had been known above 1.5 MeV. A significant share of the decay intensity proceeds through these levels, and analysis of the decay scheme of the low-lying states is not possible without knowledge of the feedings through this high-energy multiplet.

From the nuclear-orientation and internal-conversion data, we have obtained E2/M1 multipole mixing ratios for many of the low-lying transitions. The levels have been interpreted based on a calculation using the particle-plus-triaxial-rotor model. Mixing ratios calculated from this model show excellent agreement with experimental values in both magnitude and phase.

A preliminary report on this work was given at the OLNO-2 Conference,⁷ and a complete manuscript is in the final stages of preparation.⁸ A similar study of the decay of ¹⁸⁹Pt has been done. Data from that work are being analyzed.

-
1. Oregon State University, Corvallis
 2. Louisiana State University, Baton Rouge
 3. School of Physics, Georgia Institute of Technology, Atlanta
 4. University of Maryland, College Park
 5. UNISOR, Oak Ridge Institute for Science and Education, Oak Ridge, TN
 6. Present address: University of Tennessee, Knoxville
 7. M. A. Gummin *et al.*, *Hyperfine Interactions*, *in press*
 8. M. A. Gummin *et al.*, *to be published*

**NUCLEAR MAGNETIC DIPOLE AND
ELECTRIC QUADRUPOLE MOMENTS OF
¹⁸⁷Tl FROM LASER SPECTROSCOPY AND
THEIR INTERPRETATION IN THE
STRUTINSKY AND PARTICLE-PLUS-
ROTOR MODELS**

*H. A. Schuessler¹ E. C. Benck¹ F. Buchinger²
H. Iimura³ R. Wyss⁴ J. Rikovska⁵ H. K. Carter⁶
J. Kormicki^{6,7} C. R. Bingham⁸*

Collinear laser spectroscopy in ¹⁸⁷Tl has been carried⁹ out at the UNISOR separator at Oak Ridge. Heavy-ion produced neutral isotopes are excited from

the metastable 4p ²P_{3/2} level populated in a charge exchange reaction with Na. The excitation at $\lambda=535$ nm to the 7s ²S_{1/2} level, using Doppler tuning, is followed by the radiative decay to the Tl ground state at $\lambda=377$ nm. This transition is observed using a fiber optics light collection system. The signal of ¹⁸⁷Tl was observed during a single run using ion beam intensities in the order of 8×10^4 ion/s. The hyperfine constants, the isomer shift, as well as the moments and the change in mean-square charge radius between the I=1/2 and I=9/2 states for ¹⁸⁷Tl, as extracted from the data, are listed in Table 7.4.

A comparison of the results with those obtained for the heavier odd-Tl isotopes shows that the nuclear moments show only little variation with mass number. A slight decrease from $\mu=3.91$ (1) μ_N for A=193 to $\mu=3.79$ (2) μ_N for A=187 is observed for the magnetic moments of the I=9/2 states whereas those for the I=1/2 states are constant within the experimental error between A=201 and A=187 ($\mu \approx 1.59 \mu_N$). The values of the Q_s increase slowly between $Q_s=2.20$ (2) b at A=193 and $Q_s=2.43$ (5) b at A=187. We have carried out particle-triaxial-rotor (PTR-WS) and mean-field calculations, yielding Total Routhian Surfaces (TRS), for finding the deformation of ¹⁸⁷Tl. These calculations were able to describe successfully systematics in isotopic shape variations in the neighboring Pt, Au and Hg isotopes. TRS's were calculated using the deformed-mean-field approach with the Wood-Saxon potential, the Strutinsky shell correction and the monopole pairing force. The ground-state deformation parameters from the TRS calculations served as an input to the subsequent PTR-WS calculation to obtain more detailed spectroscopic properties. Both methods employ identical Wood-Saxon potentials.

Minima in the Total Routhian Surfaces at oblate deformation of $|\beta|=0.074$ (1/2⁺) and $|\beta|=0.158$ (9/2⁻) are observed. The latter value is in good agreement with the deformation found from our experimental Q_s using the strong coupling scheme ($\beta=0.15$) justified for isotopes with oblate shape for Z=81. The difference in deformation between the ground and the metastable state, indicated from the TRS's ($\delta\beta^2=0.019$), is somewhat larger than the $\delta\beta^2=0.012$ found from the isomer shift using the relation $\delta\langle r^2 \rangle_{\text{def}} = 3/5 R^2 5/(4\pi) \delta\beta^2$, where $R=1.2 A^{1/3}$. The moments calculated in the PTR-WS approach with the PTR parameters as an input, as well as after optimization of the deformation parameters, are included in Table 7.4. The moments are already well reproduced (within $\approx 10\%$) with the deformation pa-

Table 7.4. Hyperfine parameters, moments and deformation parameters for ^{187}Tl . The letters in the second column refer to: experimental values (a), results from PTR-WS calculations with deformation parameters from the Total Routhian Surfaces (b), and results from PTR-WS calculations after optimization (c).

I^π	$A(^2S_{1/2})$ [GHz]	$A(^2P_{3/2})$ [MHz]	$B(^2P_{3/2})$ [GHz]	μ [μ_N]	Q_4 [b]	β_2	β_4	γ
$1/2^+$	a:	11.7(5)	253(9)	1.55(6)				
	b:			1.74		0.074	-0.005	57°
	c:			1.57		0.10	-0.005	60°
$9/2^-$	a:	3.163(5)	64(2)	-2.71(2)	3.79(2)	-2.43(5)		
	b:			3.30	-2.27	0.16	-0.004	50°
	c:			3.57	-2.49	0.16	0.07	60°

rameters taken directly from the TRS calculations. Slight adjustments of the parameters increase the agreement further. For the $I=1/2$ state, an increase of β to $\beta=0.1$, required to fit the magnetic moment, leads to a $\delta\beta^2$ of 0.015.

In summary, the moments of ^{187}Tl are not distinctly different from those of the heavier odd isotopes. They are well explained by the TRS and PTR-WS calculations assuming oblate shape with very moderate deformation.

We have recently extended our measurements to the very deficient ^{186}Tl isotope. The ground state nuclear properties for this isotope are presently being evaluated.

DECAY OF MASS-SEPARATED ^{199}Bi

M. Zhang¹ C. R. Bingham¹ J. Ding¹
B. E. Zimmerman¹ H. K. Carter² J. Kormicki^{2,6}
P. F. Mantica, Jr.² L. Rayburn² P. K. Joshi³
J. L. Wood⁴ S. Shastry⁵

Shape coexistence in odd-A nuclei in the Pb region has been extensively studied from both an experimental and theoretical viewpoint.⁷ Because the protons occupy levels near the $Z=82$ closed shell and the neutrons occupy levels near the middle of the $N=126$ shell, there is the possibility that nearly spherical and deformed states arising from the excitation of protons across the $N=82$ shell can coexist at low energy in this region. In odd-A Pb isotopes, the $13/2^+$ deformed excited states arising from the coupling of the $i_{13/2}$ state to the deformed intruder bandhead have been found in $^{195,197}\text{Pb}$.^{8,9} The goal of the present work was to compile a more complete decay scheme for ^{199}Pb to aid in the systematic study of odd-A Pb isotopes in this region.

The decay of ^{199}Bi was studied utilizing the University Isotope Separator at Oak Ridge (UNISOR) on-line to the Holifield Heavy-Ion Research Facility tandem accelerator. Ions of ^{199}Bi were produced by bombarding a 53mg/cm^2 stack of Re foils with a 155-MeV ^{16}O beam and collected on a moving tape collector which moved the activity to a measurement station around which were placed three Ge γ -ray detectors and a Si electron detector. Multiscaled conversion electron and γ -ray singles data, as well as γ - γ and γ -electron coincidences, were collected.

1. Texas A&M University, College Station
2. Foster Radiation Laboratory, McGill University, Montreal, Canada.
3. On leave from Japan Atomic Energy Research Institute, Tokai-mura, Ibaraki, Japan.
4. Joint Institute for Heavy Ion Research, Oak Ridge, TN 87831.
5. Oxford University, OXI 3PU Oxford, U.K.
6. UNISOR, Oak Ridge Institute for Science and Education, Oak Ridge, TN
7. Vanderbilt University, Nashville, TN
8. University of Tennessee, Knoxville
9. H. A. Schuessler *et al.*, *Proceedings of the 6th International Conference on Nuclei far from Stability, Bernkastel-Kues, Germany, July 1992.*

From the data, a total of 286 transitions were attributed to the decay of ^{199}Bi , of which 149 transitions were placed in the level scheme. A total of 120 new transitions and 33 new levels were added to the previous scheme. Since the ground-state spins of ^{199}Pb and ^{199}Bi are $3/2^-$ and $9/2^-$, respectively, the bulk of the decay proceeds to the first excited $5/2^-$ state. Previous studies revealed no ground-state transitions, proposing instead an upper limit of 9.3 keV for the first excited state. We have deduced via the 1022.8 keV and 1034.0 keV gates and 1146.4 keV and 1157.5 keV gates, that each pair of these decay from the same state to both the ground and first excited states. This establishes that the energy of the first excited state is 11.2 keV.

The electron singles and coincidence data allowed for the determination of 86 (47 new) conversion coefficients and the observation of several E0 transitions, which have been interpreted to be the signature of shape-coexistent states. We have observed a 1268.1 keV transition which decays to the 436.5 keV $13/2^+$ state, which is the first positive-parity excited state. The observed α_k value is 1.3 times larger than that expected for an M1 transition. Thus, the state at 1704.6 keV is proposed to be the deformed bandhead, which, as seen in Fig. 7.11, fits well with the systematics of the neighboring Pb

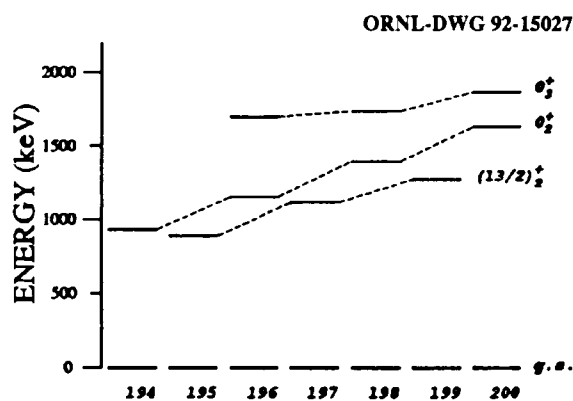


Fig. 7.11. The position of the deformed excited 0^+ states of even-A lead isotopes and $13/2^+$ states of odd-A lead isotopes with respect to the lowest level of the same spin.

isotopes. Other E0 transitions suggest possible deformed states at 1573.9, 1754.4, and 1937.2 keV.

1. University of Tennessee, Knoxville
2. UNISOR, Oak Ridge Institute for Science and Education, Oak Ridge, TN
3. Louisiana State University, Baton Rouge
4. School of Physics, Georgia Institute of Technology, Atlanta
5. State University of New York, Plattsburgh
6. Vanderbilt University, Nashville, TN
7. J. L. Wood, K. Heyde, W. Nazarewicz, M. Huyse and P. Van Duppen, *Phys. Rept.* **215**, 101 (1992)
8. J. C. Griffin *et al.*, *Nucl. Phys. A* **531**, 401 (1991)
9. J. Vanhorenbeeck *et al.*, *Nucl. Phys. A* **531**, 63 (1991)

PRODUCTION RATES OF ISOTOPES AND RESULTANT RADIOACTIVITY FOR RADIOACTIVE ION BEAM (RIB) TARGETS

L. A. Rayburn¹

The VAX version of the HETC (High Energy Transport Code) was obtained from the ORNL Radiation Shielding Information Center and installed on a Physics VAX. See Report CCC-178C for details about the code.

The first part of the code was used with incident protons of various energies to predict the production rates of isotopes from a number of anticipated RIB targets; for example: ^{40}Ca , ^{63}Cu , ^{65}Cu , ^{70}Ge , ^{76}Ge , ^{58}Ni , ^{64}Ni , ^{32}S , ^{36}S , ^{238}U and ^{64}Zn to mention a few. The isotope production cross sections were compared with measured values where possible and, in general, agreed within about a factor of two in most cases. However, it should be mentioned that there is a dearth of measured charged particle cross section values.

The second part of HETC was used to provide residual radioactivity information for RIB sources created by any incident charged particle. This part of the code is designed to study the buildup and decay of

activity in any system for which the nuclide production rates are known. The nuclides treated and other decay information are constructed from libraries of nuclide decay data and by the (input) production rates for the problem. The nuclide decay data libraries contain the half lives and decay modes (nuclide mass must be greater than 40). The code calculates the concentrations after given time intervals and can output various derived quantities: activity, mass,

gamma spectra, neutron spectra as well as others. Nuclide concentrations at a given time interval can be passed to a second calculation stage to study the subsequent decay. This part of the code has been used to treat most of the targets listed above.

1. UNISOR, Oak Ridge Institute for Science and Education, Oak Ridge, TN

8. THEORETICAL AND COMPUTATIONAL PHYSICS

INTRODUCTION

Substantial new challenges confront the nuclear science community in the U.S. today. New directives call for a redefinition of the roles that national laboratories and university-based theory groups play in the overall nuclear theory effort. In the Physics Division we have initiated two new theory programs: computational physics, and nuclear structure and astrophysics.

The computational physics program is centered around the high-performance computing and communications Grand Challenge project – “The Quantum Structure of Matter.” This project applies classical and quantum field theory to atomic, nuclear, and condensed matter physics, and combines the talents and goals of theorists in different branches of physics to understand and use the opportunities opened up by massively parallel computer architectures. Our research will advance the study of matter under strongly interacting conditions, as encountered in many

branches of energy research, including fusion plasmas, lasers, and accelerators. This work should lead to substantial advances in both the science and the associated computational mathematics of these fields.

In the Physics Division there is a new experimental program to produce radioactive heavy-ion beams that will begin to yield data in 1995. This promises a view of nuclear structure in previously unexplored areas far from stability with the possibility of increased cooperation between the fields of nuclear physics and astrophysics. We face a remarkable opportunity in the computational aspects of nuclear structure and astrophysics because of the availability of a new generation of massively parallel supercomputers. This confluence produces an opportunity to develop a comprehensive and integrated program of theoretical research that will support the developing field of radioactive ion beam physics with the melding of modern nuclear theory and contemporary high-performance computing.

ATOMIC PHYSICS

ELECTROMAGNETIC PAIR PRODUCTION IN RELATIVISTIC HEAVY-ION COLLISIONS¹

C. Bottcher and M. R. Strayer

The phenomenon of pair production by the transient electromagnetic fields produced in relativistic heavy-ion collisions, as it impinges upon atomic, nuclear, and particle physics, and the design of accelerators and detectors is surveyed. The subject is naturally divided between coherent production in peripheral collisions and incoherent production in central collisions. Examples illustrating both regimes are discussed.

1. Abstract of published paper: *Nucl. Phys. A* 544, 255c (1992) (*Proceedings of Quark Matter '91 Conference, Gatlinburg, TN, November 11-15, 1991*).

THE COULOMB THREE-BODY PROBLEM: A PROGRESS REPORT¹

C. Bottcher and D. R. Schultz

Some of the outstanding conundrums in the Coulomb three-body problem have been examined, all of which are closely interrelated. In particular, we have addressed:

- The regularization of the caustics which occur in the semiclassical breakup amplitude; e.g., when the hyperspherical angle $\alpha \rightarrow 0$, or at included angles q of order $E^{-1/4}$.
- Identification of bound orbits which analytically continue the Wannier breakup states to energies below threshold.

The first issue is resolved by going to the next approximation beyond the semiclassical time-depen-

dent formulation. Almost any approximation in which the amplitude is allowed to be complex is free of anomalies. Scrutiny of these expressions suggests that the wave function is well represented by the usual eikonal along a classical trajectory times a Gaussian *ansatz* normal to the trajectory. This concept leads to a solution of the second problem, since the *ansatz* is applicable to orbits which cross themselves without quite closing — we call these pseudoperiodic orbits. It is possible to locate extensive classes of such orbits, which, in fact, connect to the Wannier escape trajectories. Energies, resonance widths, and oscillator strengths are readily calculated. The theory is quite general, but attention is focused on rotating planar configurations of the system $e\text{-H}^+e$ (whose bound states are H^-). We assume a nonzero total angular momentum L , for which the semiclassical solutions are better behaved.

As an alternative approach, we are developing accurate time-dependent solutions of the two-electron atom. For any symmetry, the wave function is expanded in the Hylleraas representation in terms of a finite set of functions of the intrinsic coordinates (r_1, r_2, θ) . These functions are represented, in turn, as products of basis splines. As a first test of the methods, we have constructed an autoionizing state ($2s^2$) by Feshbach projection, and observed how it decays under the full interaction. The decay is exponential at a rate close to that predicted by other means. The continuum is simulated in a finite domain by adding an imaginary absorbing potential outside the range of the bound states.

1. Abstract of published paper: pp. 72-83 in *Proceedings of Workshop on Future Directions in Electron-Ion Collision Physics, Atlanta, Georgia, April 9-10, 1992* (Lawrence Livermore National Laboratory report CONF-9204186, 1992).

PARAMETRIC CORRELATIONS AND DIFFUSION IN QUANTUM SPECTRA¹

X. Yang² and J. Burgdörfer³

The evolution of the quantum spectrum as the function of a control parameter can be mapped onto the molecular dynamics of a classical many-body system. This approach is used to study the parametric motion of energy levels in classically mostly regular

and in mostly chaotic regimes. The parametric energy-level dynamics is described in terms of the velocity autocorrelation function and the friction kernel of a disordered many-body system. We show that the parametric dynamics is sensitively dependent on the underlying classical dynamics, and therefore provide new measures of quantum chaos. The transition from classically regular to chaotic motion manifests itself in the disappearance of parametric diffusion. Semiclassical arguments give analytic approximations for the spectrum of the velocity autocorrelation function, and these approximations are found to be consistent with numerical calculations for the vibronic motion of a triatomic molecule. We compare these autocorrelation functions with those found in gases, liquids, and glasses.

-
1. Abstract of published paper: *Phys. Rev. A* **46**, 2295 (1992).
 2. University of Tennessee, Knoxville.
 3. Adjunct staff member from the University of Tennessee, Knoxville.

ELECTRON-ELECTRON INTERACTION AND TWO-CENTER EFFECTS IN PROJECTILE IONIZATION AT BACKWARD EMISSION ANGLES¹

J. Wang,² C. O. Reinhold,² and J. Burgdörfer³

We analyze the electron emission spectrum into backward angles for projectile ionization in 0.5-MeV/u H^0 and He^+ on He collisions. The energy and angular distributions of the ejected electron are calculated taking into account both scattering correlations and two-center effects. Two-center effects are treated using the continuum-distorted-wave approximation and the classical-trajectory Monte Carlo method. Correlation effects are described in terms of a Born series including contributions up to second order. Both contributions are found to enhance significantly the electron-loss cross section in near-symmetric projectile-target collision systems. We find improved agreement with experiment for He^+ on He collisions. Extensions to heavier targets are also discussed.

-
1. Abstract of published paper: *Phys. Rev. A* **45**, 4507 (1992).

2. University of Tennessee, Knoxville.
3. Adjunct staff member from the University of Tennessee, Knoxville.

TORUS QUANTIZATION OF SYMMETRICALLY EXCITED HELIUM¹

J. Müller,² J. Burgdörfer,³ and D. Noid⁴

The recent discovery by Richter and Wintgen [J. Phys. B 23, L197 (1990)] that the classical helium atom is not globally ergodic has stimulated renewed interest in its semiclassical quantization. The Einstein-Brillouin-Keller quantization of Kolmogorov-Arnold-Moser tori around stable periodic orbits becomes locally possible in a selected region of phase space. Using a hyperspherical representation, we have found a dynamically confining potential allowing for a stable motion near the Wannier ridge. The resulting semiclassical eigenenergies provide a test for full quantum calculations in the limit of very high quantum numbers. The relations to frequently used group-theoretical classifications for doubly excited states and to the periodic-orbit quantization of the chaotic portion of the phase space are discussed. The extrapolation of the semiclassical quantization to low-lying states give remarkably accurate estimates for the energies of all symmetric $L=0$ states of helium.

1. Abstract of published paper: *Phys. Rev. A* 45, 1471 (1992).
2. University of Tennessee, Knoxville.
3. Adjunct staff member from the University of Tennessee, Knoxville.
4. Chemistry Division

HIGH l -STATE POPULATION IN O^{7+} PRODUCED IN ION-SOLID COLLISIONS¹

J. Kemmler,² J. Burgdörfer,³ and C. O. Reinhold⁴

The high l -state population of fast ions excited in ion-solid interactions is very different from l -state populations produced under single collision conditions. A study of the population dynamics of electronic excitation and transport within the framework of a classical transport theory for O^{2+} (2 MeV/u) ions traversing carbon foils shows good agreement with experimental results from delayed photon emission

spectroscopy. We investigate the dependence of the characteristic exponent for the power-law decay of delayed Ly_{α} and Ly_{β} radiation on the initial (n, l) distribution. From our simulations, we find evidence that the very high l -state populations produced in ion-solid collisions are the consequence of a high l -state diffusion under the influence of multiple inelastic and elastic collisions in the bulk of the solid.

1. Abstract of published paper: *NIMPR* B67, 168 (1992).
2. Centre Interdisciplinaire de la Recherche Scientifique, Caen, Cedex, France.
3. Adjunct staff member from the University of Tennessee, Knoxville.
4. University of Tennessee, Knoxville.

COULOMB-BORN THEORY OF (e,2e) COLLISIONS

J. H. Macek¹

Expansions in powers of the electron-electron interaction are standard in quantum electrodynamics, yet have been rejected in the nonrelativistic domain because such expansions cannot satisfy the correct Coulomb asymptotic conditions. For that reason, more elaborate distorted waves are employed, for example, in electron scattering from neutral systems. We have formulated expansions in powers of the electron-electron interaction rigorously using a simple modification of perturbation theory.

Consider the Hamiltonian, H , for electron-atomic hydrogen scattering

$$H = H_0 - 1/r_1 - 1/r_2 + 1/r_{12}. \quad (1)$$

The perturbation parameter 1 is introduced in the usual way

$$H = H_0 - 1/r_1 - 1/r_2 + \lambda 1/r_{12}, \quad (2)$$

and the corresponding T-matrix is written in the form

$$T(\lambda) = \left\langle \Phi_j^-(\lambda) \left| \lambda(1/r_{12} - 1/r) \right| \Psi_i^+(\lambda) \right\rangle. \quad (3)$$

Here $\Psi_i^+(\lambda)$ is the exact solution of the Schrödinger equation, and $\Phi_j^-(\lambda)$ is a solution of

$$[H_0 - (1 - \lambda)/r_1 - 1/r_2 - E]\Phi_j^-(\lambda) = 0. \quad (4)$$

The perturbation series is obtained by expanding $T(\lambda)$ in powers of λ which requires expansions of $\Phi_j^-(\lambda)$. In the usual scattering theory this is done incorrectly. When this expansion is done correctly, one readily obtains a correct expression to all orders in λ . The first term is just the Coulomb-Born amplitude for electron-hydrogen scattering, which was proposed earlier,² but rejected on fundamental grounds.³ We have applied the first-order approximation to (e,2e) experiments at high energy.

Near the Wannier threshold, we employ a semi-classical propagator to join the Coulomb functions in the reaction zone to solutions appropriate at intermediate and large distances. This gives us a normalization constant which reproduces the Wannier threshold law.

-
1. UT-ORNL Distinguished Scientist.
 2. I. J. Kang and W. D. Foland, *Phys. Rev.* **164**, 122 (1967).
 3. M. R. Rudge, *J. Phys. B* **2**, L130 (1968).

ANOMALOUS n -DEPENDENCE OF LOW-ENERGY ELECTRON CAPTURE FROM ATOMIC HYDROGEN BY MULTICHARGED IONS'

J. H. Macek² and S. Y. Ovchinnikov³

A theory of electron capture from states of high-principal quantum number n by multicharged ions is presented. We predict a capture cross section that depends upon the n of the initial state as n^β , where β is as large as 7 in some cases. This surprisingly high n -dependence explains why a small (less than 0.1%) fraction of hydrogen in high- n states contributes 30% of the capture yield in $O^{5+} + H$ collisions. The theory also predicts a strong dependence on the dipole moment of the initial state.

-
1. Abstract of published paper: *Phys. Rev. Letts.* **69**, 2357 (1992).
 2. UT-ORNL Distinguished Scientist.

3. Guest assignee from A. F. Ioffe Physical Technical Institute, St. Petersburg, Russia.

PERTURBATION THEORY WITH ARBITRARY BOUNDARY CONDITIONS FOR CHARGED-PARTICLE SCATTERING: APPLICATION TO (e,2e) EXPERIMENTS IN HELIUM'

J. H. Macek² and J. Botero³

A perturbation series of the distorted-wave Born type is developed in such a way that the slow decrease of the Coulomb potential in which the incoming and scattered particles move plays no role. We apply this approach to triple-differential cross sections for electron-impact ionization of helium at low and intermediate energies, where we use Coulomb waves with an effective charge for the incoming, scattered, and ejected electron, and show that even though these wave functions are known to satisfy the wrong Coulomb boundary conditions at infinity, they give reasonably and unexpectedly good agreement with experiment.

-
1. Abstract of published paper: *Phys. Rev. A* **45**, R8 (1992).
 2. UT-ORNL Distinguished Scientist.
 3. Escuela Colombiana de Ingeniería, Bogotá, Colombia.

CLOSE-COUPPLING CALCULATIONS FOR THE ELECTRON-IMPACT EXCITATION OF Zn^+ (ref. 1)

M. S. Pindzola,² N. R. Badnell,² R. J. W. Henry,² D. C. Griffin,³ and W. L. van Wyngaarden⁴

Electron-impact-excitation cross sections for Zn^+ are calculated in a multiple- LS -term close-coupling approximation. Total cross sections for the $4s \rightarrow 4p$ transition are compared with crossed-beams⁵ and merged-beams⁶ experiments. Taking into account cascade effects, the close-coupling calculations and

the crossed-beams measurements are found to be in reasonable agreement over a wide energy range. When only the forward-angle part of the cross section is calculated, good agreement with the merged-beams measurements is found near the excitation threshold, but at the higher energies the experimental value is somewhat lower than the theory predicts.

-
1. Abstract of published paper: *Phys. Rev. A* **44**, 5628 (1991).
 2. Auburn University, Auburn, AL.
 3. Rollins College, Winter Park, FL.
 4. California Polytech State University, San Luis Obispo, CA.
 5. Rogers et al., *Phys. Rev. A* **25**, 681 (1982).
 6. Smith et al., *Phys. Rev. Lett.* **67**, 30 (1991).

ELECTRON-IMPACT EXCITATION OF IONS¹

D. C. Griffin,² M. S. Pindzola,³ and N. R. Badnell³

Methods for performing theoretical calculations of electron-impact excitation of positive ions are reviewed and results using various levels of approximation are compared with experimental measurements. The important contributions of recombination resonances to the excitation cross sections are discussed and various theoretical methods of treating these resonances are considered. In addition to excitation of valence electrons, we also consider the contributions of inner-shell excitation followed by autoionization to the ionization cross section for cases where these indirect processes dominate the total cross section.

-
1. Abstract of published paper presented at ICPEAC XVII, Brisbane, July 1991, Section 7, IOP Publishing Ltd., 1992.
 2. Rollins College, Winter Park, FL.
 3. Auburn University, Auburn, AL.

ELECTRON IMPACT IONIZATION OF Ca⁺ (ref. 1)

N. R. Badnell,² D. C. Griffin,³ and M. S. Pindzola²

We have carried out a number of close-coupling calculations for the electron impact excitation of the $3p^5 3d 4s$ configuration of Ca⁺ using the R-matrix method, so as to determine the indirect contribution to the ionization of Ca⁺. We find that the large resonance features primarily due to capture into the $3p^5 3d^2 4s$ configuration, present when only the ⁴P and the two ²P terms of the $3p^5 3d 4s$ configuration are included in the continuum close-coupling expansion, disappear when all nine terms of this configuration are included. The resulting ionization cross section is in reasonably good agreement with experiment over the energy range where dielectronic capture-autoionization features could be expected and resolves a long-standing disagreement between theory and experiment.

-
1. Abstract of published paper: *J. Phys. B: At. Mol. Opt. Phys.* **24**, L275 (1991).
 2. Auburn University, Auburn, AL.
 3. Rollins College, Winter Park, FL.

CONVERGENCE OF THE CLOSE-COUPLED METHOD FOR THE $3p^5 3d^2$ CONFIGURATION IN Ti³⁺ (ref. 1)

D. C. Griffin,² M. S. Pindzola,³ and N. R. Badnell³

By performing 21-state and 26-state R-matrix calculations for Ti³⁺, we have explored the convergence of the close-coupling approximation for electron-impact excitation from the $3p^6 3d$ ground state to the $3p^5 3d^2$ doubly-excited states. Both calculations included all 19 terms of the $3p^5 3d^2$ configuration and they differed only in the number of singly-excited

states included. Three terms of $3p^53d^2$ are autoionizing and their excitation-autoionization contributions dominate the ionization cross section in the threshold region. Our results from either the 21-state or 26-state calculations for excitation to these three terms, when combined with the background direct cross section, are in excellent agreement with crossed-beam measurements of the ionization cross section and are an improvement over earlier 10-state R-matrix calculations. This illustrates the importance of including coupling between all terms within a doubly-excited configuration, as shown earlier in the case of Ca^+ by Badnell et al. Furthermore, the 26-state calculation shows a strong reduction in the resonance structure associated with excitation to the 16 bound terms of $3p^53d^2$, as compared to the 21-state calculation; this clearly illustrates the importance of including a sufficient number of singly-excited states in a close-coupling calculation of inner-shell excitation. Finally the 26-state calculation has also enabled us to determine valence-shell excitation cross sections from the $3p^63d$ ground state to $3p^64s$ and $3p^64p$ and from the $3p^64s$ metastable state to $3p^64p$.

-
1. Abstract of published paper: *J. Phys. B: At. Mol. Opt. Phys.* **24**, L621 (1991).
 2. Rollins College, Winter Park, FL.
 3. Auburn University, Auburn, AL.

IONIZATION AND RECOMBINATION IN TRANSITION METAL IONS¹

N. R. Badnell,² M. S. Pindzola,² D. C. Griffin,³ and H. P. Summers⁴

We discuss atomic data for transition metal ions and its use in the modeling of non-LTE magnetic fusion plasmas.

-
1. Abstract of published paper: *Phys. Scripta* **T37**, 26 (1991).
 2. Auburn University, Auburn, AL.
 3. Rollins College, Winter Park, FL.
 4. JET Joint Undertaking, Abingdon, Oxon, UK.

ELECTRON-IMPACT IONIZATION DATA FOR THE NICKEL ISONUCLEAR SEQUENCE¹

M. S. Pindzola,² D. C. Griffin,³ C. Bottcher, M. J. Buie,⁴ and D. C. Gregory

Atomic data for the electron impact ionization of ions in the nickel isonuclear sequence are reviewed. Calculations have been performed for all charge states in the distorted-wave approximation. In 8 of the 28 ions of the nickel isonuclear sequence, experiment and theory are compared. In many of the ions, excitation-autoionization contributions to the total cross section are found to be quite important. For intermediate charge state ions a large fraction of the experimental cross section may be attributed to ionization from metastable levels of low-lying excited configurations. Maxwellian collisional rate coefficients are calculated from the cross section data and presented in parametrized form.

-
1. Abstract of published paper: *Phys. Scripta* **T37**, 35 (1991).
 2. Auburn University, Auburn, AL.
 3. Rollins College, Winter Park, FL.
 4. Present address: Naval Research Lab, Washington, DC.

DIELECTRONIC RECOMBINATION BETWEEN HYPERFINE LEVELS OF THE GROUND STATE OF Bi^{82+} (ref. 1)

M. S. Pindzola,² N. R. Badnell,² and D. C. Griffin³

Dielectronic recombination cross sections between the hyperfine levels of the ground state of Bi^{82+} are calculated in a hydrogenic approximation. The radiative decay rates from the doubly excited resonances $1s(F=5)nl$ are found to be orders of magnitude stronger than the autoionizing decay rates to the $1s(F=4)$ continuum. The associated dielectronic recombination cross sections are strongly peaked towards zero energy, but their overall magnitudes are

extremely small compared to the radiative recombination background.

-
1. Abstract of published paper: *Phys. Rev. A* **45**, R7659 (1992).
 2. Auburn University, Auburn, AL.
 3. Rollins College, Winter Park, FL.

ELECTRON-IMPACT IONIZATION OF THE TUNGSTEN ATOM¹

M. S. Pindzola² and D. C. Griffin³

The near-threshold electron-impact ionization cross section for the tungsten atom is calculated in a distorted-wave approximation. A shape resonance is found to have a large effect on the total cross sections for the 6s and 5d subshells. The shape resonance in the $\ell=2$ scattering channel is most clearly defined when one examines the differential cross section with ejected energy.

-
1. Abstract of published paper: *Phys. Rev. A* **46**, 2486 (1992).
 2. Auburn University, Auburn, AL.
 3. Rollins College, Winter Park, FL.

EJECTED-ELECTRON SPECTRA IN PROTON-ATOMIC HYDROGEN COLLISIONS¹

*D. R. Schultz, R. E. Olson,² C. O. Reinhold,³
M. W. Gealy,⁴ G. W. Kerby III,⁴
Y.-Y. Hsu,⁴ and M. E. Rudd⁴*

The fundamental process of ionization in the collisions of protons with atomic hydrogen is considered at an impact energy of 70 keV by comparing experimental and theoretical doubly differential cross sections for electron ejection. This collision system provides a critical test of intermediate energy theories since effects such as electron-electron interaction (correlation) are not present and the roles of the ionization mechanism and subsequent evolution of the ejected electron in the two-center Coulomb field are isolated. Results of the classical-trajectory Monte

Carlo technique, the continuum distorted wave-eikonal initial state method and the plane wave Born approximation are compared with the present experimental data which are the first differential measurements that have been performed for the ionization of atomic hydrogen by proton impact.

-
1. Abstract of published paper: *J. Phys. B: At. Mol. Opt. Phys.* **24**, L599 (1991).
 2. University of Missouri, Rolla, MO.
 3. University of Tennessee, Knoxville, TN.
 4. University of Nebraska, Lincoln, NE.

DIFFERENTIAL CROSS SECTIONS FOR STATE-SELECTIVE ELECTRON CAPTURE IN 25-100 keV PROTON-HELIUM COLLISIONS¹

*D. R. Schultz, C. O. Reinhold,² R. E. Olson,³
and D. G. Seely⁴*

Cross sections differential in the scattering angle of the projectile are presented for electron capture summed over all states and to the 2s, 2p, 3s, 3p, 4s, and 4p states of hydrogen in 25-, 50-, and 100-keV proton-helium collisions. The classical-trajectory Monte Carlo (CTMC) technique was employed for these calculations as well as to compute total cross sections as a function of impact energy. The latter are compared with experiment to display the behavior of the integral state-selective cross sections in this energy regime. Detailed comparison is also made between the calculated angular differential cross sections and the experimental measurements of Martin et al.⁵ for capture summed over all states and of Seely et al.⁶ for capture to the 2p state. Very good overall agreement is found. Regarding the cross section for capture summed over all states, an improved agreement is demonstrated by using an alternate representation of the initial state in the CTMC method, which improves the electronic radial distribution but which cannot presently be applied to state-selective determinations.

-
1. Abstract of published paper: *Phys. Rev. A* **46**, 275 (1992).
 2. University of Tennessee, Knoxville, TN.
 3. University of Missouri, Rolla, MO.

4. Albion College, Albion, MI.
5. Rogers et al., *Phys. Rev. A* **23**, 285 (1981).
6. Smith et al., *Phys. Rev. A* **45**, R1287 (1992).

**CLASSICAL DESCRIPTION AND
CALCULATION OF IONIZATION IN
COLLISIONS OF 100 eV ELECTRONS AND
POSITRONS WITH He AND H₂ (ref. 1)**

D. R. Schultz, L. Meng,² and R. E. Olson²

In order to explore the range of applicability of the classical trajectory Monte Carlo technique concerning the phenomena associated with light-particle impact of atoms and molecules, we present calculations of the singly and doubly differential cross sections for 100 eV electron and positron impact of He and H₂. Through comparison with experimental

measurements it is noted in what regimes of ejection energy and angle the classical model describes reasonably the process of ionization by electrons. We find that reasonable agreement is obtained regarding the integrated (singly differential and total) cross sections, while the features of the doubly differential cross section which evidently come about due to quantum mechanical aspects of the collision are not reproduced. In these instances the classical cross sections reflect an averaging over electron angles and energies of the observed doubly differential cross sections. Difficulties associated with the classical model of the many electron atom which arise specifically in light-particle impact are discussed as well as a comparison with a distorted wave Born approximation for electron impact of helium.

1. Abstract of paper to be published in *Journal of Physics B* (1992).

2. University of Missouri, Rolla, MO.

COMPUTATIONAL PHYSICS

**CALCULATIONS OF PERIODIC
TRAJECTORIES FOR THE HÉNON-HEILES
HAMILTONIAN USING THE MONODROMY
METHOD¹**

K.T.R. Davies, T. E. Huston,² and M. Baranger³

The monodromy method, for calculating classical periodic trajectories, is applied to the famous Hénon-Heiles potential, which is invariant under the group D₃. The monodromy method is computationally very efficient and is used to find many families of periodic trajectories, including a number of simple bifurcations from the main families of the Hénon-Heiles potential.

**EVALUATION OF INTEGRALS USING
GENERAL PARTIAL-FRACTION
EXPANSIONS¹**

K.T.R. Davies, J.-S. Wu,² and R. W. Davies³

The function $[(x-t_1)^{n_1}(x-t_2)^{n_2}\dots(x-t_N)^{n_N}]^{-1}$, with $N, n_i \geq 1$, is explicitly expanded in partial fractions. A general recursion relation is also derived. Of particular interest are the cases $N = 2$ and $N = 3$. For $N = 2$, three partial-fraction expansions are compared, and a "symmetrical" expansion is shown to be the most useful for evaluating various finite-limit and infinite-limit principal-value integrals. Such expressions are prototypes of integrals containing products of Green's functions, which are presently being studied in intermediate-energy nuclear physics. Also, a complex-contour evaluation provides another derivation of the symmetrical partial-fraction expansions.

1. Abstract of published paper: *Chaos* **2**, 215 (1992).

2. University of Florida, Gainesville.

3. Consultant from M.I.T., Cambridge, MA.

1. Abstract of published paper: *Can. J. Phys.* **70**, 311 (1992).

2. Fayetteville State University, Fayetteville, NC.

3. GTE Laboratories, Inc., Waltham, MA.

**EXTENSION OF THE MONODROMY
METHOD TO CONSERVATIVE MAPS: THE
STANDARD MAP**

K.T.R. Davies and M. Baranger¹

The monodromy method² has been extensively used to study classical periodic motion in nonintegrable, two-dimensional Hamiltonians,²⁻⁵ which are classified as conservative flows. These studies show that the dynamical behavior of such systems are determined completely from the properties of the periodic trajectories. In particular, it is found that stable periodic trajectories lie in regular regions of phase space, while unstable ones lie in chaotic regions. However, one would like to describe the dynamics of *any* physical system entirely in terms of its periodic orbits. Because of the above work, this aim has been realized for conservative flows, but not for other types of dynamics.

We are in the process of extending the monodromy method to conservative maps, and we plan to make an extensive study of the periodic orbits of the "standard map."^{6,7} This famous map has received considerable attention by physicists who model accelerator dynamics.⁸ Also, because the monodromy method determines the stability character of each region of phase space, it is expected that it will be well suited for analyzing the delicate interplay between the periodicity and stability properties of an accelerator beam. (For a stable particle beam, one finds a type of quasiperiodicity with a "winding phase" that is *not* a rational number.) Thus, we fully expect that this project should be of considerable interest to physicists and engineers involved in the beam dynamics of accelerators (e.g., the SSC and RHIC).

For the standard map,^{6,7} the iterative equations are

$$\begin{aligned} q_{n+1} &= q_n + p_n + \frac{k}{2\pi} \sin(2\pi q_n) \pmod{1} \\ p_{n+1} &= p_n + \frac{k}{2\pi} \sin(2\pi q_n) \pmod{1}, \end{aligned} \quad (1)$$

where k is the map parameter. The Jacobian determinant of this system is unity, verifying that the mapping is conservative. Also, it can easily be shown that, for any value of k , there are two fixed points ($N \equiv$ period = 1) at $q = 0.5, p = 0$ (or 1), and at $q = 0$ (or 1), $p = 0$ (or 1). Then, for any k , there is an $N = 2$ orbit at $q = p = 0.5$ and $q = 0$ (or 1), $p = 0.5$. (There is also another $N = 2$ orbit, but its location varies with k .)

For the standard map, there are well-defined regions of regularity and of chaos, and the dynamics of this map becomes increasingly chaotic as one increases the value of the control parameter.^{6,7} Because of these features, the standard map has become an important tool for modeling in accelerator design.⁸ Thus, we plan to study this map in great detail. Our main goal is to derive various key properties of the dynamics,^{6,7} using only periodic trajectories. These properties include the following:

(1) *Construction of the "phase" (p vs. q) plots from the periodic orbits alone.* A preliminary attempt of such a construction is shown in Fig. 8.1. In the upper part of the figure (a) we show only the periodic orbits for $N \leq 16$ and for the "original" families. (The original families are those that begin at $k = 0$; any other periodic family does not originate until some $k > 0$.) The lower figure (b) shows the conventional plot obtained using many arbitrarily chosen starting points, each of which is iterated a large number of times.⁸ There are several points that should be made. First, there are a great many periodic families that bifurcate from the original families, and none of these are included in Fig. 8.1(a). In particular, the families which bifurcate from the original $N = 1, 2, 3, 4$ orbits will help to fill in much of the detail of the map in the upper, lower, and middle parts of the figure. Secondly, it is clear that in the chaotic regions in the middle of Fig. 8.1(a) the few periodic orbits shown give a very good portrait of the mapping. Third, it will be important to make a large number of phase plots for a wide range of k values, so that we have a series of "snapshots" showing the behavior spanning the range from the regular maps near $k = 0$ to the purely chaotic maps for $k \geq 4$. We will be particularly interested in the region near $k = 1$ which has been widely studied.⁶⁻⁸ Finally, it will be crucial to determine whether there exist isolated families or "islands;" i.e., families which are not directly connected to the original families or any of their bifurcations.^{3,4}

(2) *Determination of the k value at which the "last torus" disappears.* Some experts have often interpreted this phenomenon as a signal of the onset of widespread chaos. Apparently, it is related to the systematics involving the ratios of the periods of special orbits.⁶ These periods form a Fibonacci sequence, whose limiting ratio is the famous golden mean value. We expect that the monodromy method will allow one to determine this critical k value in a very accurate way.

(3) *Determination of the Lyapunov exponents for various chaotic regions.* For each unstable peri-

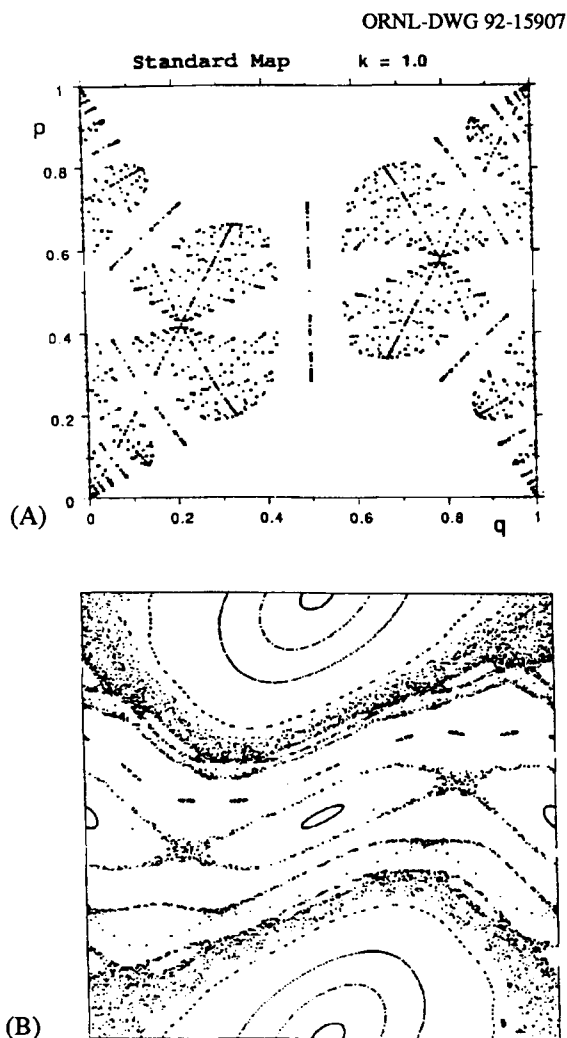


Fig. 8.1. Phase (p vs. q) plots of the standard map for $k = 1$. In (a) we plot only the original periodic families with $N \leq 16$; the small circles and small x 's indicate stable and unstable orbits, respectively. Plot (b), from Ref. 7, is a traditional graphing of a large number of nonperiodic orbits.

odic orbit, one can determine its Lyapunov exponent. We propose to examine the behavior of the periodic orbits that exist in a particular region of the phase plot. We suspect that some sort of averaging behavior will give a good estimate of a Lyapunov exponent for the given region. This then should be the same as the Lyapunov exponent that one computes by the standard method.

In summary, by using the monodromy method, we hope to be able to construct accurate phase plots

to predict the onset of widespread chaos and to determine reliable Lyapunov exponents. All of these developments will be of great value to scientists and engineers who model accelerator dynamics using various kinds for mappings.⁸

1. Consultant from M.I.T., Cambridge, MA.
2. M. Baranger, K.T.R. Davies, and J. H. Mahoney, *Ann. Phys. (N.Y.)* **186**, 95 (1988).
3. M.A.M. de Aguiar et al., *Ann. Phys. (N.Y.)* **180**, 167 (1987).
4. M. Baranger and K.T.R. Davies, *Ann. Phys. (N.Y.)* **177**, 330 (1987).
5. K.T.R. Davies, T. E. Huston, and M. Baranger, *Chaos* **2**, 215 (1992).
6. M. Tabor, pp. 134-145 and 163-167 in *Chaos and Integrability in Nonlinear Systems*, John Wiley & Sons, New York, 1989.
7. J.M.T. Thompson and H. B. Stewart, pp. 327-331 in *Nonlinear Dynamics and Chaos*, John Wiley & Sons, New York, 1986.
8. See, e.g., *Physics of Particle Accelerators, American Institute of Physics Conference Proceedings No. 184*, reports on meetings held at Fermi Laboratory, 1987 and Cornell University, 1988.

EXTENSION OF THE MONODROMY METHOD TO DISSIPATIVE SYSTEMS

K.T.R. Davies and M. Baranger¹

It appears that the monodromy method can be extended to *dissipative* systems. This means that there is much hope that the dynamics for such systems can be described in terms of periodic orbits. One of the outstanding questions is whether the attractors can be determined from the existing periodicity structures. Of course, a limit cycle *is* periodic, but in a chaotic regime it is not clear how a "strange attractor" is related to the periodic orbits. We believe that, for a dissipative system, there has never been a systematic analysis in terms of the periodic orbits (in analogy to the procedure for conservative systems²⁻⁴). Also, if the monodromy method is useful in such systems, there clearly are practical applications to a wide variety of problems in many diverse fields.

At the moment, very little is known about the application of the monodromy method to dissipative systems. However, it does appear that the method can *formally* be extended to both dissipative *flows* and

dissipative maps. The monodromy matrix will have somewhat different properties than for the analogous matrix studied previously for conservative systems.^{2,3} Nevertheless, it would seem that much of the basic machinery for determining periodic trajectories will remain in effect for the dissipative case.

For example, consider the following mapping⁵

$$\begin{aligned}x_{n+1} &= 1 + y_n - \alpha x_n^2 \\ y_{n+1} &= \beta x_n,\end{aligned}\quad (1)$$

whose transformation Jacobian has the value $-\beta$. For the choice of parameters $\alpha = 1.4$ and $\beta = 0.3$, the mapping is dissipative (since the absolute value of the Jacobian is less than unity) and gives rise to the famous Hénon attractor.⁵ One can easily find analytically the simplest periodic orbits of this map. There are two fixed points at $(x = -1.1314, y = -0.3394)$ and $(x = 0.6314, y = 0.1894)$. Then, there is a single $N = 2$ orbit at $(x = 0.9758, y = -0.1427)$ and $(x = -0.4758, y = 0.2927)$. Higher-order periodic orbits of this map can best be found by using a generalization of the monodromy method.

We propose to initiate a very thorough study of the periodic trajectories of some well-known, but simple, dissipative map such as Eq. (1). Then, if our results are encouraging, we plan to perform a similar study of a more complicated system of equations; e.g., the Lorenz or Rössler attractors.⁶ We will be especially interested in how the attractors of a chaotic regime are related to the periodic orbits. Then, the bifurcation behavior of such a dissipative system will be analyzed. We will also determine how the stability properties of a periodic orbit vary with the control parameters. Eventually, we hope to apply the monodromy method to a realistic modeling of a practical dissipative problem in engineering, medicine, global climate modeling, or some other applied field.

CHAOS EDUCATIONAL PROJECT

K.T.R. Davies

We are attempting to obtain funding for the development of a comprehensive book or syllabus on the elementary features of chaos theory. Such a book will mainly be used by high-school science students, but it could also be helpful to other students; e.g., first- or second-year undergraduates at liberal arts colleges. Our principal thrust will be the development of a large number of mathematical or computational exercises to be used as classroom teaching tools, although we intend also to focus on the cultural and philosophical implications of chaos.

This project is an outgrowth and continuation of recent workshops on chaos for high-school students. For the past two years, the Nuclear and Atomic Theory Group in the Physics Division has been conducting workshops in connection with the Laboratory's Saturday Academy of Computing and Mathematics (SACAM) program. Our workshops for the 1991-92 SACAM sessions have largely dealt with chaos and fractals, and we plan to include most of this material in the proposed book.

The motivation for this project can be summarized as follows:

a. Chaos, which has been called the third great scientific revolution of the century, pervades much of contemporary life. It is widely used in many diverse fields, including the basic sciences (mathematics, physics, chemistry, and biology), engineering, medicine, economics, meteorology, psychology, and sociology. Chaos has produced a profound revolution in science, technology, art, and philosophy. Therefore, it is important that students, even at the high-school level, acquire some appreciation of this subject.

b. Chaos is a highly mathematical subject, but a number of relatively simple mathematical exercises can be handled at the high-school level. These exercises help to give the students some feeling for the importance of various mathematical and numerical methods widely used in many fields. One of the realizations of such studies is that chaos is truly a universal science, with techniques discovered in one specialty usually having applicability to many other fields.

c. There are many qualitative and simple quantitative features of chaos that can be studied without using sophisticated computers. Thus, relatively simple "scripts," or programs, can be written in an elementary language like BASIC and run on a desktop

1. Consultant from M.I.T., Cambridge, MA.

2. M. Baranger, K.T.R. Davies, and J. H. Mahoney, *Ann. Phys. (N.Y.)* **186**, 95 (1988).

3. M.A.M. de Aguiar et al., *Ann. Phys. (N.Y.)* **180**, 167 (1987).

4. M. Baranger and K.T.R. Davies, *Ann. Phys. (N.Y.)* **177**, 330 (1987).

5. J.M.T. Thompson and H. B. Stewart, pp. 177-183 in *Nonlinear Dynamics and Chaos*, John Wiley & Sons, New York, 1986.

6. Ref. 5, pp. 212-253.

personal computer. Some problems can even be solved on a small programmable calculator. In addition, students can gain considerable insight into the theory of chaos by performing a number of purely algebraic (i.e. noncomputational) exercises.

d. On the other hand, chaos can be appreciated on the aesthetic level. The beautiful pictures of fractals that appear in many books are widely regarded as a new art form. Fractals are an integral part of chaos theory, but the connection between chaos and fractals is not well understood by high-school and college students. Thus, it is important to understand, from an elementary point of view, how fractals are constructed (e.g., from an iterative process) and how they acquire such beautiful, yet complicated, forms. Also, programs written in simple languages like TurboBASIC can produce graphically many exotic fractal shapes.

e. It is expected that this project will be followed by other programs in which new kinds of physical or mathematical theories and methods are presented at the high-school level. We are firmly convinced that high-school science students can acquire skills in constructing simple numerical algorithms for solving certain classes of problems. Future books could deal with such methods, as well as other subjects not normally studied in high school.

IMPLEMENTATION OF MUON-INDUCED FISSION ON MASSIVELY PARALLEL SUPERCOMPUTERS

*V. E. Oberacker,¹ J. C. Wells,¹ A. S. Umar,¹
C. Bottcher, and M.R. Strayer*

We study the dynamics of a muon bound to a fissioning actinide nucleus. Since the excitation energy is above the fission barrier, we can treat the fission dynamics classically; the muon is described by the time-dependent Dirac equation; i.e., it moves under the influence of the time-dependent Coulomb potential that is generated by the fissioning nucleus. Because muon and fission dynamics are coupled, we can extract information about nuclear dissipation between the outer fission barrier and the scission point (Fig. 8. 2).

In the future, we plan to test the validity of one-body (mean-field) dissipation by coupling the muon dynamics with a microscopic TDHF description of fission. (In this way, we can also study the effects of triaxial nuclear shapes in fission.) Discrepancies between theory and experiment might be caused by two-body dissipation. Another question of interest is the degree of adiabaticity of the muonic motion; this

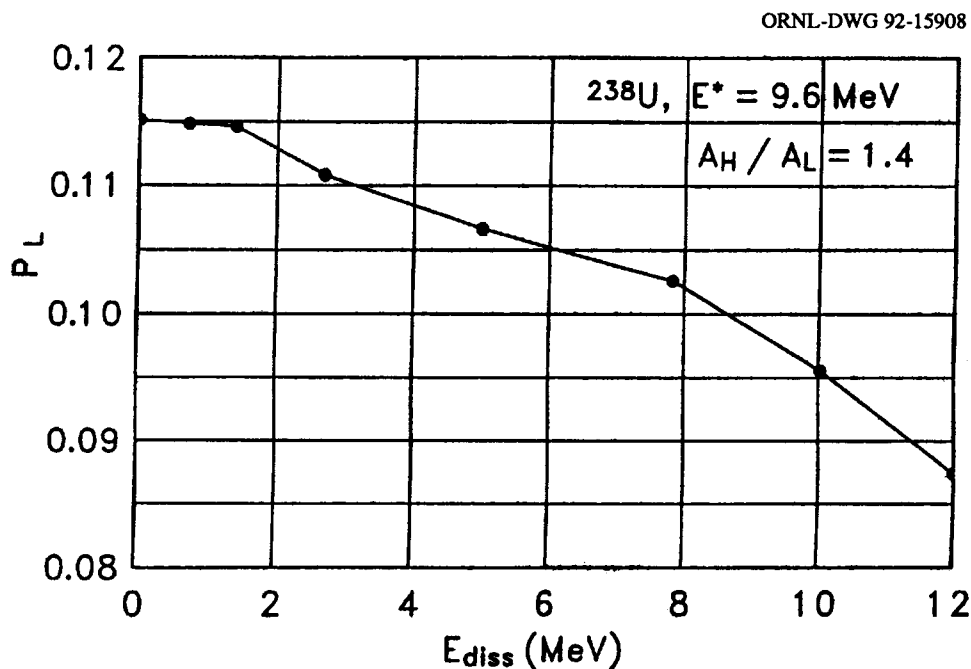


Fig. 8.2. Light fragment muon attachment probability.

can be studied by calculating a static "correlation diagram" for the transient muonic molecule on the lattice and comparing it to the expectation value of the muonic energy $E_\mu(t)$ in a dynamical run.

Current production runs have been carried out on the Cray-2 at NCSA using basis-spline collocation lattices with 29^3 mesh points. These calculations are still limited in accuracy; we would like to use lattices with 60-100 points in fission direction. To accomplish this goal, we are currently in the process of converting the code for runs on the new Intel Paragon massively-parallel supercomputer at ORNL.

1. Consultant from Vanderbilt University, Nashville, TN.

A NUMERICAL IMPLEMENTATION OF THE DIRAC EQUATION ON A HYPERCUBE MULTICOMPUTER¹

*J. C. Wells,² A. S. Umar,² V. E. Oberacker,²
C. Bottcher, M. R. Strayer, J.-S. Wu,³
J. Drake,⁴ and R. Flanery⁴*

The numerical methods used to solve the time-dependent Dirac equation on a three-dimensional Cartesian lattice are described. Efficient algorithms are required for computationally intensive studies of nonperturbative electromagnetic lepton-pair production in relativistic heavy-ion collisions. Discretization is achieved through the lattice basis-spline collocation method, in which quantum-state vectors and coordinate-space operators are expressed in terms of basis-spline functions on a spatial lattice. For relativistic lepton fields on a lattice, the fermion-doubling problem is central in the formulation of the numerical method. All numerical procedures reduce to a series of matrix-vector operations which we perform on the Intel iPSC/860 hypercube, making full use of parallelism. We discuss solutions to the problems of limited node memory and node-to-node communication overhead inherent in using distributed-memory, multiple-instruction, multiple-data-stream parallel computers.

1. Abstract of paper to be published in *International Journal of Modern Physics C*.

2. Consultant from Vanderbilt University, Nashville, TN.

3. Fayetteville State University, Fayetteville, NC.

4. Engineering Physics and Mathematics Division.

SOLUTION OF THE HELMHOLTZ-POINCARÉ WAVE EQUATION USING THE COUPLED BOUNDARY INTEGRAL EQUATIONS AND OPTIMAL SURFACE EIGENFUNCTIONS¹

*M. F. Werby,² M. K. Broadhead,² M. R. Strayer,
and C. Bottcher*

The Helmholtz-Poincaré wave equation (H-PWE) arises in many areas of classical wave-scattering theory. In particular, it can be found for the cases of acoustical scattering from submerged bounded objects and electromagnetic scattering from objects. The extended boundary integral equations (EBIE) method³⁻⁷ is derived from considering both the exterior and interior solutions of the H-PWE's. This coupled set of expressions has the advantage of not only offering a prescription for obtaining a solution for the exterior scattering problem, but it also obviates the problem of irregular values corresponding to fictitious interior eigenvalues. Once the coupled equations are derived, they can be obtained in matrix form by expanding all relevant terms in partial wave expansions, including a bi-orthogonal expansion of the Green's function. However, some freedom in the choice of the surface expansion is available since the unknown surface quantities may be expanded in a variety of ways so long as closure is obtained. Out of many possible choices, we develop an optimal method to obtain such expansions which is based on the optimum eigenfunctions related to the surface of the object. In effect, we convert part of the problem (that associated with the Fredholms integral equation of the first kind) to an eigenvalue problem of a related Hermitian operator. The methodology will be explained in detail and examples will be presented.

1. Abstract of published paper: pp. 245-258 in *Boundary Element Technology VII (Proceedings, Seventh International Conference on Boundary Element Technology, Albuquerque, New Mexico, June, 1992)* Computational Mechanics Publications, Boston and Elsevier Applied Science, New York, 1992.

2. Naval Research Laboratory, Stennis Space Center, MS.

3. P. C. Waterman, *J. Acoust. Soc. Am.* **45**, 1417 (1969).

4. P. C. Waterman, *J. Acoust. Soc. Am.* **60**, 567 (1976).

5. P. C. Waterman, pp. 61-78 in *Acoustic, Electromagnetic, and Elastic Wave Scattering - Focus on the T-Matrix Approach* (Pergamon Press, New York, 1980).

6. M. F. Werby and L. R. Green, *J. Acoust. Soc. Am.* **74**, 625 (1983).

7. M. F. Werby and S. Chin-Bing, *Int. J. Comput. Math. Appls.* **11**, 717 (1985).

SPLINE TECHNIQUES FOR SOLVING RELATIVISTIC CONSERVATION EQUATIONS¹

D. J. Dean,² C. Bottcher, M. R. Strayer, and G. Gatoff³

A new numerical method for solving the relativistic hydrodynamic equations based upon the basis-spline collocation approach is discussed. Analytical and numerical results are compared for several problems, including one-dimensional expansions and collisions for which analytical solutions exist. Methods, which may be easily and massively parallelized, are shown to give numerical results which agree to within a few percent of the analytic solutions. The relevance of the $v = z/t$ scaling solutions for the one-dimensional problem, when applied to relativistic heavy-ion collisions, is discussed. Applications to three-dimensional problems and present results for a typical three-dimensional expansion are discussed.

1. Abstract of paper submitted for publication in *International Journal of Modern Physics C*.

2. California Institute of Technology, Pasadena.

3. Oak Ridge Associated Universities Postgraduate Research Participant.

MONTE CARLO STUDY OF ONE-HOLE BAND STRUCTURE IN THE t-J MODEL¹

T. Barnes² and M. D. Kovarik³

Monte Carlo results are presented for the band structure of the lowest-lying $S_{\text{tot}} = 1/2$ one-hole band in the t-J model on 4×4 and 6×6 lattices. Measurements are reported for all $q\bar{q} \bar{k}$ states in the small-t/J regime $0 \leq t/J \leq 0.2$, and extrapolated to $0 \leq t/J \leq 0.5$. The results support the conjecture that the linear-t component of the bandwidth at small t/J vanishes proportionally to k/L^2 in the bulk limit, as was anticipated on theoretical grounds; this implies that the propagation of isolated holes is strongly hindered by the staggered magnetization of the ground state. For this initial study, a very simple trial wavefunction was used for importance sampling; it should be possible to obtain comparably accurate Monte Carlo results for band structure at appreciably larger t/J with improved importance sampling.

1. Abstract of paper to be published in *Physical Review B*.

2. UT-ORNL Collaborative Scientist.

3. Guest assignee from University of Tennessee, Knoxville.

I = 3/2 $K\pi$ SCATTERING IN THE NONRELATIVISTIC QUARK POTENTIAL MODEL¹

T. Barnes,² E. S. Swanson,³ and J. Weinstein⁴

I = 3/2 elastic $K\pi$ scattering is calculated to Born order using nonrelativistic quark wavefunctions in a constituent-exchange model. This channel is ideal for the study of nonresonant meson-meson scattering amplitudes since s-channel resonances do not contribute significantly. Standard quark-model parameters yield good agreement with the measured S- and P-wave phase shifts and with PCAC calculations of the scattering length. The P-wave phase shift is especially interesting because it is nonzero solely due to SU(3)_f symmetry-breaking effects, and is found to be in good agreement with experiment given conven-

tional values for the strange and nonstrange constituent quark masses.

1. Abstract of paper to be published in *Physical Review D*.

2. UT-ORNL Collaborative Scientist.
3. M.I.T., Cambridge, MA.
4. University of Mississippi, University.

ON THE EXCITATION SPECTRUM OF HEISENBERG SPIN LADDERS¹

T. Barnes,² E. Dagotto,³ J. Riera,³
and E. S. Swanson⁴

Heisenberg antiferromagnetic spin "ladders" (two coupled spin chains) are low-dimensional magnetic systems which, for $S = 1/2$, interpolate between half-integer-spin chains when the chains are decoupled, and effective integer-spin, one-dimensional chains in the strong coupling limit. The spin-1/2 ladder may be realized in nature by vanadyl pyrophosphate, $(VO)_2P_2O_7$. Strong-coupling perturbation theory, spin-wave theory, Lanczos techniques, and a Monte Carlo method are applied to determine the ground-state energy and the low-lying excitation spectrum of the ladder. Evidence is found of a nonzero spin gap for *all* interchain couplings $J_{\perp} > 0$. A band of spin-triplet excitations above the gap, which are referred to as "escalators," are also analyzed. These excitations are unusual for an antiferromagnet, since their long-wavelength dispersion relation behaves as $(k - k_0)^2$ (in the strong-coupling limit $J_{\perp} \gg J$, where J is the in-chain antiferromagnetic coupling). Their band is folded, with a minimum energy at $k_0 = \pi$, and a maximum between $k_1 = \pi/2$ (for $J_{\perp} = 0$) and 0 (for $J_{\perp} = \infty$). Numerical results are also given for the dynamical structure factor $S(q, \omega)$, which can be determined in neutron scattering experiments. Finally, possible experimental techniques for studying the excitation spectrum are discussed.

1. Abstract of paper to be published in *Physical Review B*.

2. UT-ORNL Collaborative Scientist.
3. Florida State University, Tallahassee.
4. M.I.T., Cambridge, MA.

DEVELOPMENT OF RELATIVISTIC HYDRODYNAMICS FOR HEAVY-ION AND ASTROPHYSICS APPLICATIONS

Z. Eitzen,¹ D. J. Dean,² M. R. Strayer,
and M. W. Guidry³

The advance of computer technology has made it increasingly possible to perform calculations involving complicated nonlinear equations, particularly those exhibiting strong discontinuities such as shock fronts. The macroscopic equations of astrophysics, whether appearing in cosmology, stellar structure, or diffuse matter tend to fall in this class. The difficulty of describing phenomena involving multiple time and distance scales, and strong discontinuities, frequently leads to the patching together of somewhat discordant models for different regimes. The Oak Ridge theory section has developed numerical methods for relativistic hydrodynamics that can be readily adapted to modeling supernovae and other explosive stellar processes in a more unified manner. In particular, we might hope to relax the customary assumptions of spherical and cylindrical symmetry. These codes are readily adaptable to massively parallel architectures, allowing us to contemplate large, three-dimensional lattices. Thus, we hope to apply sufficient computer power to significantly advance the state of supernovae and nucleosynthesis modeling.

We have initiated such a program to adapt the relativistic hydrodynamics code to the calculation of supernova explosions, without imposing the usual assumption of spherical symmetry. As an initial step in this adaptation, the code has been applied to calculations of relativistic heavy-ion collisions on Cray computers, and a version incorporating gravitation has been tested on the hypercube.

We are presently discussing a collaboration to perform such calculations with S. W. Bruenn from Florida Atlantic University and A. Mezzacappa from the University of North Carolina. We anticipate that such two-dimensional calculations of supernova explosions would allow possible effects of angular momentum and corresponding anisotropies to be studied in the core collapse and bounce.

1. UT-ORNL Science Alliance participant, summer, 1992.

2. Consultant from California Institute of Technology, Pasadena.
3. Adjunct staff member from University of Tennessee, Knoxville.

NUCLEAR PHYSICS

DYSON'S EQUATIONS FOR NUCLEON- PION-DELTA INTERACTIONS: TOWARD A SELF-CONSISTENT SOLUTION IN NUCLEAR MATTER¹

K.T.R. Davies

A formalism is developed for the self-consistent solution of Dyson's equations for the pion and the delta in cold nuclear matter. The nucleon-delta and nucleon-pion "loop integrals" are evaluated and are inserted into the pion and delta-particle propagators, respectively. The resulting pion propagator displays two distinct families of "spikes" which are dramatically different from the free-space behavior. In particular, there are significant high-momentum components of the pion which give large contributions to the nucleon-pion loop integral. Such contributions lead to severe spikes in the iterated delta propagator. Studies are made too of the sensitivity of the results of the cutoff range of the "form factor" used to evaluate the loop integrals, to the starting solution, and to the density. Also, for the densities studied here, the pion propagator exhibits pure delta-function singularities, which occur over a small range of energies just above the mass of the pion. However, it is shown that such delta functions have a negligible effect on the main calculation. Finally, this paper gives a comprehensive treatment of the main methods used to solve the nuclear matter Dyson's equations.

1. Abstract of published paper: *Ann. Phys.* **215**, 386 (1992).

RETARDATION AND DISPERSIVE EFFECTS IN THE NUCLEAR MEAN FIELD¹

C. Mahaux², K.T.R. Davies, and G. R. Satchler

The one-body potential which represents the average interaction between a particle and a medium depends upon energy. This is equivalent to a nonlocality in time. The energy dependence and the nonlocality in time are connected by a Fourier transform. The temporal nonlocality is a retardation effect because it entails that the wave function at time t is influenced only by its values at other times which

must be prior to t . This reflects a causality property. We investigate the temporal nonlocality of the nuclear mean field. A comparison is made with the temporal nonlocality of the relation between the electric displacement and the electric field in classical electrodynamics. We consider several parametrizations of the energy dependence of the imaginary part of the mean field for nucleons, as well as heavy ions. These parametrizations specify the energy dependence of the corresponding real part, because the real and imaginary parts are connected by a dispersion relation. The latter can be viewed as equivalent to the causality property. Since Hilbert transforms appear in the dispersion relation and since Fourier transforms give the correspondence between energy dependence and temporal nonlocality, we derive several properties of these transforms which are of particular interest in the present context. The most useful one is that the Fourier transform of a function $F(E)$, which is analytic in the upper half of the complex E -plane, can be expressed in terms of the Fourier transform of the imaginary part of $F(E)$ alone. We investigate several schematic models for the mean field. They fall into two main categories. These correspond to the two main definitions which have been proposed for the mean field, namely the self-energy and Feshbach's potential, respectively. Both of these definitions can be used for the nucleon-nucleus system, in which case they correspond to two different ways of handling the combined influence of ground-state correlations and antisymmetrization. The resulting two mean fields have different energy dependencies and, correspondingly, temporal nonlocalities. Feshbach's approach can also be applied to the nucleus-nucleus system. Our schematic models are semirealistic in the sense that they all take account of the "Fermi surface anomaly" for the nucleon-nucleus system or of the "threshold anomaly" for the nucleus-nucleus case. The temporal nonlocality is investigated for each model. A physical interpretation of this nonlocality is given in terms of a time delay of the response of the medium, in which an incident wave is partially trapped in nonelastic channels and subsequently re-emitted. This interpretation is buttressed by the form of the continuity equation in the presence of an energy-dependent mean field.

1. Abstract of paper to be published in *Physics Reports*.

2. University of Liege, Belgium.

ANALYSIS OF AN UNUSUAL POTENTIAL AMBIGUITY FOR $^{16}\text{O}+^{16}\text{O}$ SCATTERING¹

M. E. Brandan,² K. W. McVoy,³ and G. R. Satchler

Woods-Saxon optical-potential fits to recent measurements of $^{16}\text{O}+^{16}\text{O}$ elastic scattering at 350 MeV have been interpreted as providing clear evidence for a nuclear rainbow. Three model-independent potentials have also recently been found to reproduce these data. Two of them were indeed found to be members of a rainbow series, in which a distinctive minimum near 44° is the first or second Airy minimum of a rainbow pattern, but the scattering by the third (shallower) potential was less easy to interpret. We show here that this potential achieves its fit to the data by a different and somewhat unconventional mechanism. This serves as a reminder that ambiguities in interpretation can persist, even with as extensive and accurate a data set as this measurement provides.

1. Abstract of published paper: *Phys. Letts. B* **281**, 185 (1992).

2. Universidad Nacional Autonoma de Mexico, DF Mexico.

3. University of Wisconsin, Madison.

ELASTIC SCATTERING OF ^{11}Li AND ^{11}C FROM ^{12}C at 60 MeV/NUCLEON¹

*J. J. Kolata,² M. Zahar,² R. Smith,³ K. Lamkin,²
M. Belbot,² R. Tighe,⁴ B. M. Sherrill,⁵ N. A. Orr,⁵
J. S. Winfield,⁵ J. A. Winger,⁵ S. J. Yennello,⁵
G. R. Satchler, and A. H. Wuosmaa⁶*

The elastic scattering of the exotic "halo" nucleus ^{11}Li on ^{12}C has been studied at an energy of 60 MeV/nucleon and compared with that of the $A=11$ isobar ^{11}C . The prediction of enhanced refraction in the former system is confirmed, as is the need for very long-range absorption. No evidence is found for an Airy minimum in the farside scattering.

1. Abstract of paper submitted for publication in *Physical Review Letters*.

2. University of Notre Dame, Indiana.

3. Hospital of the University of Pennsylvania, Philadelphia.

4. Lawrence Berkeley Laboratory.
5. Michigan State University, East Lansing.
6. Argonne National Laboratory.

TEMPORAL NONLOCALITY OF NUCLEAR AND ATOMIC MEAN FIELDS¹

C. Mahaux² and G. R. Satchler

Microscopic theories of the nuclear and atomic mean fields lead to a potential which is nonlocal in time as well as in space. Some properties of the temporal nonlocality are examined, including the consequences of requiring that causality be satisfied. One of these consequences is that the temporal nonlocality is fully determined by the energy dependence of the imaginary part of the field. It is shown that different temporal nonlocalities are associated with the two basic microscopic definitions of the mean field, namely Feshbach's potential and the self energy. A physical interpretation of the temporal nonlocality is presented in terms of a time delay induced by couplings to nonelastic channels. Models for the temporal nonlocality of the nucleon-nucleus mean field are analyzed.

1. Abstract of paper to be published in *Nuclear Physics A*.

2. University of Liege, Belgium.

FURTHER STUDIES OF THE EXCITATION OF THE EVEN Zr ISOTOPES BY 70 MeV ^6Li AND OTHER IONS

D. J. Horen and G. R. Satchler

An analysis is reported elsewhere¹ of the inelastic excitation of the even Zr isotopes by ^6Li ions at 70 MeV, together with a comparison of the implied isospin structures of the transitions with those derived using other probes. Concomitant investigations of the reaction mechanisms involved that have been completed or are still in progress will be reported separately. These are largely based upon folding model calculations that allow the comparison of different reactions in a consistent way by using common transition densities. They include:

(i) Studies of the radial localizations of the interactions by modulating the transition densities with rounded or sharp radial cutoffs and calculating the cross sections as a function of the cutoff radius. These reveal which radial regions the scattering is sensitive to. In particular, it was found that 70-MeV ${}^6\text{Li}$, 35-MeV α -particles, and 160-MeV pions experience the same parts of the transition densities, typically from ~ 4 to ~ 7 fm.

(ii) Studies of the effective projectile-target nucleon interaction, another factor to be determined for each system. The ranges and strengths are determined by fitting the measured elastic scattering. This fixes the monopole component for a given model interaction, but it is possible for models that have the same monopole to differ in the higher-multipole components that are required for inelastic scattering. Various simple, local models were investigated, such as a single Yukawa or Gaussian, and a sum of Yukawa terms. Although some sensitivity was found, it is not great.

(iii) In addition, more routine studies, such as the consequences of optical potential ambiguities, comparison of coupled channels with the DWBA, reorientation effects, etc.

1. See D. J. Horen et al., "Systematics of Isospin Character of Transitions to the 2_1^+ and 3_1^- States in ${}^{90,92,94,96}\text{Zr}$," this report.

A "TOY" MODEL TO ILLUSTRATE THE DISPERSIVE AND RETARDATION PROPERTIES OF A MEAN FIELD

V. A. Madsen¹ and G. R. Satchler

Recent studies² have focused upon the general properties expected for dynamic polarization potentials; i.e., the (complex) contributions to an optical potential, or mean field, that arise from couplings to nonelastic channels, when the condition of causality is imposed. The potential U may be written

$$U(E) = V_0 + \Delta U(E) \quad (1)$$

where V_0 is the real and energy-independent (but possibly nonlocal) "bare" potential (e.g., a Hartree-Fock potential), while the polarization potential

$$\Delta U(E) = \Delta V(E) + iW(E) \quad (2)$$

arises from couplings to nonelastic channels. The real part ΔV results from virtual excitations, while the imaginary part W describes the actual absorption of flux into these channels when they are energetically open. The energy dependence translates into a nonlocality in time when a time-dependent description is used. In this representation we have the Fourier transform

$$\tilde{U}(t, t') = 2\pi \int_{-\infty}^{\infty} dE U(E) e^{iEt}. \quad (3)$$

Invariance under translation in time ensures that \tilde{U} depends only upon the temporal difference $\tau = t - t'$. The causality condition is

$$\tilde{U}(t, t') = 0 \quad \text{if } t' > t, \quad (4)$$

so that the wavefunction at time t cannot be influenced by the wavefunction at later times $t' > t$. Corresponding to Eqs. (1) and (2), we have

$$\tilde{U}(\tau) = V_0 \delta(\tau) + \Delta \tilde{V}(\tau) + i\tilde{W}(\tau), \quad (5)$$

where the bare potential V_0 corresponds to an instantaneous term, while $\Delta \tilde{V}$ and \tilde{W} are the Fourier transforms of $\Delta V(E)$ and $W(E)$.

A theorem due to Titchmarsh³ shows that the condition (4) requires that $\Delta V(E)$ and $W(E)$ are a Hilbert transform pair (i.e., satisfy dispersion relations) and that their Fourier transforms are related by

$$\begin{aligned} \Delta \tilde{V}(\tau) &= i\tilde{W}(\tau), & \tau > 0 \\ &= -i\tilde{W}(\tau), & \tau < 0. \end{aligned} \quad (6)$$

It is very helpful to have an explicit "toy" model to illustrate analytically the emergence of these and other properties. The toy consists of a system in which the projectile that is incident upon a target does not experience any bare diagonal interaction ($V_0 = 0$ above) but is coupled to a single excited state of the target by a delta function at the surface of the target. This is a very simplified version of a system in which the projectile excites surface vibrations of the target. Then by projection upon the elastic channel, we find the equivalent complex potential $\Delta U(E)$ which gives

the same elastic wavefunction and scattering. The resulting optical potential is analytic in the finite E plane except for a branch cut along the real axis from the first excited state to infinity. We then show explicitly, with careful attention to the analytic properties, how the real and imaginary parts satisfy Eqs. (4) and (6). The latter result and an explicit expression for the nonlocal time dependence of the potential are obtained by transforming the Fourier transform to momentum k -space, which results in an integrand which is analytic in the entire finite plane. The integration path in k , which comes down from $i=\infty$ along the imaginary axis and goes out to infinity along the real axis, can then be deformed into paths which yield elementary integrals. These are easily evaluated.

1. Oak Ridge Associated Universities Faculty Research Participant from Oregon State University.

2. See, for example, C. Mahaux, K.T.R. Davies, and G. R. Satchler, "Retardation and Dispersive Effects in the Nuclear Mean Field;" C. Mahaux and G. R. Satchler, "Temporal Nonlocality of Nuclear and Atomic Mean Fields," this report.

3. E. C. Titchmarsh, *Introduction to the Theory of Fourier Integrals* (Oxford University Press, Oxford, 1937).

WHERE ARE PION INELASTIC INTERACTIONS LOCALIZED?

R. L. Varner and G. R. Satchler

Further studies are underway to see which radial region of a transition density is being explored by measurements of pion inelastic scattering on various nuclei and at various energies. These are of interest because apparent anomalies in the ratios of cross sections for exciting giant quadrupole resonances (GQR) by π^+ and π^- scattering have been attributed^{1,2} to the pions only experiencing the extreme tails of the transition densities, where coupling to the continuum tends to make the neutron component dominate over the proton part. In addition, it is important to know the conditions under which the scattering may be sensitive to the detailed structure of transition densities that have been generated by microscopic nuclear structure theories (such as the RPA). This is being done by calculating cross sections using transition

densities which have been modulated by cutoff functions which eliminate the parts inside a cutoff radius $r = c$, and studying the variation with c . In a previous study,³ RPA transition densities for the GQR in ^{208}Pb were used to show that only 10% of the cross section for excitation by 162 MeV π^+ remained when a cutoff of $c \approx 8$ fm was imposed. This is in contradiction to the earlier argument,¹ using these same transition densities, to explain the π^+/π^- anomaly in this case by assuming that these pions did not experience radii smaller than about 8 fm.

Analogous studies are being made for excitation of the first 2^+ and 3^- states in the even Zr isotopes, for which open-shell RPA transition densities are also available.⁴ At energies near the (3,3) resonance, the pion scattering is sensitive to a radial region ($4 \leq r \leq 7$ fm) which is very similar to that found for excitation of these states by α -particles and ^6Li ions. However, there are indications that pions of lower energy, say 50 MeV, may be sensitive to radii as small as 2 fm.

1. B. Castel et al., *J. Phys. G* **15**, L237 (1989); *Z. Phys. A* **334**, 381 (1989); *Nucl. Phys. A* **514**, 682 (1990).

2. R. J. Peterson et al., *Nucl. Phys. A* **435**, 717 (1985); *ibid A* **459**, 445 (1986).

3. G. R. Satchler and B. Castel, *Phys. Div. Prog. Report for period ending Sept. 30, 1991*, ORNL-6689, p. 187 (1992).

4. See D. J. Horen et al., "Systematics of Isospin Character of Transitions to the 2_1^+ and 3_1^- States in $^{90,92,94,96}\text{Zr}$," this report.

A NEW EFFECTIVE INTERACTION FOR PERIPHERAL HEAVY-ION COLLISIONS

G. R. Satchler

A standard technique¹ for extracting an inelastic transition strength for a given nuclear transition excited by a particular projectile has been to find a phenomenological optical potential (frequently of Woods-Saxon form) which fits the measured elastic scattering, and then apply a deformation prescription to generate a transition potential for the inelastic scattering. The measured inelastic cross sections then have been used to deduce a deformation parameter or, more recently, a deformation length with which to characterize the transition strength. This

procedure involves assumptions about the relation of the transition density, a property of the target nucleus, to the transition potential, which is a property of the target-projectile system.

A more consistent way to compare transition strengths excited by different probes is to model the transition density itself, independently of the projectile. This then requires knowledge of an effective interaction between the projectile and each target nucleon. A minimum of three parameters, a complex "strength" and a "range," are required to specify the interaction. These can be determined by fitting the measured elastic scattering, and then applied to the inelastic scattering.

Initial studies were made using a single Yukawa or a single Gaussian for the nucleon-nucleon effective interaction, applied to elastic scattering data for $^{16,17}\text{O}$ on targets of ^{208}Pb at energies ranging from $E/A = 20$ to 94 MeV. Either Gauss or Yukawa forms gave acceptable fits, with smoothly and slowly varying strengths, although the optimum Gaussian range also varied slowly with energy from 1.65 fm at the lowest to 1.43 fm at the highest energy. On the other hand, the optimum Yukawa range was close to 0.7 fm at all energies, and this was judged to be preferable. The corresponding strengths had real and imaginary parts almost equal, with a slow energy dependence given approximately by

$$v \approx w \approx -54 = (2E / 9A) \text{ MeV}. \quad (1)$$

This Yukawa interaction was then applied successfully to data for ^{17}O scattering from $^{90,92,94,96}\text{Zr}$ and $^{112,118,124}\text{Sn}$ at $E/A = 84$ MeV. In addition, predictions were made for ^6Li scattering from the same Zr isotopes at $E/A = 11.7$ MeV, although one expects break-up effects to modify the potentials for ^6Li . To our surprise, the measured scattering was reproduced very well. Subsequent analysis² showed the optimum Yukawa range again to be close to 0.7 fm, and the strengths to be a few per cent less than given by Eq. (1).

The present need is to extend these studies to other projectiles and targets, and this is being done currently. However, it is already clear that such a simple interaction has its limitations. For example, scattering data for light systems such as $^{12}\text{C}+^{12}\text{C}$ reveal characteristics of rainbow scattering which imply sensitivity to the optical potentials somewhat inside the grazing radius.³ Our Yukawa interaction is unable to reproduce these data; the associated real

potential appears to be too weak at these smaller radii, whereas folding with a more complicated and density-dependent interaction is successful.⁴ However, our simple interaction is enjoying a measure of success for scattering that is dominated by peripheral, or grazing, collisions. Cases that are sensitive to both the slope and strength of the potential in the grazing region allow us to determine both range and strength of the effective interaction.

1. G. R. Satchler, *Direct Nuclear Reactions* (Oxford University Press, Oxford, England, 1983).

2. See D. J. Horen et al., "Systematics of Isospin Character of Transitions to the 2_1^+ and 3_1^- States in $^{90,92,94,96}\text{Zr}$," this report.

3. K. W. McVoy and G. R. Satchler, *Nucl. Phys. A* **417**, 157 (1984).

4. M. E. Brandan and G. R. Satchler, *Nucl. Phys. A* **487**, 477 (1988).

LOCAL POTENTIAL AND S-MATRIX ANALYSIS OF PION-NUCLEUS SCATTERING

G. R. Satchler, M. B. Johnson,¹
and R. S. Mackintosh²

A project has been initiated to determine local potentials which describe pion-nucleus scattering. Such potentials may provide more immediate physical insight into the scattering process than the nonlocal potentials generally used. Two approaches are being used. When the scattering can be described by a momentum-dependent potential of the Kisslinger form, an exact local equivalent can be defined analytically.³ The other approach involves a (complex) phase-shift analysis of the data followed by inversion of the S-matrix to give a local potential.⁴ This procedure has been used successfully in analyses of both nucleon and heavy-ion scattering. An initial question is whether the pion data are extensive enough that ambiguities and uncertainties in this method can be kept within reasonable bounds. Some indication that at least some data sets are adequate is given by the results of another "model-independent" local potential analysis⁵ using the Fourier-Bessel method. In addition, the phase-shift analysis alone provides information that can be used in investigations of the

optics of pion scattering without the use of an intermediate potential.

-
1. Los Alamos National Laboratory, Los Alamos, NM.
 2. The Open University, Milton Keynes, U.K.
 3. M. B. Johnson, *Phys. Rev. C* **22**, 192 (1980).
 4. S. G. Cooper, M. A. McEwan, and R. S. Mackintosh, *Phys. Rev. C* **45**, 770 (1992).
 5. E. Friedman, *Phys. Rev. C* **28**, 1264 (1983).

ORIGIN OF THE SOFT p_T SPECTRA¹

G. Gatoff² and Cheuk-Yin Wong

In high-energy collisions, the soft p_T spectra for produced mesons contain information on the motion of the quarks and antiquarks which form these mesons. We extract this information in the context of the flux-tube model with Schwinger's mechanism for particle production. We solve the Dirac equation for quarks (and antiquarks) inside a flux tube, described as an infinitely long cylinder of radius r_0 , with a uniform electric field k inside it. We calculate the production rate of quarks, antiquarks, and pions as a function of p_T . We study first a sharp transverse boundary, and find that the result deviates from the experimental soft p_T spectra, with its characteristic exponential fall. We therefore introduce a scalar potential which varies smoothly in the radial direction. With simplifying assumptions, we show how the experimental p_T spectra of pions, created in p-p collisions, determine the transverse wave function and the scalar potential that would produce it. The classical turning point for this potential is of the order of 0.6 fm. However, the potential flattens out considerably beyond that point. The wave function decays as $r^{-3/2}$, and there appears to be a considerable excursion of the quark into regions far beyond the classical turning point.

-
1. Abstract of published paper: *Phys. Rev. D* **46**, 997 (1992).
 2. Oak Ridge Associated Universities Postgraduate Research Participant.

EFFECT OF BOUNDARY ON MOMENTUM DISTRIBUTION OF QUARKS IN A QUARK-GLUON PLASMA¹

Cheuk-Yin Wong

A quark in a quark-gluon plasma can travel within the boundary of the plasma, which has a physical dimension of the order of the size of the colliding nuclei producing the plasma, in contrast to a quark in hadronic matter which travels within the boundary of a hadron. The plasma boundary affects the momentum distribution of quarks and consequently the magnitudes of signals for the search of the quark-gluon plasma.

-
1. Abstract of paper submitted for publication in *Physical Review Letters*.

THE TRANSVERSE PROFILE OF A COLOR FLUX TUBE¹

Cheuk-Yin Wong and G. Gatoff²

The p_T spectra of soft mesons produced in high-energy collisions contain information on the transverse motion of quarks and antiquarks which form these mesons. Using these data, we study the transverse profile of the color flux tube in the context of the Schwinger's mechanism for particle production by representing the transverse profile in terms of an effective transverse scalar potential. We find that the classical turning point for the potential is of the order of 0.6 fm. However, the potential flattens out considerably beyond that point. Consequently, the wave function decays surprisingly slowly in the transverse direction as $r^{-3/2}$ and extends much beyond the radius of the flux tube.

-
1. Abstract of paper to be published in the *Proceedings of Realistic Nuclear Structure*, Stony Brook, New York, May 28-30, 1992.
 2. Oak Ridge Associated Universities Postgraduate Research Participant.

NUCLEAR STOPPING POWER AND RECOILING NUCLEONS¹

Bao-An Li² and Cheuk-Yin Wong

We examine the use of the momentum distribution of recoiling nucleons to study the stopping power law of nuclear matter for incident nucleons with high energies. The dependence of the momentum distribution on the stopping-power index is studied in detail for both leading nucleons and recoiling nucleons in p+d reactions. There are two regions where the momentum distribution of the recoiling nucleons is sensitive to the stopping power law. This sensitivity can be used to study the stopping power law experimentally.

-
1. Abstract of paper to be published in *Physica Scripta*.
 2. Hahn-Meitner Institute, Berlin, Germany.

FORMATION AND DECAY OF TOROIDAL AND BUBBLE NUCLEI AND NUCLEAR EQUATION OF STATE¹

*H. M. Xu,² J. B. Natowitz,² C. A. Gagliardi,²
R. E. Tribble,² C. Y. Wong,
W. G. Lynch,³ and P. Danielewicz³*

Multifragmentation, following the formation of toroidal and bubble nuclei, is observed with an improved BUU model for central ⁹⁰Mo+⁹⁰Mo collisions. We find that the multifragmentation pattern depends sensitively on the nuclear equation of state. With a stiff equation of state, simultaneous explosion into several intermediate mass fragments (IMF) in a ring-like manner occurs due to the formation of metastable toroidal nuclei. In contrast, with a soft equation of state, simultaneous explosion into several IMF's in a volume-like manner occurs due to the formation of metastable bubble nuclei. For both cases, however, the kinetic energies of the IMF's in the center of mass are surprisingly small. We suggest the observation of nearly coplanar emission of IMF's with similar masses and energies in the center-of-mass frame as a key signature for the formation of toroidal nuclei.

-
1. Abstract of paper submitted for publication in *Physical Review Letters*.

2. Texas A&M University, College Station.
3. Michigan State University, East Lansing.

NONAPPEARANCE OF DEHNEN-SHAHIN RESONANCES IN THE POSITRONIUM CONTINUUM¹

Chun Wa Wong² and Cheuk-Yin Wong

The Dehnen-Shahin relativistic equations for the positronium are found to have no resonant solutions in both the ¹S₀ and the ³P₀ positronium continua. A certain pole singularity appearing in the ¹S₀ potential gives rise to resonances, but only if the electromagnetic interaction strength is increased 200-fold or more. The origin of the zero width property of the resonances are also understood. The same singularity even in a weak potential shows an unacceptable infrared pathology in which an infinite number of spurious bound states appear at zero energy. The strange similarity of Spence-Vary ³P₀ resonances to resonances in an infinite square-well potential is noted.

-
1. Abstract of paper submitted for publication in *Physics Letters*.
 2. University of California, Los Angeles.

EFFECT OF QUARK-GLUON PLASMA BOUNDARY ON THE MOMENTUM DISTRIBUTION OF QUARKS¹

Cheuk-Yin Wong

The boundary of a quark-gluon plasma affects the momentum distribution of quarks in the plasma. In particular, a transverse boundary leads to a transverse momentum distribution with a shape different from the thermal distribution, especially in the high transverse momentum region. In consequence, boundary effect must be taken into account if one wishes to estimate the magnitudes of signals in a search for the quark-gluon plasma.

-
1. Abstract of paper to be published in the *Proceedings of the XXII International Symposium on Multiparticle Dynamics*, Santiago de Compostela, Spain, July 13-17, 1992.

DO NUCLEONS IN ABNORMAL-PARITY STATES CONTRIBUTE TO DEFORMATION?¹

K. H. Bhatt,² C. W. Nestor, Jr.,³ and S. Raman

We consider intrinsic states of highly deformed nuclei in the framework of the universal Woods-Saxon model and show that valence nucleons in abnormal-parity high- j states contribute $\sim 20\%$ to the electric quadrupole moments of these nuclei. Similarly, we show that in the single-shell asymptotic Nilsson model this contribution is $\sim 25\%$ if reasonable effective charges are employed. We discuss, at some length, procedures used to arrive at reasonable effective charges. Both models reproduce the measured $B(E2; 0_1^+ \rightarrow 2_1^+)$ values in the rare-earth and actinide regions without the need for normalization constants. No support is found for the assumption made in the pseudo-SU(3) and the fermion dynamic symmetry models that valence nucleons in abnormal-parity high- j states do not contribute to deformation. This counterintuitive assumption leads to an underestimate of the $B(E2; 0_1^+ \rightarrow 2_1^+)$ values, which is compensated in these models by the use of appropriate normalization constants. Once the magnitudes are fixed, both models do correctly reproduce the $B(E2)$ trends.

1. Abstract of published paper: *Phys. Rev. C* **46**, 164 (1992).

2. University of Mississippi, University.

3. Computer and Telecommunications Division.

HARTREE-FOCK-BOGOLIUBOV CALCULATIONS IN CONNECTION WITH RADIOACTIVE ION BEAM FACILITY

D. R. Kegley,¹ V. E. Oberacker,² M. R. Strayer, and A. S. Umar²

The long-term goal of this project is to calculate binding energies, potential energy surfaces, and energy spectra for nuclei throughout the periodic table. This allows us to investigate the limits of nuclear stability, in particular in connection with astrophysics experiments at ORNL's Radioactive Ion Beam Facility (RIB). We also want to study new phenomena in nuclear shape isomerism (superdeformation, hyperdeformation). Starting from an effective

nucleon-nucleon interaction, we utilize various approximation schemes of microscopic many-body theory; the currently available mean-field (Hartree-Fock) code will be extended to include self-consistent pairing (Hartree-Fock-Bogoliubov). An unconstrained variation of the Hamiltonian density gives the binding energy, while a constrained variation (quadrupole and higher moments) yields a multidimensional collective potential energy surface. For a realistic description of pairing phenomena, it will be necessary to replace the zero-range Skyrme nucleon-nucleon interaction by a finite-range interaction. From a least-square fit to measured binding energies and rms radii of spherical nuclei, we can determine the parameters of the effective interaction. This fit is most easily done in a one-dimensional H-F-B code (in spherical coordinates). This code allows us also to study the pairing gap as a function of the density; in particular, in the low-density regime, one expects dramatic differences between the Nilsson-Strutinsky, H-F-B, and BCS approaches. For nuclear structure studies of deformed nuclei, we plan to extend the above studies into two- and three-space dimensions, respectively. We will develop a two-dimensional H-F-B code (using cylindrical coordinates) and a three-dimensional H-F-B code (in Cartesian coordinates). All calculations will be carried out on basis-spline collocation lattices, and we intend to do production runs on the Intel Paragon massively-parallel supercomputer at ORNL.

The H-F-B method can be extended to calculate nuclear energy spectra by the QLR (quasiparticle linear response) method. Computational techniques can be borrowed from earlier TDHF calculations.

1. Vanderbilt University, Nashville, TN.

2. Consultant from Vanderbilt University, Nashville, TN.

STUDY OF NUCLEAR DISSIPATION VIA MUON-INDUCED FISSION: A RELATIVISTIC LATTICE CALCULATION¹

V. E. Oberacker,² A. S. Umar,² J. C. Wells,² M. R. Strayer, and C. Bottcher

Excited muonic atoms in the actinide region may induce prompt nuclear fission via inverse internal conversion. We solve the time-dependent Dirac

equation for a state describing a muon in the Coulomb field of the fissioning nucleus on a three-dimensional lattice and demonstrate that the muon attachment probability to the light fission fragment is inversely proportional to the energy dissipated during fission.

1. Abstract of paper to be published in *Physics Letters*.

2. Consultant from Vanderbilt University, Nashville, TN.

STUDIES OF ELECTROMAGNETIC LEPTON-PAIR PRODUCTION WITH CAPTURE IN RELATIVISTIC HEAVY-ION COLLISIONS

J. C. Wells,¹ V. E. Oberacker,¹ A. S. Umar,¹
C. Bottcher, and M. R. Strayer

Lepton-pair production from the quantum electrodynamic (QED) vacuum during peripheral relativistic heavy-ion collisions continues to be an area of active research. We are currently studying nonperturbative QED effects in lepton-pair production with capture of the negative lepton into an atomic state of a participating heavy ion using numerical lattice solutions of the time-dependent Dirac equation in three Cartesian dimensions. Progress has been made with this approach in successfully implementing the physical interaction into the lattice solution (i.e., no screening), and in increasing the size of the lattice basis employed. The latter has been achieved through the use of improved algorithms and massively-parallel computing, and the former through a gauge transformation performed on the time-dependent electromagnetic interaction.^{2,3} Using the Intel hypercube at ORNL, our code performs 600-700 million floating-point operations per second for a lattice of 64^3 points. Convergent calculations will require approximately 100^3 lattice points and the latest supercomputer technology (i.e., Intel's Paragon).

Technical refinements in our code have produced improved results. In particular, we have learned that our solution of the fermion-doubling problem for lattice fermion dynamics² is inadequate in describing continuum excitation phenomena. Previously, we have used forward and backward derivatives (D^+ and

D^-) constructed from a Cholesky decomposition of the basis-spline-collocation representation of the second-derivative operator ($D^2 = D^+D^-$) to discretize the lower and upper components of the Dirac spinor, respectively.^{3,4} While this prescription avoids the doubled spectrum and anomalous high frequencies in the Dirac spinor indicative of fermion doubling, it does not satisfy the specified boundary conditions with sufficient accuracy. Using the Cholesky decomposition, errors develop in the continuum components of the time-dependent spinor on the boundary of the physical box which are significant compared to the magnitude of the observables.

Use of the symmetric representation of the first derivative in discretizing the Dirac spinor satisfies the boundary conditions accurately allowing the description of continuum excitations, but does not address fermion doubling. However, using the basis-spline-collocation method, fermion doubling is manifest only when the lattice spacing is approximately equal to or less than the lepton's Compton wavelength. As we are currently unable to pursue convergent calculations, we are, for the present time, using the symmetric derivatives in our calculations, choosing to defer the solution of the fermion-doubling problem until later. We have confidence that the fermion-doubling problem can be solved consistently with the boundary conditions using basis-spline collocation by one of several methods (e.g., momentum damping using Fourier analysis).

We are currently performing extensive studies of impact-parameter dependencies of muon capture probability with the goal of reproducing first-order calculations in a perturbative regime. In particular, we are attempting to produce agreement with the exponential decay of the lepton capture probability at large impact parameter predicted by low-order theories. Reproducing this exponential behavior insures that probabilities at large impact parameter are weighted correctly in cross-section integrations.

1. Consultant from Vanderbilt University, Nashville, TN.

2. J. C. Wells et al., *Phys. Rev. A* **45**, 6296 (1992).

3. J. C. Wells et al., pp. 1-32 in *Proceedings, 1991 Annual Users' Conference, Dallas, Texas, October 6-9, 1991*.

4. J. C. Wells et al., to be published in *International Journal of Modern Physics C*.

DYNAMICAL CALCULATION OF CENTRAL ENERGY DENSITIES IN RELATIVISTIC HEAVY-ION COLLISIONS'

D. J. Dean,² A. S. Umar,³ and M. R. Strayer

The 3+1 dimensional string-parton model is used to calculate energy densities and temperatures of produced mesons during relativistic heavy-ion collisions. Maximum energy densities with the experimental estimates obtained from the Bjørken formula are compared. Although the string-parton model reproduces transverse energy distributions, $dE_T/d\eta$, the dynamical energy densities of the produced mesons are three to four times smaller than estimates based on the Bjørken formula with a formation time of 1 fm/c. Various time scales which contribute to this discrepancy are discussed, and a modified interpretation of the Bjørken formula is suggested.

- 1. Abstract of paper submitted for publication in *Physical Review Letters*.
- 2. California Institute of Technology, Pasadena,
- 3. Consultant from Vanderbilt University, Nashville, TN.

SOLUTION OF A CLASS OF STURM-LIOUVILLE PROBLEMS USING THE GALERKIN METHOD WITH GLOBAL BASIS FUNCTIONS'

C. Botcher, M. R. Strayer, and M. F. Werby²

Many problems in physics and engineering can be reduced to the Sturm-Liouville (S-L) problem. For some classes of the S-L problem we develop a method that can rapidly result in computational solutions. Let us assume that we can write the problem as follows:

$$U_i = \sum_{j=1}^N a_{ij} \Psi_j, \quad \frac{d^2 U_i(r)}{dr^2} + [K(r) - \lambda_i] U_i(r) = 0, \quad (1)$$

where L is an eigenvalue and $K(r)$ is some well-behaved (i.e. positive definite) function of r . Now let k correspond to some average value of $K(r)$ over the domain of $K(r)$. The boundary conditions are general. Then we easily solve the following problem:

$$\frac{d^2 \Psi_i(r)}{dr^2} + [k - \lambda_i] \Psi_i(r) = 0. \quad (2)$$

This yields global basis functions. We determine an efficient method to obtain solutions of the form:

$$U_i = \sum_{j=1}^N a_{ij} \Psi_j, \quad (3)$$

in which we determine the best expansion coefficients a_{ij} as well as the eigenvalues L_i 's in terms of the λ_i 's and the a_{ij} 's. We also develop several perturbation methods from the technique. The method is then applied to typical problems found in acoustics and quantum mechanics.

- 1. Abstract of published paper: pp. 775-788 in *Boundary Element Technology VII (Proceedings, Seventh International Conference on Boundary Element Technology, Albuquerque, New Mexico, June, 1992)* Computational Mechanics Publications, Boston and Elsevier Applied Science, New York, 1992.
- 2. Naval Research Laboratory, Stennis Space Center, MS.

CAN MOLECULES BE SEEN BY TWO PHOTONS?'

T. Barnes²

Theoretical expectations for the $\gamma\gamma$ partial widths of weakly bound meson-meson "molecule" states such as the $K\bar{K}$ molecule candidates $f_0(975)$ and $a_0(980)$ are discussed. The theoretical consensus is that such states should have $\gamma\gamma$ partial widths about an order of magnitude smaller than expectations for $q\bar{q}$ states with similar masses. This discriminating power implies that resonance production in $\gamma\gamma$ collisions will be a useful experimental technique for identifying molecules. Experimental results for the $\gamma\gamma$ partial widths of the $f_0(975)$ and $a_0(980)$ support their identification as molecules. Other possibilities for molecules, including the $f_0(1720)$, are discussed.

- 1. Abstract of paper to be published in *Proceedings of Ninth International Workshop on Photon-Photon Collisions, San Diego, California, March 22-26, 1992*.
- 2. UT-ORNL Collaborative Scientist.

**TWO-PHOTON COUPLINGS
OF QUARKONIA WITH ARBITRARY J^{PC}**

*T. Barnes*²

Theoretical results are presented for the two-photon widths of relativistic quarkonium states with arbitrary angular momenta. These relativistic formulae are required to obtain reasonable agreement with the absolute scale of quarkonium decay rates to two photons, and have previously only been derived for spin-singlet $q\bar{q}$ states. We also evaluate these formulae numerically for $\ell \leq 3$ $q = u, d$ states in a Coulomb-plus-linear $q\bar{q}$ potential model. Light-quark higher- ℓ and radially excited $q\bar{q}$ states should be observable experimentally, as their two-photon widths are typically found to be ~ 1 KeV. The radially excited 1S_0 higher-mass quarkonium states such as $c\bar{c}$ and $b\bar{b}$ should also be observable in $\gamma\gamma$, but orbitally excited $c\bar{c}$ states with $\ell > 1$ and $b\bar{b}$ states with $\ell > 0$ are predicted to have very small two-photon widths. The helicity structure of the higher- $\ell > 0$ couplings is found to be nontrivial, with both $\lambda = 0$ and $\lambda = 2$ $\gamma\gamma$ final states contributing significantly; these results may be useful as signatures for $q\bar{q}$ states.

1. Abstract of paper to be published in *Proceedings of Ninth International Workshop on Photon-*

Photon Collisions, San Diego, California, March 22-26, 1992.

2. UT-ORNL Collaborative Scientist.

QUARK BORN DIAGRAMS: MESON-MESON SCATTERING AMPLITUDES FROM THE NONRELATIVISTIC QUARK POTENTIAL MODEL¹

*T. Barnes*²

Recent calculations of meson-meson scattering amplitudes in the nonrelativistic quark potential model, which assume that the scattering mechanism is one-gluon-exchange followed by constituent exchange (OGE+CEX), are reviewed. The scattering diagrams are referred to as "quark Born diagrams." For the cases chosen to isolate this mechanism, $I = 2\pi\pi$ and $I = 3/2 K\pi$, the theoretical results are in remarkably good agreement with experimental S- and P-wave phase shifts and PCAC scattering lengths, given standard potential-model parameters.

1. Abstract of paper to be published in *Proceedings of the XIth International Symposium on High Energy Physics Problems, Dubna, Russia, September 7-12, 1992.*

2. UT-ORNL Collaborative Scientist.

NUCLEAR STRUCTURE AND ASTROPHYSICS

SOME GENERAL CONSTRAINTS ON IDENTICAL BAND SYMMETRIES¹

*M. W. Guidry,² M. R. Strayer, C.-L. Wu,³
and D. H. Feng⁴*

It is argued on general grounds, that nearly identical bands observed for superdeformation, and less frequently for normal deformation, must be explicable in terms of a symmetry having a microscopic basis. It is assumed that the unknown symmetry is associated with a Lie algebra generated by terms bilinear in fermion creation and annihilation operators. Observed features of these bands and the general properties of Lie groups are then used to place constraints on acceptable algebras. Additional constraints are placed by assuming that the collective

spectrum is associated with a dynamical symmetry, and by examining the subgroup structure required by phenomenology. It is observed that requisite symmetry cannot be unitary, and that the simplest known group structures consistent with these minimal criteria are associated with the Ginocchio algebras employed in the fermion dynamical symmetry model. However, the arguments are general in nature, and it is proposed that they imply model-independent constraints on any candidate explanation for identical bands.

1. Abstract of paper submitted for publication in *Physics Letters B.*

2. Adjunct staff member from University of Tennessee, Knoxville.

3. JIHIR, Oak Ridge, TN.
4. Drexel University, Philadelphia, PA.

THE FERMION DYNAMICAL SYMMETRY MODEL¹

C.-L. Wu,² D. H. Feng,³ and M. W. Guidry⁴

A fundamentally new approach to nuclear structure physics is described. Although the fermion-dynamical-symmetry model (FDSM) stands in a rich tradition of symmetry-based theories, the kinds of dynamical symmetries and the manner in which they are used in the FDSM are unique. Previous applications of group theoretical methods to nuclear structure physics have resulted in two general classes of models. The first has a solid microscopic foundation, but is limited in applicability. The second has a less transparent microscopic foundation, but in its phenomenological applications is descriptive of broad ranges of nuclear structure. The FDSM attempts to combine the positive attributes of these classes, while avoiding their difficulties; it is a truncated shell model, so its microscopic pedigree is well defined, but its dynamical symmetries appear to be rich enough to encompass the basic features observed for nuclear structure in medium and heavy mass nuclei. Indeed, the examples and discussion presented in the review give strong reason to believe that all of low-energy nuclear structure may be explicable in these terms.

After an introductory chapter, the second and third chapters deal with the mathematical formulation of the model, its dynamical symmetry limits, and the comparison with the interacting boson model; Chapter 4 discusses the relationship with the geometrical model; Chapter 5 gives a variety of quantitative calculations of physical quantities; Chapter 6 discusses and provides extensive evidence for a new principle of collective motion termed the dynamical Pauli effect; Chapter 7 discusses the relationship of the FDSM to a microscopic particle-rotor model and to the traditional cranking model; Chapter 8 deals with the application of the FDSM principle to extended valence spaces termed supershells, and the application of the resulting theory to superdeformation; Chapter 9 provides a compact summary, and some provocative remarks concerning the role of microscopic dynamical symmetries in nuclear structure physics.

The emphasis in this review is on the dynamical symmetry limits of the model and on perturbation theory about those limits. However, the ground work is laid, and initial examples are given, of numerical computation of symmetry-breaking terms that will constitute the next stage of development for the FDSM.

-
1. Summary of review paper.
 2. JIHIR, Oak Ridge, TN.
 3. Drexel University, Philadelphia, PA.
 4. Adjunct staff member from University of Tennessee, Knoxville.

NUCLEAR SUPERDEFORMATION AND THE SUPERSHELL FERMION DYNAMICAL SYMMETRY MODEL¹

C.-L. Wu,² D. H. Feng,³ and M. W. Guidry⁴

The one major shell fermion dynamical symmetry model (FDSM) has been extended to multiple shells. The resulting theory is termed the supershell-FDSM (SFDSM). Many basic features of superdeformation emerge naturally from the SU(3) fermion dynamical symmetry of this model. It is found that the dynamical Pauli effect plays a vital role in the formation of low-lying superdeformed states and provides a simple criterion for predicting where SD strength is most likely to occur. The SFDSM suggests that many-body correlations that are discarded in the usual mean-field theories are responsible for the widespread occurrence of identical bands in superdeformation. In this model, the superdeformed ground band is not the usual unaligned band, but a D-pair-aligned (DPA) band that sharply crosses the excited bands. It has been proposed that the DPA band may be a key to understanding many superdeformation properties, including the sudden decay-out of superdeformed Yrast intensity.

-
1. Abstract of paper to be published in *Annals of Physics*.
 2. JIHIR, Oak Ridge, TN.
 3. Drexel University, Philadelphia, PA.
 4. Adjunct staff member from University of Tennessee, Knoxville.

THE FERMION DYNAMICAL SYMMETRY MODEL AND IDENTICAL BANDS

M. W. Guidry,¹ C.-L. Wu,² and D. H. Feng³

A new model of superdeformation is described based on an extension of the fermion dynamical symmetry model to supershells. The resulting theory is a microscopic, many-body approximation to the spherical shell model. Dynamical symmetries of the model lead to a microscopic particle-rotor model for which it is difficult for the single-particle energies to break the rotational dynamical symmetry, and for which reference moments of inertia are independent of particle number for localized regions of superdeformation. Microscopic estimates of expected symmetry-breaking terms suggest that these features may survive in a realistic Hamiltonian. This would provide an immediate microscopic explanation of the identical bands observed in many superdeformed nuclei. Further approximations lead to a mean-field cranking picture in which this feature is lost, suggesting that identical bands are essentially a many-body effect.

Thus, a solution is proposed of the identical-band puzzle that departs substantially from the traditional viewpoint. In essence, the proposed solution turns the problem on its head; identical bands are a puzzle because of our habit of thinking in mean-field and liquid-drop terms. The more correct many-body physics underlying the problem favors identical bands; it is only symmetry-breaking that keeps identical bands from being more prevalent than they are. Therefore, the more profitable question to ask is why there are so few identical bands in nature. The fact that the symmetry proposed is based on the microscopic shell structure elevates the preceding statements above the level of a tautology; the microscopic basis of the symmetry allows a realistic estimate of symmetry-breaking terms. In this picture, there is no fundamental difference between normal and superdeformations with respect to identical bands. The only difference is quantitative; symmetry-breaking terms are more efficient for normal deformation than for superdeformation, and thus are more effective in obscuring the tendency toward identical bands favored by the symmetry of the collective motion.

Thus, it is proposed that the nuclear many-body problem can exhibit more stability in macroscopic quantities such as moments of inertia than that expected from the corresponding mean-field approximation, because such approximations discard impor-

tant correlations present in the many-body problem. This idea assumes added weight because of the present assertions that the traditional mean-field approach can be derived from the FDSM approach, and that it is precisely the approximations required to accomplish this that destroy the identical band properties. Therefore, the present conjectures suggest that the identical band problem may be tangible evidence for nuclear structure effects that go beyond the mean field.

-
1. Adjunct staff member from University of Tennessee, Knoxville.
 2. JHIR, Oak Ridge, TN.
 3. Drexel University, Philadelphia, PA.

THE DYNAMICAL PAULI EFFECT

M. W. Guidry,¹ C.-L. Wu,² and D. H. Feng³

The dynamical Pauli effect (DPE) of the fermion dynamical symmetry model (FDSM) is reviewed, and a variety of experimental predictions associated with the DPE are tested against available data. It is concluded that there is strong empirical evidence from a variety of observations in support of this effect, and new experiments that can test its pervasiveness are suggested. In particular, unequivocal tests could be provided by observations of fundamental properties such as electromagnetic transition rates in nuclides that are presently unknown. Such information might become available from radioactive ion beam experiments.

It is suggested that the dynamical Pauli effect is a fundamental principle of many-body physics that unifies many well-known, but seemingly independent, properties of collective nuclear systems. For example, it is argued that there is a direct link between the dynamical Pauli effect and the appearance of gaps in the deformed single-particle spectrum, such as the ones found at nucleon numbers 98 and 152 at normal deformation, and nucleon number 64 in superdeformation.

It is shown in Fig. 8.3 that dynamical Pauli effects can often be given a simple physical interpretation in terms of a mean-field approximation to the underlying many-body theory. For example, the representation constraints for the SU(3) dynamical symmetry of the FDSM have been shown by coher-

ORNL-DWG 92-15909

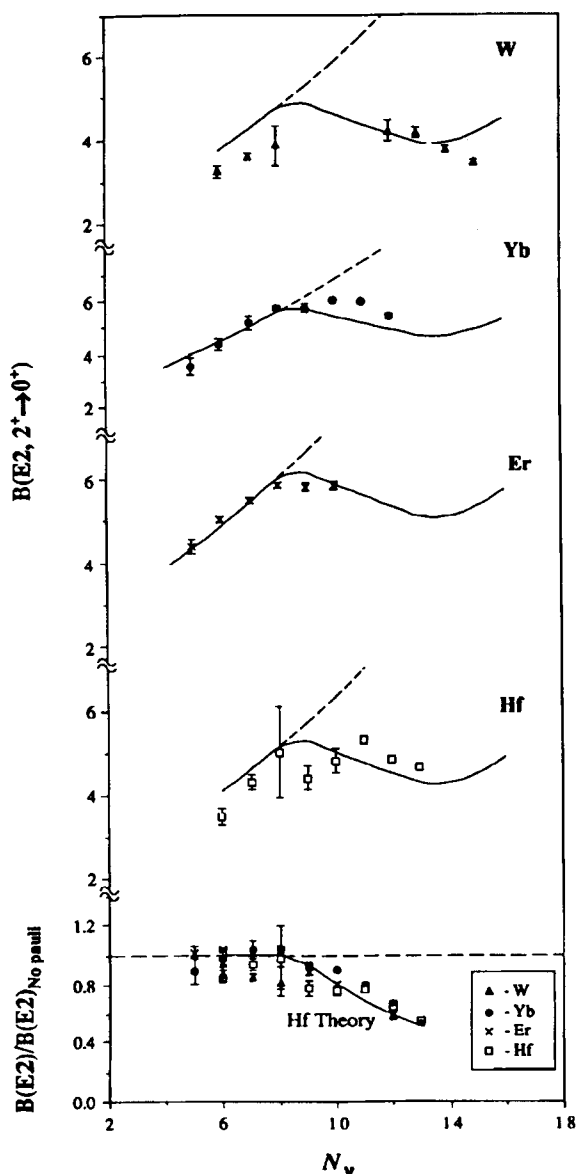


Fig. 8.3. Collective quadrupole-reduced transition rates for even-even rare-earth nuclei as a function of neutron valence pair number. Calculations are shown using the full fermion symmetry of the FDSM (solid lines), and in the boson approximation to this FDSM symmetry, which neglects the restrictions on representations implied by the Pauli principle (dashed line). The difference between these curves is the dynamical Pauli effect.

ent-state techniques to translate into Pauli-forbidden regions of the beta-gamma deformation plane. This is directly related to the occurrence of gamma degrees of freedom in such systems. Although simple physical interpretations have been attached to dynamical Pauli effects by utilizing such approximations, these effects arise at the many-body level of the symmetry theory before such simplifications are made; thus, they transcend the mean-field approximations that have been employed to express them in more familiar language.

1. Adjunct staff member from University of Tennessee, Knoxville.
2. JHIR, Oak Ridge, TN.
3. Drexel University, Philadelphia, PA.

NETWORK CALCULATIONS FOR THE PRODUCTION OF HEAVY ELEMENTS

*R. Igaras,¹ D. J. Dean,² M. R. Strayer,
M. W. Guidry,³ and F.-K. Thielemann⁴*

Understanding the synthesis of the elements is a major goal of nuclear astrophysics. Light element synthesis in the Big Bang, and the production of elements up to iron in the hydrogen burning stage of a star are much better understood than the later neutron-capture stages. The latter occur well within the last 10% of the star life cycle, and occur catastrophically. Therefore, extremely accurate hydrodynamical calculations are necessary to describe the nonequilibrium scenarios that occur, in particular the shock formation and propagation that are believed to expel the outer envelopes of the star. It is in these circumstances of high temperature and neutron fluxes that the synthesis of the heavier elements is thought to occur; the two nonequilibrium processes of importance are the s- and the r-processes.

The advent of radioactive ion beam physics implies a possibility of enhanced data quality for some input to element-production calculations, and improved theories for the extrapolation of the additional quantities required in such calculations that cannot be measured. Likewise, there are unprecedented opportunities for high-performance computation promised by the new generation of massively

parallel supercomputers. Accordingly, it is an appropriate time to evaluate the status of element-production calculations. The network codes describing the production of heavy elements in supernovae and explosive stellar-burning processes have accreted over two decades and do not generally represent state-of-the-art computation. Discussions with F.-K. Thielemann (Harvard-Smithsonian Center), J. W. Truran (University of Chicago), and J. J. Cowan (University of Oklahoma) have convinced us that there is a need for a new network code for element production that incorporates modern computational methods, and is optimized to take advantage of the new generation of supercomputers and the increased accuracy and volume of input data that could become available in the next decade.

We have initiated a project to develop such a code. The project is still in a developmental stage, with the present effort centered on evaluating algorithms for the most efficient solution of the network of differential equations describing the production of heavy elements. Once an algorithm is adopted, we intend to write a new code for a solution of this problem that will be particularly well suited to parallel systems such as the hypercube.

The environments in which the s- and r-processes take place are of the utmost importance for the predicted element production. The calculations performed so far have normally decoupled the nucleosynthesis processes from the hydrodynamical calculations; the hydro output in terms of the neutron density, nuclei densities, and temperature profiles are parameterized as a function of time and assumed as input in the nucleosynthesis codes. While this can be justified energetically, the occurrence of heavier nuclei could affect the highly unstable shock formation and propagation through a modification of the opacity to the various energy transport mechanisms. Further, a dynamical coupling between the nucleosynthesis processes and the hydrodynamics will ascertain further the exact location of nuclear formation.

In a separate contribution to this progress report, we describe the initiation of a program to calculate supernova explosions using multidimensional relativistic hydrodynamics. In the longer term, we may contemplate coupling the relativistic hydrodynamic code to the network code described in this contribution to produce a self-consistent calculation of element production in a supernova event.

1. UT-ORNL Science Alliance participant, summer, 1992.

2. Consultant from California Institute of Technology, Pasadena.

3. Adjunct staff member from University of Tennessee, Knoxville.

4. Harvard-Smithsonian Center for Astrophysics, Cambridge, MA.

HEAVY-ION TRANSFER REACTIONS TO HIGH-SPIN STATES IN THE PARTICLE-ROTOR MODEL¹

R. W. Kincaid,² H. Schecter,³ M. R. Guidry,⁴ S. Landowne⁵ R. Donangelo,³ and G. Leander⁶

Presented in this paper is a model of one-neutron transfer reactions appropriate for cases in which one of the collision partners is deformed. The model considers rotational excitation due to the Coulomb field in the entrance channel, neutron transfer between the two nuclear surfaces at the distance of closest approach, and additional rotational excitation in the final channel. The Coulomb excitation processes are described within the sudden-limit approximation using classical-limit theory, and the transfer is described in terms of spectroscopic amplitudes obtained with the particle-rotor model.

1. Abstract of paper to be published in *Physical Review C*.

2. University of Tennessee, Knoxville.

3. Universidade Federal do Rio de Janeiro, Brazil.

4. Adjunct staff member from University of Tennessee, Knoxville.

5. Argonne National Laboratory, Argonne, IL.

6. Deceased.

NUCLEAR DEFORMATIONS AS A SPONTANEOUS SYMMETRY BREAKING¹

W. Nazarewicz²

Why can certain nuclei be described in terms of intrinsic shapes with nonspherical, triaxial, or reflection-asymmetric static moments? At first glance, a violation of very fundamental symmetries such as rotational invariance, space inversion, or particle number symmetry is astonishing since strong interactions do actually conserve angular momentum, par-

ity, and baryon number. The main building blocks of the spontaneous symmetry breaking mechanism in atomic nuclei are discussed and illuminated by examples taken from atomic and nuclear physics.

1. Abstract of paper to be published in *International Review of Modern Physics E*.

2. JHIR, Oak Ridge, TN.

PROTON EMISSION FROM NUCLEI BEYOND THE PROTON DRIP LINE

S. Åberg¹, W. Nazarewicz², J. R. Beene,
and G. R. Satchler

Nuclei beyond the proton drip line are quasibound; proton decay being inhibited by the Coulomb barrier. The associated lifetimes, ranging from 10^{-6} s to a few seconds, are sufficiently long to obtain a wealth of spectroscopic information. Experimentally, few proton emitters have been discovered in the mass regions $A \sim 110, 150, \text{ and } 160$.³ It is anticipated, however, that new regions of proton-unstable nuclei will be explored by means of the radioactive nuclear beams technique.

In this work we are performing systematic calculations of half-lives and various spectroscopic properties of spherical and deformed proton-emitters.

The resonance width of a quasi-bound proton is given by

$$\Gamma = 2\pi |T_{if}|^2. \quad (1)$$

The transition amplitude, T_{if} , is given by

$$T_{if} = \langle \Psi_f(A, p) | V_N + V_C^{def} | \Psi_i(A+1) \rangle. \quad (2)$$

where $\Psi_i(A+1)$ is the wave function of the (deformed) parent nucleus, $\Psi_f(A, p)$ is the wave function of the daughter nucleus and the emitted proton (outgoing Coulomb wave), V_N is the nuclear interaction (containing a central term and a spin-orbit term), and V_C is the nonspherical part of the Coulomb potential.

For calculating G we explore and compare three methods:

1. A direct calculation of the transition amplitude (2). In the deformed case we adopt the method proposed by Bugrov and Kadenskii;⁴
2. The two-potential method of Jackson and Rhoades-Brown.⁵ Here, the wave function of the quasi-bound state is approximated through the decaying component and the outgoing wave; the latter one expressed by means of the Coulomb Green function;
3. Semiclassical approximation (WKB) (see, e.g., recent calculations for spherical nuclei⁶).

In the first phase of the project we are comparing the above methods for spherical nuclei. Very little comparison of this nature seems to have been done. The extension to deformed systems, involving coupled-channel calculations of quasi-bound states, and Coriolis coupling of valence orbitals, will be performed later according to the results of the first phase.

1. Lund Institute of Technology, Sweden.

2. JHIR, Oak Ridge, TN.

3. S. Hofmann, in *Particle Emission from Nuclei*, ed. by M. Ivascu and D. N. Poenaru (CRC, Boca Raton, 1989) Vol. 2, Chap. 2.

4. V. P. Bugrov and S. G. Kadenskii, *Sov. J. Nucl. Phys.* **49**, 967 (1989).

5. D. F. Jackson and M. J. Rhoades-Brown, *Ann. Phys. (N.Y.)* **105**, 151 (1977).

6. B. Buck, A. C. Merchant, and S. M. Perez, *Phys. Rev. C* **45**, 1688 (1992).

NEW VISTAS IN SUPERDEFORMATION¹

W. Nazarewicz²

In heavy nuclei, three regions of superdeformed (SD) shapes have been established: fission isomers in actinides, high-spin SD states around ¹⁵²Dy, and SD bands around ¹⁹²Hg. An impressive experimental and theoretical effort has been devoted to exploring the underlying physics. There is no doubt that these investigations have opened up a new, exciting field of nuclear superdeformed spectroscopy.

Hyperdeformed nuclei, i.e., with quadrupole deformations significantly larger than $\beta_2 = 0.6$ are known or predicted in several mass regions. Good examples of very elongated configurations can be found in light nuclei. For example, the hyperdeformed state in ^{12}C (three aligned alpha particles) built on the 0^+ resonant state at 10.3 MeV becomes yrast already at $I^\pi = 4^+$. The calculated low-lying reflection-asymmetric hyperdeformed minimum ($\epsilon_2 = 1$, $\epsilon_3 = 0.3$) in ^{24}Mg can be associated with the asymmetric $^{16}\text{O} + \alpha + \alpha$ (or $^{16}\text{O} + ^8\text{Be}$) structures or the symmetric hyperdeformed $\alpha + ^{16}\text{O} + \alpha$ states. Other examples are the hyperdeformed states in $^{36}\text{Ar} (^{16}\text{O} + ^{16}\text{O} + \alpha)$, $^{48}\text{Cr} (^{16}\text{O} + ^{16}\text{O} + ^{16}\text{O})$, or a six-alpha chain structure in ^{24}Mg .

In heavy nuclei the best hyperdeformed states are the so-called third minima in nuclei around ^{232}Th . In these nuclei the second saddle point is split, leading to the weak reflection-asymmetric minimum with $\beta_2 \sim 0.85$, $\beta_3 \sim 0.35$. Experimentally, the third minimum shows up as an alternating-parity microstructure of resonances near the (n,f) fission threshold. Recent calculations based on the Gogny-HF model, or the Woods-Saxon model, predict the third minima to be deeper than in the previous calculations based on the Nilsson model. Figure 8.4 displays the Woods-Saxon potential energy surface for ^{232}Th . The heights of the second and third barrier (saddle point) are 1.4 MeV and 2.9 MeV, respectively.

According to the model predictions, low-lying super and hyperdeformed configurations are expected in various mass regions, many of them being practically inaccessible with the present detector systems (too low cross sections), or inaccessible at all using

combinations of stable beams and targets. Some of those "white spots" will, hopefully, be investigated in the future—thanks to the new-generation multidetector arrays (EUROGAM, GAMMASPHERE, EUROBALL), or exotic (radioactive) ion beam facilities currently being constructed in Europe, U.S.A., and Japan.

Very little is known about the very neutron-deficient Hg nuclei with $N \sim 96$. The lightest system known from in-beam studies is ^{180}Hg . The nucleus ^{178}Hg has lifetime $\tau \sim 49$ s, while for ^{176}Hg τ drops to 34 ms, and ^{174}Hg is expected to be proton-unstable.

The potential-energy surfaces for ^{170}Hg (proton-unstable), ^{180}Hg ($\tau = 5.9$ s), ^{190}Hg ($\tau = 20$ m), ^{200}Hg (stable) are shown in Fig. 8.5. The SD minimum seen in $^{190,200}\text{Hg}$ disappears in ^{180}Hg . Note the presence of reflection-symmetric hyperdeformed minima in ^{190}Hg ($\beta_2 \sim 0.8$), ^{200}Hg ($\beta_2 \sim 1.05$), and reflection-asymmetric hyperdeformed minima in ^{180}Hg ($\beta_2 \sim 0.8$, $\beta_3 \sim 0.15$). However, when decreasing neutron number, the SD states reappear again; see the map for ^{170}Hg . Detailed calculations presented in Fig. 8.6 indicate that the excitation pattern of low-deformation, shape-coexisting configurations and SD states is symmetric with respect to the middle of the shell, i.e., $N \sim 102$. A similar situation has also been calculated for Pt and Pb isotopes.

As discussed in the proposal for the Oak Ridge Radioactive Ion Beam Facility (RIB), the new beams at RIB will provide the necessary tools to access high-spin states in the $N = Z \approx 40$ mass region, the region around ^{120}Ce , and around ^{176}Hg .

ORNL-DWG 92-15910

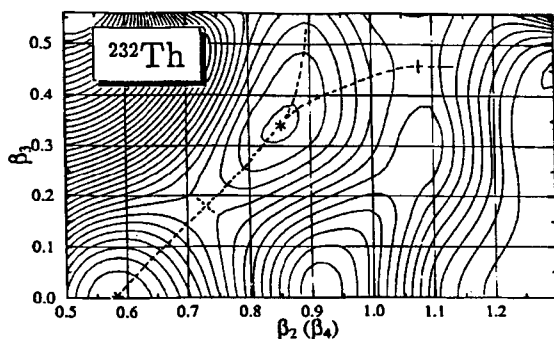


Fig. 8.4. The Woods-Saxon-Strutinsky total potential energy for ^{232}Th as a function of β_2 and β_3 . At each (β_2, β_3) point the energy was minimized with respect to β_4, β_6 . The distance between the contour lines is 0.5 MeV. (From Cwick et al., 1992).

1. Summary of invited paper: pp. 32-41 in *Proceedings of the International Conference on Nuclear Structure at High Angular Momentum, Ottawa, Canada, May 18-21, 1992*, AECL-10613, Vol. 2, 1992.

2. JHIR, Oak Ridge, TN.

DIABATICITY OF NUCLEAR MOTION: PROBLEMS AND PERSPECTIVES'

W. Nazarewicz²

The results of mean-field calculations often suggest that physical states can be related to very shallow minima of the potential energy surface (PES) or even to shell structures which do not generate a proper minimum. In the latter case, it appears that the energy

ORNL-DWG 92-15911

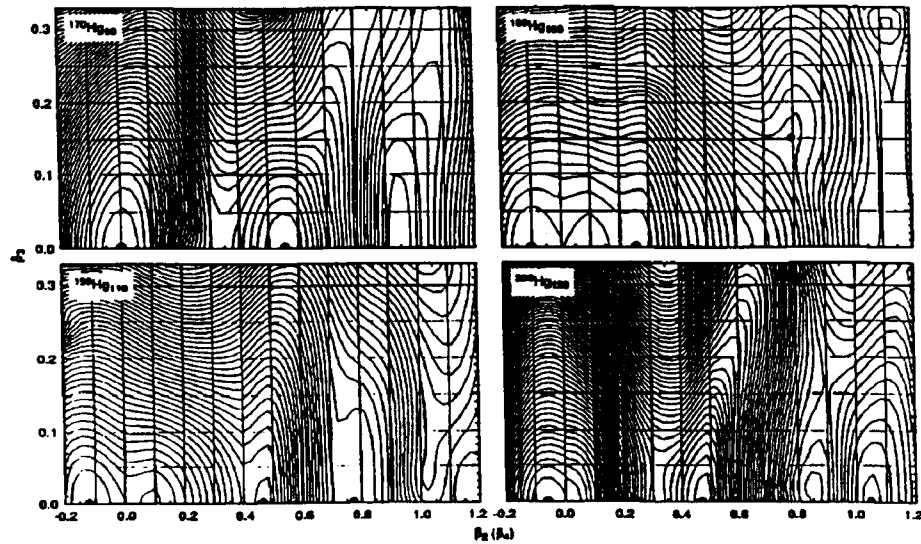


Fig. 8.5. The Woods-Saxon-Strutinsky total potential energy for $^{170,180,190,200}\text{Hg}$ as a function of β_2 and β_3 . At each (β_2, β_3) point, the energy was minimized with respect to β_4 - β_8 . The distance between the contour lines is 0.3 MeV.

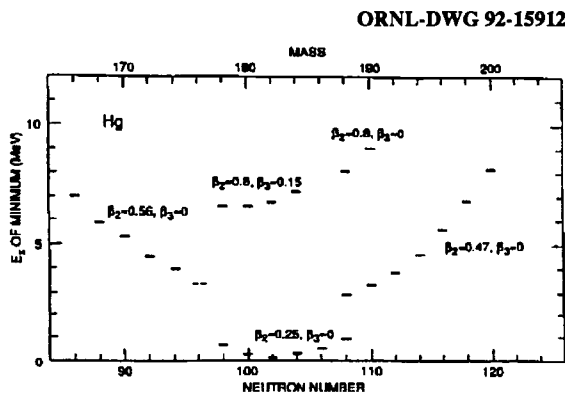


Fig. 8.6. Calculated energies of excited shape-coexisting states in even-even Hg isotopes with $86 \leq N \leq 120$.

of excited states can be estimated by removing the interaction between the different quasiparticle configurations. This has many important consequences. In standard mean-field calculations the total energy is minimized with respect to some set of collective parameters describing, e.g., the shape of a nucleus. When calculations are not constrained to a particular

intrinsic shell-model configuration, the resulting PES will be (in first approximation) the lower envelope of the set of PES associated with all possible configurations. This means that the original symmetries of the Hamiltonian are not sufficient to distinguish the physically interesting shell-model structures. It is therefore necessary to introduce auxiliary quantum numbers. Because the high- j intruder orbitals have a very distinct structure, one can label the important intrinsic configurations according to the number of occupied intruder orbitals. In order to study a given structure, one should also keep track of diabatic trajectories as a function of the deformation parameters (or constraints in HFB calculations). In particular, a new procedure must be invented to calculate the PES at those deformations for which natural and abnormal parity orbitals cross. Such an extension of the mean-field approach, referred to as the *configuration-constrained mean-field approach* has been successfully employed to many systems in various regimes of angular momentum and deformation. A particularly interesting example of the unique role of high- j orbits is seen in superdeformed high-spin nuclei, or in shape-coexisting systems.

The success of the configuration-constrained mean-field approach, inspired and strongly supported by data, leads one to question one of the underlying

assumptions of most theoretical approaches of the collective nuclear motion: the adiabatic hypothesis. This problem appears as one of the most important we shall have to address in the coming years.

The problem of the diabaticity of nuclear motion is ultimately related to the presence of self-consistent symmetries, or "effective" quantum numbers. If a self-consistent symmetry is present, it can lead to sharp crossings between energy levels with different quantum numbers. The point of degeneracy (the crossing point) has a very interesting interpretation. Unlike in the situation of complete decoupling of collective and single-particle motion (adiabatic approximation), the crossing point can be viewed as a *diabolical point* which contains an effective magnetic monopole associated with the vector potential \vec{A} . Consequently, during its collective motion, the system will always try to *go around* the point of degeneracy, analogous to the motion of a charged particle in the magnetic field of a monopole. In other words, the motion of the system is adiabatic (i.e., the system can be approximately treated semiclassically as moving along the adiabatic surface of the collective potential) only in the regions far from the point of degeneracy, where the energy splitting between different sheets of the adiabatic collective potential is large.

-
1. Summary of invited paper to be published in *Proceedings of 21st INS International Symposium on Rapidly Rotating Nuclei, Tokyo, Japan, October 26-30, 1992*, to be published in *Nuclear Physics A*.
 2. JIHIR, Oak Ridge, TN.

TRIAXIALITY AND ALTERNATING M1 STRENGTHS IN f-p-g SHELL NUCLEI¹

S. L. Tabor,² T. D. Johnson,² J. W. Holcomb,²
P. C. Womble,² J. Döring,² and W. Nazarewicz³

The appearance of alternating patterns in B(M1) strengths in f-p-g shell nuclei is surveyed. The M1 alternations in a sequence of N = 41 isotones, in conjunction with particle-rotor model calculations, is shown to provide information about changing γ deformation. In addition to other odd-A nuclei, several odd-odd nuclei are shown to exhibit alternating B(M1) values and signature inversion. Alternations have

also been reported in a four-quasiparticle band in ⁸⁶Zr, where they have been interpreted in terms of the interacting boson model.

-
1. Summary of invited paper: pp. 322-326 in *Proceedings of the International Conference on Nuclear Structure at High Angular Momentum, Ottawa, Canada, May 18-21, 1992*, AECL-10613, Vol. 2, 1992.
 2. Florida State University, Tallahassee.
 3. JIHIR, Oak Ridge, TN.

MAGNETIC DIPOLE STRENGTH IN SUPERDEFORMED NUCLEI¹

I. Hamamoto² and W. Nazarewicz²

The K^π=1⁺ intrinsic excitations and associated M1 strengths in (super)deformed nuclei are studied using the quasiparticle random phase approximation. The sum of B(M1) values in the region of E_x < 10 MeV at superdeformations is found to be several times larger than that at normal deformations, because of (i) the increase in the proton convection current contribution, and (ii) reduced pairing correlations. Moreover, at superdeformations the major part of the calculated low-lying (large) B(M1) values are concentrated in the energy region just below the neutron emission threshold. The high-lying isovector giant quadrupole resonance at superdeformed shapes is found to contain about 60% probability of "scissors" mode and carry a large B(M1) strength (see Fig. 8.7).

-
1. Abstract of paper to be published in *Physics Letters B*.
 2. JIHIR, Oak Ridge, TN.

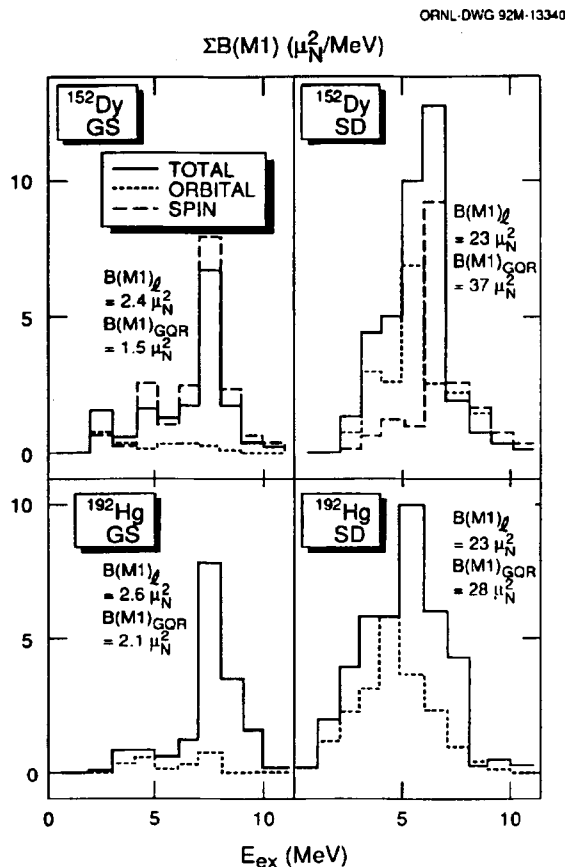


Fig. 8.7. $B(M1; g. s., K^\pi = 0^+, I^\pi = 0^+ \rightarrow K^\pi = 1^+, I^\pi = 1^+)$ values calculated in QRPA as a function of excitation energies of 1^+ states. The summed values per 1 MeV energy bin are plotted as a histogram. For reference, the $B(M1)$ values associated with spin part only ($g_l = 0$) or orbital part only ($g_s = 0$) are also shown. $B(M1)_I$ denotes the total $B(M1)$ orbital strength in the energy region below 20 MeV. This can be compared with the value for the GQR, $B(M1)_{GQR}$, which consists almost exclusively of the orbital contribution. g -factors are $g_l = g_l^{free}$ and $g_s = (0.85)g_s^{free}$. Pairing gaps (in MeV) and deformation parameters ($\Delta_p, \Delta_n, \beta_2, \beta_4$) are (1.0, 0.9, 0.14, 0.02) for the ground state of ^{152}Dy , (0.3, 0.3, 0.62, 0.12) for the SD state of ^{152}Dy , (0.5, 0.9, -0.13, -0.037) for the ground state of ^{192}Hg , and (0.3, 0.3, 0.475, 0.077) for the SD state of ^{192}Hg .

FIRST EVIDENCE FOR STATES IN Hg NUCLEI WITH DEFORMATIONS BETWEEN NORMAL- AND SUPER-DEFORMATION¹

W. C. Ma,² J. H. Hamilton,² A. V. Ramayya,²
 L. Chaturvedi,² J. K. Deng,² W. B. Gao,²
 Y. R. Jiang,² J. Kormicki,² X. W. Zhao,²
 N. R. Johnson,¹ I. Y. Lee,³ F. K. McGowan,⁴
 C. Baktash, J. D. Garrett,
 W. Nazarewicz,⁵ and R. Wyss,⁵

High-spin states in ^{186}Hg with a quadrupole deformation of $\beta_2 = 0.34(4)$ have been established from measured gamma-ray coincidences and lifetimes. These data, which provide the first evidence for a deformation midway between normal- and super-deformed, can be interpreted in terms of the $[651 1/2]$ and $[770 1/2]$ neutron configurations.

1. Abstract of paper submitted for publication in *Physical Review C*.
2. Vanderbilt University, Nashville, TN.
3. Lawrence Berkeley Laboratory.
4. Consultant.
5. JHIR, Oak Ridge, TN.

ROTATIONAL BAND STRUCTURE IN ^{75}Se ¹

T. D. Johnson,² T. Glasmacher,² J. W. Holcomb,²
 P. C. Womble,² S. L. Tabor,² and W. Nazarewicz³

The high-spin states of ^{75}Se have been investigated using the $^{59}\text{Co}(^{19}\text{F}, 2p_n)$ reaction at 55 MeV. The positive-parity band has been extended to $I^\pi = 29/2^+$ and the unfavored signature has been identified. The negative-parity band has been extended to $I^\pi = 19/2^-$ and band crossings were observed for the first time in both bands. Eleven new lifetimes were measured using the Doppler-shift attenuation method which allowed for extraction of transition strengths and transition quadrupole moments. The $B(M1)$

strengths exhibit a staggering dependent on the signature splitting. Calculations based on the Woods-Saxon-Bogoliubov cranking model explain the signature-dependent alignment process in the $g_{9/2}$ bands and predict signature inversion in all bands at high rotational frequencies. It is argued that the data are consistent with the transition from triaxial shapes with $\gamma \sim -30^\circ$, characteristic of one-quasiparticle configurations, to triaxial shapes with $\gamma \sim 30^\circ$, characteristic of a three-quasiparticle configuration containing one aligned pair of $g_{9/2}$ protons.

-
1. Abstract of published paper: *Phys. Rev. C* **46**, 516 (1992).
 2. Florida State University, Tallahassee.
 3. JHIR, Oak Ridge, TN.

ANALYSIS OF A THREE-DIMENSIONAL CRANKING IN A SIMPLE MODEL¹

W. Nazarewicz² and Z. Szymanski³

Nuclear rotational states are calculated in terms of a three-dimensional extension of the cranking model. A simple, two-level model that allows for an exact solution is employed in the analysis. Various ways to define principal axes of the rotating nucleus are discussed. The minimal energy of the system corresponds to stationary rotational motion around a principal axis.

-
1. Abstract of published paper: *Phys. Rev. C* **45**, 2771 (1992).
 2. JHIR, Oak Ridge, TN.
 3. Guest Assignee from University of Warsaw, Poland.

COLLECTIVE DIPOLE ROTATIONAL BANDS IN ¹⁹⁷Pb¹

*R. M. Clark,² R. Wadsworth,² E. S. Paul,³
C. W. Beausang,³ I. Ali,³ A. Astier,⁴
D. M. Cullen,³ P. J. Dagnall,³ P. Fallon,³
M. J. Joyce,³ M. Meyer,⁴ N. Redon,⁴
P. H. Regan,² J. F. Sharpey-Schafer,³
W. Nazarewicz,⁵ and R. Wyss⁵*

The nucleus ¹⁹⁷Pb was populated via the ¹⁸⁶W(¹⁷O,6n)¹⁹⁷Pb reaction at beam energies of 98 and 110 MeV. Two regular DI=1 bands of magnetic dipole transitions have been found. Possible interpretations in terms of collective oblate configurations involving high-K proton orbitals coupled to three $i_{13/2}$ neutrons are discussed. The similarities between several of the bands discovered in ¹⁹⁷⁻²⁰⁰Pb nuclei are emphasized.

-
1. Abstract of published paper: *Z. für Physik A* **342**, 371 (1992).
 2. University of York, England.
 3. University of Liverpool, England.
 4. Institut de Physique Nucléaire de Lyon, France.
 5. JHIR, Oak Ridge, TN.

STATIC MULTIPOLE DEFORMATIONS IN NUCLEI¹

W. Nazarewicz²

The physics of static multipole deformations in nuclei is reviewed. Nuclear static moments results from the delicate balance between the vibronic Jahn-Teller interaction (particle-vibration coupling) and the residual interaction (pairing force). Examples of various permanent nuclear deformations are discussed.

-
1. Abstract of published paper: *Prog. Part. Nucl. Phys.* **28**, 307 (1992).
 2. JHIR, Oak Ridge, TN.

ON THE QUESTION OF SPIN FITTING AND QUANTIZED ALIGNMENT IN ROTATIONAL BANDS¹

C. Baktash, W. Nazarewicz,² and R. Wyss²

Several methods employed to parameterize the spins of the superdeformed bands in terms of their observed gamma-ray energies are closely examined. It is pointed out that, since the proposed fitting procedures are variants of the Harris expansion formula, they cannot be applied to determine the unknown spins of the *excited* bands due to the possible presence of nonzero initial alignments. A comprehensive study of the normally deformed excited bands indicates that no correlation exists between the fitted spins and the experimentally known values. Therefore, there is no firm evidence for the presence of anomalous relative alignments between the superdeformed identical bands in the Hg region. Additionally, a critical review of several of the models and scenarios that purport to explain the origin of the identical bands, or the patterns of the fitted alignments is presented. It is concluded that none of these models can satisfactorily explain the identical moments of inertia in neighboring nuclei and the systematics of the observed or fitted alignments. Thus, the important question of the microscopic origin of the identical bands remains to be investigated.

1. Abstract of paper to be published in *Nuclear Physics A*.
2. JHIR, Oak Ridge, TN.

OCTUPOLE CORRELATIONS, SPIN ASSIGNMENTS, AND IDENTICAL BANDS IN ¹⁹³Hg¹

J. F. Sharpey-Schafer,² D. M. Cullen,²
 M. A. Riley,² A. Alderson,² I. Ali,²
 T. Bengtsson,³ M. A. Bentley,⁴ A. M. Bruce,⁴
 P. Fallon,² P. D. Forsyth,² F. Hanna,²
 S. M. Mullins,² W. Nazarewicz,⁵ R. Poynter,⁶
 P. Regan,⁶ J. W. Roberts,² W. Satula,⁷ J. Simpson,⁴
 G. Sletten,⁸ P. J. Twin,² R. Wadsworth,⁶
 and R. Wyss,⁵

A brief reminder is given of the evidence for the existence of octupole correlations in the superdeformed shape of ¹⁹³Hg. It is pointed out that

comparison of the data on the superdeformed bands in ¹⁹³Hg with cranked shell model calculations gives firm assignments to the signatures and parities of these bands. The spin assignments obtained are in agreement with the spin assignments given by projecting the SD bands back to zero rotational frequency and assuming the intrinsic alignment i_0 is zero. These spin assignments leave "identical" bands in ¹⁹¹Hg, ¹⁹³Hg, and ¹⁹⁴Hg with a surplus $1\hbar$ of spin relative to the superdeformed core nucleus ¹⁹²Hg. This extra $1\hbar$ is not understood.

1. Abstract of published paper: pp. 64-75 in *Proceedings of Future Directions in Nuclear Physics with 4 π Gamma-Detection Systems of the New Generation, Strasbourg, France, March 4-16, 1991*, AIP Conference Proceedings 259, New York, NY, 1992.
2. University of Liverpool, England.
3. Lund Institute of Technology, Sweden.
4. SERC Daresbury Laboratory, Warrington, England.
5. JHIR, Oak Ridge, TN.
6. University of York, England.
7. University of Warsaw, Poland.
8. Niels Bohr Institute, Risø, Denmark.

THE INFLUENCE OF PAIRING ON THE PROPERTIES OF THE A=190 SUPERDEFORMED BANDS¹

P. Fallon,² W. Nazarewicz,³ M. A. Riley,⁴
 and R. Wyss⁵

The phenomenon of superdeformed identical bands in both the A=150 and A=190 regions is reviewed. Deviations in the transition energies of the A=190 superdeformed bands at low spins are discussed in terms of variations in the moments of inertia. It is seen that simple blocking arguments predict variations in the static pair correlations at low spins. A simple expression relating the moment of inertia to the pair correlations is then used to extract the relative magnitude of the neutron (proton) pairing within superdeformed configurations. Moreover, low spin differences in the experimental moments of inertia are shown to reflect the predicted differences in the pair correlations.

1. Abstract of published paper: pp. 112-130 in *Proceedings of Future Directions in Nuclear Physics*

with 4π Gamma-Detection Systems of the New Generation, Strasbourg, France, March 4-16, 1991, AIP Conference Proceedings 259, New York, NY, 1992.

2. University of Liverpool, England.
3. JHIR, Oak Ridge, TN.
4. Florida State University, Tallahassee.
5. Royal Institute of Technology, Stockholm, Sweden.

ANOMALIES IN THE ODD-EVEN DIFFERENCE IN THE MOMENTS OF INERTIA OF ROTATIONAL BANDS

C. Baktash, J. D. Garrett, I. Hamamoto,¹
W. Nazarewicz,¹ and D. F. Winchell²

A recent comprehensive analysis of the low-spin odd-Z bands in the rare-earth region indicated that moments of inertia (MoI) of about 30% of these bands are nearly identical (to within 2%) to that of their adjacent even-even nuclei with one less proton.³ This finding runs against the naive expectation that, according to the BCS pairing theory, the MoI of the one-quasiparticle bands are typically 10-15% larger than that of the zero-quasiparticle bands in their adjacent even-even nuclei (the blocking effect). The question raised by the above study is whether this apparent "failure" of the BCS blocking happens in only a limited set of bands, namely the nearly identical bands, or occurs more frequently. Answering this question would narrow down the range of possible mechanisms that have been invoked to explain the identical bands (IB).⁴ To address this question, we have (i) evaluated the experimental fractional change in the MoI of the adjacent odd- and even-Z bands ($\Delta J_{\text{odd}} / J_e$) in the rare-earth region; and (ii) compared them with the results of pairing self-consistent cranking calculations for several bands in ^{173}Lu . Such calculations would serve to identify the shortcomings of the "standard" models in describing dynamic moments of inertia of rotational bands.

Experimentally, the fractional odd-even changes in the MoI ($\Delta J_{\text{odd}} / J_e$) were evaluated by a linear least-square fit to the slope of the relative alignment (i) as a function of spin (I). (The relative alignment is defined as the difference in the spins of two bands at a constant angular frequency.) For the majority of the bands studied, the assumption of the linearity of the (i versus I) functions were born out, indicating that ($\Delta J_{\text{odd}} / J_e$) values stay constant over an extended

range of angular frequency. Within one standard deviation, the extracted odd-even differences in the MoI are less than 2% in about 20% of the 180 bands analyzed; in good agreement with our previous study of the identical bands in this region.³

In order to answer if the standard mean-field approach can reproduce the observed odd-even variation of the MoI, several calculations of the dynamic moments of inertia were performed using the pairing self-consistent Woods-Saxon cranking model. To be able to compare the calculated results with the experimental values, a transformation has to be performed from the theoretical rotational frequency, $\omega = dE/dI_x$, and the cranking-model static and dynamic moment of inertia

$$J^{(0)} = \frac{I_x}{\omega}, \quad J^{(2)} = \frac{dI_x}{d\omega} \quad (1)$$

to the experimental frequency, ω_γ , and the experimental dynamic moment of inertia, $J_\gamma^{(2)}$, defined as

$$\omega_\gamma = \frac{dE}{dI} = \frac{E_\gamma}{2}, \quad J_\gamma^{(2)} = \frac{dI}{d\omega_\gamma} = \frac{4}{\Delta E_\gamma}. \quad (2)$$

Assuming that a rotational band has a good quantum number K, the relation between I and I_x reads:

$$I + \frac{1}{2} = \sqrt{I_x^2 + K^2}, \quad (3)$$

which leads to the relation between experimental and calculated quantities:

$$\begin{aligned} \omega_\gamma &= \sqrt{\omega^2 + \frac{K^2}{(J^{(0)})^2}}, \quad J_\lambda^{(2)} \\ &= J^{(2)} \left\{ 1 + \frac{K^{(2)} J^{(0)} - J^{(2)}}{I_x^2 J^{(0)}} \right\}^{-1}. \end{aligned} \quad (4)$$

Figure 8.8 shows the calculated fractional changes in the MoI of four rotational bands in ^{173}Lu , where the rotational frequency is defined with respect to the cranking x-axis. The BCS pairing gaps of all bands were adjusted self consistently, while the shape parameters were kept fixed at values appropriate for the reference band, namely the ground state band in

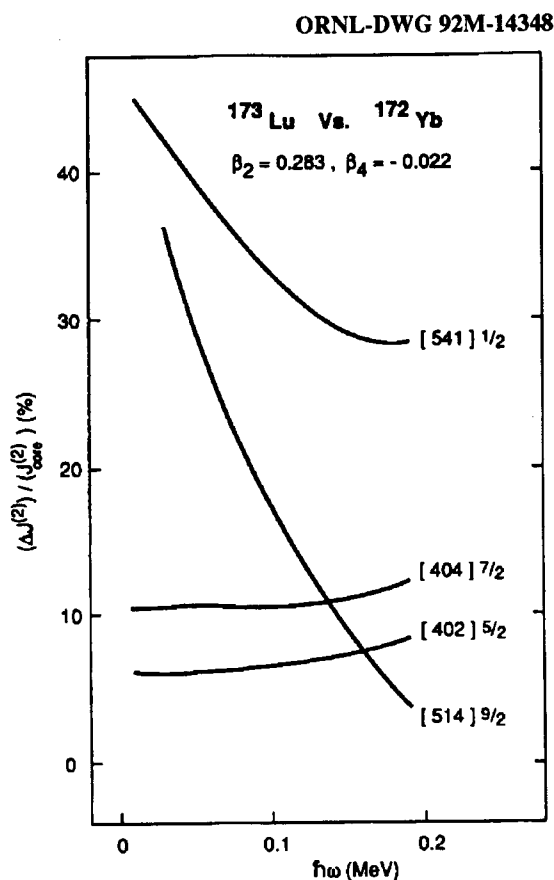


Fig. 8.8. Calculated fractional odd-even difference in the dynamic moments of inertia of four rotational bands in ^{173}Lu for cranking around the x-axis. The shape parameters were kept fixed at the indicated values, appropriate for the ^{172}Yb core.

^{172}Yb . Interestingly, the calculated fractional changes for the $[402]5/2$ and $[404]7/2$ bands are nearly *constant* and close to the above-mentioned value of 10% expected from the BCS theory. In contrast, the predicted fractional variations of the $[514]9/2$ and $[541]1/2$ intruder orbitals are large and *nonconstant*.

Figure 8.9 gives the calculated variations of these orbitals following the application of transformations given in Eq. (4), and are to be compared with the corresponding experimental results shown to the right. The solid curves in this figure (corresponding to the ^{172}Yb shape parameters) indicate a significantly smaller odd-even difference in the calculated MoI of the high-K bands compared to the values given in Fig. 8.8. The $K=1/2$ orbitals remain unchanged under this transformation. The calculated

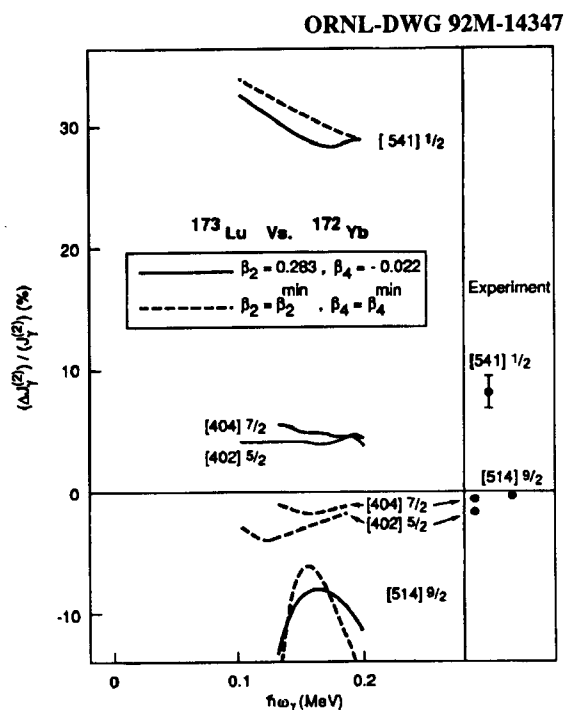


Fig. 8.9. Calculated fractional odd-even difference in the dynamic moments of inertia of four rotational bands in ^{173}Lu after application of the transformation given in Eq. (4). The dashed curves were obtained following minimization with respect to the shape parameters. The corresponding frequency-averaged, experimental values are given on the righthand side.

variations of the high-K bands are further reduced if the shape polarization of these valence orbitals is accounted for (dashed curves in Fig. 8.9). Indeed, these calculations successfully reproduce the identical bands based on the $[402]5/2$ and $[404]7/2$ high-K orbitals. It is noteworthy that *two equally important* factors give rise to these “identical bands:” (i) transformation from the x-axis to the tilted cranking axis given in Eq. (4) (cf. solid curves in Figs. 8.8 and 8.9); and (ii) shape polarization effects (cf. solid and dashed curves in Fig. 8.9).

In contrast, the predicted variation of the MoI of both the low-K $[541]1/2$ and the high-K $[514]9/2$ intruder orbitals remain large and *nonconstant* in Fig. 8.9. Failure of these calculations to reproduce the IB based on the $[514]9/2$ orbital indicates that large K values alone are not sufficient to produce identical bands. An even more important lesson is the

fact that the largest discrepancy between the experimental and calculated value is observed for the non-identical band based on the [541]1/2 orbital. That is, nonidentical bands may provide an even more stringent test of these calculations than the identical bands. To further document the strengths and weaknesses of the conventional models, we have initiated a systematic investigation of the MoI of the odd-Z rotational bands in the rare-earth region.

1. JIHIR, Oak Ridge, TN.
2. University of Pennsylvania, Philadelphia.
3. C. Baktash et al., *Phys. Rev. Lett.* **69**, 1500 (1992).
4. C. Baktash, W. Nazarewicz, and R. Wyss, *Nuclear Physics* (in press).

TRIAXIAL HEXADECAPOLE DEFORMATIONS IN ATOMIC NUCLEI

S. Åberg¹ and W. Nazarewicz²

Experimentally, very little is known about higher-order hexadecapole moments, $\alpha_{4\mu}$, $\mu > 0$. For instance, there is some evidence from alpha-particle scattering studies² for the nonaxial hexadecapole deformations, α_{42} and α_{44} , around ¹⁶⁸Er. On the theoretical side, the nonaxial hexadecapole moments are expected to be important, particularly at high spins, where the axial-symmetry is broken due to the angular momentum alignment of high-j nucleons. The interesting deformation is the one with $\mu = 4$. In the presence of nonvanishing hexadecapole moments α_{40} , α_{42} , and α_{44} , one may expect small hexadecapole perturbations of rotational bands.

A generalized parametrization of the hexadecapole deformation has been proposed by Rohozinski and Sobiczewski.³ In the presence of the three symmetry planes, the hexadecapole tensor can be parametrized by means of three parameters, β_4 , γ_4 , and δ_4 . The properties of this parametrization can be tested using a semiclassical single-j shell model. The hexadecapole field associated with the lowest one-quasiparticle excitation can be written as

$$V_4 = \kappa_4 \beta_4 j^4 z \left\{ \frac{2}{\sqrt{30}} \cos \delta_4 - \sqrt{\frac{2}{21}} \sin \delta_4 \cos \left(\gamma_4 + \frac{\pi}{3} \right) \right\}, \quad (1)$$

where $0 \leq \delta_4 \leq \pi$ and $0 \leq \gamma_4 \leq \pi/3$. The field V_4 leads to a modification of the quadrupole triaxial deformation, γ_2 , as a function of the shell filling.

Microscopic calculations have been performed within the cranked Nilsson-Strutinsky scheme. The usual condition of fixing δ_4 and γ_4 for given β_4 and γ is released, and the full hexadecapole tensor is included in the minimization procedure.

1. JIHIR, Oak Ridge, TN.
2. I. M. Govil et al., *Phys. Rev. C* **33**, 793 (1986); *Phys. Rev. C* **36**, 1442 (1987).
3. S. G. Rohozinski and A. Sobiczewski, *Acta Phys. Pol. B* **12**, 1001 (1981).

NUCLEAR SUPERDEFORMATION: PAST, PRESENT, AND FUTURE¹

W. Nazarewicz²

The study of high-spin states in nuclei is an extremely broad subject. Many of the bands of states observed at high spin require an interpretation in terms of shapes that are different from the ground state.

Recently, this has been given an additional dimension with the discovery of superdeformed (SD) high-spin bands in heavy atomic nuclei. Superdeformed high-spin bands, together with fission isomers, are the most spectacular examples of shape coexistence. They are characterized by an unusually large distortion, and occur at high angular momenta. To date, the superdeformed bands have been observed in a number of nuclei from the A~150 (Gd-Dy) and A~190 (Hg-Pb) mass regions. Contrary to the Gd-Dy region, where the superdeformed bands are built upon aligned many-quasiparticle configurations and, therefore, are seen at rather high angular momenta, in the Hg-Pb region the lowest observed spins in superdeformed bands are as low as $10\hbar$.

The main objective of this talk is to discuss recent developments in the physics of nuclear superdeformation and review the perspectives for future studies.

A sizable amount of high-spin data on SD states makes it possible, for the first time, to test many fine details of the shell structure at very large elongations. Moreover, it offers an opportunity to probe exotic orbitals that appear at normal deformations at com-

pletely different regions of particle number and rotational frequency. In particular, spectroscopy of superdeformed nuclear states opens up an exciting possibility to probe new properties of the nuclear mean field. The unusually deformed atomic nucleus can serve as a microscopic laboratory of quantum-mechanical symmetries of a three-dimensional harmonic oscillator. The quantum numbers and coupling schemes characteristic of weakly deformed systems are expected to be modified in the superdeformed world. Consequently, new classification schemes have to be introduced. They can be directly related to certain geometrical properties of the nuclear shape.

New possibilities in the field of superdeformation have been opened up by the discovery of multiple SD bands within one nucleus. The excited SD configurations turned out to have markedly different structures, as compared with the SD Yrast bands, suggesting a change in the intrinsic configurations. Calculations based on the deformed shell model theory explain many observed properties of SD bands in terms of characteristic *intruder* orbitals originating from the high-N oscillator shells and approaching the Fermi surface at large deformations. Because of their large intrinsic angular momenta, these states are strongly influenced by the Coriolis force. It has been

shown that the observed variations in the moments of inertia in the SD bands can be attributed to the number of high-N states occupied. The different high-N occupations have also been shown to explain the deformation variations with the particle number.

One of the most remarkable and puzzling current issues is the observation of identical g-ray sequences in different nuclei. Such *twinned* bands have first been found in SD systems. Various recent scenarios aiming at explanation of identical bands, such as pseudospin alignment, supersymmetry, triplet pairing, strong coupling, etc., will be discussed.

A comment will be made on (i) the possible quenching of pairing correlations at large elongations, (ii) the presence of low-lying octupole correlations at SD and hyperdeformed shapes, and (iii) the existence of intermediate-deformation structures.

Some future perspectives, e.g., superdeformed spectroscopy with radioactive ion beams, will be outlined.

1. Summary of invited talk presented at the *Seventh Nordic Meeting on Nuclear Physics, Vigsø, Denmark, August, 1992.*

2. JIHIR, Oak Ridge, TN.

9. LASER AND ELECTRO-OPTICS LAB

DEVELOPMENT OF AN INFRARED INTERFEROMETER/POLARIMETER SYSTEM FOR ITER

C. H. Ma and D. P. Hutchinson

The objective of this project is to use the Alcator-C-Mod tokamak as a test bed to demonstrate the system feasibility of an infrared interferometer/polarimeter for measurements of electron density and plasma current profiles in the International Thermonuclear Experimental Reactor (ITER). The system utilizes a cw CO₂ laser at a wavelength of 10.6 μm. Polarization-modulation techniques have been used to achieve the high sensitivity required for the measurements. During the past year, a mock-up system of the C-Mod polarimeter has been designed, constructed, and calibrated at this Laboratory and will be integrated into the existing two-color interferometer on C-Mod at MIT.¹ The polarimeter is a modification of a previous system developed for CIT.² The modifications are the result of two major improvements to the signal-processing scheme and the modulation system: (1) use of the two lock-in amplifier scheme to increase the sensitivity and (2) modification of the electronics to improve the time resolution.

A schematic diagram of the polarimeter system is shown in Fig. 9.1. An acousto-optic Bragg cell diffracts approximately 50% of the laser power into a reference beam. This acousto-optic cell also introduces a frequency shift Df of 40 MHz in the diffracted beam. The probing beam is passed through a polarization modulator and a plasma simulator, and is mixed with the reference beam. An electro-optic polarization-modulation technique has been utilized to improve the sensitivity and time response of the polarimetry. Cadmium telluride (CdTe) crystal polarization rotators are used as the modulators and the plasma simulator. The modulator consists of a ZnSe Fresnel $\lambda/4$ rhomb, and a CdTe crystal of $4 \times 4 \times 50$ mm operating with a half-wave voltage of 4.24 kV. The frequency of the modulation is approximately 1 MHz. An indium-doped CdTe crystal of $12.5 \times 12.5 \times 50.8$ mm is used in the plasma simulator. A solenoid of 7.6-mm i.d., 97-mm o.d., and 65-mm length pro-

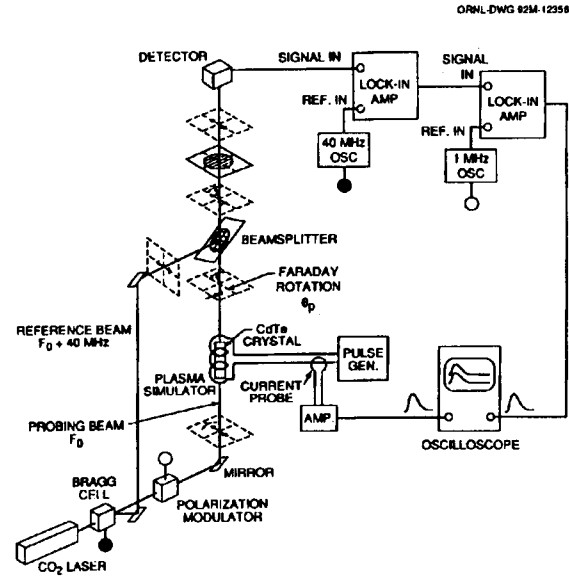


Fig. 9.1. Experimental configuration for the polarization-modulation CO₂ laser polarimeter.

duces a magnetic flux density of approximately 2.7 kG at a dc current of 3.5 A. The detector is a liquid-nitrogen-cooled HgCdTe photovoltaic diode. The output V_s of the detector can be expressed by the following relation:

$$V_s = \frac{1}{2} R P_p J_1(2\theta_p) \sin(2\theta_p) \sin(\omega_m t) + R(P_p P_r)^{1/2} \cos[\theta_p \theta_m \sin(\omega_m t)] \cos(\Delta\omega t = \phi) \quad (1)$$

+ terms of dc and other frequencies

where R is the responsivity of the detector, θ_m is the amplitude of the modulation angle, ω_m is the modulation frequency, ϕ is the phase shift due to plasma density, θ_p is the poloidal field-induced Faraday rotation in plasma, $J_1(2\theta_m)$ is the Bessel function of the first kind with order 1, and θ_p and θ_r are the power of the probing and the reference beam at the detector, respectively. In the previous system, the output signal was analyzed by only one lock-in amplifier

synchronized to a modulation frequency of 70 KHz. This system utilizes two lock-in amplifiers connected in series. The first one is synchronously detected at 40 MHz, and its output is fed into the second lock-in amplifier which is synchronized to the modulation frequency of approximately 1 MHz. The output voltage of the second amplifier is given by

$$V = V_o \sin(\theta_p) \quad (2)$$

where $V_o = 2AR(P_p P_r)^{1/2} J_1(\theta_m)$ and A is the total gain of the amplifiers. The maximum values of q_p in C-Mod and ITER are calculated to be 0.71° and 1.1° , respectively.³ Therefore, V can be considered as a direct measure of θ_p and Eq. (2) becomes

$$\theta_p = V/V_o \quad (3)$$

The calibration constant V_o can be obtained by inserting a mechanical polarization rotator in the path of the probing beam, setting its rotation at few degrees, and measuring the value of V without the pulse current in the plasma simulator. The use of the two lock-in amplifier scheme in the present system has not only reduced the RF pick-up noise but has also greatly improved the sensitivity of the system.

1. T. Luke and J. H. Irby, *Bull. Am. Phys. Soc.* **35**, 1997 (1990).

2. C. H. Ma, D. P. Hutchinson, and K. L. Vander Sluis, *Rev. Sci. Instrum.* **59**, 1629 (1988).

3. C. H. Ma, D. P. Hutchinson, and J. Irby, *Bull. Am. Phys. Soc.* **37** (1992).

CO₂ LASER THOMSON SCATTERING ALPHA PARTICLE DIAG- NOSTIC

*R. K. Richards, D. P. Hutchinson,
and C. H. Ma*

A proof-of-principle test of an alpha particle diagnostic based on CO₂ laser Thomson scattering has been completed. The diagnostic is being developed for the measurement of the velocity distribution of fusion product alpha particles in an ignited thermonuclear reactor.^{1,2} Because such a reactor does not exist, the diagnostic was tested on a nonburning

plasma experiment — the Advanced Toroidal Facility (ATF). With no energetic alpha particles, the test was performed by a measurement of the plasma electrons. For the test, the diagnostic was configured to duplicate the requirements for an alpha-particle measurement — i.e., the measurement of a small scattered signal ($\leq 10^{-9}$ W) in the presence of a high power source laser ($\geq 10^6$ W) at small scattering angles ($\leq 1^\circ$). The goals of this test were to eliminate stray laser light which would produce a background signal at the receiver and to maintain alignment between the pulsed laser and receiver beams (which was set at 0.86°), while performing scattering measurements on the plasma. This test and its results are detailed in ref. 3. The test proved successful, as indicated in Fig. 9.2, with the measurement of an electron resonance feature near the electron plasma frequency and represents the first demonstration of a

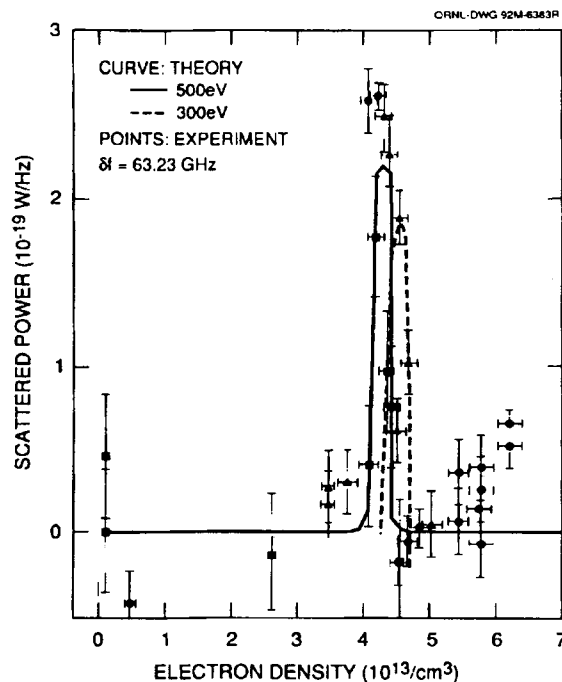


Fig. 9.2. The measured scattered power from the ATF plasma versus electron density at a frequency shift of 63.23 ± 1 GHz from the laser line. Three sets of experimental data (taken on three separate days) are compared to a calculation of the resonance for the electron temperature of 500 eV (solid curve) and 300 eV (dotted curve), the variation of temperatures during the experiment.

diagnostic technique capable of measurements of confined alpha particles in a burning fusion plasma.

The next step in the development and testing of this diagnostic is the measurement of a fast ion-tail population. In the plasma device Alcator C-Mod at MIT, which has just started operation, the plasma parameters with ion-cyclotron heating are expected to produce hot-ion tails which resemble the distributions of fusion-product alpha particles both in density and velocity. A diagnostic system is currently being developed for this measurement. Part of this development is the increase in laser pulse length over the 1 μ sec used in the proof-of-principle test. The longer

pulse is needed for an increased signal-to-noise ratio necessary for a temperature measurement.

1. D. P. Hutchinson, K. L. Vander Sluis, J. Sheffield, and D. J. Sigmar, *Rev. Sci. Instrum.* **56**, 1075 (1985).

2. R. K. Richards, C. A. Bennett, L. K. Fletcher, H. T. Hunter, and D. P. Hutchinson, *Rev. Sci. Instrum.* **59**, 1556 (1988).

3. R. K. Richards, D. P. Hutchinson, C. A. Bennett, H. T. Hunter, and C. H. Ma, to be published in *Applied Physics Letters*.

10. COMPILATIONS AND EVALUATIONS

CONTROLLED FUSION ATOMIC DATA CENTER

H. B. Gilbody,¹ D. C. Gregory, C. C. Havener, M. I. Kirkpatrick, E. W. McDaniel,² F. W. Meyer, T. J. Morgan,³ R. A. Phaneuf,⁴ M. S. Pindzola,⁵ D. R. Schultz, and E. W. Thomas²

The mission of the Controlled Fusion Atomic Data Center (CFADC) is to compile, evaluate, and disseminate atomic and molecular data pertinent to fusion energy research. To these ends, the CFADC maintains a bibliographic database, publishes data compilations, and participates in an international network of atomic data centers. These activities are supported by the equivalent of 1.2 full-time Physics Division staff members and five expert consultants under contract. Ongoing components and accomplishments in these areas are summarized below.

1. The CFADC Bibliographic Database

Through journal searches performed primarily by a network of expert consultants, the CFADC maintains a PC-based, on-line database of references to articles of interest to fusion energy research, covering the period from 1978 to the present. The database currently contains approximately 24,500 entries and increases by about 1000 each year. Requests for queries of the database are answered at the rate of about three per week. Bibliographic entries are periodically provided to the International Atomic Energy Agency (IAEA) to be published in the "International Bulletin on Atomic and Molecular Data for Fusion," most recently for the period from October 1990 to March 1992. In addition, efforts have been initiated to restore, from tape archives, the bibliographic entries dating from c. 1950 to 1978. Initial funding has been received to adapt the bibliographic system to a new user-accessible computer workstation. This workstation, which will be accessible through INTERNET, will allow a much more widespread and flexible availability to this database, as well as to the growing numerical atomic databases

derived from CFADC publications and the international exchange of information.

2. The Compilation and Evaluation of Data

The CFADC undertakes projects to recommend atomic and molecular data and has published the series "Atomic Data for Fusion" (ORNL-6086 V. 1, 3-5 and ORNL-6551 V. 1-3), commonly referred to as the "Redbooks." The feasibility of reinitiating the process of compiling and recommending data for electron-impact processes relevant to fusion in a joint effort with NIST and JILA is currently being evaluated. This work would be published as Volume 2 of the Redbook series. In addition, members of the CFADC and its associates regularly contribute works to provide evaluated data to research and review journals. For example, owing to the need for state-selective capture cross sections for fully stripped ions colliding with atomic hydrogen for plasma diagnostic applications, a collaboration with the IAEA and the Japanese data centers at NIFS and JAERI has led to a set of recommended cross sections. Also, an effort has been initiated in response to the needs of the fusion community in modelling the edge plasma layer for the International Thermonuclear Experimental Reactor to collect data in this newly emphasized regime and to perform new theoretical calculations.

3. International Cooperation

Through a network of international data centers, coordinated by the International Atomic Energy Agency, the CFADC cooperates in distributing evaluated data in the ALADDIN format and in assessing the status and needs concerning atomic and molecular data for fusion research. In addition, efforts to produce or encourage the production of data to address the highest priority needs continue to be made. During the past year, members of the CFADC have participated in several IAEA meetings regarding the data center network and have been contributors to advisory groups charged with making recommendations on such issues as atomic data for hydrogen

recycling and helium removal from next-step fusion reactors.

1. Consultant, Queen's University, Belfast, Northern Ireland
2. Consultant, Georgia Institute of Technology, Atlanta, Georgia
3. Consultant, Wesleyan University, Middletown, Connecticut
4. Present address: Dept. of Physics, Univ. of Nevada, Reno, NV
5. Consultant, Auburn University, Auburn, Alabama

NUCLEAR DATA PROJECT

*Y. A. Akevali, M. R. Lay, M. J. Martin, S. Rab,¹
and M. R. Schmorak²*

The Nuclear Data Project (NDP) is one of five data evaluation centers comprising the U.S. Nuclear Data Network (USNDN). The Project is responsible for the evaluation of nuclear structure information in the mass region $A \geq 199$. The NDP maintains a complete computer-indexed library of reports and published articles in experimental nuclear structure physics as well as copies of the Evaluated Nuclear Structure Data and Nuclear Structure Reference files (ENSDF, NSR).

The Editor-in-Chief of the *Nuclear Data Sheets* is a member of the Nuclear Data Project staff. All mass chains from the 14 centers in the International Nuclear Data Network are edited here, and the Editor-in-Chief has the ultimate responsibility for the quality of the mass chains entered into ENSDF and, thus, for what is published in the *Nuclear Data Sheets*.

Data Evaluation. During this report period, NDP staff members prepared revised evaluations for the $A = 230, 235, 239,$ and 245 mass chains. These evaluations have been published or are in press in the *Nuclear Data Sheets*.

Mass Chain Editing and Review. NDP staff members edited and/or reviewed 14 mass chains.

Information Services. NDP staff members responded to requests for specific information by researchers outside the evaluation center. Responses took the form of searches of the ENSDF and NSR files and personal consultation. A list of reports and preprints received by the NDP is prepared and distributed monthly to division staff members.

Research. NDP staff members have participated in research with other groups in the division. Discussion of these activities may be found in the research section of this report.

-
1. Visitor from Kuwait Institute for Scientific Research, Kuwait, and partial support provided by Joint Institute for Heavy Ion Research, ORNL.
 2. Consultant.

11. PUBLICATIONS

List Prepared by Shirley J. Ball

The following list of publications includes primarily those articles by Physics Division staff members and associates which appeared in print from October 1991 through September 1992. Articles pending publication as of September 30, 1992, are listed immediately following this section.

BOOK, JOURNAL, AND PROCEEDINGS ARTICLES

Ackleh, E. S., and T. Barnes

"Two-Photon Width of Singlet Positronium and Quarkonium with Arbitrary Total Angular Momentum," *Phys. Rev. D* **45**, 232-40 (Jan. 1992)

Ackleh, E. S., T. Barnes, and F. E. Close

"Two-Photon Helicity Selection Rules and Widths for Positronium and Quarkonium States with Arbitrary Angular Momenta," *Phys. Rev. D* **46**, 2257-60 (Sept. 1992)

Akovali, Y. A.

"Nuclear Data Sheets for A= 213," *Nucl. Data Sheets* **66**, 237-79 (May 1992)

Akovali, Y. A.

"Nuclear Data Sheets for A= 247," *Nucl. Data Sheets* **66**, 505-34 (June 1992)

Akovali, Y. A.

"Nuclear Data Sheets for A= 243," *Nucl. Data Sheets* **66**, 897-930 (Aug. 1992)

Akovali, Y. A.

"Nuclear Data Sheets for A = 245," *Nucl. Data Sheets* **67**, 153-93 (Sept. 1992)

Albert, C. J., D. J. Ernst, M. R. Strayer, and C. Bottcher (Invited Presentation)

"Electromagnetic Lepton-Pair Production in Relativistic Collisions," pp.255-66 in Proceedings, Conference on Computational Quantum Physics, Nashville, Tenn., May 22-25, 1991, AIP Conference Proceedings 260, American Institute of Physics, New York, 1992

Albrecht, R., T. C. Awes, C. Baktash, P. Beckmann, F. Berger, M. Bloomer, D. Bock, R. Bock, G. Claesson, G. Clewing, L. Dragon, A. Eklund, R. L. Ferguson, A. Franz, S. Garpman, R. Glasow, H. A. Gustafsson, H. H. Gutbrod, M. Hartig, G. Hoelker, J. Idh, P. Jacobs, K. H. Kampert, B. W. Kolb, P. Kristiansson, H. Loehner, I. Lund, F. E. Obenshain, A. Oskarsson, I. Otterlund, T. Peitzmann, S. Persson, F. Plasil, A. M. Poskanzer, M. Purschke, H. G. Ritter, B. Roters, S. Saini, R. Santo, H. R. Schmidt, R. Schmidt, S. P. Sorensen, K. Steffens, P. Steinhauser, E. Stenlund, D. Stueken, M. L. Tincknell, A. Twyhues, and G. R. Young

"Bose-Einstein Correlations in the Target Fragmentation Region in 200 A GeV ^{16}O + Nucleus Collisions," *Z. Phys. C* **53**, 225-37 (Feb. 1992)

Albrecht, R., T. C. Awes, C. Baktash, P. Beckmann, F. Berger, M. Bloomer, D. Bock, R. Bock, G. Claesson, G. Clewing, L. Dragon, A. Eklund, R. Ferguson, A. Franz, S. I. A. Garpman, R. Glasow, H. A. Gustafsson, H. H. Gutbrod, J. Idh, P. Jacobs, K. H. Kampert, B. W. Kolb, H. Loehner, I. Lund, F. E. Obenshain, A. Oskarsson, I. Otterlund, T. Peitzmann, F. Plasil, A. M. Poskanzer, M. Purschke, H. G. Ritter, S. Saini, R. Santo, H. R. Schmidt, S. P. Sorensen, K. Steffens, E. Stenlund, D. Stueken, and G. R. Young

“Multiplicity and Pseudorapidity Distributions of Charged Particles from ^{32}S Induced Heavy Ion Interactions at 200 A GeV,” *Z. Phys. C* **55**, 539 ff. (1992)

Albrecht, R., T. C. Awes, P. Beckmann, F. Berger, D. Bock, R. Bock, G. Claesson, G. Clewing, L. Dragon, A. Eklund, R. L. Ferguson, A. Franz, S. Garpman, R. Glasow, H. A. Gustafsson, H. H. Gutbrod, G. Hoelker, J. Idh, P. Jacobs, K. H. Kampert, B. W. Kolb, P. Kristiansson, I. Y. Lee, H. Loehner, I. Lund, F. E. Obenshain, A. Oskarsson, I. Otterlund, T. Peitzmann, F. Plasil, A. M. Poskanzer, M. Purschke, H. G. Ritter, R. Santo, S. Saini, H. R. Schmidt, S. P. Sorensen, K. Steffens, D. Stueken, E. Stenlund, M. L. Tincknell, and G. R. Young

“Upper Limit for Thermal Direct Photon Production in Heavy-Ion Collisions at 60 and 200 A GeV,” *Z. Phys. C* **51**, 1-10 (July 1991)

Albrecht, R., T. C. Awes, C. Baktash, P. Beckmann, F. Berger, R. Bock, G. Claesson, G. Clewing, L. Dragon, A. Eklund, R. L. Ferguson, A. Franz, S. Garpman, R. Glasow, H. A. Gustafsson, H. H. Gutbrod, J. Idh, P. Jacobs, K. H. Kampert, B. W. Kolb, P. Kristiansson, I. Y. Lee, H. Loehner, I. Lund, F. E. Obenshain, A. Oskarsson, I. Otterlund, T. Peitzmann, S. Persson, F. Plasil, A. M. Poskanzer, M. Purschke, H. G. Ritter, S. Saini, R. Santo, H. R. Schmidt, T. Siemiarczuk, S. P. Sorensen, E. Stenlund, M. L. Tincknell, and G. R. Young

“Distributions of Transverse Energy and Forward Energy in ^{16}O - and ^{32}S -Induced Heavy-Ion Collisions at 60 A and 200 A GeV,” *Phys. Rev. C* **44**, 2736-52 (Dec. 1991)

Alton, G. D.

“A Simple, High-Efficiency, Negative Surface Ionization Source,” Fourth International Conference on Ion Sources, Bensheim, Germany, Sept. 30-Oct. 4, 1991, *Rev. Sci. Instrum.* **63**, 2453-54 (Apr. 1992)

Alton, G. D.

“A Pulsed-Mode, High-Intensity, Heavy Negative Ion Source,” Fourth International Conference on Ion Sources, Bensheim, Germany, Sept. 30-Oct. 4, 1991, *Rev. Sci. Instrum.* **63**, 2455-57 (Apr. 1992)

Alton, G. D.

“A Multiple-Sample, Cesium-Sputter, Negative Ion Source,” Fourth International Conference on Ion Sources, Bensheim, Germany, Sept. 30-Oct. 4, 1991, *Rev. Sci. Instrum.* **63**, 2450-52 (Apr. 1992)

Alton, G. D.

“Design Aspects for a Pulsed-Mode, High-Intensity, Heavy Negative Ion Source,” pp. 1937-39 in *Proceedings, 1991 IEEE Particle Accelerator Conference, San Francisco, Calif., May 6-9, 1991, Vol. 3, IEEE Catalog No. 91CH3038-7, World Scientific Publishing, Singapore, 1991*

Alton, G. D., H. K. Carter, C. M. Jones, J. Kormicki, and D. K. Olsen

“Element/Target-Dependent Release Times and Release Efficiencies for the Proposed OREB Facility,” pp. 95-100 in *Radioactive Nuclear Beams 1991* (Proceedings, Second International Conference on Radioactive Nuclear Beams, Louvain-la-Neuve, Belgium, Aug. 19-21, 1991), IOP Publishing, Bristol, England, 1992

Alton, G. D., H. K. Carter, I. Y. Lee, C. M. Jones, J. Kormicki, and D. K. Olsen

“Studies of the Release Properties of ISOL-Target Materials Using Ion Implantation,” *Nucl. Instrum. Methods Phys. Res.* **B66**, 492-502 (1992)

- Alton, G. D., R. A. Sparrow, and R. E. Olson
"Plasma as a High-Charge-State Projectile Stripping Medium," *Phys. Rev. A* **45**, 5957-63 (Apr. 1992)
- Andersson, L. R., H. Cederquist, A. Barany, L. Liljeby, C. Biedermann, J. C. Levin, N. Keller, S. B. Elston, J. P. Gibbons, and I.A. Sellin
"One- and Two-Step Double-Electron Capture in Slow Ar⁶⁺-He Collisions," *Phys. Rev. A* **45**, R4-R7 (Jan. 1992)
- Aronson, S., M. J. Murtagh, M. Starks, X. T. Liu, G. A. Pettit, Z. Zhang, L. A. Ewell, J. C. Hill, F. K. Wahn, J. B. Costales, M. N. Namboodiri, T. C. Sangster, J. H. Thomas, A. Gavron, L. Waters, W. L. Kehoe, S. G. Steadman, T. C. Awes, F. E. Obenshain, S. Saini, G. R. Young, J. Chang, S.-Y. Fung, J. H. Kang, J. Kreke, X. He, S. P. Sorensen, E. C. Cornell, and C. F. Maguire (Invited Presentation)
"Calorimeter/Absorber Optimization for a RHIC Dimuon Experiment (RD-10 Project)," pp. 153-79 in *Proceedings, Symposium on RHIC Detector R&D, Upton, N.Y., Oct. 10-11, 1991, BNL Report BNL52321 (1992)*
- Auble, R. L., Editor
"Holifield Heavy Ion Research Facility Newsletter," Issue No. 45 (1991)
- Auble, R. L., Editor
"Holifield Heavy Ion Research Facility Newsletter," Issue No. 46 (1991)
- Auble, R. L., Editor
"Holifield Heavy Ion Research Facility Newsletter," Issue No. 47 (1992)
- Awes, T. C., F. E. Obenshain, F. Plasil, S. Saini, S. P. Sorensen, and G. R. Young
"A Simple Method of Shower Localization and Identification in Laterally Segmented Calorimeters," *Nucl. Instrum. Methods Phys. Res. A* **311**, 130-38 (Jan. 1992)
- Baktash, C. (Invited Presentation)
"Finite-Temperature Effects in Warm Nuclei: Recent Developments and Open Questions," pp. 423-43 in *Proceedings, Conference on "Future Directions in Nuclear Physics with 4 π Gamma Detection Systems of the New Generation," Strasbourg, France, Mar. 4-16, 1991, AIP Conference Proceedings 259, American Institute of Physics, New York, 1992*
- Baktash, C., J. D. Garrett, D. F. Winchell, and A. Smith
"Low-Spin Identical Bands in Neighboring Odd-A and Even-Even Nuclei: A Possible Challenge to Mean-Field Theories," *Phys. Rev. Lett.* **69**, 1500-03 (Sept. 1992)
- Barnes, T.
"Two-Photon Couplings of Quarkonia with Arbitrary Angular Momenta," pp. 498-502 in *Hadron '91 (Proceedings, Fourth International Conference on Hadron Spectroscopy, College Park, Md., Aug. 12-16, 1991), World Scientific Publishing, Singapore, 1992*
- Barnes, T. (Invited Presentation)
"The t-J Model at Small t/J: Numerical, Perturbative, and Supersymmetric Results," pp. 503-14 in *High Temperature Superconductivity (Proceedings, Workshop on Electronic Structure and Mechanisms for High Temperature Superconductivity, Miami, Fla., Jan. 3-9, 1991), Plenum Publishing, New York, 1992*
- Barnes, T., A. E. Jacobs, M. D. Kovarik, and W. G. Macready
"Detailed Lanczos Study of One- and Two-Hole Band Structure and Finite-Size Effects in the t-J Model," *Phys. Rev. B* **45**, 256-65 (Jan. 1992)

Barnes, T., and E. S. Swanson

“Diagrammatic Approach to Meson-Meson Scattering in the Nonrelativistic Quark Potential Model,”
Phys. Rev. D **46**, 131-59 (July 1992)

Beene, J. R., and F. E. Bertrand (Invited Presentation)

“Giant Resonances and Intermediate Energy Heavy Ions: Electromagnetic Decay Experiments,”
Proceedings, Fourth International Conference on Nucleus-Nucleus Collisions, Kanazawa, Japan, June
10-14, 1991, Nucl. Phys. A**538**, 553c-64c (1992)

Benhenni, M., S. M. Shafroth, J. K. Swenson, M. Schulz, J. P. Giese, H. Schone, C. R. Vane, P. F. Dittner,
and S. Datz (Invited Presentation)

“Evidence for Interference Between Resonant and Nonresonant Transfer and Excitation,” pp. 693-98 in
Proceedings, XVII International Conference on the Physics of Electronic and Atomic Collisions,
Brisbane, Australia, July 10-14, 1991, IOP Publishing, Bristol, England, 1992

Bhatt, K. H., C. W. Nestor, Jr., and S. Raman

“Do Nucleons in Abnormal-Parity States Contribute to Deformation?,” Phys. Rev. C **46**, 164-80 (July
1992)

Bloomer, M. A., P. Jacobs, R. Albrecht, T. C. Awes, P. Beckmann, F. Berger, D. Bock, R. Bock,
G. Claesson, G. Clewing, R. Debbe, L. Dragon, A. Eklund, R. L. Ferguson, S. Fokin, A. Franz,
S. Garpman, R. Glasow, H. A. Gustafsson, H. H. Gutbrod, O. Hansen, M. Hartig, G. Hoelker, J. Idh,
M. Ippolitov, K. H. Kampert, K. Karadjev, B. W. Kolb, A. Lebedev, H. Loehner, I. Lund, V. Manko,
B. Moskowitz, F. E. Obenshain, A. Oskarsson, I. Otterlund, T. Peitzmann, F. Plasil, A. M. Poskanzer,
M. Purschke, H. G. Ritter, B. Roters, S. Saini, R. Santo, H. R. Schmidt, K. Soderstrom, S. P. Sorensen,
K. Steffens, P. Steinhauser, E. Stenlund, D. Stueken, A. Twyhues, A. Vinogradov, and G. R. Young
“Intermittency in $^{32}\text{S}+\text{S}$ and $^{32}\text{S}+\text{Au}$ Collisions at the CERN SPS,” Proceedings, Ninth International
Conference on Ultra-Relativistic Nucleus-Nucleus Collisions (Quark Matter '91), Gatlinburg, Tenn.,
Nov. 11-15, 1991, Nucl. Phys. A**544**, 543c-46c (July 1992)

Botcher, C., M. J. Rhoades-Brown, and M. R. Strayer

“Approximate Analytic Formula Used to Estimate Electron-Capture Cross Sections at Relativistic
Energies,” Phys. Rev. A **44**, 4769-70 (Oct. 1991)

Botcher, C., and M. R. Strayer (Invited Presentation)

“Electromagnetic Pair Production in Relativistic Heavy-Ion Collisions,” Proceedings, Ninth Interna-
tional Conference on Ultra-Relativistic Nucleus-Nucleus Collisions (Quark Matter '91), Gatlinburg,
Tenn., Nov. 11-15, 1991, Nucl. Phys. A**544**, 255c-65c (July 1992)

Botcher, C., and M. R. Strayer (Invited Presentation)

“Ultrarelativistic Atomic Collisions,” pp. 371-80 in Proceedings, XVII International Conference on the
Physics of Electronic and Atomic Collisions, Brisbane, Australia, July 10-16, 1991, IOP Publishing,
Bristol, England, 1992

Botcher, C., and M. R. Strayer (Invited Presentation)

“The Electromagnetic Scenario for Higgs Production in Large Colliders,” pp. 183-209 in Proceedings,
Workshop on Beam-Beam and Beam-Radiation Interactions: High Intensity and Nonlinear Effects, Los
Angeles, Calif., May 13-16, 1991, World Scientific Publishing, Singapore, 1992

Botcher, C., and M. R. Strayer (Invited Presentation)

“Coherent Lepton Pair Production from Relativistic Heavy-Ion Collisions,” pp. 191-200 in Proceedings,
Pittsburgh Workshop on Soft Lepton Pair and Photon Production, Pittsburgh, Penn., Sept. 6-8, 1990,
Nova Science Publishers, New York, 1992

- Brandan, M. E., K. W. McVoy, and G. R. Satchler
"Analysis of an Unusual Potential Ambiguity for $^{16}\text{O}+^{16}\text{O}$ Scattering," *Phys. Lett. B* **281**, 185-90 (May 1992)
- Burgdorfer, J. (Invited Presentation)
"Dynamic Screening and Wake Effects on Electronic Excitation in Ion-Solid and Ion-Surface Collisions," Proceedings, International Conference on Atomic Collisions in Solids, University of Salford, U.K., July 28-Aug. 2, 1991, *Nucl. Instrum. Methods Phys. Res. B* **67**, 1-20 (Apr. 1992)
- Burgdorfer, J., P. Lerner, and F. W. Meyer
"Above-Surface Neutralization of Highly Charged Ions: The Classical Over-the-Barrier Model," *Phys. Rev. A* **44**, 5674-85 (Nov. 1991)
- Butsch, R., D.J. Hofman, C.P. Montoya, P. Paul, and M. Thoennessen
"Time Scales for Fusion-Fission and Quasifission from Giant Dipole Resonance Decay," *Phys. Rev. C* **44**, 1515-27 (Oct. 1991)
- Casten, R. F., J. D'Auria, C. Davids, J. Garrett, M. Nitschke, B. Sherrill, D. Vieira, M. Wiescher, and E. Zganjar
"The IsoSpin Laboratory (ISL) - Research Opportunities with Radioactive Nuclear Beams" (Report of the Steering Committee), Los Alamos National Laboratory Report LALP91-51 (1991)
- Clark, R. M., R. Wadsworth, E. S. Paul, C. W. Beausang, I. Ali, A. Astier, D. M. Cullen, P. J. Dagnall, P. Fallon, M. J. Joyce, M. Meyer, N. Redon, P. H. Regan, W. Nazarewicz, and R. Wyss
"First Observation of a Collective Dipole Rotational Band in the A~200 Mass Region," *Phys. Lett. B* **275**, 247-51 (Jan. 1992)
- Clark, R. M., R. Wadsworth, E. S. Paul, C. W. Beausang, I. Ali, A. Astier, D. M. Cullen, P. J. Dagnall, P. Fallon, M. J. Joyce, M. Meyer, N. Redon, P. H. Regan, J. F. Sharpey-Schafer, W. Nazarewicz, and R. Wyss
"Collective Dipole Rotational Bands in ^{197}Pb ," *Z. Phys. A* **342**, 371-72 (1992)
- Close, F. E., and Z. P. Li
"A Unified Formalism for $\gamma\gamma\rightarrow\text{Meson}$ and $\psi\rightarrow X$ with Possible Tests for Hybrid and Gluonic Hadrons," *Z. Phys. C* **54**, 147-62 (Apr. 1992)
- Connelly, J. P., H. Crannell, L. W. Fagg, J. T. O'Brien, M. Petraitis, D. I. Sober, S. Raman, J. R. Deininger, and S. E. Williamson
"Magnetic Dipole Strength in ^{46}Ca Observed with 180° Electron Scattering," *Phys. Lett. B* **277**, 38386 (Mar. 1992)
- Datz, S., P. F. Dittner, J. Gomez del Campo, H. F. Krause, T. M. Rosseel, and C. R. Vane (Invited Presentation)
"Electron Ion Interactions in Crystal Channels: Collisions in Ultra-Dense Electron Media," *Z. Phys. D* **21**, (Suppl.: Proceedings, Fifth International Conference on the Physics of Highly Charged Ions, Giessen, West Germany, Sept. 10-14, 1990), S45-50 (1991)
- Datz, S., P. F. Dittner, J. Gomez del Campo, H. F. Krause, T. M. Rosseel, C. R. Vane, Y. Iwata, K. Komaki, M. Kimura, Y. Yamazaki, F. Fujimoto, and Y. Honda (Invited Presentation)
"Resonant Coherent Excitation of Mg^{11+} : Electronic Collisions of State Specified Short-Lived Excited States in a Crystal Channel," Proceedings, 13th Werner Brandt Workshop on the Interaction of Charged Particles with Matter, Nara, Japan, November 12-18, 1990, *Radiation Effects and Defects in Solids* **117**, 73 ff. (1991)

218 Physics Division Progress Report

- Datz, S., P. F. Dittner, H. F. Krause, C. R. Vane, A. Belkacem, B. Feinberg, H. Gould, R. Schuch, H. Knudsen, and P. Hvelplund
"Measurements of Pair Production in Relativistic Heavy Particle Coulomb Collisions," CERN Annual Report for 1990, Vol.2, p.27 (1991)
- Datz, S., and M. Larsson
"Radiative Lifetimes for all Vibrational Levels in the $X^1\Sigma^+$ State of HeH^+ and Its Relevance to Dissociative Recombination Experiments in Ion Storage Rings," Phys. Scr. **46**, 343-47 (1992)
- Datz, S., C. R. Vane, H. F. Krause, and P. F. Dittner (Invited Presentation)
"Dielectronic Excitation and Recombination in Crystal Channels," pp.311-18 in Recombination of Atomic Ions (Proceedings, NATO Workshop on Resonant Transfer and Excitation in Channeling, Belfast, Northern Ireland, Oct. 7-9, 1991), Plenum Publishing, New York, 1992
- Davies, K. T. R.
"Dyson's Equations for Nucleon-Pion-Delta Interactions: Toward a Self-Consistent Solution in Nuclear Matter," Ann. Phys. (N.Y.) **215**, 386-456 (May 1992)
- Davies, K. T. R., Huston, T. E., and M. Baranger
"Calculations of Periodic Trajectories for the Hénon-Heiles Hamiltonian Using the Monodromy Method," Chaos **2**, 215-24 (1992)
- Davies, K. T. R., J. S. Wu, and R. W. Davies
"Evaluation of Integrals Using General Partial-Fraction Expansions," Can. J. Phys. **70**, 311-29 (May 1992)
- Dean, D. J., A. S. Umar, J.-S. Wu, and M. R. Strayer
"A Dynamical String-Parton Model for Relativistic Heavy-Ion Collisions," Phys. Rev. C **45**, 400-14 (Jan. 1992)
- Dean, D. J., A. S. Umar, J.-S. Wu, and M. R. Strayer (Invited Presentation)
"A Dynamical Picture of Hadron-Hadron Collisions with the String-Parton Model," pp. 159-71 in Proceedings, Conference on Computational Quantum Physics, Nashville, Tenn., May 22-25, 1991, AIP Conference Proceedings 260, American Institute of Physics, New York, 1992
- Dellwo, J., Y. Liu, D. J. Pegg, and G. D. Alton
"Near-Threshold Photodetachment of the Li^- Ion," Phys. Rev. A **45**, 1544-47 (Feb. 1992)
- Dittner, P. F., and S. Datz (Invited Presentation)
"Early Measurements of Dielectronic Recombination: Multiply Charged Ions," pp.133-41 in Recombination of Atomic Ions (Proceedings, NATO Workshop on Resonant Transfer and Excitation in Channeling, Belfast, Northern Ireland, Oct. 7-9, 1991), Plenum Publishing, New York, 1992
- Dittner, P. F., C. R. Vane, H. F. Krause, J. Gomez del Campo, N. L. Jones, P. Zeijlmans van Emmichoven, U. Bechtold, and S. Datz
"Search for a Narrow Resonant Transfer and Excitation Resonance of Titanium Projectiles Channeled in a Gold Crystal," Phys. Rev. A **45**, 2935-39 (Mar. 1992)
- Dooley, K., E. S. Swanson, and T. Barnes
"A Prediction of Spin-0 and -2 Vector-Meson Molecules. A New Model of the $\theta_2(1720)$," Phys. Lett. B **275**, 478-86 (Jan. 1992)

Dragon, L., R. Albrecht, T. C. Awes, P. Beckman, F. Berger, D. Bock, R. Bock, G. Claesson, G. Clewing, A. Eklund, R. Ferguson, A. Franz, S. Garpman, R. Glasow, H. A. Gustafsson, H. H. Gutbrod, G. Hoelker, J. Idh, P. Jacobs, K. H. Kampert, B. W. Kolb, H. Loehner, I. Lund, F. E. Obenshain, A. Oskarsson, I. Otterlund, T. Peitzmann, F. Plasil, A. M. Poskanzer, M. Purschke, H. G. Ritter, S. Saini, R. Santo, H. R. Schmidt, S. P. Sorensen, K. Steffens, E. Stenlund, D. Stueken, M. L. Tincknell, and G. R. Young
"Search for Direct Thermal Photons in Heavy-Ion Collisions at the SPS," pp. 13-19 in Proceedings, Pittsburgh Workshop on Soft Lepton Pair and Photon Production, Pittsburgh, Penn., Sept. 6-8, 1990, Nova Science Publishers, New York, 1992

Gao, W. B., I. Y. Lee, C. Baktash, R. Wyss, J. H. Hamilton, C. M. Steele, C. H. Yu, N. R. Johnson, and F. K. McGowan
"High Spin Spectroscopy and Lifetime Measurements in ^{169}Hf ," Phys. Rev. C **44**, 1380-96 (Oct. 1991)

Garrett, J. D., J. R. German, L. Courtney, and J. M. Espino (Invited Presentation)
"The Distribution of Nuclear Quantum States in 'Cold' Rotating Nuclei," pp. 345-57 in Proceedings, Conference on "Future Directions in Nuclear Physics with 4π Gamma Detection Systems of the New Generation," Strasbourg, France, Mar. 4-16, 1991, AIP Conference Proceedings 259, American Institute of Physics, New York, 1992

Gatoff, G., and C. Y. Wong
"Origin of the Soft p_T Spectra," Phys. Rev. D **46**, 997-1006 (Aug. 1992)

Griffin, D. C., M. S. Pindzola, and N. R. Badnell
"Convergence of the Close-Coupling Method for the $3p^5 3d^2$ Configuration in Ti^{3+} ," J. Phys. B **24**, L621-29 (Dec. 1991)

Gronidin, G. (Invited Presentation)
"A Monte Carlo Study of the Light $Q^2\bar{Q}^2$ System," pp.783-88 in Hadron'91 (Proceedings, 4th International Conference on Hadron Spectroscopy, College Park, Md., Aug. 12-16, 1991), World Scientific Publishing, Singapore, 1992

Gronidin, G. (Invited Presentation)
"Monte Carlo Simulation of a Dynamical Fermion Problem: The Light $q\bar{q}^{-2}$ System," pp.292-308 in Proceedings, Conference on Computational Quantum Physics, Nashville, Tenn., May 22-25, 1991, AIP Conference Proceedings 260, American Institute of Physics, New York, 1992

Hamilton, J. H. (Invited Presentation)
"New Approaches to Studies of Exotic Nuclei," Proceedings, International School of Nuclear Physics: 4π High Resolution Gamma Ray Spectroscopy, published in Prog. Part. Nucl. Phys., Vol. 28 (1992)

Havener, C. C., F. W. Meyer, and R. A. Phaneuf (Invited Presentation)
"Electron Capture in Very Low Energy Collisions of Multicharged Ions with H and D in Merged Beams," pp.381-90 in Proceedings, XVII International Conference on the Physics of Electronic and Atomic Collisions, Brisbane, Australia, July 10-16, 1991, IOP Publishing, Bristol, England, 1992

Havener, C. C., M. P. Nesnidal, M. R. Porter, and R. A. Phaneuf (Invited Presentation)
"Electron Capture in Slow Collisions of Multicharged Ions with Hydrogen Atoms Using Merged Beams," Z. Phys. D **21** (Suppl.: Proceedings of the Fifth International Conference on the Physics of Highly Charged Ions, Giessen, Germany, Sept. 10-14, 1991), S243-44 (1991)

220 Physics Division Progress Report

- Haynes, D. L., C. M. Jones, R. C. Juras, M. J. Meigs, J. E. Raatz, and J. B. Schroeder
"A Simple, Inexpensive Voltage Grading Resistor for Large Electrostatic Accelerators," Nucl. Instrum. Methods Phys. Res. A320, 400-02 (Aug. 1992)
- Horen, D. J., F. E. Bertrand, J. R. Beene, G. R. Satchler, W. Mittig, A. C. C. Villari, Y. Schutz, Z. Wenlong, E. Plagnol, and A. Gillibert
"Isospin Character of the Giant Quadrupole Transition in ^{124}Sn ," Phys. Rev. C 44, 2385-89 (Dec. 1991)
- Horen, D. J., C. L. Morris, S. J. Seestrom, F. W. Hersman, J. R. Calarco, M. Holtrop, M. Leuschner, M. Rawool-Sullivan, R. W. Garnett, S. J. Greene, M. A. Plum, and J. D. Zumbro
"Isospin Character of the Transition to the 0.803-MeV State in ^{206}Pb from π^{\pm} Scattering at 180 MeV," Phys. Rev. C 46, 499-503 (Aug. 1992)
- Ikezoe, H., N. Shikazona, Y. Nagame, T. Ohtsuki, Y. Sugiyama, Y. Tomita, K. Ideno, I. Kanno, H. J. Kim, B. J. Qi, and A. Iwamoto (Invited Presentation)
"Charged Particle Emissions in Fission Process," Proceedings, 4th International Conference on Nucleus-Nucleus Collisions, Kanazawa, Japan, June 10-14, 1991, Nucl. Phys. A538, 299c-306c (1992)
- International Hybrid Spectrometer Consortium, including H.O. Cohn
"Neutral-Strange-Particle Production in 200-GeV/c $p/\pi^+/K^+$ Interactions on Au, Ag, and Mg," Phys. Rev. D 45, 734 (Feb. 1992)
- Jacobs, P., M. A. Bloomer, R. Albrecht, T. C. Awes, P. Beckmann, F. Berger, D. Bock, R. Bock, G. Claesson, G. Clewing, R. Debbe, L. Dragon, A. Eklund, R. L. Ferguson, S. Fokin, A. Franz, S. Garpman, R. Glasow, H. A. Gustafsson, H. H. Gutbrod, O. Hansen, M. Hartig, G. Hoelker, J. Idh, M. Ippolitov, K. H. Kampert, K. Karadjev, B. W. Kolb, A. Lebedev, H. Loehner, I. Lund, V. Manko, B. Moskowitz, F. E. Obenshain, A. Oskarsson, I. Otterlund, T. Peitzmann, F. Plasil, A. M. Poskanzer, M. Purschke, H. G. Ritter, B. Roters, S. Saini, R. Santo, H. R. Schmidt, K. Soderstrom, S. P. Sorensen, K. Steffens, P. Steinhauser, E. Stenlund, D. Stueken, A. Twyhues, A. Vinogradov, and G. R. Young
"Intermittency in 200 GeV/Nucleon S+S Collisions," Proceedings, Workshop on Dynamical Fluctuations and Correlations in Nuclear Collisions, Aussois, France, Mar. 16-20, 1992, Nucl. Phys. A545, 311c-20c (Aug. 1992)
- Jin, H.-Q., L. L. Riedinger, C.-H. Yu, W. Nazarewicz, R. Wyss, J.-Y. Zhang, C. Baktash, J. D. Garrett, N. R. Johnson, I. Y. Lee, and F. K. McGowan
"Electromagnetic Properties of the $[303]5/2, 7/2$ Pseudo-Spin Doublet in ^{175}Re ," Phys. Lett. B 277, 387-92 (Mar. 1992)
- Johnson, N. R. (Invited Presentation)
"Collective Properties and Shapes of Nuclei at Very High Spins," Proceedings, International School of Nuclear Physics— 4π High Resolution Gamma-Ray Spectroscopy, Erice, Italy, Sept. 20-28, 1991, Prog. Part. Nucl. Phys. 28, 215-24 (1992)
- Johnson, T. D., T. Glasmacher, J. W. Holcomb, P. C. Womble, S. L. Tabor, and W. Nazarewicz
"Rotational Band Structure in ^{75}Se ," Phys. Rev. C 46, 516-31 (Aug. 1992)
- Kampert, K. H., R. Albrecht, T. C. Awes, P. Beckmann, F. Berger, M. Bloomer, D. Bock, R. Bock, G. Claesson, G. Clewing, R. Debbe, L. Dragon, A. Eklund, R. L. Ferguson, S. Fokin, A. Franz, S. Garpman, R. Glasow, H. A. Gustafsson, H. H. Gutbrod, O. Hansen, M. Hartig, G. Hoelker, J. Idh, M. Ippolitov, P. Jacobs, K. Karadjev, B. W. Kolb, A. Lebedev, H. Loehner, I. Lund, V. Manko, B. Moskowitz, F. E. Obenshain, A. Oskarsson, I. Otterlund, T. Peitzmann, F. Plasil, A. M. Poskanzer,

- M. Purschke, H. G. Ritter, B. Roters, S. Saini, R. Santo, H. R. Schmidt, R. Schmidt, S. P. Sorensen, K. Steffens, P. Steinhauser, E. Stenlund, D. Stueken, A. Vinogradov, H. Wegener, and G. R. Young (Invited Presentation)
"Recent Results from the WA80 Experiment at CERN," Proceedings, Ninth International Conference on Ultra-Relativistic Nucleus-Nucleus Collisions (Quark Matter '91), Gatlinburg, Tenn., Nov. 11-15, 1991, Nucl. Phys. A544, 183c-96c (July 1992)
- Keller, N., O. Heil, J. Kemmler, M. W. Lucas, R. Maier, H. Rothard, I. A. Sellin, and K. O. Groneveld
"Continuum Electrons in Coincidence with the Charge State of Target Ions," Phys. Rev. A 44, 4407-11 (Oct. 1991)
- Kemmler, J., J. Burgdorfer, and C. O. Reinhold
"High I State Population in O^{7+} Produced in Ion-Solid Collisions," Proceedings, International Conference on Atomic Collisions in Solids, University of Salford, U.K., July 28-Aug. 2, 1991, Nucl. Instrum. Methods Phys. Res. B67, 168-72 (Apr. 1992)
- Korolija, M., D. Shapira, N. Cindro, J. Gomez del Campo, H. J. Kim, K. Teh, and J. Y. Shea (Invited Presentation)
"Interferometric Studies from p-p-Fragment Coincidences," pp. 165 ff. in Proceedings, 7th International Adriatic Conference on Nuclear Physics, Croatia, Yugoslavia, May 27-June 1, 1991, World Scientific Publishing, Singapore, 1991
- Lee, I. Y. (Invited Presentation)
"The GAMMASPHERE," International School of Nuclear Physics - 4π High Resolution Gamma-Ray Spectroscopy, Erice, Italy, Sept. 20-28, 1991, published in Prog. Part. Nucl. Phys., Vol. 28 (1992)
- Lee, I. Y. (Invited Presentation)
"The GAMMASPHERE," pp. 90-103 in Proceedings, International Conference on New Nuclear Physics with Advanced Techniques, Crete, Greece, June 23-29, 1991, World Scientific Publishing, Singapore, 1992
- Lee, I. Y. (Invited Presentation)
"Proposal of Physics with Exotic Beams at Oak Ridge," pp. 369-75 in Proceedings, International Conference on New Nuclear Physics with Advanced Techniques, Crete, Greece, June 23-29, 1991, World Scientific Publishing, Singapore, 1992
- Lee, I. Y., C. Baktash, J. R. Beene, M. L. Halbert, D. C. Hensley, N. R. Johnson, F. K. McGowan, M. A. Riley, and D. G. Sarantites
"Quantitative Studies of Continuum Gamma-Ray Correlations in ^{170}Hf ," Phys. Rev. C 46, 597-603 (Aug. 1992)
- LEP Collaborations, including H. O. Cohn, Yu. Kamyshkov, F. Plasil, and K. F. Read
"Electroweak Parameters of the Z^0 Resonance and the Standard Model," Phys. Lett. B 276, 247 (Feb. 1992)
- L3 Collaboration, including H. O. Cohn, Yu. Kamyshkov, F. Plasil, and K. F. Read
"Measurement of the Strong Coupling Constant α_s for Bottom Quarks at the Z^0 Resonance," Phys. Lett. B 271, 463 (Nov. 1991)
- L3 Collaboration, including H. O. Cohn, Yu. Kamyshkov, F. Plasil, and K. F. Read
"Search for Lepton Flavor Violation in Z^0 Decays," Phys. Lett. B 271, 455 (Nov. 1991)

222 Physics Division Progress Report

- L3 Collaboration, including H. O. Cohn, Yu. Kamyshkov, F. Plasil, and K. F. Read
"Measurement of the Lifetime of B-Hadrons and a Determination of $|V_{cb}|$," Phys. Lett. B **270**, 111 (Nov. 1991)
- L3 Collaboration, including H. O. Cohn, Yu. Kamyshkov, F. Plasil, and K. F. Read
"A Direct Determination of the Number of Light Neutrino Families from $e^+e^- \rightarrow \nu\bar{\nu}\gamma$ at LEP," Phys. Lett. B **275**, 209 (Jan. 1992)
- L3 Collaboration, including H. O. Cohn, Yu. Kamyshkov, F. Plasil, and K. F. Read
"Search for the Neutral Higgs Boson at LEP," Phys. Lett. B **283**, 454 (June 1992)
- L3 Collaboration, including H. O. Cohn, Yu. Kamyshkov, F. Plasil, and K. F. Read
"Studies of Hadronic Event Structure and Comparisons with QCD Models at the Z^0 Resonance," Z.Phys. C **55**, 39 (1992)
- Macek, J. H.
"Reply to A.Salin: Some Remarks on Strong-Potential Born Expansions for Ion-Atom Collisions," J.Phys. B **24**, 5121-32 (Dec. 1991)
- Mantica, P. F., Jr., B. E. Zimmerman, W. B. Walters, J. Rikovska, and N. J. Stone
"Level Structure of ^{126}Xe : Population of Low-Spin Levels in the Decay of $1^+ ^{126}\text{Cs}$ and Theoretical Description of Adjacent Even-Even Xe Nuclides," Phys. Rev. C **45**, 1586-96 (Apr. 1992)
- McGowan, F. K., N. R. Johnson, C. Baktash, I. Y. Lee, Y. Schutz, J. C. Wells, and A. Larabee
"Transition Quadrupole Moments of High-Spin States in $^{162,163}\text{Yb}$," Nucl. Phys. A **539**, 276-94 (Mar. 1992)
- Meyer, F. W., S. H. Overbury, C. C. Havener, P. A. Zeijlmans van Emmichoven, J. Burgdorfer, and D. M. Zehner
"Electron Emission During Interactions of Multicharged N and Ar Ions with Au(110) and Cu(001) Surfaces," Phys. Rev. A **44**, 7214-28 (Dec. 1991)
- Mowat, J. R., J. A. Tanis, R. R. Haar, J. L. Forest, T. Ellison, C. Foster, W. Jacobs, T. Rinckel, P. F. Dittner, W. G. Graham, M. W. Clark, D. E. Schneider, and M. P. Stockli (Invited Presentation)
"A Measurement of the Dielectronic Recombination of He^+ Ions," pp.203-08 in Recombination of Atomic Ions (Proceedings, NATO Workshop on Resonant Transfer and Excitation in Channeling, Belfast, Northern Ireland, Oct. 7-9, 1991), Plenum Publishing, New York, 1992
- Muller, J., J. Burgdorfer, and D. W. Noid
"Semiclassical Eigenenergies in the Wake of Fast Ions in Solids," pp.449-60 in Quantum Chaos (Proceedings, Miniworkshop on Quantum Chaos, Trieste, Italy, June 4-July 6, 1990), World Scientific Publishing, Singapore, 1991
- Muller, J., J. Burgdorfer, and D. Noid
"Torus Quantization of Symmetrically Excited Helium," Phys. Rev. A **45**, 1471-78 (Feb. 1992)
- Nazarewicz, W. (Invited Presentation)
"Static Multipole Deformations in Nuclei," Proceedings, International School on Nuclear Physics - 4π High Resolution Gamma Ray Spectroscopy, Erice, Sicily, Sept. 20-29, 1991, Prog. Part. Nucl. Phys. **28**, 307-30 (1992)

- Nazarewicz, W., and J. Dobaczewski
“Dynamical Symmetries, Multiclustering and Octupole Susceptibility in Superdeformed and Hyperdeformed Nuclei,” *Phys. Rev. Lett.* **26**, 154-57 (Jan. 1992)
- Nazarewicz, W., J. Dobaczewski, and P. VanIsacker (Invited Presentation)
“Shell Model Calculations at Superdeformed Shapes,” pp.30-51 in *Proceedings, Workshop–Symposium on Future Directions in Nuclear Physics with 4π Gamma Detection Systems of the New Generation*, Strasbourg, France, Mar. 4-16, 1991, AIP Conference Proceedings 259, American Institute of Physics, New York, 1992
- Nazarewicz, W. and Z. Szymanski
“Analysis of a Three-Dimensional Cranking in A Simple Model,” *Phys. Rev. C* **45**, 2771-81 (June 1992)
- Nazarewicz, W., and S. L. Tabor
“Octupole Shapes and Shape Changes at High Spins in the $Z \approx 58$, $N \approx 88$ Nuclei,” *Phys. Rev. C* **45**, 2226-37 (May 1992)
- Olsen, D. K., G. D. Alton, C. Baktash, H. K. Carter, D. T. Dowling, J. D. Garrett, D. L. Haynes, C. M. Jones, R. C. Juras, S. N. Lane, I. Y. Lee, M. J. Meigs, G. D. Mills, S. W. Mosko, B. A. Tatum, and K. S. Toth
“Radioactive Beams with the HHIRF Accelerators,” pp. 2604-06 in *Proceedings, 1991 IEEE Particle Accelerator Conference*, San Francisco, Calif., May 6-9, 1991, Vol.4, IEEE Catalog No. 91CH3038-7, World Scientific Publishing, Singapore, 1991
- Olsen, D. K., G. D. Alton, C. Baktash, H. K. Carter, D. T. Dowling, J. D. Garrett, D. L. Haynes, C. M. Jones, R. C. Juras, S. N. Lane, I. Y. Lee, M. J. Meigs, G. D. Mills, S. W. Mosko, B. A. Tatum, and K. S. Toth
“The Extension of the HHIRF Accelerators to Produce Radioactive Ion Beams,” pp.131-36 in Radioactive Nuclear Beams 1991 (Proceedings, Second International Conference on Radioactive Nuclear Beams, Louvain-la-Neuve, Belgium, Aug. 19-21, 1991), IOP Publishing, Bristol, England, 1992
- Palacz, M., Z. Sujkowski, J. Nyberg, J. Bacelar, J. Jongman, W. Urban, W. Hesselink, J. Nasser, A. Plompen, and R. Wyss
“High Spin States in ^{131}Ce ,” *Z. Phys. A* **338**, 467-68 (1991)
- Pegg, D. J.
“Correlation in Photodetachment,” pp. 348-58 in Atomic and Molecular Physics (Proceedings, Third U.S./Mexico Symposium, Moralos, Mexico, Mar. 13-16, 1991), World Scientific Publishing, Singapore, 1991
- Phaneuf, R. A., F. W. Meyer, D. C. Gregory, C. C. Havener, P. A. Zeijlmans van Emmichoven, S. H. Overbury, D. M. Zehner, G. H. Dunn, J. S. Thompson, E. K. Wahlin, and A. C. H. Smith (Invited Presentation)
“Low-Energy Collisions of Multiply Charged Ions with Electrons, Atoms and Surfaces,” pp. 403-17 in Atomic and Molecular Physics (Proceedings, Third U.S./Mexico Symposium, Moralos, Mexico, Mar. 13-16, 1991), World Scientific Publishing, Singapore, 1991
- Pindzola, M. S., N. R. Badnell, and D. C. Griffin
“Dielectronic Recombination Between Hyperfine Levels of the Ground State of Bi^{82+} ,” *Phys. Rev. A* **45**, R7659-62 (June 1992)

- Pindzola, M. S., N. R. Badnell, R. J. W. Henry, D. C. Griffin, and W. L. vanWyngaarden
"Close-Coupling Calculations for the Electron-Impact Excitation of Zn," *Phys. Rev. A* **44**, 5628-35 (Nov. 1991)
- Plasil, F., R. Albrecht, T. C. Awes, C. Baktash, P. Beckmann, F. Berger, R. Bock, G. Claesson, G. Clewing, L. Dragon, A. Eklund, R. L. Ferguson, A. Franz, S. Garpman, R. Glasow, H. A. Gustafsson, H. H. Gutbrod, J. Idh, P. Jacobs, K. H. Kampert, B. W. Kolb, P. Kristiansson, I. Y. Lee, H. Loehner, I. Lund, F. E. Obenshain, A. Oskarsson, I. Otterlund, T. Peitzmann, S. Persson, A. M. Poskanzer, M. Purschke, H. G. Ritter, S. Saini, R. Santo, H. R. Schmidt, T. Siemiarczuk, S. P. Sorensen, K. Steffens, E. Stenlund, D. Stucken, M. L. Tincknell, and G. R. Young (Invited Presentation)
"Nucleus-Nucleus Collisions at 60 to 200 GeV/Nucleon: Results from the WA80 Experiment at CERN," pp. 1104-05 in Vol. II, Proceedings, 25th International Conference on High Energy Physics, Singapore, Aug. 2-8, 1990, South East Asia Theoretical Physics Association and Physical Society of Japan, 1991
- Raman, S., L. W. Fagg, and R. S. Hicks
"Giant Magnetic Resonances," pp. 355-533 in Electric and Magnetic Giant Resonances in Nuclei, International Review of Nuclear Physics, Vol. 7, World Scientific Publishing, Singapore, 1991
- Raman, S., E. T. Journey, J. W. Starner, and J. E. Lynn
"Thermal-Neutron Capture by Silicon Isotopes," *Phys. Rev. C* **46**, 972-83 (Sept. 1992)
- Raman, S., and J. E. Lynn (Invited Presentation)
"Mechanism of (n, γ) Reaction at Low Neutron Energies," pp. 107-15 in Proceedings, Beijing International Symposium on Fast Neutron Physics, Beijing, China, Sept. 9-13, 1991, World Scientific Publishing, Singapore, 1992
- Reinhold, C. O., J. Burgdorfer, J. Kemmler, and P. Koschar
"Simulation of Convoy-Electron Emission," *Phys. Rev. A* **45**, R2655-58 (Mar. 1992)
- Roberts, M. L., P. D. Felsher, G. J. Weisel, Z. Chen, C. R. Howell, W. Tornow, R. L. Walter, and D. J. Horen
"Measurement of $A\gamma(\theta)$ for $n+^{208}\text{Pb}$ from 6 to 10 MeV and the Neutron-Nucleus Interaction over the Energy Range from Bound States at -17 MeV up to Scattering at 40 MeV," *Phys. Rev. C* **44**, 2006-24 (Nov. 1991)
- Satchler, G. R.
Book Review: Heavy Ion Reactions: Lecture Notes, Volume 1, Elementary Processes, *Science* **252**, 1325 (May 1991)
- Satchler, G. R.
"Local Potential Model for Pion-Nucleus and π^+/π^- Excitation Ratios," *Nucl. Phys. A* **540**, 533-76 (Apr. 1992)
- Satchler, G. R., M. K. Singham, and M. B. Johnson
"Comment on 'Pion Scattering from ^{39}K and ^{58}Ni ' and Virtual Excitation Effects on Elastic Scattering." *Phys. Rev. C* **45**, 2027-29 (Apr. 1992)
- Satula, W., S. Cwiok, W. Nazarewicz, R. Wyss, and A. Johnson
"Structure of Superdeformed States in Au-Ra Nuclei," *Nucl. Phys. A* **529**, 289-314 (July 1991)

Schmorak, M. R.

"Nuclear Data Sheets for A= 239," Nucl. Data Sheets **66**, 839-96 (Aug. 1992)

Shafroth, S. M., M. Benhenni, J. K. Swenson, M. Schulz, J. P. Giese, H. Schone, C. R. Vane, P. F. Dittner, and S. Datz

"Resonant Transfer Excitation: Interference Effects," pp.301-10 in Recombination of Atomic Ions (Proceedings, NATO Workshop on Resonant Transfer and Excitation in Channeling, Belfast, Northern Ireland, Oct. 7-9, 1991), Plenum Publishing, New York, 1992

Shapira, D., J. Gomez del Campo, H. Kim, E. L. Chavez, J. P. Wielecko, J. Y. Shea, C. F. Maguire, M. Korolija, N. Cindro, and K. Teh

"Toward a Unified Dynamic Model for Heavy Ion Reactions — Exclusive Measurements of Br+Al and Ni+Mg at Incident Energies Near 10 MeV/amu," pp. 121 ff. in Proceedings, 7th International Conference on Nuclear Physics, Croatia, Yugoslavia, May 27-June 1, 1991, World Scientific Publishing, Singapore, 1991

Sharma, R. P., L. E. Rehn, P. M. Baldo, J. W. Downey, B. Kestel, R. Vane, H. F. Krause, and P. F. Dittner

"Ion Channeling Investigations in High T_c Materials," Proceedings, 14th International Conference on Atomic Collisions in Solids, Salford, U.K., July 28-Aug. 2, 1991, Nucl. Instrum. Methods Phys. Res. **B67**, 194-98 (Apr. 1992)

Sobotka, L. G., L. Gallamore, A. Chbihi, D. G. Sarantites, D. W. Stracener, W. Bauer, D. R. Bowman, N. Carlin, R. T. DeSouza, C.K. Gelbke, W. G. Gong, S. Hannuschke, Y. D. Kim, W. G. Lynch, R. Ronningen, M. B. Tsang, F. Zhu, J. R. Beene, M. L. Halbert, and M. Thoennesen

"Particle Multiplicity Dependence of High-Energy Photon Production in a Heavy-Ion Reaction," Phys. Rev. C **44**, R2257-61 (Dec. 1991); Erratum: Phys. Rev. C **46**, 819-21 (Aug. 1992)

Sorensen, S. P., R. Albrecht, T. C. Awes, C. Baktash, P. Beckmann, F. Berger, R. Bock, G. Claesson, G. Clewing, L. Dragon, A. Eklund, R. L. Ferguson, A. Franz, S. Garpman, R. Glasow, H. A. Gustafsson, H. H. Gutbrod, J. Idh, P. Jacobs, K. H. Kampert, B. W. Kolb, P. Kristiansson, I. Y. Lee, H. Loehner, I. Lund, F. E. Obenshain, A. Oskarsson, I. Otterlund, T. Peitzmann, S. Persson, F. Plasil, A. M. Poskanzer, M. Purschke, H. G. Ritter, S. Saini, R. Santo, H. R. Schmidt, T. Siemiarczuk, E. Stenlund, M. L. Tincknell, and G. R. Young (Invited Presentation)

"Transverse and Forward Energy Measurements in Nucleus-Nucleus Collisions at 60 and 200 GeV/Nucleon," pp.55-64 in Proceedings, Hadron Structure'91 (Physics and Applications, Vol. 16), Stara Lesna, Czechoslovakia, Sept. 16-20, 1991, Slovak Academy of Sciences, Bratislava, Czechoslovakia, 1991

Sorensen, S. P., R. Albrecht, T. C. Awes, C. Baktash, P. Beckmann, F. Berger, R. Bock, G. Claesson, G. Clewing, L. Dragon, A. Eklund, R. L. Ferguson, A. Franz, S. Garpman, R. Glasow, H. A. Gustafsson, H. H. Gutbrod, J. Idh, P. Jacobs, K. H. Kampert, B. W. Kolb, P. Kristiansson, I. Y. Lee, H. Loehner, I. Lund, F. E. Obenshain, A. Oskarsson, I. Otterlund, T. Peitzmann, S. Persson, F. Plasil, A. M. Poskanzer, M. Purschke, H. G. Ritter, S. Saini, R. Santo, H. R. Schmidt, T. Siemiarczuk, E. Stenlund, M. L. Tincknell, and G. R. Young (Invited Presentation)

"Nuclear Stopping Power," pp. 582-91 in Proceedings, XXI International Symposium on Multiparticle Dynamics, Wuhan, China, Sept. 23-27, 1991, World Scientific Publishing, Singapore, 1992

Tatum, B. A.

"Vacuum and Beam Diagnostic Controls for ORIC Beam Lines," pp.1519-21 in Proceedings, 1991 Particle Accelerator Conference, San Francisco, Calif., May 6-9, 1991, Vol.3, IEEE Catalog No. 91CH3038-7, World Scientific Publishing, Singapore, 1991

226 Physics Division Progress Report

- Teichmann, S.G., S. B. Gazes, M. E. Mason, R. B. Roberts, and H. J. Kim
"Breakup-Fusion as a Source of Prompt Neutrons in Low-Energy $^{28}\text{Si}+^{98}\text{Mo}$, ^{58}Ni Reactions," *Phys. Lett. B* **283**, 37-41 (1992)
- Thoennessen, M., and J. R. Beene
"Nuclear Dissipation and the Feeding of Superdeformed Bands," *Phys. Rev. C* **45**, 873-75 (Feb. 1992)
- Thoennessen, M., J. R. Beene, F. E. Bertrand, C. Baktash, M. L. Halbert, D. J. Horen, D. C. Hensley, D. G. Sarantites, W. Spang, D. W. Stracener, and R. L. Varner,
"Large Deformation in $A \sim 170$ Nuclei at High Excitation Energies," *Phys. Lett. B* **282**, 288-92 (May 1992)
- Toth, K. S., C. R. Bingham, H. J. Kim, J. W. McConnell, J. D. Robertson, and D. C. Sousa
"Limits of Stability for Proton Rich Nuclei," pp.237-42 in Radioactive Nuclear Beams 1991 (Proceedings, Second International Conference on Radioactive Nuclear Beams, Louvain-la-Neuve, Belgium, Aug. 19-21, 1991), IOP Publishing, Bristol, England, 1992
- Toth, K. S., H. J. Kim, J. W. McConnell, C. R. Bingham, and D. C. Sousa
"Alpha Decays of Light Uranium Isotopes," *Phys. Rev. C* **45**, 856-59 (Feb. 1992)
- Toth, K. S., K. S. Vierinen, M. O. Kortelahti, D. C. Sousa, J. M. Nitschke, and P. A. Wilmarth
"Investigation of $A = 155$ and $A = 151$ Nuclides: Identification of the $^{155}\text{Tm}_{s_{1/2}}$ Isomer and of the ^{155}Yb β -Decay Branch," *Phys. Rev. C* **44**, 1868-77 (Nov. 1991)
- Toth, K. S., K. S. Vierinen, J. M. Nitschke, P. A. Wilmarth, and R. M. Chasteler
"Alpha-Decaying Low-Spin Levels in ^{155}Lu and ^{157}Lu ," *Z. Phys. A* **340**, 343-44 (1991)
- Umar, A. S., D. J. Dean, and M. R. Strayer
"A Dynamical String-Parton Model for Relativistic Heavy-Ion Collisions," Proceedings, Ninth International Conference on Ultra-Relativistic Nucleus-Nucleus Collisions (Quark Matter '91), Gatlinburg, Tenn., Nov. 11-15, 1991, *Nucl. Phys. A* **544**, 475c-78c (July 1992)
- Umar, A. S., M. R. Strayer, J.-S. Wu, D. J. Dean, and M. C. Guclu
"Nuclear Hartree-Fock Calculations with Splines," *Phys. Rev. C* **44**, 2512-21 (Dec. 1991)
- Utsunomiya, H., Y.-W. Lui, D. R. Haenni, H. Dejbakhsh, L. Cooke, B. K. Srivastava, W. Turmel, D. O'Kelley, R. P. Schmitt, D. Shapira, J. Gomez del Campo, A. Ray, and T. Udagawa
"Breakup of ^7Li Near the α -t Threshold and a Possible Probe of Radiative-Capture Processes," *Phys. Rev. Lett.* **65**, 847-50 (Aug. 1990)
- Vane, C. R., P. F. Dittner, H. F. Krause, J. Gomez del Campo, N. L. Jones, P. Zeijlmans van Emmichoven, U. Bechtold, and S. Datz (Invited Presentation)
"Energy Loss Dependence of X-Rays Emitted by Titanium Ions Channeled in a Thin Gold Single Crystal," Proceedings, International Conference on Atomic Collisions in Solids, University of Salford, United Kingdom, July 28-Aug. 2, 1991, *Nucl. Instrum. Methods Phys. Res.* **B67**, 256-61 (1992)
- Wahlin, E. K., J. S. Thompson, G. H. Dunn, R. A. Phaneuf, D. C. Gregory, and A. C. H. Smith (Invited Presentation)
"Electron-Impact Excitation of Multiply-Charged Ions Using Energy Loss in Merged Beams: $e + \text{Si}^{3+}(3s^2S_{1/2}) \rightarrow e + \text{Si}^{3+}(3p^2P_{1/2,3/2})$," *Z. Phys. D* **21** (Suppl.: Proceedings of the Fifth International Conference on the Physics of Highly Charged Ions, Giessen, West Germany, Sept. 10-14, 1991), S3538 (1991)

- Walkiewicz, T. A., S. Raman, E. T. Jurney, J. W. Starner, and J. E. Lynn
"Thermal-Neutron Capture by Magnesium Isotopes," *Phys. Rev. C* **45**, 1597-608 (Apr. 1992)
- Wang, J., C. O. Reinhold, and J. Burgdorfer
"Electron-Electron Interaction and Two-Center Effects in Projectile Ionization at Backward Emission Angles," *Phys. Rev. A* **45**, 4507-18 (Apr. 1992)
- Wang, J., C. O. Reinhold, and J. Burgdorfer
"Electron Loss at Backward Observation Angles," *Phys. Rev. A* **44**, 7243-51 (Dec. 1991)
- Wang, T. F., E. A. Henry, J. A. Becker, A. Kuhnert, M. A. Stoyer, S. W. Yates, M. J. Brinkman, J. A. Cizewski, A. O. Macchiavelli, F. S. Stephens, M. A. Deleplanque, R. M. Diamond, J. E. Draper, F. A. Azaiez, W. H. Kelly, W. Korten, E. Rubel, and Y. A. Akovali
"First Lifetime Measurements of Dipole Collective Bands in Neutron-Deficient Lead Nuclei," *Phys. Rev. Lett.* **69**, 1737-40 (Sept. 1992)
- Wells, J. C., C. Bottcher, J. Drake, R. Flanery, V. E. Oberacker, M. R. Strayer, A. S. Umar, and J.-S. Wu
"Numerical Methods for the Dirac Equation," pp.1-32 in Proceedings, Intel Supercomputer Users' Group 1991 International Users' Conference, Dallas, Texas, Oct. 6-9, 1991, Intel Corporation, Supercomputer Systems Division (Nov. 1991)
- Wells, J. C., V. E. Oberacker, A. S. Umar, C. Bottcher, M. R. Strayer, and J.-S. Wu (Invited Presentation)
"Nonperturbative Electromagnetic Muon-Pair Production with Capture in Peripheral Relativistic Heavy Ion Collisions," pp. 215-27 in Proceedings, Conference on Computational Quantum Physics, Nashville, Tenn., May 22-25, 1991, AIP Conference Proceedings 260, American Institute of Physics, New York, 1992
- Wells, J. C., V. E. Oberacker, A. S. Umar, C. Bottcher, M. R. Strayer, J.-S. Wu, and G. Plunien
"Nonperturbative Electromagnetic Lepton-Pair Production in Peripheral Relativistic Heavy-Ion Collisions," *Phys. Rev. A* **45**, 6296-312 (May 1992)
- Winchell, D. F., D. O. Ludwigsen, and J. D. Garrett
"The Mass Dependence of Moments of Inertia of Rapidly-Rotating Nuclei," *Phys. Lett. B* **289**, 267-70 (Sept. 1992)
- Woody, C., D. Lissauer, J. Gomez del Campo, A. Ray, D. Shapira, M. Tincknell, R. Clark, C. Erd, J. Schurkraft, and W. Willis
"Status of Soft Photons in Experiment E855," pp. 21-28 in Proceedings, Pittsburgh Workshop on Soft Lepton Pair and Photon Production, Pittsburgh, Penn., Sept. 6-8, 1990, Nova Science Publishers, New York, 1992
- Wu, J. S., C. Bottcher, M. R. Strayer, and C. M. Shakin (Invited Presentation)
"Particle Production Through Two-Photon Processes in Relativistic Heavy-Ion Colliders," pp. 47-58 in Proceedings, Conference on Computational Quantum Physics, Nashville, Tenn., May 22-25, 1991, AIP Conference Proceedings 260, American Institute of Physics, New York, 1992
- Wu, J. S., M. J. Rhoades-Brown, C. Bottcher, and M. R. Strayer
"Detailed Analysis of the Background e^+e^- Spectra Generated by Relativistic Heavy-Ion Beam Crossing," *Nucl. Instrum. Methods Phys. Res. A* **311**, 249-57 (Jan. 1992)
- Xu, Y., K. S. Krane, M. A. Gummin, M. Jarrio, J. L. Wood, E. F. Zganjar, and H. K. Carter
"Shape Coexistence and Electric Monopole Transitions in ^{184}Pt ," *Phys. Rev. Lett.* **68**, 3853-56 (June 1992)

228 Physics Division Progress Report

Young, G. R. (Invited Presentation)

"Experimental Challenges at RHIC and LHC," Proceedings, Ninth International Conference on Ultra-Relativistic Nucleus-Nucleus Collisions, Gatlinburg, Tenn., Nov. 11-15, 1991, Nucl. Phys. A544, 391c-403c (July 1992)

Young, G. R. (Invited Presentation)

"Physics and Experiments at RHIC," Proceedings, Fourth International Conference on Nucleus-Nucleus Collisions, Kanazawa, Japan, June 10-14, 1991, Nucl. Phys. A538, 649c-58c (1992)

Zhang, J. Y., X. He, C. C. Shih, S. P. Sorensen, and C. Y. Wong

"Transverse Energy and Forward Energy Production in a High Energy Nuclear Collision Model," Phys. Rev. C 46, 748-53 (Aug. 1992)

Zhu, S., L. Chaturvedi, J. H. Hamilton, A. V. Ramayya, C. Girit, J. Kormicki, X. W. Zhao, W. B. Gao,

N. R. Johnson, I. Y. Lee, F. K. McGowan, M. L. Halbert, M. Riley, M. O. Kortelahti, and J. D. Cole
"High Spin States in ^{65}Ga , ^{67}Ga and Their Collective Behavior at High Angular Momentum," Chinese J. Nucl. Phys. 13, 331-38 (1991)

PROGRESS REPORT

Ball, J. B., F. E. Bertrand, S. Datz, C. M. Jones, F. Plasil, R. L. Robinson, and M. R. Strayer

Physics Division Progress Report for Period Ending September 30, 1991, ORNL-6689 (Mar. 1992)

THESIS

Gao, W.

"Triple Energy Correlation Study of Continuum γ -Rays in Cerium-130," dissertation presented for the Ph.D. degree, Vanderbilt University, 1991; advisor I.Y. Lee

TOPICAL REPORTS

Auble, R. L.

Preliminary Hazard Screening, Physics Division, ORNL, ORNL/CF-92/67 (Apr. 1992)

Basher, A. M. H.

Development of a Remote Control Console for the HIRF 25-MV Tandem Accelerator, ORNL/TM11928 (Oct. 1991)

Raman, S., B. L. Broadhead, J. K. Dickens, R. L. Walker, and J. L. Botts

Analyses of Physics Specimens in Fuel Pins 1 and 2 Irradiated in the Dounreay Prototype Fast Reactor, ORNL-6632 (Oct. 1991)

ARTICLES PENDING PUBLICATION

Alton, G. D. (Invited Presentation)

"Ion Sources for Accelerators in Material Research," Proceedings, Second European Conference on Accelerators in Applied Research and Technology, Frankfurt, Germany, Sept. 3-7, 1991

Alton, G. D. (Invited Presentation)

"Ion Sources for Use in Analytical, Industrial, and Nuclear Applications," Proceedings, Third International Conference on Applications of Nuclear Techniques, Mykonos, Greece, June 6-13, 1992

Alton, G. D., M. R. Dinehart, D. T. Dowling, D.L. Haynes, C. A. Irizarry, C. M. Jones, R. C. Juras, S. N. Lane, C. T. LeCroy, R. L. McPherson, M. J. Meigs, G. D. Mills, S. W. Mosko, S.N. Murray, D. K. Olsen, and B. A. Tatum

"Oak Ridge 25URC Tandem Accelerator – 1991 SNEAP Lab Report," Proceedings, Symposium of Northeastern Accelerator Personnel, Albuquerque, New Mexico, Oct. 15-19, 1991

Alton, G. D., M. R. Dinehart, D. T. Dowling, D. L. Haynes, C. A. Irizarry, C. M. Jones, R. C. Juras, S. N. Lane, C. T. LeCroy, M. J. Meigs, G. D. Mills, S. W. Mosko, S. N. Murray, D. K. Olsen, and B. A. Tatum

"Oak Ridge 25URC Tandem Accelerator — 1992 SNEAP Lab Report," Proceedings, Symposium of Northeastern Accelerator Personnel, Hull, Canada, Sept. 23-25, 1992

Alton, G. D., D. L. Haynes, G. D. Mills, and D. K. Olsen

"Selection and Design of the Oak Ridge Radioactive Ion Beam Facility Target/Ion Source," Proceedings, 6th International Conference on Electrostatic Accelerators and Associated Boosters, Legnaro, Italy, June 1-5, 1992

Alton, G. D., and M. T. Johnson

"Performance Characteristics of a Multiple-Sample, Cesium-Sputter, Negative Ion Source," Proceedings, 6th International Conference on Electrostatic Accelerators and Associated Boosters, Montegrotto Terme, Padova, Italy, June 1-5, 1992

Alton, G. D., M. T. Johnson, and G. D. Mills

"A Simple Positive/Negative Surface Ionization Source," Proceedings, 6th International Conference on Electrostatic Accelerators and Associated Boosters, Legnaro, Italy, June 1-5, 1992

Alton, G. D., D. H. Olive, M. L. Pinkham, and J. R. Olive

"A Scaled Sigmund Theory Model for Determining Sputter Ratios," Proceedings, Second International Conference on Swift Heavy Ions in Matter (SHIM 92), Bensheim/Darmstadt, Germany, May 19-22, 1992

Ayik, S., and D. Boilley

"Memory Effects in Damping of Collective Vibrations," Proceedings, Eighth Winter Workshop on Nuclear Dynamics, Jackson Hole, Wy., Jan. 18-25, 1992

Baktash, C., J. D. Garrett, D. F. Winchell, and A. Smith (Invited Presentation)

"Low-Spin Identical Bands in Odd-A Nuclei," Proceedings, International Conference on Nuclear Structure at High Angular Momentum, Ottawa, Canada, May 18-22, 1992

Baktash, C., W. Nazarewicz, and R. Wyss

"On the Question of Spin Fitting and Quantitized Alignment in Rotational Bands," Nuclear Physics A

Barnes, T. (Invited Presentation)

"Can Molecules Be Seen by Two Photons," Proceedings, Ninth International Workshop on Photon-Photon Collisions, San Diego, Calif., Mar. 22-26, 1992

Barnes, T. (Invited Presentation)

"Two-Photon Couplings of Quarkonia with Arbitrary J^{PC} ," Proceedings, Ninth International Workshop on Photon-Photon Collisions, San Diego, Calif., Mar. 22-26, 1992

230 Physics Division Progress Report

Barnes, T., E. Dagotto, J. Riera, and E. S. Swanson

"On the Excitation of Heisenberg Spin Ladders," *Physical Review B*

Barnes, T., and M. D. Kovarik

"Monte Carlo Study of One-Hole Band Structure in the t - J Model," *Physical Review B*

Barreto, J., D. G. Sarantites, R. J. Charity, N. G. Nicolis, L. G. Sobotka, D. W. Stracener, D. C. Hensley, J. R. Beene, M. Halbert, and C. Baktash

"Charged Particles as Probes to Study Entrance Channel Effects in the Composite System ^{164}Yb ," Proceedings, Eighth Winter Workshop on Nuclear Dynamics, Jackson Hole, Wy., Jan. 18-25, 1992

Baxter, A. M., T. L. Khoo, M. E. Bleich, M. P. Carpenter, I. Ahmad, R. V. F. Janssens, E. F. Moore, I. G. Bearden, J. R. Beene, and I. Y. Lee

"Compton Suppression Tests on Ge and BGO Prototype Detectors for GAMMASPHERE," *Nuclear Instruments and Methods in Physics Research*

Baxter, A. M., T. L. Khoo, M. E. Bleich, M. P. Carpenter, I. Ahmad, R. V. F. Janssens, E. F. Moore, I. G. Bearden, J. R. Beene, and I. Y. Lee

"Compton Suppression Tests on Ge and BGO Prototype Detectors for GAMMASPHERE," Proceedings, International Conference on Nuclear Structure at High Angular Momentum, Ottawa, Canada, May 18-21, 1992

Beck, C., B. Djerroud, F. Haas, R. M. Freeman, A. Hachem, B. Heusch, A. Morsad, M. Vuillet-a-Cilles, M. Youlal, Y. Abe, R. Dayras, J. P. Wieleczko, R. Legrain, E. Pollaco, A. Ray, D. Shapira, J. Gomez del Campo, H. J. Kim, B. Shiva Kumar, D. Blumenthal, S. Cavallaro, E. deFilippo, G. Lanzano, A. Pagano, M. L. Sperduto, T. Matsuse, and S. J. Sanders

"Asymmetrical Fission and Statistical Emission of Complex Fragments from the Highly Excited ^{47}V Compound Nucleus," Proceedings, XXX International Winter Meeting on Nuclear Physics, Bormio, Italy, Jan. 27-Feb. 1, 1992

Beene, J. R.

"Monte Carlo Simulations and the Honeycomb Prototype, GAMMASPHERE Technical Note/ORNL 1," Prepared for the GAMMASPHERE Steering Committee, Lawrence Berkeley Laboratory

Beene, J. R., and F. E. Bertrand

"Giant Resonances and Intermediate Energy Heavy Ions: Electromagnetic Decay," *Nuclear Physics at GANIL 1989-1991*, GANIL Report

Bengtsson, R. (Invited Presentation)

"Nuclear Orientation Measurements and Their Contribution to Our Understanding of the Structure of Nuclei," Proceedings, Second International Conference on On-Line Nuclear Orientation and Related Topics, Oak Ridge, Tenn., Oct. 16-19, 1991, *Hyperfine Interactions*

Bengtsson, R.

"Intruder States and Low Energy Nuclear Spectroscopy," Proceedings, Conference on Nuclear Shapes and Nuclear Structure at Low Excitation Energies, Corsica, France, June 3-7, 1991

Bingham, C. R. (Invited Presentation)

"Laser Spectroscopy and Laser Ion Source Development at UNISOR," Proceedings, Symposium on Reflections and Directions in Low Energy Heavy-Ion Physics, Oak Ridge, Tenn., Oct. 14, 1991

- Bingham, C. R., Y. A. Akovali, H. K. Carter, W. D. Hamilton, M. M. Jarrio, M. B. Kassim, J. Kormicki, J. Schwarzenberg, K. S. Toth, and M. Zhang
"New Mass Differences and α -Decay Rates for Au and Pt Isotopes," Proceedings, 6th International Conference on Nuclei Far from Stability, Bernkastel-Kues, Germany, July 19-24, 1992
- Booth, M. G., J. Rikovska, N. J. Stone, B. E. Zimmerman, W. B. Walters, P. F. Mantica, Jr., H. K. Carter, and B. D. Kern
"On-Line Nuclear Orientation of ^{116m}Sb , ^{116}In , and ^{114}Sb ," Hyperfine Interactions
- Bottcher, C., and M. R. Strayer (Invited Presentation)
"Calculations of Pair Production by Monte Carlo Methods," Proceedings, Third IMACS Symposium on Computational Acoustics, Cambridge, Massachusetts, June 26-28, 1991
- Bottcher, C., and M. R. Strayer (Invited Presentation)
"Spline Methods for Conservation Equations," Proceedings, Third IMACS Symposium on Computational Acoustics, Cambridge, Massachusetts, June 26-28, 1991
- Breitenbach, J., R. A. Braga, J. L. Wood, P. B. Semmes, and J. Kormicki
"Deformation Studies in the Extremely Neutron-Deficient Praseodymium, Neodymium, and Promethium Isotopes," Proceedings, 6th International Conference on Nuclei Far from Stability and 9th International Conference on Atomic Masses and Fundamental Constants, Bernkastel, Germany, July 19-24, 1992
- Britton, C. L., Jr., E. J. Kennedy, R. A. Todd, A. L. Wintenberg, and G. R. Young
"A Four-Channel Bipolar Monolithic Preamplifier for RHIC Dimuon Pad Readout," Proceedings, Nuclear Science Symposium, Santa Fe, New Mexico, Nov. 2-5, 1991, IEEE Transactions in Nuclear Science
- Buchinger, F., H.A. Schuessler, E.C. Benck, H. Iimura, Y.F. Li, C. Bingham, and H.K. Carter
"Isotope Shift Measurements on the Neutron-Deficient Thallium Isotopes," Hyperfine Interactions
- Burgdorfer, J., and F. Meyer
"Image Acceleration of Multiply Charged Ions by Metallic Surfaces," Physical Review Letters
- Burgdorfer, J., and F. Meyer (Invited Presentation)
"Above-Surface Neutralization of Highly Charged Ions: The Formation of Hollow Atoms," Proceedings, Nobel Symposium on Heavy-Ion Spectroscopy and QED Effects in Atomic Systems," Saltsjobaden, Sweden, June 29-July 3, 1992
- Charity, R. J., J. Barreto, L. G. Sobotka, D. G. Sarantites, D. W. Stracener, A. Chbihi, N.G. Nicolis, R. Auble, C. Baktash, J. R. Beene, F. Bertrand, M. Halbert, D. C. Hensley, D. J. Horen, C. Ludemann, M. Thoennessen, and R. Varner
"The Mechanism for the Disassembly of Excited ^{16}O Projectiles into Four Alpha Particles," Physical Review C
- Charity, R. J., J. L. Barreto, L. G. Sobotka, D. G. Sarantites, D. W. Stracener, A. Chbihi, N. G. Nicolis, R. Auble, C. Baktash, J. R. Beene, F. Bertrand, M. Halbert, D. C. Hensley, D. J. Horen, C. Ludemann, M. Thoennessen, and R. Varner
"The Mechanism for the Disassembly of Excited ^{16}O Projectiles into Alpha Particles," Proceedings, Eighth Winter Workshop on Nuclear Dynamics, Jackson Hole, Wy., Jan. 18-25, 1992

- Crater, H. W., R. L. Becker, C. Y. Wong, and P. VanAlstine
"Nonperturbative Solution of Two-Body Dirac Equations for Quantum Electrodynamics and Related Field Theories," *Physical Review D*
- Crater, H. W., P. VanAlstine, R. L. Becker, and C. Y. Wong (Invited Presentation)
"Meson Spectra from Two-Body Dirac Equations with Minimal Interactions," *Proceedings, 4th International Conference on Hadron Spectroscopy, College Park, Md., Aug. 12-16, 1992*
- Cullen, D. M., I. Y. Lee, C. Baktash, J. D. Garrett, N. R. Johnson, F. K. McGowan, and D. F. Winchell
"X-Ray Yields of Superdeformed States in ^{193}Hg ," *Physical Review C*
- Dai, J., and J. Liu
"Supersymmetry-Induced Non-Oblique Radiative Corrections to Atomic Parity Violation," *Physics Letters B*
- Dai, J., M. J. Savage, J. Liu, and R. Springer
"Low Energy Effective Hamiltonian for $\Delta I = 1$ Nuclear Parity Violation and Nucleonic Strangeness," *Physics Letters B*
- Datz, S.
"Channeling: A Marriage of Atomic Collision Physics and Material Science," *Zeitschrift fuer Physik D*
- Datz, S. (Invited Presentation)
"Atomic Collision Physics – A Summary and Some Projections," *Proceedings, Nobel Symposium on Heavy-Ion Spectroscopy and QED Effects in Atomic Systems, Saltsjobaden, Sweden, June 29-July 3, 1992*
- Davies, K. T. R., M. L. Glasser, and R. W. Davies
"Quadrature Relations for Finite-Limit, Principal-Value Integrals," *Canadian Journal of Physics*
- Davies, K. T. R., M. L. Glasser, and R. W. Davies
"Periodic Orbits Generated from Conformal Mappings," *Revista Tecnica*
- Dean, D. J., C. Bottcher, M. R. Strayer, and G. Gatoff
"Spline Techniques for Solving Relativistic Conservation Equations," *International Journal of Modern Physics C*
- Dean, D. J., M. Gyulassy, B. Muller, E. A. Remler, M. R. Strayer, A. S. Umar, and J.-S. Wu
"Multiparticle Production in Lepton-Nucleus Collisions and Relativistic String Models," *Physical Review C*
- Dean, D. J., A. S. Umar, and M. R. Strayer
"Dynamical Calculation of Central Energy Densities in Relativistic Heavy-Ion Collisions," *Physical Review Letters*
- Dellwo, J., Y. Liu, C. Y. Tang, D. J. Pegg, and G. D. Alton
"Photodetachment Cross Sections for Li^- ," *Physical Review A*
- Dellwo, J., Y. Liu, C. Y. Tang, D. J. Pegg, and G. D. Alton
"An Investigation of Li^- Photodetachment in the Vicinity of the $2^2P+\epsilon s$ Threshold," *Nuclear Instruments and Methods in Physics Research*

- Deng, J. K., J. H. Hamilton, A. V. Ramayya, W. C. Ma, X. W. Zhao, J. Kormicki, W. D. Hamilton, P. F. Mantica, H.K. Carter, N. Severijns, and L. Vanneste
"On-Line Nuclear Orientation of ^{70}As ," Proceedings, Second International Conference on On-Line Nuclear Orientation and Related Topics, Oak Ridge, Tenn., Oct. 16-19, 1991, Hyperfine Interactions
- Deng, J. K., J. H. Hamilton, A. V. Ramayya, J. Rikovska, N. J. Stone, W. L. Croft, R. B. Piercey, J. C. Morgan, and P. F. Mantica
"Test of a Symmetrical Four-Detector Compton Polarimeter Using Low Temperature Nuclear Orientation," Proceedings, Second International Conference on On-Line Nuclear Orientation and Related Topics, Oak Ridge, Tenn., Oct. 16-19, 1991, Hyperfine Interactions
- Deveney, E. E., Q. C. Kessel, R. J. Fuller, M. P. Reaves, S. M. Shafroth, and N. Jones (Invited Presentation)
"Possible Two-Electron Excitations in C^{3+} Following 1 MeV/u Collisions with Atomic Targets; $Z= 2, 10, 18,$ and $36,$ " Proceedings, 12th International Conference on the Application of Accelerators in Research and Industry, Denton, Texas, Nov. 2-5, 1992
- Gaither, C. C., III, M. Breinig, J.W. Berryman, B.F. Hasson, and J.D. Richards
"Coincident Detection of Electrons Ejected at Large Angles and Target Recoil Ions Produced in Multiply-Ionizing Collisions for the 1-MeV/u $\text{O}^{q+} + \text{Ar}$ System, Physical Review A
- Garrett, J. D. (Invited Presentation)
"The Case for Exotic Beams at the Holifield Heavy Ion Research Facility," Proceedings, Symposium on Reflections and Directions in Low-Energy Heavy-Ion Physics, Oak Ridge, Tenn., Oct. 14-15, 1991
- Garrett, J. D. (Invited Presentation)
"Exotic Nuclear Shapes and Configurations That Can Be Studied at High Spin Using Radioactive Ion Beams," Proceedings, International Workshop on the Physics and Techniques of Secondary Nuclear Beams, Dourdan, France, Mar. 23-25, 1992
- Garrett, J. D. (Invited Presentation)
"North American Radioactive Beam Initiatives," Proceedings, International Workshop on the Physics and Techniques of Secondary Nuclear Beams, Dourdan, France, Mar. 23-25, 1992
- Garrett, J. D. (Invited Presentation)
"High Spin Studies with Radioactive Ion Beams," Proceedings, Workshop on Large Gamma-Ray Detector Arrays, Chalk River, Ontario, May 22-23, 1992
- Garrett, J. D. (Invited Presentation)
"Prospects for Studies of Astrophysical Interest with Radioactive Ion Beams," Proceedings, Second International Symposium on Nuclear Astrophysics – *Nuclei in the Cosmos 1992*, Karlsruhe, Germany, July 6-10, 1992
- Gatoff, G.
"2+1-Dimensional Chromohydrodynamics for Relativistic Heavy-Ion Collisions," Physical Review D
- Gummin, M. A., K. S. Krane, Y. Xu, T. Lam, E. Zganjar, J. B. Breitenbach, B. E. Zimmerman, P. F. Mantica, Jr., and H. K. Carter
"Nuclear Structure Studies of ^{187}Ir via On-Line Nuclear Orientation," Proceedings, Second International Conference on On-Line Nuclear Orientation and Related Topics, Oak Ridge, Tenn., Oct. 16-19, 1991, Hyperfine Interactions

234 Physics Division Progress Report

Hamamota, I., and W. Nazarewicz

"Magnetic Dipole Strength in Superdeformed Nuclei," *Physics Letters B*

Havener, C. C., M. A. Haque, A. C. H. Smith, S. Urbain, and P. A. Zeijlmans van Emmichoven (Invited Presentation)

"Low-Energy Measurements of Electron Capture by Multicharged Ions from Excited Hydrogen Atoms," *Proceedings, VIth International Conference on the Physics of Highly Charged Ions, Manhattan, Kan., Sept. 28-Oct. 2, 1992*

Horen, D. J., R. L. Auble, J. Gomez del Campo, G. R. Satchler, R. L. Varner, J. R. Beene, B. Lund, V. R. Brown, P. L. Anthony, and V. A. Madsen

"Systematics of Isospin Character of Transitions to the 2_1^+ and 3_1^- States in $^{90,92,94,96}\text{Zr}$," *Physical Review C*

Horen, D. J., R. L. Auble, J. Gomez del Campo, R. L. Varner, J. R. Beene, G. R. Satchler, B. Lund, V. R. Brown, P. L. Anthony, and V. A. Madsen

"Different Effects of Valence Neutrons on the Isospin Character of Transitions to the First 2^+ and 3^- States of $^{90,92,94,96}\text{Zr}$," *Physics Letters B*

Hughes, I. G., R. Behrisch, and A. P. Martinelli (Invited Presentation)

"Depth Profiling of Deuterium Using Nuclear Reaction Analysis," *Proceedings, Twelfth International Conference on the Application of Accelerators in Research and Industry, Denton, Texas, Nov. 2-5, 1992*

Hughes, I. G., C. C. Havener, S. H. Overbury, M. T. Robinson, D. M. Zehner, P. A. Zeijlmans van Emmichoven, and F. W. Meyer

"Incident Ion Charge State Dependence of Electron Emission During Slow Multicharged Ion-Surface Interactions," *Proceedings, VIth International Conference on the Physics of Highly-Charged Ions (HCI92), Manhattan, Kan., Sept. 28-Oct. 2, 1992*

Ignatyuk, A. V., J. L. Weil, S. Raman, and S. Kahane

"Density of Discrete Levels in ^{116}Sn ," *Physical Review C*

Janev, R. K., R. A. Phaneuf, and H. Tawara

"Recommended Cross Sections for State-Selective Electron Capture in Collisions of C^{6+} and O^{8+} Ions with Atomic Hydrogen," *Atomic Data and Nuclear Data Tables*

Johnson, N. R. (Invited Presentation)

"The Shapes and Collective Behavior of Rapidly Rotating Nuclei," *Proceedings, International Symposium on the Spectroscopy and Structure of Molecules and Nuclei, Tallahassee, Fla., Mar. 27-28, 1992*

Johnson, N. R., F. K. McGowan, D. F. Winchell, J. C. Wells, C. Baktash, L. Chaturvedi, W. B. Gao, J. D. Garrett, I. Y. Lee, W. C. Ma, S. Pilotte, and C.-H. Yu (Invited Presentation)

"Transition Probabilities Up to $I=36^+$ in ^{160}Yb Nuclei," *Proceedings, International Conference on Nuclear Structure at High Angular Momentum, Ottawa, Canada, May 18-21, 1992*

Jones, N. L., and P. F. Dittner

"Improved Voltage Gradient Control System Electrostatic Accelerators," *Proceedings, 6th International Conference on Electrostatic Accelerators and Associated Boosters, Montegrotto Terme, Padova, Italy, June 1-5, 1992*

- Joshi, P., S. J. Robinson, P. F. Mantica, E. F. Zganjar, D. Rupnik, R. L. Gill, W. B. Walters, H. K. Carter, C. R. Bingham, J. Kormicki, A. V. Ramayya, W. C. Ma, and J. H. Hamilton
"Lifetimes of the 0_2^+ Configuration in ^{186}Hg and ^{188}Hg ," Proceedings, 6th International Conference on Nuclei Far from Stability and the 9th International Conference on Atomic Masses and Fundamental Constants, Bernkastel, Germany, July 19-24, 1992
- Kolata, J. J., M. Zahar, R. Smith, K. Lamkin, M. Belbot, R. Tighe, B. M. Sherrill, N. A. Orr, J. S. Winfield, J. A. Winger, S. J. Yennello, G. R. Satchler, and A. H. Wuosmaa
"Elastic Scattering of ^{11}Li and ^{11}C at 60 MeV/Nucleon," Physical Review Letters
- Kovarik, M.D., B.M. Elrick, A.E. Jacobs, and W. G. Macready
"Hubbard Model in the Strong-Coupling Approximation," Physical Review B
- Lee, I.Y., C. Baktash, D. Cullen, J.D. Garrett, N. R. Johnson, F. K. McGowan, D. F. Winchell, and C. H. Yu (Invited Presentation)
"Lifetimes of the Low Spin States in the Superdeformed Band of ^{192}Hg ," Proceedings, International Conference on High Angular Momentum, Ottawa, Canada, May 18-21, 1992
- Lee, I. Y., C. Baktash, D. M. Cullen, J. D. Garrett, N. R. Johnson, F. K. McGowan, D. F. Winchell, and C. H. Yu
"Lifetimes of Low Spin States in the Superdeformed Band of ^{192}Hg ," Physical Review Letters
- Lee, I. Y., H. Xie, C. Baktash, W. B. Gao, J. D. Garrett, N. R. Johnson, F. K. McGowan, and R. Wyss
"Lifetime Measurements for Continuum Gamma Rays in ^{164}Yb and ^{170}Hf ," Nuclear Physics A
- Liu, J., C. Y. Wong, C. C. Shih, and R. C. Wang
"Massless Schwinger Model and Fragmentation Functions," Physica Scripta
- Ma, C. H., L. R. Baylor, D. P. Hutchinson, M. Murakami, and J. B. Wilgen
"Density Profile Measurement Using a Multichannel Difluoromethane Laser Interferometer System on ATF," Proceedings, Ninth Topical Conference on High-Temperature Plasma Diagnostics, Santa Fe, N.M., Mar. 15-19, 1992
- Ma, W. C., J. H. Hamilton, A.V. Ramayya, L. Chaturvedi, J. K. Deng, W. B. Gao, Y. R. Jiang, J. Kormicki, X. W. Zhao, N. R. Johnson, I. Y. Lee, F. K. McGowan, C. Baktash, J. D. Garrett, W. Nazarewicz, and R. Wyss
"First Evidence for States in Hg Nuclei with Deformations Between Normal- and Super-Deformation," Physical Review Letters
- Macek, J., and S. Y. Ovchinnikov
"Anomalous n-Dependence of Low-Energy Electron Capture from Atomic Hydrogen by Multicharged Ions," Physical Review Letters
- Mahaux, C., K. T. R. Davies, and G. R. Satchler
"Retardation and Dispersive Effects in the Nuclear Mean Field," Physics Reports
- Mahaux, C., and G. R. Satchler
"Temporal Nonlocality of Nuclear and Atomic Mean Fields," Nuclear Physics A
- Mantica, P. F., P.K. Joshi, S. J. Robinson, E. F. Zganjar, R. L. Gill, W. B. Walters, D. Rupnik, H. K. Carter, J. Kormicki, and C. R. Bingham
"Lifetime Measurements in $^{118,120}\text{Xe}$," Proceedings, 6th International Conference on Nuclei Far from Stability and 9th International Conference on Atomic Masses and Fundamental Constants, BernkastelKues, Germany, July 19-24, 1992

- Mantica, P. F., B. D. Kern, B. E. Zimmerman, W. B. Walters, J. Rikovska, and N. J. Stone
"The Measurement of Beta Asymmetries at UNISOR/NOF Using External Plastic Scintillator Detectors," Proceedings, Second International Conference on On-Line Nuclear Orientation and Related Topics, Oak Ridge, Tenn., Oct. 16-19, 1991, Hyperfine Interactions
- Martin, M. J. (Invited Presentation)
"Quality Control, Checks and Balances in ENSDF," Proceedings, Joint American Nuclear Society/ European Nuclear Society 1992 International Conference, Chicago, Ill., Nov. 15-20, 1992
- Melles, M., C. O. Reinhold, and J. Burgdorfer (Invited Presentation)
"Classical and Quantum Dynamics of the Impulsively Driven Hydrogen Atom," Proceedings, Twelfth International Conference on the Application of Accelerators in Research and Industry, Denton, Texas, Nov. 2-5, 1992
- Muller, A., A. Frank, J. Haselbauer, G. Hofmann, J. Neumann, U. Pracht, E. Salzborn, S. Schennach, W. Spies, M. Stenke, O. Uwira, R. Volpel, M. Wagner, R. Becker, E. Jennewein, M. Kleinod, U. Probstel, R. A. Phaneuf, G. H. Dunn, E. M. Bernstein, N. Angert, and P. H. Mokler
"Recombination of Highly Charged Ions with Free Electrons," Proceedings, 8th APS Topical Conference on Atomic Processes in Plasmas, Portland, Maine, Aug. 25-29, 1991
- Nazarewicz, W.
"Nuclear Deformations as a Spontaneous Symmetry Breaking," International Journal of Modern Physics E
- Nazarewicz, W. (Invited Presentation)
"Reflection Asymmetric Shapes in Atomic Nuclei," Proceedings, Nuclear Shapes and Nuclear Structure at Low Excitation Energies, Cargese, France, June 3-7, 1991
- Nazarewicz, N. (Invited Presentation)
"Theory at UNISOR and JHIR: A Historical View," Proceedings, International Symposium on Reflections and Directions in Low-Energy Heavy-Ion Physics, Oak Ridge, Tenn., Oct. 14-15, 1991
- Nazarewicz, W. (Invited Presentation)
"New Vistas in Superdeformation," Proceedings, International Conference on Nuclear Structure at High Angular Momentum, Ottawa, Canada, May 18-21, 1992
- Oberacker, V. E., A. S. Umar, J. C. Wells, M. R. Strayer, and C. Bottcher
"Study of Nuclear Dissipation via Muon-Induced Fission: A Relativistic Lattice Calculations," Physics Letters B
- Olsen, D. K. (Invited Presentation)
"Opportunities with Accelerated Radioactive Ion Beams," Proceedings, 6th International Conference on Electrostatic Accelerators and Associated Boosters, Legnaro, Italy, June 1-5, 1992
- Olsen, D. K., G. D. Alton, C. Baktash, D. T. Dowling, J. D. Garrett, D. L. Haynes, C. M. Jones, R. C. Juras, S. N. Lane, I. Y. Lee, M. J. Meigs, G. D. Mills, S. W. Mosko, B. A. Tatum, K. S. Toth, and H. K. Carter
"The ORNL Radioactive Ion Beam Project with the ORIC Accelerator," Proc. 13th International Conference on Cyclotrons and Their Applications, Vancouver, Canada, July 6-10, 1992
- Ortiz, M. E., E. R. Chavez, A. Dacal, J. Gomez del Campo, Y. D. Chan, and R. G. Stokstad
"The $^{14}\text{N}+^{10}\text{B}$ System Measured at $E(^{14}\text{N})=248\text{ MeV}$," Revista Mexicana de Fisica

- Phaneuf, R. A. (Invited Presentation)
"Assessment of Ion-Atom Collision Data for Magnetic Fusion Plasma Edge Modelling," Proceedings, Meeting of the IAEA Coordinated Research Programme on "Atomic and Molecular Data for Fusion Edge Plasmas," Vienna, Austria, September 24-26, 1990, Nuclear Fusion, Supplement
- Phaneuf, R. A. (Invited Presentation)
"Progress in Collisions of Multiply Charged Ions," Proceedings, 8th APS Topical Conference on Atomic Processes in Plasmas, Portland, Maine, Aug. 25-29, 1991
- Phaneuf, R. A., R. K. Janev, H. Tawara, M. Kimura, P. S. Krstic, G. Peach, and M. A. Mazing (Invited Article)
"Status and Critical Assessment of the Database for Collisions of Be⁹⁺ Ions with H, H₂, and He," Nuclear Fusion, Supplement
- Raman, S. (Invited Presentation)
"Low-Lying Collective Quadrupole Strengths in Even-Even Nuclei," Proceedings, Second International Symposium on Nuclear Excited States, Lodz, Poland, June 22-26, 1992
- Raman, S., J. L. Campbell, A. Prindle, R. Gunnink, and J. C. Palathingal
"Unsuitability of ¹⁵⁷Tb for Light-Neutrino Rest-Mass Studies," Physical Review C
- Ray, A., and D. Shapira
"Orbiting: Toward a Unified Model of Nucleus-Nucleus Collision or Excitation of Nuclear Molecular States in Heavy Ion Collisions?," Proceedings, International Symposium – *Toward a Unified Picture of Nuclear Dynamics*, Nikko, Japan, June 6-8, 1991
- Reinhold, C. O., J. Burgdorfer, J. Kemmler, and P. Koschar
"Simulation of Convoy Electron Emission," Annual Report, Johan Wolfgang Goethe Universitat, Frankfurt, Germany
- Richards, J. D., M. Breinig, C. C. Gaither, J. W. Berryman, and B. F. Hasson
"The Detection of Two Electrons in Low-Lying Continuum States of a Single Projectile Ion Resulting from the Collision of a 10.7-MeV Ag⁴⁺," Physical Review A
- Richards, R. K., D. P. Hutchinson, C. A. Bennett, H. T. Hunter, and C. H. Ma
"Measurement of CO₂ Laser Small-Angle Thomson Scattering on a Magnetically Confined Plasma," Applied Physics Letters
- Schuessler, H. A., E. C. Benck, F. Buchinger, H. Iimura, Y. F. Li, C. Bingham, and H. K. Carter
"Nuclear Moments of the Neutron-Deficient Thallium Isotopes," Proceedings, Second International Conference on On-Line Nuclear Orientation and Related Topics, Oak Ridge, Tenn., Oct. 16-19, 1991, Hyperfine Interactions
- Sellin, I. A., J. Levin, R. Miller, N. Keller, Y. Azuma, H. G. Berry, N. Berrah-Mansour, and D. Lindle (Invited Presentation)
"Comparison of Double and Single Ionization in He by Photons and by Charged Projectiles," Proceedings, Spring-8 Workshop on Atomic Physics at High Brilliance Synchrotron Radiation Facilities, Himeji, Japan, Mar. 23-24, 1992
- Stachel, J., and G. R. Young
"Relativistic Heavy Ion Physics at CERN and BNL," Annual Review of Nuclear and Particle Science

Stoyer, M. A., E. A. Henry, Y. A. Akovali, J. A. Becker, C. R. Bingham, J. Breitenbach, H. K. Carter, R. W. Hoff, M. Jarrio, P. Joshi, J. Kormicki, A. Kuhnert, P. F. Mantica, T. F. Wang, J. L. Wood, and M. Zhang

"Search for Population of Superdeformed States in ^{194}Pb Using ^{194}Bi β^+ Decay," *Physical Review C*

Theine, K., A. P. Byrne, H. Hubel, M. Murzel, R. Chapman, D. Clarke, F. Khazaie, J. C. Lisle, J. N. Mo, J. D. Garrett, H. Ryde, and R. Wyss

"High-Spin Structure of ^{167}W and ^{168}W ," *Nuclear Physics A*

Thoennessen, M., and J. R. Beene (Invited Presentation)

"Nuclear Dissipation and the Giant Dipole Resonance," *Proceedings, International Symposium on Reflections and Directions in Low Energy Heavy Ion Physics, Oak Ridge, Tenn., Oct. 14-15, 1991*

Thoennessen, M., and J. R. Beene (Invited Presentation)

"Dissipation and the Population of Compound Nuclei," *Proceedings, Eighth Winter Workshop on Nuclear Dynamics, Jackson Hole, Wy., Jan. 18-25, 1992*

Toth, K. S., C. N. Davids, Y. A. Akovali, B. B. Back, R. R. Betts, K. Bindra, C. R. Bingham, H. K. Carter, W. Chung, Y. Hatsukawa, D. J. Henderson, W. Kutschera, T. Lauritsen, P. F. Mantica, D. M. Moltz, A. V. Ramayya, J. D. Robertson, and W. B. Walters

"Investigation of Proton-Rich Platinum and Mercury Isotopes with the Fragment Mass Analyzer at ATLAS and the Isotope Separator at UNISOR," *Proceedings, 6th International Conference on Nuclei Far from Stability, Bernkastel-Kues, Germany, July 19-24, 1992*

Toth, K. S., H. J. Kim, J. W. McConnell, C. R. Bingham, and D. C. Sousa

"The α -Decay Properties of Light Uranium Isotopes," *Proceedings, 6th International Conference on Nuclei Far from Stability, Bernkastel-Kues, Germany, July 19-24, 1992*

Toth, K. S., J. M. Nitschke, D. C. Sousa, K. S. Vierinen, and P. A. Wilmarth

"Study of Short-Lived Rare Earth Nuclei Near the Proton Drip Line," *Proceedings, 6th International Conference on Nuclei Far from Stability, Bernkastel-Kues, Germany, July 19-24, 1992*

Toth, K. S., D. C. Sousa, P. A. Wilmarth, J. M. Nitschke, and K. S. Vierinen

"The ($\text{EC} + \beta^+$) Decay of ^{147}Tm ," *Physical Review C*

Vane, C. R., S. Datz, P. F. Dittner, H. F. Krause, C. Bottcher, M. Strayer, R. Schuch, H. Gao, and R. Hutton

"Electron-Positron Pair Production in Coulomb Collisions of Ultrarelativistic Sulfur Ions with Fixed Targets," *Physical Review A*

Vegh, L., and R. L. Becker

"Selective Population of Ionic States Produced in Photoionization by Linearly Polarized Light," *Physical Review A*

Wells, J. C., A. S. Umar, V. E. Oberacker, C. Bottcher, M. R. Strayer, J.-S. Wu, J. Dranke, and R. Flanery

"A Numerical Implementation of the Dirac Equation on a Hypercube Multicomputer," *International Journal of Modern Physics C*

Wong, C. Y.

"Effect of Boundary on Momentum Distribution of Quarks in a Quark-Gluon Plasma," *Physical Review Letters*

- Wong, C. Y., and G. Gattoff (Invited Presentation)
"The Transverse Profile of a Color Flux Tube," Proceedings, Realistic Nuclear Structure, Stony Brook, N.Y., May 28-30, 1992
- Wong, C. Y., J. Liu, R. C. Wang, and C. C. Shih
"Fragmentation of A Charge Pair in Two-Dimensional QED," Physical Review D
- Wood, J. L., J. Schwarzenberg, E. F. Zganjar, and D. Rupnik
"Detailed Nuclear Structure Studies Far from Stability," Proceedings, Second International Conference on On-Line Nuclear Orientation and Related Topics, Oak Ridge, Tenn., Oct. 16-19, 1991, Hyperfine Interactions
- Wu, C.-L., D. H. Feng, and M. W. Guidry (Invited Article)
"Nuclear Superdeformation and the Supershell Fermion Dynamical Symmetry Model," Annals of Physics (N.Y.)
- Wyss, R.
"Rotational Band Structure of Intruder Configurations: Success and Limitations of the Cranked Shell Model," Proceedings, Workshop on Reflections and Directions in Low Energy Heavy-Ion Physics, Oak Ridge, Tenn., Oct. 14-15, 1991
- Xu, Y., K. S. Krane, M. A. Gummin, J. L. Wood, M. M. Jarro, J. B. Breitenbach, E. Zganjar, D. Rupnik, H. K. Carter, P. F. Mantica, Jr., and B. E. Zimmerman
"On-Line Nuclear Orientation Study of ^{184}Au ," Proceedings, Second International Conference on On-Line Nuclear Orientation and Related Topics, Oak Ridge, Tenn., Oct. 16-19, 1991, Hyperfine Interactions
- Young, G. R. (Invited Presentation)
"Electronics for the RHIC PHENIX Detector," Proceedings, Conference on Electronics for Future Colliders, Chestnut Ridge, N.Y., May 19-21, 1992
- Young, G. R. (Invited Presentation)
"Physics from Photon and Lepton-Pair Spectra," Proceedings, NATO Advanced Study Institute, Lucca, Italy, July 12-24, 1992
- Zeijlmans van Emmichoven, P. A., C. C. Havener, I. G. Hughes, S. H. Overbury, M. T. Robinson, D. M. Zehner, and F. W. Meyer
"Electron Emission During Multicharged Ion-Metal Surface Interactions," Proceedings, 14th Werner Brandt Workshop on Charged-Particle Penetration Phenomena, Oak Ridge, Tenn., Apr. 30-May 1, 1992
- Zeijlmans van Emmichoven, P. A., C. C. Havener, I. G. Hughes, D. M. Zehner, and F. W. Meyer
"Analysis of Low Energy Electron Emission Arising During Slow Multicharged Ion-Surface Interactions," Proceedings, VIth International Conference on the Physics of Highly-Charged Ions (HCI92), Manhattan, Kan., Sept. 28-Oct. 2, 1992
- Zeijlmans van Emmichoven, P. A., C. C. Havener, I. G. Hughes, D. M. Zehner, and F. W. Meyer
"Emission of Low-Energy Electrons from Multicharged Ions Interacting with Metal Surfaces," Physical Review A

Zhu, S., X. Zhao, J. H. Hamilton, A. V. Ramayya, W.-C. Ma, L. K. Peker, J. Kormicki, X. Hong, W. B. Gao, J. K. Deng, I. Y. Lee, N. R. Johnson, F. K. McGowan, C. E. Bemis, J. D. Cole, R. Aryaeinejad, G. Ter-Akopian, and Yu. Oganessian (Invited Presentation)

"Higher Spin States in Neutron Rich Nuclei," Proceedings, XV Symposium on Nuclear Physics, Oaxtepec, Mexico, Jan. 7-10, 1992

Zimmerman, B. E., W. B. Walters, P. F. Mantica, Jr., H. K. Carter, M. G. Booth, J. Rikovska, and N. J. Stone

"Determination of the Magnetic Dipole Moment of ^{114}Sb Via On-Line Nuclear Orientation," Proceedings, Second International Conference on On-Line Nuclear Orientation and Related Topics, Oak Ridge, Tenn., Oct. 16-19, 1991, Hyperfine Interactions

Zimmerman, B. E., W. B. Walters, P. F. Mantica, Jr., J. Kormicki, H. K. Carter, J. Rikovska, N. J. Stone, and B. Kern

"Level Structure of the Odd-Odd Nuclei ^{114}I ," Proceedings, 6th International Conference on Nuclei Far from Stability, Bernkastel-Kues, Germany, July 20-24, 1992

12. PAPERS PRESENTED AT SCIENTIFIC AND TECHNICAL MEETINGS

October 1991 Through September 1992

List Prepared by Shirley J. Ball

1991

Intel Supercomputer Users' Group 1991 International Users' Conference, Dallas, Texas, Oct. 6-9, 1991

Wells, J. C., C. Bottcher, J. Drake, R. Flanery, V. E. Oberacker, M. R. Strayer, A. S. Umar, and J.-S. Wu
"Numerical Methods for the Dirac Equation"

NATO Workshop on Resonant Transfer and Excitation in Channeling, Belfast, Northern Ireland, Oct. 7-9, 1991

Datz, S., C. R. Vane, H. F. Krause, and P. F. Dittner (Invited Presentation)
"Dielectronic Excitation and Recombination in Crystal Channels"

Dittner, P. F., and S. Datz (Invited Presentation)
"Early Measurements of Dielectronic Recombination of Multiply Charged Ions"

Mowat, J. R., J. A. Tanis, R. R. Haar, J. L. Forest, T. Ellison, C. Foster, W. Jacobs, R. Rinckel, P. F. Dittner, W. G. Graham, M. W. Clark, D. E. Schneider, and M. P. Stockli (Invited Presentation)
"A Measurement of the Dielectronic Recombination of He⁺ Ions"

Shafroth, S. M., M. Benhenni, J. K. Swenson, M. Schulz, J. P. Giese, H. Schone, C. R. Vane, P. F. Dittner, and S. Datz (Invited Presentation)
"Resonant Transfer Excitation: Interference Effects"

Symposium on RHIC Detector R&D, Upton, N.Y., Oct. 10-11, 1991

Aronson, S., M. J. Murtagh, M. Starks, X. T. Liu, G. A. Petitt, Z. Zhang, L. A. Ewell, J. C. Hill, F. K. Wohn, J. B. Costales, M. N. Namboodiri, T. C. Sangster, J. H. Thomas, A. Gavron, L. Waters, W. L. Kehoe, S. G. Steadman, T. C. Awes, F. E. Obenshain, S. Saini, G. R. Young, J. Chang, S.-Y. Fung, J. H. Kang, J. Kreke, X. He, S. P. Sorensen, E. C. Cornell, and C. F. Maguire (Invited Presentation)
"Calorimeter/Absorber Optimization for a RHIC Dimuon Experiment (RD-10 Project)"

Symposium on Reflections and Directions in Low Energy Heavy-Ion Physics, Oak Ridge, Tenn., Oct. 14-15, 1991

Bingham, C. R. (Invited Presentation)
"Laser Spectroscopy and Laser Ion Source Development at UNISOR"

Garrett, J. D. (Invited Presentation)

“The Case for Exotic Beams at the Holifield Heavy Ion Research Facility”

Nazarewicz, W. (Invited Presentation)

“Theory at UNISOR and JHIR: A Historical View”

Thoennessen, M., and J. R. Beene (Invited Presentation)

“Nuclear Dissipation and the Giant Dipole Resonance”

Wyss, R.

“Rotational Band Structure of Intruder Configurations: Success and Limitations of the Cranked Shell Model”

Tenth International School on Nuclear Physics, Neutron Physics, and Nuclear Energy, Varna, Bulgaria, Oct. 14-19, 1991

Guidry, M. W.

“Nuclear Masses in the Fermion Dynamical Symmetry Model and Some Applications in Nuclear Astrophysics”

Guidry, M. W.

“The Fermion Dynamical Symmetry Model of Superdeformation”

Symposium of Northeastern Accelerator Personnel, Albuquerque, N.M., Oct. 15-19, 1991

Alton, G. D., M. R. Dinehart, D. T. Dowling, D. L. Haynes, C. A. Irizarry, C. M. Jones, R. C. Juras, S. N. Lane, C. T. Lecroy, R. L. McPherson, M. J. Meigs, G. D. Mills, S. W. Mosko, S. N. Murray, D. K. Olsen, and B. A. Tatum

“Oak Ridge 25URC Tandem Accelerator – 1991 SNEAP Lab Report”

Jones, N.

“EN-12 at ORNL”

Second International Conference on On-Line Nuclear Orientation and Related Topics, Oak Ridge, Tenn., Oct. 16-19, 1991

Bengtsson, B. R. (Invited Presentation)

“Nuclear Orientation Measurements and Their Contribution to Our Understanding of the Structure of Nuclei”

Butler-Moore, K., A. V. Ramayya, J. H. Hamilton, J. K. Deng, J. Kormicki, W. Ma, P. F. Mantica, Jr., H. K. Carter, R. B. Piercey, J. C. Morgan, and W. D. Hamilton

“Off-Line Nuclear Orientation Studies on ^{96}Mo ”

Deng, J. K., J. H. Hamilton, A. V. Ramayya, W. C. Ma, X. W. Zhao, J. Kormicki, W. D. Hamilton, P. F. Mantica, H. K. Carter, N. Severijns, and L. Vanneste

“On-Line Nuclear Orientation of ^{70}As ”

Deng, J. K., J. H. Hamilton, A. V. Ramayya, J. Rikovska, N. J. Stone, W. L. Croft, R. B. Piercey, J. C. Morgan, and P. F. Mantica

“Test of a Symmetrical Four-Detector Compton Polarimeter Using Low Temperature Nuclear Orientation”

Gummin, M. A., K. S. Krane, Y. Xu, T. Lam, E. Zganjar, J. B. Breitenbach, B. E. Zimmerman, P. F. Mantica, Jr., and H. K. Carter

“Nuclear Structure Studies of ^{187}Ir via On-Line Nuclear Orientation”

Mantica, P. F., Jr., B. D. Kern, B. E. Zimmerman, W. B. Walters, J. Rikovska, and N. J. Stone

“The Measurement of Beta Asymmetries at UNISOR/NOF Using External Plastic Scintillator Detectors”

Schuessler, H. A., E. C. Benck, F. Buchinger, H. Iimura, Y. F. Li, C. R. Bingham, and H. K. Carter
(Invited Presentation)

“Laser Spectroscopy of the Very Neutron-Deficient Thallium Isotopes”

Semmes, P. B.

“Nuclear Spins and Moments: Fundamental Structural Information”

Wood, J. L., J. Schwarzenberg, E. F. Zganjar, and D. Rupnik

“Detailed Nuclear Structure Studies Far from Stability”

Xu, Y., K. S. Krane, M. A. Gummin, J. L. Wood, M. M. Jarrio, J. B. Breitenbach, E. Zganjar, D. Rupnik, H. K. Carter, P. F. Mantica, Jr., and B. E. Zimmerman

“On-Line Nuclear Orientation Study of ^{184}Au ”

Zimmerman, B. E., W. B. Walters, P. F. Mantica, Jr., H. K. Carter, N. J. Stone, J. Rikovska, and B. D. Kern

“Nuclear Orientation and Decay of I-114 and I-116”

Workshop on Giant Resonances and Related Phenomena, Notre Dame, Ind., Oct. 21-23, 1991

Beene, J. R. (Invited Presentation)

“Electromagnetic Decay of Giant Resonances”

Horen, D. J. (Invited Presentation)

“Measurement of Isospin Character of Nuclear Transitions by Inelastic Heavy-Ion Scattering and Comparisons with Other Probes”

44th Annual Gaseous Electronics Conference, Albuquerque, N. M., Oct. 22-25, 1991

Meyer, F. W., S. H. Overbury, C. C. Havener, P. A. Zeijlmans van Emmichoven, and D. M. Zehner
(Invited Presentation)

“Evidence for Above- and Sub-Surface Neutralization During Interactions of Highly Charged Ions with a Metal Plate”

American Physical Society Meeting, Division of Nuclear Physics, East Lansing, Mich., Oct. 24-26, 1991

Baktash, C., I. Frosch, C. M. Steele, W. B. Gao, J. D. Garrett, N. R. Johnson, I. Y. Lee, F. K. McGowan, J. H. McNeill, J. C. Wells, and H. Xie

“Identical Bands and Integer Alignments in the Normally-Deformed Bands of ^{171}Hf ,” Bull. Am. Phys. Soc. **36**, 2156 (Sept. 1991)

244 Physics Division Progress Report

- Charity, R. J., J. Barreto, L. G. Sobotka, D. G. Sarantites, D. W. Stracener, A. Chbihi, N. G. Nicolis, R. Auble, C. Baktash, J. R. Beene, F. Bertrand, M. Halbert, D. C. Hensley, D. Horen, C. Ludemann, M. Thoennessen, and R. Varner
"On the Mechanism for the 4α Breakup of Excited Oxygen Projectiles," *Bull. Am. Phys. Soc.* **36**, 2134 (Sept. 1991)
- Garrett, J. D., J. R. German, and L. Courtney
"The Distribution of Nuclear Quantum States in 'Cold' Rotating Nuclei," *Bull. Am. Phys. Soc.* **36**, 2149 (Sept. 1991)
- Gross, E. E., D. C. Hensley, M.L. Halbert, J. R. Beene, F.E. Bertrand, G. Vourvopoulos, and D. L. Humphrey
" ^{26}Mg Nuclear Structure from $^{26}\text{Mg}(200\text{ MeV}) + ^{208}\text{Pb}$ Scattering," *Bull. Am. Phys. Soc.* **36**, 2132 (Sept. 1991)
- Jin, H.-Q., L. L. Riedinger, C.-H. Yu, W. Nazarewicz, R. Wyss, J.-Y. Zhang, C. Baktash, J. D. Garrett, N. R. Johnson, I. Y. Lee, and F. K. McGowan
"Electromagnetic Properties of the $5/2, 7/2[303]$ Pseudospin Doublet in ^{175}Re ," *Bull. Am. Phys. Soc.* **36**, 2156 (Sept. 1991)
- Liu, X. T., Z. Z. Zhang, G. A. Pettit, P. Mikelsons, and G. R. Young
"Discriminant Function Analysis for Muon Identification," *Bull. Am. Phys. Soc.* **36**, 2129 (Sept. 1991)
- Moltz, D. M., J. D'Auria, J. Batchelder, L. Buchmann, M. Dombisky, P. McNeely, T. Ognibene, P. Reeder, and K. Toth
"Mass Difference Measurements from the Decay of ^{76}Rb and ^{75}Rb ," *Bull. Am. Phys. Soc.* **36**, 2139 (Sept. 1991)
- Petratis, M., J. P. Connelly, H. Crannell, L. W. Fagg, J. T. O'Brien, D. I. Sober, S. Raman, J. R. Deininger, and S. E. Williamson
"Electroexcitation of Low-Multipolarity Transitions in $^{32,34}\text{S}$," *Bull. Am. Phys. Soc.* **36**, 2125 (Sept. 1991)
- Ramakrishnan, E., M. Thoennessen, J. R. Beene, R. L. Auble, C. Baktash, F. E. Bertrand, M. L. Halbert, D. J. Horen, P. Mueller, D. H. Olive, and R. L. Varner
"Search for Entrance Channel Effects in Excited Sn Nuclei," *Bull. Am. Phys. Soc.* **36**, 2116 (Sept. 1991)
- Sobotka, L. G., L. Gallamore, A. Chbihi, D.G. Sarantites, D. W. Stracener, W. Bauer, D. R. Bowman, N. Carlin, R. T. Desouza, C. K. Gelbke, W. G. Gong, S. Hannuschke, Y. D. Kim, W. G. Lynch, R. Ronningen, M. B. Tsang, F. Zhu, J. R. Beene, M. L. Halbert, and M. Thoennessen
"The Particle Multiplicity Dependence of High Energy Photon Production in a Heavy-Ion Reaction," *Bull. Am. Phys. Soc.* **36**, 2151 (Sept. 1991)
- Stelson, P. H., E. Chavez, D. Shapira, J. Gomez del Campo, H. J. Kim, A. Dacal, and M. Ortiz
"Measurement of DIC at Subbarrier Energies for Several Heavy Ion Systems," *Bull. Am. Phys. Soc.* **36**, 2141 (Sept. 1991)
- Stracener, D. W., D. G. Sarantites, A. Chbihi, N. G. Nicolis, M. Halbert, C. Baktash, I. Y. Lee, D. C. Hensley, F. McGowan, J. R. Beene, N. R. Johnson, and F. Bertrand
"On the Mechanism for the 4α Breakup of Excited Oxygen Projectiles," *Bull. Am. Phys. Soc.* **36**, 2134 (Sept. 1991)

Thoennessen, M., J. R. Beene, C. Baktash, F. E. Bertrand, M. L. Halbert, D. C. Hensley, D. J. Horen, R. L. Varner, W. Spang, D. G. Sarantites, and D. W. Stracener
"Evidence for Hyperdeformation in A~170 Nuclei," Bull. Am. Phys. Soc. 36, 2156 (Sept. 1991)

Weil, J. L., A. V. Ignatyuk, S. Raman, and S. Kahane
"Level Density Fits for ^{114}Sn ," Bull. Am. Phys. Soc. 36, 2118 (Sept. 1991)

Yu, C.-H., L. L. Riedinger, H. Q. Jin, C. Baktash, J. D. Garrett, and I. Y. Lee,
"The Nearly Identical Bands Between ^{180}Ir and Its Neighboring Odd-A Nuclei," Bull. Am. Phys. Soc. 36, 2156 (Sept. 1991)

Zhang, J.-Y., H.-Q. Jin, C.-H. Yu, and J. D. Garrett
"Constant-N Contours and Empirical Proton-Neutron Interactions for Rare Earth Nuclei," Bull. Am. Phys. Soc. 36, 2144 (Sept. 1991)

Nuclear Science Symposium, Santa Fe, N.M., Nov. 2-5, 1991

Britton, C. L., Jr., E. J. Kennedy, R. A. Todd, A. L. Wintenberg, and G. R. Young
"A Four-Channel Bipolar Monolithic Preamplifier for RHIC Dimuon Pad Readout"

Annual Meeting of the Division of Plasma Physics, American Physical Society, Tampa, Fla., Nov. 4-8, 1991

Richards, R. K., D. P. Hutchinson, and C. A. Bennett
"Recent Results from an Alpha Particle Diagnostic Proof of Principle," Bull. Am. Phys. Soc. 36, 2492 (Oct. 1991)

Annual Meeting of Southeastern Section of the American Physical Society, Durham, N.C., Nov. 11-13, 1991

Deveney, E.F., Q. C. Kessel, R. J. Fuller, M. Reaves, S. M. Shafroth, Y. Clifton, L. D. Hendrick, D. M. Peterson, U. Bechtold, and N. Jones
"Evidence for Simultaneous Capture and Excitation of Electrons by C^{3+} to 2s,2p," Bull. Am. Phys. Soc. 36, 2732 (Nov. 1991)

Garrett, J. D. (Invited Presentation)
"Prospects for Studies of Astrophysical Interest with Radioactive Beams," Bull. Am. Phys. Soc. 36, 2739 (Nov. 1991)

Ninth International Conference on Ultra-Relativistic Nucleus-Nucleus Collisions (Quark Matter '91), Gatlinburg, Tenn., Nov. 11-15, 1991

Bloomer, M. A., P. Jacobs, R. Albrecht, T. C. Awes, P. Beckmann, F. Berger, D. Bock, R. Bock, G. Claesson, G. Clewing, R. Debbe, L. Dragon, A. Eklund, R. L. Ferguson, S. Fokin, A. Franz, S. Garpman, R. Glasow, H. A. Gustafsson, H. H. Gutbrod, O. Hansen, M. Hartig, G. Hoelker, J. Idh, M. Ippolitov, K. H. Kampert, K. Karadjev, B. W. Kolb, A. Lebedev, H. Loehner, I. Lund, V. Manko, B. Moskowit, F. E. Obenshain, A. Oskarsson, I. Otterlund, T. Peitzmann, F. Plasil, A. M. Poskanzer, M. Purschke, H. G. Ritter, B. Roters, S. Saini, R. Santo, H. R. Schmidt, K. Soderstrom, S. P. Sorensen, K. Steffens, P. Steinhauser, E. Stenlund, D. Stueken, A. Twyhues, A. Vinogradov, and G. R. Young
"Intermittency in $^{32}\text{S}+\text{S}$ and $^{32}\text{S}+\text{Au}$ Collisions at the CERN SPS"

Bottcher, C., and M. R. Strayer (Invited Presentation)
"Electromagnetic Pair Production in Relativistic Heavy-Ion Collisions"

Kampert, K. H., R. Albrecht, T. C. Awes, P. Beckmann, F. Berger, M. Bloomer, D. Bock, R. Bock, G. Claesson, G. Clewing, R. Debbe, L. Dragon, A. Eklund, R. L. Ferguson, S. Fokin, A. Franz, S. Garpman, R. Glasow, H. A. Gustafsson, H. H. Gutbrod, O. Hansen, M. Hartig, G. Hoelker, J. Idh, M. Ippolitov, P. Jacobs, K. Karadjev, B. W. Kolb, A. Lebedev, H. Loehner, I. Lund, V. Manko, B. Moskowit, F. E. Obenshain, A. Oskarsson, I. Otterlund, T. Peitzmann, F. Plasil, A. M. Poskanzer, M. Purschke, H. G. Ritter, B. Roters, S. Saini, R. Santo, H. R. Schmidt, R. Schmidt, S. P. Sorensen, K. Steffens, P. Steinhauser, E. Stenlund, D. Stueken, A. Vinogradov, H. Wegener, and G. R. Young (Invited Presentation)

“Recent Results from the WA80 Experiment at CERN”

Liu, J., C. Y. Wong, C. C. Shih, and R. C. Wang

“Study of Particle Production with QED₂”

Shih, C. C., X. C. He, J. Y. Zhang, S. Sorensen, and C. Y. Wong

“Signature of Multiple Collisions in Proton-Nucleus Reactions”

Umar, A.S., D.J. Dean, and M.R. Strayer

“A Dynamical String-Parton Model for Relativistic Heavy-Ion Collisions”

Young, G. R. (Invited Presentation)

“Experimental Challenges at RHIC and LHC”

Zhang, J. Y., X. C. He, C. C. Shih, S. Sorensen, and C. Y. Wong

“Study of the Transverse Energy Distribution in Pseudorapidity”

1992

XV Symposium on Nuclear Physics, Oaxtepec, Mexico, Jan. 7-10, 1992

Zhu, S., X. Zhao, J. H. Hamilton, A. V. Ramayya, W.-C. Ma, L. K. Peker, J. Kormicki, X. Hong, W. B. Gao, J. K. Deng, I. Y. Lee, N. R. Johnson, F. K. McGowan, C. E. Bemis, J. D. Cole, R. Aryaeinejad, G. Ter-Akopian, and Yu. Oganessian (Invited Presentation)

“Higher Spin States in Neutron Rich Nuclei”

Eighth Winter Workshop on Nuclear Dynamics, Jackson Hole, Wy., Jan. 18-25, 1992

Ayik, S., and D. Boilley

“Memory Effects in Damping of Collective Vibrations”

Barreto, J., D. G. Sarantites, R. J. Charity, N. G. Nicolis, L. G. Sobotka, D. W. Stracener, D. C. Hensley, J. R. Beene, M. Halbert, and C. Baktash

“Charged Particles as Probes to Study Entrance Channel Effects in the Composite System ¹⁶⁴Yb”

Charity, R. J., J. L. Barreto, L. G. Sobotka, D. G. Sarantites, D. W. Stracener, A. Chbihi, N. G. Nicolis, R. Auble, C. Baktash, J. R. Beene, F. Bertrand, M. Halbert, D. C. Hensley, D. J. Horen, C. Ludemann, M. Thoennessen, and R. Varner

“The Mechanism for the Disassembly of Excited ¹⁶O Projectiles into Alpha Particles”

Thoennessen, M., and J. R. Beene (Invited Presentation)

“Dissipation and the Population of Compound Nuclei”

XXX International Winter Meeting on Nuclear Physics, Bormio, Italy, Jan. 27-Feb. 1, 1992

Beck, C., B. Djerroud, F. Haas, R. M. Freeman, A. Hachem, B. Heusch, A. Morsad, M. Vuillet-a-Cilles, M. Youlal, Y. Abe, R. Dayras, J. P. Wieleczo, R. Legrain, E. Pollaco, A. Ray, D. Shapira, J. Gomez del Campo, H. J. Kim, B. Shiva Kumar, D. Blumenthal, S. Cavallaro, E. deFilippo, G. Lanzano, A. Pagano, M. L. Sperduto, T. Masuse, and S. J. Sanders
"Asymmetrical Fission and Statistical Emission of Complex Fragments from the Highly Excited ^{47}V Compound Nucleus"

Ninth Topical Conference on High-Temperature Plasma Diagnostics, Santa Fe, N.M., Mar. 15-19, 1992

Hutchinson, D. P., R. K. Richards, C. A. Bennett, and C. H. Ma
"Proof-of-Principle of a Diagnostic for D-T Fusion-Product Alpha Particles"

Ma, C. H., L. R. Baylor, D. P. Hutchinson, M. Murakami, and J. B. Wilgen
"Density Profile Measurement Using a Multichannel Difluoromethane Laser Interferometer System on ATF"

Workshop on Dynamical Fluctuations and Correlations in Nuclear Collisions, Aussois, France, Mar. 16-20, 1992

Jacobs, P., M. A. Bloomer, R. Albrecht, T. C. Awes, P. Beckmann, F. Berger, D. Bock, R. Bock, G. Claesson, G. Clewing, R. Debbe, L. Dragon, A. Eklund, R. L. Ferguson, S. Fokin, A. Franz, S. Garpman, R. Glasow, H. A. Gustafsson, H. H. Gutbrod, O. Hansen, M. Hartig, G. Hoelker, J. Idh, M. Ippolitov, K. H. Kampert, K. Karadjev, B. W. Kolb, A. Lebedev, H. Loehner, I. Lund, V. Manko, B. Moskowitz, F. E. Obenshain, A. Oskarsson, I. Otterlund, T. Peitzmann, F. Plasil, A. M. Poskanzer, M. Purschke, H. G. Ritter, B. Roters, S. Saini, R. Santo, H. R. Schmidt, K. Soderstrom, S. P. Sorensen, K. Steffens, P. Steinauser, E. Stenlund, D. Stueken, A. Twyhues, A. Vinogradov, and G. R. Young
"Intermittency in 200 GeV/Nucleon S+S Collisions"

Ninth International Workshop on Photon-Photon Collisions, San Diego, Calif., Mar. 22-26, 1992

Barnes, T. (Invited Presentation)
"Can Molecules Be Seen by Two Photons?"

Barnes, T. (Invited Presentation)
"Two-Photon Couplings of Quarkonia with Arbitrary J^{PC} "

Spring-8 Workshop on Atomic Physics at High Brilliance Synchrotron Radiation Facilities, Himeji, Japan, Mar. 23-24, 1992

Sellin, I. A., J. Levin, R. Miller, N. Keller, Y. Azuma, H. G. Berry, N. Berrah-Mansour, and D. Lindle (Invited Presentation)
"Comparison of Double and Single Ionization in He by Photons and by Charged Projectiles"

International Workshop on the Physics and Techniques of Secondary Nuclear Beams, Dourdan, France, Mar. 23-25, 1992

Garrett, J. D. (Invited Presentation)
"Exotic Nuclear Shapes and Configurations That Can Be Studied at High Spin Using Radioactive Ion Beams"

Garrett, J. D. (Invited Presentation)

“North American Radioactive Beam Initiatives”

International Symposium on the Spectroscopy and Structure of Molecules and Nuclei, Tallahassee, Fla., Mar. 27-28, 1992

Johnson, N. R. (Invited Presentation)

“The Shapes and Collective Behavior of Rapidly Rotating Nuclei”

Annual Meeting of the American Chemical Society, San Francisco, Calif., Apr. 5-10, 1992

Baktash, C. (Invited Presentation)

“Nuclear Structure and Astrophysics Studies at the Proposed Oak Ridge Exotic Beam Facility”

Workshop on Future Directions in Electron-Ion Collision Physics, Atlanta, Ga., Apr. 9-10, 1992

Botcher, C., D. H. Madison, and D. R. Schultz (Invited Presentation)

“Towards a Time-Dependent Description of Electron-Atom/Ion Collisions: Two Electron Systems”

Botcher, C., and D. R. Schultz (Invited Presentation)

“The Coulomb Three-Body Problem: A Progress Report”

American Physical Society Meeting, Washington, D.C., Apr. 20-24, 1992

Baktash, C. (Invited Presentation)

“Identical Moments of Inertia in Neighboring Odd-A and Even-Even Nuclei: A Crisis in Nuclear Pair Correlations,” *Bull. Am. Phys. Soc.* **37**, 892 (Apr. 1992)

Chavez, E., A. Dacal, M. E. Ortiz, J. Gomez del Campo, H. J. Kim, D. Shapira, P.H. Stelson, and J. P. Wieleczko

“Total Momentum Transfer and Compound-Nucleus Formation and Decay in $^{79}\text{Br}(930\text{ MeV})+^{27}\text{Al}$,” *Bull. Am. Phys. Soc.* **37**, 871 (Apr. 1992)

Davids, C.N., B. B. Back, R. R. Betts, K. Bindra, W. Chung, M. Freer, J. Gehring, D. J. Henderson, W. Kutschera, T. Lauritsen, C. R. Bingham, D. M. Moltz, A. V. Ramayya, J. D. Robertson, and W. B. Walters

“First Results from the Fragment Mass Analyzer at ATLAS,” *Bull. Am. Phys. Soc.* **37**, 1021 (Apr. 1992)

Garrett, J. D.

“Level Repulsion and Chaos in the Nuclear Quantum System,” *Bull. Am. Phys. Soc.* **37**, 1015 (Apr. 1992)

Horen, D. J., C. L. Morris, S. J. Seestrom-Morris, F. W. Hersman, J. R. Calarco, M. Holtrop, M. Leuschner, M. Rawool, R. Garnett, S. Greene, M. Plum, and J. Zumbro

“Isospin Character of Transitions to Bound States of ^{206}Pb from π^\pm Scattering at 180 MeV,” *Bull. Am. Phys. Soc.* **37**, 916 (Apr. 1992)

Jurney, E. T., J. W. Starner, J. E. Lynn, and S. Raman

“Check of the Smith and Wapstra Mass Doublet Measurements,” *Bull. Am. Phys. Soc.* **37**, 902 (Apr. 1992)

Lewis, J. M., S. Pilotte, C.-H. Yu, L. L. Riedinger, C. Baktash, J. D. Garrett, N. R. Johnson, I.Y. Lee, and F. K. McGowan

"Rotational Bands in ^{191}Tl ," Bull. Am. Phys. Soc. 37, 1029 (Apr. 1992)

Ludwigsen, D. O., D. F. Winchell, and J. D. Garrett

"The Mass Dependence of Moments of Inertia of Rapidly-Rotating Nuclei," Bull. Am. Phys. Soc. 37, 980 (Apr. 1992)

Metlay, M., J. X. Saladin, M. S. Kaplan, D. F. Winchell, I. Y. Lee, C. Baktash, M. L. Halbert, M. A. Riley, A. Virtanen, and O. Dietzsch

"Multipolarity of Continuum Transitions in ^{130}Ce ," Bull. Am. Phys. Soc. 37, 996 (Apr. 1992)

Ramakrishnan, M. Thoennessen, J. R. Beene, R. L. Auble, C. Baktash, F. E. Bertrand, M. L. Halbert, D. J. Horen, P. Mueller, D. H. Olive, and R. L. Varner

"Differences in Compound Nucleus Population of ^{150}Er and ^{160}Er ," Bull. Am. Phys. Soc. 37, 870 (Apr. 1992)

Winchell, D. F., C. Baktash, J. D. Garrett, N. R. Johnson, I. Y. Lee, F. K. McGowan, M. L. Halbert, D. C. Hensley, M. S. Kaplan, J. X. Saladin, and U. J. Huttmeier

"High Spin and Shape Change in ^{83}Sr ," Bull. Am. Phys. Soc. 37, 937 (Apr. 1992)

14th Werner Brandt Workshop on Charged-Particle Penetration Phenomena, Oak Ridge, Tenn., Apr. 30-May 1, 1992

Zeijlmans van Emmichoven, P. A., C. C. Havener, I. G. Hughes, S. H. Overbury, M. T. Robinson, D. M. Zehner, and F. W. Meyer

"Electron Emission During Multicharged Ion-Metal Surface Interactions"

International Conference on Nuclear Structure at High Angular Momentum, Ottawa, Canada, May 18-22, 1992

Baktash, C., J. D. Garrett, D. F. Winchell, and A. Smith (Invited Presentation)

"Low-Spin Identical Bands in Neighboring Odd-A and Even-Even Nuclei: A Challenge to Mean-Field Theories"

Baktash, C., W. Nazarewicz, and R. Wyss

"On the Question of Spin Fitting and Quantized Alignment in Rotational Bands"

Baxter, A. M., T. L. Khoo, M. E. Bleich, M. P. Carpenter, I. Ahmad, R. V. F. Janssens, E. F. Moore, I. G. Bearden, J. R. Beene, and I. Y. Lee

"Compton Suppression Tests on Ge and BGO Prototype Detectors for GAMMASPHERE"

Bearden, I. G., R. V. F. Janssens, M. P. Carpenter, I. Ahmad, P. J. Daly, M. W. Drigert, U. Gary, T. L. Khoo, T. Lauritsen, W. Reviol, and R. Wyss

"Higher Superdeformed Band Members in ^{190}Hg : Evidence for a Band Interaction?"

Clark, R. M., R. Wadsworth, E. S. Paul, C. W. Beausang, I. Ali, A. Astier, D. M. Cullen, P. J. Dagnall, P. Fallon, M. J. Joyce, M. Meyer, N. Redon, P. H. Regan, J. F. Sharpey-Schafer, W. Nazarewicz, and R. Wyss

"Collective Dipole Rotational Bands in the A~ 200 Region"

250 Physics Division Progress Report

Fallon, P., W. Nazarewicz, M. A. Riley and R. Wyss
"Differences in 'Identical' Superdeformed Bands"

Galindo-Urbarri, A., H. R. Andrews, G. C. Ball, T. E. Drake, G. Hackmann, V. P. Janzen, S. M. Mullins, L. Persson, D. C. Radford, J. C. Waddington, D. Ward, and R. Wyss
"New Features in the Spectrum of ^{152}Dy : Evidence for Hyperdeformation?"

Garrett, J. D.
"Level Repulsion and Chaos in the Nuclear Quantum System"

Guidry, M.
"The Fermion Dynamical Symmetry Model of Superdeformation"

Guidry, M.
"Transfer Reactions and High-Spin Nuclear Structure"

Ibbotson, R., D. Cline, M. Devline, K. G. Helmer, A. E. Kavka, B. Kotlinski, A. Renalds, E. G. Vogt, C. Y. Wu, P. A. Butler, N. Clarkson, T. H. Hoare, G. D. Jones, C. A. White, J. R. Hughes, R. J. Pounter, P. Regan, R. Wadsworth, D. L. Watson, T. Czosnyka, J. Srebrny, W. Urban, R. A. Cunningham, and I. Y. Lee
"Octupole Deformation in ^{148}Nd "

Janzen, V. P., H. R. Andrews, T. E. Dranke, D. Fossan, A. Galindo-Urbarri, B. Haas, A. Omar, D. LaFosse, R. Hughes, S. Mullins, E. Paul, L. Persson, S. Pilotte, D. Prevost, D. C. Radford, J. Rodriguez, M. Sawicki, H. Schnare, H. Timmers, P. Unrau, J. C. Waddington, R. Wadsworth, D. Ward, J. Wilson, R. Wyss, and G. Zwartz
"Intruder Bands in $Z=51$ $^{109-115}\text{Sb}$ "

Jin, H. Q., V. P. Janzen, L. L. Riedinger, C.-H. Yu, C. Baktash, J. D. Garrett, N. R. Johnson, I. Y. Lee, F. K. McGowan, P. B. Semmes, and J.-Y. Zhang
"Studies of High-Spin Phenomena in Ir and Re Nuclei"

Johnson, N. R., F. K. McGowan, D. F. Winchell, J. C. Wells, C. Baktash, L. Chaturvedi, W. B. Gao, J. D. Garrett, I. Y. Lee, W. C. Ma, S. Pilotte, and C.-H. Yu (Invited Presentation)
"Transition Probabilities and Collective Properties Up to $I=36^+$ in Light Yb Nuclei"

Lee, I. Y., C. Baktash, D. M. Cullen, J. D. Garrett, N. R. Johnson, F. K. McGowan, D. F. Winchell, and C. H. Yu (Invited Presentation)
"Lifetimes of Low Spin States in the Superdeformed Band of ^{192}Hg "

Lewis, J. M., L. L. Riedinger, C.-H. Yu, C. Baktash, J. D. Garrett, N. R. Johnson, and I. Y. Lee
"Rotational Bands in ^{191}Tl "

Nazarewicz, W. (Invited Presentation)
"New Vistas in Superdeformation"

Stoyer, M. A., E. A. Henry, J. A. Becker, R. W. Hoff, A. Kuhnert, T. F. Wang, J. Breitenbach, M. Jarrio, J. L. Wood, Y. A. Akovali, C. R. Bingham, M. Zhang, P. Joshi, H. K. Carter, J. Kormicki, and P. Mantica
"Search for Population of Superdeformed States in ^{194}Pb Using ^{194}Bi β^+ Decay"

Timmers, H., J. Simpson, M. A. Riley, T. Bengtsson, M. A. Bentley, F. Hanna, S. M. Mullins, J. F. SharpeySchafer, R. Wyss, J. R. Hughes, D. B. Fossan, Y. Liang, R. Ma, and N. Xu
"High-Spin γ -Ray Spectroscopy of $^{121,122}\text{Xe}$ "

Winchell, D. F., D. O. Ludwigsen, and J. D. Garrett
"The Mass Dependence of Moments of Inertia of Rapidly-Rotating Nuclei"

Yu, C.-H., H. Q. Jin, J.M. Lewis, W. F. Mueller, L. L. Riedinger, C. Baktash, J. D. Garrett, N. R. Johnson, I. Y. Lee, F. K. McGowan, and D. Winchell
"High Spin Studies of ^{181}Au "

Yu, C.-H., H. Q. Jin, L. L. Riedinger, C. Baktash, J. D. Garrett, I. Y. Lee, W. Nazarewicz, and R. Wyss
"The Nearly Identical Bands in Odd-Odd ^{180}Ir and Its Neighboring Odd-A Nuclei"

Conference on Electronics for Future Colliders, Chestnut Ridge, N.Y., May 19-21, 1992

Young, G. R. (Invited Presentation)
"Electronics for the RHIC PHENIX Detector"

Second International Conference on Swift Heavy Ions in Matter (SHIM 92), Bensheim/Darmstadt, Germany, May 19-22, 1992

Alton, G. D., D. H. Olive, and J. R. Olive
"A Scaled Sigmund Theory Model for Determining Sputter Ratios"

Alton, G. D., R. A. Sparrow, and R. E. Olson
"Computational Evaluation of the Stripping Properties of a Plasma"

American Physical Society, Division of Atomic, Molecular, and Optical Physics, Chicago, Ill., May 20-22, 1992

Andersson, L. R., and J. Burgdorfer
"Radiative Electron Capture into Near-Threshold States of Highly Charged Ions," *Bull. Am. Phys. Soc.* **37**, 1071 (May 1992)

Burgdorfer, J. (Invited Presentation)
"Above-Surface Neutralization of Multiply Charged Ions: Transient Formation of 'Hollow' Atoms," *Bull. Am. Phys. Soc.* **37**, 1128 (May 1992)

Dellwo, J., Y. Liu, D. J. Pegg, and G. D. Alton
"Electron Affinity of Li," *Bull. Am. Phys. Soc.* **37**, 1142 (May 1992)

Elston, S. B., J. P. Gibbons, R. DeSerio, N. Keller, I. A. Sellin, S. Ricz, J. Vegh, and D. Berenyi
"Measurement of Projectile ELC Emission Distributions Produced in Intermediate Velocity Collisions of O^{5+} with He and Ar Gas Targets," *Bull. Am. Phys. Soc.* **37**, 1073 (May 1992)

Gaither, C. C., III, M. Breinig, J. W. Berryman, B. F. Hansen, and J. D. Richards
"Angular Distributions of Electrons Ejected at Large Angles in Multiply Ionizing Collisions Between O^{q+} ($q=4,7$) and Ar," *Bull. Am. Phys. Soc.* **37**, 1070 (May 1992)

252 Physics Division Progress Report

- Guo, X. Q., E. W. Bell, J. S. Thompson, G. H. Dunn, R. A. Phaneuf, D. C. Gregory, and A. C. H. Smith
"Electron-Impact Excitation of Ar^{7+} Using a Merged-Beams Technique," *Bull. Am. Phys. Soc.* **37**, 1068 (May 1992)
- Havener, C.C., P. A. Zeijlmans van Emmichoven, and R. A. Phaneuf
"Low-Energy Measurements of Electron Capture by Multicharged Ions from Excited Hydrogen Atoms," *Bull. Am. Phys. Soc.* **37**, 1116 (May 1992)
- Keller, N., R. D. Miller, L. R. Andersson, J.C. Levin, S.B. Elston, I. A. Sellin, C. Biedermann, and L. Liljeby
"State-Selective Electron Capture in Very-Slow Ne^{4+} -He Collisions," *Bull. Am. Phys. Soc.* **37**, 1071 (May 1992)
- Meyer, F. W. (Invited Presentation)
"The Production of 'Hollow Atoms' in Slow Multicharged Ion-Surface Interactions," *Bull. Am. Phys. Soc.* **37**, 1128 (May 1992)
- Muller, J., and J. Burgdorfer
"Semiclassical Description of High-Lying Doubly Excited ^1S States of Helium-Like Systems," *Bull. Am. Phys. Soc.* **37**, 1090 (May 1992)
- Ovchinnikov, S., and J. H. Macek
"Anomalous n-Dependence of Cross Sections for Capture from High Rydberg States of Atomic Hydrogen," *Bull. Am. Phys. Soc.* **37**, 1097 (May 1992)
- Reinhold, C. O., and J. Burgdorfer
"Classical and Quantum Mechanical Ionization in Fast Ion-Atom Collisions," *Bull. Am. Phys. Soc.* **37**, 1072 (May 1992)
- Reinhold, C. O., J. Burgdorfer, and J. Kemmler
"Forward Electron Emission in Fast H^0 - C-Foil Collisions," *Bull. Am. Phys. Soc.* **37**, 1072 (May 1992)
- Szabo, G., J. Wang, and J. Burgdorfer
"Electron Loss to Continuum from Rydberg States," *Bull. Am. Phys. Soc.* **37**, 1107 (May 1992)
- Vane, C.R., S.Datz, P.F. Dittner, H.F. Krause, R.Schuch, H.Gao, and R.Hutton
"Production of Electron-Positron Pairs in Coulomb Collisions of Ultrarelativistic Heavy Particles," *Bull. Am. Phys. Soc.* **37**, 1084 (May 1992)
- Yang, X., and J. Burgdorfer
"Parametric Correlations and Diffusion in Quantum Spectra," *Bull. Am. Phys. Soc.* **37**, 1096 (May 1992)
- Zeijlmans van Emmichoven, P. A., D. C. Gregory, C. C. Havener, J. S. Thompson, E. W. Bell, and X. Guo
"Electron-Impact Ionization of Multicharged Silicon Ions," *Bull. Am. Phys. Soc.* **37**, 1068 (May 1992)
- Zeijlmans van Emmichoven, P. A., C. C. Havener, I. G. Hughes, F. W. Meyer, and D. M. Zehner
"Emission of Low-Energy Continuum Electrons During Multicharged-Ion Surface Collisions," *Bull. Am. Phys. Soc.* **37**, 1072 (May 1992)

Workshop on Large Gamma-Ray Detector Arrays, Chalk River, Ontario, May 22-23, 1992

Garrett, J. D. (Invited Presentation)
"High Spin Studies with Radioactive Ion Beams"

Realistic Nuclear Structure, Stony Brook, N.Y., May 28-30, 1992

Wong, C. Y., and G. Gatoff (Invited Presentation)
"The Transverse Profile of a Color Flux Tube"

7th International Conference on Boundary Element Technology, Albuquerque, N.M., June 1992

Bottcher, C., M. R. Strayer, and M. F. Werby
"Solution of a Class of Sturm-Liouville Problems Using the Galerkin Method with Global Basis Functions"

Werby, M. F., M. K. Broadhead, M. R. Strayer, and C. Bottcher
"Solution of the Helmholtz-Poincaré Wave Equation Using the Coupled Boundary Integral Equations and Optimal Surface Eigenfunctions"

6th International Conference on Electrostatic Accelerators and Associated Boosters, Legnaro, Italy, June 1-5, 1992

Alton, G. D.
"The Performance Characteristics of a Simple, High-Efficiency, Negative Surface-Ionization Source"

Alton, G. D.
"Performance Characteristics of a Multiple-Sample, Cesium-Sputter Negative Ion Source"

Alton, G. D., D. L. Haynes, G. D. Mills, and D. K. Olsen
"Selection and Design of the Oak Ridge Radioactive Ion Beam Facility ISOL / Target Ion Source"

Jones, N. L., and P. F. Dittner
"Improved Voltage Gradient Control System Electrostatic Accelerators"

Juras, R. C., G. D. Alton, C. Baktash, D. T. Dowling, J. D. Garrett, D. L. Haynes, C. M. Jones, S. N. Lane, I. Y. Lee, M. J. Meigs, G. D. Mills, S. W. Mosko, D. K. Olsen, B.A. Tatum, K. S. Toth, and H. K. Carter
"The ORNL Radioactive Ion Beam Project with the 25MV Tandem Accelerator"

Olsen, D. K. (Invited Presentation)
"Opportunities with Radioactive Nuclear Beams"

Third International Conference on Applications of Nuclear Techniques, Mykonos, Greece, June 6-13, 1992

Alton, G. D. (Invited Presentation)
"Ion Sources for Use in Analytical, Industrial, and Nuclear Applications"

Canadian Association of Physicists' 1992 Congress, Windsor, Ontario, June 14-17, 1992

Phaneuf, R. A. (Invited Presentation)
"Progress in Collisions of Highly Charged Ions"

Second International Symposium on Nuclear Excited States, Lodz, Poland, June 22-26, 1992

Raman, S. (Invited Presentation)

“Low-Lying Collective Quadrupole Strengths in Even-Even Nuclei”

1992 International Conference on Plasma Physics, Innsbruck, Austria, June 29-July 3, 1992

Hutchinson, D. P., R. K. Richards, and C. H. Ma

“A Proof-of-Principle Test of a CO₂ Laser-Based Alpha Particle Diagnostic for Ignited Plasmas”

Nobel Symposium on Heavy-Ion Spectroscopy and QED Effects in Atomic Systems, Saltsjobaden, Sweden, June 29-July 3, 1992

Burgdorfer, J., and F. Meyer (Invited Presentation)

“Above-Surface Neutralization of Highly Charged Ions: The Formation of Hollow Atoms”

Datz, S. (Invited Presentation)

“Atomic Collision Physics— A Summary and Some Projections”

13th International Conference on Cyclotrons and Their Applications, Vancouver, Canada, July 6-10, 1992

Olsen, D. K., G. D. Alton, C. Baktash, D. T. Dowling, J. D. Garrett, D. L. Haynes, C. M. Jones, R. C. Juras, S. N. Lane, I. Y. Lee, M. J. Meigs, G. D. Mills, S. W. Mosko, B. A. Tatum, K. S. Toth, and H. K. Carter

“The ORNL Radioactive Ion Beam Project with the ORIC Accelerator”

Second International Symposium on Nuclear Astrophysics — *Nuclei in the Cosmos*, Karlsruhe, Germany, July 6-10, 1992

Garrett, J. D. (Invited Presentation)

“Prospects for Studies of Astrophysical Interest with Radioactive Beams”

NATO Advanced Study Institute, Lucca, Italy, July 12-24, 1992

Young, G. R. (Invited Presentation)

“Physics from Photon and Lepton-Pair Spectra”

International Symposium on Multiparticle Dynamics, Santiago de Compostela, Spain, July 13-17, 1992

Wong, C. Y. (Invited Presentation)

“Effect of Quark-Gluon Plasma Boundary on the Momentum Distribution of Quarks”

6th International Conference on Nuclei Far from Stability and 9th International Conference on Atomic Masses and Fundamental Constants, Bernkastel-Kues, Germany, July 19-24, 1992

Bingham, C.R., Y. A. Akovali, H. K. Carter, W. D. Hamilton, M. M. Jarrio, M. B. Kassim, J. Kormicki, J. Schwarzenberg, K. S. Toth, and M. Zhang

“New Mass Differences and α -Decay Rates for Au and Pt Isotopes”

Breitenbach, J., R. A. Braga, J. L. Wood, P. B. Semmes, and J. Kormicki

“Deformation Studies in the Extremely Neutron-Deficient Praseodymium, Neodymium, and Promethium Isotopes”

Joshi, P. K., P. F. Mantica, S. J. Robinson, E. F. Zganjar, R. L. Gill, H. K. Carter, J. Kormicki, D. Rupnik, W. B. Walters, and C. R. Bingham

“Lifetime of the O_2^+ Configuration in ^{188}Hg ”

Mantica, P. F., P. K. Joshi, S. J. Robinson, E. F. Zganjar, R. L. Gill, W. B. Walters, D. Rupnik, H. K. Carter, J. Kormicki, and C. R. Bingham

“Lifetime Measurements in ^{120}Xe ”

Schuessler, H. A., E. C. Benck, F. Buckinger, R. Wyss, C. R. Bingham, H. K. Carter, and I. Rikovska-Stone

“Deformation of $^{187,189}\text{Tl}$ from Laser Spectroscopy and Its Interpretation in the Strutinsky and Particle Plus Rotor Models”

Toth, K. S., C. N. Davids, B. B. Back, R. R. Betts, K. Bindra, C. R. Bingham, W. Chung, M. Freer, J. Gehring, D. J. Henderson, W. Kutschera, T. Lauritsen, D. M. Moltz, A. V. Ramayya, J. D. Robertson, and W. B. Walters

“Investigation of Proton-Rich Platinum Isotopes with the Fragment Mass Analyzer at ATLAS”

Toth, K. S., H. J. Kim, J. W. McConnell, C. R. Bingham, and D. C. Sousa

“The α -Decay Properties of Light Uranium Isotopes”

Toth, K. S., J. M. Nitschke, D. C. Sousa, K. S. Vierinen, and P. A. Wilmarth

“Study of Short-Lived Rare Earth Nuclei Near the Proton Drip Line”

Zhu, S., X. Zhao, K. Butler-Moore, J. H. Hamilton, A. V. Ramayya, Q. Lu, W.-C. Ma, L. K. Peker, J. Kormicki, X. Hong, W. B. Gao, J. K. Deng, J. D. Cole, R. Aryaeinejad, I. Y. Lee, N. R. Johnson, F. K. McGowan, C. E. Bemis, G. Ter-Akopian, and Yu. Oganessian

“High Spin States in Neutron Rich Nuclei from Spontaneous Fission”

Zimmerman, B. E., W. B. Walters, P. F. Mantica, Jr., J. Kormicki, H. K. Carter, J. Rikovska, N. J. Stone, and B. Kern

“Level Structure of the Odd-Odd Nuclei ^{114}Tl ”

International Nuclear Physics Conference, Wiesbaden, Germany, July 26-Aug. 1, 1992

Gatoff, G., and C. Y. Wong

“On the Origin of the Soft p_T Spectra”

Horen, D. J.

“Measurement of the Isospin Character of Nuclear Transitions by Inelastic Heavy-Ion Scattering and Comparison with Other Probes”

Toth, K. S., J. M. Nitschke, D. C. Sousa, K. S. Vierinen, and P. A. Wilmarth

“Investigation of Rare-Earth Nuclei at or near the Proton Drip Line”

XXVI International Conference on High Energy Physics, Dallas, Texas, Aug. 6-12, 1992

Plasil, F., R. Albrecht, T. C. Awes, C. Baktash, P. Beckmann, F. Berger, M. Bloomer, D. Bock, R. Bock, G. Claesson, G. Clewing, L. Dragon, A. Eklund, R. L. Ferguson, A. Franz, S. Garpman, R. Glasow, H. A. Gustafsson, H. H. Gutbrod, M. Hartig, G. Hoelker, J. Idh, P. Jacobs, K. H. Kampert, B. W. Kolb, H. Loehner, I. Lund, F. E. Obenshain, A. Oskarsson, I. Otterlund, T. Peitzmann, S. Persson, A. M. Poskanzer, M. Purschke, H. G. Ritter, B. Roters, S. Saini, R. Santo, H. R. Schmidt, R. Schmidt, T. Siemiarczuk, S. P. Sorensen, K. Steffens, P. Steinhauser, E. Stenlund, D. Stueken, M. L. Tincknell, A. Twyhues, and G. R. Young

“Photon Measurements and Global Event Characteristics from Nucleus-Nucleus Collisions at 60 and 200 GeV/Nucleon”

7th Nordic Meeting on Nuclear Physics, Vigso, Kursuscenter, Denmark, Aug. 17-21, 1992

Carlsson, H., M. Bergstrom, A. Brockstedt, L. P. Ekstrom, J. Lyttkens-Linden, H. Ryde, R. A. Bark, G. B. Hagemann, J. D. Garrett, R. Chapman, D. Clarke, F. Khazaie, J. C. Lisle, and J. N. Mo

“Backbending Phenomena and Proton-Neutron Interactions in ^{171}Re ”

9th International Conference on Hyperfine Interactions, Toyonaka, Japan, Aug. 17-21, 1992

Booth, M. G., J. Rikavska, N. J. Stone, B. E. Zimmerman, W. B. Walters, P. F. Mantica, H. K. Carter, and B. D. Kern

“Magnetic Dipole Moment of ^{114}Sb by On-Line Nuclear Orientation”

American Chemical Society Meeting, Washington, D.C., Aug. 24-28, 1992

Baktash, C. (Invited Presentation)

“Identical Moments of Inertia in Neighboring Odd-A and Even-Even Nuclei: A Crisis for Nuclear Pair Correlations”

Zganjar, E. F.

“The Electric Monopole Transition: Nuclear Structure and Nuclear Spectroscopy”

XI International Seminar on High Energy Physics Problems, Dubna, Russia, Sept. 7-12, 1992

Barnes, T. (Invited Presentation)

“Quark Born Diagrams: Meson-Meson Scattering Amplitudes from the Nonrelativistic Quark Potential Model”

International School of Nuclear Physics, 14th Course: *Heavy Ion Collisions at Intermediate and Relativistic Energies*, Erice, Sicily, Sept. 7-16, 1992

Cindro, N., M. Korolija, and D. Shapira

“Two-Proton Correlations from Heavy-Ion Collisions: Determining the Reaction Zone of Ni+Ni by the Hanbury-Brown/Twiss Effect”

Symposium of Northeastern Accelerator Personnel, Hull, Canada, Sept. 23-25, 1992

Alton, G. D., M. R. Dinehart, D. T. Dowling, D. L. Haynes, C. A. Irizarry, C. M. Jones, R. C. Juras, S. N. Lane, C. T. LeCroy, M. J. Meigs, G. D. Mills, S. W. Mosko, S. N. Murray, D. K. Olsen, and B. A. Tatum

“Oak Ridge 25URC Tandem Accelerator — 1992 SNEAP Lab Report”

Meigs, M., G. D. Alton, D. T. Dowling, D. L. Haynes, C. M. Jones, R. C. Juras, S. N. Lane, G. D. Mills, S. W. Mosko, D. K. Olsen, and B. A. Tatum

“Radioactive Ion Beam Production Challenges at the Holifield Heavy Ion Research Facility”

First International Symposium on Nuclear Physics in the Universe, Oak Ridge, Tenn., Sept. 25, 1992

Smith, M. S. (Invited Presentation)

“Experimental, Computational, and Observational Analysis of Primordial Nucleosynthesis”

Vth International Conference on the Physics of Highly-Charged Ions, Manhattan, Kan., Sept. 28-Oct. 2, 1992

Guo, X. Q., E. W. Bell, J. S. Thompson, G. H. Dunn, M. E. Bannister, R. A. Phaneuf, and A. C. H. Smith

“Backscattering in Electron-Impact Excitation of Multiply Charged Ions”

Havener, C. C., M. A. Haque, A. C. H. Smith, S. Urbain, and P. A. Zeijlmans van Emmichoven (Invited Presentation)

“Low-Energy Measurements of Electron Capture by Multicharged Ions from Excited Hydrogen Atoms”

Hughes, I. G., C. C. Havener, S. H. Overbury, M. T. Robinson, D. M. Zehner,

P. A. Zeijlmans van Emmichoven, and F.W. Meyer

“Incident Ion Charge State Dependence of Electron Emission During Slow Multicharged Ion-Surface Interactions”

Irby, V. D. (Invited Presentation)

“Saddle-Point Shifts in Ionizing Collisions”

Meyer, F. W., J. Burgdorfer, I. G. Hughes, S. H. Overbury, D. M. Zehner, and

P. A. Zeijlmans van Emmichoven

“Neutralization of Slow Multicharged Ions above a Cesium Au Surface”

Ovchinnikov, S.Y., and J. Macek (Invited Presentation)

“Theory of Electron Ejection from Surfaces by Highly Charged Ion Impact”

Segner, F., J. W. Berryman, and M. Breinig

“Coincidence Measurements Between Recoil-Ions and Electrons Ejected at Large Angles”

Zeijlmans van Emmichoven, P. A., C. C. Havener, I. G. Hughes, D. M. Zehner, and F. W. Meyer

“Analysis of Low Energy Electron Emission Arising During Slow Multicharged Ion-Surface Interactions”

14th International Conference on Plasma Physics and Controlled Nuclear Fusion Research, Wurzburg, Germany, Sept. 30-Oct.7, 1992

Richards, R. K., D. P. Hutchinson, and C. H. Ma

“Experimental Test of an Alpha Particle Diagnostic for ITER Based on CO₂ Laser Thomson Scattering”

13. GENERAL INFORMATION

PERSONNEL CHANGES

New Staff Members

D. R. Schultz, University of Missouri, Rolla, Missouri

Division Postdoctoral Associates

M. E. Bannister, Princeton University, Princeton, New Jersey
E. Chavez-Lomeli, Universidad Nacional Autonoma de Mexico, Mexico City, Mexico
D. M. Cullen, University of Liverpool, Liverpool, England
L. Folkerts, Kernfysisch Versneller Institute, Groningen, the Netherlands
G. Gatoff, Universite de Paris XI, Orsay, France
M. M. Gensini, Institute for Transuranium Elements, Karlsruhe, Germany
I. G. Hughes, Joint European Tokamak Project, Oxfordshire, England
V. D. Irby, University of Missouri, Rolla, Missouri
J. Liu, University of Miami, Coral Gables, Florida
P. E. Mueller, University of Illinois, Urbana, Illinois
A. Ray, University of Tennessee, Knoxville, Tennessee
S. Saini, University of Tennessee, Knoxville, Tennessee
M. S. Smith, California Institute of Technology, Pasadena, California
D. F. Winchell, University of Pittsburgh, Pittsburgh, Pennsylvania
P. Zeijlmans van Emmichoven, Rijksuniversiteit te Utrecht, Utrecht, the Netherlands

Staff Assignments

C. Bottcher, 5-month assignment at University of California, Santa Barbara

Staff Transfers and Terminations

A. Scientific Staff

D. P. Hutchinson (transferred to Instrumentation and Controls Division)
I-Y. Lee (accepted position with Lawrence Berkeley Laboratory)
R. A. Phaneuf (accepted position with University of Nevada, Reno)
P. H. Stelson (deceased)

B. Administrative and Technical Staff

C. A. Irizarry, Accelerator Operations (transferred to Office of Operational Readiness and Safety)
A. B. Livingston, Administrative Assistant (retirement)
R. W. Miles, HHIRF Facility Operations and Development (transferred to Plant Protection Shift Operations)

Temporary Assignments

A. Visiting Scientists

J. L. Blankenship, Retired - ORNL
R. DeSerio, University of Tennessee, Knoxville, Tennessee
G. H. Dunn, Joint Institute for Laboratory Astrophysics (JILA), University of Colorado,
Boulder, Colorado
Y. V. Efremenko, Institute for Theoretical and Experimental Physics (ITEP), Moscow, Russia
A. M. Gordeev, Institute for Theoretical and Experimental Physics (ITEP), Moscow, Russia
X-L. Han, University of Tennessee, Knoxville, Tennessee, and Jilin University, Changchun,
People's Republic of China
Y. Hatsukawa, Japan Atomic Energy Research Institute (JAERI), Ibaraki, Japan
H. Iimura, Japan Atomic Energy Research Institute (JAERI), Ibaraki, Japan
Y. A. Kamyshkov, Institute for Theoretical and Experimental Physics (ITEP), Moscow, Russia
J. Kormicki, Vanderbilt University, Nashville, Tennessee
K. M. Likin, General Physics Institute, Russian Academy of Sciences, Moscow, Russia
F. K. McGowan, Retired - ORNL
A. A. Nikitin, Institute for Theoretical and Experimental Physics, Moscow, Russia
D. V. Onoprienko, Institute for Theoretical and Experimental Physics (ITEP), Moscow, Russia
S. Ovchinnikov, Ioffe Physical Technical Institute, Leningrad, Russia
S. Rab, Kuwait Institute for Scientific Research, Kuwait
B-H. Sa, Institute of Atomic Energy, Beijing, People's Republic of China
A. Y. Savin, Institute for Theoretical and Experimental Physics (ITEP), Moscow, Russia
M. R. Schmorak, Retired - ORNL
K. D. Shmakov, Institute for Theoretical and Experimental Physics (ITEP), Moscow, Russia
A. V. Smirnov, Institute for Theoretical and Experimental Physics (ITEP), Moscow, Russia
A. C. H. Smith, University College London, London, England
E. I. Tarkovski, Institute for Theoretical and Experimental Physics (ITEP), Moscow, Russia

B. Visiting Postdoctoral Research Associates

J. Botero, University of Tennessee, Knoxville, Tennessee
X. Guo, University of Colorado, Boulder, Colorado
X. He, University of Tennessee, Knoxville, Tennessee
J. Kemmler, University of Tennessee, Knoxville, Tennessee
M. D. Kovarik, University of Tennessee, Knoxville, Tennessee
J. C. Levin, University of Tennessee, Knoxville, Tennessee
P. F. Mantica, Jr., Oak Ridge Associated Universities (UNISOR), Oak Ridge, Tennessee
R. D. Miller, University of Tennessee, Knoxville, Tennessee
C. O. Reinhold-Larsson, University of Tennessee, Knoxville, Tennessee
C-Y. Tang, University of Tennessee, Knoxville, Tennessee
C-H. Yu, University of Tennessee, Knoxville, Tennessee

C. Graduate Students

S. S. Ackleh, Cumberland College, Williamsburg, Kentucky
L. R. Andersson, Manne Siegbahn Institute of Physics, Stockholm, Sweden
E. W. Bell, Joint Institute for Laboratory Astrophysics (JILA), University of Colorado,
Boulder, Colorado
J. W. Berryman, University of Tennessee, Knoxville, Tennessee

R. L. Clark, Vanderbilt University, Nashville, Tennessee
D. J. Dean, Vanderbilt University, Nashville, Tennessee
J. Dellwo, University of Tennessee, Knoxville, Tennessee
D. D. Desai, University of Tennessee, Knoxville, Tennessee
X. Dong, University of Tennessee, Knoxville, Tennessee
K. L. Dooley, University of Tennessee, Knoxville, Tennessee
C. C. Gaither, University of Tennessee, Knoxville, Tennessee
W-B. Gao, Vanderbilt University, Nashville, Tennessee
G. L. Gauthier, Universite Claude Bernard, Villeurbanne Cedex, France
G. R. J. Grondin, University of Toronto, Toronto, Canada
B. F. Hasson, University of Tennessee, Knoxville, Tennessee
H. Jin, University of Tennessee, Knoxville, Tennessee
P. K. Joshi, Louisiana State University, Baton Rouge, Louisiana
N. Keller, University of Tennessee, Knoxville, Tennessee
D. Kerek, Royal Institute of Technology, Stockholm, Sweden/University of Tennessee,
Knoxville, Tennessee
J. G. Kreke, University of Tennessee, Knoxville, Tennessee
R. Minniti, University of Tennessee, Knoxville, Tennessee
J. Mueller, University of Frankfurt, Frankfurt, Germany
D. H. Olive, Jr., Vanderbilt University, Nashville, Tennessee
L. S. Pibida, University of Tennessee, Knoxville, Tennessee
J. D. Richards, University of Tennessee, Knoxville, Tennessee
F. W. Segner, University of Frankfurt, Frankfurt, Germany
G. A. Torshizi, University of Tennessee, Knoxville, Tennessee
J. Wang, University of Tennessee, Knoxville, Tennessee
R. C. Whaley, University of Tennessee, Knoxville, Tennessee
X. Yang, University of Tennessee, Knoxville, Tennessee
M. Zhang, University of Tennessee, Knoxville, Tennessee

D. Joint Institute for Heavy Ion Research (JIHIR) Guests

S. G. Aberg, Lund Institute of Technology, Lund, Sweden
Y. S. Chen, Institute of Atomic Energy, Beijing, People's Republic of China
R. Donangelo, Cidade Universitaria, Rio de Janeiro, Brazil
W. M. Greiner, University of Frankfurt, Frankfurt, Germany
I. Hamamoto-Kuroda, Lund Institute of Technology, Lund, Sweden
M. Korolija, Ruder Boskovic Institute, Croatia, Yugoslavia
W. Nazarewicz, Warsaw Technical University, Warsaw, Poland
Z. Szymanski, University of Warsaw, Warsaw, Poland
C-L. Wu, Jilin University, Changchun, People's Republic of China
R. A. Wyss, Royal Institute of Technology, Stockholm, Sweden
J. Y. Zhang, Lanzhou University, Lanzhou, People's Republic of China
W-Q. Zhao, Institute of High Energy Physics, Beijing, People's Republic of China

E. ORAU Faculty Research Participant

V. A. Madsen, Oregon State University, Corvallis, Oregon

F. ORAU Laboratory Graduate Research Participants

D. H. Olive, Jr., Vanderbilt University, Nashville, Tennessee
J. C. Wells, Vanderbilt University, Nashville, Tennessee

262 Physics Division Progress Report

G. ORAU Computational Science Graduate Fellowship

C. J. Lundy, University of Missouri, Rolla, Missouri

H. Oak Ridge Science and Engineering Research Semester (ORSERS) Participants

M. T. Johnson, Hamline University, Saint Paul, Minnesota

D. K. Love, Tuskegee University, Tuskegee, Alabama

M. L. Pinkham, Loyola University, New Orleans, Louisiana

S. M. Winder, University of North Carolina, Asheville, North Carolina

I. Great Lakes Colleges Association/Associated Colleges of the Midwest (GLCA/ACM) Science Program Participant

A. Sahibzada, Wabash College, Crawfordsville, Indiana

J. Individual Student Research Participants

M-B. Liu, University of Tennessee, Knoxville, Tennessee

M. Papantonakis, Berea College, Berea, Kentucky

Summer Assignments

A. HBCU/Faculty Research Program Participants

A. M. H. Basher, South Carolina State College, Orangeburg, South Carolina

M. A. Haque, Alcorn State University, Lorman, Mississippi

B. Other Visiting Faculty

K. H. Bhatt, University of Mississippi, University, Mississippi

C. University of Tennessee/ORNL Science Alliance Undergraduate Program Participants

M. D. Barrett, Texas A&M University, College Station, Texas

Z. A. Eitzen, University of Maryland, College Park, Maryland

R. R. Igharas, University of Tennessee, Knoxville, Tennessee

M. L. Lewis, Hastings College, Hastings, Nebraska

S. Mioduszewski, North Carolina State University, Raleigh, North Carolina

M. E. Rupright, University of Tennessee, Knoxville, Tennessee

L. L. Straus, Clemson University, Clemson, South Carolina

S. R. Young, California State University, Sacramento, California

PHYSICS DIVISION SEMINARS: OCTOBER 1991—SEPTEMBER 1992

Seminars arranged by the Physics Division and announced in the ORNL Technical Calendar are listed below. During the period of this report, S. (Ram) Raman served as Seminar Chairman.

Oct. 10	Claude Mahaux Universite de Liege Liege, Belgium	The Complex Shell Model
Oct. 17	Christian Erd Vienna Technical University Vienna, Austria	Soft Photon Production in 350-GeV Proton-Nucleus Collisions
Nov. 14	Zdzislaw Szymanski University of Warsaw Warsaw, Poland	Nuclear Cranking About an Arbitrary Axis
Nov. 15	Friedel Thielemann Harvard University Cambridge, Massachusetts	Nucleosynthesis in Stars and Supernovae
Nov. 18	Grzegorz Wilk Soltan Institute for Nuclear Studies Warsaw, Poland	Interacting Gluon Model in Proton-Nucleus Collisions
Nov. 21	Jacek Dobaczewski University of Warsaw Warsaw, Poland	Nuclear Structure at the Particle Drip Line
Nov. 27	Konstantin Golovanivsky Patrice Lumumba University Moscow, Russia	Physics and Applications of the GYRAC
Jan. 2	Ben-Hao Sa China Institute of Atomic Energy Beijing, China	Correlations in the Disassembly of Hot Nuclei
Jan. 9	Robert V. F. Janssens Argonne National Laboratory Argonne, Illinois	Superdeformed Nuclei Near $A = 100$
Jan. 23	Robert Compton ORNL Health and Safety Division	Carbon Clusters
Jan. 30	Alfred S. Schlachter Lawrence Berkeley National Laboratory Berkeley, California	Advanced Light Source: Photon Beams of Unprecedented Brightness
Feb. 13	James R. Thompson ORNL Solid State Division	Better High T_c Superconducting Materials with Ion-Induced Defects

Feb. 20	Walter Greiner University of Frankfurt Frankfurt, Germany	Cluster Radioactivity
Feb. 27	Ron Gill Brookhaven National Laboratory Upton, New York	Study of Neutron-Rich Nuclei at Reactor-Based Isotope Separators
Feb. 28	Ilya Fabrikant University of Nebraska Lincoln, Nebraska	Low-Energy Electron Alkali Atom Scattering and Atom-Atom Interactions
Mar. 26	Michel Baranger Massachusetts Institute of Technology Cambridge, Massachusetts	Poincaré's Dream
Mar. 26	Vladimir Zelevinsky Niels Bohr Institute Copenhagen, Denmark	Level and Width Statistics for an Open System
Apr. 10	Roger Hegstrom Wake Forest University Winston-Salem, North Carolina	Handedness of the Universe
May 4	Helmut Winter Institut für Kernphysik der Universität Münster Münster, Germany	Grazing Ion-Surface Collisions
May 21	Christopher Gould North Carolina State University Raleigh, North Carolina	Neutron Transmission Test of Time Reversal Invariance
June 11	Jean-Claude Dousse University of Fribourg Fribourg, Switzerland	<i>L</i> - and <i>M</i> -Shell Ionization Probabilities from <i>K</i> X-ray Spectra Induced by Light and Heavy Ions
July 9	Juhani Keinonen University of Helsinki Helsinki, Finland	Measurement of Stopping Power with the Doppler Shift Attenuation Method
July 14	Hermann Wollnik University of Giessen Giessen, Germany	On-Line Isotope Separators
July 16	Eric Lynn Los Alamos National Laboratory Los Alamos, New Mexico	Relevance of Nuclear Energy Levels to Quantum Chaos
July 23	Sven Åberg Lund Institute of Technology Lund, Sweden	Quantum Chaos and Nuclear Rotation Damping

- | | | |
|---------|--|---|
| Aug. 6 | Takeshi Udagawa
University of Texas
Austin, Texas | Δ Excitation in Nuclei and the Decay of Δ |
| Aug. 13 | Stefan Frauendorf
Central Institute for Nuclear Research
Rossendorf, Germany | Shapes of Sodium Clusters |
| Aug. 21 | Ikuko Hamamoto
University of Lund
Lund, Sweden | Octupole and Quadrupole Deformations in
Large Fermion Systems (Metal Clusters) |
| Aug. 27 | Yurii Demkov
St. Petersburg State University
St. Petersburg, Russia | J. C. Maxwell and the Mendeleev Tables |

SCIENTIFIC MEETINGS HELD DURING THIS PERIOD

**Joint Meeting of the USNDN and the
Panel on Basic Nuclear Data Compilations**
Oak Ridge, Tennessee, October 3-4, 1991

M. J. Martin, organizer

**Symposium on Reflections and Directions
in Low Energy Heavy-Ion Physics**
Oak Ridge, Tennessee, October 14-15, 1991

J. H. Hamilton (Vanderbilt) and R. L. Robinson, organizers

**Second International Conference on
On-Line Nuclear Orientation and Related Topics**
Oak Ridge, Tennessee, October 16-19, 1991

K. S. Krane (Oregon State), H. K. Carter,
and R. L. Robinson, organizers

Quark Matter '91

Gatlinburg, Tennessee, November 10-15, 1991

F. Plasil, organizer

Workshop on Microscopic Origin of Nuclear Deformation
Oak Ridge, Tennessee, November 25, 1991

D. H. Feng (Drexel), M. W. Guidry,
and W. Nazarewicz, organizers

Workshop on Nuclear Structure Models
Oak Ridge, Tennessee, March 16-25, 1992
R. Bengtsson and W. Nazarewicz, organizers

**A Symposium on Nuclear Reactions to Commemorate
the Sixty-fifth Birthday of G. R. Satchler**
Oak Ridge, Tennessee, April 15-16, 1992

M. R. Strayer, organizer

First Symposium on Nuclear Physics in the Universe
Oak Ridge, Tennessee, September 24-26, 1992

M. R. Strayer and M. W. Guidry, organizers

PHYSICS DIVISION

AUGUST 1982

J. B. BALL, DIRECTOR
J. K. THACKER, SEC.

DIVISION OPERATIONS
C. M. JONES, DOM ♦
O. J. MORRIS, SEC. ♦
R. L. AUBLE, DRORCO
R. L. MORRIS, LOC
G. D. MILLS, EPO
S. W. MOSKO, ERC
R. K. RICHARDS, LSO
D. L. HAYNES, LRC
R. H. BROWN
J. L. CAMERON
L. M. WALDEN

ICAC
PAE
OEHP

ADMINISTRATIVE SUPPORT
J. C. CORELAND
L. S. MORSEY

FAM

SPECIAL ASSIGNMENTS
S. RAMAN, SEMINARS
M. R. LAY, LIBRARY
F. E. BERTRAND, STUDENTS

RIB PROJECT
D. K. OLSEN
O. J. MORRIS, SEC. ♦

TARGET/ION SOURCE PHYSICS
G. D. ALTON
G. D. MILLS
D. L. HAYNES
C. A. REED ♦

ORAU

PROJECT ENGINEERING
R. C. IRVING, EC, TEM
S. W. MOSKO, CSN ♦
D. T. DOWLING
D. L. HAYNES ♦
M. J. MEIGS
S. A. TATUM
S. N. LANE, CHART
E. T. LACROIX
S. N. MURRAY

RIB FACILITY DEVELOPMENT
R. L. ROBINSON
F. P. ERVIN, SEC.

ADVANCED FACILITIES
C. M. JONES ♦
R. L. AUBLE ♦
M. E. WHITLEY

DEVELOPMENT SUPPORT
D. L. HAYNES ♦
S. W. MOSKO ♦

FACILITY MAINTENANCE
S. N. LANE ♦

UNISOR
H. K. CARTER
D. L. HAYNES
P. F. MANITCA
C. A. REED ♦
C. N. THOMAS ♦

JOINT INSTITUTE
W. KAZAROWICZ
J. B. SMITH, SEC.
J. C. STEWART, SEC.

HIGH-ENERGY EXPERIMENTAL PHYSICS
F. PLASIL
S. J. BALL, SEC.

HIGH-ENERGY NUCLEAR PHYSICS
G. R. YOUNG
T. C. JAMES
H. J. IGM
F. E. OBERSHAIN
S. SAN
S. P. SORRENSEN

UT

PARTICLE PHYSICS
H. O. COHN
K. F. REAG, JR.
Y. A. MITSKHOV

CS
ITEP

NUCLEAR SCIENCE APPLICATIONS
S. RAMAN
M. M. GENSINI

NUCLEAR DATA PROJECT
M. J. MARTIN
Y. A. KOVALEV
M. R. LAY
S. NAB

LOW/MEDIUM ENERGY EXPERIMENTAL PHYSICS
F. E. BERTRAND
J. R. HEATH, SEC.
C. R. WALLACE, SEC.

NUCLEAR REACTION SPECTROSCOPY
J. R. BEENE
J. GOMEZ DEL CAMPO
M. L. HALBERT
D. SHARON
R. L. VARNER ♦
M. KOROLLIA
P. E. MUELLER
D. W. STRACENER

UT
UT
UT
UT

NUCLEAR STRUCTURE AND RIB PHYSICS
J. D. GARRETT
R. P. AUBLE ♦
C. BAKTASH
N. R. JOHNSON
L. Y. LEE
K. S. TULLEN
D. F. WINCHELL
C. R. SINGHAM
J. C. WELLS

UT
TTU

DETECTOR/ELECTRONICS COMPUTER DEVELOPMENT
W. T. MILNER
J. W. MCCONNELL
R. L. VARNER ♦
C. N. THOMAS ♦
J. L. BLANKENSHIP

ORAU

ATOMIC PHYSICS RESEARCH
S. DATZ
F. W. THANNY, SEC.
L. H. SANDRI, SEC.

ACCELERATOR-BASED ATOMIC PHYSICS
P. F. DITNER
N. L. JONES
H. F. KRAUSE
M. BREING
S. B. ELSTON
J. J. PEGG
I. A. BELLIN

UT
UT
UT
UT

ECR-BASED ATOMIC COLLISION PHYSICS
F. W. MEYER
J. W. HALE
C. C. HAVENER
M. E. BANNISTER
I. G. HUGHES

LASER ELECTRO-OPTICS LABORATORY
C. H. MA
R. K. RICHARDS
D. P. HUTCHINSON

IMC

CONTROLLED-FUSION ATOMIC DATA CENTER
D. R. SCHULTZ
M. I. KIRKPATRICK

THEORETICAL AND COMPUTATIONAL PHYSICS
M. R. STRAYER
A. S. TATE, SEC.

THEORETICAL PHYSICS
C. BOTTCHE ♦
K. T. R. DAVIES
G. R. SCHULTER
C. Y. WONG
J. H. MACEK
J. BURGDORFER
G. GATOFF
M. W. GUIDRY

DS
UT
UT

CENTER FOR COMPUTATIONALLY INTENSIVE PHYSICS
C. BOTTCHE ♦
F. E. BARNES
M. R. STRAYER

CS

♦ DUAL CAPACITY
OR - UNIVERSITY OF OKLAHOMA
UT - UNIVERSITY OF TENNESSEE
ITEP - INSTITUTE FOR THEORETICAL AND EXPERIMENTAL PHYSICS (MOSCOW)
OEHP - OFFICE OF ENVIRONMENTAL AND HEALTH ORAL - OAK RIDGE ASSOCIATED UNIVERSITY
PAE - PLANT AND EQUIPMENT DIVISION
FAM - FINANCE AND MATERIALS DIVISION
ICAC - INSTITUTE FOR COMPUTATIONAL AND COMPUTATIONAL CHEMISTRY
TTU - TEXAS TECH UNIVERSITY

INTERNAL DISTRIBUTION

1. E. D. Aebischer
2. Y. A. Akovali
3. G. D. Alton
4. T. D. Anderson
5. B. R. Appleton
6. L. D. Armstrong
7. R. L. Auble
8. T. C. Awes
9. C. Baktash
- 10-88. J. B. Ball
89. S. J. Ball
90. M. Beckerman
91. J. R. Beene
92. C. E. Bemis, Jr.
93. F. E. Bertrand
94. J. A. Biggerstaff
95. C. R. Bingham
96. Biology Library
97. H. R. Brashear
98. M. Breinig
99. J. Burgdorfer
100. H. K. Carter
- 101-102. Central Research Library
103. H. O. Cohn
104. D. F. Craig
105. S. Datz
106. K. T. R. Davies
107. P. F. Dittner
108. D. T. Dowling
109. B. G. Eads
110. S. B. Elston
111. F. P. Ervin
112. J. D. Garrett
113. R. K. Genung
114. J. Gomez del Campo
115. M. B. Goolsby
116. J. H. Greene
117. D. S. Griffith
118. M. W. Guidry
119. E. C. Halbert
120. M. L. Halbert
121. J. W. Hale
122. J. A. Harvey
123. C. C. Havener
124. D. L. Haynes
125. J. R. Heath
126. R. B. Honea
127. D. J. Horen
128. D. P. Hutchinson
129. N. R. Johnson
130. C. M. Jones
131. N. L. Jones
132. R. C. Juras
133. S. V. Kaye
134. H. J. Kim
135. P. W. King, III
136. M. I. Kirkpatrick
137. H. F. Krause
138. E. H. Krieg, Jr.
- 139-140. Laboratory Records Department
141. Laboratory Records, ORNL R.C.
142. S. N. Lane
143. M. R. Lay
144. C. H. Ma
145. J. H. Macek
146. A. P. Malinauskas
147. M. J. Martin
148. O. J. McBride
149. J. W. McConnell
150. D. W. McDonald
151. F. K. McGowan
152. G. S. McNeilly
153. S. A. Meacham
154. P. E. Melroy
155. F. W. Meyer
156. W. T. Milner
157. S. W. Mosko
158. W. Nazarewicz
159. F. E. Obenshain
160. D. K. Olsen
161. ORNL - Y-12 Technical Library
Document Reference Section
162. F. M. Ownby
163. R. W. Peelle
164. D. J. Pegg
165. Physics Division Library
166. F. Plasil
167. M. L. Poutsma

- | | |
|----------------------|-----------------------|
| 168. L. Rayburn | 186. S. P. Sorensen |
| 169. S. Raman | 187. M. R. Strayer |
| 170. K. F. Read | 188. A. S. Tate |
| 171. J. B. Richard | 189. B. A. Tatum |
| 172. R. K. Richards | 190. J. K. Thacker |
| 173. J. B. Roberto | 191. K. S. Toth |
| 174. R. L. Robinson | 192. C. R. Vane |
| 175. T. M. Rosseel | 193. R. L. Varner |
| 176. T. H. Row | 194. C. R. Wallace |
| 177. L. J. Saddiq | 195. K. M. Wallace |
| 178. M. J. Saltmarsh | 196. R. C. Ward |
| 179. G. R. Satchler | 197. D. A. Waters |
| 180. D. R. Schultz | 198. J. C. Wells, Jr. |
| 181. I. A. Sellin | 199. G. E. Whitesides |
| 182. D. Shapira | 200. M. Whitley |
| 183. J. Sheffield | 201. B. Y. Wilkes |
| 184. W. D. Shults | 202. C-Y. Wong |
| 185. C. S. Sims | 203. G. R. Young |

EXTERNAL DISTRIBUTION

204. P. R. Adzic, Boris Kidric Institute of Nuclear Science - Vinca, Laboratory of Physics, P.O. Box 522, 11001 Belgrade, Yugoslavia
205. J. M. Alexander, Department of Physics, SUNY at Stony Brook, Stony Brook NY 11794
206. B. J. Allen, Physics Division, Australian Atomic Energy Commission, Sutherland, N.S.W., Australia
207. J. Russia Andersen, Institute of Physics, Aarhus University, DK-8000, Aarhus C, Denmark
208. Sakir Ayik, Physics Department, Tennessee Technological University, Cookeville, TN 38505
209. A. B. Balantekin, Department of Physics, University of Wisconsin, 1150 University Avenue, Madison, WI 53706
210. Charles A. Barnes, Division of Physics and Astronomy, California Institute of Technology, Pasadena, CA 91125
211. G. A. Bastin, Centre de Spectrometrie Nucleaire et de Spectrometrie de Masse, B. P. 104, 91406 Orsay, France
212. Bates Linear Accelerator, P. O. Box 95, Middleton, MA 01949
213. F. D. Becchetti, Department of Physics-Randall Lab., University of Michigan, Ann Arbor, MI 48109-1120
214. H. Behrens, Zentralstelle fur Atomkernenergie-Dokumentation, Kernforschungszentrum Karlsruhe 7514, Eggenstein-Leopoldshafen-2, Germany
215. Ingmar Bergstrom, Nobel Institute of Physics, Stockholm 50, Sweden
216. B. L. Berman, Department of Physics, The George Washington University, Washington, DC 20052
217. Biblioteca, Dep. de Fisica (Tandar), CNEA, Av. Libertador 8250, 1429 Buenos Aires, Argentina
218. Bibliotheque - Madame Belle, Universite de Grenoble, Institut des Sciences Nucleaires, 53, rue des Martyrs, B. P. 21, 38 Grenoble, France
219. P. Blasi, Universita di Fierenza, Largo E. Fermi 2, 50125 Fierenza, Italy
220. S. D. Bloom, Lawrence Livermore National Laboratory, P. O. Box 808, Livermore, CA 94550
221. H. G. Blosser, NSCL/Cyclotron Laboratory, Michigan State University, East Lansing, MI 48824
222. R. Bock, Gesellschaft fur Schwerionenforschung, Postfach 11 05 41, 6100 Darmstadt, Germany
223. H. Bohn, Physik-Department E12, Technische Universitat, 8046 Garching bei Munchen, Germany

224. A. Bohr, Copenhagen University, Niels Bohr Institute, Blegdamsvej 17, Copenhagen, Denmark
225. José-Luis Boldú, Secretary for the Coordination of Science, Instituto de Física, Universidad Nacional Autonoma de Mexico, Apartado Postal 20-364, 01000 Mexico, D.F.
226. William Brantley, Department of Physics, Furman University, Greenville, SC 29613
227. Peter Braun-Munzinger, Department of Physics, SUNY at Stony Brook, Stony Brook, NY 11794
228. L. B. Bridwell, Office of the President, S.W. Missouri State University, 901 South National, Springfield, MO 65804
229. J. S. Briggs, Theoretical Physics Division, Atomic Energy Research Establishment, Harwell, Didcot, Oxfordshire OX 11 ORA, England
230. J. A. Brink, Library Division, The Merensky Institute of Physics, University of Stellenbosch, Stellenbosch, Republic of South Africa
231. H. C. Britt, Lawrence Livermore Laboratory, P. O. Box 808, Livermore, CA 94550
232. Ricardo Americo Broglia, Niels Bohr Institute, Blegdamsvej 17, 2100 Copenhagen O, Denmark
233. D. A. Bromley, Nuclear Structure Laboratory, Yale University, New Haven, CT 06520
234. Peter Anthony Butler, University of Liverpool, P. O. Box 147, Liverpool L69 3X, United Kingdom
235. T. A. Cahill, Director, Crocker Nuclear Laboratory, University of California, Davis, CA 95616
236. R. Caplar, Ruder Boskovic Institute, Bijenicka 54, 41001 Zagreb, Croatia, Yugoslavia
237. Jose L. S. Carvalho, Instituto de Radioprotecao e Dosimetria, C.N.E.N., Av. das Americas km 11,5 Barra de Tijuca - R. J., 22700 - Rio de Janeiro, R. J. Brazil
238. Yong Shou Chen, Institute of Atomic Energy, Academia Sinica, P. O. Box 275, Beijing, China
239. F. E. Chukreev, Kurchatov Institute of Atomic Energy, Kurchatov Square, 123 182 Moscow, Russia
240. N. Cindro, Ruder Boskovic Institute, Bijenicka 54, 41001 Zagreb, Yugoslavia
241. David Clark, Lawrence Berkeley Laboratory, University of California, Berkeley, CA 94720
242. Douglas Cline, Nuclear Structure Research Laboratory, University of Rochester, Rochester, NY 14627
243. J. D. Cole, EG&G Idaho, Inc., TRA 652, Idaho Falls, ID 83415
244. University of Colorado, Department of Physics, Boulder, CO 80309
245. D. H. Crandall, Branch Chief for Experimental Research, Applied Plasma Physics Division, Office of Fusion Energy, ER 542, G-226, GTN, U.S. Department of Energy, Washington, DC 20545
246. Walter Croft, Department of Physics and Astronomy, Mississippi State University, Drawer 5167, Mississippi State, MS 39762-5167
247. F. L. Culler, Office of the President, Electric Power Research Institute, P. O. Box 10412, 3412 Hillview Avenue, Palo Alto, CA 94303
248. R. E. Culp, Martin Marietta Denver Aerospace, P.O. Box 179, M/S # PO540, Denver, CO 80201
249. T. J. Curtin, Director, Office of Research and Grants Administration, Texas Women's University, Box 22939, TWU Station, Denton, TX 76204
250. R. Y. Cusson, Physics Department, Duke University, Durham, NC 27706
251. Cyclotron Library, Indiana University Cyclotron Facility, 2401 Milo B. Sampson Lane, Bloomington, IN 47405
252. B. A. Dahling, Lawrence Livermore National Laboratory, Livermore, CA 94550
253. Solange de Barros, Head, Department of Nuclear Physics, Universidade Federal do Rio de Janeiro, Instituto de Fisica - Department Fisica Nuclear, Centro de Tecnologia - Bloco A, Ilha do Fundao - Rio de Janeiro, Brasil
254. Adriano de Lima, Physics Laboratory, University of Coimbra, Coimbra, Portugal
255. Departamento de Física, Faculdade de Ciências de Lisboa, Universidade de Lisboa, Campo Grande, ed. C1, piso 4, 1700-Lisboa, Portugal
256. Dipartimento di Fisica, Università di Pisa, Piazza Torricelli, 2, 56100 Pisa, Italy
257. Claude Detraz, Director, GANIL, B.P. 5027, 14021 Caen Cedex, France

272 Physics Division Progress Report

258. Antonio D'Onofrio, Istituto Nazionale di Fisica Nucleare, Sezione di Napoli, Mostra D'Oltremare Pad. 20, 80125 Napoli, Italy
259. R. M. Diamond, Chemistry Division, Lawrence Berkeley Laboratory, Berkeley, CA 94720
260. Olacio Dietzsch, Depto. de Fisica Experimental, Instituto de Fisica, Universidade de Sao Paulo, Cx. Postal 20516, Sao Paulo, S.P., Brazil
261. Jerzy Dudek, Centre de Recherches Nucleaires, Division de Physique Nucleaire, B.P. 20, 67037 Strasbourg Cedex, France
262. J. L. Duggan, Department of Physics, North Texas State University, Denton, TX 76203
263. K. A. Erb, National Science Foundation, Rm. 341, 1800 G Street NW, Washington, DC 20550
264. John R. Erskine, U.S. Department of Energy, Division of Nuclear Physics, ER-23, GTN, Washington, DC 20585
265. U. Facchini, Physics Department, University of Milan, Via Salidini 50, Milan, Italy
266. Amand Faessler, Institut fur Theoretische Physik, Universitat Tubingen, Auf der Morgenstelle 14, D-7400 Tubingen, Germany
267. D. H. Feng, Department of Physics, Drexel University, Philadelphia, PA 19104
268. M. P. Fewell, Australian National University, Canberra, 2600 Australia
269. J. S. Forster, Nuclear Physics Branch, Atomic Energy of Canada Limited, Chalk River Nuclear Laboratories, Chalk River, Ontario, Canada K0J 1J0
270. J. D. Fox, Department of Physics, Florida State University, Tallahassee, FL 32306
271. I. M. Frank, Laboratory for Nuclear Reactions, Dubna Joint Institute for Nuclear Research, Dubna, Moscow Oblast, Russia
272. Umesh Garg, Department of Physics, University of Notre Dame, Notre Dame, IN 46556
273. Claus-Konrad Gelbke, National Superconducting Cyclotron Laboratory, Michigan State University, East Lansing, MI 48824
274. F. Lester Ginn, Program Manager, Research Management Branch, Department of Energy, Oak Ridge Operations, Post Office Box 2008, Oak Ridge, TN 37831-6269
- 275-284. GLCA-ORS, Attention: R. R. Winters, Denison University, Granville, OH 43023
285. Alan Goodman, Department of Physics, Tulane University, New Orleans, LA 70118
286. Harvey A. Gould, Lawrence Berkeley Laboratory, 1 Cyclotron Blvd., Berkeley, CA 94720
287. H. E. Gove, Nuclear Structure Laboratory, University of Rochester, Bldg. 510A, Rochester, NY 14627
288. Walter Greiner, Institut fur Theoretische Physik der Universitat Frankfurt Main, Robert Mayer-Strasse 8-10, Germany
289. E. E. Gross, 115 Pitch Pine Lane, Chapel Hill, NC 27514
290. H. Grunder, Continuous Electron Beam Accelerator Facility (CEBAF), 12070 Jefferson Avenue, Newport News, VA 23606
291. M. Grypeos, University of Thessaloniki, Department of Theoretical Physics, Thessaloniki, Greece
292. H. H. Gutbrod, Gesellschaft fr Schwerionenforschung, Postfach 11 05 41, 6100 Darmstadt 1, Germany
293. F. Haas, CRN-PNIW, Rue du Loess, 67037 Strasbourg Cedex, France
294. J. H. Hamilton, Department of Physics, Vanderbilt University, Nashville, TN 37203
295. Ole Hansen, Brookhaven National Laboratory, Bldg. 901A, Upton, NY 19973
296. Yuichi Hatsukawa, Japan Atomic Energy Research Institute, Department of Radioisotopes, Tokai, Ibaraki 319-11, Japan
297. J. S. Hattula, Department of Physics, University of Jyvaskyla, Seminaarinkatu 15, SF-40100 Jyvaskyla 10, Finland
298. R. L. Heath, Idaho National Engineering Laboratory, EG&G Idaho, Inc., P. O. Box 1625, Idaho Falls, ID 83401
299. David L. Hendrie, Director, Division of Nuclear Physics, ER 23, Mail Station J-309, U.S. Department of Energy, Washington, DC 20585
300. Ronald Henry, Vice President for Academic Affairs, Auburn University, 208 Samford Hall, Auburn University, AL 36849-5108

301. Bent Herskind, Niels Bohr Institute, Riso, DK-4000 Roskilde, Denmark
302. Kris L. Heyde, Institute of Theoretical Physics, University of Ghent, Proeftvinstraat 42, B9000 Ghent, Belgium
303. Rainer Hippler, Universitat Bielefeld, Fakultat fur Physik, University of Bielefeld, Postfach 8640, 4800 Bielefeld 1, Germany
304. William A. Hoffman, Director, Oak Ridge Science Semester, Denison University, Granville, OH 43023
305. Harry D. Holmgren, Department of Physics, University of Maryland, College Park, MD 20742
306. J. R. Huizenga, Department of Physics and Astronomy, University of Rochester, Rochester, NY 14627
307. P. Hvelplund, Institute of Physics, Aarhus University, DK-8000, Aarhus C, Denmark
308. H. R. McK. Hyder, A.W. Wright Nuclear Structure Laboratory, Yale University, P.O. Box 666, 272 Whitney Ave., New Haven, CT 06511
309. M. V. Hynes, Department of Physics, Los Alamos National Laboratory, University of California, Los Alamos, NM 97545
310. Francesco Iachello, Department of Physics, Yale University, New Haven, CT 06520
311. University of Illinois at Urbana-Champaign, Department of Physics, Urbana, IL 61801
312. Institute of Physics, High Energy and Nuclear Physics Library, C. Postal 20.516,0100 - Sao Paulo, S.P., Brasil
313. Hideki Iimura, Department of Chemistry, Japan Atomic Energy Research Institute, Tokai-mura, Ibaraki 319-11, Japan
314. I. Iori, Istituto di Science Fisiche, Aldo Pontromoli, Via Celoria 16, 20133 Milano, Italy
315. Iowa State University, Department of Physics, Ames, IA 50011
316. J. M. Irvine, Department of Physics, University of Manchester, Oxford Rd., GB-Manchester M13 9 PL, United Kingdom
317. Beth Jinkerson, ORAU/SEED, Oak Ridge, TN 37831-0117
318. R. C. Johnson, University of Surrey, Guildford, Surrey GU2 5XH, United Kingdom
319. R. Kamermans, Fysisch Laboratorium, Rijksuniversiteit Utrecht, P. O. Box 80.000, 3508 TA UTRECHT, The Netherlands
320. H. Kamitsubo, Head, Cyclotron Laboratory, Institute of Physical and Chemical Research, Wako-shi, Saitama, 351 Japan
321. D. G. Kamke, Ruhr-Universitat Bochum, Dynamitron Tandem Laboratory, Universitätsstr., 150 Gibaunde NT, Postfach 1021 48, 4360 Bochum 1, Germany
322. University of Kansas, Department of Physics, Lawrence, KS 66045
323. Mika Karhu, SSC Laboratory, International Coordination Dept., Mail Stop 1070, 2550 Beckleymeade Ave., Dallas, TX 75237
324. Norihisa Kato, Department of Physics, Kyushu University, 33 Fukuoka, 812, Japan
325. H. Kawakami, Institute for Nuclear Study, University of Tokyo, Midori-cho, Tokyo, Japan
326. J. O. Kephart, Department of Electrical Engineering, Stanford University, Stanford, CA 94305
327. B. D. Kern, Department of Physics & Astronomy, University of Kentucky, Lexington, KY 40506
328. Uwe Keyser, Institut F. Metallphysik und Nukleare, Festkoerperphysik Techn.-Universitaet, D3300 Braunschweig, Mendelssohnstr. 3, Germany
329. Jae Yool Kim, High Energy Physics Laboratory, Department of Physics, Chonnam National University, Kwangju 500-757, Korea
330. R. K. Klein, Department of Electrical Engineering, Stanford University, Stanford, CA 94305
331. P. K. Kloepfel, Continuous Electron Beam Accelerator Facility, 12070 Jefferson Avenue, Newport News, VA 23606
332. H. Knudsen, Institute of Physics, Aarhus University, DK-8000, Aarhus C, Denmark
333. S. Koicki, Boris Kidric Institute of Nuclear Science - Vinca, Laboratory of Physics, P.O. Box 522, 11001 Beograd, Yugoslavia
334. Steven E. Koonin, Kellogg Radiation Laboratory, California Institute of Technology, Pasadena, CA 91125

274 Physics Division Progress Report

335. Jan Kormicki, Department of Physics, Vanderbilt University, P.O. Box 1807, Station B, Nashville, TN 37235
336. M. O. Kortelahti, Physics Department, University of Jyväskylä, Seminaarink 15, 40100 Jyväskylä, Finland
337. K. S. Krane, Department of Physics, Oregon State University, Corvallis, OR 97331-6507
338. B. Krishnarajulu, Department of Physics, Gulbarga University, Gulbarga 585106, India
339. Jozef Kristiak, Fyzikalny Ustav, Centra Elektro-fyzikalneho Vyskumu, Slovenskej Akademie Vied, 842 28 Bratislava, Dubravska Cesta 9, Czechoslovakia
340. Thomas J. Kvale, Department of Physics & Astronomy, University of Toledo, Toledo, OH 43606
341. I. Y. Lee, Nuclear Science Division, Lawrence Berkeley Laboratory, 1 Cyclotron Road, Berkeley, CA 94720
342. Michel LeTourmel, Centre de Recherches Nucleaires, Service des Accelerateurs, B. P. 20 CRO, 67037 Strasbourg Cedex, France
343. Librarian, Atomic Energy Centre, P. O. Box No. 164, Ramna, Dacca, Bangladesh
344. Librarian, Chen Kin-hai, Institute of Modern Physics, Academia Sinica, P. O. Box 31, Lanzhou, People's Republic of China
345. Librarian, Cyclotron Laboratory, Michigan State University, East Lansing, MI 48824
346. Librarian, Cyclotron Laboratory, RIKEN (The Institute of Physical and Chemical Research), Wako-shi, Saitama 351, Japan
347. Librarian, Department of Physics, Georgia State University, Atlanta, GA 30303
348. Librarian, Fermi National Accelerator Lab., P.O. Box 500, Batavia, IL 60510
349. Librarian, GANIL, B. P. No. 5027, 14004 Caen Cedex, France
350. Librarian, GSI, Postfach 11 05 41, 6100 Darmstadt, Germany
351. Librarian, Institut des Sciences Nucleaires, B. P. No. 257 - Centre de Tri, 38044 Grenoble Cedex, France
352. Librarian, Institute of Nuclear Research of the Hungarian Academy of Sciences, P.O. Box 51, Debrecen, H-4001 Hungary
353. Librarian, International Centre for Theoretical Physics, Miramare, P.O.B. 586, 84100 Trieste, Italy
354. Librarian, MERT Division Library, Oak Ridge Associated Universities, P. O. Box 117, Oak Ridge, TN 37831-0117
355. Librarian, Nuclear Physics Group, Department of Physics, Schuster Laboratory, The University, Manchester, M13 9PL, United Kingdom
356. Librarian, Nuclear Physics Group, Institute of Physics, Academia Sinica, Taipei, Taiwan 11529, Republic of China
357. Librarian, Nuclear Physics Lab, University of Oxford, 1 Keble Rd., Oxford OX1 3PH, United Kingdom
358. Librarian, Physics Department, 374 Bausch and Lomb Building, University of Rochester, Rochester, NY 14627
359. Librarian, Research Center for Nuclear Physics, Osaka University, 10-1 Mihogaoka, Ibaraki, Osaka, 567 Japan
360. Librarian, Saha Institute of Nuclear Physics, Sector-I, Block-AF, Bidhan Nagar, Calcutta-700064, India
361. Librarian, Universidade de Sao Paulo, Instituto de Fisica - Biblioteca Depto Fisica Nuclear, Caixa Postal, 20516 - 01498 - Sao Paulo, Brasil
362. Librarian, University of Illinois, Nuclear Physics Laboratory, 23 Stadium Drive, Champaign, IL 61820
363. Librarian, Texas Accelerator Center, Building 2, 4802 Research Forest Drive, The Woodlands, TX 77381
364. Library, Institute for Nuclear Study, University of Tokyo, Midori-cho, Tanashi, Tokyo 188, Japan

365. Library of the Institute of Atomic Energy, Beijing, People's Republic of China
366. Library, Beijing National Tandem Accelerator Laboratory, Institute of Atomic Energy, P.O. Box 275 (80), Beijing 102413, China
367. Rainer M. Lieder, Institut fur Kernphysik, Postfach 1913, 5170 Julich, Germany
368. J. S. Lilley, Daresbury Laboratory, GB-Warrington WA4 4AD Cheshire, England
369. J. C. Lisle, Dept. of Physics, Schuster Laboratory, Manchester University, Manchester M13 9 M13 9 PL, United Kingdom
370. H. Lizurej, Jagellonian University, Institute of Physics, Reymonta 4, 30-059 Krakow 16, Poland
371. Tom Lonnroth, Department of Physics, Abo Akademi, Porthansgatan 3, SF-20500 Turku, Finland
372. Malcolm Macfarlane, Department of Physics, Indiana University, Bloomington, IN 47405
373. A. D. MacKellar, Department of Physics and Astronomy, University of Kentucky, Lexington, KY 40506-0055
374. G. Madurga, Departameto de Fisica Atomica y Nuclear, Facultad de Ciencias, Universidad de Sevilla, Sevilla, Spain
375. Claude Charles Mahaux, Institut de Physique B5 Universite de Liege, Sait Tilman, B-4000 Liege 1, Belgium
376. Robert S. Marianelli, Division of Chemical Sciences, Office of Basic Energy Sciences, U.S. Department of Energy, Mail Station G-334, GTN, Washington, DC 20545
377. Mario Mariscotti, Comision Nacional de Energia Atomica, Departamento de Fisica, Avenida del Libertador 8250, 1429 Buenos Aires, Argentina
378. Niels Marquardt, Universitat Dortmund Lehrstuhl fur Beschleunigerphysik, P.O. Box 500 500, D-4600 Dortmund 50, Germany
379. Felix Marti, NSCL, Michigan State University, East Lansing, MI 48824
380. J. V. Martinez, Division of Chemical Sciences, Mail Stop J309 GTN, U.S. Department of Energy, Washington, DC 20585
381. V. Massidda, Departamento de Fisica, C.N.E.A., Buenos Aires, Argentina
382. Floyd D. McDaniel, Department of Physics, North Texas State University, Denton, TX 76203
383. J. B. McGrory, Division of Nuclear Physics, ER 23, G-236/GTN, U.S. Department of Energy, Washington, DC 20585
384. G. K. Mehta, Director, Nuclear Science Centre, JNU Campus, Post Box No. 10502, New Delhi-110067, India
385. Eugen Merzbacher, University of North Carolina, Department of Physics and Astronomy, Chapel Hill, NC 27514
386. R. J. Meyer, Nuclear Physics Department, Fysisch Laboratorium Rijksuniversiteit, P. O. Box 80 000, 3508 TA Utrecht, The Netherlands
387. R. Middleton, Department of Physics, University of Pennsylvania, Philadelphia, PA 19104
388. E. Migneco, INFN Laboratorio Nazionale del Sud, Corso Italia 57, 95127 Catania, Italy
389. Alice C. Mignerey, Department of Chemistry, University of Maryland, College Park, MD 20742
390. J. C. D. Milton, Physics Division, Atomic Energy of Canada Ltd., Chalk River, Canada KOJ 1J0
391. MIT, Laboratory for Nuclear Science, Intermediate Energy Group, c/o Secretary 26-441, Cambridge, MA 02139
392. University of Minnesota, Physics Department, 116 Church Street SW, Minneapolis, MN 55455
393. C. D. Moak, 332 Louisiana Avenue, Oak Ridge, TN 37830
394. G. C. Morrison, Department of Physics, University of Birmingham, Birmingham B15 2TT, England
395. U. Mosel, Institut fur Theoretische Physik, Universitat Giessen, 6300 Giessen, Germany
396. Brian W. Moudry, c/o Ms. Helene Perry, Department of Physics, Loyola College, Baltimore, MD 21210
397. Shoji Nagamiya, Department of Physics, Columbia University, New York, NY 10027
398. M. A. Nagarajan, Daresbury Laboratory, GB-Warrington WA4 4AD Cheshire, England

276 Physics Division Progress Report

399. Y. Nakamura, JPL, Systems Analysis Section, California Institute of Technology, 4800 Oak Grove Drive, Pasadena, CA 91103
400. John H. Neiler, 853 West Outer Drive, Oak Ridge, TN 37830
401. Nebojsa Neskovic, Boris Kidric Institute of Nuclear Science - Vinca, Institute for Research in Physics, P.O. Box 522, 11001 Belgrade - Yugoslavia
402. John Newton, Dept. of Nuclear Physics, The Australian National University, P. O. Box 4, Canberra ACT 2600, Australia
403. Ray Nix, Nuclear Theory, T-9, MS B279, Los Alamos National Laboratory, Los Alamos, NM 87545
404. Ranier W. Novotny, II. Physikalisches Institut, Justus-Liebig Universitat, Heinrich-Buff-Ring 16, 6300 Giessen, Germany
- 405-485. Oak Ridge Associated Universities, Office of Information Services, P.O. Box 117, Oak Ridge, TN 37831-0117
486. Yu.Ts. Oganessian, Laboratory for Nuclear Reactions, Dubna Joint Institute for Nuclear Research, Dubna, Moscow Oblast, Russia
487. Office of Assistant Manager for Energy Research and Development, Department of Energy, Oak Ridge Operations Office, Oak Ridge, TN 37830
488. Yuko Okamoto, Particle Theory Group, Department of Physics, Nara Women's University, Nara-shi 630, Japan
489. Masumi Oshima, Japan Atomic Energy Research Institute, Tokai Establishment, Tokai-mura, Naka-gun, Ibaraki-ken 319-11, Japan
490. Ingvar Otterlund, Division of Cosmic and Subatomic Physics, University of Lund, Slvegatan 14, S-233 62 Lund, Sweden
491. R. H. Pantell, Department of Electrical Engineering, Stanford University, Stanford, CA 94305
492. H. Park, Department of Electrical Engineering, Stanford University, Stanford, CA 94305
493. Peter Paul, Department of Physics, S.U.N.Y. at Stony Brook, Stony Brook, NY 11794
494. Max Peisach, Southern Universities Nuclear Institute, P. O. Box 17, Faure, 7131, Republic of South Africa
495. Rodney (Buz) Piercey, Department of Physics and Astronomy, Mississippi State University, Drawer 5167, Mississippi State, MS 39762-5167
496. University of Pittsburgh, Department of Physics, Pittsburgh, PA 15260
497. A.J.M. Plompen and J.P.S. van Schagen, Fakulteit Natuurkunde en Sterrenkunde, Postbus 7161, 1007 AM Amsterdam, Netherlands
498. J. G. Pochodzalla, Gessellschaft fur Schwerionenforschung, Postfach 11 05 41, Darmstadt 1, Germany
499. R. E. Pollock, Department of Physics, Indiana University, Bloomington, IN 47405
500. A. M. Poskanzer, Nuclear Science Division, Lawrence Berkeley Laboratory, Berkeley, CA 94720
501. F. Pougheon, Institut de Physique Nucleaire, B.P. No. 1, 91406 Orsay, France
502. B. Povh, Max Planck Institut fur Kernphysik, 69 Heidelberg, Saupfercheckweg, Postfach 124B, Germany
503. James Purcell, Department of Physics, Georgia State University, Atlanta, GA 30303
504. A. V. Ramayya, Department of Physics, Vanderbilt University, Nashville, TN 37203
505. Jacobo Rapaport, Department of Physics, Ohio University, Athens, OH 45701-0640
506. John Rasmussen, Lawrence Berkeley Laboratory, Building 70A, Berkeley, CA 94720
507. Patrick Richard, Physics Department, Kansas State University, Manhattan, KS 66506
508. Shela Robinson, Department of Physics & Astronomy, Western Kentucky University, Bowling Green, KY 42101
509. Steve Robinson, Department of Physics, Tennessee Technological University, P.O. Box 505, Cookeville, TN 38505
510. L. Rosen, Los Alamos National Laboratory, P. O. Box 1663, Los Alamos, NM 87544

511. Marcos Rosenbaum, Director, Instituto de Ciencias Nucleares, Universidad Nacional Autonoma de Mexico, Circuito Exterior, Ciudad Universitaria, Delegación Coyoacán, Apartado Postal 70-360, 04510 Mexico D.F.
512. D. G. Sarantites, Department of Chemistry, Washington University, St. Louis, MO 63130
513. V. Sarantseva, Head, Publishing Department, Joint Institute for Nuclear Research, Head Post Office, P. O. Box 79, Moscow, Russia
514. J. P. Schiffer, Physics Division, Argonne National Laboratory, 9700 South Cass Avenue, Argonne, IL 60439
515. K. D. Schilling, Research Center Rossendorf Inc., Institute for Nuclear and Hadronic Physics, PF 19, D-(0)-8051 Dresden, Germany
516. Hans A. Schuessler, Department of Physics, Texas A&M University, College Station, TX 77843
517. Hermann Schweickert, Cyclotron Laboratory, Kernforschungszentrum Karlsruhe, Institut für Applied Physik, P. O. Box 3640, D-7500 Karlsruhe 1, Germany
518. David K. Scott, National Superconducting Cyclotron Laboratory, Michigan State University, East Lansing, MI 48824
519. S. Seki, Tandem Accelerator Center, University of Tsukuba, Ibaraki 305, Japan
520. J.P.F. Sellschop, Department of Physics, University of Witwatersrand, Johannesburg, South Africa
521. P. B. Semmes, Physics Department, Tennessee Technological University, Cookeville, TN 38505
522. M. H. Sergolle, Director, Institut de Physique Nucleaire - Orsay , B.P. N° 1, 91406 Orsay Cedex, France
523. Nathal Severijns, Instituut voor Kern-en Stralingsfysika, K U Leuven, Celestijnenlaan 200 D, B-3001 Heverlee, Belgium
524. J. C. C. Sharp, Information Officer, Daresbury Laboratory, Science Research Council, Daresbury, Warrington WA4 4AD, England
525. J. F. Sharpey-Schafer, Oliver Lodge Laboratory, The University, P. O. Box 147, Liverpool, L69 3BX, United Kingdom
526. N. Shikazono, Division of Physics, Japan Atomic Energy Research Institute, Tokai Research Institute, Postal Area Number 319-11, Tokai-mura, Naka-gun, Ibaraki-ken, Japan
527. P. J. Siemens, Department of Physics, Oregon State University, Corvallis, OR 97331
528. R. H. Siemssen, Kernfysisch Versneller Instituut der Rijksuniversiteit Zernikelaan 25, 9747 AA Groningen, The Netherlands
529. C. Signorini, INFN Laboratorio Nazionale di Legnaro, Via Romea 4, 35020 Legnaro-Padova, Italy
530. Raghuvir Singh, North Eastern Hill University, Department of Physics, Laitumkhrah, Shillong-793003, India
531. S. J. Skorka, Tandem Accelerator Laboratory, University of Munich, Munich, Germany
532. Carl Sofield, Nuclear Physics Division, Bldg. 477, AERE Harwell, Oxfordshire OX 11 ORA, England
533. Hsu Loke Soo, Department of Physics, Nanyang University, Singapore 22, Republic of Singapore
534. C. Speth, Institut für Kernphysik, KFA, Julich, Postfach 1913, D-5170 Julich, Germany
535. Spett.le Biblioteca, Laboratori Nazionali del Gran Sasso (INFN), S.S. 17 bis km. 18+910, 67010 Assergi (AQ), Italy
536. T. Springer, Institut für Festkörperforschung der KFA Julich GmbH, Postfach 1913, D-5170 Julich 1, Germany
537. Stanford University, Department of Physics, Stanford, CA 94305
538. Stephen G. Steadman, Massachusetts Institute of Technology, Room 26-411, Cambridge, MA 02139
539. Alberto Stefanini, Instituto Nazionale di Fisica Nucleare, Laboratori Nazionali di Legnaro, 35020 Legnaro (Padova), Italy

540. Donald K. Stevens, Office of Basic Energy Sciences, U.S. Department of Energy, Mail Station J-304, GTN, Washington, DC 20585
541. R. G. Stokstad, Lawrence Berkeley Laboratory, Bldg. 88, Berkeley, CA 94720
542. N. Stolterfoht, Hahn-Meitner-Institut für Kernforschung Berlin GmbH, Bereich Kern - und Strahlenphysik, D-1000 Berlin 39, Germany
543. Nick Stone, University of Oxford, Clarendon Laboratory, Parks Road, Oxford OX1 3PU, England
544. Kazusuke Sugiyama, Department of Nuclear Engineering, Faculty of Engineering, Tohoku University, Sendai, Japan
545. J. K. Swenson, Department of Physics, University of North Carolina, Chapel Hill, NC 27514
546. T. J. Symons, Nuclear Science Division, Lawrence Berkeley Laboratory, 1 Cyclotron Road, Berkeley, CA 94720
547. Hiroyuki Tawara, Institute of Plasma Physics, Nagoya University, Chikusa-ku Nagoya 464, Japan
548. Lee C. Teng, Fermi National Accelerator Laboratory, Accelerator Division, P. O. Box 500, Batavia, IL 60510
549. The High Energy Group, Institute of Physics, Academia Sinica, Nankang, Taipei, Taiwan, ROC
550. Gurgun M. Ter-Akopian, Laboratory of Nuclear Reactions, JINR, 14198 Dubna, Russia
551. Mauro Donizette Tonasse, Faculdades Integradas de Uberaba, Avenida Afranio de Azevedo no. 115, UBERABA - MG - Brazil
552. P. J. Twin, University of Liverpool, P.O. Box 147, Liverpool L69 3BX, United Kingdom
553. J. P. Unik, Argonne National Laboratory, Building 200, Argonne, IL 60439
554. Robert Vandenbosch, Department of Chemistry, University of Washington, Seattle, WA 98195
555. A. van der Woude, Kernfysisch Versnellend Instituut der Rijksuniversiteit, Universiteitscomplex Paddepoel, Groningen, The Netherlands
556. H. Verheul, Natuurkundig Laboratorium der Vrije Universiteit de Boelelaan 1081, Amsterdam, The Netherlands
557. VICKSI, Sekretariat, Hahn-Meitner Institut für Kernforschung Berlin GmbH, Postfach 39 01 28, D-1000 Berlin 39, Germany
558. Virginia Polytechnic Institute and State University, Department of Physics, Blacksburg, VA 24061
559. A. J. A. Virtanen, Department of Physics, University of Jyväskylä, Seminaarinkatu 15, SF-40100 Jyväskylä, Finland
560. W. von Oertzen, Hahn-Meitner Institut für Kernforschung, Berlin GmbH, Germany
561. George Vourvopoulos, Department of Physics, Western Kentucky University, Bowling Green, KY 42101
562. Thomas A. Walkiewicz, Edinboro University, Department of Chemistry & Physics, P.O. Box 589, Wetsell Ridge Road, Edinboro, PA 16412
563. William Walters, Department of Chemistry, University of Maryland, College Park, MD 20742
564. A. H. Wapstra, Institute Voor Kernfysisch Onderzoek, Ooster Ringdijk 18, Amsterdam, The Netherlands
565. David Ward, Nuclear Physics Branch, Chalk River Nuclear Laboratories, Ontario, Canada KOJ 1J0
566. H. E. Wegner, Department of Physics, 901A, Brookhaven National Laboratory, Upton, NY 11973
567. J. L. Weil, Department of Physics and Astronomy, University of Kentucky, Lexington, KY 40506
568. D. C. Weisser, Department of Nuclear Physics, Institute of Advanced Studies, The Australian National University, P. O. Box 4, Canberra ACT 2600, Australia
569. W. G. Weitkamp, Nuclear Physics Laboratory, G-10, University of Washington, Seattle, WA 98195
570. Robert A. Weller, 1687 Station B, Vanderbilt University, Nashville, TN 37235

- 571. Joseph Weneser, Department of Physics, Bldg. 510, Brookhaven National Laboratory, Upton, NY 11973
- 572. B. H. Wildenthal, Department of Physics & Astronomy, University of New Mexico, 800 Yale NE, Albuquerque, NM 87131
- 573. University of Wisconsin, Department of Physics, Madison, WI 53706
- 574. J. L. Wood, School of Chemistry, Georgia Institute of Technology, Atlanta, GA 30332
- 575. Alexander Xenoulis, Van de Graaff Laboratory, Nuclear Research Center, Demokritos, Aghia Paraskevi Attikis, Athens, Greece
- 576. Takashi Yamazaki, Research Center for Nuclear Physics, Osaka University (Suita Campus), Ibaraki, Osaka, 567 Japan
- 577. Yasunori Yamazaki, Research Laboratory for Nuclear Reactors, Tokyo Institute of Technology, Tokyo, Japan
- 578. Fujia Yang, Director, Institute of Modern Physics, Fudan University, Shanghai, People's Republic of China
- 579. D. Youngblood, Cyclotron Institute, Texas A&M University, College Station, TX 77940
- 580. E. F. Zganjar, Department of Physics and Astronomy, Louisiana State University, Baton Rouge, LA 70803
- 581. K. Ziegler, Hahn-Meitner Institut für Kernforschung Berlin GmbH, Postfach 39 01 28, D-1000 Berlin 39, Germany
- 582-642. Given distribution as shown in DOE/TIC-4500 under UC-410 - General Physics

